Oxidative Medicine and Cellular Longevity

From Regulated Cell Death to Adaptive Stress Strategies: Convergence and Divergence in Eukaryotic Cells

Lead Guest Editor: Karin Thevissen
Guest Editors: Paula Ludovico and Sabrina Büttner

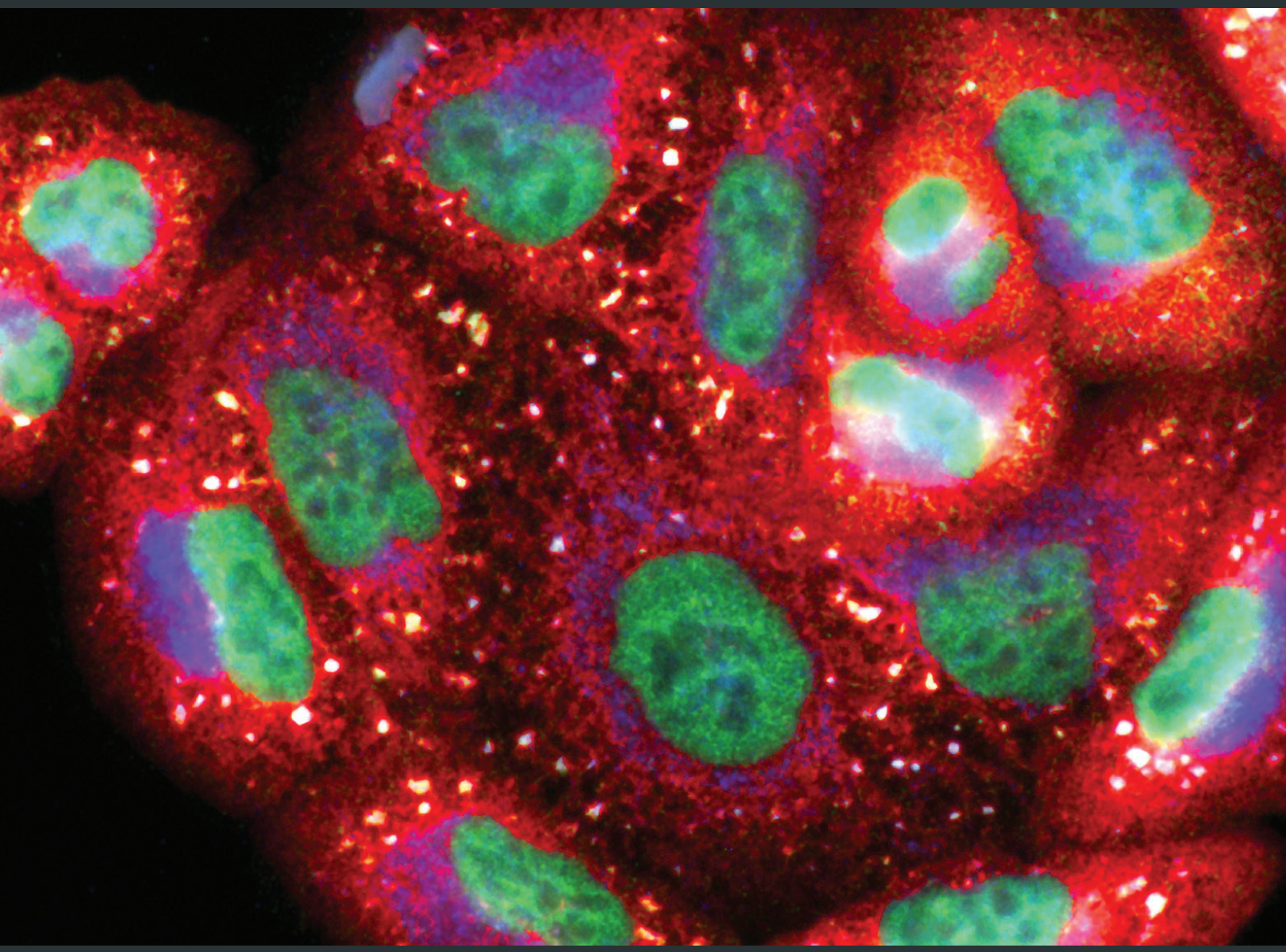

From Regulated Cell Death to Adaptive Stress Strategies: Convergence and Divergence in Eukaryotic Cells

Oxidative Medicine and Cellular Longevity

From Regulated Cell Death to Adaptive Stress Strategies: Convergence and Divergence in Eukaryotic Cells

Lead Guest Editor: Karin Thevissen
Guest Editors: Paula Ludovico and Sabrina Büttner

Editorial Board

Contents

Hindawi
Oxidative Medicine and Cellular Longevity
Volume 2018, Article ID 2480462, 2 pages
https://doi.org/10.1155/2018/2480462

Editorial

From Regulated Cell Death to Adaptive Stress Strategies: Convergence and Divergence in Eukaryotic Cells

Sabrina Büttner,[1,2] Paula Ludovico,[3,4] and Karin Thevissen[5]

[1]*Department of Molecular Biosciences, The Wenner-Gren Institute, Stockholm University, 10691 Stockholm, Sweden*
[2]*Institute of Molecular Biosciences, University of Graz, 8010 Graz, Austria*
[3]*Life and Health Sciences Research Institute (ICVS), School of Medicine, University of Minho, 4710-057 Braga, Portugal*
[4]*ICVS/3B's-PT Government Associate Laboratory, Braga/Guimarães, Portugal*
[5]*Centre of Microbial and Plant Genetics (CMPG), Kasteelpark Arenberg 20, 3001 Heverlee, Belgium*

Correspondence should be addressed to Karin Thevissen; karin.thevissen@kuleuven.be

Received 28 March 2018; Accepted 28 March 2018; Published 24 June 2018

Regulated cell death (RCD) encompasses different active forms of cell death ranging from apoptosis to necrosis or autophagy that are governed by distinct and highly sophisticated molecular pathways. An event intimately associated with RCD and RCD-associated pathologies, such as neurodegenerative or proliferative disorders, is redox homeostasis. A better understanding of how a cell responds to RCD induced by oxidative stress will undoubtedly uncover novel adaptive stress strategies, thereby providing more insights towards pro- or anti-RCD therapies.

This special issue unites 7 reviews and 5 original research articles. Various eukaryotic cell systems are discussed and include yeast, pathogenic fungi, zebrafish, and cancer cells. To uncover the complex network of the different and often interwoven RCD pathways and their association with oxidative stress, as well as for drug discovery purposes, lower eukaryotic cell model systems, including the budding yeast *Saccharomyces cerevisiae*, are used. In addition, due to the high conservation of RCD-related cellular processes, yeast can be used to study human pathologies caused by deviations in RCD. Moreover, the analysis of cell death routes solely present/induced in yeast and other fungi might point to novel therapeutic strategies to combat fungal infections.

To set the scene, K. F. Cooper describes the interplay between autophagy and apoptosis, thereby focusing in particular on the role of reactive oxygen species (ROS) in these processes. In addition, the molecular mechanisms underlying the induction and execution of RCD upon diverse types of stress and their association with oxidative stress have been addressed. Natural RCD-inducing scenarios such as ageing or disease have been considered as well as RCD induction upon challenge with external toxins. K. Mohammad et al. contributed with a relevant and timely review to the mechanisms of the liponecrotic mode of RCD induced by exogenous palmitoleic acid in the yeast *S. cerevisiae*. This review integrates liponecrotic RCD in different RCD scenarios, including age-related cell death modalities. In this respect, M. R. Yeaman et al. also provided a review on novel antifungal peptides that induce RCD in pathogenic fungi. Given the increasing impact of fungal infections on society due to the increasing emergence of resistance development and the relatively small armoury of antifungal compounds, antifungal agents that induce fungal cell death via a novel mode of action are of high relevance. Moreover, D. Wilkinson et al. contributed an original research article demonstrating that spatio-temporal metabolic differentiation within yeast colonies of different ages exists. They based their research on a comprehensive transcriptomic analysis and found that crucial metabolic reprogramming events arise during colony ageing, thereby supporting a role for mitochondria in this differentiation process. D. Wilkinson et al. also provided a review on the relevance of long noncoding RNAs (lncRNA) in differentiated subpopulations of yeast colonies and biofilms. Different cell types differ in their

complements of lncRNA, which target diverse functional categories of genes in different cell subpopulations and specific colony types. These contributions highlight how *S. cerevisiae* colonies have become an excellent model for studying various aspects of microbial multicellularity, including cell differentiation and communication. In an original contribution, R. Zadrag-Tecza et al. used *S. cerevisiae* to study the impact of increased cell size on replicative ageing. An analysis of yeast cells harbouring differing genome copy numbers, ranging from haploid to tetraploid, provides evidence for a correlation between an increase in cell volume achieved via additional genome copies and the reproductive as well as the postreproductive lifespan.

Besides that, analysis of adaptive stress strategies or tolerance mechanisms elicited by different organisms under RCD stress or oxidative stress in general is of great interest. This knowledge can be exploited to develop effective combination therapy. In this respect, K. Vriens et al. contributed a study on the tolerance mechanisms that are induced by amphotericin B in yeast and in the human pathogen *Candida albicans* using a microfluidics platform. They show that the fungicidal action of amphotericin B can be increased by inhibiting the nitric oxide-dependent tolerance pathway via the NO synthase inhibitor L-NAME. This resulted in a fungicidal combination treatment based on AMB and L-NAME.

Redox homeostasis and cell death were also addressed in different diseases and models with therapeutic aims. M. Cobbaut and J. Van Lint discussed the role of protein kinase D (PKD) isoforms as regulators of the oxidative stress response. They highlight the differential activation of the specific PKD isoforms upon increased oxidative burden and the signaling pathways mediating their downstream effects as well as their isoform-specific characteristics. H. Gu et al. provided a review on the occurrence of radioresistance in gastric cancer, which is one of the primary causes responsible for therapeutic failure and recurrence of cancer and linked to ROS. In an original contribution, A. A. Kulkarni et al. used a transgenic nitroreductase-expressing zebrafish model treated with the prodrug metronidazole to demonstrate that ROS can be generated in a beta cell-specific manner. This hybrid chemical/genetic approach allows monitoring of ROS generation in beta cells in situ, and its manipulation, for instance by antioxidants, is shown to be protective for beta cells under conditions of elevated ROS production.

P. Davalli et al. contributed with a review on the DNA damage response (DDR) as a target for oxidative-based cancer therapy. DDR is deeply affected and sensitive to redox homeostasis since ROS regulate several enzymes of this repair pathway. The authors reviewed mechanisms contributing to ROS homeostasis, the ROS-sensitive proteins in DDR, and how DDR could be targeted in cancer therapy by using DDR inhibitors combined with ROS-inducing drugs. In an original article, S. V. Kostyuk et al. analysed the response of several human cell types to cell-free DNA differing in GC content and grade of oxidation. They provide insights into the different expression patterns of the transcription factors NF-κB and NRF2 following treatment with distinct DNA species. While oxidized cell-free DNA elicited a very fast and intense inflammatory response, often leading to apoptosis, nonoxidized species rich in GC rather triggered a weaker response, promoting cell survival possibly via hormesis.

In conclusion, this special issue will provide more insights into RCD and into tolerance mechanisms elicited in cells experiencing RCD. Such information can prove very valuable in designing novel (combinatorial) pro- or anti-RCD therapies.

Disclosure

Sabrina Büttner and Paula Ludovico shared as first authors.

Acknowledgments

The editors would like to thank all authors who submitted their research to this special issue, as well as all reviewers for their valuable contribution.

Sabrina Büttner
Paula Ludovico
Karin Thevissen

Hindawi
Oxidative Medicine and Cellular Longevity
Volume 2018, Article ID 4701275, 13 pages
https://doi.org/10.1155/2018/4701275

Review Article

Till Death Do Us Part: The Marriage of Autophagy and Apoptosis

Katrina F. Cooper

Department of Molecular Biology, Graduate School of Biological Sciences, Rowan University, Stratford, NJ 08084, USA

Correspondence should be addressed to Katrina F. Cooper; cooperka@rowan.edu

Received 24 October 2017; Revised 2 January 2018; Accepted 8 January 2018; Published 8 May 2018

Academic Editor: Karin Thevissen

Autophagy is a widely conserved catabolic process that is necessary for maintaining cellular homeostasis under normal physiological conditions and driving the cell to switch back to this status quo under times of starvation, hypoxia, and oxidative stress. The potential similarities and differences between basal autophagy and stimulus-induced autophagy are still largely unknown. Both act by clearing aberrant or unnecessary cytoplasmic material, such as misfolded proteins, supernumerary and defective organelles. The relationship between reactive oxygen species (ROS) and autophagy is complex. Cellular ROS is predominantly derived from mitochondria. Autophagy is triggered by this event, and by clearing the defective organelles effectively, it lowers cellular ROS thereby restoring cellular homeostasis. However, if cellular homeostasis cannot be reached, the cells can switch back and choose a regulated cell death response. Intriguingly, the autophagic and cell death machines both respond to the same stresses and share key regulatory proteins, suggesting that the pathways are intricately connected. Here, the intersection between autophagy and apoptosis is discussed with a particular focus on the role ROS plays.

1. Introduction

Autophagy was discovered in 1963 as a lysosome-mediated degradation process for nonessential or damaged cellular constituents [1]. Since then, work pioneered in yeast [2, 3] has revealed that this widely conserved catabolic process is both highly regulated and a crucial integration point in cell physiology, [4, 5]. There are three main autophagic pathways that have been shown to coexist in mammalian cells called macroautophagy, microautophagy, and chaperone-mediated autophagy (CMA). Macroautophagy involves the formation of a doubled membrane structure called the autophagosome that fuses with the lysosome thereby transferring its luminal content for degradation [6]. Microautophagy refers to the process where cytosolic proteins are directly engulfed by the lysosome [7]. CMA, as its name suggests, utilzes cytosolic chaperones to deliver proteins to the surface of the lysosomes whereupon they unfold and cross the lysosomal membrane [8].

The subject of this review is the highly conserved process of macroautophagy, which here on out will be referred to as "autophagy." Although more nuanced in higher eukaryotes, many of the AuTophaGy (Atg) genes and processes (outlined in Figure 1) initially defined in yeast are conserved [9, 10]. This significant body of work has also resulted in many different types of selective autophagy being identified. For example, mitophagy, pexophagy, and lipophagy represent the lysosomal degradation of mitochondria, peroxisome, and lipids, respectively. Given this wide range of substrates, understanding the molecular details of how the various components are both recognized and processed is now at the forefront of autophagy research [9]. Unfortunately, the recent explosion of published studies has also led to considerable terminology confusion. For example, the term canonical and noncanonical autophagy has been widely used in the literature to describe autophagy events that use different molecular signatures [11–13]. Recently, leaders in the field have reached a consensus on what these signatures should be called [10].

As stated above, autophagy maintains cellular homeostasis under normal physiological conditions and in response to exogenous stimuli. Increased levels of intracellular reactive

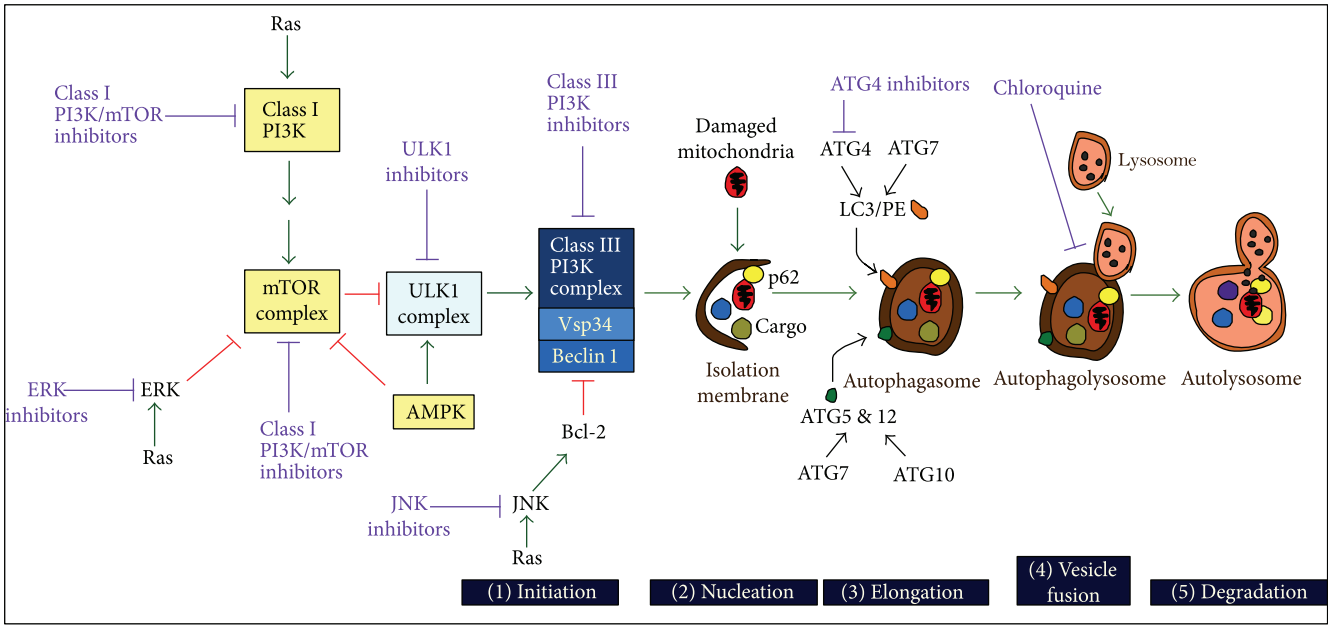

Figure 1: Schematic overview the five stages of the autophagy pathway. The execution point of where known pharmacological inhibitors act are written in purple. See text for details.

oxygen species (ROS) which arise predominantly from defective mitochondria also trigger autophagy. In turn, the increased autophagic flux drives down ROS by the consumption of damaged organelles (Figure 2). Thus, excess ROS upregulates autophagic flux, and in turn, this catabolic cellular process restores physiological ROS levels. As such, stimulus-induced autophagy underlies and sustains an adaptive response to stress with cytoprotective functions. However, when the levels of ROS become overwhelming, a nonautophagic regulated cell death (RCD) response is initiated suggesting that autophagy and RCD pathways are tightly linked [14]. How this switch is made is presently unclear. In this review, the relationship between ROS, autophagy and cell death are discussed. In addition, current knowledge about the crosstalk between autophagy and apoptosis is also reviewed. Lastly, cell death pathways have also been through a recent nomenclature classification [15]. For the purposes of this review, the type of RCD pathway will be referred to by its subtype. Thus, when referring to apoptosis, unless specified differently, I will be referring to both intrinsic and extrinsic mechanisms.

2. The Process of Autophagy

The word autophagy is fittingly derived from the Greek words for *self* (auto) and *eating* (phagy). It is a multistep catabolic process acting as a critical cellular response to nutrient and oxygen deprivation. Thereafter, free amino acids, free fatty acids, and ATP are recycled back into the cytoplasm for biomolecule synthesis. In mammals, there are five key control points, namely, initiation, nucleation, elongation, and lysosomal fusion and degradation of autophagosome contents. These stages are outlined in Figure 1, and the reader is referred to many excellent and recent reviews that provide more details on the role individual proteins play [16–18]. In short, initiation of the preautophagosomal membranes, which can be derived from the endoplasmic reticulum (ER) [19], begins with the activation of the ULK1 kinase complex. This complex is activated by cellular stress via mTORC inhibition and/or AMP-activated protein kinase (AMPK) activation [20]. ULK1 phosphorylates Atg13 and Fip200 to form an ULK1/2-mAtg13-Fip200 complex that is stabilized by Atg10 [16]. ULK1 activation promotes the recruitment of a multiprotein complex with class III phosphatidylinositol 3-kinase (PI3K) activity. This complex consists of 4 proteins which are scaffolded by Beclin-1, whose role upon release from the antiapoptotic protein Bcl-2, is to activate the vacuolar sorting protein Vps34 [21]. Maturation of the growing autophagosome membrane requires the complexes to recruit two ubiquitin-like conjugation systems. Both these systems involve the E1-like Atg7 [22, 23] which initiates the conjugation of LC3 with phosphatidylethanolamine (LC3/PE) and Atg5 with Atg12. Incorporation of these complexes into the autophagosome membrane is an essential process. Likewise, Atg4, the protease that cleaves and thereby activates LC3, is required the formation of the LC3-PE complex [24]. To end the program, the autophagosome fuses with the lysosome to form the autophagolysosome. The SNARE protein Stx17 [25] is essential for this process. Upon completion, the contents of the autophagosomes are degraded by the lysosomal hydrolases producing amino acids and lipids for protein and other macromolecular synthesis and metabolism.

In the past decade, the molecular mechanisms by which cargos are identified and consequently sequestrated within autophagosomes have been revealed. Best understood is the role the adaptor protein p62 plays in mitophagy. Here, p62 binds to defective and surplus mitochondria that are marked by ubiquitin thereby entrapping them in the autophagasome

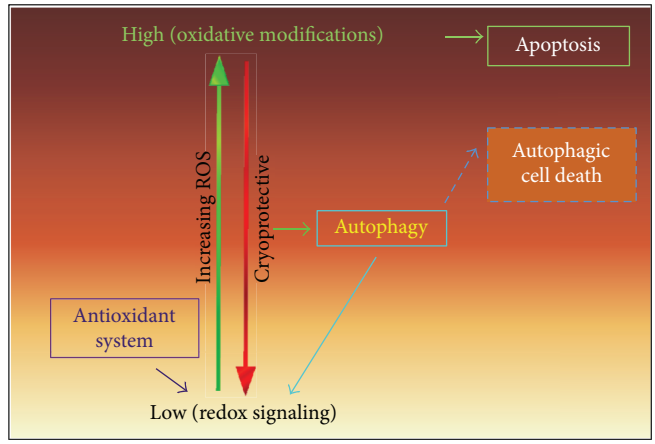

Figure 2: Diagram showing the closely linked relationship between ROS levels, autophagy, and apoptosis. See text for details.

by binding to the autophagosome marker protein LC3 [26–28]. More recently, other selective autophagy receptors which include Nbr1, Ndp52, Vcp, and Optineurin have been characterized and the reader is referred to recent reviews for more detailed information [29, 30].

3. ROS Balance

How cells decide to switch from cellular homeostasis to apoptotic pathways upon ROS stress is not well understood. Understanding this is critical, as many types of cancers, especially established tumors, have adopted enhanced autophagy as a mechanism to survive in unfavorable environments. As a result, autophagic inhibition represents a new therapeutic tool to drive cells into regulated cell death (RCD) pathways [31]. However, a caveat to this approach is that, although rare, in some contexts, components of the autophagy machinery are used in autophagic cell death pathways [15, 17, 32]. Autophagic cell death is another area that has recently been redefined, the details of which are beyond the scope of this current review [10]. That being said, this reclassification is important as many reported studies of autophagic cell death may be due to defective apoptotic machinery [33]. However, autophagic cell death, although rare, does exist and is classified as an event that has to be retarded by pharmacological or genetic inhibition of autophagy. Given the fact that multiple components of the macroautophagy machinery have autophagy-independent functions ([34] and see below), it is recommended that before etiologically attributing a cell death event to macroautophagy, the involvement of at least two different proteins of the macroautophagy apparatus is shown to be required [10]. To date, three types of autophagic cell death have met with these more stringent criteria, autosis, ferroptosis, and more recently necroptosis [17, 35, 36]. Paradoxically, the loss of autophagy also contributes to de novo tumor formation, as autophagy is required to remove genotoxic materials that prevent malignant transformations [15]. Consistent with this hypothesis, mouse models of oncogene-driven caners with defective autophagy display accelerated tumor development. However, the tumors were benign and autophagy was essential for the progression to a more malignant state [33]. The favored model from these studies is that autophagy inhibits the initiation of tumorigenesis but promotes the survival of established tumors [37]. More recently, however, in certain contexts, the presence or absence of p53 and key Atg proteins dictates tumor growth in certain K-Ras-driven mouse models [38]. Thus, the relationship between autophagy, tumor suppressor genes, and oncogenes certainly warrants future studies.

3.1. ROS. ROS is classified as a heterogeneous group of molecules generated naturally in cellular metabolism from diatomic oxygen [39]. The group includes the highly reactive free oxygen radicals (superoxide anion O_2^-, hydroxyl radical OH^-) and the stable 'diffusible' non-radical oxidant, hydrogen peroxide (H_2O_2). Their formation begins with the univalent reduction of oxygen to produce superoxide radical O_2^- (see Figure 3). This predominantly occurs in the mitochondria as a result of electron leakage during normal respiration in the electron transport chain [40]. O_2^- is also produced from other sources: in peroxisomes through β-oxidation of fatty acids and flavin oxidase activity [41]; in the endoplasmic reticulum (ER) from protein oxidation of molecular oxygen [42]; and by enzymatic reduction of molecular oxygen with xanthine/xanthine oxidase, uncoupled nitric oxide synthases (NOS), cytochrome P-450 isoforms, and NADPH-dependent oxidases (NOXs) being key contributors [39]. As O_2^- is highly reactive with the ability to convert to the toxic OH^- radical, it is rapidly converted to the more stable and membrane-diffusible ROS H_2O_2 [43]. This occurs either spontaneously or through the actions of superoxide dismutases (SOD1 and SOD 2 [44]).

3.2. Antioxidants. How cells process intracellular H_2O_2 is intricately linked to their cell fate. It can be converted to water (ROS detoxification) or the genotoxic hydroxyl radical by different enzymes. Lastly, it can be used as a signaling molecule in a process coined redox signaling (Figure 3). ROS detoxification is executed by a variety of enzymes, the key players being catalase, glutathione peroxidases (GPXs),

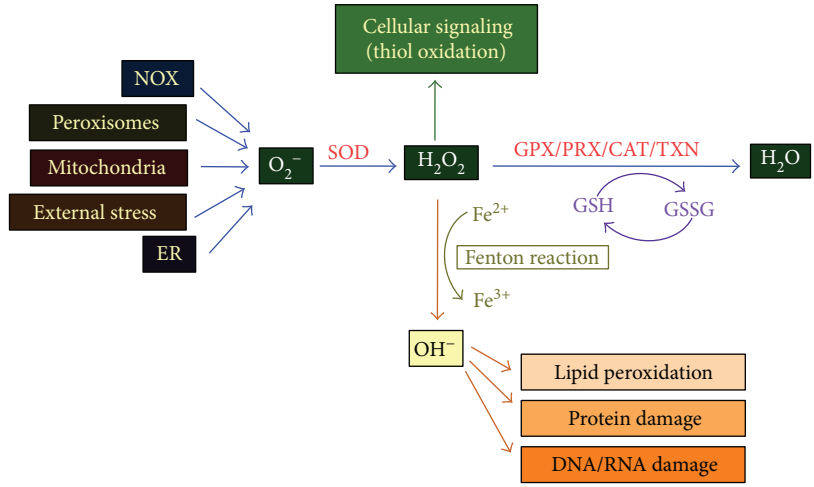

Figure 3: Schematic illustration of the mechanism involved in reactive oxygen species (ROS) formation and elimination. Endogenous forms of ROS arise from NADPH oxidase (NOX) as well as the organelles shown. The cytosolic superoxide (O_2^-) is converted into hydrogen peroxide (H_2O_2) by superoxide dismutase (SOD). H_2O_2 has three fates. It can be detoxified to water by glutathione peroxidase (GPX) peroxiredoxin (PRx), thioredoxin (TRX), and catalase (CAT). The reduced form of glutathione (GSH) promotes this reaction whereas oxidation to glutathione disulfide GSSH results in intracellular redox. H_2O_2 can be converted to the cytotoxic hydroxyl radical (OH^-) via the Fenton reaction resulting in irreversible damage to lipids, proteins, and DNA. Lastly, H_2O_2 can also be used as a signaling molecule by oxidizing critical thiols within proteins to regulate numerous biological processes.

peroxiredoxins, glutathione peroxidases (GSH-Px or GPx), and thioredoxin (TXN). Whilst PRXs are associated with H_2O_2 scavenging, the GPX family of proteins (GPX1–8) catalyzes the reduction of H_2O_2 to H_2O by oxidizing reduced glutathione (GSH) to glutathione disulfide (GSSG). Consistent with this, GSH oxidation to GSSG results in intracellular redox imbalance which is reflected by a decreased GSH:GSSG ratio [45]. Other antioxidants are vitamin C, vitamin E, and carotenoids. Conversion of H_2O_2 to the damaging free hydroxyl radicals occurs by the Fenton reaction where free iron (Fe^{2+}) reacts with H_2O_2. This insoluble radical has strong oxidizing potential and causes irreversible oxidative damage to virtually any cellular macromolecules within the vicinity of their production [46, 47]. Thus, cellular levels of H_2O_2 and OH^- are maintained by a balance between oxidant and antioxidant responses.

3.3. Role of Transcription Factors. The transcription factor Nrf2 (nuclear factor erythroid 2-related factor 2) [48] plays a key role in both ROS detoxification, prevention of OH^- production, and redox balance [49]. Following exposure to oxidants or electrophiles, Nrf2 accumulates in the nucleus where it upregulates four groups of genes encoding detoxification and antioxidant enzymes. These include those needed for the biosynthesis and maintenance of GSH [50], cytosolic thioredoxin (TXN), thioredoxin reductase (TXNRD), and sulfiredoxin (SRXN), all of which reduce oxidized protein thiols [51]. In addition, genomic studies have revealed that Nrf2 regulates over 600 genes [52] including those required for inhibition of inflammation and the repair or removal of damaged proteins. This has resulted in Nrf2 being named "the master regulator of antioxidant responses" [53]. As befitting this principal role, Nrf2 itself is tightly controlled by ubiquitin-mediated proteolysis which is inhibited following oxidative stress (see below for details) [54].

Worth mentioning is that Nrf2 indirectly helps to modulate ROS levels by regulating free Fe(II) homeostasis. This is achieved by the upregulation of genes encoding members of the ferritin complex, which detoxifies Fe(II) by converting it into Fe(III). This complex also sequesters iron within its own structure that prevents it from being accessed by the Fenton reaction, thus reducing the production of OH^- radicals from ROS [55, 56]. Given this role, it comes as no surprise that iron excess can significantly promote tumorigenesis [57, 58]. This has led to the emergence of using iron chelation or transferrin receptor-neutralizing antibodies, to treat cancer [59]. However, the molecular mechanisms by which iron excess promotes tumorigenesis remain unclear. Recently, the tumor suppressor p53 was identified as a protein that can ligate the heme iron using one cysteine side chain. This promotes p53 nuclear export and degradation by ubiquitin-mediated proteolysis [60]. Lastly, although beyond the scope of this review, it is important to mention that other transcription factor families, for example, Forkhead box O (FoxO) and nuclear factor-κB (NF-κB), also regulate antioxidant gene expression [53].

4. ROS as a Signaling Molecule

Since the 1990's, the model that cellular oxidant production is inherently damaging has been replaced by a more complex scenario in which regulated oxidant production functions as important physiological regulators of intracellular signaling pathways [61]. These include cellular proliferation and differentiation as well as stress-responsive programs

[62]. This posttranslational modification is achieved by H_2O_2-mediated oxidation of reactive cysteine residues found within redox-sensitive signaling proteins. Importantly, this reaction, in which the sulfhydryl group undergoes deprotonation and oxidation, is reversible being easily reduced back to reduced cysteine by either enzymatic systems (thioredoxin/thioredoxin reductase system) or nonenzymatic reactions (thiol/disulfide exchange). This reversibility provides the on/off switch, a character of that is essential for signaling. An emerging theme is that antioxidant proteins also actively participate in redox signaling [61]. For example, they catalyze the reduction of oxidized proteins as well as binding to signaling intermediates thereby activating downstream effectors such as p38 MAPK and the c-Jun N-terminal kinase (JNK) [61]. However, when ROS levels cannot reach homeostasis, the reversible SOH derivative can be hyperoxidized to the irreversible and damaging SO_2H derivative [63].

Given the potential of this posttranslational modification to affect a wide range of cellular processes, large-scale proteomic approaches have been used to identify proteins that potentially possess modulatory cysteine residues [64–66]. The results identified many phosphatases that are well established signaling molecules [67, 68]. A more recent study has identified that many mitochondrial proteins contain potentially reactive cysteines [69]. Intriguingly, apart from the protease Atg4, no other autophagy proteins were identified in these screens. However, two groups have proposed that the superoxide acts as a signal to activate mitophagy by depolarizing the mitochondrial inner membrane. These depolarized mitochondria become fragmented and recruit Park2, the mitophagy E3 ubiquitin ligase [70, 71].

5. RNS as a Signaling Molecule

Although not the subject of this review, in addition to ROS, cells contain reactive nitrogen species (RNS) mostly in the form of nitric oxide (NO^-). Nitric oxide is generated by the mitochondria and acts as a cell signaling molecule in many physiological processes including mitochondrial biogenesis and bioenergetics [72, 73]. NO^- itself is not highly toxic as it is efficiently removed by its rapid diffusion through tissues into red blood cells, where it is converted to nitrate by reaction with oxyhemoglobin [74]. However, when both superoxide O_2^- and NO^- are synthesized within a few cell diameters of each other, they will combine spontaneously to form peroxynitrite ($ONOO^-$) that can mediate cellular damage in a wide range of conditions [75]. Small amounts of peroxynitrite may also spontaneously decompose to yield NO_2^- and the hydroxyl radical [76]. Similar to ROS, RNS can add posttranslational modifications to proteins by S-nitrosylation of reactive cysteines [77]. Importantly, Drp1, the GTPase that regulates mitochondrial fission, is posttranslationally modified in such a manner [78]. In addition, several proteins that bind to the core fission/fusion proteins also contain redox-sensitive motifs [79]. Taken together, this data suggests that RNS and ROS both regulate mitochondrial morphology via posttranslational modification.

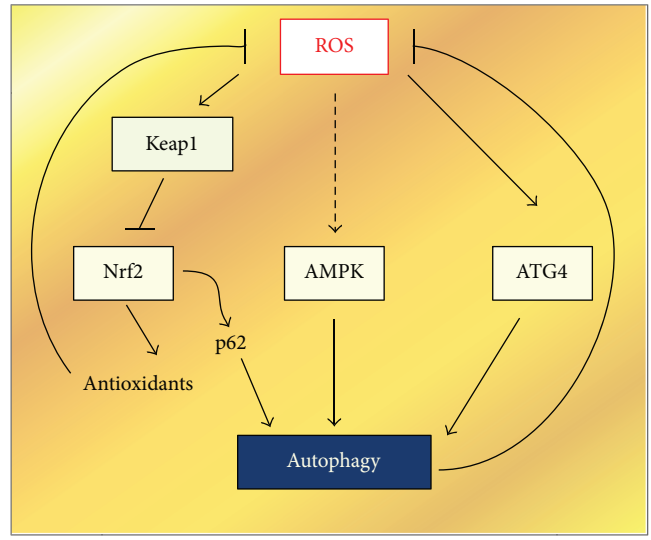

Figure 4: Diagram depicting the genetic relationship between ROS and autophagy initiation. The dotted lines represent an indirect relationship.

6. Direct Effect of ROS on Autophagy

It is well established that ROS can induce autophagy, as this is a major mechanism used to exsanguinate superfluous cellular ROS. In turn, autophagy drives down the levels of ROS as it consumes damaged mitochondria, the major source of ROS. This "pas de deux" represents a finely tuned negative feedback mechanism by which autophagy eliminates the source of oxidative stress and protects the cell from oxidative damage. Increased intracellular ROS that is accompanied with increased autophagic flux is triggered by many factors including starvation, hypoxia, TNFα (tumor necrosis factor α), and NGF (nerve growth factor) deprivation [80, 81]. Consistent with this, studies have shown that treatment of make cells with the ROS scavenger N-acetyl cysteine (NAC) decreases both cellular ROS production and autophagy, implicating redox thiol signaling as an important regulator of autophagy. Likewise, exogenous H_2O_2 and suppressed NF-κB activation of mTOR mimics these effects [82]. These findings are consistent with H_2O_2 effects being mediated through the production of ROS and redox signaling. However, the precise molecular details on how ROS crosstalks with the autophagic machinery are still unclear. In the last few years, it has emerged that redox imbalance has a pivotal role in driving the process. Consistent with this, two proteins Atg4 and Keap1, which have opposing roles in promoting or inhibiting autophagy, respectively, are regulated by redox signaling. Lastly, AMPK, which is a major inducer of autophagy in response to starvation, may also indirectly play a role (see Figure 4).

6.1. ATG4. Atg4 is the only mammalian protein whose redox regulation has been shown to be necessary for the progression of autophagy [24]. Atg4 is a protease which is active in a reducing environment where it cleaves the C-terminal domain of LC3. This allows LC3 conjugation with

phosphoethanolamine (PE) which is a hallmark of, and necessary for, autophagosome formation. Upon oxidation of an active cysteine residue (C81), the protease activity is inhibited, resulting in increased autophagy. These results were obtained in 2007, and although it has also been speculated that other enzymes involved in the initiation and elongation stages of autophagosome formation may also be regulated by redox signaling, no concrete evidence has been reported.

6.2. AMPK. AMPK an established indirect regulator of autophagy [20, 83, 84]. During normal physiological conditions, cellular homeostasis is maintained by strictly matching the generation and consumption of ATP. When ATP levels become low, they are replenished by autophagic recycling of unnecessary cytoplasmic material, such as misfolded proteins, supernumerary, or defective organelles [18]. AMPK is critical for this process as it is an energy sensor, being activated by increased levels of ADP and AMP [84, 85]. This AMP:ATP imbalance can be stimulated by multiple stresses including amino acid starvation, glucose withdrawal, hypoxia, and H_2O_2 [86]. Given this role, it is not surprising that AMPK is regulated by the intracellular redox status, being activated by Trx1 during energy starvation which promotes access by AMPK to two key cysteine residues in the catalytic subunit [87]. Once activated, AMPK can initiate autophagy by several ways. It negatively regulates components of the mTOR signaling cascade [88, 89] as well as directly activating the ULK1 kinase [90] (Figure 1). Furthermore, in yeast, it has recently been shown that following glucose starvation, the AMPK homologue Snf1 is recruited to the outer mitochondrial membrane, where it phosphorylates the Atr homologue Mec1. This is then required for recruitment of Atg1 (ULK1 homologue) thereby allowing the Snf1-Mec1-Atg1 module to maintain mitochondrial respiration by initialing autophagy during glucose starvation [91]. Although the molecular mechanisms still remain unclear, Atg1 may maintain mitochondrial respiration by directly or indirectly phosphorylating key mitochondrial proteins which are essential for respiration [91].

The very fast induction of autophagy following ROS exposure suggests that a rapid on/off molecular switch may regulate initiation of autophagy. Some research has implicated that AMPK could play a role as, following hypoxia, it is activated in an AMP:ATP-independent manner [92, 93]. In support of a rapid switch, is the observation that following ROS induction, GSH is excluded from cells. This consequently permits the accumulation of redox-sensitive proteins in their oxidized form. Also, chemically oxidized GSH can induce autophagy in the absence of an autophagic stimulus [94, 95]. This result serves to strengthen the key role redox homeostasis plays in autophagy commitment.

6.3. Others. Other proteins also indirectly respond to increased cellular ROS. These include high mobility group box 1 (Hmgb1, a nuclear protein that is released extracellularly in response to cytokines), Ras, and various kinases, Atm, Akt, Erk, JNK, and Perk to name a few [96]. In recent years, the role these proteins play in regulating autophagy has become increasingly important as their signaling capabilities have been linked to cancer cell progression [97]. A classic example is oncogenic Kras signaling, which is an established driver of pancreatic ductal adenocarcinoma (PDAC). More recently, tumor growth has been shown to be contingent on stromal inputs that are derived from fibroblasts of the pancreatic tumor microenvironment [98]. These observations have initiated test therapies that couple an established autophagy inhibitor (chloroquine) with kinase inhibitors [33].

6.4. Keap1 and p62. Different to Atg4, the Kelch-like ECH-associated protein 1 (Keap1) is a redox-sensitive protein that indirectly negatively regulates autophagy in response to ROS [99]. Keap1 serves as a substrate adaptor protein for the (Keap1)-Cullin 3 (Cul3) E3 ubiquitin ligase complex [100]. Under normal physiological conditions, this complex is responsible for the rapid turnover of the transcription factor Nrf2. However, Keap1 is equipped with reactive cysteine residues which, upon exposure to oxidants, causes a conformational change which impairs its ability to trap Nrf2 for ubiquitylation and degradation [101]. The resulting stable Nrf2 then translocates to the nucleus where it upregulates antioxidant genes [102]. Stable Nrf2 can also be created by competitive binding of p62 to the Nrf2-binding site on Keap1. p62 as mentioned above, is the autophagic adaptor protein that brings dysfunctional mitochondria to the phagosome [103]. Therefore, increased free p62 levels activate the Nrf2 pathway. p62 is also an Nrf2 target gene, thus creating a positive regulatory loop [104]. p62 also promotes the expression of other signaling proteins including NF-κB and mTor1 [105, 106] and thus has gained notoriety as a signaling hub [107]. Intriguingly none of these functions depend on the ubiquitin-associated or LC3-interacting region domains of p62 [105], but they are linked to cytosolic p62 levels which are regulated by autophagy via by its LIR domain that binds to LC3 on autophagasomal membranes [105]. As in vivo studies have shown that overexpression of p62 is carcinogenic in hepatocellular carcinoma [108], it has been suggested that homeostatic maintenance cytosolic p62 levels contributes to the final outcome of the tumorigenic process [107]. This has led to the idea that a critical role of autophagy is to prevent p62-driven tumor initiation and malignant transformation.

7. Autophagy and Apoptosis—Till Death Do We Part

Both autophagy and apoptosis respond to similar stresses. However, the molecular mechanisms that dictate cell fate decisions are only just emerging. What is striking is that proteins that were originally thought to be required for just one pathway have now been shown to play a role in both. Thus, the decision to commit cellular suicide following stress may be controlled by many factors as opposed to a simple molecular switch. What is also apparent is that our understanding of how apoptosis repurposes the ATG machinery to promote cell death far outweighs the current knowledge of how autophagy inhibits apoptosis. This is somewhat surprising as there are a large number of examples in the

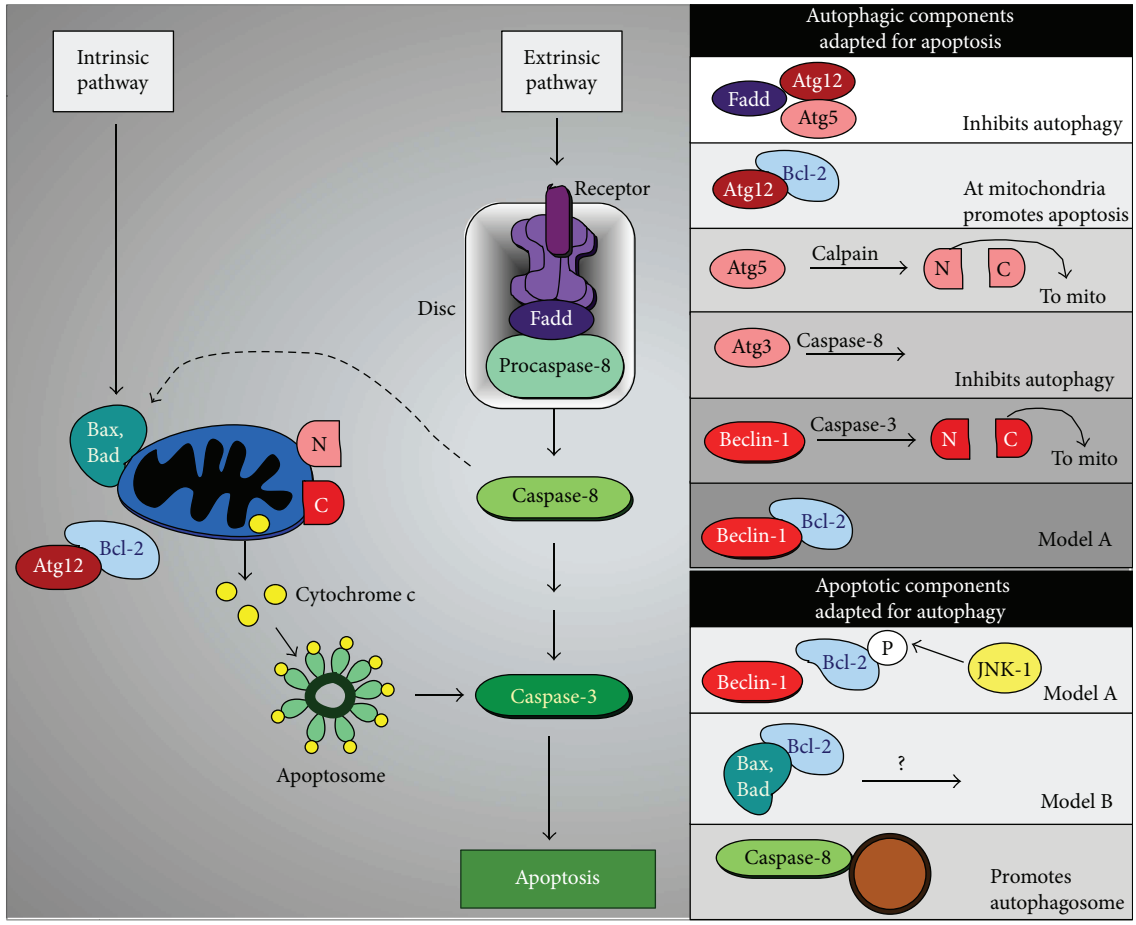

Figure 5: Diagram showing the intricate relationship between autophagy and the extrinsic and intrinsic apoptotic pathways. See text for details.

literature where autophagy protects against apoptosis. The salient points of this symbiotic relationship are discussed below and summarized in Figure 5. Further details can be found in many excellent reviews and original papers cited therein [14, 109–112]. The overwhelming recent explosion of data has though served to emphasize that, like all marriages, the relationship is complex. What is becoming clear however is that in a narcissistic manner, each pathway steals and adapts proteins from the other pathway to promote its own mechanism.

7.1. Brief Outline of Apoptosis. The cast of characters that play a role in the intersection of apoptosis and autophagy are derived from two distinct but connected apoptotic pathways, intrinsic and extrinsic apoptosis (outlined in Figure 5) and described in many excellent reviews [113, 114], so only the salient details are given below. The *intrinsic pathway* is characterized by pro- and antideath signals converging at mitochondrial membranes. These consequently become permeabilized (MOMP—mitochondrial outer membrane permeabilization), leading to the release of mitochondrial intermembrane proteins including cytochrome c. Rapid cell death follows as MOMP triggers both caspase activation on the apoptosome and blocks caspase inhibitors. Together, this starts a cascade of active caspases which cleave hundreds of cellular substrates ending in cellular demise. The Bcl-2 family of proteins consists of proapoptotic and prosurvival proteins which together control MOMP. Under basal conditions, the prosurvival proteins, Bcl-2, Bcl-X_L, and Mcl-1, inhibit MOMP in two ways. First, they directly bind and inhibit the proapoptotic effector proteins Bax and Bak, which form the pores in the mitochondrial membrane. Second, they bind to BH3-only proteins such as Bim which prevents them from activating Bax [115].

The *extrinsic* receptor-mediated apoptosis pathway is triggered by the ligation of death receptors with their cognate ligands. This stimulates receptor clustering resulting in the recruitment of cytoplasmic adapter proteins, important amongst which is Fadd. Fadd then associates with procaspase-8 leading to the formation of a death-inducing signaling complex (DISC). This results in the dimerization and catalytic activation of caspase-8, which can then directly cleave and activate caspase-3 [116]. Both intrinsic and extrinsic pathways result in caspase-3 activation that is linked to the initiation of the execution phase of apoptosis. Crosstalk between the two pathways is mediated by caspase-8 cleavage and activation of BID. BID is a BH3-interacting domain death agonist, the product of which

(truncated BID; tBID) is required in some cell types for death receptor-induced apoptosis [117].

7.2. Beclin-1 and Bcl-2. The best described relationship between autophagic and apoptotic proteins is the complex relationship between Beclin-1, the antiapoptotic proteins, Bcl-2 [118] (plus family members Mcl1-1 and Bcl-X_L) and the prodeath protein Bax [119]. In this ménage à trois Bcl-2 plays a key role as under normal physiological conditions, its interaction with Beclin-1 and Bax inhibits autophagy and apoptosis, respectively [118]. Currently, there is no consensus on the molecular mechanisms that define this relationship. Furthermore, it is complicated as there are two distinct cellular pools of Bcl-2, one at the ER where it is bound to Beclin-1, [118, 120], and the other at mitochondria where it is bound to Bax. In the original model, (model A, in Figure 5) under autophagy-inducing conditions, a BH3-only protein, (either Bik, Bad, or Nova) competitively binds to Bcl-2, thereby displacing it from Beclin-1 [118, 121]. This displacement is augmented by JNK1 phosphorylation of Bcl-2 and required for Beclin-1 to activate Vps34 resulting in the nucleation of an isolation membrane thereby promoting autophagy [122]. As Bcl-2 has a higher affinity for Bax than Beclin-1, this low level phosphorylation of Bcl-2 is not enough for it to be dissociated from mitochondrial Bax. This proapoptosis move occurs if the stress signal becomes overwhelming and requires Bcl-2 hyperphosphorylation [122].

Many inducers of autophagy also cause cell death, which lead David Vauz and colleagues to challenge this model. In a series of elegant genetic and biochemical experiments, his group demonstrated that in the absence of Bax and Bak, antagonizing or altering the levels of prosurvival Bcl-2 family members has no detectable impact on autophagy [121]. This then suggests a model (model B in Figure 5) in which the effects of Bcl-2 on autophagy are an indirect consequence of its inhibition of apoptosis by associating with Bax and Bad. Thus, as both Beclin-1 and Bcl-2 are key regulators of autophagy and apoptosis, respectively, it is imperative that these opposing models be resolved. As it seems to be the case in many studies, both models could be correct but context specific.

7.3. Caspases. Caspases are cysteine proteases that traditionally are principle mediators of apoptotic cell death [123]. In recent years, they have been shown to shift the balance of cellular homeostasis towards apoptosis by dismantling several key Atg proteins, including Atg3, Vps34, and Beclin-1. The culprit caspases are 3 and 8 that cleave PI3K members (Vps34 and Beclin-1) and Atg3, respectively [124–126]. Worthy of note is that the proteolytic product of Beclin-1 (and caplain cleaved Atg5, see below) translocates to the outer mitochondrial membrane and exhibits a proapoptotic activity [125, 127]. Thus, the apoptotic machinery not only inactivates autophagy but also repurposes proteins to promote cell death. Consistent with this theme, the cleavage of Beclin-1 is enhanced by Bax thereby further suppressing autophagy [127]. As neither the N- nor C-terminal fragments of Beclin-1 can interact with Vps34, the cleavage of Beclin-1 has been shown to be a critical event whereby caspases inhibit autophagy [128, 129]. Consistent with this, a noncleavable Beclin-1 mutant can restore autophagy [130].

Unexpectedly, it has also been shown that caspases can also promote autophagy under certain contexts. As stated above, caspase-8 is activated by DISC, a multiprotein signaling platform. In the absence of DISC, caspase-8 can still be activated from procaspase-8 by being recruited to autophagosomes. Its localization to the autophagosome this is executed by binding either to the autophagic cargo receptor p62 or through an interaction between the adaptor protein Fadd and Atg5 [128]. It remains unclear if this mechanism promotes apoptosis or autophagy pathways as both scenarios have been reported in the literature in different tumor types [128, 131]. The most likely scenario is that these contradictory functions are likely to be context specific. Ascribing which function caspase-8 is playing at the autophagosome is worth while as this mechanism has been successfully exploited to render cancerous cell lines responsive to further pharmacological treatment [132].

Other caspases also have been reported to have proautophagic roles [133]. Similar to caspase-8, their prosurvival survival role at present appears to be context specific [134–136]. For more details, I refer the reader to an excellent recent review [133]. Further research needs to be executed to define the exact mechanism by which these caspases execute their proautophagic role. To summarize the relationship of caspases with apoptosis is surprisingly complex, with different caspases augmenting prosurvival or death pathways [133].

7.4. Atg5 and Atg12. Atg5 and Atg12 are two members of the ubiquitin-like conjugation systems that are needed for autophagosome formation. As stated earlier, the ubiquitin-like protein Atg12 is transferred from Atg7 the E1-like enzyme, via Atg10 (E2-like) to form a covalent attachment with Atg5 [137–139]. The Atg12–5 conjugate is essential for autophagy. More recently, procell death roles have emerged for both Atg5 and Atg12 in their unconjugated forms. Atg5 is cleaved by caplains (which are cysteine proteases activated by cellular stress) and plays a key role in the initiation of apoptosis [140]. Following cleavage, the N-terminal of Atg5 translocates to the mitochondria, where it mediates the release of cytochrome c by interacting with Bcl-X_L to promote apoptosis [141]. More recently, unconjugated Atg12 also been ascribed a procell death function by two quite separate autophagy-independent mechanisms. Firstly, free Atg12 binds to and inactivates mitochondrial Bcl-2 family members [142]. Secondly, Atg12 can conjugate to Atg3 where it promotes mitochondrial fusion and restricts mitochondrial mass [143]. Lastly, although not involved in mediating apoptosis, the Atg12–Atg3 conjugate promotes basal autophagy and endolysosomal trafficking [144]. Taken together, these observations serve to demonstrate the flexibility of repurposing Atg proteins for different roles dependent upon the cellular circumstances. Despite these discoveries, it remains to be seen if any or a combination of these interactions represents a key event where autophagy and apoptosis diverge in response to specific signals.

8. Conclusions

This review has summarized how cells maintain cellular ROS levels as well as discussing the complicated relationship between autophagy and apoptosis. The last decade has seen an explosion of reports that has lead to an increased understanding of how these pathways communicate. Importantly, the overriding theme evolving from these studies is that the relationship between autophagy and apoptosis is intertwined, with proteins from both pathways being repurposed for the benefit of the other. What is also emerging is that these new roles (also known as *night job*) of proteins whose "*day job*" is firmly established are, in many cases, context specific. Given the consideration that many chemotherapeutic regimes both inhibit apoptosis and/or autophagy [5, 33, 97], it is of great importance that both the molecular mechanisms and context-specific job assignment be defined for these multifunctional proteins.

Conflicts of Interest

The author declares no conflict of interest.

Acknowledgments

The author thanks Randy Strich for the critical reading of this manuscript. Katrina F. Cooper is supported by the National Institutes of Health Award (GM113196).

References

[1] C. De Duve, "The lysosome," *Scientific American*, vol. 208, no. 5, pp. 64–73, 1963.

[2] K. Takeshige, M. Baba, S. Tsuboi, T. Noda, and Y. Ohsumi, "Autophagy in yeast demonstrated with proteinase-deficient mutants and conditions for its induction," *The Journal of Cell Biology*, vol. 119, no. 2, pp. 301–311, 1992.

[3] M. Tsukada and Y. Ohsumi, "Isolation and characterization of autophagy-defective mutants of *Saccharomyces cerevisiae*," *FEBS Letters*, vol. 333, no. 1-2, pp. 169–174, 1993.

[4] E. White, "Deconvoluting the context-dependent role for autophagy in cancer," *Nature Reviews Cancer*, vol. 12, no. 6, pp. 401–410, 2012.

[5] C. G. Towers and A. Thorburn, "Therapeutic targeting of autophagy," *eBioMedicine*, vol. 14, pp. 15–23, 2016.

[6] D. J. Klionsky, "The molecular machinery of autophagy: unanswered questions," *Journal of Cell Science*, vol. 118, no. 1, pp. 7–18, 2005.

[7] W. W. Li, J. Li, and J. K. Bao, "Microautophagy: lesser-known self-eating," *Cellular and Molecular Life Sciences*, vol. 69, no. 7, pp. 1125–1136, 2012.

[8] S. Kaushik and A. M. Cuervo, "Chaperone-mediated autophagy: a unique way to enter the lysosome world," *Trends in Cell Biology*, vol. 22, no. 8, pp. 407–417, 2012.

[9] N. T. Ktistakis and S. A. Tooze, "Digesting the expanding mechanisms of autophagy," *Trends in Cell Biology*, vol. 26, no. 8, pp. 624–635, 2016.

[10] L. Galluzzi, E. H. Baehrecke, A. Ballabio et al., "Molecular definitions of autophagy and related processes," *The EMBO Journal*, vol. 36, no. 13, pp. 1811–1836, 2017.

[11] M. Niso-Santano, S. A. Malik, F. Pietrocola et al., "Unsaturated fatty acids induce non-canonical autophagy," *The EMBO Journal*, vol. 34, no. 8, pp. 1025–1041, 2015.

[12] J. Martinez, R. S. Malireddi, Q. Lu et al., "Molecular characterization of LC3-associated phagocytosis reveals distinct roles for Rubicon, NOX2 and autophagy proteins," *Nature Cell Biology*, vol. 17, no. 7, pp. 893–906, 2015.

[13] K. Huang and D. Liu, "Targeting non-canonical autophagy overcomes erlotinib resistance in tongue cancer," *Tumor Biology*, vol. 37, no. 7, pp. 9625–9633, 2016.

[14] A. D. Rubinstein and A. Kimchi, "Life in the balance - a mechanistic view of the crosstalk between autophagy and apoptosis," *Journal of Cell Science*, vol. 125, no. 22, pp. 5259–5268, 2012.

[15] L. Galluzzi, J. M. Bravo-San Pedro, I. Vitale et al., "Essential versus accessory aspects of cell death: recommendations of the NCCD 2015," *Cell Death and Differentiation*, vol. 22, no. 1, pp. 58–73, 2015.

[16] C. A. Lamb, T. Yoshimori, and S. A. Tooze, "The autophagosome: origins unknown, biogenesis complex," *Nature Reviews Molecular Cell Biology*, vol. 14, no. 12, pp. 759–774, 2013.

[17] Y. Liu and B. Levine, "Autosis and autophagic cell death: the dark side of autophagy," *Cell Death and Differentiation*, vol. 22, no. 3, pp. 367–376, 2015.

[18] Z. Yin, C. Pascual, and D. J. Klionsky, "Autophagy: machinery and regulation," *Microbial Cell*, vol. 3, no. 12, pp. 588–596, 2016.

[19] K. Matsunaga, E. Morita, T. Saitoh et al., "Autophagy requires endoplasmic reticulum targeting of the PI3-kinase complex via Atg14L," *The Journal of Cell Biology*, vol. 190, no. 4, pp. 511–521, 2010.

[20] S. Alers, A. S. Loffler, S. Wesselborg, and B. Stork, "Role of AMPK-mTOR-Ulk1/2 in the regulation of autophagy: cross talk, shortcuts, and feedbacks," *Molecular and Cellular Biology*, vol. 32, no. 1, pp. 2–11, 2012.

[21] C. He and B. Levine, "The Beclin 1 interactome," *Current Opinion in Cell Biology*, vol. 22, no. 2, pp. 140–149, 2010.

[22] I. Tanida, E. Tanida-Miyake, T. Ueno, and E. Kominami, "The human homolog of *Saccharomyces cerevisiae* Apg7p is a protein-activating enzyme for multiple substrates including human Apg12p, GATE-16, GABARAP, and MAP-LC3," *Journal of Biological Chemistry*, vol. 276, no. 3, pp. 1701–1706, 2001.

[23] N. Mizushima, "Autophagy: process and function," *Genes & Development*, vol. 21, no. 22, pp. 2861–2873, 2007.

[24] R. Scherz-Shouval, E. Shvets, E. Fass, H. Shorer, L. Gil, and Z. Elazar, "Reactive oxygen species are essential for autophagy and specifically regulate the activity of Atg4," *The EMBO Journal*, vol. 26, no. 7, pp. 1749–1760, 2007.

[25] E. Itakura, C. Kishi-Itakura, and N. Mizushima, "The hairpin-type tail-anchored SNARE syntaxin 17 targets to autophagosomes for fusion with endosomes/lysosomes," *Cell*, vol. 151, no. 6, pp. 1256–1269, 2012.

[26] G. Bjorkoy, T. Lamark, A. Brech et al., "p62/SQSTM1 forms protein aggregates degraded by autophagy and has a protective effect on huntingtin-induced cell death," *The Journal of Cell Biology*, vol. 171, no. 4, pp. 603–614, 2005.

[27] M. Komatsu, S. Waguri, M. Koike et al., "Homeostatic levels of p62 control cytoplasmic inclusion body formation in autophagy-deficient mice," *Cell*, vol. 131, no. 6, pp. 1149–1163, 2007.

[28] Y. Ichimura, T. Kumanomidou, Y. S. Sou et al., "Structural basis for sorting mechanism of p62 in selective autophagy," *Journal of Biological Chemistry*, vol. 283, no. 33, pp. 22847–22857, 2008.

[29] M. Lippai and P. Low, "The role of the selective adaptor p62 and ubiquitin-like proteins in autophagy," *BioMed Research International*, vol. 2014, Article ID 832704, 11 pages, 2014.

[30] V. Rogov, V. Dotsch, T. Johansen, and V. Kirkin, "Interactions between autophagy receptors and ubiquitin-like proteins form the molecular basis for selective autophagy," *Molecular Cell*, vol. 53, no. 2, pp. 167–178, 2014.

[31] L. Galluzzi, J. M. Bravo-San Pedro, B. Levine, D. R. Green, and G. Kroemer, "Pharmacological modulation of autophagy: therapeutic potential and persisting obstacles," *Nature Reviews Drug Discovery*, vol. 16, no. 7, pp. 487–511, 2017.

[32] M. Gao, P. Monian, Q. Pan, W. Zhang, J. Xiang, and X. Jiang, "Ferroptosis is an autophagic cell death process," *Cell Research*, vol. 26, no. 9, pp. 1021–1032, 2016.

[33] V. W. Rebecca and R. K. Amaravadi, "Emerging strategies to effectively target autophagy in cancer," *Oncogene*, vol. 35, no. 1, pp. 1–11, 2016.

[34] S. Hwang, N. S. Maloney, M. W. Bruinsma et al., "Nondegradative role of Atg5-Atg12/Atg16L1 autophagy protein complex in antiviral activity of interferon gamma," *Cell Host & Microbe*, vol. 11, no. 4, pp. 397–409, 2012.

[35] Y. Xie, W. Hou, X. Song et al., "Ferroptosis: process and function," *Cell Death and Differentiation*, vol. 23, no. 3, pp. 369–379, 2016.

[36] R. Weinlich, A. Oberst, H. M. Beere, and D. R. Green, "Necroptosis in development, inflammation and disease," *Nature Reviews Molecular Cell Biology*, vol. 18, no. 2, pp. 127–136, 2017.

[37] X.-H. Ma, S. Piao, D. Wang et al., "Measurements of tumor cell autophagy predict invasiveness, resistance to chemotherapy, and survival in melanoma," *Clinical Cancer Research*, vol. 17, no. 10, pp. 3478–3489, 2011.

[38] A. Yang, N. V. Rajeshkumar, X. Wang et al., "Autophagy is critical for pancreatic tumor growth and progression in tumors with p53 alterations," *Cancer Discovery*, vol. 4, no. 8, pp. 905–913, 2014.

[39] J. K. Kwee, "A paradoxical chemoresistance and tumor suppressive role of antioxidant in solid cancer cells: a strange case of Dr. Jekyll and Mr. Hyde," *BioMed Research International*, vol. 2014, Article ID 209845, 9 pages, 2014.

[40] D. E. Handy and J. Loscalzo, "Redox regulation of mitochondrial function," *Antioxidants & Redox Signaling*, vol. 16, no. 11, pp. 1323–1367, 2012.

[41] M. Schrader and H. D. Fahimi, "Peroxisomes and oxidative stress," *Biochimica et Biophysica Acta (BBA) - Molecular Cell Research*, vol. 1763, no. 12, pp. 1755–1766, 2006.

[42] J. D. Malhotra and R. J. Kaufman, "Endoplasmic reticulum stress and oxidative stress: a vicious cycle or a double-edged sword?," *Antioxidants & Redox Signaling*, vol. 9, no. 12, pp. 2277–2294, 2007.

[43] C. C. Winterbourn, "The biological chemistry of hydrogen peroxide," *Methods in Enzymology*, vol. 528, pp. 3–25, 2013.

[44] S. I. Liochev and I. Fridovich, "The effects of superoxide dismutase on H_2O_2 formation," *Free Radical Biology & Medicine*, vol. 42, no. 10, pp. 1465–1469, 2007.

[45] M. L. Circu and T. Y. Aw, "Glutathione and modulation of cell apoptosis," *Biochimica et Biophysica Acta (BBA) - Molecular Cell Research*, vol. 1823, no. 10, pp. 1767–1777, 2012.

[46] D. Trachootham, W. Lu, M. A. Ogasawara, R. D. Nilsa, and P. Huang, "Redox regulation of cell survival," *Antioxidants & Redox Signaling*, vol. 10, no. 8, pp. 1343–1374, 2008.

[47] J. Navarro-Yepes, M. Burns, A. Anandhan et al., "Oxidative stress, redox signaling, and autophagy: cell death versus survival," *Antioxidants & Redox Signaling*, vol. 21, no. 1, pp. 66–85, 2014.

[48] P. Moi, K. Chan, I. Asunis, A. Cao, and Y. W. Kan, "Isolation of NF-E2-related factor 2 (Nrf2), a NF-E2-like basic leucine zipper transcriptional activator that binds to the tandem NF-E2/AP1 repeat of the beta-globin locus control region," *Proceedings of the National Academy of Sciences*, vol. 91, no. 21, pp. 9926–9930, 1994.

[49] J. D. Hayes and A. T. Dinkova-Kostova, "The Nrf2 regulatory network provides an interface between redox and intermediary metabolism," *Trends in Biochemical Sciences*, vol. 39, no. 4, pp. 199–218, 2014.

[50] T. W. Kensler, N. Wakabayashi, and S. Biswal, "Cell survival responses to environmental stresses via the Keap1-Nrf2-ARE pathway," *Annual Review of Pharmacology and Toxicology*, vol. 47, no. 1, pp. 89–116, 2007.

[51] J. Lu and A. Holmgren, "The thioredoxin antioxidant system," *Free Radical Biology and Medicine*, vol. 66, pp. 75–87, 2014.

[52] D. Malhotra, E. Portales-Casamar, A. Singh et al., "Global mapping of binding sites for Nrf2 identifies novel targets in cell survival response through ChIP-Seq profiling and network analysis," *Nucleic Acids Research*, vol. 38, no. 17, pp. 5718–5734, 2010.

[53] C. Gorrini, I. S. Harris, and T. W. Mak, "Modulation of oxidative stress as an anticancer strategy," *Nature Reviews Drug Discovery*, vol. 12, no. 12, pp. 931–947, 2013.

[54] N. F. Villeneuve, A. Lau, and D. D. Zhang, "Regulation of the Nrf2-Keap1 antioxidant response by the ubiquitin proteasome system: an insight into cullin-ring ubiquitin ligases," *Antioxidants & Redox Signaling*, vol. 13, no. 11, pp. 1699–1712, 2010.

[55] B. N. Chorley, M. R. Campbell, X. Wang et al., "Identification of novel NRF2-regulated genes by ChIP-Seq: influence on retinoid X receptor alpha," *Nucleic Acids Research*, vol. 40, no. 15, pp. 7416–7429, 2012.

[56] K. Orino, L. Lehman, Y. Tsuji, H. Ayaki, S. V. Torti, and F. M. Torti, "Ferritin and the response to oxidative stress," *Biochemical Journal*, vol. 357, no. 1, pp. 241–247, 2001.

[57] E. D. Weinberg, "The role of iron in cancer," *European Journal of Cancer Prevention*, vol. 5, no. 1, pp. 19–36, 1996.

[58] S. V. Torti and F. M. Torti, "Iron and cancer: more ore to be mined," *Nature Reviews Cancer*, vol. 13, no. 5, pp. 342–355, 2013.

[59] J. L. Buss, B. T. Greene, J. Turner, F. M. Torti, and S. V. Torti, "Iron chelators in cancer chemotherapy," *Current Topics in Medicinal Chemistry*, vol. 4, no. 15, pp. 1623–1635, 2004.

[60] J. Shen, X. Sheng, Z. Chang et al., "Iron metabolism regulates p53 signaling through direct heme-p53 interaction and modulation of p53 localization, stability, and function," *Cell Reports*, vol. 7, no. 1, pp. 180–193, 2014.

[61] T. Finkel, "Signal transduction by reactive oxygen species," *The Journal of Cell Biology*, vol. 194, no. 1, pp. 7–15, 2011.

[62] S. G. Rhee, "Cell signaling. H_2O_2, a necessary evil for cell signaling," *Science*, vol. 312, no. 5782, pp. 1882-1883, 2006.

[63] G. Filomeni, E. Desideri, S. Cardaci, G. Rotilio, and M. R. Ciriolo, "Under the ROS: thiol network is the principal suspect for autophagy commitment," *Autophagy*, vol. 6, no. 7, pp. 999–1005, 2010.

[64] E. Weerapana, C. Wang, G. M. Simon et al., "Quantitative reactivity profiling predicts functional cysteines in proteomes," *Nature*, vol. 468, no. 7325, pp. 790–795, 2010.

[65] Y. Yasueda, T. Tamura, A. Fujisawa et al., "A set of organelle-localizable reactive molecules for mitochondrial chemical proteomics in living cells and brain tissues," *Journal of the American Chemical Society*, vol. 138, no. 24, pp. 7592–7602, 2016.

[66] N. J. Pace and E. Weerapana, "A competitive chemical-proteomic platform to identify zinc-binding cysteines," *ACS Chemical Biology*, vol. 9, no. 1, pp. 258–265, 2013.

[67] T. C. Meng, T. Fukada, and N. K. Tonks, "Reversible oxidation and inactivation of protein tyrosine phosphatases in vivo," *Molecular Cell*, vol. 9, no. 2, pp. 387–399, 2002.

[68] S. R. Lee, K. S. Kwon, S. R. Kim, and S. G. Rhee, "Reversible inactivation of protein-tyrosine phosphatase 1B in A431 cells stimulated with epidermal growth factor," *The Journal of Biological Chemistry*, vol. 273, no. 25, pp. 15366–15372, 1998.

[69] D. W. Bak, M. D. Pizzagalli, and E. Weerapana, "Identifying functional cysteine residues in the mitochondria," *ACS Chemical Biology*, vol. 12, no. 4, pp. 947–957, 2017.

[70] Y. Wang, Y. Nartiss, B. Steipe, G. A. McQuibban, and P. K. Kim, "ROS-induced mitochondrial depolarization initiates PARK2/PARKIN-dependent mitochondrial degradation by autophagy," *Autophagy*, vol. 8, no. 10, pp. 1462–1476, 2012.

[71] J. Y. Yang and W. Y. Yang, "Spatiotemporally controlled initiation of Parkin-mediated mitophagy within single cells," *Autophagy*, vol. 7, no. 10, pp. 1230–1238, 2011.

[72] D. M. Dudzinski, J. Igarashi, D. Greif, and T. Michel, "The regulation and pharmacology of endothelial nitric oxide synthase," *Annual Review of Pharmacology and Toxicology*, vol. 46, no. 1, pp. 235–276, 2006.

[73] P. Pacher, J. S. Beckman, and L. Liaudet, "Nitric oxide and peroxynitrite in health and disease," *Physiological Reviews*, vol. 87, no. 1, pp. 315–424, 2007.

[74] M. S. Joshi, T. B. Ferguson, T. H. Han et al., "Nitric oxide is consumed, rather than conserved, by reaction with oxyhemoglobin under physiological conditions," *Proceedings of the National Academy of Sciences*, vol. 99, no. 16, pp. 10341–10346, 2002.

[75] A. Valerio and E. Nisoli, "Nitric oxide, interorganelle communication, and energy flow: a novel route to slow aging," *Frontiers in Cell and Developmental Biology*, vol. 3, 2015.

[76] R. Radi, T. P. Cosgrove, J. S. Beckman, and B. A. Freeman, "Peroxynitrite-induced luminol chemiluminescence," *Biochemical Journal*, vol. 290, no. 1, pp. 51–57, 1993.

[77] D. W. Bak and E. Weerapana, "Cysteine-mediated redox signalling in the mitochondria," *Molecular BioSystems*, vol. 11, no. 3, pp. 678–697, 2015.

[78] D. H. Cho, T. Nakamura, J. Fang et al., "S-Nitrosylation of Drp1 mediates β-amyloid-related mitochondrial fission and neuronal injury," *Science*, vol. 324, no. 5923, pp. 102–105, 2009.

[79] P. H. Willems, R. Rossignol, C. E. Dieteren, M. P. Murphy, and W. J. Koopman, "Redox homeostasis and mitochondrial dynamics," *Cell Metabolism*, vol. 22, no. 2, pp. 207–218, 2015.

[80] R. A. Kirkland, R. M. Adibhatla, J. F. Hatcher, and J. L. Franklin, "Loss of cardiolipin and mitochondria during programmed neuronal death: evidence of a role for lipid peroxidation and autophagy," *Neuroscience*, vol. 115, no. 2, pp. 587–602, 2002.

[81] R. A. Kirkland, G. M. Saavedra, and J. L. Franklin, "Rapid activation of antioxidant defenses by nerve growth factor suppresses reactive oxygen species during neuronal apoptosis: evidence for a role in cytochrome c redistribution," *Journal of Neuroscience*, vol. 27, no. 42, pp. 11315–11326, 2007.

[82] M. Djavaheri-Mergny, M. Amelotti, J. Mathieu et al., "NF-κB activation represses tumor necrosis factor-α-induced autophagy," *Journal of Biological Chemistry*, vol. 281, no. 41, pp. 30373–30382, 2006.

[83] D. G. Hardie, "AMPK and autophagy get connected," *The EMBO Journal*, vol. 30, no. 4, pp. 634-635, 2011.

[84] D. G. Hardie, "AMPK: positive and negative regulation, and its role in whole-body energy homeostasis," *Current Opinion in Cell Biology*, vol. 33, pp. 1–7, 2015.

[85] D. G. Hardie, F. A. Ross, and S. A. Hawley, "AMPK: a nutrient and energy sensor that maintains energy homeostasis," *Nature Reviews Molecular Cell Biology*, vol. 13, no. 4, pp. 251–262, 2012.

[86] R. C. Russell, H. X. Yuan, and K. L. Guan, "Autophagy regulation by nutrient signaling," *Cell Research*, vol. 24, no. 1, pp. 42–57, 2014.

[87] D. Shao, S. Oka, T. Liu et al., "A redox-dependent mechanism for regulation of AMPK activation by thioredoxin1 during energy starvation," *Cell Metabolism*, vol. 19, no. 2, pp. 232–245, 2014.

[88] K. Inoki, T. Zhu, and K. L. Guan, "TSC2 mediates cellular energy response to control cell growth and survival," *Cell*, vol. 115, no. 5, pp. 577–590, 2003.

[89] R. J. Shaw, N. Bardeesy, B. D. Manning et al., "The LKB1 tumor suppressor negatively regulates mTOR signaling," *Cancer Cell*, vol. 6, no. 1, pp. 91–99, 2004.

[90] M. Bach, M. Larance, D. E. James, and G. Ramm, "The serine/threonine kinase ULK1 is a target of multiple phosphorylation events," *Biochemical Journal*, vol. 440, no. 2, pp. 283–291, 2011.

[91] C. Yi, J. Tong, P. Lu et al., "Formation of a Snf1-Mec1-Atg1 module on mitochondria governs energy deprivation-induced autophagy by regulating mitochondrial respiration," *Developmental Cell*, vol. 41, no. 1, pp. 59–71.e4, 2017.

[92] I. Papandreou, A. L. Lim, K. Laderoute, and N. C. Denko, "Hypoxia signals autophagy in tumor cells via AMPK activity, independent of HIF-1, BNIP3, and BNIP3L," *Cell Death & Differentiation*, vol. 15, no. 10, pp. 1572–1581, 2008.

[93] B. M. Emerling, F. Weinberg, C. Snyder et al., "Hypoxic activation of AMPK is dependent on mitochondrial ROS but independent of an increase in AMP/ATP ratio," *Free Radical Biology and Medicine*, vol. 46, no. 10, pp. 1386–1391, 2009.

[94] E. Desideri, G. Filomeni, and M. R. Ciriolo, "Glutathione participates in the modulation of starvation-induced autophagy in carcinoma cells," *Autophagy*, vol. 8, no. 12, pp. 1769–1781, 2012.

[95] H. Mancilla, R. Maldonado, K. Cereceda et al., "Glutathione depletion induces spermatogonial cell autophagy," *Journal of Cellular Biochemistry*, vol. 116, no. 10, pp. 2283–2292, 2015.

[96] S. Sridharan, K. Jain, and A. Basu, "Regulation of autophagy by kinases," *Cancer*, vol. 3, no. 4, pp. 2630–2654, 2011.

[97] J. M. M. Levy, C. G. Towers, and A. Thorburn, "Targeting autophagy in cancer," *Nature Reviews Cancer*, vol. 17, no. 9, pp. 528–542, 2017.

[98] E. S. Knudsen, U. Balaji, E. Freinkman, P. McCue, and A. K. Witkiewicz, "Unique metabolic features of pancreatic cancer stroma: relevance to the tumor compartment, prognosis, and invasive potential," *Oncotarget*, vol. 7, no. 48, pp. 78396–78411, 2016.

[99] K. Itoh, N. Wakabayashi, Y. Katoh et al., "Keap1 represses nuclear activation of antioxidant responsive elements by Nrf2 through binding to the amino-terminal Neh2 domain," *Genes & Development*, vol. 13, no. 1, pp. 76–86, 1999.

[100] S. B. Cullinan, J. D. Gordan, J. Jin, J. W. Harper, and J. A. Diehl, "The Keap1-BTB protein is an adaptor that bridges Nrf2 to a Cul3-based E3 ligase: oxidative stress sensing by a Cul3-Keap1 ligase," *Molecular and Cellular Biology*, vol. 24, no. 19, pp. 8477–8486, 2004.

[101] A. T. Dinkova-Kostova, R. V. Kostov, and P. Canning, "Keap1, the cysteine-based mammalian intracellular sensor for electrophiles and oxidants," *Archives of Biochemistry and Biophysics*, vol. 617, pp. 84–93, 2017.

[102] K. Taguchi, H. Motohashi, and M. Yamamoto, "Molecular mechanisms of the Keap1-Nrf2 pathway in stress response and cancer evolution," *Genes to Cells*, vol. 16, no. 2, pp. 123–140, 2011.

[103] S. Geisler, K. M. Holmstrom, D. Skujat et al., "PINK1/Parkin-mediated mitophagy is dependent on VDAC1 and p62/SQSTM1," *Nature Cell Biology*, vol. 12, no. 2, pp. 119–131, 2010.

[104] Y. Katsuragi, Y. Ichimura, and M. Komatsu, "p62/SQSTM1 functions as a signaling hub and an autophagy adaptor," *FEBS Journal*, vol. 282, no. 24, pp. 4672–4678, 2015.

[105] J. Moscat and M. T. Diaz-Meco, "p62 at the crossroads of autophagy, apoptosis, and cancer," *Cell*, vol. 137, no. 6, pp. 1001–1004, 2009.

[106] A. Duran, R. Amanchy, J. F. Linares et al., "p62 is a key regulator of nutrient sensing in the mTORC1 pathway," *Molecular Cell*, vol. 44, no. 1, pp. 134–146, 2011.

[107] J. Moscat, M. Karin, and M. T. Diaz-Meco, "p62 in cancer: signaling adaptor beyond autophagy," *Cell*, vol. 167, no. 3, pp. 606–609, 2016.

[108] A. Umemura, F. He, K. Taniguchi et al., "p62, upregulated during preneoplasia, induces hepatocellular carcinogenesis by maintaining survival of stressed HCC-initiating cells," *Cancer Cell*, vol. 29, no. 6, pp. 935–948, 2016.

[109] T. Yonekawa and A. Thorburn, "Autophagy and cell death," *Essays in Biochemistry*, vol. 55, pp. 105–117, 2013.

[110] L. A. Booth, S. Tavallai, H. A. Hamed, N. Cruickshanks, and P. Dent, "The role of cell signalling in the crosstalk between autophagy and apoptosis," *Cellular Signalling*, vol. 26, no. 3, pp. 549–555, 2014.

[111] G. Marino, M. Niso-Santano, E. H. Baehrecke, and G. Kroemer, "Self-consumption: the interplay of autophagy and apoptosis," *Nature Reviews Molecular Cell Biology*, vol. 15, no. 2, pp. 81–94, 2014.

[112] Y. Fuchs and H. Steller, "Live to die another way: modes of programmed cell death and the signals emanating from dying cells," *Nature Reviews Molecular Cell Biology*, vol. 16, no. 6, pp. 329–344, 2015.

[113] S. W. G. Tait and D. R. Green, "Mitochondrial regulation of cell death," *Cold Spring Harbor Perspectives in Biology*, vol. 5, no. 9, 2013.

[114] A. Ashkenazi and G. Salvesen, "Regulated cell death: signaling and mechanisms," *Annual Review of Cell and Developmental Biology*, vol. 30, no. 1, pp. 337–356, 2014.

[115] R. J. Youle and A. Strasser, "The BCL-2 protein family: opposing activities that mediate cell death," *Nature Reviews Molecular Cell Biology*, vol. 9, no. 1, pp. 47–59, 2008.

[116] S. Elmore, "Apoptosis: a review of programmed cell death," *Toxicologic Pathology*, vol. 35, no. 4, pp. 495–516, 2007.

[117] C. Kantari and H. Walczak, "Caspase-8 and bid: caught in the act between death receptors and mitochondria," *Biochimica et Biophysica Acta (BBA) - Molecular Cell Research*, vol. 1813, no. 4, pp. 558–563, 2011.

[118] M. C. Maiuri, A. Criollo, and G. Kroemer, "Crosstalk between apoptosis and autophagy within the Beclin 1 interactome," *The EMBO Journal*, vol. 29, no. 3, pp. 515-516, 2010.

[119] L. Galluzzi, O. Kepp, and G. Kroemer, "Mitochondria: master regulators of danger signalling," *Nature Reviews Molecular Cell Biology*, vol. 13, no. 12, pp. 780–788, 2012.

[120] J. P. Decuypere, J. B. Parys, and G. Bultynck, "Regulation of the autophagic bcl-2/Beclin 1 interaction," *Cell*, vol. 1, no. 4, pp. 284–312, 2012.

[121] L. M. Lindqvist, M. Heinlein, D. C. S. Huang, and D. L. Vaux, "Prosurvival Bcl-2 family members affect autophagy only indirectly, by inhibiting Bax and Bak," *Proceedings of the National Academy of Sciences*, vol. 111, no. 23, pp. 8512–8517, 2014.

[122] M. C. Bassik, L. Scorrano, S. A. Oakes, T. Pozzan, and S. J. Korsmeyer, "Phosphorylation of BCL-2 regulates ER Ca2+ homeostasis and apoptosis," *The EMBO Journal*, vol. 23, no. 5, pp. 1207–1216, 2004.

[123] S. J. Riedl and Y. Shi, "Molecular mechanisms of caspase regulation during apoptosis," *Nature Reviews Molecular Cell Biology*, vol. 5, no. 11, pp. 897–907, 2004.

[124] O. Oral, D. Oz-Arslan, Z. Itah et al., "Cleavage of Atg3 protein by caspase-8 regulates autophagy during receptor-activated cell death," *Apoptosis*, vol. 17, no. 8, pp. 810–820, 2012.

[125] V. M. S. Betin and J. D. Lane, "Caspase cleavage of Atg4D stimulates GABARAP-L1 processing and triggers mitochondrial targeting and apoptosis," *Journal of Cell Science*, vol. 122, no. 14, pp. 2554–2566, 2009.

[126] J. M. Norman, G. M. Cohen, and E. T. Bampton, "The in vitro cleavage of the hAtg proteins by cell death proteases," *Autophagy*, vol. 6, no. 8, pp. 1042–1056, 2010.

[127] E. Wirawan, L. Vande Walle, K. Kersse et al., "Caspase-mediated cleavage of Beclin-1 inactivates Beclin-1-induced autophagy and enhances apoptosis by promoting the release of proapoptotic factors from mitochondria," *Cell Death & Disease*, vol. 1, no. 1, article e18, 2010.

[128] M. M. Young, Y. Takahashi, O. Khan et al., "Autophagosomal membrane serves as platform for intracellular death-inducing signaling complex (iDISC)-mediated caspase-8 activation and apoptosis," *Journal of Biological Chemistry*, vol. 287, no. 15, pp. 12455–12468, 2012.

[129] D. H. Cho, Y. K. Jo, J. J. Hwang, Y. M. Lee, S. A. Roh, and J. C. Kim, "Caspase-mediated cleavage of ATG6/Beclin-1 links apoptosis to autophagy in HeLa cells," *Cancer Letters*, vol. 274, no. 1, pp. 95–100, 2009.

[130] A. Oberstein, P. D. Jeffrey, and Y. Shi, "Crystal structure of the Bcl-X_L-Beclin 1 peptide complex: Beclin 1 is a novel BH3-only protein," *Journal of Biological Chemistry*, vol. 282, no. 17, pp. 13123–13132, 2007.

[131] W. Hou, J. Han, C. Lu, L. A. Goldstein, and H. Rabinowich, "Autophagic degradation of active caspase-8: a crosstalk mechanism between autophagy and apoptosis," *Autophagy*, vol. 6, no. 7, pp. 891–900, 2010.

[132] S. Huang, K. Okamoto, C. Yu, and F. A. Sinicrope, "p62/sequestosome-1 up-regulation promotes ABT-263-induced caspase-8 aggregation/activation on the autophagosome," *Journal of Biological Chemistry*, vol. 288, no. 47, pp. 33654–33666, 2013.

[133] P. Tsapras and I. P. Nezis, "Caspase involvement in autophagy," *Cell Death and Differentiation*, vol. 24, no. 8, pp. 1369–1379, 2017.

[134] Q. Sun, W. Gao, P. Loughran et al., "Caspase 1 activation is protective against hepatocyte cell death by up-regulating Beclin 1 protein and mitochondrial autophagy in the setting of redox stress," *Journal of Biological Chemistry*, vol. 288, no. 22, pp. 15947–15958, 2013.

[135] M. Tiwari, L. K. Sharma, D. Vanegas et al., "A nonapoptotic role for CASP2/caspase 2: modulation of autophagy," *Autophagy*, vol. 10, no. 6, pp. 1054–1070, 2014.

[136] H. S. Jeong, H. Y. Choi, E. R. Lee et al., "Involvement of caspase-9 in autophagy-mediated cell survival pathway," *Biochimica et Biophysica Acta (BBA) - Molecular Cell Research*, vol. 1813, no. 1, pp. 80–90, 2011.

[137] N. Mizushima, T. Noda, T. Yoshimori et al., "A protein conjugation system essential for autophagy," *Nature*, vol. 395, no. 6700, pp. 395–398, 1998.

[138] Y. Ichimura, T. Kirisako, T. Takao et al., "A ubiquitin-like system mediates protein lipidation," *Nature*, vol. 408, no. 6811, pp. 488–492, 2000.

[139] K. Suzuki, T. Kirisako, Y. Kamada, N. Mizushima, T. Noda, and Y. Ohsumi, "The pre-autophagosomal structure organized by concerted functions of APG genes is essential for autophagosome formation," *The EMBO Journal*, vol. 20, no. 21, pp. 5971–5981, 2001.

[140] S. Yousefi and H. U. Simon, "Apoptosis regulation by autophagy gene 5," *Critical Reviews in Oncology/Hematology*, vol. 63, no. 3, pp. 241–244, 2007.

[141] S. Yousefi, R. Perozzo, I. Schmid et al., "Calpain-mediated cleavage of Atg5 switches autophagy to apoptosis," *Nature Cell Biology*, vol. 8, no. 10, pp. 1124–1132, 2006.

[142] A. D. Rubinstein, M. Eisenstein, Y. Ber, S. Bialik, and A. Kimchi, "The autophagy protein Atg12 associates with antiapoptotic Bcl-2 family members to promote mitochondrial apoptosis," *Molecular Cell*, vol. 44, no. 5, pp. 698–709, 2011.

[143] L. Radoshevich, L. Murrow, N. Chen et al., "ATG12 conjugation to ATG3 regulates mitochondrial homeostasis and cell death," *Cell*, vol. 142, no. 4, pp. 590–600, 2010.

[144] L. Murrow and J. Debnath, "ATG12-ATG3 connects basal autophagy and late endosome function," *Autophagy*, vol. 11, no. 6, pp. 961-962, 2015.

Hindawi
Oxidative Medicine and Cellular Longevity
Volume 2018, Article ID 2138502, 10 pages
https://doi.org/10.1155/2018/2138502

Review Article

Function and Regulation of Protein Kinase D in Oxidative Stress: A Tale of Isoforms

Mathias Cobbaut[1,2] **and Johan Van Lint**[1,2]

[1]*Department of Cellular and Molecular Medicine, Faculty of Medicine, KU Leuven, Leuven, Belgium*
[2]*Leuven Cancer Institute (LKI), KU Leuven, Leuven, Belgium*

Correspondence should be addressed to Johan Van Lint; johan.vanlint@kuleuven.be

Received 27 October 2017; Accepted 19 February 2018; Published 26 April 2018

Academic Editor: Sabrina Büttner

Oxidative stress is a condition that arises when cells are faced with levels of reactive oxygen species (ROS) that destabilize the homeostatic redox balance. High levels of ROS can cause damage to macromolecules including DNA, lipids, and proteins, eventually resulting in cell death. Moderate levels of ROS however serve as signaling molecules that can drive and potentiate several cellular phenotypes. Increased levels of ROS are associated with a number of diseases including neurological disorders and cancer. In cancer, increased ROS levels can contribute to cancer cell survival and proliferation via the activation of several signaling pathways. One of the downstream effectors of increased ROS is the protein kinase D (PKD) family of kinases. In this review, we will discuss the regulation and function of this family of ROS-activated kinases and describe their unique isoform-specific features, in terms of both kinase regulation and signaling output.

1. Oxidative Stress: Causes and Consequences

Oxidative stress is a condition that develops when the cellular redox balance is disturbed by an excessive buildup of reactive oxygen species (ROS). ROS mainly occur as a byproduct of normal cellular metabolism, due to the leak of 1–3% of electrons utilized in the mitochondrial electron transport chain for the reduction of oxygen to water, resulting in the production of superoxide [1]. Besides this "collateral" production of ROS, they are also produced deliberately. ROS (mainly H_2O_2) are generated by oxidases in peroxisomes, for example, during β-oxidation of fatty acids and flavin oxidase activity [2]. Furthermore, ROS are also produced in the endoplasmic reticulum during oxidation of maturating proteins in the ER, which helps to stabilize them during folding [3]. Another source of ROS is the production of H_2O_2 by nicotinamide adenine dinucleotide (NADPH) oxidase complexes (NOX) in granulocytes and macrophages to kill pathogens [4]. NOX enzymes are also activated by growth factor signaling. Via the activation of kinases and by oxidizing the active-site cysteines of Tyr and lipid phosphatases, the NOX-generated ROS can potentiate the growth factor signaling output [5–8]. While ROS produced in these contexts serve a purpose, their levels should be tightly controlled, since excessive levels of ROS can cause damage to macromolecules (such as DNA, proteins, and lipids) and cause severe mitochondrial damage, causing it to leak cytochrome c resulting in apoptosis [9–16]. To this end, cells have several antioxidant mechanisms in place to prevent the excessive buildup of ROS. These are both enzymatic (e.g., superoxide dismutases, thioredoxin reductases, and glutaredoxins) and nonenzymatic (e.g., ascorbic acid, α-tocopherol, and glutathione) in nature [17–20]. A disturbed redox balance is associated with a variety of pathologies, including cardiovascular disease, fibrosis, neurological disease, and cancer [21–25]. Interestingly, several cancer cell lines have been shown to harbor increased levels of ROS in comparison to nontransformed cells [26, 27]. This elevated ROS is thought to come from diverse sources: altered metabolism and mitochondrial functions, mutations in mtDNA, enhanced growth factor signaling, and activation of oncogenes such as mutant forms of Ras and c-Myc [3, 28–30]. For example, it was shown that

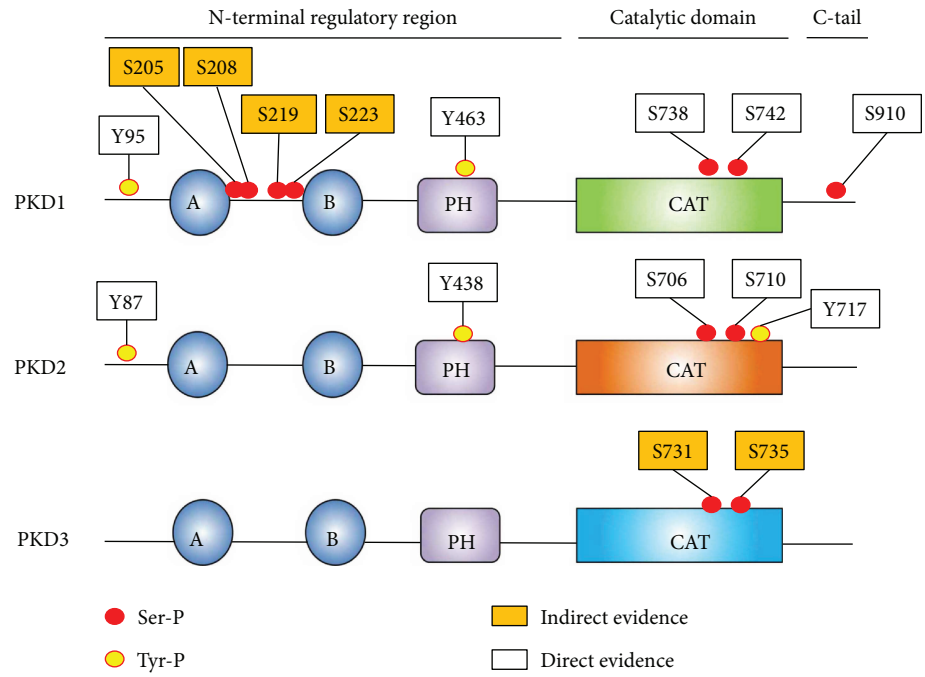

Figure 1: Domain organization and phosphorylation sites of PKD1/2/3 in oxidative stress conditions. Tyr phosphorylation sites are indicated with yellow-coloured circles, and Ser phosphorylation sites are indicated with red-coloured circles. "Direct evidence" indicates that the sites have been shown to be phosphorylated via immunoblotting with a site-specific antibody or via mass spectrometry. "Indirect evidence" indicates data obtained via site-directed mutagenesis or readouts dependent on general phosphorylation (such as PhosTag gels). A and B denote C1a and C1b domains, PH denotes the pleckstrin homology domain, and CAT denotes the kinase domain.

exogenous expression of H-RasG12V in 3T3 cells increases their proliferation rate, an event dependent on increased ROS levels [31]. Furthermore it was shown that H-RasG12V increases ROS levels by activating NOX4 [32]. Besides Ras, c-Myc has also been shown to increase ROS levels in cancer cells, leading to DNA damage and genomic instability, thereby promoting cancer development [33, 34]. Moderate levels of ROS result in the activation of several signaling cascades contributing to either increased proliferation or enhanced survival of cancer cells. For example, upregulation of the PI3K/Akt pathway (e.g., via the inactivation of PTEN), MAP kinase pathways such as Erk1/2 and JNK (although the latter is also involved in ROS-induced apoptosis), and the NF-κB pathway has been observed [31, 35–37]. An important downstream regulator of the oxidative stress response is protein kinase D (PKD). The mechanisms leading to the activation of different PKD isoforms in cells undergoing oxidative stress, as well as the signaling consequences of this activation will be discussed in this review.

2. Protein Kinase D

2.1. The PKD Family: Isoforms and Domain Organization. The human PKD family consists of three isoforms in humans (PKD1, PKD2, and PKD3) and belongs to the Ca^{2+}/calmodulin-dependent protein kinase (CAMK) group of Ser/Thr kinases. PKD1 is the largest member, with 912 amino acids and a molecular mass of 115 kDa. PKD2 and PKD3 are smaller with molecular masses of 105 kDa and 110 kDa, respectively [38].

PKDs are modular enzymes that contain a long N-terminal regulatory region followed by a catalytic domain and a C-terminal extension (C-tail) (Figure 1). The N-terminal part of the protein contains several regions and domains involved in kinase autoregulation, localization, and binding to interactors.

At the extreme N-terminus, PKD1/2 contain a hydrophobic Ala(/Pro)-rich stretch (not found in PKD3), which has been hypothesized to insert in membranes [39]. This region is followed by two diacylglycerol (DAG) binding C1 domains. Because of this feature, PKDs were first classified as members of the protein kinase C (PKC) family [40]. However, the catalytic domain of PKD1 shows higher homology CAM kinases and has similar substrate and inhibitor specificity which resulted in the classification of PKDs as members of the CAMK group [41, 42]. While the C1b domain binds PDB with high affinity, DAG is preferably bound by the C1a domain [43]. In PKD, the C1a and C1b domains are separated by a large linker of approximately 70 amino acids (compared to the linker in PKC isoforms that is much shorter, for example, 8 amino acids in cPKC isoforms). Additionally, the C1a-C1b linker in PKD has important functional properties. Phosphorylation of Ser-205/208 and Ser-219/223 in the linker has been shown to generate a 14-3-3 binding site, which is crucial for ASK1 binding and downstream JNK activation in H_2O_2-stimulated cells (see further [44]).

The C1 domains are connected to the pleckstrin homology (PH) domain by a large linker enriched in acidic amino acids (sometimes denoted as the acidic domain). The

potential regulatory role of this acidic stretch is not fully explored, but it has been suggested in an early study that it could play a role in PKD activation. This idea resulted from the observation that basic peptides and proteins (such as protamine sulfate, myelin basic protein, and histone H1) could inhibit PKD *in vitro*. On the other hand, polyanionic molecules such as heparin or dextran sulfate are capable of activating PKD, without phosphatidylserine/12-O-tetradecanoylphorbol-13-acetate (PS/TPA) [45]. Therefore, the authors hypothesized that polyanionic molecules could disrupt an intramolecular interaction between the acidic domain and a basic stretch elsewhere in the protein [45]. This hypothesis however has not been further explored. The PH domain itself functions as a negative regulator of kinase activity. A full deletion, as well as partial deletions of the PH domain, renders the kinase constitutively active [46]. Pleckstrin homology domains are known interacting modules for phosphoinositides. However, only a small number of these have lipid-binding capabilities, for which the requirements are well defined [47–49]. Structural analysis of the available NMR structures of PKD PH domains in the protein databank (2COA and 2D9Z) reveals that the PH domains of PKD lack the necessary amino acids to interact with phosphatidylinositol phosphate head groups. Hence, the PH domain of PKD does not seem to serve as a lipid-interaction module, but rather serves as a protein interaction module. Important binding partners in the context of PKD activation are G$\beta\gamma$ isoforms. Binding of PKD to G$\beta\gamma$ heterodimers has been proven to directly activate immunoprecipitated PKD1 *in vitro* [50]. Also, incubation of permeabilized HeLa cells with G$\beta\gamma$ causes PKD activation, and when competing free PH domain was added, activation was decreased [50]. Seemingly in contrast to this finding, transfection studies showed that cotransfection of G$\beta\gamma$ isoforms with phospholipase C (PLC) β2/3 isoforms was necessary to activate PKD. However, only certain G$\beta\gamma$ isoforms could activate PKD1 and PLCβ2/3, while other G$\beta\gamma$ isoforms could activate PLCβ2/3 but not PKD1 [51]. This indicates that structural compatibility between G$\beta\gamma$ and the PH domain is required for activation of PKD, besides DAG generation by PLCβ2/3.

The N-terminal regulatory region is followed by the catalytic domain. Notably, PKDs are non-RD kinases, that is, they do not contain an Arg in their catalytic loop (HRD motif). However, while these non-RD kinases normally are not dependent on activation loop phosphorylation, PKDs are (in most cases) dependent on activation loop Ser-738/742 (hPKD1 numbering) phosphorylation for their activity [52]. The catalytic domain is followed by a C-terminal extension (C-tail). The C-terminal portion of the tail is not conserved and may contribute to isoform-specific functions such as differential localization [53]. At the extreme C-terminus, PKD1/2 contains a PDZ-domain binding motif (type I: X-(Ser/Thr)-X-ϕ, where X is any amino acid and ϕ is a hydrophobic amino acid), which contains an autophosphorylation site [54]. The tail is likely also important in the regulation of PKD activity, since it has been shown that PKD1 C-terminal epitope tags increase *in vitro* autocatalytic activity and activity towards the peptide substrate syntide-2 compared to N-terminally tagged PKD1 [55].

2.2. Activation Models of PKD

2.2.1. Classical PKD Activation. In most instances, activation of PKD begins with diacylglycerol formation at membranes (e.g., after phospholipase C activation downstream of receptor tyrosine kinase or G-protein-coupled receptor activation, Figure 2(a)), although several exceptions have been discovered [56–68]. PKD binds to local pools of DAG via its C1 domains, which results in a conformational change, abrogating an autoinhibitory mechanism. At this stage, PKD expectedly autophosphorylates at the C-tail Ser-910 residue. This idea is supported by the fact that deletion of C1a and/or C1b in PKD1 results in an increased basal autocatalytic activity towards the Ser-910 autophosphorylation site and increased activity towards peptide substrate [69]. It is noteworthy that a deletion of the C1 domains does not increase basal activity towards protein substrates, nor in an increase of Ser-738/742 autophosphorylation *in vitro* [70]. Furthermore, Ser-910 phosphorylation does not require prior activation loop Ser-738/742 phosphorylation, since a S738/742A mutant still autophosphorylates Ser-910 while substrate phosphorylation is abolished [71]. This partially activated conformation likely allows PKCs (which colocalize at DAG-containing microenvironments via their respective C1 domains) to phosphorylate PKD at the activation loop Ser-738/742 residues. This phosphorylation will in turn stabilize a conformation in which the autoinhibition by the PH domain is relieved. This has been shown in a study by Waldron and Rozengurt where PKD1 bearing nonphosphorylatable Ser to Ala substitutions in the activation loop could not be activated, but when combined with a PH domain deletion (PKD1 S738/742A ΔPH), the kinase showed high basal activity towards Syntide-2. This activity could not be further stimulated with PDB in cellulo, an enzymatic profile that is comparable to PKD1 ΔPH [72]. This indicates that the role of activation loop phosphorylation is to stabilize the active conformation after the release of the PH domain. Indeed, in an isolated catalytic domain construct, Ser-738/742 substitution with Ala has a similar activity to that with a WT PKD1 catalytic domain construct [72]. This fully active PKD species will then act locally on substrates or relocate intracellularly to exert its function. All three isoforms can be activated by DAG in an activation loop phosphorylation-dependent manner. It should be noted however that there are differences in their regulation. For example, PKD3 does not contain a C-terminal Ser autophosphorylation site. Since it has been suggested that the phosphorylation of this site primes for subsequent autophosphorylation of the second Ser site in the activation loop (i.e., Ser-742) in PKD1, it is possible that PKD3 does not autophosphorylate at this residue [71]. Furthermore, the C1 domains of the different isoforms display different affinities for DAG [43], and a deletion of the C1 domains in PKD2 results in an inactivation rather than the activating effect seen for PKD1 [73], likely pointing to differences in their activation mechanisms.

2.2.2. PKD Activation in Oxidative Stress: An Isoform-Specific Matter. In oxidative stress conditions, the activation

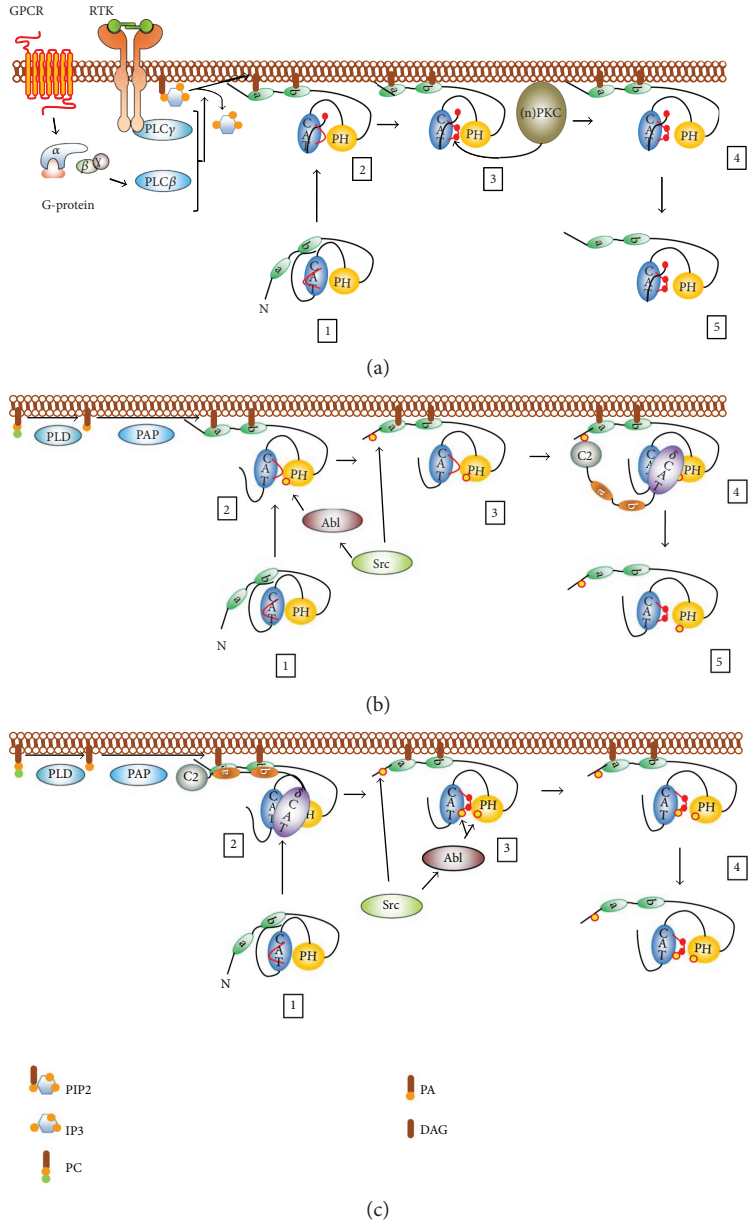

Figure 2: (a) Classical activation of PKD downstream of phospholipase C activity. (1) PKD1 is in an inactive resting conformation: the C1 and PH domains autoinhibit PKD activity. (2) PKD1 is recruited to DAG-containing microenvironments at the plasma membrane, which alleviates the autoinhibition exerted by the C1 domains. In this conformation, PKD has increased activity towards peptide substrates, but not towards proteins, indicative of an "unstable" open or "half-open" conformation. At this point, PKD can also exert autocatalytic activity towards Ser-910. (3) The abovementioned conformational changes and Ser-910 phosphorylation structure the kinase core for subsequent Ser-738 and Ser-742 phosphorylation by upstream PKCs. (4) Activation loop Ser phosphorylation stabilizes the PH-CAT module in an "open" conformation allowing for full PKD activity. (5) PKD1 is released from the membrane and translocates to several compartments to exert its functions. (b) Activation of PKD1 in oxidative stress conditions. (1) PKD1 is in a resting state, confer (a). (2) Activation is initiated by phosphorylation of Tyr-463 in the PH domain, which allows the recruitment of PKD to DAG generated by phospholipase D (PLD) activity at the outer mitochondrial membrane. (3) A subsequent conformational change allows for N-terminal phosphorylation at Tyr-95. (4) PKCδ docks to PKD1 via pTyr-95 and phosphorylates PKD1 at the activation loop Ser-738/742 residues. (5) PKD1 reaches full activity and initiates downstream signaling. (c) Activation of PKD2 in oxidative stress conditions. (1) PKD2 is in a resting state, confer (a). (2) PKD2 is recruited to DAG generated by phospholipase D (PLD) and phosphatidic acid phosphatase (PAP) activity at the outer mitochondrial membrane via its C1 domains, where it colocalizes and interacts with PKCδ without the need for Tyr-95 phosphorylation. PKCδ phosphorylates PKD2 at the activation loop Ser-706/710 residues. (3) PKD2 is phosphorylated at Tyr residues, including Tyr-87, Tyr-438, and Tyr-717, with no determined hierarchy. (4) An active and Tyr-phosphorylated PKD2 species is released from the membrane to exert its functions. PIP2: phosphatidylinositol 4,5-bisphosphate; IP3: inositol 1,4,5-trisphosphate; PC: phosphatidylcholine; PA: phosphatidic acid; DAG: diacylglycerol. Tyr phosphorylation sites are indicated with yellow-coloured circles, and Ser phosphorylation sites are indicated with red-coloured circles.

mechanism for PKD1 has historically been most studied and is well established. In contrast to classical activation by DAG downstream of G-protein-coupled receptors (GPCRs) or receptor tyrosine kinases (RTKs) through plasma membrane PLCs, activation of PKD1 in oxidative stress conditions is initiated by mitochondrial DAG production through phospholipase D (and phosphatidic acid phosphatase (PAP)) activity and generally requires the hierarchical phosphorylation of two Tyr residues in order to activate the kinase (Figures 1 and 2(b)) [74].

First, PKD1 is phosphorylated in the PH domain at Tyr-463 by Abl [75]. This initiates a conformational change, allowing for Src-mediated N-terminal phosphorylation at Tyr-95 [75, 76]. This residue is embedded in a motif that resembles the pTyr recognition motif for the C2 domain of PKCδ. PKCδ docks to the pTyr motif and consequently phosphorylates the activation loop Ser-738/742 residues, an event shown to be crucial for PKD1 activity in oxidative stress (Figures 1 and 2(b)) [76–78]. In transformed cells, Ser-910 is found not to be phosphorylated in oxidative stress conditions and thus not part of the activation mechanism [77]. Recent data indicates some remarkable isoform-specific differences in the activation mechanism during oxidative stress. Indeed, in PKD2, Tyr phosphorylation does not prime for activation loop Ser-706/710 phosphorylation, but rather the opposite: activation loop Ser phosphorylation is necessary for subsequent Tyr phosphorylation of PKD2 (Figure 2(c)) [79]. How can this divergence be explained? A possible explanation is that in PKD1, phosphorylation of Tyr-463 in the PH domain is needed to promote the deinhibited state of the PH domain-catalytic domain interaction. This allows for subsequent activation loop Ser-738/742 phosphorylation, which further stabilizes the active conformation. N-terminal Tyr-95 phosphorylation is necessary to increase the affinity of PKD1 for PKCδ in this step. In PKD2, Tyr kinases likely have no access to the autoinhibited conformation. Activation of the kinase is in this case fully dependent on activation loop Ser-706/710 phosphorylation to stabilize the open conformation of the kinase after DAG binding. This active form of PKD2 can then be accessed by Tyr kinases. Rather than being involved in the activation of PKD2, the role of Tyr phosphorylation in the PKD2 PH domain could be to dock specific interactors in oxidative stress, since the PH domain in PKDs acts as a protein-protein interaction hub, and the sequence surrounding the Tyr residue is in agreement with the PTB domain consensus sequence NXXY [80]. N-terminal phosphorylation in PKD2 on the other hand could be beneficial to stabilize the PKD2-PKCδ interaction. It should be noted however that there is no difference in the association with PKCδ between WT PKD2 and an N-terminal Tyr-Phe substituted mutant (PKD2 Y87F) during acute oxidative stress experiments [79]. This indicates that concentration of both kinases on DAG microenvironments on the outer mitochondrial membrane (OMM) can drive the interaction between PKCδ and PKD2 during acute stress, overruling the need for additional affinity contacts. However, Tyr-87 phosphorylation might be beneficial at regions of lower protein densities to increase the PKCδ-PKD2 affinity and to maintain PKD2 phosphorylation at the activation loop, for example, after dissociation from the OMM. In line with this, a recent study showed decreased activation loop phosphorylation of a PKD2 Y87F mutant when activated in focal adhesions [81]. Besides this differential activation mechanism, PKD2 is also differentially phosphorylated during oxidative stress. Indeed, PKD2 but not PKD1, is phosphorylated at Tyr in the P + 1 loop just before the APE motif. This is remarkable considering the fact that the activation segment is 100% conserved between the isoforms and highly conserved in all Ser/Thr kinases. This differential phosphorylation is due to a motif just C-terminal of the activation segment, which likely influences recognition by the upstream kinase c-Abl. This indicates a highly regulated signaling output towards the different isoforms in oxidative stress conditions. While no effects were seen on substrate selectivity on a peptide array, the phosphorylation of this site is shown to increase peptide substrate turnover *in vitro* [79].

PKD3 was long thought not to be activated in oxidative stress because it lacks an N-terminal Tyr residue. However, PKD3 was recently shown to be activated via oxidative stress in fibroblasts, which is reversible by treatment with the PKC inhibitor GF109203X [82]. This indicates that PKC can phosphorylate both PKD2 and PKD3 without Tyr phosphorylation at the N-terminus during acute stress.

Besides isoform-specific behavior in oxidative stress conditions, certain cell-type-specific behavior was also observed. PKD1 activation in primary neuronal cells is associated with an increase in Ser-910 autophosphorylation (Figure 1) (this is in contrast with transformed cell lines) [83]. This effect has also been shown in another study in neuronal cells, where Ser-910 phosphorylation was shown to prime for activation loop phosphorylation of PKD1 [84]. Intriguingly, PKD1 activation does not involve Tyr phosphorylation in these studies [83, 84].

2.3. PKD Signaling in Oxidative Stress. Once activated, PKDs regulate several pathways downstream of oxidative stress. The best studied signaling output is towards the nuclear factor kappa-light-chain-enhancer of the activated B cell (NF-κB) pathway. PKD1 signals to NF-κB via the IKK complex, which results in the consequential degradation of IκB, but the exact mechanism has not been elucidated yet [85]. NF-κB activity results in upregulation of mnSOD, which detoxifies the cell from mROS, but also generates H_2O_2, a tumor-promoting signaling molecule [86]. Additionally, it was recently shown that ROS-induced PKD1-mediated NF-κB activity results in the upregulation of epidermal growth factor receptor (EGFR) signaling components (EGFR and its ligand TGFα) in pancreatic cancer downstream of oncogenic Ras [87]. While PKD-induced NF-κB activity in transformed cells contributes to tumor development, this pathway has recently also been shown to contribute to the physiological steady-state survival of neuronal cells. Indeed, in these cells, the PKD-NF-κB-SOD2 axis is constitutively active and protects against oxidative damage [88]. In a model of excitotoxic neurodegeneration, which results in endoplasmic reticulum stress and mitochondrial dysfunction, high levels of ROS, and oxidative stress damage, the authors

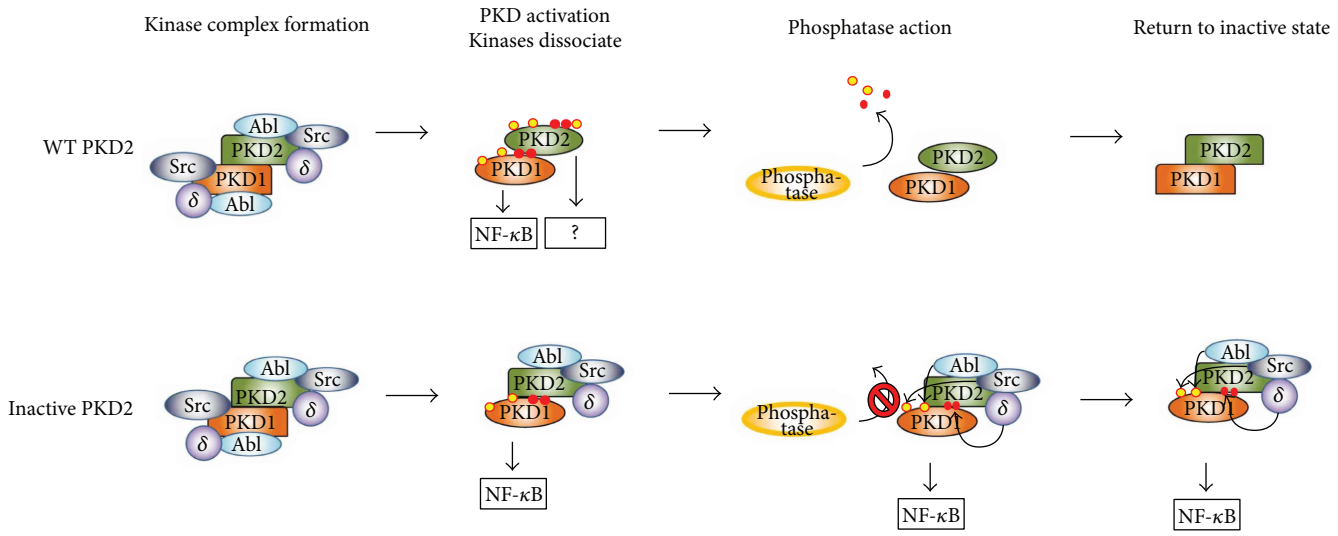

Figure 3: Putative function of PKD2 in NF-κB signaling, based on observations with inactive PKD2. Upon exposure to oxidative stress, a kinase complex comprising dimeric PKD1/2, Src, Abl, and PKCδ is assembled on the outer mitochondrial membrane. In a WT PKD1/2 dimer, the upstream kinases phosphorylate PKD1/2, which causes loss of affinity and consequentially the release of upstream kinases. PKD1 and PKD2 are both activated, but only PKD1 signals to NF-κB. When PKD2 cannot be phosphorylated because of mutations, the upstream kinases retain their affinity for PKD2 and can keep PKD1 phosphorylated (since they will have a similar affinity for PKD1 when it is dephosphorylated). In conjunction with this, the inactive conformation of PKD2, resulting from the fact that it cannot be phosphorylated, could protect PKD1 from phosphatase action. Both these phenomena could explain the enhanced NF-κB signaling output seen with inactive PKD2 mutants. Tyr phosphorylation sites are indicated with yellow-coloured circles, and Ser phosphorylation sites are indicated with red-coloured circles.

showed that PKD1 is rapidly deactivated after a short burst of activity, resulting in the loss of NF-κB signaling and impeding neuronal survival [88]. These findings were further substantiated *in vivo* using patient samples and an ischemic mouse model [88]. Another recent study in hippocampal primary neurons showed that PKD1 is transiently activated during oxidative stress, but no changes in NF-κB signaling were observed by the authors [83]. Notably, while activity and activation loop Ser-738/742 phosphorylation are necessary for signaling output to NF-κB by PKD1, for PKD2, the inverse has been shown [77, 89]. Indeed, a kinase-dead PKD2 D695A (DFG to AFG) mutant strongly stimulates NF-κB signaling, as do an inactivated S706/710A or Y717F mutants, while WT PKD2 (i.e., activated) or an activation loop phosphomimetic S706/710E mutant displays no increased signaling output in oxidative stress conditions [79, 89]. The reason for this isoform-specific behavior in oxidative stress is not known. One possibility is that PKD2 itself does not signal to NF-κB but acts as a scaffold for PKD1, which phosphorylates an isoform-specific substrate in the NF-κB pathway. Indeed, PKD1 and PKD2 are known to form heterodimers [90]. The fact that PKD2 cannot be phosphorylated by its upstream kinases through S706/710A or Y717F mutations could "trap" the upstream kinase complex (i.e., PKCδ, Abl, and potentially Src) on inactive PKD2. Due to dimer formation of PKD2 with PKD1, the latter is kept phosphorylated by the upstream kinases held in proximity by PKD2, potentiating its activity on NF-κB (Figure 3). In addition, the inactive conformation of the PKD2 monomer in the heterodimer could protect PKD1 from phosphatases (Figure 3). It should be noted however that it is unknown whether an Asp-Ala substitution in the DFG motif of the PKD2 activation segment has an effect on the ability of PKCδ and Abl to phosphorylate Ser-706/710 and Tyr-717 residues. Additionally, PKD2 can potentially enhance PKD1-mediated signaling by recruiting NF-κB signaling components via its PH domain in a Tyr-438 phosphorylation-dependent manner. Indeed, a phosphomimetic mutant of this residue displays increased signaling output to NF-κB in the absence of H_2O_2 when combined with an inactivating D695A mutation, but not when combined with a S706/710E mutant [89].

Besides the effects of PKDs on NF-κB, other PKD-dependent signaling functions have been described. For example, PKD1 inhibits mitochondrial depolarization and decreases cytochrome c release upon oxidative stress in mouse embryonic fibroblasts, effectively protecting them from apoptosis [91]. Interestingly, this behavior is isoform-specific, since cells expressing PKD2/3 do not display this phenotype. In hepatocytes, PKD1 has also been shown to protect cells from apoptosis by downregulating JNK signaling [92]. In epithelioid RIE-1 cells, PKD1 not only signals to NF-κB but also reduces p38 phosphorylation, both of which contribute to protection from apoptosis [93]. No alterations were seen in JNK signaling in this context [93]. PKD1 also phosphorylates Hsp27 in response to oxidative stress [94, 95]. In neuronal cells, Hsp27 phosphorylation protects from ischemia-induced apoptosis by suppressing JNK activity [95].

Notably, all of the PKD1 functions described above result in prosurvival signals in oxidative stress. However, in a PKC-independent pathway, oxidative stress-induced PKD1 activity can also activate JNK downstream of death-associated

protein kinase (DAPK), which results in a prodeath signal and increased necrotic cell death [96]. Furthermore, in bovine aortic ECs (BAECs), PKD1 has been shown to activate JNK via association with its upstream kinase ASK1. This association is dependent on 14-3-3 binding to PKD1, potentially via Ser-205/208 and Ser-219/223 autophosphorylation (Figure 1). The consequence of JNK activation in these cells has not been explored [44]. PKD1 also has been shown to phosphorylate Vps34 in oxidative stress [97]. Vps34 is a PI3 kinase and its phosphorylation by PKD1 leads to an activation and consequential increase of PI(3)P, resulting in increased autophagy and presumably cell death [97].

3. Concluding Remarks and Perspectives

The activation, regulation, and signaling properties of protein kinase D isoforms in oxidative stress come with intriguing questions that require further exploration. The remarkable isoform-specific differences point to a highly specific regulation of these kinases. Isoform-specific behavior in oxidative stress is also seen for other kinase families. For example, Akt isoforms are differentially regulated in oxidative stress, where Akt2 is specifically inactivated after H_2O_2 stimulation via the generation of a disulfide bond [98]. Besides their differential regulation, PKD isoforms also display distinct signaling properties. A striking example of this is their different signaling output to NF-κB. While activated PKD1 in oxidative stress signals to NF-κB, it has been shown that for PKD2, inactive forms stimulate the NF-κB signaling output [79, 89]. However, the functional relevance of inactive PKD2 is unclear, since it is also activated during oxidative stress, likely to an even larger extent than PKD1 [79]. The role of WT PKD2 in NF-κB signaling as part of a PKD1-PKD2 heterodimer is likely twofold: (1) to recruit NF-κB signaling components via its PH domain and (2) to enhance complex formation with upstream kinases to enhance PKD1 activation. An important question is whether there are other, currently unknown pathways activated PKD2 contributes to in oxidative stress.

Isoform-specific signaling behavior in redox signaling is also observed within the PKC family. For example, in the protection of the heart from ischemic events, the related nPKCs PKCδ and PKCε play opposing roles, with PKCε being cardioprotective while PKCδ increases damage induced by ischemia both *in vitro* and *in vivo* [99].

Another level of complexity lies within cell-type-specific behavior of PKDs in oxidative stress, both in their regulation and in their signaling properties. For example, as mentioned before, in neuronal cells, PKD1 activation does not always involve Tyr phosphorylation, but rather Ser-910 phosphorylation, and it does not contribute to an increased NF-κB signaling output in these cells [83, 84]. Moreover, a recent study shows a loss of homeostatic NF-κB signaling output during increased oxidative stress due to a rapid downregulation of PKD1 activity [88].

In conclusion, future studies should be carefully carried out to dissect the ROS-mediated regulation and functional roles of the individual PKD isoforms in different cell types, in order to understand the full extent of PKD-mediated signaling in oxidative stress.

Disclosure

Mathias Cobbaut's present address is The Francis Crick Institute, London, United Kingdom.

Conflicts of Interest

The authors declare that there is no conflict of interest regarding the publication of this paper.

References

[1] C. L. Quinlan, J. R. Treberg, I. V. Perevoshchikova, A. L. Orr, and M. D. Brand, "Native rates of superoxide production from multiple sites in isolated mitochondria measured using endogenous reporters," *Free Radical Biology & Medicine*, vol. 53, no. 9, pp. 1807–1817, 2012.

[2] M. Schrader and H. D. Fahimi, "Peroxisomes and oxidative stress," *Biochimica et Biophysica Acta (BBA) - Molecular Cell Research*, vol. 1763, no. 12, pp. 1755–1766, 2006.

[3] B. Bhandary, A. Marahatta, H. R. Kim, and H. J. Chae, "An involvement of oxidative stress in endoplasmic reticulum stress and its associated diseases," *International Journal of Molecular Sciences*, vol. 14, no. 1, pp. 434–456, 2013.

[4] B. Rada and T. L. Leto, "Oxidative innate immune defenses by Nox/Duox family NADPH oxidases," *Contributions to Microbiology*, vol. 15, pp. 164–187, 2008.

[5] M. Sundaresan, Z. X. Yu, V. J. Ferrans, K. Irani, and T. Finkel, "Requirement for generation of H_2O_2 for platelet-derived growth factor signal transduction," *Science*, vol. 270, no. 5234, pp. 296–299, 1995.

[6] Y. S. Bae, S. W. Kang, M. S. Seo et al., "Epidermal growth factor (EGF)-induced generation of hydrogen peroxide. Role in EGF receptor-mediated tyrosine phosphorylation," *The Journal of Biological Chemistry*, vol. 272, no. 1, pp. 217–221, 1997.

[7] S. R. Lee, K. S. Yang, J. Kwon, C. Lee, W. Jeong, and S. G. Rhee, "Reversible inactivation of the tumor suppressor PTEN by H_2O_2," *The Journal of Biological Chemistry*, vol. 277, no. 23, pp. 20336–20342, 2002.

[8] E. Giannoni, F. Buricchi, G. Raugei, G. Ramponi, and P. Chiarugi, "Intracellular reactive oxygen species activate Src tyrosine kinase during cell adhesion and anchorage-dependent cell growth," *Molecular and Cellular Biology*, vol. 25, no. 15, pp. 6391–6403, 2005.

[9] A. W. Girotti, "Mechanisms of lipid peroxidation," *Journal of Free Radicals in Biology & Medicine*, vol. 1, no. 2, pp. 87–95, 1985.

[10] M. S. Cooke, M. D. Evans, M. Dizdaroglu, and J. Lunec, "Oxidative DNA damage: mechanisms, mutation, and disease," *The FASEB Journal*, vol. 17, no. 10, pp. 1195–1214, 2003.

[11] A. L. Jackson, R. Chen, and L. A. Loeb, "Induction of microsatellite instability by oxidative DNA damage," *Proceedings of the National Academy of Sciences of the United States of America*, vol. 95, no. 21, pp. 12468–12473, 1998.

[12] R. Ghosh and D. L. Mitchell, "Effect of oxidative DNA damage in promoter elements on transcription factor binding," *Nucleic Acids Research*, vol. 27, no. 15, pp. 3213–3218, 1999.

[13] E. Cadenas, "Mitochondrial free radical production and cell signaling," *Molecular Aspects of Medicine*, vol. 25, no. 1-2, pp. 17–26, 2004.

[14] H. U. Simon, A. Haj-Yehia, and F. Levi-Schaffer, "Role of reactive oxygen species (ROS) in apoptosis induction," *Apoptosis*, vol. 5, no. 5, pp. 415–418, 2000.

[15] K. J. Davies, "Protein damage and degradation by oxygen radicals. I. General aspects," *The Journal of Biological Chemistry*, vol. 262, no. 20, pp. 9895–9901, 1987.

[16] E. R. Stadtman, "Metal ion-catalyzed oxidation of proteins: biochemical mechanism and biological consequences," *Free Radical Biology & Medicine*, vol. 9, no. 4, pp. 315–325, 1990.

[17] S. Gromer, S. Urig, and K. Becker, "The thioredoxin system—from science to clinic," *Medicinal Research Reviews*, vol. 24, no. 1, pp. 40–89, 2004.

[18] S. Curello, C. Ceconi, C. Bigoli, R. Ferrari, A. Albertini, and C. Guarnieri, "Changes in the cardiac glutathione status after ischemia and reperfusion," *Experientia*, vol. 41, no. 1, pp. 42-43, 1985.

[19] D. Sheehan, G. Meade, V. M. Foley, and C. A. Dowd, "Structure, function and evolution of glutathione transferases: implications for classification of non-mammalian members of an ancient enzyme superfamily," *Biochemical Journal*, vol. 360, no. 1, pp. 1–16, 2001.

[20] H. Sies, "Glutathione and its role in cellular functions," *Free Radical Biology & Medicine*, vol. 27, no. 9-10, pp. 916–921, 1999.

[21] N. S. Dhalla, R. M. Temsah, and T. Netticadan, "Role of oxidative stress in cardiovascular diseases," *Journal of Hypertension*, vol. 18, no. 6, pp. 655–673, 2000.

[22] D. Kienhofer, S. Boeltz, and M. H. Hoffmann, "Reactive oxygen homeostasis — the balance for preventing autoimmunity," *Lupus*, vol. 25, no. 8, pp. 943–954, 2016.

[23] K. Richter and T. Kietzmann, "Reactive oxygen species and fibrosis: further evidence of a significant liaison," *Cell and Tissue Research*, vol. 365, no. 3, pp. 591–605, 2016.

[24] A. Popa-Wagner, S. Mitran, S. Sivanesan, E. Chang, and A. M. Buga, "ROS and brain diseases: the good, the bad, and the ugly," *Oxidative Medicine and Cellular Longevity*, vol. 2013, Article ID 963520, 14 pages, 2013.

[25] G. Y. Liou and P. Storz, "Reactive oxygen species in cancer," *Free Radical Research*, vol. 44, no. 5, pp. 479–496, 2010.

[26] T. P. Szatrowski and C. F. Nathan, "Production of large amounts of hydrogen peroxide by human tumor cells," *Cancer Research*, vol. 51, no. 3, pp. 794–798, 1991.

[27] R. A. Cairns, I. S. Harris, and T. W. Mak, "Regulation of cancer cell metabolism," *Nature Reviews Cancer*, vol. 11, no. 2, pp. 85–95, 2011.

[28] A. Chatterjee, E. Mambo, and D. Sidransky, "Mitochondrial DNA mutations in human cancer," *Oncogene*, vol. 25, no. 34, pp. 4663–4674, 2006.

[29] H. C. Lee, P. H. Yin, J. C. Lin et al., "Mitochondrial genome instability and mtDNA depletion in human cancers," *Annals of the New York Academy of Sciences*, vol. 1042, no. 1, pp. 109–122, 2005.

[30] E. Mambo, A. Chatterjee, M. Xing et al., "Tumor-specific changes in mtDNA content in human cancer," *International Journal of Cancer*, vol. 116, no. 6, pp. 920–924, 2005.

[31] K. Irani, Y. Xia, J. L. Zweier et al., "Mitogenic signaling mediated by oxidants in Ras-transformed fibroblasts," *Science*, vol. 275, no. 5306, pp. 1649–1652, 1997.

[32] U. Weyemi, O. Lagente-Chevallier, M. Boufraqech et al., "ROS-generating NADPH oxidase NOX4 is a critical mediator in oncogenic H-Ras-induced DNA damage and subsequent senescence," *Oncogene*, vol. 31, no. 9, pp. 1117–1129, 2012.

[33] O. Vafa, M. Wade, S. Kern et al., "c-Myc can induce DNA damage, increase reactive oxygen species, and mitigate p53 function: a mechanism for oncogene-induced genetic instability," *Molecular Cell*, vol. 9, no. 5, pp. 1031–1044, 2002.

[34] A. Maya-Mendoza, J. Ostrakova, M. Kosar et al., "Myc and Ras oncogenes engage different energy metabolism programs and evoke distinct patterns of oxidative and DNA replication stress," *Molecular Oncology*, vol. 9, no. 3, pp. 601–616, 2015.

[35] C. W. Lin, L. Y. Yang, S. C. Shen, and Y. C. Chen, "IGF-I plus E2 induces proliferation via activation of ROS-dependent ERKs and JNKs in human breast carcinoma cells," *Journal of Cellular Physiology*, vol. 212, no. 3, pp. 666–674, 2007.

[36] L. Z. Liu, X. W. Hu, C. Xia et al., "Reactive oxygen species regulate epidermal growth factor-induced vascular endothelial growth factor and hypoxia-inducible factor-1α expression through activation of AKT and P70S6K1 in human ovarian cancer cells," *Free Radical Biology & Medicine*, vol. 41, no. 10, pp. 1521–1533, 2006.

[37] N. R. Leslie, D. Bennett, Y. E. Lindsay, H. Stewart, A. Gray, and C. P. Downes, "Redox regulation of PI 3-kinase signalling via inactivation of PTEN," *The EMBO Journal*, vol. 22, no. 20, pp. 5501–5510, 2003.

[38] E. Rozengurt, O. Rey, and R. T. Waldron, "Protein kinase D signaling," *The Journal of Biological Chemistry*, vol. 280, no. 14, pp. 13205–13208, 2005.

[39] V. Malhotra and F. Campelo, "PKD regulates membrane fission to generate TGN to cell surface transport carriers," *Cold Spring Harbor Perspectives in Biology*, vol. 3, no. 2, 2011.

[40] F. J. Johannes, J. Prestle, S. Eis, P. Oberhagemann, and K. Pfizenmaier, "PKCu is a novel, atypical member of the protein kinase C family," *The Journal of Biological Chemistry*, vol. 269, no. 8, pp. 6140–6148, 1994.

[41] E. Rozengurt, J. Sinnett-Smith, J. Van Lint, and A. M. Valverde, "Protein kinase D (PKD): a novel target for diacylglycerol and phorbol esters," *Mutation Research*, vol. 333, no. 1-2, pp. 153–160, 1995.

[42] J. V. Van Lint, J. Sinnett-Smith, and E. Rozengurt, "Expression and characterization of PKD, a phorbol ester and diacylglycerol-stimulated serine protein kinase," *The Journal of Biological Chemistry*, vol. 270, no. 3, pp. 1455–1461, 1995.

[43] J. Chen, F. Deng, J. Li, and Q. J. Wang, "Selective binding of phorbol esters and diacylglycerol by individual C1 domains of the PKD family," *The Biochemical Journal*, vol. 411, no. 2, pp. 333–342, 2008.

[44] W. Zhang, S. Zheng, P. Storz, and W. Min, "Protein kinase D specifically mediates apoptosis signal-regulating kinase 1-JNK signaling induced by H_2O_2 but not tumor necrosis factor," *The Journal of Biological Chemistry*, vol. 280, no. 19, pp. 19036–19044, 2005.

[45] M. Gschwendt, F. J. Johannes, W. Kittstein, and F. Marks, "Regulation of protein kinase Cmu by basic peptides and heparin. Putative role of an acidic domain in the activation of the kinase," *The Journal of Biological Chemistry*, vol. 272, no. 33, pp. 20742–20746, 1997.

[46] T. Iglesias and E. Rozengurt, "Protein kinase D activation by mutations within its pleckstrin homology domain," *The*

Journal of Biological Chemistry, vol. 273, no. 1, pp. 410–416, 1998.

[47] M. A. Lemmon, "Pleckstrin homology domains: not just for phosphoinositides," *Biochemical Society Transactions*, vol. 32, no. 5, pp. 707–711, 2004.

[48] W. S. Park, W. D. Heo, J. H. Whalen et al., "Comprehensive identification of PIP3-regulated PH domains from *C. elegans* to *H. sapiens* by model prediction and live imaging," *Molecular Cell*, vol. 30, no. 3, pp. 381–392, 2008.

[49] K. Scheffzek and S. Welti, "Pleckstrin homology (PH) like domains — versatile modules in protein-protein interaction platforms," *FEBS Letters*, vol. 586, no. 17, pp. 2662–2673, 2012.

[50] C. Jamora, N. Yamanouye, J. Van Lint et al., "G$\beta\gamma$-mediated regulation of Golgi organization is through the direct activation of protein kinase D," *Cell*, vol. 98, no. 1, pp. 59–68, 1999.

[51] W. W. Lau, A. S. Chan, L. S. Poon, J. Zhu, and Y. H. Wong, "G$\beta\gamma$-mediated activation of protein kinase D exhibits subunit specificity and requires G$\beta\gamma$-responsive phospholipase Cβ isoforms," *Cell Communication and Signaling*, vol. 11, no. 1, p. 22, 2013.

[52] R. T. Waldron, O. Rey, T. Iglesias, T. Tugal, D. Cantrell, and E. Rozengurt, "Activation loop Ser744 and Ser748 in protein kinase D are transphosphorylated in vivo," *The Journal of Biological Chemistry*, vol. 276, no. 35, pp. 32606–32615, 2001.

[53] R. Papazyan, E. Rozengurt, and O. Rey, "The C-terminal tail of protein kinase D2 and protein kinase D3 regulates their intracellular distribution," *Biochemical and Biophysical Research Communications*, vol. 342, no. 3, pp. 685–689, 2006.

[54] L. Sanchez-Ruiloba, N. Cabrera-Poch, M. Rodriguez-Martinez et al., "Protein kinase D intracellular localization and activity control kinase D-interacting substrate of 220-kDa traffic through a postsynaptic density-95/discs large/zonula occludens-1-binding motif," *The Journal of Biological Chemistry*, vol. 281, no. 27, pp. 18888–18900, 2006.

[55] W. Qiu, F. Zhang, and S. F. Steinberg, "The protein kinase D1 COOH terminus: marker or regulator of enzyme activity?," *American Journal of Physiology Cell physiology*, vol. 307, no. 7, pp. C606–C610, 2014.

[56] M. S. Kim, F. Wang, P. Puthanveetil et al., "Cleavage of protein kinase D after acute hypoinsulinemia prevents excessive lipoprotein lipase-mediated cardiac triglyceride accumulation," *Diabetes*, vol. 58, no. 11, pp. 2464–2475, 2009.

[57] T. Vantus, D. Vertommen, X. Saelens et al., "Doxorubicin-induced activation of protein kinase D1 through caspase-mediated proteolytic cleavage: identification of two cleavage sites by microsequencing," *Cellular Signalling*, vol. 16, no. 6, pp. 703–709, 2004.

[58] J. Lemonnier, C. Ghayor, J. Guicheux, and J. Caverzasio, "Protein kinase C-independent activation of protein kinase D is involved in BMP-2-induced activation of stress mitogen-activated protein kinases JNK and p38 and osteoblastic cell differentiation," *The Journal of Biological Chemistry*, vol. 279, no. 1, pp. 259–264, 2003.

[59] W. M. Cheung, W. W. Ng, and A. W. Kung, "Dimethyl sulfoxide as an inducer of differentiation in preosteoblast MC3T3-E1 cells," *FEBS Letters*, vol. 580, no. 1, pp. 121–126, 2006.

[60] D. Y. Kim, K. H. Park, M. S. Jung et al., "Ginsenoside Rh2(S) induces differentiation and mineralization of MC3T3-E1 cells through activation of the PKD/AMPK signaling pathways," *International Journal of Molecular Medicine*, vol. 28, no. 5, pp. 753–759, 2011.

[61] M. D. Bradford and S. P. Soltoff, "P2X7 receptors activate protein kinase D and p42/p44 mitogen-activated protein kinase (MAPK) downstream of protein kinase C," *The Biochemical Journal*, vol. 366, no. 3, pp. 745–755, 2002.

[62] J. E. Park, Y. I. Kim, and A. K. Yi, "Protein kinase D1: a new component in TLR9 signaling," *Journal of Immunology*, vol. 181, no. 3, pp. 2044–2055, 2008.

[63] F. Rezaee, N. Meednu, J. A. Emo et al., "Polyinosinic : polycytidylic acid induces protein kinase D-dependent disassembly of apical junctions and barrier dysfunction in airway epithelial cells," *The Journal of Allergy and Clinical Immunology*, vol. 128, no. 1216–1224, article e11, 2011.

[64] J. Yuan, L. W. Slice, and E. Rozengurt, "Activation of protein kinase D by signaling through Rho and the α subunit of the heterotrimeric G protein G13," *The Journal of Biological Chemistry*, vol. 276, no. 42, pp. 38619–38627, 2001.

[65] T. Eiseler, H. Doppler, I. K. Yan, K. Kitatani, K. Mizuno, and P. Storz, "Protein kinase D1 regulates cofilin-mediated F-actin reorganization and cell motility through slingshot," *Nature Cell Biology*, vol. 11, no. 5, pp. 545–556, 2009.

[66] H. Doppler, L. I. Bastea, S. Borges, S. J. Spratley, S. E. Pearce, and P. Storz, "Protein kinase D isoforms differentially modulate cofilin-driven directed cell migration," *PLoS One*, vol. 9, no. 5, article e98090, 2014.

[67] G. V. Pusapati, T. Eiseler, A. Rykx et al., "Protein kinase D regulates RhoA activity via rhotekin phosphorylation," *The Journal of Biological Chemistry*, vol. 287, no. 12, pp. 9473–9483, 2012.

[68] V. McEneaney, B. J. Harvey, and W. Thomas, "Aldosterone rapidly activates protein kinase D via a mineralocorticoid receptor/EGFR *trans*-activation pathway in the M1 kidney CCD cell line," *The Journal of Steroid Biochemistry and Molecular Biology*, vol. 107, no. 3-5, pp. 180–190, 2007.

[69] T. Iglesias and E. Rozengurt, "Protein kinase D activation by deletion of its cysteine-rich motifs," *FEBS Letters*, vol. 454, no. 1-2, pp. 53–56, 1999.

[70] V. O. Rybin, J. Guo, E. Harleton, F. Zhang, and S. F. Steinberg, "Regulatory domain determinants that control PKD1 activity," *The Journal of Biological Chemistry*, vol. 287, no. 27, pp. 22609–22615, 2012.

[71] V. O. Rybin, J. Guo, and S. F. Steinberg, "Protein kinase D1 autophosphorylation via distinct mechanisms at Ser744/Ser748 and Ser916," *The Journal of Biological Chemistry*, vol. 284, no. 4, pp. 2332–2343, 2009.

[72] R. T. Waldron and E. Rozengurt, "Protein kinase C phosphorylates protein kinase D activation loop Ser744 and Ser748 and releases autoinhibition by the pleckstrin homology domain," *The Journal of Biological Chemistry*, vol. 278, no. 1, pp. 154–163, 2003.

[73] A. Auer, J. von Blume, S. Sturany et al., "Role of the regulatory domain of protein kinase D2 in phorbol ester binding, catalytic activity, and nucleocytoplasmic shuttling," *Molecular Biology of the Cell*, vol. 16, no. 9, pp. 4375–4385, 2005.

[74] C. F. Cowell, H. Doppler, I. K. Yan, A. Hausser, Y. Umezawa, and P. Storz, "Mitochondrial diacylglycerol initiates protein-kinase D1-mediated ROS signaling," *Journal of Cell Science*, vol. 122, no. 7, pp. 919–928, 2009.

[75] P. Storz, H. Doppler, F. J. Johannes, and A. Toker, "Tyrosine phosphorylation of protein kinase D in the pleckstrin homology domain leads to activation," *The Journal of Biological Chemistry*, vol. 278, no. 20, pp. 17969–17976, 2003.

[76] H. Doppler and P. Storz, "A novel tyrosine phosphorylation site in protein kinase D contributes to oxidative stress-mediated activation," *The Journal of Biological Chemistry*, vol. 282, no. 44, pp. 31873–31881, 2007.

[77] P. Storz, H. Doppler, and A. Toker, "Activation loop phosphorylation controls protein kinase D-dependent activation of nuclear factor κB," *Molecular Pharmacology*, vol. 66, no. 4, pp. 870–879, 2004.

[78] R. T. Waldron and E. Rozengurt, "Oxidative stress induces protein kinase D activation in intact cells. Involvement of Src and dependence on protein kinase C," *The Journal Biological Chemistry*, vol. 275, no. 22, pp. 17114–17121, 2000.

[79] M. Cobbaut, R. Derua, H. Doppler et al., "Differential regulation of PKD isoforms in oxidative stress conditions through phosphorylation of a conserved Tyr in the P+1 loop," *Scientific Reports*, vol. 7, no. 1, p. 887, 2017.

[80] M. J. Smith, W. R. Hardy, J. M. Murphy, N. Jones, and T. Pawson, "Screening for PTB domain binding partners and ligand specificity using proteome-derived NPXY peptide arrays," *Molecular and Cellular Biology*, vol. 26, no. 22, pp. 8461–8474, 2006.

[81] N. Durand, L. I. Bastea, H. Doppler, T. Eiseler, and P. Storz, "Src-mediated tyrosine phosphorylation of protein kinase D2 at focal adhesions regulates cell adhesion," *Scientific Reports*, vol. 7, no. 1, p. 9524, 2017.

[82] W. Qiu and S. F. Steinberg, "Phos-tag SDS-PAGE resolves agonist- and isoform-specific activation patterns for PKD2 and PKD3 in cardiomyocytes and cardiac fibroblasts," *Journal of Molecular and Cellular Cardiology*, vol. 99, pp. 14–22, 2016.

[83] H. Liliom, K. Tarnok, Z. Abraham, B. Racz, A. Hausser, and K. Schlett, "Protein kinase D exerts neuroprotective functions during oxidative stress via nuclear factor kappa B-independent signaling pathways," *Journal of Neurochemistry*, vol. 142, no. 6, pp. 948–961, 2017.

[84] A. Asaithambi, A. Kanthasamy, H. Saminathan, V. Anantharam, and A. G. Kanthasamy, "Protein kinase D1 (PKD1) activation mediates a compensatory protective response during early stages of oxidative stress-induced neuronal degeneration," *Molecular Neurodegeneration*, vol. 6, no. 1, p. 43, 2011.

[85] P. Storz and A. Toker, "Protein kinase D mediates a stress-induced NF-κB activation and survival pathway," *The EMBO Journal*, vol. 22, no. 1, pp. 109–120, 2003.

[86] P. Storz, H. Doppler, and A. Toker, "Protein kinase D mediates mitochondrion-to-nucleus signaling and detoxification from mitochondrial reactive oxygen species," *Molecular and Cellular Biology*, vol. 25, no. 19, pp. 8520–8530, 2005.

[87] G. Y. Liou, H. Doppler, K. E. DelGiorno et al., "Mutant KRas-induced mitochondrial oxidative stress in acinar cells upregulates EGFR signaling to drive formation of pancreatic precancerous lesions," *Cell Reports*, vol. 14, no. 10, pp. 2325–2336, 2016.

[88] J. Pose-Utrilla, L. Garcia-Guerra, A. Del Puerto et al., "Excitotoxic inactivation of constitutive oxidative stress detoxification pathway in neurons can be rescued by PKD1," *Nature Communications*, vol. 8, no. 1, p. 2275, 2017.

[89] T. Mihailovic, M. Marx, A. Auer et al., "Protein kinase D2 mediates activation of nuclear factor κB by Bcr-Abl in Bcr-Abl$^+$ human myeloid leukemia cells," *Cancer Research*, vol. 64, no. 24, pp. 8939–8944, 2004.

[90] C. Aicart-Ramos, S. D. He, M. Land, and C. S. Rubin, "A novel conserved domain mediates dimerization of protein kinase D (PKD) isoforms: dimerization is essential for PKD-dependent regulation of secretion and innate immunity," *The Journal of Biological Chemistry*, vol. 291, no. 45, pp. 23516–23531, 2016.

[91] T. Zhang, P. Sell, U. Braun, and M. Leitges, "PKD1 protein is involved in reactive oxygen species-mediated mitochondrial depolarization in cooperation with protein kinase Cδ (PKCδ)," *The Journal of Biological Chemistry*, vol. 290, no. 16, pp. 10472–10485, 2015.

[92] Y. Wang, J. M. Schattenberg, R. M. Rigoli, P. Storz, and M. J. Czaja, "Hepatocyte resistance to oxidative stress is dependent on protein kinase C-mediated down-regulation of c-Jun/AP-1," *The Journal of Biological Chemistry*, vol. 279, no. 30, pp. 31089–31097, 2004.

[93] J. Song, J. Li, J. Qiao, S. Jain, B. Mark Evers, and D. H. Chung, "PKD prevents H_2O_2-induced apoptosis via NF-κB and p38 MAPK in RIE-1 cells," *Biochemical and Biophysical Research Communications.*, vol. 378, no. 3, pp. 610–614, 2009.

[94] H. Doppler, P. Storz, J. Li, M. J. Comb, and A. Toker, "A phosphorylation state-specific antibody recognizes Hsp27, a novel substrate of protein kinase D," *The Journal of Biological Chemistry*, vol. 280, no. 15, pp. 15013–15019, 2005.

[95] R. A. Stetler, Y. Gao, L. Zhang et al., "Phosphorylation of HSP27 by protein kinase D is essential for mediating neuroprotection against ischemic neuronal injury," *The Journal of Neuroscience*, vol. 32, no. 8, pp. 2667–2682, 2012.

[96] A. Eisenberg-Lerner and A. Kimchi, "DAP kinase regulates JNK signaling by binding and activating protein kinase D under oxidative stress," *Cell Death and Differentiation*, vol. 14, no. 11, pp. 1908–1915, 2007.

[97] A. Eisenberg-Lerner and A. Kimchi, "PKD is a kinase of Vps34 that mediates ROS-induced autophagy downstream of DAPk," *Cell Death and Differentiation*, vol. 19, no. 5, pp. 788–797, 2012.

[98] R. Wani, J. Qian, L. Yin et al., "Isoform-specific regulation of Akt by PDGF-induced reactive oxygen species," *Proceedings of the National Academy of Sciences of the United States of America*, vol. 108, no. 26, pp. 10550–10555, 2011.

[99] L. Chen, H. Hahn, G. Wu et al., "Opposing cardioprotective actions and parallel hypertrophic effects of δPKC and εPKC," *Proceedings of the National Academy of Sciences of the United States of America*, vol. 98, no. 20, pp. 11114–11119, 2001.

Hindawi
Oxidative Medicine and Cellular Longevity
Volume 2018, Article ID 5473817, 20 pages
https://doi.org/10.1155/2018/5473817

Review Article

Regulated Cell Death as a Therapeutic Target for Novel Antifungal Peptides and Biologics

Michael R. Yeaman,[1,2,3,4] **Sabrina Büttner**,[5,6] **and Karin Thevissen**[7]

[1]*Division of Molecular Medicine, Los Angeles County Harbor-UCLA Medical Center, Torrance, CA 90502, USA*
[2]*Division of Infectious Diseases, Los Angeles County Harbor-UCLA Medical Center, Torrance, CA 90502, USA*
[3]*Los Angeles Biomedical Research Institute at Harbor-UCLA Medical Center, Torrance, CA 90502, USA*
[4]*The David Geffen School of Medicine at UCLA, Los Angeles, CA 90024, USA*
[5]*Department of Molecular Biosciences, The Wenner-Gren Institute, Stockholm University, Stockholm, Sweden*
[6]*Institute of Molecular Biosciences, University of Graz, Graz, Austria*
[7]*Centre of Microbial and Plant Genetics (CMPG), KU Leuven, Leuven, Belgium*

Correspondence should be addressed to Michael R. Yeaman; MRYeaman@ucla.edu

Received 13 December 2017; Accepted 7 March 2018; Published 26 April 2018

Academic Editor: Alessandra Ricelli

The rise of microbial pathogens refractory to conventional antibiotics represents one of the most urgent and global public health concerns for the 21st century. Emergence of *Candida auris* isolates and the persistence of invasive mold infections that resist existing treatment and cause severe illness has underscored the threat of drug-resistant fungal infections. To meet these growing challenges, mechanistically novel agents and strategies are needed that surpass the conventional fungistatic or fungicidal drug actions. Host defense peptides have long been misunderstood as indiscriminant membrane detergents. However, evidence gathered over the past decade clearly points to their sophisticated and selective mechanisms of action, including exploiting regulated cell death pathways of their target pathogens. Such peptides perturb transmembrane potential and mitochondrial energetics, inducing phosphatidylserine accessibility and metacaspase activation in fungi. These mechanisms are often multimodal, affording target pathogens fewer resistance options as compared to traditional small molecule drugs. Here, recent advances in the field are examined regarding regulated cell death subroutines as potential therapeutic targets for innovative anti-infective peptides against pathogenic fungi. Furthering knowledge of protective host defense peptide interactions with target pathogens is key to advancing and applying novel prophylactic and therapeutic countermeasures to fungal resistance and pathogenesis.

1. Significance of Fungal Infections

1.1. Medical Burden of Fungal Infection. In the last two decades, *Candida* species have emerged as the third most common pathogen of nosocomial septicemia, accounting for 5–10% of all hospital-acquired bloodstream infections [1–3]. Overall incidence of candidemia now surpasses incidences of bacteremia due to *Escherichia coli* or *Klebsiella* species [4, 5]. Furthermore, *Candida* species are the most common cause of deep-seated fungal infections in patients who have extensive burns [6] or have undergone transplantation [7–9]. Additionally, *Candida* species are among the most common causes of catheter-related fungal infections [10]. Despite modest advances in antifungal therapy, attributable mortality of candidemia remains approximately 40% [11]. The emergence of highly antifungal-resistant species such as *C. auris* compounds these concerns [12]. Likewise, life-threatening infections caused by *Aspergillus*, *Rhizopus*, and *Mucor* species are seen with increasing incidence as the numbers of patients having immunosuppression in settings of hematopoietic or solid organ transplant, cytotoxic cancer chemotherapy, and related conditions increase [13, 14]. Collectively, these fungal

infections have unacceptably high mortality rates that may exceed 50%, even with gold-standard antifungal therapy.

1.2. Urgent Need for Innovative Solutions. Convergence of increasing populations at risk of serious fungal infections, emerging resistance to conventional antifungal agents, and a paucity of development of mechanistically novel antifungal therapeutics portends a significant public health concern.

1.2.1. Burgeoning Populations at Risk. Populations of individuals at risk of severe fungal infections are rapidly expanding in scope and number worldwide and are related to several trends with respect to the global population demographics, including the following:

(1) Aging. Immune waning and senescence have significant negative impacts on host defense against infection [15, 16]. Infection is now the attributable cause of mortality in nearly one-third of all individuals aged 65 years or older [17]. Estimates project that by 2050, the number of persons ≥ 65 years of age will reach 1.5 billion, and those aged ≥ 80 years will reach 395 million [18, 19]. Thus, along with risk factors imposed by age-related comorbidities, the growing cohort of aging individuals portends significant increases in opportunistic and pathogenic fungal infections.

(2) Cancer. Infection is a significant risk factor for morbidity in cancer patients and is a leading cause of attributable death in malignancy [16]. Beyond systemic impacts due to cancer itself, cytotoxic chemotherapy renders patients functionally immunosuppressed, thereby affecting key cell-mediated effectors such as granulocytes and macrophages [20]. Further, hospitalization, long-term in-dwelling catheterization, and chronic exposure to antibiotics enhance their risks of fungal infection [21]. Projections by the World Health Organization and others estimate a dramatic increase in cancer incidence and prevalence in the next two decades [22].

(3) Surgery. With other healthcare-associated risk factors, infections due to surgical procedures are rising in incidence and associated with worse outcomes [23]. Moreover, obesity, diabetes, smoking, hypertension, coronary artery disease, and chronic obstructive pulmonary disease [24] are pre and postsurgical risks of infection. Compounding this issue is the wide use of broad-spectrum antibiotic prophylaxis in relation to surgery, which together with immune suppression can increase risks for opportunistic fungal infections.

(4) Transplant. Successful transplantation almost always requires prolonged or even life-long immune suppressive therapy. It follows that infectious complications remain a leading cause of morbidity and mortality in settings of organ or hematologic transplantation [25]. Opportunistic fungal pathogens are among the most dangerous etiologies of these infections and can emerge when the host is rendered immunocompromised by regimens necessary for engraftment. In part due to the rise of antifungal resistance, opportunistic fungal infections are increasingly common in transplantation [26].

(5) Autoimmunity. Autoimmune diseases affect 5–10% of the population worldwide [27], translating to hundreds of millions of lives impacted. Autoimmune diseases are burgeoning globally [28], and as a group are equivalent in prevalence to heart disease, and twice that of cancer [29, 30]. Immune-modifying therapies used to treat autoimmune diseases have significant risks for life-threatening infection, including those caused by opportunistic and pathogenic fungi [31, 32].

1.2.2. Resistance to Existing Antimycotics. Fungal infections are often difficult to treat for several reasons: (1) few selective targets in these eukaryotic pathogens as compared to the human host; (2) increasing resistance to conventional antifungal agents which have advanced little in the past 50 years; and (3) the lack of mechanistically novel antifungal agents developed for clinical application. As a result, an additional concern is the emergence of resistance to antifungal agents, which are commonly used to prevent and treat disseminated candidiasis. Azole-resistant *Candida* strains are being isolated with increasing frequency, even in patients without AIDS [1, 2]. Although a limited number of antifungal drugs have been developed, experience with antibacterial agents predicts that resistance to novel antifungal drugs will emerge as their use increases [33]. Multiple factors have led to the continuous increase of reported antifungal resistance in the laboratory and in clinical failures due to resistance in human infection. For example, the fact that with few exceptions, the antifungal agents used in clinical medicine today are largely the same as those used for the prior several decades. Thus, as is the case for antibacterial resistance, exposing countless generations of fungal organisms to such agents necessarily affords a survival advantage to those pathogens capable of resistance. Key themes of concern include *Candida parapsilosis*, *C. krusei*, and *C. glabrata* clinical isolates that routinely exhibit reduced susceptibility to multiple antifungal agents [12]. While perhaps less common in incidence than infections due to *C. albicans*, these fungal pathogens can often represent serious or life-threatening bloodstream and invasive infections. Moreover, the advent of pan-resistant species of *Candida*, such as *C. auris*, is among the most significant public health concerns related to fungal infections in recent memory [12]. In addition, infections due to opportunistic or pathogenic molds remain an urgent issue. Infections caused by *Aspergillus*, *Rhizopus*, *Mucor*, and related molds are angioinvasive and destructive, often leading to necrotic and irreversible tissue damage. Infections caused by these Mucoromycotina, and those due to *Cryptococcus*, are typically treated with cytotoxic levels of amphotericin B and typically resist less toxic azoles or echinocandins [33]. Echinocandins are the newest class of antifungals introduced for human therapy in the last decade. However, recent development of echinocandin resistance has been reported via point mutations in *FKS* genes that encode the echinocandin targets (reviewed in [34]), supporting the urgent need to identify novel antifungal agents.

1.2.3. Paucity of Antifungal Development. Amphotericin B was originally discovered in the 1950s, and has been used clinical to treat fungal infections for approximately 50 years. Over that same span of time, remarkable few mechanistically novel antifungal compounds have reached regulatory approval for clinical use. These include 5-flucytosine (1963), the azoles fluconazole (1990) and voriconazole (2002), and the echinocandin caspofungin (2003), posoconazole (2006), and anidulafungin (2007) [33]. Thus, the pharmacopeia of approved antifungal agents for bloodstream or other invasive infections is essentially encompassed by just three mechanistic classes: polyenes, azoles, and echinocandins. While echinocandins are technically considered to have cyclic-peptide-like structures, the scope of the discussion herein focuses on noncyclic host defense and synthetic peptide compounds. Likewise, the many factors contributing to a significant reduction of industry investment in developing novel antifungal agents is beyond the scope of this discussion. Suffice it to say there is now an urgent need to discover and develop structurally and mechanistically new antifungal agents to meet the growing threat of life-threatening infections due to these pathogens.

2. Regulated Cell Death in Fungi

An important new area of discovery with great potential to reveal conceptually as well as mechanistically novel targets for next-generation antifungal therapeutics is regulated cell death (RCD), previously referred to as programmed cell death (PCD). For the last two decades, the occurrence of RCD in unicellular eukaryotes has been a topic of intensive study, and fungi have been shown to succumb to several distinct subroutines of regulated cell death. The majority of these studies have been carried out in the well-established model system *Saccharomyces cerevisiae*. According to the classification of cell death modalities suggested by the Nomenclature Committee on Cell Death 2018 and the recent guidelines for cell death nomenclature in yeast [35, 36], *S. cerevisiae* and likely other fungi can undergo at least three distinct types of RCD: intrinsic apoptosis (formerly **type I PCD**), autophagic cell death (formerly **type II PCD**), and regulated necrosis (formerly **type III PCD**). While considerable efforts have historically been focused on gaining a greater mechanistic and biological understanding of these RCD pathways in *S. cerevisiae*, recent studies have also provided new insights into RCD in human pathogenic fungi, including *Candida* and *Aspergillus* species. Here, we summarize the basic concepts and significant advances in this regard.

2.1. Biological Roles of Regulated Cell Death in Fungi. The signals, mechanisms, and pathways through which eukaryotic cells functionally age, wane, and ultimately meet death is equally important to their origin, development, and maturation. Thus, RCD has evolved as a means for populations of cells to most efficiently—and least disruptively—censor those individual cells that either do not actively contribute to the larger microbial community or that detract from it. Example settings in which RCD is particularly meaningful in this regard include reproduction, establishment of colonies, quorum sensing and metastatic dissemination from existing colonies or abscesses, biofilm maturation and survival in the face of antifungal agents, and many other processes necessary for survival and pathogenesis. Thus, there is sound rationale supporting fungal RCD as an innovative and mechanistically novel target of next generation antifungal therapeutics.

While the sense of an apoptotic program in unicellular organisms might not be as obvious as in metazoans, emerging data depict scenarios in which the death of damaged or old cells favors the survival of a clonal population [37]. RCD has been shown to occur during physiological scenarios such as unsuccessful mating [38], differentiation of a yeast colony [39], or replicative and chronological aging [40–42]. While replicative aging refers to the number of cell divisions an individual mother cell can undergo, chronological aging reflects the time nondividing cells stay viable in stationary phase. In both aging scenarios, apoptosis serves the elimination of cells that may be old, irreversibly injured, or which have dysfunctions that are detrimental to the larger fungal cell population. Aside from this, the apoptotic program can also be hijacked by competing fungal populations, for example via secretion of killer toxins that trigger cell death in susceptible strains [43].

In aggregate, the RCD subroutines can be induced by a plethora of different stimuli and scenarios, ranging from signaling molecules necessary for survival and reproduction to existing environmental and host threats, including antifungal agents. The relative dependence on distinct molecular players and events for activation of specific RCD pathways appears to be subject to conditional contexts in which the organism encounters a specific stress signal [44]. Based on their molecular and biochemical characteristics, the apoptotic mode of cell death has been subdivided into extrinsic and intrinsic apoptosis [35]. While extrinsic apoptosis is initiated by activation of specific transmembrane receptors that subsequently trigger cellular demise, intrinsic apoptosis can be induced by a variety of cellular stresses that all converge on mitochondria-mediated cell death processes. While yeast does most probably not succumb to the typical extrinsic apoptosis, intrinsic apoptosis does exist and represents the best studied RCD scenario in yeast so far. Morphologically, this mode of cell death is characterized by hallmark features, including systematic DNA fragmentation, nuclear condensation, exposure of phosphatidylserine at the outer leaflet of the plasma membrane, and accumulation of reactive oxygen species.

The fundamental molecular machinery governing apoptotic cell death appears to be evolutionary conserved, and numerous counterparts of mammalian key effectors of apoptosis have been identified in yeast in the past two decades [45–47]. For instance, these include orthologues of the apoptosis-inducing factor (Aif1) and Endonuclease G (Nuc1). When released from mitochondria upon an apoptotic insult and translocation to the nucleus, they cause DNA fragmentation and subsequent cell death [48, 49]. For Endonuclease G, this process involves the mitochondrial adenine translocator, implying the formation and actuation of a mitochondrial permeability transition pore in yeast apoptosis [48].

Mitochondrial features such as hyperpolarization, oxidative burst and generation of reactive oxygen species (ROS), dissipation of mitochondrial transmembrane potential, release of cytochrome *C*, loss of cytochrome *C* oxidase activity, or mitochondrial fragmentation have all been shown to contribute to apoptotic death to varying extents depending on respective triggers and scenarios [50]. Even so, variations on these themes have been observed among differing fungal organisms, including opportunistic yeast and pathogenic fungi, as discussed below.

2.2. Regulated Cell Death Subroutines in Saccharomyces cerevisiae. Although *S. cerevisiae* is not a typical human pathogen, the emergence of opportunistic *S. cerevisiae* infections has been reported in patients with chronic disease, cancer, and immunosuppression [51]. Moreover, considerable insights into RCD have been gained through studies using this organism as a model. The following discussion considers the genetic and mechanistic aspects of RCD in *S. cerevisiae* in this light, particularly given many of the RCD determinants and pathways have homologous systems in high priority human pathogens, including *Candida* species and pathogenic molds.

2.2.1. Intrinsic Apoptosis (Type I PCD). Intrinsic apoptosis is perhaps the most well-known of RCD pathways, through which cellular constituents are systematically degraded by caspase-dependent or -independent mechanisms. Comparable to mammalian intrinsic apoptosis, apoptosis in yeast is accompanied by release of cytochrome *C* from mitochondria, thus impairing oxidative phosphorylation. However, the participation of cytosolic cytochrome *C* in the formation of apoptosomes, as is observed in mammalian cells, has not yet been demonstrated in yeast.

To date, one orthologue of mammalian caspases has been identified in *S. cerevisiae*: the metacaspase Yca1 (alias Mca1) [52]. Despite different cleavage specificities of caspases (targeting aspartate-X dyads) and metacaspases (targeting lysine-X or arginine-X dyads), these proteases share a common evolutionary origin and are integral to cell death execution. Notably, the protein TSN (Tudor staphylococcal nuclease) has been established as the first common substrate of caspases and metacaspases, arguing for stringent functional conservation despite phylogenetic distance [53]. Approximately 40% of the apoptotic scenarios investigated in *S. cerevisiae* to date depend at least in part on the presence of Yca1 as executor of cellular destruction [54]. The fact that caspase-like activities have been detected even in cells lacking Yca1 indicates that additional proteases with caspase-like activity contribute to RCD in yeast [55]. One such protease may be the separin Esp1, a highly conserved protease that facilitates sister chromatid separation during metaphase to anaphase transition via cleavage of Scc1 (alias Mcd1), a subunit of the cohesion complex [56]. Esp1 belongs to the CD clan (superfamily) of cysteine proteases, a group of proteases that also includes caspases, transamidases, and bacterial gingipains [56]. During hydrogen peroxide-induced apoptosis, cleavage of Scc1 by Esp1 yields a C-terminal Scc1-fragment that relocalizes from the nucleus to the mitochondria, causing the dissipation of mitochondrial transmembrane potential, cytochrome *C* release, and cell death [57]. Several additional proteases have been associated with yeast apoptosis. Among these, the HtrA2/Omi-orthologous serine protease Nma111 is involved in oxidative stress-induced cell death [58] and responsible for the proapoptotic cleavage of the yeast inhibitor-of-apoptosis protein Bir1 [59]. Likewise, the serine carboxypeptidase Kex1 is involved in cell death execution upon treatment with hypochlorite and acetic acid as well as defects in N-glycosylation [60, 61].

Numerous endogenous and exogenous triggers have been reported to initiate intrinsic apoptotic cell death pathways in yeast, through metacaspase-dependent as well as metacaspase-independent pathways [45–47]. Among the endogenous triggers are for instance DNA damage and replication stress [62], defects in N-glycosylation [61], chronological or replicative aging [41, 42], perturbations in cytoskeleton dynamics [63], and impaired mRNA stability [64]. Likewise, a diverse set of exogenous stimuli for yeast apoptosis has been identified, including treatment with low doses of acetic acid and hydrogen peroxide, hyperosmotic stress, heat, high salt concentrations, UV irradiation, heavy metals such as iron, copper, and manganese, ceramide, amiodarone, aspirin, diverse antitumor agents, and many more [45, 46, 65]. Relevant to pathogenesis, specific host defense factors have been shown to act via induction of the intrinsic pathway of apoptosis in various fungi, including *S. cerevisiae*. For instance, peptides from the dermaseptin family produced by amphibians trigger Aif1-dependent apoptosis [66], and the plant-derived defense peptide osmotin kills by activation of Ras-dependent apoptosis [67]. Interestingly, this mode of cell death requires the binding of osmotin to the plasma membrane receptor Pho36 and might thus constitute a variant of extrinsic apoptosis (also see Section (4), below).

Homologues of mammalian proteins integral to the mitochondrial pathway of intrinsic apoptosis have been shown to be functional in yeast and to act through conserved cell death machinery. For instance, heterologous expression of the human proapoptotic protein Bax in yeast causes outer mitochondrial membrane permeabilization, cytochrome *C* release, and cell death [45]. Simultaneous heterologous expression of the human antiapoptotic regulators Bcl-2 or Bcl-XL prevents Bax-induced death and enhances yeast resistance to the apoptotic stimuli H_2O_2 and acetic acid [50]. Thus, the intrinsic pathway of apoptosis in yeast can be complemented by human or other mammalian homologues, again highlighting the functional conservation of the apoptotic program.

2.2.2. Autophagic Cell Death (Type II PCD). Autophagy represents the degradation pathway in eukaryotic cells through which the bulk of intracellular molecular turnover occurs, including breakdown of a wide range of cytoplasmic material such as aggregated proteins, organelles, and in some cases, pathogen determinants. During macroautophagy, cargo destined for degradation is sequestered into double-membraned vesicles termed autophagosomes and targeted to the vacuole for subsequent degradation and recycling. Discovered more than half a century ago, autophagy is now recognized as a catabolic process required for the coordinated regulation of cell

development, infection control, aging, and other physiological and pathophysiological fates, including cell death. Similar to other RCD subroutines, the fundamental autophagic mechanisms and molecules are conserved across the evolutionary spectrum from microbes to man. Indeed, most of the autophagy-related (*ATG*) genes and pathways have been identified and characterized in yeast cells under nutrient limiting and other stress conditions [68, 69]. While autophagy mostly represents a prosurvival and longevity-ensuring program, excessive autophagy can also contribute to cell death, in particular during development [70]. Autophagic cell death is characterized by increased numbers of autophagosomes along with aberrant protein and organelle turnover. Evidence suggests that autophagic cell death occurs in yeast cells, but the precise contribution of distinct autophagic processes to cell death execution is relatively unexplored [46]. Even so, data supporting this concept are emerging. Heterologous expression of mammalian p53 in yeast causes cell death accompanied by an upregulation of autophagy, and deletion of *ATG1* and *ATG5* partly restores survival [71]. In addition, selective leucine starvation causes a mode of death that requires the presence of essential autophagy regulators such as Atg8 [72]. Indications for an involvement of excessive autophagy targeting mitochondria (mitophagy) derive from studies showing that cells lacking the mitophagy regulator Uth1 are no longer susceptible to cell death induced by expression of mammalian Bax [73]. However, as Bax also causes mitochondria-mediated apoptosis in yeast, the precise contributions of mitophagy to Bax-mediated yeast cell death requires further investigation.

2.2.3. Regulated Necrosis (Type III PCD). Historically, necrosis has been predominantly considered to represent a purely coincidental mode of cell death upon extreme, biochemical, immunological, or mechanical insult that results in membrane rupture, swelling of organelles, and indiscriminant spilling of cell content into its surroundings. In recent years, a more specific view of necrosis has emerged, representing a more fine-tuned and regulated mechanism with implications in inflammatory responses in a variety of physiological conditions [74, 75]. In mammalian cells, the cascade of molecular events and signaling pathways that ultimately leads to necrotic RCD often involves proteases such as calpains and cathepsins, as well as the kinases RIP1 and RIP3 [74]. While most of our knowledge of regulated necrosis comes from mammalian systems, studies demonstrating this form of RCD existing in yeast have been published [76]. During chronological aging, a portion of dying cells exhibit typical hallmarks of necrosis, including loss of membrane integrity and nucleocytosolic redistribution of Nhp6A, the yeast counterpart of mammalian high mobility group box-1 protein HMGB1 [77]. This necrotic, age-associated cell death is inhibited by spermidine, a natural polyamine whose levels decline during the aging process. Spermidine inhibits cell death via an epigenetic process that involves histone H3 deacetylation and induction of autophagy. Thus, the ability of distinct pharmacological and genetic interventions to modulate this process argues that necrotic cell death is highly regulated. In this respect, deletion of distinct histone acetyltransferases blocks regulated necrosis as well [77]. Furthermore, peroxisomal function, perturbation of vacuolar function, and pH homeostasis as well as excess palmitoleic acid and elevated levels of free fatty acids have been associated with regulated necrotic cell death [78–82]. In counterbalance, high levels of the vacuolar protease Pep4, the yeast orthologue of mammalian cathepsin D, prevent both apoptotic and necrotic death during yeast chronological aging. Notably, the inhibition of apoptosis requires the proteolytic activity of native Pep4, while the suppression of necrosis is facilitated by the short propeptide version of Pep4 [83].

2.3. Regulated Cell Death in Candida Species. *Candida albicans* represents the main model system to study fungal pathogenicity and virulence, and RCD of *C. albicans* has been observed upon exposure to various antifungals and other stressors (Figure 1). *Candida* species have been shown to undergo RCD with typical characteristics of intrinsic apoptosis, whereas other forms of RCD such as autophagic cell death and regulated necrosis remain largely unexplored in this organism [84]. Among the triggers for such apoptotic pathways are for instance acetic acid and hydrogen peroxide [85], antifungal peptides from plants [86, 87], and other sources [88, 89], as well as a variety of botanicals such as perillaldehyde, honokiol, baicalin, and cinnamaldehyde [90–93]. In addition, clinical antifungal agents, including caspofungin and micafungin, two echinocandins that disturb cell wall biogenesis, can promote RCD in *C. albicans* [94, 95]. In most of these scenarios, apoptotic death of *Candida* is accompanied by an accumulation of reactive oxygen species and mitochondrial dysfunction [91, 92, 96].

As in *S. cerevisiae*, one metacaspase (Mca1) has been identified in *C. albicans* to date, and Mca1-dependent as well as -independent apoptotic cell death scenarios have been detected [84]. *C. albicans* cells lacking Mca1 are more resistant to oxidative stress-induced cell death than parental organisms [97]. Of note, increased caspase activity has been observed in relation to induction of apoptosis in *C. albicans* exposed to other stimuli, for instance the quorum sensing molecule farnesol [98, 99], the plant-derived macrocyclic bisbibenzyl plagiochin E [96] or silibinin [100]. In contrast, cell death resulting from caspofungin is executed through a Mca1-independent manner but instead requires Aif1 [94, 101].

Amphotericin B, an antifungal agent in clinical use for more than 30 years, triggers apoptotic death of *C. albicans* [85, 102] and inhibits biofilm formation of *C. albicans*, *C. krusei*, and *C. parapsilosis* [103]. Its fungicidal effects are accompanied by increased caspase activities, and concomitant exposure to caspase inhibitors provides cytoprotection. Interestingly, simultaneous pharmacological inhibition of histone deacetylation enhances amphotericin B-induced apoptosis of established *Candida* biofilms [103]. Furthermore, earlier studies connected apoptotic death in *C. albicans* to increased Ras signaling [104] and defects in glutathione synthesis [105]. More recently, human lactoferrin has been reported to induce apoptosis in *C. albicans* via binding and inhibition of the plasma membrane H^+-ATPase Pma1, which eventually results in disturbed ion homeostasis,

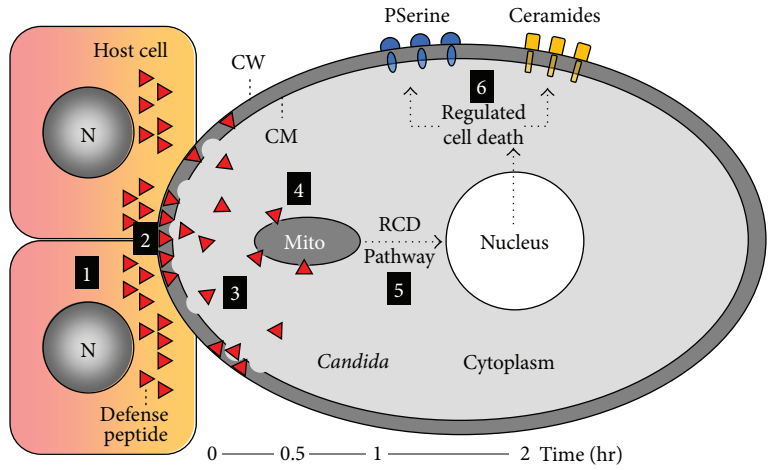

Figure 1: Model of host defense peptide mechanisms versus *C. albicans*. (1) Host cells activated by *C. albicans* deploy prestored and upregulate nuclear- (N-) encoded host defense peptides that directly interact with *C. albicans* to (2) target electronegative cell wall components (e.g., glycosylceramide or all specific cell proteins); (3) permeabilization of the cytoplasmic membrane during or following entry into the cytoplasm; (4) target the electronegative phospholipid composition and transnegative potential ($\Delta\psi$) of mitochondria (Mito); (5) perturb mitochondrial functions essential to cell cycle and trafficking, as well as de-energization and respiratory decoupling activation of caspase and/or metacaspase pathway responses; (6) combined effects of cell envelope damage and mitochondrial dysfunction invokes the regulated cell death response which corresponds to hallmark features of apoptosis, including phosphatidylserine (PS) expression. This integrated model is supported by recent publications [115, 125, 131]. It should be understood that different antifungal peptides may exert different mechanisms or a different mechanistic sequence. For example, in the case of plant defensins, the sequence of membrane perturbation and ceramide accumulation has not yet been resolved. It could well be that ceramide accumulation is a first consequence of interaction with glucosylceramides (e.g., step 2; as with RsAFP2). Alternatively, membrane perturbation could potentially be a consequence of the induction of RCD and hence, only appears at step 6.

mitochondrial dysfunction, and death [106]. Moreover, host cells seem to be able to utilize the apoptotic program of fungal pathogens as a defense system. For example, interaction with macrophages induces metacaspase activation and apoptosis in *C. albicans* [107]. In this process, distinct metacaspase substrates involved in glycolysis and protein quality control were decreased [107].

It should be understood that a given fungal organism may employ distinct apoptotic pathways, depending on multiple factors in context. For example, cell density may affect nutritional availability or activate quorum sensing pathways leading to apoptosis [108]. Thus, the effects of farnesol or other signals with respect to quorum sensing, biofilm formation, and cell death may vary depending on the microenvironmental conditions in context of infection and the strategies of fungal growth characteristics therein (e.g., yeast versus hyphae).

2.4. Regulated Cell Death in Pathogenic Molds. Compared to *Saccharomyces* or *Candida* species, less is known regarding RCD in *Aspergillus* species (Ascomycetes) or their Mucoromycotina cousins, *Rhizopus* or *Mucor*. However, recent data point to parallels in RCD among pathogenic fungi. Farnesol-induced quorum-sensing mechanisms may exist in *Aspergillus*, ultimately yielding RCD [109]. For example, in *A. nidulans*, farnesol induces the expression of an apoptosis-inducing factor (AIF-) like mitochondrial oxidoreductase, mitochondrial ATPase inhibitor, and cytochrome *C* peroxidase. As a result, ROS accumulation and mitochondrial fragmentation is observed, consistent with a process of caspase-independent apoptosis in this organism. Early studies also suggest that *Mucor* species have explicit RCD responses to stress. For instance, the HMG-CoA reductase inhibitor lovastatin can inhibit posttranslational modification of proteins, including prenylation. Following exposure to lovastatin, *M. racemosus* arrested sporangiospore germination, yielding profound cytoplasmic condensation and DNA fragmentation [110]. More recent studies reported that specific sesterterpene-type metabolites, including ophiobolins A and B, can induce apoptosis in *Mucor* species [111]. The calcineurin pathway governs key virulence and antifungal resistance pathways in *Rhizopus* as well as in other pathogenic molds such as *Mucor*. Interestingly, when exposed to the calcineurin inhibitor tacrolimus, the fungistatic triazole agents posaconazole and itraconazole became fungicidal for *R. oryzae* [112]. This effect was accompanied by DNA fragmentation, phosphatidylserine externalization, ROS accumulation, and activation of caspase-like functions. From these examples, there is considerable evidence supporting the view that caspase-dependent and -independent pathways of RCD exist in pathogenic molds and yeasts.

3. Regulated Cell Death as an Antifungal Peptide Target

Host defense peptides (HDPs) of different structural scaffolds occurring naturally or engineered have now been shown to activate fungal RCD by way of key mechanisms, including perturbation of quorum sensing, mitochondrial

Table 1: Main classes of host defense peptides (HDPs) shown to induce RCD.

Main classes of RCD-inducing antifungal peptides*		
Name	Source	Mode of action apart from RCD induction and mitochondrial dysfunction
A. Helical and extended peptides		
Periplanetasin-2	Cockroach (*Periplaneta americana)*	Lipid peroxidation, caspase activation
Scolopendin	Centipedes Class *Chilopoda*	Metacaspase activation
Lactoferrin	Bovine/human	Metacaspase activation, inhibition of membrane H^+-ATPase Pma1
B. γ–core containing peptides		
Plant defensin RsAFP2	Radish (*Raphanus sativus)*	Interaction with fungal-specific glucosylceramide, induction of cell wall stress, ceramide accumulation, septin mislocalization, metacaspase independent
Plant defensin HsAFP1	Coral bell (*Heuchera sanguinea)*	Interaction with PA and PI phospholipids, accumulation at buds and septa, internalization, pH dependent activity in vitro
Plant defensin-like peptide ApDef-1	*Adenanthera pavonina*	Cell cycle dysfunction, metacaspase activation
Insect defensin Coprisin	Dung beetle Family *Scarabaeoidea*	Dysfunctional mitochondrial $\Delta\psi$ and cytochrome C release
Fungal defensin-like peptide NFAP	*Neosartorya fischeri*	Cell wall dysfunction, accumulation of nuclei at broken hyphal tips
Fungal defensin-like peptide AFP	*Aspergillus giganteus*	Cell wall perturbation
Neutrophil defensin hNP-1	Human	Membrane permeabilization and depolarization
Beta defensin hβD-2	Human	RCD modulated by Bcr1 and Ssd1 proteins in *C. albicans*
Kinocidins (e.g., CXCL4, CXCL8)	Mammalian	Perturb membrane energetics and inhibit macromolecular synthesis; pH-related activity in vitro; RCD modulated by Bcr1 and Ssd1 proteins in *C. albicans*

*Note that Histatin-5 and plant defensin-like peptide LpDef1 were not integrated in the table as their potential induction of RCD is still under investigation.

function, autophagy or mitophagy, disruption of replication or reproductive mechanisms, and/or interference with cell cycle and aging. A particularly attractive aspect of targeting RCD in developing novel antifungal agents relates to the potential minimization of unintended consequences of inflammation that may accompany death of fungal cells exposed to cytotoxic agents that induce unregulated necrotic death. The following discussion focuses on selected examples from recent studies that offer insights into the RCD-inducing mechanisms of host defense peptides and how they might be exploited as novel antifungal agents and strategies. Recent and prior evidence is considered from studies of RCD mechanisms differentially induced by distinctive classes of antifungal HDPs (summarized in Table 1).

3.1. Helical and Extended Peptides. Perhaps the most widely recognized structural class of peptides having antifungal activity are those exhibiting α–helical or extended structures. Examples of this group of molecules for which evidence of RCD has been reported are discussed below.

3.1.1. Periplanetasin-2. This peptide has recently been isolated from the cockroach *Periplaneta americana* and studied in terms of its mechanism of action against *C. albicans* [113]. The synthetic amide version of the peptide led to lipid peroxidation, accumulation of ROS, externalization of phosphatidylserine, dissipation of $\Delta\psi$, and loss of cytochrome *C* from mitochondria, with activation of caspases, DNA fragmentation, and eventual cell death. Therefore, by inducing insurmountable oxidative stress, it appears that periplanetasin-2 evokes intrinsic apoptosis in *C. albicans*.

3.1.2. Scolopendin. Scolopendins are recently identified antimicrobial peptides of centipedes [89]. A prototype scolopendin was found to induce apoptosis in *C. albicans*, as evidenced by mitochondrial dysfunction, ROS accumulation, cytochrome *C* release, deenergization, phosphatidylserine externalization, chromatin condensation and fragmentation, and cell death. These RCD mechanisms were associated with metacaspase activation.

3.1.3. Lactoferrin. Lactoferrin is one of the most extensively studied HDPs. In early work, Andres et al. showed that this peptide induces apoptotic cell death in *C. albicans* via K+ channel-mediated K+ efflux [114]. More recently, this same group has shown lactoferrin to induce apoptosis by inhibiting the membrane H+-ATPase Pma1, leading to subsequent mitochondrial dysfunction [106]. Interestingly, Yount et al. previously noted that toxicity of human beta-defensin 2 (hβD-2) and crotamine toxin corresponded to common structure-activity relationships promoting targeting of eukaryotic K+ channels, including that of *C. albicans* [115]. Human lactoferrin has also been found to trigger caspase-dependent cell death in *Saccharomyces* [116].

3.1.4. Histatin-5. It remains unclear whether the antifungal peptide histatin-5, found in human saliva and oral secretions, induces apoptosis in *C. albicans*. Investigations by Vylkova et al. showed that histatin-5 evokes osmotic stress responses [117], and ensuing studies by Sun et al. demonstrated it to perturb ATPase functions in *C. albicans* [118]. Prior to those studies, Helmerhorst et al. demonstrated that histatin-5 exerts its antifungal activity through the formation of reactive oxygen species [119] and also showed histatin-5 to target fungal energetic systems and to cause mitochondrial dysfunction [120]. Collectively, such findings strongly implied RCD-like mechanisms. However, studies by Wunder et al. reported that histatin-5 does not exert its antifungal mechanisms via apoptosis [121].

3.2. γ–Core Peptides. Cysteine-stabilized (CS) HDPs across the phylogenetic continuum share a 12–18 residue multidimensional structure-function feature known as the γ–core [115, 122]. While this structure-function signature is conserved across a vast evolutionary distance, accessory sequences have adapted to optimize functions in distinct host anatomic and microbiologic niches. For instance, this fundamental motif is conserved in peptides of the defensin, CSαβ, and many other distinct peptide families originating from bacteria, fungi, plants, insects, and humans [123], but the accessory domains have undergone evolutionary radiation. Examples of apoptosis-inducing γ–core peptides that have antifungal efficacy are considered below.

3.2.1. Plant Defensins RsAFP2 and HsAFP1. As with all defensin-family polypeptides of plants, RsAFP1, RsAFP2, and HsAFP1 are cysteine-stabilized, cationic peptides containing a multidimensional γ–core motif [122, 124]. Plant defensins are in general characterized by broad-spectrum antifungal activity and typically have minimal toxicity to plant or human cells in vitro [125]. Originating from the common radish plant family member *Raphanus sativus* and the coral bell *Heuchera sanguinea*, the respective plant defensins RsAFP2 and HsAFP1 are models for studying apoptotic mechanisms of action versus *C. albicans*. Aerts et al. were perhaps the first to demonstrate that a plant defensin (RsAFP2) can induce intrinsic apoptosis in *C. albicans*, independent of the metacaspase Mca1 [86]. This observation was followed by a report on the induction of apoptosis of *C. albicans* by another plant defensin, HsAFP1 [87]. Interestingly, HsAFP1 was the first plant defensin for which a direct interaction with a fungal-specific lipid-based receptor was demonstrated [126], however at that time, this receptor could not be identified. Later studies by Thevissen and coworkers demonstrated that RsAFP2 interacts with fungal-specific glucosylceramides (GlcCer) [127]. The GlcCer constituents are present in the cell membrane and wall of susceptible fungi. As RsAFP2 cannot interact (or does so to a substantially lesser extent) with structurally distinct GlcCer from plant or human cells [127], the induction of RCD is selective to organisms that contain the fungal-specific sphingolipid receptor. This relationship explains why RsAFP2 is not active against the emerging fungal pathogen *Candida glabrata*, as this organism does not produce GlcCer due to a lack of the *GCS1* gene encoding glucosylceramide synthase [128]. Subsequently, Thevissen et al. demonstrated that RsAFP2 is not internalized in the cell per se, but associates with the cell envelope, resulting in cell wall stress, septin mislocalization, and accumulation of ceramides in *C. albicans* [129]. The latter effects are likely responsible for the induction of apoptosis; however, the exact mechanism yielding RCD relative to the RsAFP2-induced ceramide accumulation is hitherto unknown. Thus, multiple lines of evidence suggest this peptide induces RCD by way of targeting mitochondrial and cell cycle functions.

These antifungal effects of RsAFP2 were also found to be synergistic with caspofungin in mitigating the pathogenic consequences of *C. albicans* biofilms [130]. In the case of HsAFP1, the identity of the fungal-specific membrane receptor has not yet been elucidated. Its fungicidal action exploits the oxidative respiratory chain in *C. albicans* to cause hyperaccumulation of ROS among other phenotypic markers of apoptotic death. Interestingly, genes associated with conferring susceptibility to this peptide were those mediating mitochondrial response and related stress-induced functions [87]. Very recent evidence indicates that HsAFP1 can bind to phosphatidic acid (PA) and to a lesser extent, to various phosphatidyl inositol moieties [131]. Specifically, this peptide accumulates at the cell surface of yeast cells with intact membranes, most notably at the buds and septa, and is subsequently internalized. Further, PA was found to play an influential role in the internalization of HsAFP1, as yeast expressing reduced PA levels internalized less of this peptide (Thevissen, unpublished data). However, additional as yet unknown fungal-specific processes and targets also appear to be playing a role in HsAFP1 internalization. Likewise, in the case of the plant defensin NaD1, cell wall components have been implicated in its internalization [132, 133]. Microbicidal effects resulting from induction of RCD, such as energy perturbation and membrane permeabilization, are presumably secondary effects that ensue following HsAFP1 internalization [131].

3.2.2. Plant Defensin-Like Peptides. The seeds of the leguminous plant *Adenanthera pavonina* are the source of a recently identified peptide that exerts apoptotic mechanisms of action against fungi [134]. This defensin-like plant polypeptide termed ApDef-1 causes cell cycle dysfunction and concomitant intracellular ROS accumulation and chromatin condensation prior to metacaspase activation and cell death by intrinsic apoptosis. It is not yet known if ApDef-1 triggers these effects through general stress responses or if prototypic fungal pathogens such as *C. albicans* or pathogenic molds are susceptible to this mechanism of action. The LpDef1 peptide recently isolated from the seeds of *Lecythis pisonis* causes the accumulation of ROS and mitochondrial dysfunction in *C. albicans*, pointing towards RCD as mechanism of action [135].

3.2.3. Insect Defensin Coprisin. Coprisin is an antimicrobial peptide from the dung beetle with features of the broader insect defensin family [136, 137]. In its 43 amino acid form, there are two Cys-disulfide bonds that stabilize its

characteristic CS–$\alpha\beta$ structure. Lee et al. reported this form of coprisin to exert energy- and salt-dependent mechanisms of RCD in *C. albicans* [138]. These activities include accumulation of intracellular ROS, dysfunctional mitochondrial $\Delta\psi$ and cytochrome *C* release, phosphatidylserine externalization, and metacaspase activation, leading to apoptotic death of *C. albicans*.

3.2.4. Fungal Defensin-Like Peptides. Along with higher eukaryotic organisms, fungi themselves appear to have exploited RCD over an evolutionary timespan as a means to protect themselves from other competing fungal organisms. For example, the *Neosartorya fischeri* antifungal protein (NFAP) is a basic, cysteine-rich, extracellular antifungal protein with structural similarity to defensins [139]. This peptide is characterized by a β–barrel topology, constituting five highly twisted antiparallel β–strands, stabilized by disulfide bridges. However, in contrast to its β–defensin relatives, NFAP contains a hydrophobic core [140]. Homologues of this peptide have also been isolated from *Aspergillus giganteus* (*Aspergillus giganteus* antifungal protein (AFP)), *Aspergillus clavatus* (*Aspergillus clavatus* antifungal protein (AcAMP)), and *Aspergillus niger* (*Aspergillus niger* antifungal protein (ANAFP)) [141, 142]. Specifically, NFAP is produced by the *N. fischeri* NRRL 181 isolate (anamorph: *Aspergillus fischerianus*). Heterologous expression of the *nfap* gene in the NFAP-sensitive *A. nidulans* revealed the induction of intrinsic apoptosis, as well as damage and dysfunction of the cell wall, the destruction of chitin filaments, and the accumulation of nuclei at the broken hyphal tips [143].

3.2.5. Human Defensins. Human neutrophil defensin-1 (hNP-1) and human beta-defensin 2 (hβD-2) are among the most predominant of the host defense peptides elaborated within neutrophils and expressed by the integument (epithelial barriers), respectively. Notably, hβD-2 has been shown to perturb mitochondrial energetics and induce phosphatidylserine accessibility in *C. albicans* [115]. Such results indicate that these peptides exert their candidacidal mechanisms at least in part via a RCD response involving mitochondrial targeting. These effects were influenced by pH and occurred in relationship to altered cell membrane permeability. Similar mechanisms of anticandidal activity have been observed for hNP-1. Extending on these findings, two genes have now been identified in HDP resistance in *C. albicans* and *S. cerevisiae*. Gank et al. showed that the gene *SSD1* is integral to the ability of these fungi to survive in the face of human defensins [144]. Moreover, an *ssd1* null *C. albicans* strain was significantly less virulent in a mouse model of infection as compared to its wild-type counterpart. Subsequent investigations by Jung et al. demonstrated that the regulatory gene *BCR1* also contributes to host defense peptide resistance in *C. albicans* likely via a pathway that intersects that of *SSD1* [145]. Of note, a synthetic β–hairpin peptide (RP-13) that lacks a γ–core motif did not exert anticandidal activities identical to those of hNP-1 or hβD-2.

3.2.6. Kinocidins. Kinocidins are chemokines that exert direct microbicidal activities and potentiate functions of synergistic immune effectors, such as leukocytes [123, 146, 147]. These host defense peptides have common structural configurations comprising three modular domains: (1) N-terminal domain containing the chemokine cysteine motif; (2) interposing γ–core domain; and (3) C-terminal microbicidal helical domain [147, 148]. All mammalian kinocidins are characterized by this structural pattern. Human kinocidins representing all four conventional chemokine cysteine array structure groups (C, CC, CXC, and CX_3C) have been identified and demonstrated to have direct microbicidal activity against human pathogens [147], and congeners of these molecules have been engineered for enhanced antimicrobial activity [149, 150]. The two predominant groups of kinocidins are distinguished as α (CXC) or β (CC and other). Examples of α–kinocidins (CXC) include platelet factor-4 (PF-4; CXCL4) and platelet basic peptide (PBP; CXCL7), interleukin-8 (CXCL8), monokine induced by interferon-γ (MIG-9; CXCL9), interferon-γ inducible protein-10 kDa (IP-10; CXCL10), and interferon-inducible T cell α-chemoattractant (I-TAC9; CXCL11) [123, 147, 151]. Specific examples of β–kinocidins (CC and other subgroups) include monocyte chemoattractant protein-1 (MCP-1; CCL2), macrophage inflammatory protein-1 (MIP-1; CCL3), RANTES (regulated upon activation, normal T cell expressed/secreted; CCL5), and lymphotactin (CL1). The importance of these concepts and roles for host defense peptides having more than just antimicrobial activity are reviewed elsewhere [146, 152].

Kinocidin holoproteins and their modular peptide domains exert direct antifungal activities which are conditionally dependent. For example, kinocidins CXCL1 (GRO-a), CXCL8 (IL-8), CCL5 (RANTES), and CL1 (lymphotactin) exert significant candidacidal efficacy at pH 5.5 but little or no activity at pH 7.5 in vitro [147]. The fungicidal effect of the CXCL8 holoprotein was observed with as little as 1 nmol/ml, with complete sterilization of a 6 log CFU inoculum of *C. albicans* exposure to 5 nmol/ml of this protein. Importantly, the hemipeptide of CXCL8 containing the γ–core and microbicidal helix accounted for all of the antifungal activity of the holoprotein. For example, the isolated microbicidal helix of CXCL8 at 0.5 nmol/ml exerted sterilization of a 6 log inoculum of this organism in the same solution phase assay in vitro. Interestingly, whereas the kinocidins typically exert strong anti-*C. albicans* activity at pH 5.5, their efficacy is considerably less at pH 7.5. This pattern of activity is opposite to that of these peptides versus bacteria, which generally is substantially greater at pH 7.5 than pH 5.5 in vitro.

Mechanisms of kinocidin antifungal action have been studied using *C. albicans* clinical isolates and genetic mutants. For example, a synthetic peptide congener (RP-1) designed on the microbicidal helices of mammalian CXCL4 (PF-4) family kinocidins caused invagination and permeabilization of the cell membrane, condensation of cytoplasmic macromolecules, and loss of mitochondrial energetics in wild-type *C. albicans* [145, 153]. Gank et al. and Jung et al. demonstrated that Ssd1 and Bcr1 proteins function in a pathway that is integral to the survival of this organism in the face of low concentrations RP-1 and other host defense peptides [144, 145]. To gain further mechanistic insights, *C. albicans*

wild type, Δ*ssd1*/Δ*ssd1* null, *SSD1* complemented and forced overexpression mutants were exposed to RP-1 under distinct pH conditions simulating bloodstream (pH 7.5) or abscess (pH 5.5) contexts in vitro. Mechanisms of action were then evaluated using multiparametric flow cytometry assay devised to simultaneously assess six modes of activity (osmotic homeostasis; macromolecular condensation; cell membrane permeability; mitochondrial energetics; phosphatidylserine display; and caspase-like protease activity) [153]. *SSD1* expression inversely correlated with antimicrobial peptide susceptibility, mitochondrial deenergization and phosphatidylserine accessibility. Moreover, *SSD1* expression corresponded to mitigation of membrane permeability (assessed by propidium iodide staining, PI) and caspase-like protease induction and was greater at pH 7.5 than pH 5.5. Collectively, these results suggest that RP-1 and perhaps other host defense peptides induce RCD in *C. albicans* which can be modulated to some extent by Ssd1 protein. Similar studies focusing on Δ*bcr1*/Δ*bcr1* mutants of *C. albicans* demonstrated that the Bcr1 protein functions downstream of Ssd1 to mediate low level resistance to RP-1 and perhaps other host defense peptides by fostering homeostatic membrane integrity and mitochondrial energetics in vitro [145]. Furthermore, a homozygous null mutant of *SSD1* (Δ*ssd1*/Δ*ssd1*) was significantly less virulent in a murine model of hematogenous candidiasis [144]. Thus, the Ssd1-mediated pathway also plays an important role in the survival of *C. albicans* during infection in vivo.

3.3. Other Regulated Cell Death-Inducing Peptides. A variety of other natural peptides and proteins have been shown to induce apoptosis in yeast. Examples include osmotin [67], melittin [154], the aspergillocidal peptide PAF of *Penicillium chrysogenum* [155], the surfactant protein WH1 fungin produced by *Bacillus amyloliquefaciens* [156], a truncated derivative of dermaseptin S3 [66], yeast pheromone [157], psacotheacin [158], and the killer toxins produced by the yeast *Kluyveromyces lactis* [159]. Other peptides for which evidence exists of apoptosis-related mechanisms of action are reviewed in De Brucker et al. [160]. Additional examples of peptides that exert antifungal activity but for which RCD has not been substantiated are reviewed in [161].

4. Development of Peptide Anti-Infectives Targeting Fungal RCD

Meritorious attempts have been made to translate the potent and rapid in vitro antimicrobial activities of naturally occurring host defense and related peptides of higher organisms into novel anti-infective drugs. For a variety of reasons, this goal has proven quite elusive to date. Even so, exciting advances are emerging regarding structure, mechanism, and development of peptide-based agents. In the following discussion, the main challenges experienced to date and opportunities on the horizon are reviewed.

4.1. In Vitro to In Vivo Translation. There have been numerous examples of antibacterial peptide efficacy in animal models of infection. However, few of these agents have successfully reached phase III clinical trials, and no host defense peptide isolated from higher organisms or engineered mimetic thereof has achieved regulatory approval for use in clinical therapy [162, 163]. Even less progress has been made with respect to development of peptide therapeutics targeting fungal infections. There are only few reports that document in vivo efficacy of antifungal peptides. In this respect, Tavares et al. demonstrated efficacy of the native plant antifungal peptide RsAFP2 when administered prophylactically in a mouse candidiasis model [164]. Moreover, combined therapy of PAF, the small antifungal protein from *Penicillium chrysogenum*, and amphotericin B (AMB), which act synergistically in vitro, was more effective than either AMB or PAF treatment alone in a mouse model for invasive pulmonary aspergillosis [165]. Aside from toxicologic and pharmacologic barriers (see below), one significant issue in this respect is the reality that in vitro activity does not consistently translate to in vivo efficacy. As discussed above, the challenge of context likely plays a major role in this regard. For example, many published methods assess antimicrobial peptide efficacy in austere buffer systems that lack relevant physiologic constituents or conditions. Complicating this issue is the observation that even the most bioactive peptides can exhibit little or no efficacy in complex media (e.g., Mueller-Hinton or Brain-Heart Infusion broth) often used for standard MIC testing. Thus, the relevance of in vitro susceptibility testing of any antimicrobial peptide should be considered in relation to these limitations. A more relevant but more cost- and labor-intensive method involves testing peptide compounds in blood biomatrices, including whole blood, plasma, and serum ex vivo [166]. This method has two important advances over assays done in buffer systems: (1) peptides must overcome binding to molecular or cellular constituents present in the matrix and (2) additive or synergistic functions of a peptide with other host defense mechanisms can be assessed, for example, potentiation of neutrophil opsonophagocytosis and intracellular killing [146].

Translation of in vitro activity to in vivo efficacy has also been limited with respect to antifungal peptide efficacy. Gank et al. correlated in vitro hypersusceptibility of *C. albicans* to host defense peptides with in vivo hypovirulence in a murine model of hematogenous dissemination [144]. Very recently, Cools et al. demonstrated that truncated HsAFP1-based peptides spanning the γ–core were very active in combination with caspofungin against biofilms in vitro. However, translation to in vivo conditions failed due to the interaction of the truncated peptides with serum albumins [167], which could not be resolved by their subsequent PEGylation or cyclization. Interestingly, however, native HsAFP1 still displayed activity in the presence of serum albumins, possibly owing to its structured configuration. Hence, it is plausible that the use of native HDPs or their engineered congeners, alone or in combination with standard antimycotics, bears great potential to combat fungal infections including those resistant to current therapies.

4.2. Off-Target Effects and Toxicity. One key challenge to therapeutic development of peptide antifungal agents relates to the undefined toxicity of certain candidates tested

clinically to date. Several examples of anti-infective peptide candidates failing in preclinical development or early-stage clinical trials have been cited for reasons largely due to off-target effects and toxicity. Notable cases in this regard have been reviewed elsewhere [151, 168, 169]. As detailed above, evidence strongly supports the concept that some host defense peptides and engineered congeners thereof act at least in part by inducing or eventuating RCD in fungal target cells. This double-edged sword is likely a result of multiple convergent issues: (1) unicellular (e.g., fungi) and multicellular (e.g., mammals) eukaryotes share common molecular machineries and signal-response pathways that are responsible for RCD; (2) evolutionary, structural, and functional parallels exist among families of host defense peptides, venoms, and toxins [115]. For example, reciprocal structure-function relationships exist among human defensins such as hBD-2 and venoms/neurotoxins such as rattlesnake crotamine sharing related γ–core structural motifs [115, 170]. Mechanistic data and computational modeling also support such relationships. For example, hBD-2 and crotamine each significantly perturb mitochondrial energetics and induce phosphatidylserine accessibility of *C. albicans* and human endothelial cells in vitro [115]. Likewise, Aarbiou et al. showed that hNP-1 and LL-37 induce death of human lung epithelia and human immortalized T lymphocytes (Jurkat T cells) by mitochondrial injury [171]. In support of these concepts, Zhu et al. reported that mutations of two residues in a core consensus insect defensin sequence possessing a structural signature related to toxogenic effects of scorpion venoms could convert a defensin into a neurotoxin [172]. Similarly, Vriens et al. reported on the mutation of one residue in the sequence of the antifungal plant defensin PDF2.3 from *Arabidopsis thaliana* (AtPDF2.3), thereby converting its partial scorpion toxin signature into the full toxin signature [171–173]. As a consequence, this mutant AtPDF2.3 was characterized by antifungal activity and inhibitory activity toward mammalian Kv1.2 and Kv1.6 potassium channels [173]. Therefore, untoward toxicologic mechanisms and determinants that may reside in host defense peptides chosen to serve as antifungal templates will need to be addressed during preclinical and clinical development.

In balance, there are important opportunities pertaining to the potential for host defense peptides or their mimetics to be developed as novel antifungal agents targeting RCD. For example, crotamine was found to occlude eukaryotic (mammalian $K_v1.2$ or *C. albicans* CAK) potassium channels in molecular simulations using NMR structures. However, while hBD-2 engaged them with lower affinity, it did not occlude either of these mammalian or prokaryotic potassium channels (*Escherichia coli* KcsA) [115]. This finding suggests there are definable structure-activity features that may guide the differentiation of antimicrobial activity from host cell toxicities. Likewise, the means by which antifungal peptides or their congeners target cells may be exploited or used to improve selective toxicity. For instance, RsAFP2 has been shown to interact directly with fungal-specific glucosylceramides [127]. Interestingly, while RsAFP2 is not internalized following this interaction, a related antifungal peptide (HsAFP1) does undergo internalization and may induce RCD in target organisms. Moreover, plant defensin NaD1 is unable to permeabilize fungal cell membranes or kill target cells when the β-glucan layer is removed, suggesting a specific target or vulnerable process localizes to this layer [133]. Li et al. have reported Ssa1/2 to be a key cell envelope-binding protein for histatin-5 in targeting *C. albicans* [174]. In the case of plant defensin MtDef4, its internalization is energy dependent and mediated through endocytosis in *Neurospora crassa* [175]. Nonetheless, to date there are few other examples of specific receptors for antifungal peptides, and only limited information exists on their exact mechanisms of uptake or selective toxicity.

One notable advance that may facilitate development of antifungal peptide drugs relates to the recent discovery that peptides evolved to target or govern mitochondrial functions in eukaryotic cells contain sequence domains that exert potent antimicrobial activity in vitro [176, 177]. This interesting area is based on the evolutionary progression that led to eukaryotic symbiosis with prokaryotes in the form of mitochondria. Many of these peptides or engineered mimetics thereof induce classic features of RCD in fungi but not in human cell lines. Thus, subtle structural and/or mechanistic features may be designed into peptides to afford greater selective toxicity that targets fungal RCD as an anti-infective strategy. Moreover, particularly advantageous aspects of antifungal peptides that are ultimately developed to target RCD include their likelihood to mitigate a proinflammatory storm of necrotic cell death that may result from antifungal agents inducing survival countermeasures of the target organism.

4.3. Pharmacologic Uncertainties. An essential concept has been recognized with respect to naturally occurring antimicrobial peptides, and which has direct implications on the development of antifungal peptide therapeutics: distinct peptides have evolved in context to optimally defend distinct anatomic, physiologic, and microbiologic niches in their host [122, 123, 151]. For example, the human α–defensins hNP-1, -2, -3, and -4 are exclusively confined to neutrophil granules. These peptides must be able to function in settings of reduced pH and high levels of reactive oxygen species that are integral to the microbicidal milieu of neutrophil phagolysosomes. By comparison, α–defensins HD-5 and HD-5 (alias, cryptdins) are expressed by Paneth cells of small intestine villus crypts. Similarly, human β–defensins such as hBD-2 are only predominantly expressed by skin and cutaneous epithelial barrier cells such as keratinocytes. Importantly, while hNPs, HDs, and hBDs share the cysteine array characteristic of the defensin peptide family [170], they differ in sequence and composition as likely optimized to best defend the distinct niches in which they are expressed. It follows that attempts to deploy these peptides or their non-natural congeners as systemic antimicrobials have largely met with loss of activity or poor efficacy, degradation or lack of durable availability, and/or toxicity when placed out of context.

Defining the conditional optima for peptide antimicrobial activities is an area that remains to be fully explored. Even so, several aspects of the microenvironment in which

antimicrobial peptides best function to target pathogens and spare hosts have been studied. These include ion or salt concentrations, pH, protein binding, and growth phase/status of the target organism, among other factors [151, 178, 179]. Lakshminarayanan et al. demonstrated that conditions which alter transmembrane potential and membrane rigidity protect *C. albicans* from lethality due to tetravalent peptide B4010 (4 copies of the sequence RGRKVVRR linked through a branched lysine) [180]. Another challenge to development of peptide anti-infectives is their vulnerability to proteolytic degradation by a variety of proteases encountered systemically, be they en route to or enriched within sites of infection. For example, metalloproteases, trypsin, and chymotrypsin as well other proteases can cleave peptides into nonfunctional fragments. In addition, proteases generated by the pathogens themselves have been demonstrated to serve as resistance mechanisms to certain host defense peptides [181–185].

Various strategies have been used to circumvent the issues of proteolytic degradation that could negatively affect pharmacology of anti-infective peptides. A specific approach that may facilitate therapeutic advancement is the structural design of antifungal peptides or mimetics that retain potent and multimodal mechanisms of action but which are less susceptible or inert to rapid degradation. For example, use of nonnatural amino acids (e.g., D- versus L-enantiomeric amino acids), peptoid platforms and cyclization are methods that have been explored in reducing enzyme vulnerability of lead candidate templates as a means to improve half-life, distribution, and other pharmacokinetic parameters [151, 169]. Notable in this latter regard is the θ (theta) family of defensins that are found in leukocytes of Old World monkeys and orangutans, which are cyclic peptides generated by a posttranslational ligation event of two truncated α–defensin substrates [186]. Likewise, cyclic orbitide peptides from *Euphorbiaceae* spp. and novel cyclodepsipeptides of fungal organisms represent intriguing antifungal templates [187, 188]. Indeed, naturally occurring peptide-based molecules have illustrated success in this regard and are approved for clinical use as antifungals. For example, echinocandins are peptide-based compounds that inhibit the synthesis of cell wall glucan in fungi including *Candida* spp. and *Cryptococcus neoformans* and often have fungistatic activity against some pathogenic molds (e.g., *Aspergillus*). Members of this antifungal class (caspofungin, micafungin, and anidulafungin) are highly complex cyclic hexapeptoids conjugated to N-linked lipids that competitively inhibit 1,3–β glucan synthase [189]. Echinocandin therapeutics are derived from the papulacandin family of naturally occurring antifungals originally isolated from *Papularia* spp. of marine fungi. However, while these agents are technically peptide-based, they are quite distinct from mammalian or plant host defense peptides. Ultrashort peptides, including amidated sequences [190], may offer new insights into antifungal peptide therapeutic agents or strategies. Other approaches include liposomal formulation, continuous infusion, and topical applications.

Opportunities also exist for innovative approaches to development of antifungal peptides based on natural designs and their biological roles in a certain context. For example, specific peptides also have distinct functions under differing conditions and are processed in context to render distinctive functional modules. These themes are established for many kinocidins including CXCL4 and CXCL8, which undergo context-specific cleavage by relevant proteases to yield fully autonomous microbicidal helices [148, 179, 191]. Interestingly, their helical domains exhibit differences in antimicrobial spectra and have greater antifungal activity at pH 5.5 than pH 7.5. Innovative approaches based on such natural processing may afford strategic opportunities to exploit contextually optimized antifungal peptide structures or mechanisms. For example, context-activated protides are synthetic, multimodular propeptides designed to sense and be activated in direct response to strategic microbial or host signals—including proteases and other enzymes—in contexts of infection [123, 192]. Thus, these agents are intended to have complementary advantages with respect to their therapeutic potential. First, they are designed to intensify in the immediate proximity of infection, targeting derivative antimicrobial effector modules to microbes. Second, in contrast to conventional antibiotics which select for resistant pathogens, protides are biased to favor organisms that lack or do not express virulence determinant activators and are poorly or nonpathogenic. Thus, beyond enhanced efficacy and improved targeting of the infecting microbe, context-activated protides have the intriguing potential to shift the evolution of pathogens in favor of nonpathogenic phenotypes. Context-activated protide lead candidates are currently in the process of preclinical development.

Perhaps even more specific to the potential development of biologics targeted for fungal efficacy are recently invented proteins and peptides that induce cell death by exploiting regulated cell death evolutionary relationships [176]. These molecules are designed in part based upon the structure-function relationships of nuclear-encoded proteins that regulate mitochondrial function. As with the context-activated protide platform, the molecules in this technology platform are in the preclinical stage of development.

4.4. Sourcing and Manufacturing Issues. Isolation of naturally occurring antimicrobial peptides from native organisms or synthesis of natural or engineered forms of these molecules has historically been seen as time-, labor-, and cost-intensive for feasible commercial development. Therefore, expression systems are most commonly considered for bulk production necessary for commodity-scale use. However, by virtue of their antimicrobial activities, heterologous expression in microbial systems (e.g., *E. coli*) can present issues regarding generation of large amounts of bioactive compound [193]. In this regard, codon-use bias, intracellular granule storage, and misfolding have been among the key pitfalls encountered. To partially circumvent these issues, heterologous expression in the eukaryotes *Pichia pastoris* and *Penicillium chrysogenum* has been proven successful for production of various types of plant defensins [194] and other cysteine-rich, cationic, antifungal peptides [195], respectively. However, the above issues may remain considerable barriers in terms of sourcing and manufacturing of anti-infective peptides, directing production by means other

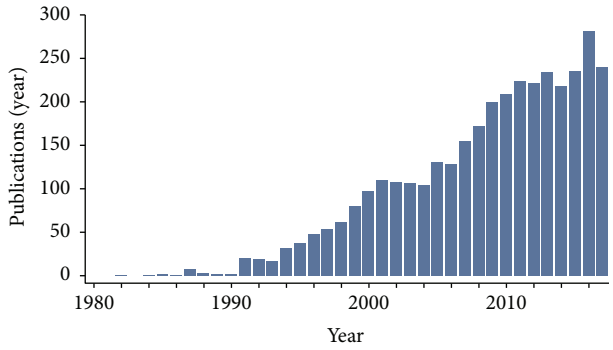

Figure 2: Trajectory of antifungal peptide publications 1980–2017. [Clarivate Analytics accessed Nov 2017].

than classical culture and recovery systems. However, recent advances in peptide expression and other innovative approaches including solid-state synthesis have provided new and practical methods to surmount many of these issues. A notable example in this regard was the large-scale heterologous expression of the defensin-family peptide plectasin, from the saprophytic fungus *Pseudoplectania nigrella*. Generation of this cysteine-stabilized peptide at a commodity scale and GMP quality as necessary for human clinical trials provides proof of concept that such peptides can be produced as therapeutics [196]. In addition, the number and diversity of regulatory approved peptide-based therapeutics is growing rapidly, demonstrating how peptides or biologics targeting microbial RCD or other mechanisms can overcome sourcing and manufacturing barriers [197].

5. Prospectus

Host defense peptides from natural sources have long held promise to serve as templates for novel anti-infective agents. This optimism stems from the rapid and potent antimicrobial efficacies of many such compounds, which often exert multimodal mechanisms of action that are considerably less prone to resistance development than static small molecules. The scope of structural and functional features of antifungal peptides has burgeoned in recent years (Figure 2). This trend is expected to accelerate in the coming decade, given the urgency with which novel antifungal and other antimicrobial agents are needed to meet the growing threat of resistance. Many pathogenic fungi are highly refractory to existing anti-infective agents, resulting in high rates of morbidity and mortality. Compounding this challenge are the significant increases in the projected incidence and prevalence of conditions predisposing to invasive fungal infections, including cancer, respiratory diseases such as chronic obstructive pulmonary disease (COPD), organ transplantation, and others. As reviewed herein, of special importance is the opportunity for innovative peptides or mimetics thereof to exploit RCD pathways in fungi as novel therapeutic targets. This strategy has multiple conceptual advantages, including mechanistic novelty and the mitigation of inflammatory storm responses that may occur as fungi attempt to counteract traditional antifungal agents. For example, fungi such as *Candida albicans* may create a systemic and cytokine storm-like effect following the application of antifungal therapy. Likewise, other fungal pathogens may participate in immune reconstitution inflammatory syndromes (IRIS) in the setting of infection in immune compromised hosts. Therefore, controlling fungal infections through regulated cell death has the potential to minimize or avoid these unintended consequences of conventional antifungal therapy.

To realize the potential for evolutionary-proven efficacy of natural antifungal peptides as innovative therapeutics, an intensive and coordinated research and development process is needed, including: (1) host and fungal science to better understand and optimize fungal RCD as a selective target for peptide-based therapeutics; (2) structure-mechanism relationship studies to define the key sequence and/or 3-dimensional determinants of peptides that selectively induce RCD in fungal cell targets; (3) medicinal chemistry to minimize or eliminate off-target host cell toxicity and optimize the pharmacologic delivery of antifungal peptide therapeutics; and (4) feasible and cost-efficient methods for generating commodity-scale peptide anti-infective drugs at GMP quality for clinical use. Achieving these goals appears to be in reach with sustained prioritization of novel antifungal agents to meet the rising tide of fungal infections anticipated in the coming decades.

Conflicts of Interest

The authors declare that they have no conflicts of interest.

References

[1] G. D. Brown, D. W. Denning, N. A. R. Gow, S. M. Levitz, M. G. Netea, and T. C. White, "Hidden killers: human fungal infections," *Science Translational Medicine*, vol. 4, no. 165, article 165rv13, 2012.

[2] B. Calvo, A. S. A. Melo, A. Perozo-Mena et al., "First report of *Candida auris* in America: clinical and microbiological aspects of 18 episodes of candidemia," *Journal of Infection*, vol. 73, no. 4, pp. 369–374, 2016.

[3] S. Corcione, R. Angilletta, S. Raviolo et al., "Epidemiology and risk factors for mortality in bloodstream infection by CP-Kp, ESBL-E, Candida and CDI: a single center retrospective study," *European Journal of Internal Medicine*, vol. 48, pp. 44–49, 2018.

[4] M. B. Edmond, S. E. Wallace, D. K. McClish, M. A. Pfaller, R. N. Jones, and R. P. Wenzel, "Nosocomial bloodstream infections in United States hospitals: a three-year analysis," *Clinical Infectious Diseases*, vol. 29, no. 2, pp. 239–244, 1999.

[5] M. S. Rangel-Frausto, T. Wiblin, H. M. Blumberg et al., "National epidemiology of mycoses survey (NEMIS): variations in rates of bloodstream infections due to *Candida* species in seven surgical intensive care units and six neonatal intensive care units," *Clinical Infectious Diseases*, vol. 29, no. 2, pp. 253–258, 1999.

[6] O. Ekenna, R. J. Sherertz, and H. Bingham, "Natural history of bloodstream infections in a burn patient population: the importance of candidemia," *American Journal of Infection Control*, vol. 21, no. 4, pp. 189–195, 1993.

[7] D. R. Andes, N. Safdar, J. W. Baddley et al., "The epidemiology and outcomes of invasive *Candida* infections among organ transplant recipients in the United States: results of the Transplant-Associated Infection Surveillance Network (TRANSNET)," *Transplant Infectious Disease*, vol. 18, no. 6, pp. 921–931, 2016.

[8] P. Castaldo, R. J. Stratta, R. P. Wood et al., "Clinical spectrum of fungal infections after orthotopic liver transplantation," *Archives of Surgery*, vol. 126, no. 2, pp. 149–156, 1991.

[9] J. M. Rabkin, S. L. Oroloff, C. L. Corless et al., "Association of fungal infection and increased mortality in liver transplant recipients," *The American Journal of Surgery*, vol. 179, no. 5, pp. 426–430, 2000.

[10] P. M. Arnow, E. M. Quimosing, and M. Beach, "Consequences of intravascular catheter sepsis," *Clinical Infectious Diseases*, vol. 16, no. 6, pp. 778–784, 1993.

[11] S. B. Wey, M. Mori, M. A. Pfaller, R. F. Woolson, and R. P. Wenzel, "Hospital-acquired candidemia. The attributable mortality and excess length of stay," *Archives of Internal Medicine*, vol. 148, no. 12, pp. 2642–2645, 1988.

[12] S. R. Lockhart, K. A. Etienne, S. Vallabhaneni et al., "Simultaneous emergence of multidrug-resistant *Candida auris* on 3 continents confirmed by whole-genome sequencing and epidemiological analyses," *Clinical Infectious Diseases*, vol. 64, no. 2, pp. 134–140, 2017.

[13] A. P. Douglas, S. C.-A. Chen, and M. A. Slavin, "Emerging infections caused by non-*Aspergillus* filamentous fungi," *Clinical Microbiology and Infection*, vol. 22, no. 8, pp. 670–680, 2016.

[14] R. E. Lewis and D. P. Kontoyiannis, "Epidemiology and treatment of mucormycosis," *Future Microbiology*, vol. 8, no. 9, pp. 1163–1175, 2013.

[15] M. G. Dorrington and D. M. E. Bowdish, "Immunosenescence and novel vaccination strategies for the elderly," *Frontiers in Immunology*, vol. 4, p. 171, 2013.

[16] K. A. Thursky and L. J. Worth, "Can mortality of cancer patients with fever and neutropenia be improved?," *Current Opinion in Infectious Diseases*, vol. 28, no. 6, pp. 505–513, 2015.

[17] K. A. Kline and D. M. E. Bowdish, "Infection in an aging population," *Current Opinion in Microbiology*, vol. 29, pp. 63–67, 2016.

[18] WHO, "Are you ready? What you need to know about ageing," December 2017. http://www.who.int/world-health-day/2012/toolkit/background/en/.

[19] "WPAM.pdf," December 2017 https://www.nia.nih.gov/sites/default/files/2017-06/WPAM.pdf.

[20] J. Truong, E. K. Lee, M. E. Trudeau, and K. K. W. Chan, "Interpreting febrile neutropenia rates from randomized, controlled trials for consideration of primary prophylaxis in the real world: a systematic review and meta-analysis," *Annals of Oncology*, vol. 27, no. 4, pp. 608–618, 2016.

[21] T. Holland, V. G. Fowler Jr., and S. A. Shelburne III, "Invasive gram-positive bacterial infection in cancer patients," *Clinical Infectious Diseases*, vol. 59, Supplement 5, pp. S331–S334, 2014.

[22] M. J. Hayat, N. Howlader, M. E. Reichman, and B. K. Edwards, "Cancer statistics, trends, and multiple primary cancer analyses from the Surveillance, Epidemiology, and End Results (SEER) Program," *The Oncologist*, vol. 12, no. 1, pp. 20–37, 2007.

[23] P. L. Owens, M. L. Barrett, S. Raetzman, M. Maggard-Gibbons, and C. A. Steiner, "Surgical site infections following ambulatory surgery procedures," *JAMA*, vol. 311, no. 7, pp. 709–716, 2014.

[24] J. T. Wiseman, S. Fernandes-Taylor, M. L. Barnes et al., "Predictors of surgical site infection after hospital discharge in patients undergoing major vascular surgery," *Journal of Vascular Surgery*, vol. 62, no. 4, pp. 1023–31.e5, 2015.

[25] P. Dorschner, L. M. McElroy, and M. G. Ison, "Nosocomial infections within the first month of solid organ transplantation," *Transplant Infectious Disease*, vol. 16, no. 2, pp. 171–187, 2014.

[26] E. J. Polvi, X. Li, T. R. O'Meara, M. D. Leach, and L. E. Cowen, "Opportunistic yeast pathogens: reservoirs, virulence mechanisms, and therapeutic strategies," *Cellular and Molecular Life Sciences*, vol. 72, no. 12, pp. 2261–2287, 2015.

[27] Y. Shoenfeld, C. Selmi, E. Zimlichman, and M. E. Gershwin, "The autoimmunologist: geoepidemiology, a new center of gravity, and prime time for autoimmunity," *Journal of Autoimmunity*, vol. 31, no. 4, pp. 325–330, 2008.

[28] N. Agmon-Levin, Z. Lian, and Y. Shoenfeld, "Explosion of autoimmune diseases and the mosaic of old and novel factors," *Cellular & Molecular Immunology*, vol. 8, no. 3, pp. 189–192, 2011.

[29] S. E. Gabriel and K. Michaud, "Epidemiological studies in incidence, prevalence, mortality, and comorbidity of the rheumatic diseases," *Arthritis Research & Therapy*, vol. 11, no. 3, p. 229, 2009.

[30] S. J. Walsh and L. M. Rau, "Autoimmune diseases: a leading cause of death among young and middle-aged women in the United States," *American Journal of Public Health*, vol. 90, no. 9, pp. 1463–1466, 2000.

[31] A. Winkelmann, M. Loebermann, E. C. Reisinger, H.-P. Hartung, and U. K. Zettl, "Disease-modifying therapies and infectious risks in multiple sclerosis," *Nature Reviews Neurology*, vol. 12, no. 4, pp. 217–233, 2016.

[32] M. R. Yeaman and J. P. Hennessey Jr., "Innovative approaches to improve anti-infective vaccine efficacy," *Annual Review of Pharmacology and Toxicology*, vol. 57, no. 1, pp. 189–222, 2017.

[33] T. Roemer and D. J. Krysan, "Antifungal drug development: challenges, unmet clinical needs, and new approaches," *Cold Spring Harbor Perspectives in Medicine*, vol. 4, no. 5, 2014.

[34] N. P. Wiederhold, "Antifungal resistance: current trends and future strategies to combat," *Infection and Drug Resistance*, vol. 10, pp. 249–259, 2017.

[35] L. Galluzzi, I. Vitale, S. A. Aaronson et al., "Molecular mechanisms of cell death: recommendations of the Nomenclature Committee on Cell Death 2018," *Cell Death & Differentiation*, vol. 25, no. 3, pp. 486–541, 2018.

[36] D. Carmona-Gutierrez, M. A. Bauer, A. Zimmermann et al., "Guidelines and recommendations on yeast cell death nomenclature," *Microbial Cell*, vol. 5, no. 1, pp. 4–31, 2018.

[37] S. Büttner, T. Eisenberg, E. Herker, D. Carmona-Gutierrez, G. Kroemer, and F. Madeo, "Why yeast cells can undergo apoptosis: death in times of peace, love, and war," *The Journal of Cell Biology*, vol. 175, no. 4, pp. 521–525, 2006.

[38] F. F. Severin and A. A. Hyman, "Pheromone induces programmed cell death in *S. cerevisiae*," *Current Biology*, vol. 12, no. 7, pp. R233–R235, 2002.

[39] L. Váchová and Z. Palková, "Physiological regulation of yeast cell death in multicellular colonies is triggered by ammonia," *The Journal of Cell Biology*, vol. 169, no. 5, pp. 711–717, 2005.

[40] P. Fabrizio, L. Battistella, R. Vardavas et al., "Superoxide is a mediator of an altruistic aging program in *Saccharomyces cerevisiae*," *The Journal of Cell Biology*, vol. 166, no. 7, pp. 1055–1067, 2004.

[41] E. Herker, H. Jungwirth, K. A. Lehmann et al., "Chronological aging leads to apoptosis in yeast," *Journal of Cell Biology*, vol. 164, no. 4, pp. 501–507, 2004.

[42] P. Laun, A. Pichova, F. Madeo et al., "Aged mother cells of *Saccharomyces cerevisiae* show markers of oxidative stress and apoptosis," *Molecular Microbiology*, vol. 39, no. 5, pp. 1166–1173, 2001.

[43] J. Reiter, E. Herker, F. Madeo, and M. J. Schmitt, "Viral killer toxins induce caspase-mediated apoptosis in yeast," *Journal of Cell Biology*, vol. 168, no. 3, pp. 353–358, 2005.

[44] G. Banfalvi, "*Mille modis morimur*: we die in a thousand ways," *Apoptosis*, vol. 22, no. 2, pp. 169–174, 2017.

[45] D. Carmona-Gutierrez, T. Eisenberg, S. Büttner, C. Meisinger, G. Kroemer, and F. Madeo, "Apoptosis in yeast: triggers, pathways, subroutines," *Cell Death & Differentiation*, vol. 17, no. 5, pp. 763–773, 2010.

[46] C. Falcone and C. Mazzoni, "External and internal triggers of cell death in yeast," *Cellular and Molecular Life Sciences*, vol. 73, no. 11-12, pp. 2237–2250, 2016.

[47] R. Strich, "Programmed cell death initiation and execution in budding yeast," *Genetics*, vol. 200, no. 4, pp. 1003–1014, 2015.

[48] S. Büttner, T. Eisenberg, D. Carmona-Gutierrez et al., "Endonuclease G regulates budding yeast life and death," *Molecular Cell*, vol. 25, no. 2, pp. 233–246, 2007.

[49] S. Wissing, P. Ludovico, E. Herker et al., "An AIF orthologue regulates apoptosis in yeast," *Journal of Cell Biology*, vol. 166, no. 7, pp. 969–974, 2004.

[50] T. Eisenberg, S. Büttner, G. Kroemer, and F. Madeo, "The mitochondrial pathway in yeast apoptosis," *Apoptosis*, vol. 12, no. 5, pp. 1011–1023, 2007.

[51] J. N. Algazaq, K. Akrami, F. Martinez, A. McCutchan, and A. R. Bharti, "*Saccharomyces cerevisiae* laryngitis and oral lesions in a patient with laryngeal carcinoma," *Case Reports in Infectious Diseases*, vol. 2017, Article ID 2941527, 4 pages, 2017.

[52] F. Madeo, E. Herker, C. Maldener et al., "A caspase-related protease regulates apoptosis in yeast," *Molecular Cell*, vol. 9, no. 4, pp. 911–917, 2002.

[53] J. F. Sundström, A. Vaculova, A. P. Smertenko et al., "Tudor staphylococcal nuclease is an evolutionarily conserved component of the programmed cell death degradome," *Nature Cell Biology*, vol. 11, no. 11, pp. 1347–1354, 2009.

[54] F. Madeo, D. Carmona-Gutierrez, J. Ring, S. Büttner, T. Eisenberg, and G. Kroemer, "Caspase-dependent and caspase-independent cell death pathways in yeast," *Biochemical and Biophysical Research Communications*, vol. 382, no. 2, pp. 227–231, 2009.

[55] D. Wilkinson and M. Ramsdale, "Proteases and caspase-like activity in the yeast *Saccharomyces cerevisiae*," *Biochemical Society Transactions*, vol. 39, no. 5, pp. 1502–1508, 2011.

[56] F. Uhlmann, D. Wernic, M. A. Poupart, E. V. Koonin, and K. Nasmyth, "Cleavage of cohesin by the CD clan protease separin triggers anaphase in yeast," *Cell*, vol. 103, no. 3, pp. 375–386, 2000.

[57] H. Yang, Q. Ren, and Z. Zhang, "Cleavage of Mcd1 by caspase-like protease Esp1 promotes apoptosis in budding yeast," *Molecular Biology of the Cell*, vol. 19, no. 5, pp. 2127–2134, 2008.

[58] B. Fahrenkrog, U. Sauder, and U. Aebi, "The *S. cerevisiae* HtrA-like protein Nma111p is a nuclear serine protease that mediates yeast apoptosis," *Journal of Cell Science*, vol. 117, no. 1, Part 1, pp. 115–126, 2004.

[59] D. Walter, S. Wissing, F. Madeo, and B. Fahrenkrog, "The inhibitor-of-apoptosis protein Bir1p protects against apoptosis in *S. cerevisiae* and is a substrate for the yeast homologue of Omi/HtrA2," *Journal of Cell Science*, vol. 119, no. 9, pp. 1843–1851, 2006.

[60] D. Carmona-Gutierrez, A. Alavian-Ghavanini, L. Habernig et al., "The cell death protease Kex1p is essential for hypochlorite-induced apoptosis in yeast," *Cell Cycle*, vol. 12, no. 11, pp. 1704–1712, 2014.

[61] P. Hauptmann, C. Riel, L. A. Kunz-Schughart, K. U. Frohlich, F. Madeo, and L. Lehle, "Defects in N-glycosylation induce apoptosis in yeast," *Molecular Microbiology*, vol. 59, no. 3, pp. 765–778, 2006.

[62] M. Weinberger, L. Ramachandran, L. Feng et al., "Apoptosis in budding yeast caused by defects in initiation of DNA replication," *Journal of Cell Science*, vol. 118, no. 15, Part 15, pp. 3543–3553, 2005.

[63] C. W. Gourlay, L. N. Carpp, P. Timpson, S. J. Winder, and K. R. Ayscough, "A role for the actin cytoskeleton in cell death and aging in yeast," *Journal of Cell Biology*, vol. 164, no. 6, pp. 803–809, 2004.

[64] C. Mazzoni, E. Herker, V. Palermo et al., "Yeast caspase 1 links messenger RNA stability to apoptosis in yeast," *EMBO Reports*, vol. 6, no. 11, pp. 1076–1081, 2005.

[65] B. Almeida, A. Silva, A. Mesquita, B. Sampaio-Marques, F. Rodrigues, and P. Ludovico, "Drug-induced apoptosis in yeast," *Biochimica et Biophysica Acta (BBA) - Molecular Cell Research*, vol. 1783, no. 7, pp. 1436–1448, 2008.

[66] C. O. Morton, S. C. Dos Santos, and P. Coote, "An amphibian-derived, cationic, α-helical antimicrobial peptide kills yeast by caspase-independent but AIF-dependent programmed cell death," *Molecular Microbiology*, vol. 65, no. 2, pp. 494–507, 2007.

[67] M. L. Narasimhan, B. Damsz, M. A. Coca et al., "A plant defense response effector induces microbial apoptosis," *Molecular Cell*, vol. 8, no. 4, pp. 921–930, 2001.

[68] F. Reggiori and D. J. Klionsky, "Autophagic processes in yeast: mechanism, machinery and regulation," *Genetics*, vol. 194, no. 2, pp. 341–361, 2013.

[69] X. Wen and D. J. Klionsky, "An overview of macroautophagy in yeast," *Journal of Molecular Biology*, vol. 428, no. 9, Part A, pp. 1681–1699, 2016.

[70] N. Kourtis and N. Tavernarakis, "Autophagy and cell death in model organisms," *Cell Death & Differentiation*, vol. 16, no. 1, pp. 21–30, 2009.

[71] M. Leão, S. Gomes, C. Bessa et al., "Studying p53 family proteins in yeast: induction of autophagic cell death and modulation by interactors and small molecules," *Experimental Cell Research*, vol. 330, no. 1, pp. 164–177, 2015.

[72] S. A. Dziedzic and A. B. Caplan, "Autophagy proteins play cytoprotective and cytocidal roles in leucine starvation-induced cell death in *Saccharomyces cerevisiae*," *Autophagy*, vol. 8, no. 5, pp. 731–738, 2014.

[73] N. Camougrand, A. Grelaud-Coq, E. Marza, M. Priault, J. J. Bessoule, and S. Manon, "The product of the *UTH1* gene, required for Bax-induced cell death in yeast, is involved in the response to rapamycin," *Molecular Microbiology*, vol. 47, no. 2, pp. 495–506, 2003.

[74] L. Galluzzi, T. Vanden Berghe, N. Vanlangenakker et al., "Programmed necrosis: from molecules to health and disease," *International Review of Cell and Molecular Biology*, vol. 289, pp. 1–35, 2011.

[75] L. Galluzzi, O. Kepp, F. K.-M. Chan, and G. Kroemer, "Necroptosis: mechanisms and relevance to disease," *Annual Review of Pathology*, vol. 12, no. 1, pp. 103–130, 2017.

[76] T. Eisenberg, D. Carmona-Gutierrez, S. Büttner, N. Tavernarakis, and F. Madeo, "Necrosis in yeast," *Apoptosis*, vol. 15, no. 3, pp. 257–268, 2010.

[77] T. Eisenberg, H. Knauer, A. Schauer et al., "Induction of autophagy by spermidine promotes longevity," *Nature Cell Biology*, vol. 11, no. 11, pp. 1305–1314, 2009.

[78] E. Bener Aksam, H. Jungwirth, S. D. Kohlwein et al., "Absence of the peroxiredoxin Pmp20 causes peroxisomal protein leakage and necrotic cell death," *Free Radical Biology & Medicine*, vol. 45, no. 8, pp. 1115–1124, 2008.

[79] H. Jungwirth, J. Ring, T. Mayer et al., "Loss of peroxisome function triggers necrosis," *FEBS Letters*, vol. 582, no. 19, pp. 2882–2886, 2008.

[80] V. R. Richard, A. Beach, A. Piano et al., "Mechanism of liponecrosis, a distinct mode of programmed cell death," *Cell Cycle*, vol. 13, no. 23, pp. 3707–3726, 2014.

[81] P. Rockenfeller, J. Ring, V. Muschett et al., "Fatty acids trigger mitochondrion-dependent necrosis," *Cell Cycle*, vol. 9, no. 14, pp. 2836–2842, 2010.

[82] A. Schauer, H. Knauer, C. Ruckenstuhl et al., "Vacuolar functions determine the mode of cell death," *Biochimica et Biophysica Acta (BBA) - Molecular Cell Research*, vol. 1793, no. 3, pp. 540–545, 2009.

[83] D. Carmona-Gutierrez, A. Reisenbichler, P. Heimbucher et al., "Ceramide triggers metacaspase-independent mitochondrial cell death in yeast," *Cell Cycle*, vol. 10, no. 22, pp. 3973–3978, 2014.

[84] S.-J. Lin and N. Austriaco, "Aging and cell death in the other yeasts, *Schizosaccharomyces pombe* and *Candida albicans*," *FEMS Yeast Research*, vol. 14, no. 1, pp. 119–135, 2014.

[85] A. J. Phillips, I. Sudbery, and M. Ramsdale, "Apoptosis induced by environmental stresses and amphotericin B in *Candida albicans*," *Proceedings of the National Academy of Sciences of the United States of America*, vol. 100, no. 24, pp. 14327–14332, 2011.

[86] A. M. Aerts, D. Carmona-Gutierrez, S. Lefevre et al., "The antifungal plant defensin RsAFP2 from radish induces apoptosis in a metacaspase independent way in *Candida albicans*," *FEBS Letters*, vol. 583, no. 15, pp. 2513–2516, 2009.

[87] A. M. Aerts, L. Bammens, G. Govaert et al., "The antifungal plant Defensin HsAFP1 from *Heuchera sanguinea* induces apoptosis in *Candida albicans*," *Frontiers in Microbiology*, vol. 2, p. 47, 2011.

[88] H. Lee and D. G. Lee, "Fungicide Bac8c triggers attenuation of mitochondrial homeostasis and caspase-dependent apoptotic death," *Biochimie*, vol. 133, pp. 80–86, 2017.

[89] H. Lee, J.-S. Hwang, and D. G. Lee, "Scolopendin, an antimicrobial peptide from centipede, attenuates mitochondrial functions and triggers apoptosis in *Candida albicans*," *Biochemical Journal*, vol. 474, no. 5, pp. 635–645, 2017.

[90] S. N. Khan, S. Khan, J. Iqbal, R. Khan, and A. U. Khan, "Enhanced killing and antibiofilm activity of encapsulated cinnamaldehyde against *Candida albicans*," *Frontiers in Microbiology*, vol. 8, p. 1641, 2017.

[91] L. Sun, K. Liao, and D. Wang, "Honokiol induces superoxide production by targeting mitochondrial respiratory chain complex I in *Candida albicans*," *PLoS One*, vol. 12, no. 8, article e0184003, 2017.

[92] H. Tian, S. Qu, Y. Wang et al., "Calcium and oxidative stress mediate perillaldehyde-induced apoptosis in *Candida albicans*," *Applied Microbiology and Biotechnology*, vol. 101, no. 8, pp. 3335–3345, 2017.

[93] T. Wang, G. Shi, J. Shao et al., "*In vitro* antifungal activity of baicalin against *Candida albicans* biofilms via apoptotic induction," *Microbial Pathogenesis*, vol. 87, pp. 21–29, 2015.

[94] C. Chin, F. Donaghey, K. Helming, M. McCarthy, S. Rogers, and N. Austriaco, "Deletion of *AIF1* but not of *YCA1*/*MCA1* protects *Saccharomyces cerevisiae* and *Candida albicans* cells from caspofungin-induced programmed cell death," *Microbial Cell*, vol. 1, no. 2, pp. 58–63, 2014.

[95] F. Shirazi and D. P. Kontoyiannis, "Micafungin triggers caspase-dependent apoptosis in *Candida albicans* and *Candida parapsilosis* biofilms, including caspofungin nonsusceptible isolates," *Virulence*, vol. 6, no. 4, pp. 385–394, 2015.

[96] X.-Z. Wu, W.-Q. Chang, A.-X. Cheng, L.-M. Sun, and H.-X. Lou, "Plagiochin E, an antifungal active macrocyclic bis(bibenzyl), induced apoptosis in *Candida albicans* through a metacaspase-dependent apoptotic pathway," *Biochimica et Biophysica Acta (BBA) - General Subjects*, vol. 1800, no. 4, pp. 439–447, 2010.

[97] Y. Cao, S. Huang, B. Dai et al., "*Candida albicans* cells lacking CaMCA1-encoded metacaspase show resistance to oxidative stress-induced death and change in energy metabolism," *Fungal Genetics and Biology*, vol. 46, no. 2, pp. 183–189, 2009.

[98] T. Léger, C. Garcia, M. Ounissi, G. Lelandais, and J.-M. Camadro, "The metacaspase (Mca1p) has a dual role in farnesol-induced apoptosis in *Candida albicans*," *Molecular & Cellular Proteomics*, vol. 14, no. 1, pp. 93–108, 2014.

[99] M. E. Shirtliff, B. P. Krom, R. A. M. Meijering et al., "Farnesol-induced apoptosis in *Candida albicans*," *Antimicrobial Agents and Chemotherapy*, vol. 53, no. 6, pp. 2392–2401, 2009.

[100] D. G. Yun and D. G. Lee, "Silibinin triggers yeast apoptosis related to mitochondrial Ca^{2+} influx in *Candida albicans*," *The International Journal of Biochemistry & Cell Biology*, vol. 80, pp. 1–9, 2016.

[101] F. Ma, Y. Zhang, Y. Wang et al., "Role of Aif1 in regulation of cell death under environmental stress in *Candida albicans*," *Yeast*, vol. 33, no. 9, pp. 493–506, 2016.

[102] M. Ramsdale, "Programmed cell death in pathogenic fungi," *Biochimica et Biophysica Acta (BBA) - Molecular Cell Research*, vol. 1783, no. 7, pp. 1369–1380, 2008.

[103] R. S. Al-Dhaheri and L. J. Douglas, "Apoptosis in *Candida* biofilms exposed to amphotericin B," *Journal of Medical Microbiology*, vol. 59, no. 2, pp. 149–157, 2010.

[104] A. J. Phillips, J. D. Crowe, and M. Ramsdale, "Ras pathway signaling accelerates programmed cell death in the pathogenic fungus *Candida albicans*," *Proceedings of the National*

Academy of Sciences of the United States of America, vol. 103, no. 3, pp. 726–731, 2006.

[105] Y.-U. Baek, Y.-R. Kim, H.-S. Yim, and S.-O. Kang, "Disruption of γ-glutamylcysteine synthetase results in absolute glutathione auxotrophy and apoptosis in *Candida albicans*," *FEBS Letters*, vol. 556, no. 1–3, pp. 47–52, 2004.

[106] M. T. Andrés, M. Acosta-Zaldívar, and J. F. Fierro, "Antifungal mechanism of action of lactoferrin: identification of H^+-ATPase (P_{3A}-type) as a new apoptotic-cell membrane receptor," *Antimicrobial Agents and Chemotherapy*, vol. 60, no. 7, pp. 4206–4216, 2016.

[107] V. Cabezón, V. Vialás, A. Gil-Bona et al., "Apoptosis of *Candida albicans* during the interaction with murine macrophages: proteomics and cell-death marker monitoring," *Journal of Proteome Research*, vol. 15, no. 5, pp. 1418–1434, 2016.

[108] T. Wongsuk, P. Pumeesat, and N. Luplertlop, "Fungal quorum sensing molecules: role in fungal morphogenesis and pathogenicity," *Journal of Basic Microbiology*, vol. 56, no. 5, pp. 440–447, 2016.

[109] T. M. Dinamarco, M. H. S. Goldman, and G. H. Goldman, "Farnesol-induced cell death in the filamentous fungus *Aspergillus nidulans*," *Biochemical Society Transactions*, vol. 39, no. 5, pp. 1544–1548, 2011.

[110] L. V. Roze and J. E. Linz, "Lovastatin triggers an apoptosis-like cell death process in the fungus *Mucor racemosus*," *Fungal Genetics and Biology*, vol. 25, no. 2, pp. 119–133, 1998.

[111] K. Krizsán, O. Bencsik, I. Nyilasi, L. Galgóczy, C. Vágvölgyi, and T. Papp, "Effect of the sesterterpene-type metabolites, ophiobolins a and B, on zygomycetes fungi," *FEMS Microbiology Letters*, vol. 313, no. 2, pp. 135–140, 2010.

[112] F. Shirazi and D. P. Kontoyiannis, "The calcineurin pathway inhibitor tacrolimus enhances the *in vitro* activity of azoles against *Mucorales* via apoptosis," *Eukaryotic Cell*, vol. 12, no. 9, pp. 1225–1234, 2013.

[113] J. Yun, J.-S. Hwang, and D. G. Lee, "The antifungal activity of the peptide, periplanetasin-2, derived from American cockroach Periplaneta americana," *Biochemical Journal*, vol. 474, no. 17, pp. 3027–3043, 2017.

[114] M. T. Andrés, M. Viejo-Díaz, and J. F. Fierro, "Human lactoferrin induces apoptosis-like cell death in *Candida albicans*: critical role of K^+-channel-mediated K^+ efflux," *Antimicrobial Agents and Chemotherapy*, vol. 52, no. 11, pp. 4081–4088, 2008.

[115] N. Y. Yount, D. Kupferwasser, A. Spisni et al., "Selective reciprocity in antimicrobial activity versus cytotoxicity of hBD-2 and crotamine," *Proceedings of the National Academy of Sciences of the United States of America*, vol. 106, no. 35, pp. 14972–14977, 2009.

[116] M. Acosta-Zaldívar, M. T. Andrés, A. Rego, C. S. Pereira, J. F. Fierro, and M. Côrte-Real, "Human lactoferrin triggers a mitochondrial- and caspase-dependent regulated cell death in *Saccharomyces cerevisiae*," *Apoptosis*, vol. 21, no. 2, pp. 163–173, 2016.

[117] S. Vylkova, W. S. Jang, W. Li, N. Nayyar, and M. Edgerton, "Histatin 5 initiates osmotic stress response in *Candida albicans* via activation of the Hog1 mitogen-activated protein kinase pathway," *Eukaryotic Cell*, vol. 6, no. 10, pp. 1876–1888, 2007.

[118] J. N. Sun, W. Li, W. S. Jang, N. Nayyar, M. D. Sutton, and M. Edgerton, "Uptake of the antifungal cationic peptide Histatin 5 by *Candida albicans* Ssa2p requires binding to non-conventional sites within the ATPase domain," *Molecular Microbiology*, vol. 70, no. 5, pp. 1246–1260, 2008.

[119] E. J. Helmerhorst, R. F. Troxler, and F. G. Oppenheim, "The human salivary peptide histatin 5 exerts its antifungal activity through the formation of reactive oxygen species," *Proceedings of the National Academy of Sciences of the United States of America*, vol. 98, no. 25, pp. 14637–14642, 2001.

[120] E. J. Helmerhorst, W. van't Hof, P. Breeuwer et al., "Characterization of histatin 5 with respect to amphipathicity, hydrophobicity, and effects on cell and mitochondrial membrane integrity excludes a candidacidal mechanism of pore formation," *Journal of Biological Chemistry*, vol. 276, no. 8, pp. 5643–5649, 2001.

[121] D. Wunder, J. Dong, D. Baev, and M. Edgerton, "Human salivary histatin 5 fungicidal action does not induce programmed cell death pathways in *Candida albicans*," *Antimicrobial Agents and Chemotherapy*, vol. 48, no. 1, pp. 110–115, 2004.

[122] N. Y. Yount and M. R. Yeaman, "Multidimensional signatures in antimicrobial peptides," *Proceedings of the National Academy of Sciences of the United States of America*, vol. 101, no. 19, pp. 7363–7368, 2004.

[123] M. R. Yeaman and N. Y. Yount, "Unifying themes in host defence effector polypeptides," *Nature Reviews Microbiology*, vol. 5, no. 9, pp. 727–740, 2007.

[124] K. Vriens, T. L. Cools, P. J. Harvey et al., "Synergistic activity of the plant defensin HsAFP1 and caspofungin against *Candida albicans* biofilms and planktonic cultures," *PLoS One*, vol. 10, no. 8, article e0132701, 2015.

[125] T. L. Cools, C. Struyfs, B. P. A. Cammue, and K. Thevissen, "Antifungal plant defensins: increased insight in their mode of action as a basis for their use to combat fungal infections," *Future Microbiology*, vol. 12, no. 5, pp. 441–454, 2017.

[126] K. Thevissen, R. W. Osborn, D. P. Acland, and W. F. Broekaert, "Specific, high affinity binding sites for an antifungal plant defensin on *Neurospora crassa* hyphae and microsomal membranes," *Journal of Biological Chemistry*, vol. 272, no. 51, pp. 32176–32181, 1997.

[127] K. Thevissen, D. C. Warnecke, I. E. J. A. François et al., "Defensins from insects and plants interact with fungal glucosylceramides," *Journal of Biological Chemistry*, vol. 279, no. 6, pp. 3900–3905, 2004.

[128] K. Saito, N. Takakuwa, M. Ohnishi, and Y. Oda, "Presence of glucosylceramide in yeast and its relation to alkali tolerance of yeast," *Applied Microbiology and Biotechnology*, vol. 71, no. 4, pp. 515–521, 2006.

[129] K. Thevissen, P. de Mello Tavares, D. Xu et al., "The plant defensin RsAFP2 induces cell wall stress, septin mislocalization and accumulation of ceramides in *Candida albicans*," *Molecular Microbiology*, vol. 84, no. 1, pp. 166–180, 2012.

[130] K. Vriens, T. L. Cools, P. J. Harvey et al., "The radish defensins RsAFP1 and RsAFP2 act synergistically with caspofungin against *Candida albicans* biofilms," *Peptides*, vol. 75, pp. 71–79, 2016.

[131] T. L. Cools, K. Vriens, C. Struyfs et al., "The antifungal plant Defensin HsAFP1 is a phosphatidic acid-interacting peptide inducing membrane permeabilization," *Frontiers in Microbiology*, vol. 8, 2017.

[132] B. M. E. Hayes, M. R. Bleackley, J. L. Wiltshire, M. A. Anderson, A. Traven, and N. L. van der Weerden, "Identification and

mechanism of action of the plant defensin NaD1 as a new member of the antifungal drug arsenal against *Candida albicans*," *Antimicrobial Agents and Chemotherapy*, vol. 57, no. 8, pp. 3667–3675, 2013.

[133] N. L. van der Weerden, R. E. W. Hancock, and M. A. Anderson, "Permeabilization of fungal hyphae by the plant defensin NaD1 occurs through a cell wall-dependent process," *Journal of Biological Chemistry*, vol. 285, no. 48, pp. 37513–37520, 2010.

[134] J. R. Soares, E. José Tenório de Melo, M. da Cunha et al., "Interaction between the plant *Ap*Def$_1$ defensin and *Saccharomyces cerevisiae* results in yeast death through a cell cycle- and caspase-dependent process occurring *via* uncontrolled oxidative stress," *Biochimica et Biophysica Acta (BBA) - General Subjects*, vol. 1861, no. 1, pp. 3429–3443, 2017.

[135] M. E. B. Vieira, I. M. Vasconcelos, O. L. T. Machado, V. M. Gomes, and A. d. O. Carvalho, "Isolation, characterization and mechanism of action of an antimicrobial peptide from *Lecythis pisonis* seeds with inhibitory activity against *Candida albicans*," *Acta Biochimica et Biophysica Sinica*, vol. 47, no. 9, pp. 716–729, 2015.

[136] J.-S. Hwang, J. Lee, Y.-J. Kim et al., "Isolation and characterization of a defensin-like peptide (coprisin) from the dung beetle, Copris tripartitus," *International Journal of Peptides*, vol. 2009, Article ID 136284, 5 pages, 2009.

[137] J. K. Kang, J. S. Hwang, H. J. Nam et al., "The insect peptide coprisin prevents *Clostridium difficile*-mediated acute inflammation and mucosal damage through selective antimicrobial activity," *Antimicrobial Agents and Chemotherapy*, vol. 55, no. 10, pp. 4850–4857, 2011.

[138] J. Lee, J.-S. Hwang, I.-S. Hwang et al., "Coprisin-induced antifungal effects in *Candida albicans* correlate with apoptotic mechanisms," *Free Radical Biology & Medicine*, vol. 52, no. 11-12, pp. 2302–2311, 2012.

[139] L. Kovács, M. Virágh, M. Takó, T. Papp, C. Vágvölgyi, and L. Galgóczy, "Isolation and characterization of *Neosartorya fischeri* antifungal protein (NFAP)," *Peptides*, vol. 32, no. 8, pp. 1724–1731, 2011.

[140] L. Galgóczy, A. Borics, M. Virágh et al., "Structural determinants of *Neosartorya fischeri* antifungal protein (NFAP) for folding, stability and antifungal activity," *Scientific Reports*, vol. 7, no. 1, p. 1963, 2017.

[141] M. Hajji, K. Jellouli, N. Hmidet, R. Balti, A. Sellami-Kamoun, and M. Nasri, "A highly thermostable antimicrobial peptide from *Aspergillus clavatus* ES1: biochemical and molecular characterization," *Journal of Industrial Microbiology & Biotechnology*, vol. 37, no. 8, pp. 805–813, 2010.

[142] V. Meyer, "A small protein that fights fungi: AFP as a new promising antifungal agent of biotechnological value," *Applied Microbiology and Biotechnology*, vol. 78, no. 1, pp. 17–28, 2008.

[143] L. Galgóczy, L. Kovács, Z. Karácsony, M. Virágh, Z. Hamari, and C. Vágvölgyi, "Investigation of the antimicrobial effect of Neosartorya fischeri antifungal protein (NFAP) after heterologous expression in Aspergillus nidulans," *Microbiology*, vol. 159, Part 2, pp. 411–419, 2013.

[144] K. D. Gank, M. R. Yeaman, S. Kojima et al., "*SSD1* is integral to host defense peptide resistance in *Candida albicans*," *Eukaryotic Cell*, vol. 7, no. 8, pp. 1318–1327, 2008.

[145] S.-I. Jung, J. S. Finkel, N. V. Solis et al., "Bcr1 functions downstream of Ssd1 to mediate antimicrobial peptide resistance in *Candida albicans*," *Eukaryotic Cell*, vol. 12, no. 3, pp. 411–419, 2013.

[146] M. R. Yeaman, "Platelets: at the nexus of antimicrobial defence," *Nature Reviews Microbiology*, vol. 12, no. 6, pp. 426–437, 2014.

[147] N. Y. Yount, A. J. Waring, K. D. Gank, W. H. Welch, D. Kupferwasser, and M. R. Yeaman, "Structural correlates of antimicrobial efficacy in IL-8 and related human kinocidins," *Biochimica et Biophysica Acta (BBA) - Biomembranes*, vol. 1768, no. 3, pp. 598–608, 2007.

[148] M. R. Yeaman, N. Y. Yount, A. J. Waring et al., "Modular determinants of antimicrobial activity in platelet factor-4 family kinocidins," *Biochimica et Biophysica Acta (BBA) - Biomembranes*, vol. 1768, no. 3, pp. 609–619, 2007.

[149] M. R. Yeaman, A. J. Shen, and Center LABRIAH-UM, "Antimicrobial peptides and derived metapeptides," 2017, https://www.google.com/patents/US9133257.

[150] N. Y. Yount and M. Yeaman, "Antimicrobial kinocidin compositions and methods of use," 2016, Google Patents, https://www.google.se/patents/US9428566.

[151] N. Y. Yount and M. R. Yeaman, "Emerging themes and therapeutic prospects for anti-infective peptides," *Annual Review of Pharmacology and Toxicology*, vol. 52, no. 1, pp. 337–360, 2012.

[152] R. E. W. Hancock, E. F. Haney, and E. E. Gill, "The immunology of host defence peptides: beyond antimicrobial activity," *Nature Reviews Immunology*, vol. 16, no. 5, pp. 321–334, 2016.

[153] S. Chaili, S. Filler, N. Yount et al., "SSD1 modulates pathways of cell response enabling *Candida albicans* resistance to host defense peptides," in *53rd Interscience Conference on Antimicrobial Agents & Chemotherapy*, Denver, CO, USA, 2013.

[154] C. Park and D. G. Lee, "Melittin induces apoptotic features in *Candida albicans*," *Biochemical and Biophysical Research Communications*, vol. 394, no. 1, pp. 170–172, 2010.

[155] E. Leiter, H. Szappanos, C. Oberparleiter et al., "Antifungal protein PAF severely affects the integrity of the plasma membrane of *Aspergillus nidulans* and induces an apoptosis-like phenotype," *Antimicrobial Agents and Chemotherapy*, vol. 49, no. 6, pp. 2445–2453, 2005.

[156] G. Qi, F. Zhu, P. Du et al., "Lipopeptide induces apoptosis in fungal cells by a mitochondria-dependent pathway," *Peptides*, vol. 31, no. 11, pp. 1978–1986, 2010.

[157] A. I. Pozniakovsky, D. A. Knorre, O. V. Markova, A. A. Hyman, V. P. Skulachev, and F. F. Severin, "Role of mitochondria in the pheromone- and amiodarone-induced programmed death of yeast," *Journal of Cell Biology*, vol. 168, no. 2, pp. 257–269, 2005.

[158] B. Hwang, J.-S. Hwang, J. Lee, and D. G. Lee, "The antimicrobial peptide, psacotheasin induces reactive oxygen species and triggers apoptosis in *Candida albicans*," *Biochemical and Biophysical Research Communications*, vol. 405, no. 2, pp. 267–271, 2011.

[159] R. Klassen and F. Meinhardt, "Induction of DNA damage and apoptosis in *Saccharomyces cerevisiae* by a yeast killer toxin," *Cellular Microbiology*, vol. 7, no. 3, pp. 393–401, 2005.

[160] K. De Brucker, B. P. A. Cammue, and K. Thevissen, "Apoptosis-inducing antifungal peptides and proteins," *Biochemical Society Transactions*, vol. 39, no. 5, pp. 1527–1532, 2011.

[161] A. Matejuk, Q. Leng, M. D. Begum et al., "Peptide-based antifungal therapies against emerging infections," *Drugs of the Future*, vol. 35, no. 3, p. 197, 2010.

[162] S.-J. Kang, S. J. Park, T. Mishig-Ochir, and B.-J. Lee, "Antimicrobial peptides: therapeutic potentials," *Expert Review of Anti-Infective Therapy*, vol. 12, no. 12, pp. 1477–1486, 2014.

[163] M. Mahlapuu, J. Håkansson, L. Ringstad, and C. Björn, "Antimicrobial peptides: an emerging category of therapeutic agents," *Frontiers in Cellular and Infection Microbiology*, vol. 6, p. 194, 2016.

[164] P. M. Tavares, K. Thevissen, B. P. A. Cammue et al., "In vitro activity of the antifungal plant defensin RsAFP2 against *Candida* isolates and its in vivo efficacy in prophylactic murine models of candidiasis," *Antimicrobial Agents and Chemotherapy*, vol. 52, no. 12, pp. 4522–4525, 2008.

[165] Z. Palicz, T. Gáll, É. Leiter et al., "Application of a low molecular weight antifungal protein from *Penicillium chrysogenum* (PAF) to treat pulmonary aspergillosis in mice," *Emerging Microbes & Infections*, vol. 5, no. 11, article e114, 2016.

[166] M. R. Yeaman, D. Cheng, B. Desai et al., "Susceptibility to thrombin-induced platelet microbicidal protein is associated with increased fluconazole efficacy against experimental endocarditis due to *Candida albicans*," *Antimicrobial Agents and Chemotherapy*, vol. 48, no. 8, pp. 3051–3056, 2004.

[167] T. L. Cools, C. Struyfs, J. W. Drijfhout et al., "A linear 19-mer plant defensin-derived peptide acts synergistically with caspofungin against *Candida albicans* biofilms," *Frontiers in Microbiology*, vol. 8, p. 2051, 2017.

[168] C. D. Fjell, J. A. Hiss, R. E. W. Hancock, and G. Schneider, "Designing antimicrobial peptides: form follows function," *Nature Reviews Drug Discovery*, vol. 11, no. 1, pp. 37–51, 2011.

[169] R. E. W. Hancock and H.-G. Sahl, "Antimicrobial and host-defense peptides as new anti-infective therapeutic strategies," *Nature Biotechnology*, vol. 24, no. 12, pp. 1551–1557, 2006.

[170] N. Y. Yount and M. R. Yeaman, "Structural congruence among membrane-active host defense polypeptides of diverse phylogeny," *Biochimica et Biophysica Acta (BBA) - Biomembranes*, vol. 1758, no. 9, pp. 1373–1386, 2006.

[171] J. Aarbiou, G. S. Tjabringa, R. M. Verhoosel et al., "Mechanisms of cell death induced by the neutrophil antimicrobial peptides α-defensins and LL-37," *Inflammation Research*, vol. 55, no. 3, pp. 119–127, 2006.

[172] S. Zhu, S. Peigneur, B. Gao, Y. Umetsu, S. Ohki, and J. Tytgat, "Experimental conversion of a defensin into a neurotoxin: implications for origin of toxic function," *Molecular Biology and Evolution*, vol. 31, no. 3, pp. 546–559, 2014.

[173] K. Vriens, S. Peigneur, B. De Coninck, J. Tytgat, B. P. A. Cammue, and K. Thevissen, "The antifungal plant defensin AtPDF2.3 from *Arabidopsis thaliana* blocks potassium channels," *Scientific Reports*, vol. 6, no. 1, article 32121, 2016.

[174] X. S. Li, M. S. Reddy, D. Baev, and M. Edgerton, "*Candida albicans* Ssa1/2p is the cell envelope binding protein for human salivary histatin 5," *Journal of Biological Chemistry*, vol. 278, no. 31, pp. 28553–28561, 2003.

[175] K. El-Mounadi, K. T. Islam, P. Hernández-Ortiz, N. D. Read, and D. M. Shah, "Antifungal mechanisms of a plant defensin MtDef4 are not conserved between the ascomycete fungi Neurospora crassa and Fusarium graminearum," *Molecular Microbiology*, vol. 100, no. 3, pp. 542–559, 2016.

[176] M. R. Yeaman, N. Y. Yount, and E. P. Brass, "Peptides and methods for inducing cell death," Google Patents, 2013, Available from: https://www.google.se/patents/US8492333.

[177] M. R. Yeaman, N. Y. Yount, and E. P. Brass, "Peptides and methods for inducing cell death," US9562083 B2, 2017, http://www.google.se/patents/US9562083.

[178] N. Y. Yount and M. R. Yeaman, "Immunocontinuum: perspectives in antimicrobial peptide mechanisms of action and resistance," *Protein & Peptide Letters*, vol. 12, no. 1, pp. 49–67, 2005.

[179] N. Y. Yount, S. E. Cohen, D. Kupferwasser et al., "Context mediates antimicrobial efficacy of kinocidin congener peptide RP-1," *PLoS One*, vol. 6, no. 11, article e26727, 2011.

[180] R. Lakshminarayanan, S. Liu, J. Li et al., "Synthetic multivalent antifungal peptides effective against fungi," *PLoS One*, vol. 9, no. 2, article e87730, 2014.

[181] A. Falanga, L. Lombardi, G. Franci et al., "Marine antimicrobial peptides: nature provides templates for the design of novel compounds against pathogenic bacteria," *International Journal of Molecular Sciences*, vol. 17, no. 12, 2016.

[182] H.-K. Kang, C. Kim, C. H. Seo, and Y. Park, "The therapeutic applications of antimicrobial peptides (AMPs): a patent review," *Journal of Microbiology*, vol. 55, no. 1, pp. 1–12, 2017.

[183] O. Nešuta, M. Budešínský, R. Hadravová, L. Monincová, J. Humpolicková, and V. Cerovský, "How proteases from *Enterococcus faecalis* contribute to its resistance to short α-helical antimicrobial peptides," *Pathogens and Disease*, vol. 75, no. 7, 2017.

[184] P. V. Panteleev, S. V. Balandin, V. T. Ivanov, and T. V. Ovchinnikova, "A therapeutic potential of animal β-hairpin antimicrobial peptides," *Current Medicinal Chemistry*, vol. 24, no. 17, pp. 1724–1746, 2017.

[185] J. Wiesner and A. Vilcinskas, "Antimicrobial peptides: the ancient arm of the human immune system," *Virulence*, vol. 1, no. 5, pp. 440–464, 2014.

[186] Y. Q. Tang, J. Yuan, G. Osapay et al., "A cyclic antimicrobial peptide produced in primate leukocytes by the ligation of two truncated α-defensins," *Science*, vol. 286, no. 5439, pp. 498–502, 1999.

[187] S. D. Ramalho, M. E. F. Pinto, D. Ferreira, and V. S. Bolzani, "Biologically active orbitides from the Euphorbiaceae family," *Planta Medica*, 2017.

[188] C. Steiniger, S. Hoffmann, A. Mainz et al., "Harnessing fungal nonribosomal cyclodepsipeptide synthetases for mechanistic insights and tailored engineering," *Chemical Science*, vol. 8, no. 11, pp. 7834–7843, 2017.

[189] K. D. James, C. P. Laudeman, N. B. Malkar, R. Krishnan, and K. Polowy, "Structure-activity relationships of a series of echinocandins and the discovery of CD101, a highly stable and soluble echinocandin with distinctive pharmacokinetic properties," *Antimicrobial Agents and Chemotherapy*, vol. 61, no. 2, pp. e01541–e01516, 2016.

[190] T. Thery, Y. O'Callaghan, N. O'Brien, and E. K. Arendt, "Optimisation of the antifungal potency of the amidated peptide H-Orn-Orn-Trp-Trp-NH2 against food contaminants," *International Journal of Food Microbiology*, vol. 265, pp. 40–48, 2018.

[191] N. Y. Yount, K. D. Gank, Y. Q. Xiong et al., "Platelet microbicidal protein 1: structural themes of a multifunctional antimicrobial peptide," *Antimicrobial Agents and Chemotherapy*, vol. 48, no. 11, pp. 4395–4404, 2004.

[192] M. R. Yeaman, N. Y. Yount, J. E. Edwards Jr., and E. P. Brass, "Multifunctional context-activated protides and methods of

use," 2013, US8592375 B2, http://www.google.ch/patents/US8592375.

[193] L. R. S. Gazzaneo, V. Pandolfi, A. L. S. de Jesus, S. Crovella, A. M. Benko-Iseppon, and A. C. de Freitas, "Heterologous expression systems for plant defensin expression: examples of success and pitfalls," *Current Protein & Peptide Science*, vol. 18, no. 4, pp. 391–399, 2017.

[194] K. Vriens, B. P. A. Cammue, and K. Thevissen, "Antifungal plant defensins: mechanisms of action and production," *Molecules*, vol. 19, no. 8, pp. 12280–12303, 2014.

[195] C. Sonderegger, L. Galgóczy, S. Garrigues et al., "A *Penicillium chrysogenum*-based expression system for the production of small, cysteine-rich antifungal proteins for structural and functional analyses," *Microbial Cell Factories*, vol. 15, no. 1, p. 192, 2016.

[196] P. H. Mygind, R. L. Fischer, K. M. Schnorr et al., "Plectasin is a peptide antibiotic with therapeutic potential from a saprophytic fungus," *Nature*, vol. 437, no. 7061, pp. 975–980, 2005.

[197] S. S. Usmani, G. Bedi, J. S. Samuel et al., "THPdb: database of FDA-approved peptide and protein therapeutics," *PLoS One*, vol. 12, no. 7, article e0181748, 2017.

Hindawi
Oxidative Medicine and Cellular Longevity
Volume 2018, Article ID 1324739, 8 pages
https://doi.org/10.1155/2018/1324739

Research Article

An *In Vivo* Zebrafish Model for Interrogating ROS-Mediated Pancreatic β-Cell Injury, Response, and Prevention

Abhishek A. Kulkarni,[1,2] **Abass M. Conteh**,[1,2] **Cody A. Sorrell**,[3] **Anjali Mirmira**,[3] **Sarah A. Tersey**,[1,3] **Raghavendra G. Mirmira**,[1,2,3,4] **Amelia K. Linnemann**,[1,2,3,4] **and Ryan M. Anderson**[1,3,4]

[1]*Center for Diabetes and Metabolic Disease, Indiana University School of Medicine, Indianapolis, IN 46202, USA*
[2]*Department of Biochemistry and Molecular Biology, Indiana University School of Medicine, Indianapolis, IN 46202, USA*
[3]*Department of Pediatrics, Indiana University School of Medicine, Indianapolis, IN 46202, USA*
[4]*Department of Cellular and Integrative Physiology, Indiana University School of Medicine, Indianapolis, IN 46202, USA*

Correspondence should be addressed to Amelia K. Linnemann; aklinnem@iu.edu and Ryan M. Anderson; ryanande@iu.edu

Received 1 November 2017; Accepted 23 January 2018; Published 28 March 2018

Academic Editor: Paula Ludovico

It is well known that a chronic state of elevated reactive oxygen species (ROS) in pancreatic β-cells impairs their ability to release insulin in response to elevated plasma glucose. Moreover, at its extreme, unmitigated ROS drives regulated cell death. This dysfunctional state of ROS buildup can result both from genetic predisposition and environmental factors such as obesity and overnutrition. Importantly, excessive ROS buildup may underlie metabolic pathologies such as type 2 diabetes mellitus. The ability to monitor ROS dynamics in β-cells in situ and to manipulate it via genetic, pharmacological, and environmental means would accelerate the development of novel therapeutics that could abate this pathology. Currently, there is a lack of models with these attributes that are available to the field. In this study, we use a zebrafish model to demonstrate that ROS can be generated in a β-cell-specific manner using a hybrid chemical genetic approach. Using a transgenic nitroreductase-expressing zebrafish line, *Tg(ins:Flag-NTR)*^{s950}, treated with the prodrug metronidazole (MTZ), we found that ROS is rapidly and explicitly generated in β-cells. Furthermore, the level of ROS generated was proportional to the dosage of prodrug added to the system. At high doses of MTZ, caspase 3 was rapidly cleaved, β-cells underwent regulated cell death, and macrophages were recruited to the islet to phagocytose the debris. Based on our findings, we propose a model for the mechanism of NTR/MTZ action in transgenic eukaryotic cells and demonstrate the robust utility of this system to model ROS-related disease pathology.

1. Introduction

The generation of reactive oxygen species (ROS)—including peroxides, superoxides, and oxygen radicals—in excess of ROS mitigation mechanisms, results in cellular dysfunction and triggers regulated cell death under extreme circumstances [1]. Cells of metabolically active tissues are predisposed to high levels of ROS production, and thus, metabolic diseases such as type 2 diabetes mellitus (T2DM) are often associated with excessive ROS generation and resulting oxidative stress [2]. T2DM is characterized by chronic hyperglycemia resulting from the dysfunction of insulin-secreting pancreatic β-cells in the setting of overnutrition and obesity [3]. This dysfunction may be driven in part by the generation of excessive ROS, which likely results from the low endogenous levels of antioxidant enzymes in β-cells [4]. ROS diminishes the expression of insulin in β-cells, impairs glucose-stimulated insulin secretion, and promotes β-cell apoptosis [5, 6]. The availability of a vertebrate model to study factors that regulate ROS dynamics in the islet in situ would accelerate the discovery and testing of novel therapeutics for a variety of metabolic diseases, including T2DM. The zebrafish, *Danio rerio*, is a robust model to interrogate the pathogenesis of metabolic disease and the efficacy of experimental therapeutics [7, 8].

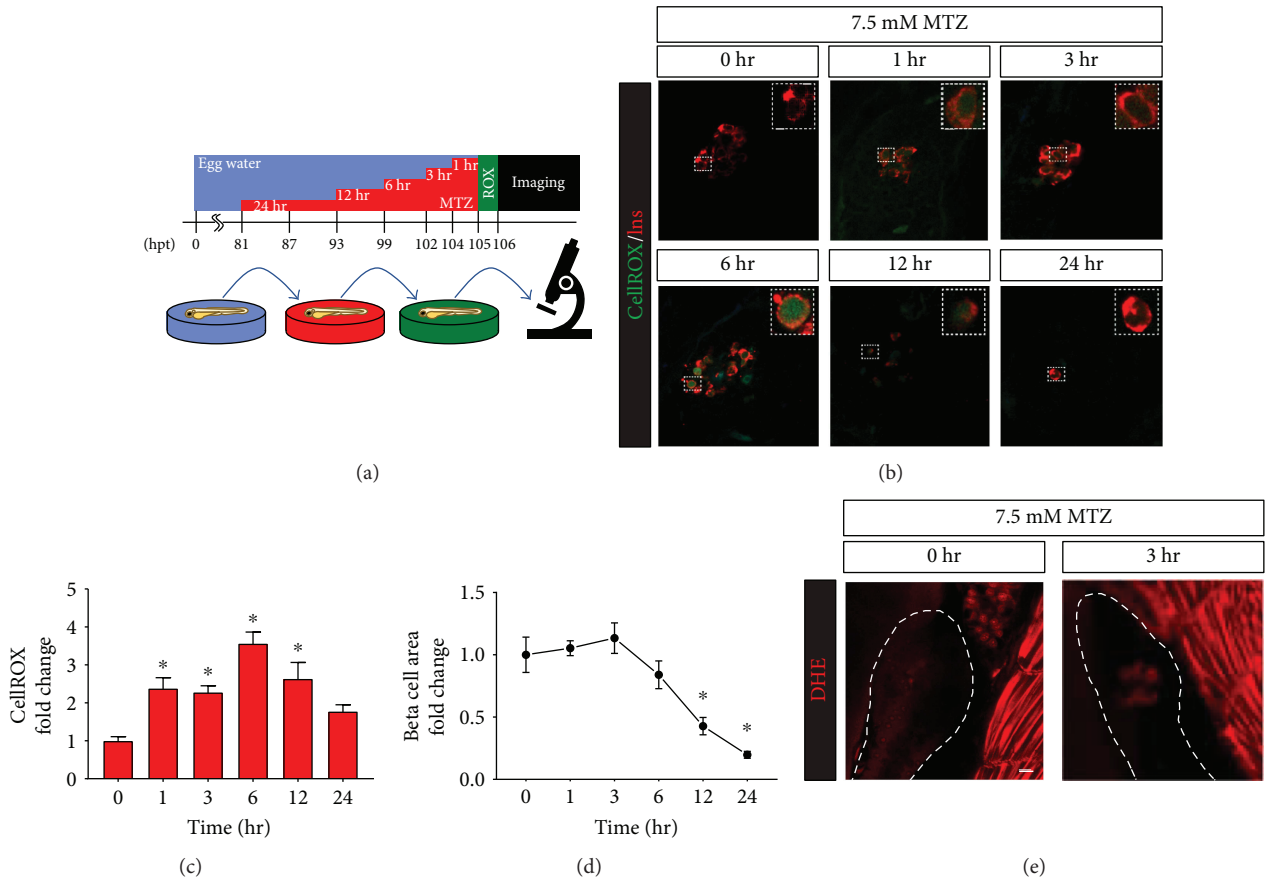

FIGURE 1: Time-dependent metronidazole induction of β-cell-specific ROS. (a) Schematic of MTZ treatments and imaging. Zebrafish (NTR$^+$) larvae were treated with MTZ or vehicle for 0, 1, 3, 6, 12, or 24 hours with a "staggered start" such that all treatments were completed simultaneously; larvae were then incubated with CellROX green stain at 105 hpf and fixed/analyzed at 106 hpf. (b) Representative immunofluorescence images of zebrafish pancreatic islets stained with insulin antibody and CellROX green after 7.5 mM MTZ treatments. Magnified insets (bounded by dashed boxes) highlight the dose-dependent increase in CellROX green signal in β-cells. (c) Quantification of CellROX green intensity in insulin-positive β-cells showing a significant increase in ROS generation after 1, 3, 6, and 12 hours of MTZ treatment as compared to vehicle-treated controls ($n = 12$ for each condition). (d) MTZ treatment caused a significant decrease in β-cell area after 12 or 24 hours of treatment as compared to untreated controls. (e) Representative immunofluorescence images of zebrafish pancreatic islets treated for 3 hours with 0 or 7.5 mM MTZ and stained with 5 μM DHE. Dotted lines demarcate the boundaries of the pancreas. Graphed data are presented as mean ± SEM ($^*p < 0.05$). Statistical significance was determined by one-way ANOVA followed by post hoc Holm-Sidak test. Scale bar indicates 10 μm.

The oxygen-insensitive NAD(P)H nitroreductase (NTR, *NfsB*) enzyme, cloned from *E. coli*, has been harnessed to drive tissue-specific cell ablation in various transgenic zebrafish models. When NTR-expressing transgenic zebrafish lines, such as *Tg(ins:Flag-NTR)^{s950}*, are treated with the antibiotic metronidazole (MTZ), this prodrug is metabolized into cytotoxins that are retained by NTR-expressing β-cells, rapidly inducing their death [9]. While the precise mechanisms of MTZ-induced cell toxicity have not been characterized in NTR-expressing transgenic lines, existing research provides some insight: nitroreduction of MTZ may produce cytotoxic nitroradical metabolites, which can cross-link DNA [10–12]. In this study, we use transgenic NTR$^+$ zebrafish to demonstrate their suitability for modeling ROS generation, cellular responses to ROS, and pharmaceutical interventions *in vivo*. Together, our findings suggest that zebrafish are a superb model for ROS-related disorders.

2. Results

2.1. Metronidazole Induces β-Cell ROS Generation in an NTR- and Dose-Dependent Manner. The nitroreductase-metronidazole (NTR-MTZ) system has been widely implemented as a tool to efficiently ablate cells in a tissue-specific and temporally controllable manner [13]. However, the molecular mechanisms driving its induction of regulated cell death are not fully understood. To determine if ROS are generated in MTZ-treated NTR-expressing cells, we used *Tg(ins:Flag-NTR)^{s950}* transgenic zebrafish that express insulin promoter-driven NTR in the pancreatic β-cells. Heterozygous transgenic larvae were immersed in a solution of MTZ for 0, 1, 3, 6, 12, or 24 hr, then stained with CellROX green to indicate ROS (Figure 1(a)). Incubation start times were staggered such that all larvae were at 106 hours postfertilization (hpf) at analysis. We began treatments with 7.5 mM

MTZ, a dose which is effective to ablate β-cells after 24 hr exposure [14]. With 1 hour of treatment, we observed ROS staining specifically in β-cell nuclei, whereas adjacent islet cells were not stained (Figure 1(b)). With longer treatments, ROS levels increased by almost 4-fold relative to untreated controls, reaching a peak intensity with 6 hours of treatment, then showing less increase with 12 or 24 hours of treatment (Figure 1(c)). We attribute this diminished staining to the attrition of β-cells via regulated cell death mechanisms and their clearance by phagocytes (Figure 1(d)), as well as the neogenesis of β-cells that have not yet generated detectable ROS. Importantly, neither MTZ nor the transgene was toxic alone; ROS generation in β-cells required both components ([9], data not shown). To further confirm that the CellROX green staining that we observed was truly representative of MTZ-induced cellular ROS and not artefactual (i.e., simply due to an interaction of CellROX green with the reduced nitroradical form of metronidazole), we next incubated MTZ-treated transgenic larvae in 5 μM dihydroethidium (DHE). Upon its oxidation to 2OH-ethidium by superoxide, this cell-permeant dye is excited at 405 nm and emits a bright red fluorescence at 570 nm [15]. In 106 hpf *Tg(ins:Flag-NTR)*^{s950} larvae that were not treated with MTZ, we detected no specific pancreatic fluorescence in any sample (Figure 1(e); $n = 13$). In contrast, in transgenic larvae treated with 7.5 mM MTZ for 3 hours, we observed strong fluorescence in β-cells in every case (Figure 1(e); $n = 14$). These data indicate that superoxide is generated in transgenic β-cells in response to MTZ.

Next, we hypothesized that the level of ROS generated in the NTR$^+$ β-cells would be directly dependent on the concentration of MTZ present. To investigate if there is a dose-dependent relationship, we treated embryos with both low (2.5 mM) and high (7.5 mM) concentrations of MTZ using the same experimental paradigm indicated in Figure 1(a). As expected, there was no ROS generation in the untreated control β-cells (Figure 2(a)). With 1 hour of treatment, the 2.5 mM dose did not show significant ROS generation, but 7.5 mM MTZ induced a more than 4-fold increase in ROS levels as compared to untreated controls (Figures 2(b)–2(d)). With 6 hours of treatment, the 2.5 mM treatment did not result in significant ROS generation, though it trended upward, while the 7.5 mM dose caused a nearly 6-fold rise in ROS levels relative to untreated controls. Consistent with our previous observations, the measured ROS levels were no different than baseline with 24-hour treatment of either the 2.5 mM or 7.5 mM MTZ. Despite the lower levels of ROS observed with 2.5 mM treatment, there was a dramatic reduction in the number of β-cells at the 24-hour time point (Figure 1(b)). Thus, even though induced ROS levels are lower with the 2.5 mM dose, this dose is sufficient to induce cell death over a 24-hour period.

2.2. MTZ-Induced ROS Generation Leads to Immune Cell Recruitment and β-Cell Apoptosis. Many studies have correlated the production of ROS with the induction of apoptotic cell death [15–17]. Therefore, to determine whether the generation of ROS is correlated with the induction of β-cell apoptosis in this system, we analyzed cleaved caspase 3 (Casp3*) in islet β-cells after following the same MTZ treatment paradigm shown in Figure 1(a). Casp3* is the active form of caspase 3 and an indicator of the activated apoptotic pathway. We did not detect significant Casp3* staining in the untreated controls or with a 1-hour MTZ treatment (Figures 3(a)–3(d)). However, with a 6-hour treatment, Casp3* was significantly increased with 7.5 mM MTZ, but not 2.5 mM relative to untreated controls, following a pattern similar to ROS generation (Figures 2(d) and 3(d)). As before, with 24 hours of treatment, almost all β-cells were ablated by both concentrations of MTZ (Figures 3(b) and 3(c)).

It has been demonstrated that ROS-injured β-cells release factors that attract immune cells [18]. Consistent with this finding, we show that generation of ROS in β-cells is coincident with the infiltration of *Tg(mpeg1:GFP)* + macrophages into the islet; this is first apparent with a 3-hour treatment, and peak infiltration is seen with 6 hours of MTZ treatment—when the ROS staining was also measured at its highest levels. Additionally, engulfment of β-cells by macrophages is first observed with a 12-hour MTZ treatment, a time point that is coincident with the observed drop in the β-cell area (Figures 1(d) and 3(e)).

2.3. Antioxidants Protect β-Cells from MTZ-Induced ROS Generation. We hypothesized that the generation of ROS in β-cells could be mitigated in our zebrafish model by the addition of small molecule antioxidants to the water. To test this hypothesis, we used the common antioxidant *N*-acetyl-L-cysteine (NAC). We treated zebrafish larvae with an intermediate dose of 5 mM MTZ with the goal of using a dose that was strong enough to induce a rapid ROS response, but that would not overwhelm other treatments. MTZ treatments were supplemented with 100 μM NAC and ROS intensity was measured at multiple time points (Figure 4). With either a 1- or 6-hour treatment of MTZ, NAC significantly reduced the levels of ROS staining in β-cells. Consistent with all other treatments, there was no significant difference with a 24-hour treatment, which again could be attributed to the ablation of nearly all β-cells in the presence of MTZ treatment alone. Together, we conclude that MTZ drives the production of ROS in β-cells in the presence of NTR. Additionally, a known antioxidant was effective at mitigating this effect, suggesting that other novel compounds might be uncovered through screening approaches in this zebrafish system.

3. Discussion

3.1. Mechanism of Cell Ablation by MTZ-NTR. NTR (*NfsB*) is a type 1 oxygen-insensitive nitroreductase that catalyzes the full reduction of nitroaromatic compounds under anaerobic conditions [19]. In anaerobes, MTZ serves as a prodrug that is metabolized by NTR to generate cytotoxic derivatives capable of blocking DNA synthesis and inducing DNA damage [20]. In our study, we found that MTZ also induces ROS generation in the presence of NTR. This is consistent with the hypothesis that under aerobic conditions, as when expressed in mammalian cells, NTR might generate superoxide and derivative reactive oxygen species, potentially through a type 2-like "futile reduction cycle" (Figure 5) [21].

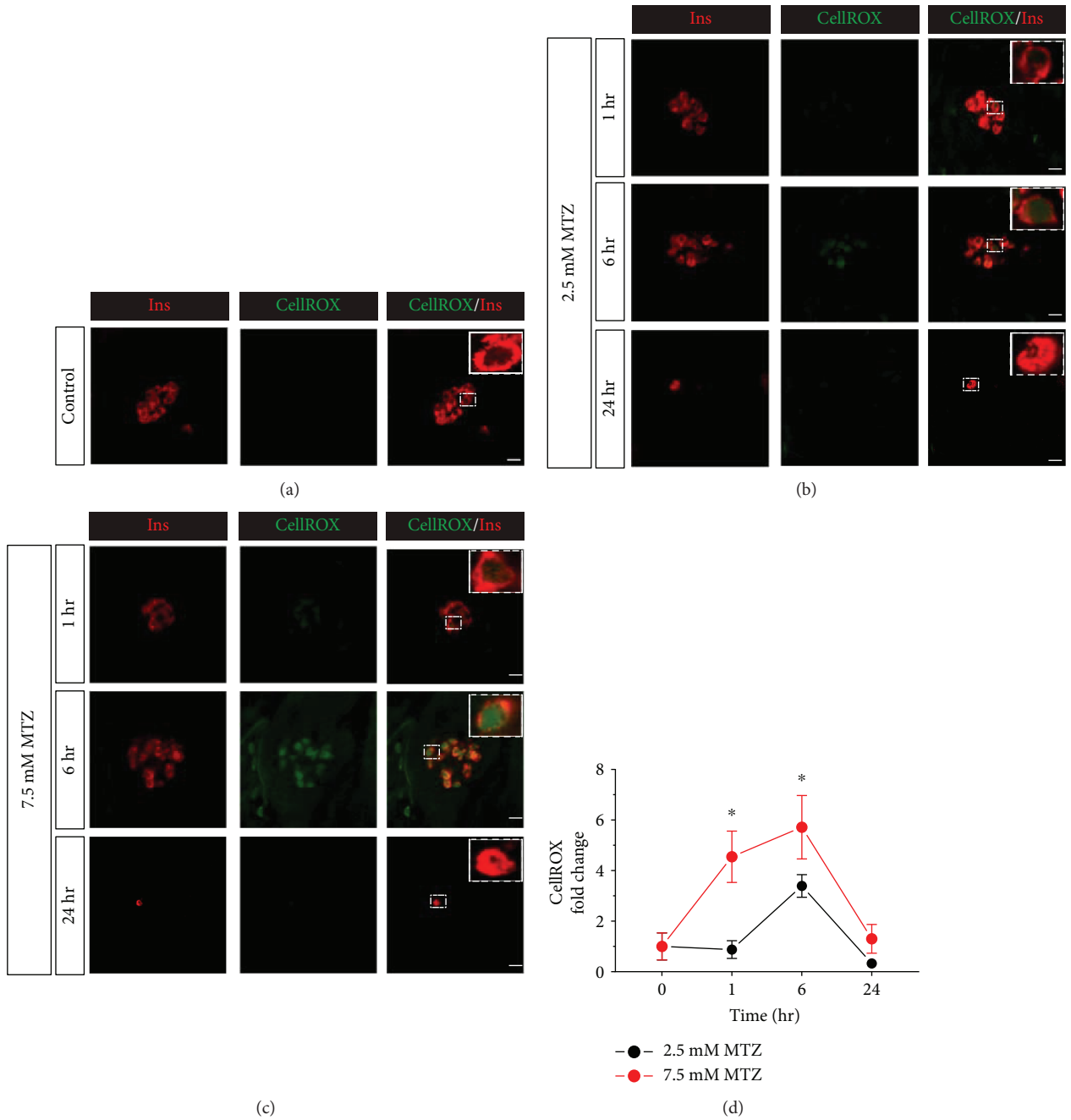

Figure 2: Metronidazole induces ROS generation in a dose-dependent manner. (a) Representative image of vehicle-treated zebrafish islets ($n = 12$) at 106 hpf. (b) Representative image of islets of zebrafish (NTR^+) larvae ($n = 12$ per condition) treated with 2.5 mM and 7.5 mM MTZ at different time points. (c) Quantification of CellROX intensity shows a significant increase after 1 or 6 hours of treatment in the β-cells of 7.5 mM MTZ-treated embryos, as compared to untreated controls. Data are presented as mean ± SEM ($^*p < 0.05$). Statistical significance was determined by one-way ANOVA followed by post hoc Holm-Sidak test. Scale bar indicates 10 μm.

3.2. Utility of MTZ-NTR Zebrafish System as a Disease Model beyond Just Cell Ablation. As a β-cell ablation system, the relevance of Ins:NTR/MTZ to type 1 diabetes is evident. However, chronic ROS production and associated β-cell dysfunction are also critical to the pathology of type 2 diabetes even before β-cell mass is diminished. Intriguingly, because the generation of ROS by NTR in this model is dependent on the dose of MTZ treatment, this provides a compelling opportunity to manipulate ROS under varied contexts. For instance, many other disease conditions like type 2 diabetes, atherosclerosis, diabetic neuropathy, and cancer arise as a result of chronic ROS generation in specific tissues [22]. To model such cases, low concentrations of MTZ can be used for generating persistent ROS conditions and studying the effects. Future studies will determine whether lower levels of ROS can be induced by MTZ treatments

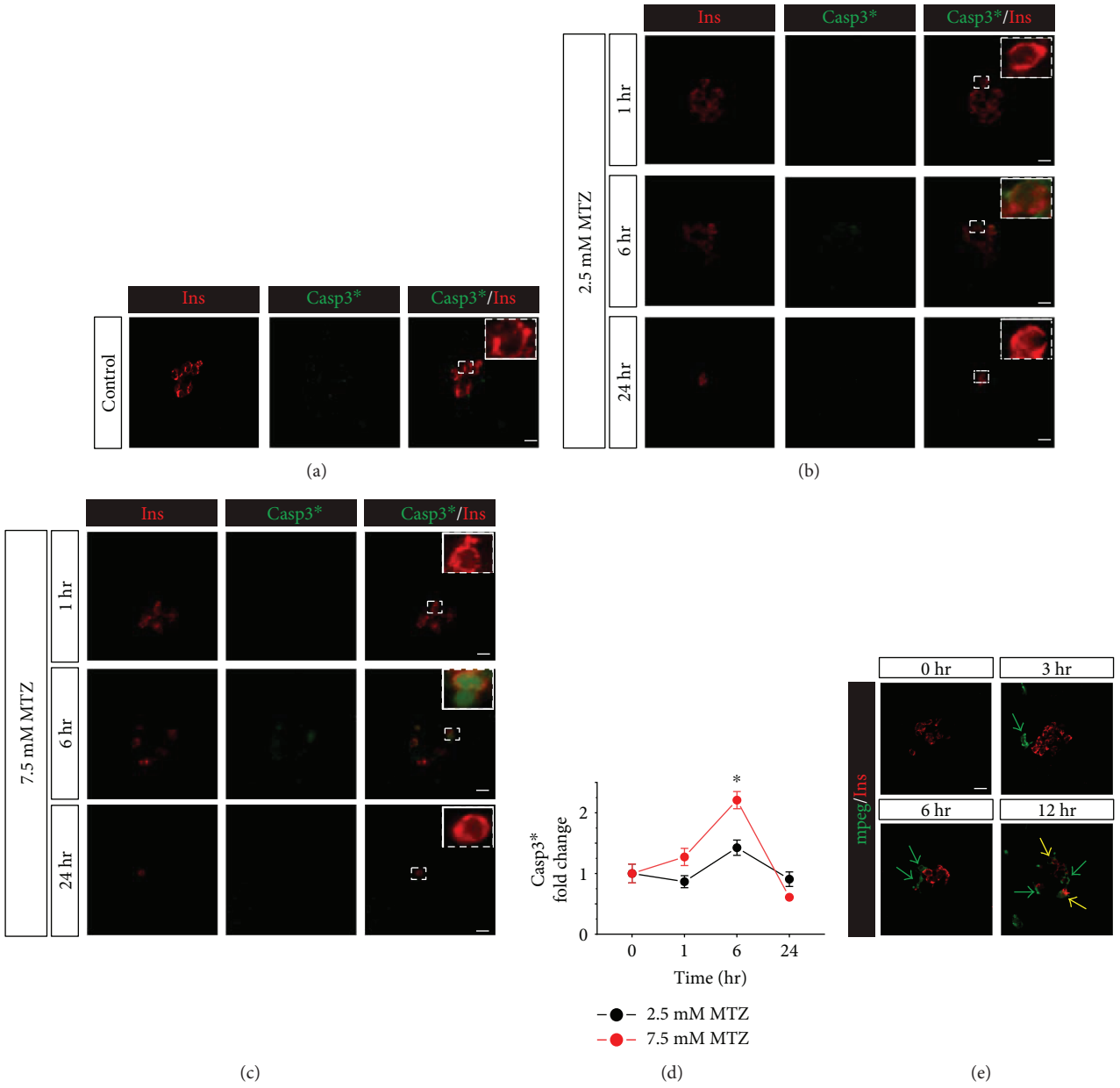

FIGURE 3: Metronidazole induces apoptosis signaling in β-cells. (a) Representative image of vehicle-treated zebrafish islets ($n = 12$) after fixing at 106 hpf. (b) Representative image of islets of zebrafish (NTR$^+$) larvae ($n = 12$ per condition) treated with 2.5 mM or 7.5 mM MTZ at different time points and immune-stained for insulin and cleaved caspase 3 (Casp3*). (c) Quantification of Casp3* intensity shows a significant increase after 6 hours of treatment in the β-cells of 7.5 mM MTZ-treated embryos compared to vehicle. (d) Representative immunofluorescence images of zebrafish (*mpeg*+) islets ($N = 6$/condition) treated with 7.5 mM MTZ showing macrophage invasion into islets (green arrows) and their engulfment of β-cells (yellow arrows). Data are presented as mean ± SEM ($^*p < 0.05$). Statistical significance was determined by one-way ANOVA followed by post hoc Holm-Sidak test. Scale bar indicates 10 μm.

that are sufficient to impair β-cell function, but not to induce cell death.

Zebrafish proves to be an outstanding model organism for studying ROS generation and ROS-related pathologies. The MTZ-NTR system seems to work exceptionally well for cell-specific ablation. However, with the added possibility of precisely modulating the ROS generation using MTZ dosing and antioxidants like NAC, this makes zebrafish a particularly flexible model.

4. Methods

4.1. Zebrafish Maintenance and Embryo Collection. Wild-type (AB), *Tg(ins:Flag-NTR)*^{s950} (ZDB-ALT-130930-5) [23], and *Tg(mpeg1:GFP)* (ZDB-ALT-120117-1) zebrafish were maintained at 28.5°C in a recirculating aquaculture system enclosed in a cabinet and subjected to a 14-/10-hour light/dark cycle in accordance with institutional policies under IACUC oversight. Heterozygous outcrossed embryos

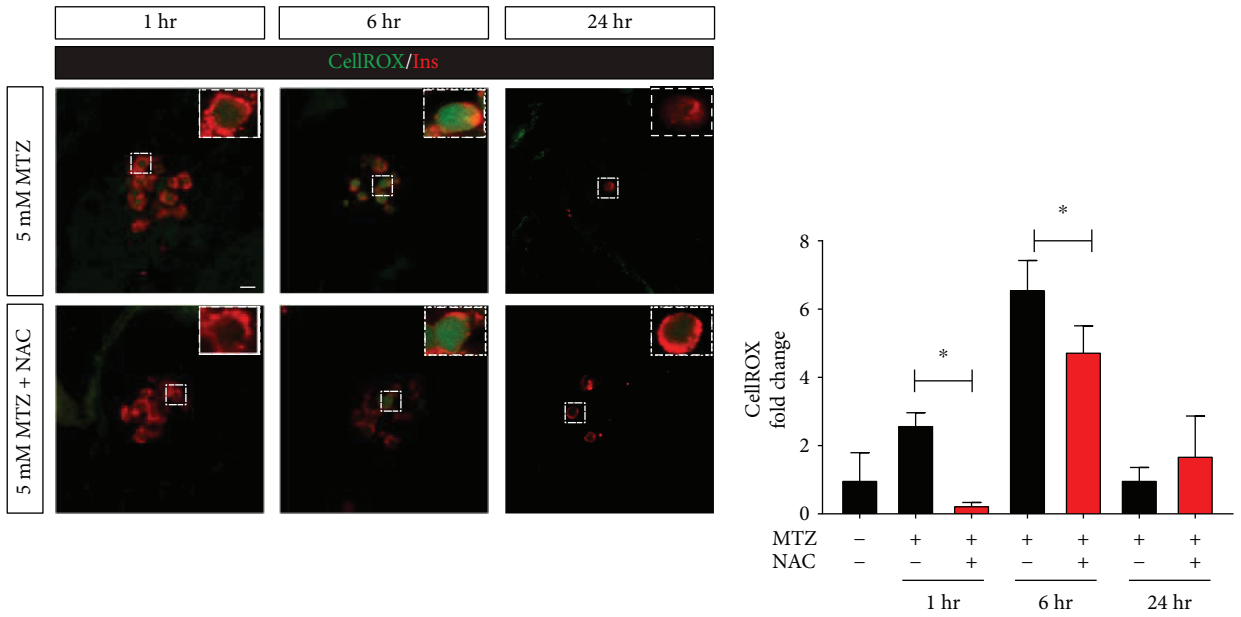

Figure 4: Antioxidant treatment protects from metronidazole-induced ROS generation in β-cells. Zebrafish larvae ($n = 12$ per condition) were treated with 5 mM metronidazole ± *N*-acetyl-L-cysteine (NAC) for 1, 6, or 24 hours followed by an assessment of ROS using CellROX green stain. (a) Representative images of islets of 106 hpf zebrafish (NTR^+) embryos treated with 5 mM MTZ ± NAC at different time points. (b) Quantification of CellROX green intensity shows NAC-mediated protection from MTZ-induced ROS in β-cells after 1 or 6 hours of treatment. Data are presented as mean ± SEM ($^*p < 0.05$). Statistical significance was determined by Student's *t*-test. Scale bar indicates 10 μm.

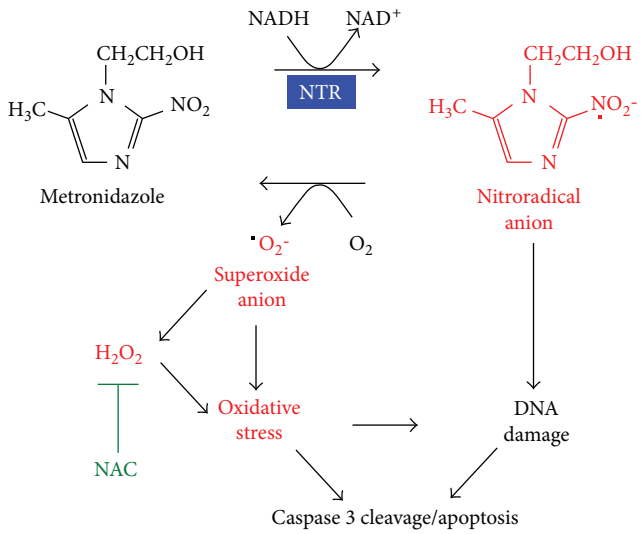

Figure 5: Proposed mechanism of metronidazole-nitroreductase-mediated cell ablation. In the aerobic setting of NTR-expressing eukaryotic cells, we propose that MTZ is reduced to a nitroradical anion by electron transfer from NADH, in a type 2-like mechanism. This radical may be cytotoxic and directly induces DNA damage and apoptosis. Alternately, this radical may regenerate back to metronidazole by electron transfer to O_2, concurrently forming superoxide anion and ROS derivatives. This, in turn, drives increased cellular-oxidative stress and triggering of regulated cell death.

bearing the *Tg(ins:Flag-NTR)*^{s950} allele were collected at spawning and maintained in a 28.5°C incubator in egg water-filled petri dishes. Transgenic zebrafish larvae were genotyped by epifluorescence at 80 hpf using a Leica M205FA dissecting microscope.

4.2. Chemical Treatments. 1-Phenyl-2-thiourea (PTU; Acros #207250250) supplementation at 0.003% was used to prevent pigmentation in all embryos after gastrulation stages. Metronidazole (Sigma #095K093) solutions of 2.5 mM, 5 mM, and 7.5 mM were prepared in egg water (0.1% instant ocean salt, 0.0075% calcium sulfate) that was supplemented with PTU. For antioxidant treatments, egg water, either with or without 5 mM MTZ, was supplemented with 100 μM *N*-acetyl L-cysteine (NAC; Acros #160280250), which was diluted from a 100 mM stock prepared in ddH_2O. Control treatments for MTZ and NAC used egg water alone.

4.3. ROS Staining, Immunofluorescence, and Image Collection. Cellular ROS was detected using a CellROX green reagent (Invitrogen #C10444); live larvae were transferred to 1.5 ml microcentrifuge tubes, washed with egg water, then incubated in the dark for 1 hr at 28.5°C with 10 μM CellROX green diluted in egg water. At the conclusion of each experiment, larvae were washed in egg water then fixed with 3% formaldehyde in a PEM buffer (0.21 M PIPES, 1 mM $MgSO_4$, 2 mM EGTA, and pH 7) at 4°C overnight. Fixed larvae were washed with PBS and deyolked, then antibody staining was performed as described [24]. The following concentrations of primary antibodies were used: 1 : 200 guinea

pig anti-insulin (Invitrogen #180067), 1 : 200 rabbit anti-cleaved caspase 3 (Cell Signaling Technologies #9661S), and 1 : 100 mouse anti-glucagon (Sigma #SAB4200685). Primary antibodies were detected with 1 : 500 dilutions of complementary Alexa-conjugated secondary antibodies (Jackson ImmunoResearch). DNA was stained with TO-PRO3 (Thermo Fisher #T3605) diluted 1 : 500. After staining, larvae were mounted on slides in VECTASHIELD (Vector Labs H-1000), and confocal imaging was performed with a Zeiss LSM700 microscope. The confocal stacks of pancreatic islets were analyzed with CellProfiler software [25]. For detection of superoxide in situ in live pancreatic β-cells, heterozygous *Tg(ins:Flag-NTR)*^{s950} larvae were treated with 7.5 mM MTZ for 3 hours then placed in 5 μM dihydroethidium (Thermo Fisher #D1168) + 0.02% DMSO for 30 minutes in dark conditions. Larvae were then paralyzed with 0.01% tricaine (Sigma #A-5040), mounted on glass-bottom petri dishes (Mattek #P35G-0-10-C) in 0.5% low melt agarose (Sigma #A9414), and imaged with a Zeiss LSM700 confocal microscope.

4.4. Statistical Analysis. The data are presented as the means ± standard error of the mean (SEM). The data analyses were performed using the GraphPad Prism 7.1 software package. Significant differences between the mean values were determined using Student's *t*-test, where two means were compared, and one-way analysis of variance (ANOVA) followed by post hoc Holm-Sidak test when more than two means were compared. The differences were considered statistically significant at $p < 0.05$.

Conflicts of Interest

The authors declare that there is no conflict of interests regarding the publication of this paper.

Acknowledgments

This work is supported by March of Dimes research Grant MOD1-FY14-327 (to Ryan M. Anderson); NIH Grant K01 DK102492; startup funds from School of Medicine, Indiana University, and the Herman B Wells Center for Pediatric Research (to Amelia K. Linnemann); and NIH Grant R01 DK105588 (to Raghavendra G. Mirmira). In addition, this study utilized core services provided by Diabetes Research Center Award P30 DK097512 from the National Institutes of Health (to Indiana University).

References

[1] H. Kaneto, N. Katakami, M. Matsuhisa, and T. Matsuoka, "Role of reactive oxygen species in the progression of type 2 diabetes and atherosclerosis," *Mediators of Inflammation*, vol. 2010, Article ID 453892, 11 pages, 2010.

[2] U. C. S. Yadav, V. Rani, G. Deep, R. K. Singh, and K. Palle, "Oxidative stress in metabolic disorders: pathogenesis, prevention, and therapeutics," *Oxidative Medicine and Cellular Longevity*, vol. 2016, Article ID 9137629, 3 pages, 2016.

[3] T. Ogihara and R. G. Mirmira, "An islet in distress: β cell failure in type 2 diabetes," *Journal of Diabetes Investigation*, vol. 1, no. 4, pp. 123–133, 2010.

[4] H. Ha, I.-A. Hwang, J. H. Park, and H. B. Lee, "Role of reactive oxygen species in the pathogenesis of diabetic nephropathy," *Diabetes Research and Clinical Practice*, vol. 82, pp. S42–S45, 2008.

[5] R. P. Robertson and J. S. Harmon, "Pancreatic islet β-cell and oxidative stress: the importance of glutathione peroxidase," *FEBS Letters*, vol. 581, no. 19, pp. 3743–3748, 2007.

[6] N. Hou, S. Torii, N. Saito, M. Hosaka, and T. Takeuchi, "Reactive oxygen species-mediated pancreatic β-cell death is regulated by interactions between stress-activated protein kinases, p38 and c-Jun N-terminal kinase, and mitogen-activated protein kinase phosphatases," *Endocrinology*, vol. 149, no. 4, pp. 1654–1665, 2008.

[7] C. A. MacRae and R. T. Peterson, "Zebrafish as tools for drug discovery," *Reviews Drug Discovery*, vol. 14, no. 10, pp. 721–731, 2015.

[8] T. P. Barros, W. K. Alderton, H. M. Reynolds, A. G. Roach, and S. Berghmans, "Zebrafish: an emerging technology for *in vivo* pharmacological assessment to identify potential safety liabilities in early drug discovery," *British Journal of Pharmacology*, vol. 154, no. 7, pp. 1400–1413, 2008.

[9] S. Curado, R. M. Anderson, B. Jungblut, J. Mumm, E. Schroeter, and D. Y. R. Stainier, "Conditional targeted cell ablation in zebrafish: a new tool for regeneration studies," *Developmental Dynamics*, vol. 236, no. 4, pp. 1025–1035, 2007.

[10] J. R. Mathias, Z. Zhang, M. T. Saxena, and J. S. Mumm, "Enhanced cell-specific ablation in zebrafish using a triple mutant of *Escherichia coli* nitroreductase," *Zebrafish*, vol. 11, no. 2, pp. 85–97, 2014.

[11] R. N. Felmer and J. A. Clark, "The gene suicide system Ntr/CB1954 causes ablation of differentiated 3T3L1 adipocytes by apoptosis," *Biological Research*, vol. 37, no. 3, pp. 449–460, 2004.

[12] R. J. Knox, F. Friedlos, M. Jarman, and J. J. Roberts, "A new cytotoxic, DNA interstrand crosslinking agent, 5-(aziridin-1-yl)-4-hydroxylamino-2-nitrobenzamide, is formed from 5-(aziridin-1-yl)-2,4-dinitrobenzamide (CB 1954) by a nitroreductase enzyme in Walker carcinoma cells," *Biochemical Pharmacology*, vol. 37, no. 24, pp. 4661–4669, 1988.

[13] D. T. White and J. S. Mumm, "The nitroreductase system of inducible targeted ablation facilitates cell-specific regenerative studies in zebrafish," *Methods*, vol. 62, no. 3, pp. 232–240, 2013.

[14] L. Ye, M. A. Robertson, T. L. Mastracci, and R. M. Anderson, "An insulin signaling feedback loop regulates pancreas progenitor cell differentiation during islet development and regeneration," *Developmental Biology*, vol. 409, no. 2, pp. 354–369, 2016.

[15] R. R. Nazarewicz, A. Bikineyeva, and S. I. Dikalov, "Rapid and specific measurements of superoxide using fluorescence spectroscopy," *Journal of Biomolecular Screening*, vol. 18, no. 4, pp. 498–503, 2013.

[16] H.-U. Simon, A. Haj-Yehia, and F. Levi-Schaffer, "Role of reactive oxygen species (ROS) in apoptosis induction," *Apoptosis*, vol. 5, no. 5, pp. 415–418, 2000.

[17] M. L. Circu and T. Y. Aw, "Reactive oxygen species, cellular redox systems, and apoptosis," *Free Radical Biology and Medicine*, vol. 48, no. 6, pp. 749–762, 2010.

[18] C. D. Gregory and A. Devitt, "The macrophage and the apoptotic cell: an innate immune interaction viewed simplistically?," *Immunology*, vol. 113, pp. 1–14, 2004.

[19] J. Whiteway, P. Koziarz, J. Veall et al., "Oxygen-insensitive nitroreductases: analysis of the roles of nfsA and nfsB in development of resistance to 5-nitrofuran derivatives in *Escherichia coli*," *Journal of Bacteriology*, vol. 180, no. 21, pp. 5529–5539, 1998.

[20] G. Sisson, J. Y. Jeong, A. Goodwin et al., "Metronidazole activation is mutagenic and causes DNA fragmentation in *Helicobacter pylori* and in *Escherichia coli* containing a cloned *H. pylori rdxA*$^+$ (nitroreductase) gene," *Journal of Bacteriology*, vol. 182, no. 18, pp. 5091–5096, 2000.

[21] I. M. de Oliveira, A. Zanotto-Filho, J. C. F. Moreira, D. Bonatto, and J. A. P. Henriques, "The role of two putative nitroreductases, Frm2p and Hbn1p, in the oxidative stress response in *Saccharomyces cerevisiae*," *Yeast*, vol. 27, no. 2, pp. n/a–102, 2010.

[22] J. D. Lambeth, "Nox enzymes, ROS, and chronic disease: an example of antagonistic pleiotropy," *Free Radical Biology and Medicine*, vol. 43, no. 3, pp. 332–347, 2007.

[23] O. Andersson, B. A. Adams, D. Yoo et al., "Adenosine signaling promotes regeneration of pancreatic β cells in vivo," *Cell Metabolism*, vol. 15, no. 6, pp. 885–894, 2012.

[24] L. Ye, M. A. Robertson, D. Hesselson, D. Y. R. Stainier, and R. M. Anderson, "Glucagon is essential for alpha cell transdifferentiation and beta cell neogenesis," *Development*, vol. 142, no. 8, pp. 1407–1417, 2015.

[25] *BioTechniques - CellProfiler™: Free, Versatile Software for Automated Biological Image Analysis*, October 2017, https://www.biotechniques.com/biotechniques/BiotechniquesJournal/2007/January/CellProfiler-free-versatile-software-for-automated-biological-image-analysis/biotechniques-40380.html.

Hindawi
Oxidative Medicine and Cellular Longevity
Volume 2018, Article ID 5801209, 8 pages
https://doi.org/10.1155/2018/5801209

Review Article

Reactive Oxygen Species-Mediated Tumor Microenvironment Transformation: The Mechanism of Radioresistant Gastric Cancer

Huifeng Gu,[1] **Tianhe Huang**,[2] **Yicheng Shen**,[3] **Yin Liu**,[1] **Fuling Zhou**,[4] **Yanxia Jin**,[4] **Haseeb Sattar**,[5] **and Yongchang Wei**[1]

[1]*Department of Radiation and Medical Oncology, Zhongnan Hospital, Wuhan University, Wuhan, Hubei 430071, China*
[2]*Department of Clinical Oncology, First Affiliated Hospital, Medical School of Xi'an Jiaotong University, Xi'an, Shanxi 710061, China*
[3]*School of Medicine, University of Texas Medical Branch, Galveston, TX 77555, USA*
[4]*Department of Hematology, Zhongnan Hospital, Wuhan University, Wuhan, Hubei 430071, China*
[5]*Department of Clinical Pharmacy, Wuhan Union Hospital, Affiliated to Tongji Medical College, Huazhong University of Science and Technology, Wuhan, Hubei 430022, China*

Correspondence should be addressed to Yongchang Wei; weiyongchang@whu.edu.cn

Received 7 October 2017; Revised 30 January 2018; Accepted 26 February 2018; Published 27 March 2018

Academic Editor: Karin Thevissen

Radioresistance is one of the primary causes responsible for therapeutic failure and recurrence of cancer. It is well documented that reactive oxygen species (ROS) contribute to the initiation and development of gastric cancer (GC), and the levels of ROS are significantly increased in patients with GC accompanied with abnormal expressions of multiple inflammatory factors. It is also well documented that ROS can activate cancer cells and inflammatory cells, stimulating the release of a variety of inflammatory cytokines, which subsequently mediates the tumor microenvironment (TME) and promotes cancer stem cell (CSC) maintenance as well as renewal and epithelial-mesenchymal transition (EMT), ultimately resulting in radioresistance and recurrence of GC.

1. Introduction

Gastric cancer (GC) is the second most frequently diagnosed cancer and the second leading cause of cancer-related mortality in China [1]. Almost one million new cases are estimated to occur worldwide every year [2]. Radiotherapy (RT) can optimize outcomes in patients with gastric cancer [3]. However, the impact of RT is hindered by a frequent development of resistance to the treatment [4]. Radiotherapy causes tissue damage in two different ways, a direct damaging effect from radiotherapy itself and an indirect effect resulting from the alteration of cellular pathways [5]. Radiotherapy can generate DNA breaks and induce cell apoptosis to indirectly militate against the antitumor treatment by inducing the reactive oxygen species (ROS). ROS are products of an excessive oxidative phosphorylation in mitochondria, as well as products of peroxisome-mediated β-oxidation of branched and very long-chain fatty acids (VLCFAs) [6], which regulate a variety of important signaling pathways for cell proliferation and survival.

Chronic low-level increased ROS can activate the change of the tumor microenvironment. Radiotherapy typically causes chronic oxidative stress and induces higher levels of ROS. The haemal levels of ROS in gastric cancer patients are obviously increased, along with the abnormal expression of factors such as P38 which modulates the expression of inflammatory factors [7–9]. ROS also directly alter the tumor microenvironment by activating cancer cells and inflammatory cells, which in turn release a variety of inflammatory factors to promote CSC renewal [10], leading to therapeutic resistance [11].

1.1. Effects of Radiotherapy in Gastric Cancer

1.1.1. ROS-Associated Radioresistance in Gastric Cancer. The biological effects of radiotherapy are mainly a consequence of DNA damage, such as breaks in the double-strand (ds)

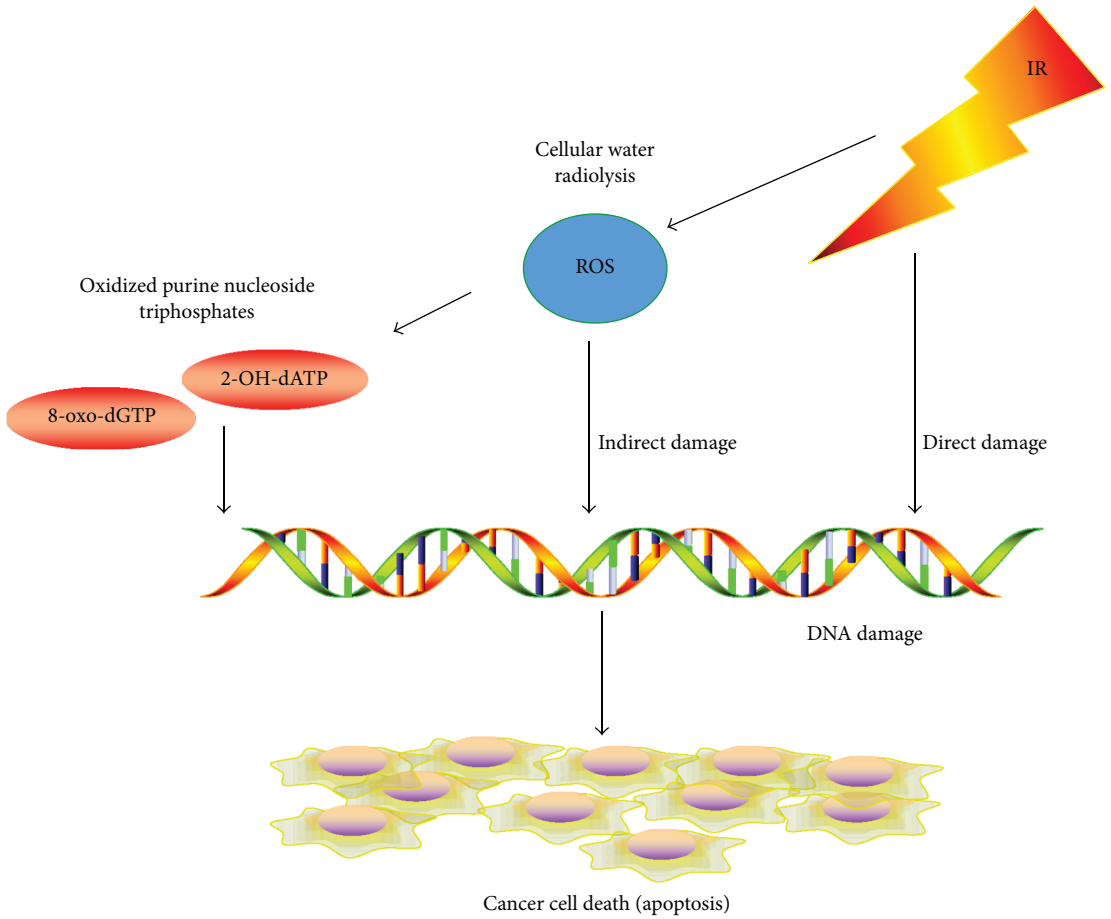

Figure 1: Radiotherapy and ROS promote antitumor effects. Radiotherapy irradiation causes cellular death through direct DNA breaks and indirect ROS effects. ROS induces 8-oxo-dGTP and 2-OH-dATP into genomic DNA, which leads to tumor cell apoptosis.

structure. These breaks can be directly caused by interactions between rays and DNA molecules, or indirectly from ROS-related cellular water radiolysis [12] (summarized in Figure 1). High levels of ROS suppress tumor growth through the inhibition of cell proliferation and induction of apoptosis and senescence. Incorporation of oxidized purine nucleoside triphosphates, such as 8-oxo-2′-deoxyguanosine triphosphate (8-oxo-dGTP) and 2-hydroxy-2′-deoxyadenosine triphosphate (2-OH-dATP), into genomic DNA plays an important role in apoptosis induced by ROS [13]. In addition, some studies confirm that tumor-infiltrating lymphocyte (TIL) can be attracted by ROS and exert their antitumor effects [14]. However, some cancer cells can survive ROS by activation of DNA repair and the antioxidant system [15]. Consequently, both activation of cellular DNA damage checkpoints and the ability to repair DNA in cells like CSCs contribute to cellular survival after receiving radiotherapy [10].

1.1.2. ROS-Related Alterations in the Tumor Microenvironment after Radiotherapy. Radiotherapy can break the DNA of tumor cells and increase the levels of ROS, leading to damage in tumor cells and changes in the microenvironment. After radiotherapy exposure, normal and tumor tissues show inflammatory responses, including vascular trauma, tissue edema, and hypoxia. Pulmonary fibrosis is one of the most undesired side effects of RT. Studies have confirmed that some RT can cause acute lung injury, and the connective tissue growth factor (CTGF) mediates a chronic inflammatory response resulting in pulmonary fibrosis [16, 17]. Myofibroblast expansion and progressive deposition of the extracellular matrix can be observed in this process. The radiotherapy-induced vascular trauma, tissue self-healing, and immune cell infiltration usually cause an increased demand for oxygen, and the following hypoxic environment activates hypoxia-inducible factors (HIFs) [11]. The HIFs, particularly HIF-1α and HIF-2α, regulate tumor cell proliferation, migration, and angiogenesis by regulating glucose metabolism and ROS production [18, 19]. The hypoxia also influences the immune system by recruiting immune cells, such as tumor-associated macrophages (TAMs), T-cells, B-cells, and myeloid-derived suppressor cells (MDSCs) [20]. Whether HIFs function positively or negatively in the tumor immune response is not clearly understood. In addition, RT causes tumor cell death and inflammatory infiltration, which induce the release of tumor antigens and trigger antigen-presenting cells [21]. RT also promotes dendritic cell (DC) recruitment and a T-cell immune response through RT-induced IgM targeting of the necrotic tumor cells. The inflammatory environment within tumors can also attract TAMs and T-cells to suppress or promote tumor growth [22]. The microenvironment is deeply

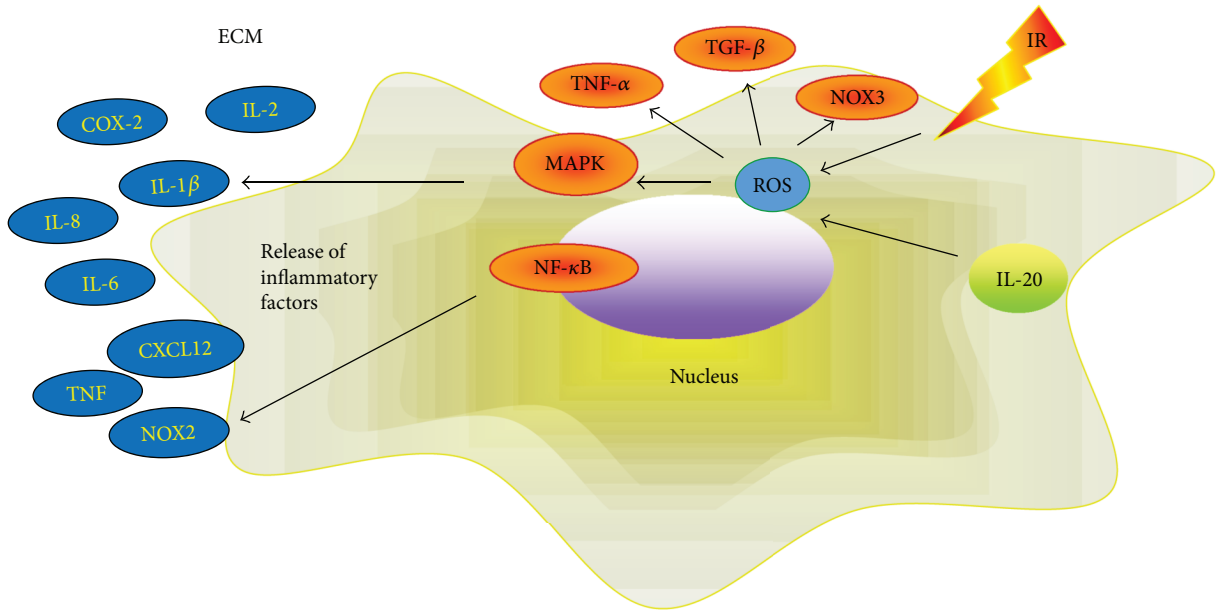

Figure 2: ROS mediate TME alterations. ROS can activate TNF-α, TGF-β, MAPK, NOX3, and NF-κB signaling pathways and promote the release of inflammatory factors TNF, NOX2, IL-6, IL-2, IL-8, and CXCL12, leading to tumor microenvironment changes and the development of tumors.

Table 1: ROS and TME-relevant signaling.

ROS target	Factors	Signaling pathways	Function	References
P38	TLR2/6	P38 MAPK, JNK	Translocation of NF-κB to the nucleus	[26]
NF-κB	IL-1β, IL-6, COX-2, IL-2, IL-8, TNF, NOX2, CXCL12	STAT3, NF-κB p65	Regulation of tumor proliferation and apoptosis	[23, 27]
TNF	TNFs	TNF, NF-κB, JNK	Cell survival or death	[27]
TGF-β		TGF	EMT inducer	[28, 30]
NOX-3	NADPH	MAPK, STAT1	Inflammation and apoptosis	[31]

changed after RT in response to the effects of ROS, which results in the transformation of TME and contributes to resistant cancer cells.

1.2. ROS-Mediated Tumor Microenvironment Transformation in Gastric Cancer Patients. Elevated levels of ROS are closely related to changes in the tumor microenvironment. The interaction between ROS and inflammation is an important pathogenic factor for GC carcinogenesis. Studies have shown that inflammatory mediators, such as cytokines and growth factors, can regulate nitrogen oxides (NOX) to produce ROS [23]. IL-20 stimulates ROS production through the activation of the signal transducer and activator of transcription 3 (STAT3), protein kinase B (AKT)/phospho-c-Jun NH(2)-terminal kinase (JNK)/extracellular signal-regulated kinase (ERK) signals [24]. As an effector molecule, ROS attract white blood cells involved in inflammation and tissue damage. Many studies have shown that ROS participate in carcinogenesis by activating inflammatory mediators, thus triggering an inflammatory microenvironment [25]. In Kupffer cells, ROS induce the release of inflammatory mediators by activating P38 to revitalize mitogen-activated protein kinase (MAPK) and nuclear factor-kappa B (NF-κB) [26]. High levels of ROS can also activate tumor necrosis factor alpha (TNF-α), protein (p65), and transforming growth factor beta (TGF-β) and downregulate the inhibitor of kappa B alpha (IκBα) to mediate the release of inflammatory mediators [23, 27, 28]. In addition, inflammatory cytokines can be released through the signal transducer and activator of transcription 1 (STAT1) signaling pathway, which is activated by ROS [29, 30]. ROS activate NF-κB, TNF-α, and STAT3 signaling pathways in inflammatory cells and tumor cells to release TNF, NOX2, IL-6, IL-2, IL-8, and CXCL12 involved in the change of TME [23, 27] (summarized in Figure 2 and Table 1). Our former researches and other groups have confirmed that patients with GC are in a status of oxidative stress [32] accompanied by abnormal expression of a variety of inflammatory factors, including IL-1β, IL-6, and COX-2. Therefore, ROS may stimulate tumor cells to proliferate and resist apoptosis while promoting the development and progression of GC by impacting the tumor microenvironment.

1.3. Transformed Tumor Microenvironment Promotes Gastric Cancer Development and Radiotherapy Resistance.

Table 2: CSCs involve in the mechanisms of radioresistance.

Mechanism	Signaling pathways	References
Protection of DNA repair	PARP	[35]
	ATR-Chk1	[36]
	ATR-Cnk1, ATM-Chk2	[37]
	Chk1, Chk2	[38]
	ATM-ZEB1-Chk1	[39]
	Myc-Chk1 and Chk2	[40]
	AKT/cyclin D1/Cdk4	[41]
	Upregulated DNA repair genes	[42, 43]
Protection of ROS scavenging	Nrf2 signaling pathway	[44–46]
	The Prdx family of antioxidant enzymes	[47, 48]
Protection of TME change	HIF-mediated mechanisms and negative immune responses	[14, 18, 49, 50]

Radioresistant GC cells have stem cell-like features. Several studies have shown that cancer stem cells (CSCs) play an important role in developing resistance and recurrence of cancer. The change of the tumor microenvironment after radiotherapy can activate CSC renewal and epithelial-mesenchymal transition (EMT) [33, 34]. CSCs display an EMT phenotype that is resistant to conventional therapies. Self-renewal of such cells is the main cause for treatment resistance and recurrence of GC (summarized in Table 2). In some human and mouse mammary tumors, ROS levels in CSCs are lower than those found in corresponding non-tumorigenic cells (NTCs). Compared to NTCs, CSCs show less DNA damage and are more viable. A highly activated free radical scavenger system contributes to lower levels of ROS in CSCs. Pharmacologic depletion of ROS scavengers in CSCs significantly decreases their ability to form colonies, leading to increased radiosensitivity [51]. These suggest that, similar to stem cells, CSCs in tumors can enhance reactive oxygen defense and reduce ROS levels, which may lead to cancer radiotherapy resistance [15]. Recent reports confirm that ROS are associated with GC stem cell markers CD133, CD166, and CD44 [52–54]; ROS can also regulate EMT-related indicators, such as E-cadherin, N-cadherin, snail, and twist [55].

EMT is crucial not only in regulating tissue development but also in tumor invasion and metastasis [56]. The change of the microenvironment plays an important role in the development of tumors, stem cell transfer, and self-renewal. ROS change the tumor microenvironment by regulating a variety of cell signaling pathways to promote CSC transformation [57, 58]. ROS also regulate the activity of NF-κB, which is an important mediator of the release of inflammatory factors by tumor cells [59, 60]. In breast cancer, head and neck squamous cell carcinoma, gastric cancer, and glioma, IL-6 promotes stem cell self-renewal through the classical IL-6R/gp130/STAT3 signaling pathway [61] (summarized in Figure 3). An elevated level of IL-6 is related to cancer cell proliferation, angiogenesis, and metastasis via stimulation of MAPK, STAT3, and AKT signaling pathways [62, 63]. IL-6 accelerates EMT through an altered expression of N-cadherin, E-cadherin, twist, snail, and vimentin, which results in cancer metastasis. It is reported that the levels of ROS, IL-6, COX2, and TNF-α are abnormally increased in patients with GC. Therefore, ROS may activate NF-κB to cause GC cells and cancer-associated fibroblast cells (CAFs) to release IL-6, thus mediating tumor metastasis and self-renewal that will consequently facilitate CSC self-renewal and maintenance. The activation of the cellular DNA damage checkpoint and the ability of DNA repair in CSCs result in their survival of radiotherapy, thus establishing radioresistance in GC cells.

1.4. Targeting ROS and ROS-Associated Tumor Microenvironment Signaling Pathways. Recently, multiple medicinal and chemical therapies are investigated to target the factors and signaling pathways associated with ROS-mediated TME alteration, ROS-mediated DNA damage, and apoptosis (summarized in Table 3). Selenium nanoparticles (SeNPs) possess special chemical and physical properties and generate ROS in cells to provide a novel strategy for the rational design and synthesis of chemo-radiosensitizing therapeutic materials [65]; SeNPs are also confirmed to affect on TNF and IRF1 to induce ROS-mediated activation of necroptosis [70]. There are also reports demonstrating that an increased level of ROS is a feasible strategy to improve radiotherapy efficacy [64–66]. Most of the drugs like bortezomib, celecoxib, 5-FU, and other compounds are validated to enhance the generation of ROS. Other reports suggest that microRNAs and other materials can repress the factors in ROS-mediated TME and enhance radiosensitivity in numerous cancer cells, including GC cells [72, 73]. Nonetheless, the mechanisms of ROS-mediated TME alteration in GC are not explicitly understood, particularly regarding key genes and proteins that influence the signaling pathways within the TME, inflammatory factors releasing, CSCs, EMT, and ROS scavenging.

2. Conclusion

The purpose of radiotherapy is to eliminate tumor cells, but spare normal cells and tissues from radiotherapy damage. However, currently single-course radiotherapy cannot provide sufficiently high-dosage radiotherapy for effective treatment of GC. While ROS can be induced chronically during multiple rounds of radiotherapy, its antitumor effect may be compromised. Within the tumor microenvironment, radiotherapy and several key cytokines can promote ROS production, consequently suppressing the antioxidant system. Patients with GC suffer from chronic oxidative stress and have higher levels of locally induced ROS, which leads to an abnormal expression of cytokines and inflammatory factors. ROS can activate a variety of signal molecules, such as MAPK, NF-κB, TNF-α, and TGF-β that transform the TME by releasing inflammatory factors, including IL-1β, IL-6, COX-2, TNF, and NOX2. These inflammatory factors promote the development and progression of GC through cellular proliferation and apoptosis signal pathways. The GC stem cell markers like CD133, CD166, and CD44 are also associated with ROS and EMT markers. ROS can also activate several cell signal pathways to regulate the CSCs. ROS-

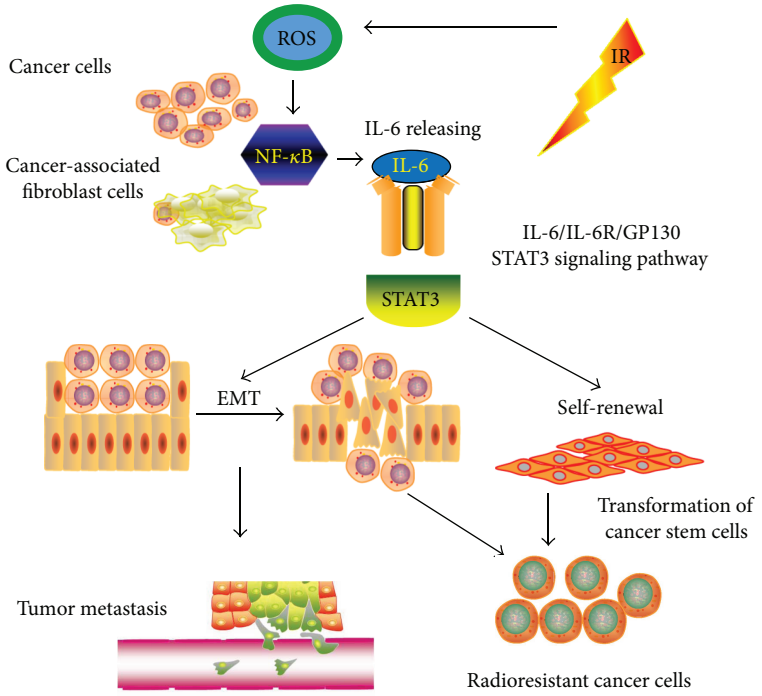

Figure 3: The IL-6R/gp130/STAT3 signaling pathway. The IL-6 secreted by tumor cells and CAFs through the ROS-mediated NF-κB signaling pathway can promote tumor metastasis, radioresistance, and CSC self-renewal. IL-6 promotes GC metastasis and CSC self-renewal through the classical IL-6R/gp130/STAT3 signaling pathway.

Table 3: Novel therapies targeting the ROS-mediated TME alteration.

Therapy	Target	Material type	Mechanism	References
BEMER electromagnetic field therapy	ROS	Cancer cell lines	Enhanced ROS formation and induced DNA damage	[64]
X-ray responsive selenium nanoparticles	ROS	HeLa and NIH3T3 cells	ROS overproduction causing the cell apoptosis	[65]
Diisopropylamine dichloroacetate	ROS	Human esophageal squamous cell carcinoma cell lines Eca-109 and TE-13	Modulated mitochondrial oxidation	[66]
Bortezomib, romidepsin	NF-κB	Human NSCLC cell lines (A549)	Increasing ROS and stimulating the extrinsic pathway of apoptosis	[67]
Bortezomib	ROS, Noxa	Mantle-cell lymphoma cell lines and patients	Cytotoxic effect through ROS generation and Noxa induction	[68]
Celecoxib, 5-FU	ROS	Human squamous cell lines (SNU-1041 and SNU-1076), orthotopic tongue cancer mouse model	Inhibiting the AKT pathway and enhancing ROS production	[69]
Selenium nanoparticles	TNF, IRF1	Human prostate adenocarcinoma cell line (PC-3)	Causing TNF and IRF1-induced ROS-mediated necroptosis	[70]
miR-139-5p	Multiple genes	Breast cancer patients, human breast cancer cell line (MCF7), xenograft mouse model	Suppression of gene networks of DNA repair and ROS defense	[71]
Ursolic acid		BGC-823 human adenocarcinoma gastric cancer cell line	Enhanced G2/M arrest, increasing ROS, promoting apoptosis	[72]
miR-200c nanoparticles	CSC	Human gastric adenocarcinoma cell lines (BGC823, SGC7901, and MKN45) and an immortalized human gastric mucosa cell line (GES-1)	Impairing ROS generation and DNA repair by the miR-200c	[73]

activated NF-κB mediates the release of IL-6 in GC, breast cancer, glioma, and HNSCC. The IL6R/gp130/STAT3 signal pathway regulates CSC renewal and cancer metastasis which leads to radiotherapy resistance. Further investigation of treatment options addressing the pathways associated with ROS in GC may increase the sensitivity of radiotherapy in patients with GC. Since inflammatory factors play an important role in ROS-mediated TME alteration and CSCs, anti-inflammatory drugs, such as NSAIDs and glucocorticoids, can be used to regulate the release of inflammatory factors and restore the aberrant TME. In addition, an optimal dosage of radiotherapy in less therapeutic frames of radiotherapy, along with other strategies to increase radiosensitivity, may significantly augment effective ROS levels for GC treatment.

Additional Points

Highlights. (i) This review focuses on recent advances in the research of radiotherapy-mediated tumor microenvironment changes in gastric cancer. (ii) There is accumulating evidence that reactive oxygen species induce the transformation of the tumor microenvironment that promotes cancer stem cells and epithelial-mesenchymal transition. (iii) This review proposes key targets for improving the radiosensitivity of gastric cancer.

Conflicts of Interest

The authors declare that there is no conflict of interest.

Authors' Contributions

All authors drafted the manuscript and approved the final version of the manuscript.

Acknowledgments

This study was supported by the National Natural Science Foundation of China (Grant no. 81673033 to Yongchang Wei).

References

[1] W. Chen, R. Zheng, P. D. Baade et al., "Cancer statistics in China, 2015," *CA: A Cancer Journal for Clinicians*, vol. 66, no. 2, pp. 115–132, 2016.

[2] L. A. Torre, F. Bray, R. L. Siegel, J. Ferlay, J. Lortet-Tieulent, and A. Jemal, "Global cancer statistics, 2012," *CA: a Cancer Journal for Clinicians*, vol. 65, no. 2, pp. 87–108, 2015.

[3] J. Ng and P. Lee, "The role of radiotherapy in localized esophageal and gastric cancer," *Hematology/Oncology Clinics of North America*, vol. 31, no. 3, pp. 453–468, 2017.

[4] H. H. Hartgrink, E. P. Jansen, N. C. van Grieken, and C. J. van de Velde, "Gastric cancer," *The Lancet*, vol. 374, no. 9688, pp. 477–490, 2009.

[5] I. Szumiel, "Ionizing radiation-induced oxidative stress, epigenetic changes and genomic instability: the pivotal role of mitochondria," *International Journal of Radiation Biology*, vol. 91, no. 1, pp. 1–12, 2015.

[6] J. Zhang, D. N. Tripathi, J. Jing et al., "ATM functions at the peroxisome to induce pexophagy in response to ROS," *Nature Cell Biology*, vol. 17, no. 10, pp. 1259–1269, 2015.

[7] T. Huang, F. Wang-Johanning, F. Zhou, H. Kallon, and Y. Wei, "MicroRNAs serve as a bridge between oxidative stress and gastric cancer (review)," *International Journal of Oncology*, vol. 49, no. 5, pp. 1791–1800, 2016.

[8] T. Huang, F. Zhou, F. Wang-Johanning, K. Nan, and Y. Wei, "Depression accelerates the development of gastric cancer through reactive oxygen species-activated ABL1 (review)," *Oncology Reports*, vol. 36, no. 5, pp. 2435–2443, 2016.

[9] H. Tu, H. Sun, Y. Lin et al., "Oxidative stress upregulates PDCD4 expression in patients with gastric cancer via miR-21," *Current Pharmaceutical Design*, vol. 20, no. 11, pp. 1917–1923, 2014.

[10] S. Bao, Q. Wu, R. E. McLendon et al., "Glioma stem cells promote radioresistance by preferential activation of the DNA damage response," *Nature*, vol. 444, no. 7120, pp. 756–760, 2006.

[11] D. Triner and Y. M. Shah, "Hypoxia-inducible factors: a central link between inflammation and cancer," *The Journal of Clinical Investigation*, vol. 126, no. 10, pp. 3689–3698, 2016.

[12] S. Le Caër, "Water radiolysis: influence of oxide surfaces on H_2 production under ionizing radiation," *Water*, vol. 3, no. 1, pp. 235–253, 2011.

[13] J. Ichikawa, D. Tsuchimoto, S. Oka et al., "Oxidation of mitochondrial deoxynucleotide pools by exposure to sodium nitroprusside induces cell death," *DNA Repair*, vol. 7, no. 3, pp. 418–430, 2008.

[14] H. E. Barker, J. T. Paget, A. A. Khan, and K. J. Harrington, "The tumour microenvironment after radiotherapy: mechanisms of resistance and recurrence," *Nature Reviews Cancer*, vol. 15, no. 7, pp. 409–425, 2015.

[15] M. Diehn, R. W. Cho, N. A. Lobo et al., "Association of reactive oxygen species levels and radioresistance in cancer stem cells," *Nature*, vol. 458, no. 7239, pp. 780–783, 2009.

[16] C. I. Diakos, K. A. Charles, D. C. McMillan, and S. J. Clarke, "Cancer-related inflammation and treatment effectiveness," *The Lancet Oncology*, vol. 15, no. 11, pp. e493–e503, 2014.

[17] S. Bickelhaupt, C. Erbel, C. Timke et al., "Effects of CTGF blockade on attenuation and reversal of radiation-induced pulmonary fibrosis," *Journal of the National Cancer Institute*, vol. 109, no. 8, 2017.

[18] S. Rey, L. Schito, M. Koritzinsky, and B. G. Wouters, "Molecular targeting of hypoxia in radiotherapy," *Advanced Drug Delivery Reviews*, vol. 109, pp. 45–62, 2017.

[19] B. Thienpont, J. Steinbacher, H. Zhao et al., "Tumour hypoxia causes DNA hypermethylation by reducing TET activity," *Nature*, vol. 537, no. 7618, pp. 63–68, 2016.

[20] F. Klug, H. Prakash, P. E. Huber et al., "Low-dose irradiation programs macrophage differentiation to an $iNOS^+$/M1 phenotype that orchestrates effective T cell immunotherapy," *Cancer Cell*, vol. 24, no. 5, pp. 589–602, 2013.

[21] F. G. Herrera, J. Bourhis, and G. Coukos, "Radiotherapy combination opportunities leveraging immunity for the next oncology practice," *CA: A Cancer Journal for Clinicians*, vol. 67, no. 1, pp. 65–85, 2017.

[22] T. Blankenstein, P. G. Coulie, E. Gilboa, and E. M. Jaffee, "The determinants of tumour immunogenicity," *Nature Reviews. Cancer*, vol. 12, no. 4, pp. 307–313, 2012.

[23] S. Prasad, S. C. Gupta, and A. K. Tyagi, "Reactive oxygen species (ROS) and cancer: role of antioxidative nutraceuticals," *Cancer Letters*, vol. 387, pp. 95–105, 2017.

[24] Y. H. Hsu, C. C. Wei, D. B. Shieh, C. H. Chan, and M. S. Chang, "Anti-IL-20 monoclonal antibody alleviates inflammation in oral cancer and suppresses tumor growth," *Molecular Cancer Research*, vol. 10, no. 11, pp. 1430–1439, 2012.

[25] T. Monkkonen and J. Debnath, "Inflammatory signaling cascades and autophagy in cancer," *Autophagy*, pp. 1–9, 2017.

[26] H. Wang, L. Wang, N. L. Li et al., "Subanesthetic isoflurane reduces zymosan-induced inflammation in murine Kupffer cells by inhibiting ROS-activated p38 MAPK/NF-κB signaling," *Oxidative Medicine and Cellular Longevity*, vol. 2014, Article ID 851692, 13 pages, 2014.

[27] H. Blaser, C. Dostert, T. W. Mak, and D. Brenner, "TNF and ROS crosstalk in inflammation," *Trends in Cell Biology*, vol. 26, no. 4, pp. 249–261, 2016.

[28] S. Petanidis, E. Kioseoglou, K. Domvri et al., "In vitro and ex vivo vanadium antitumor activity in (TGF-β)-induced EMT. Synergistic activity with carboplatin and correlation with tumor metastasis in cancer patients," *The International Journal of Biochemistry & Cell Biology*, vol. 74, pp. 121–134, 2016.

[29] A. Valavanidis, T. Vlachogianni, K. Fiotakis, and S. Loridas, "Pulmonary oxidative stress, inflammation and cancer: respirable particulate matter, fibrous dusts and ozone as major causes of lung carcinogenesis through reactive oxygen species mechanisms," *International Journal of Environmental Research and Public Health*, vol. 10, no. 9, pp. 3886–3907, 2013.

[30] G. Oruqaj, S. Karnati, V. Vijayan et al., "Compromised peroxisomes in idiopathic pulmonary fibrosis, a vicious cycle inducing a higher fibrotic response via TGF-β signaling," *Proceedings of the National Academy of Sciences of the United States of America*, vol. 112, no. 16, pp. E2048–E2057, 2015.

[31] T. Kaur, V. Borse, S. Sheth et al., "Adenosine A_1 receptor protects against cisplatin ototoxicity by suppressing the NOX3/STAT1 inflammatory pathway in the cochlea," *The Journal of Neuroscience*, vol. 36, no. 14, pp. 3962–3977, 2016.

[32] Y. C. Wei, F. L. Zhou, D. L. He et al., "Oxidative stress in depressive patients with gastric adenocarcinoma," *International Journal of Neuropsychopharmacology*, vol. 12, no. 8, pp. 1089–1096, 2009.

[33] Y. Hayakawa, H. Ariyama, J. Stancikova et al., "Mist1 expressing gastric stem cells maintain the normal and neoplastic gastric epithelium and are supported by a perivascular stem cell niche," *Cancer Cell*, vol. 28, no. 6, pp. 800–814, 2015.

[34] J. C. Santos, E. Carrasco-Garcia, M. Garcia-Puga et al., "SOX9 elevation acts with canonical WNT signaling to drive gastric cancer progression," *Cancer Research*, vol. 76, no. 22, pp. 6735–6746, 2016.

[35] Y. Liu, M. L. Burness, R. Martin-Trevino et al., "RAD51 mediates resistance of cancer stem cells to PARP inhibition in triple-negative breast cancer," *Clinical Cancer Research*, vol. 23, no. 2, pp. 514–522, 2017.

[36] M. Ogrunc, R. I. Martinez-Zamudio, P. B. Sadoun et al., "USP1 regulates cellular senescence by controlling genomic integrity," *Cell Reports*, vol. 15, no. 7, pp. 1401–1411, 2016.

[37] S. Natarajan, F. Begum, J. Gim et al., "High mobility group A2 protects cancer cells against telomere dysfunction," *Oncotarget*, vol. 7, no. 11, pp. 12761–12782, 2016.

[38] I. Iacobucci, A. G. Di Rora, M. V. Falzacappa et al., "In vitro and in vivo single-agent efficacy of checkpoint kinase inhibition in acute lymphoblastic leukemia," *Journal of Hematology & Oncology*, vol. 8, no. 1, p. 125, 2015.

[39] P. Zhang, Y. Wei, L. Wang et al., "ATM-mediated stabilization of ZEB1 promotes DNA damage response and radioresistance through CHK1," *Nature Cell Biology*, vol. 16, no. 9, pp. 864–875, 2014.

[40] W. J. Wang, S. P. Wu, J. B. Liu et al., "MYC regulation of CHK1 and CHK2 promotes radioresistance in a stem cell-like population of nasopharyngeal carcinoma cells," *Cancer Research*, vol. 73, no. 3, pp. 1219–1231, 2013.

[41] T. Shimura, N. Noma, T. Oikawa et al., "Activation of the AKT/cyclin D1/Cdk4 survival signaling pathway in radioresistant cancer stem cells," *Oncogene*, vol. 1, no. 6, article e12, 2012.

[42] C. Mayr, A. Wagner, M. Loeffelberger et al., "The BMI1 inhibitor PTC-209 is a potential compound to halt cellular growth in biliary tract cancer cells," *Oncotarget*, vol. 7, no. 1, pp. 745–758, 2016.

[43] C. Saygin, A. Wiechert, V. S. Rao et al., "CD55 regulates self-renewal and cisplatin resistance in endometrioid tumors," *The Journal of Experimental Medicine*, vol. 214, no. 9, pp. 2715–2732, 2017.

[44] B. C. Lu, J. Li, W. F. Yu, G. Z. Zhang, H. M. Wang, and H. M. Ma, "Elevated expression of Nrf2 mediates multidrug resistance in $CD133^+$ head and neck squamous cell carcinoma stem cells," *Oncology Letters*, vol. 12, no. 6, pp. 4333–4338, 2016.

[45] A. Sparaneo, F. P. Fabrizio, and L. A. Muscarella, "Nrf2 and notch signaling in lung cancer: near the crossroad," *Oxidative Medicine and Cellular Longevity*, vol. 2016, Article ID 7316492, 17 pages, 2016.

[46] Y. Mitsuishi, H. Motohashi, and M. Yamamoto, "The Keap1–Nrf2 system in cancers: stress response and anabolic metabolism," *Frontiers in Oncology*, vol. 2, p. 200, 2012.

[47] R. Wang, J. Wei, S. Zhang et al., "Peroxiredoxin 2 is essential for maintaining cancer stem cell-like phenotype through activation of Hedgehog signaling pathway in colon cancer," *Oncotarget*, vol. 7, no. 52, pp. 86816–86828, 2016.

[48] A. Perkins, K. J. Nelson, D. Parsonage, L. B. Poole, and P. A. Karplus, "Peroxiredoxins: guardians against oxidative stress and modulators of peroxide signaling," *Trends in Biochemical Sciences*, vol. 40, no. 8, pp. 435–445, 2015.

[49] V. Kumar and D. I. Gabrilovich, "Hypoxia-inducible factors in regulation of immune responses in tumour microenvironment," *Immunology*, vol. 143, no. 4, pp. 512–519, 2014.

[50] J. Bensimon, D. Biard, V. Paget et al., "Forced extinction of CD24 stem-like breast cancer marker alone promotes radiation resistance through the control of oxidative stress," *Molecular Carcinogenesis*, vol. 55, no. 3, pp. 245–254, 2016.

[51] I. Skvortsova, P. Debbage, V. Kumar, and S. Skvortsov, "Radiation resistance: cancer stem cells (CSCs) and their enigmatic pro-survival signaling," *Seminars in Cancer Biology*, vol. 35, pp. 39–44, 2015.

[52] M. Krause, A. Dubrovska, A. Linge, and M. Baumann, "Cancer stem cells: radioresistance, prediction of radiotherapy outcome and specific targets for combined treatments," *Advanced Drug Delivery Reviews*, vol. 109, pp. 63–73, 2016.

[53] M. E. Prince, R. Sivanandan, A. Kaczorowski et al., "Identification of a subpopulation of cells with cancer stem cell properties in head and neck squamous cell carcinoma," *Proceedings of the*

National Academy of Sciences of the United States of America, vol. 104, no. 3, pp. 973–978, 2007.

[54] M. Zoller, "CD44: can a cancer-initiating cell profit from an abundantly expressed molecule?," *Nature Reviews Cancer*, vol. 11, no. 4, pp. 254–267, 2011.

[55] H. Kinugasa, K. A. Whelan, K. Tanaka et al., "Mitochondrial SOD2 regulates epithelial–mesenchymal transition and cell populations defined by differential CD44 expression," *Oncogene*, vol. 34, no. 41, pp. 5229–5239, 2015.

[56] V. J. Findlay, C. Wang, D. K. Watson, and E. R. Camp, "Epithelial-to-mesenchymal transition and the cancer stem cell phenotype: insights from cancer biology with therapeutic implications for colorectal cancer," *Cancer Gene Therapy*, vol. 21, no. 5, pp. 181–187, 2014.

[57] P. Csermely, J. Hodsagi, T. Korcsmaros et al., "Cancer stem cells display extremely large evolvability: alternating plastic and rigid networks as a potential mechanism: network models, novel therapeutic target strategies, and the contributions of hypoxia, inflammation and cellular senescence," *Seminars in Cancer Biology*, vol. 30, pp. 42–51, 2015.

[58] P. H. Nguyen, J. Giraud, L. Chambonnier et al., "Characterization of biomarkers of tumorigenic and chemoresistant cancer stem cells in human gastric carcinoma," *Clinical Cancer Research*, vol. 23, no. 6, pp. 1586–1597, 2016.

[59] S. Nakajima and M. Kitamura, "Bidirectional regulation of NF-κB by reactive oxygen species: a role of unfolded protein response," *Free Radical Biology and Medicine*, vol. 65, pp. 162–174, 2013.

[60] D. Capece, D. Verzella, A. Tessitore, E. Alesse, C. Capalbo, and F. Zazzeroni, "Cancer secretome and inflammation: the bright and the dark sides of NF-κB," *Seminars in Cell & Developmental Biology*, 2017.

[61] R. Bharti, G. Dey, and M. Mandal, "Cancer development, chemoresistance, epithelial to mesenchymal transition and stem cells: a snapshot of IL-6 mediated involvement," *Cancer Letters*, vol. 375, no. 1, pp. 51–61, 2016.

[62] K. Middleton, J. Jones, Z. Lwin, and J. I. Coward, "Interleukin-6: an angiogenic target in solid tumours," *Critical Reviews in Oncology/Hematology*, vol. 89, no. 1, pp. 129–139, 2014.

[63] S. Cohen, I. Bruchim, D. Graiver et al., "Platinum-resistance in ovarian cancer cells is mediated by IL-6 secretion via the increased expression of its target cIAP-2," *Journal of Molecular Medicine*, vol. 91, no. 3, pp. 357–368, 2013.

[64] K. Storch, E. Dickreuter, A. Artati, J. Adamski, and N. Cordes, "BEMER electromagnetic field therapy reduces cancer cell radioresistance by enhanced ROS formation and induced DNA damage," *PLoS One*, vol. 11, no. 12, article e0167931, 2016.

[65] B. Yu, T. Liu, Y. Du, Z. Luo, W. Zheng, and T. Chen, "X-ray-responsive selenium nanoparticles for enhanced cancer chemo-radiotherapy," *Colloids and Surfaces B: Biointerfaces*, vol. 139, pp. 180–189, 2016.

[66] G. Dong, Q. Chen, F. Jiang et al., "Diisopropylamine dichloroacetate enhances radiosensitization in esophageal squamous cell carcinoma by increasing mitochondria-derived reactive oxygen species levels," *Oncotarget*, vol. 7, no. 42, pp. 68170–68178, 2016.

[67] S. Karthik, R. Sankar, K. Varunkumar, C. Anusha, and V. Ravikumar, "Blocking NF-κB sensitizes non-small cell lung cancer cells to histone deacetylase inhibitor induced extrinsic apoptosis through generation of reactive oxygen species," *Biomedicine & Pharmacotherapy*, vol. 69, pp. 337–344, 2015.

[68] P. Perez-Galan, G. Roue, N. Villamor, E. Montserrat, E. Campo, and D. Colomer, "The proteasome inhibitor bortezomib induces apoptosis in mantle-cell lymphoma through generation of ROS and Noxa activation independent of p53 status," *Blood*, vol. 107, no. 1, pp. 257–264, 2006.

[69] M. W. Sung, D. Y. Lee, S. W. Park et al., "Celecoxib enhances the inhibitory effect of 5-FU on human squamous cell carcinoma proliferation by ROS production," *The Laryngoscope*, vol. 127, no. 4, pp. E117–E123, 2017.

[70] P. Sonkusre and S. S. Cameotra, "Biogenic selenium nanoparticles induce ROS-mediated necroptosis in PC-3 cancer cells through *TNF* activation," *Journal of Nanobiotechnology*, vol. 15, no. 1, p. 43, 2017.

[71] M. Pajic, D. Froio, S. Daly et al., "miR-139-5p modulates radiotherapy resistance in breast cancer by repressing multiple gene networks of DNA repair and ROS defense," *Cancer Research*, vol. 78, no. 2, pp. 501–515, 2018.

[72] Y. Yang, M. Jiang, J. Hu et al., "Enhancement of radiation effects by ursolic acid in BGC-823 human adenocarcinoma gastric cancer cell line," *PLoS One*, vol. 10, no. 7, article e0133169, 2015.

[73] F. B. Cui, Q. Liu, R. T. Li et al., "Enhancement of radiotherapy efficacy by miR-200c-loaded gelatinase-stimuli PEG-Pep-PCL nanoparticles in gastric cancer cells," *International Journal of Nanomedicine*, vol. 9, pp. 2345–2358, 2014.

Hindawi
Oxidative Medicine and Cellular Longevity
Volume 2018, Article ID 2389523, 21 pages
https://doi.org/10.1155/2018/2389523

Review Article

Targeting Oxidatively Induced DNA Damage Response in Cancer: Opportunities for Novel Cancer Therapies

Pierpaola Davalli,[1] **Gaetano Marverti**,[1] **Angela Lauriola**,[2] **and Domenico D'Arca**[1,3]

[1]*Department of Biomedical, Metabolic and Neural Sciences, University of Modena and Reggio Emilia, 41125 Modena, Italy*
[2]*Department of Life Sciences, University of Modena and Reggio Emilia, 41125 Modena, Italy*
[3]*Istituto Nazionale di Biostrutture e Biosistemi, 00136 Roma, Italy*

Correspondence should be addressed to Domenico D'Arca; domenico.darca@unimore.it

Received 21 September 2017; Accepted 22 January 2018; Published 27 March 2018

Academic Editor: Paula Ludovico

Cancer is a death cause in economically developed countries that results growing also in developing countries. Improved outcome through targeted interventions faces the scarce selectivity of the therapies and the development of resistance to them that compromise the therapeutic effects. Genomic instability is a typical cancer hallmark due to DNA damage by genetic mutations, reactive oxygen and nitrogen species, ionizing radiation, and chemotherapeutic agents. DNA lesions can induce and/or support various diseases, including cancer. The DNA damage response (DDR) is a crucial signaling-transduction network that promotes cell cycle arrest or cell death to repair DNA lesions. DDR dysregulation favors tumor growth as downregulated or defective DDR generates genomic instability, while upregulated DDR may confer treatment resistance. Redox homeostasis deeply and capillary affects DDR as ROS activate/inhibit proteins and enzymes integral to DDR both in healthy and cancer cells, although by different routes. DDR regulation through modulating ROS homeostasis is under investigation as anticancer opportunity, also in combination with other treatments since ROS affect DDR differently in the patients during cancer development and treatment. Here, we highlight ROS-sensitive proteins whose regulation in oxidatively induced DDR might allow for selective strategies against cancer that are better tailored to the patients.

1. Introduction

Human cancer is the primary death cause in economically developed countries and the second death cause in developing countries. Adoption of cancer-associated lifestyles as smoking, physical inactivity, and "westernized" diets and the increasing number of aging people are major causes for cancer expansion [1]. Targeted therapy has improved the outcome for specific cancer types; however, intrinsic or acquired resistance to the therapies remains an inevitable challenge for the patients [2–4]. Several features like cell composition of the tumor, tumor microenvironment, and drug efficiency lead tumor cells to overwhelm the therapies through the same mechanisms that healthy cells utilize for surviving under adverse conditions. In addition, many therapies are scarcely selective for cancer cells and damage healthy cells thus compromising the therapeutic effect [5–7]. Almost all human tumors are characterized by genomic instability, which essentially derives from deoxyribonucleic acid (DNA) damage generated by reactive oxygen/nitrogen species (ROS/RNS, usually referred as ROS), ionizing radiation, and chemotherapeutic agents, besides occasional genetic mutations, so that DNA damage is direct and indirect target of a wide number of anticancer treatments [8–11]. Eukaryotic cells have developed a sophisticated signaling-transduction mechanism, named DNA damage response (DDR), that maintains cell genome integrity by acting as an efficacious network. DDR can detect DNA lesions and arrest the cell cycle both temporary (checkpoint control activation) and permanently (senescence) or promote cell death (apoptosis). DDR sets cell fate depending on mode and level of DNA damage after comparing its severity and cell potentiality to survive. Aberrant repair mechanisms, mutations, and polymorphisms of genes involved in DNA repair contribute to

human cancer onset, development, and progression [12–15]. DDR defects that are detectable in human tumors allow classifying the patients for appropriate therapy. Tumor cells often shift their ratio between DNA damage and DNA repair activities in favor of repair that leads to stabilize DNA lesions, as the repairing system cannot identify gene mutations. The lesion extent may exceed the repairing capability of the cell and generate resistance to DNA-targeted therapies [16–18]. Mechanism-based-targeted therapies are preferentially administered as single-target therapies often induce resistance through restoring basal cancer pathways [19–21]. Oxidatively induced DDR has aroused increasing interest since when ROS are no more considered causing exclusive molecular damage or palliative effect against anticancer drugs. ROS together with related molecules and enzymes contribute to physiological functions and pathological alterations of DDR. Oscillations of the redox equilibrium under the cell death threshold can affect the stringency of DDR through modulating its pathways and mechanisms [22–24]. ROS participate to the complex crosstalk of DDR and autophagy that contributes to treatment resistance of cancer cells and their subsequent regrowth through the DNA repair mechanisms [25–29]. Depending on their level, ROS coordinate intracellular redox signaling by acting as messengers in both healthy and cancer cells, although through different pathways. The imbalance between ROS/RNS production and elimination favors their accumulation, subjecting both healthy and cancerous cells to the oxidative/nitrosative stress (collectively named oxidative stress, OS). Cancer cells proliferate in a constitutive OS state, as their hallmark, that may generate resistance to ROS-based anticancer interventions when the antioxidant system of the cell is proportional to its OS level or evolve towards cell death when ROS are subjected to spontaneous or therapeutically induced further increase [30–35].

Here, we briefly prospect possible points of therapeutic intervention in oxidatively induced DDR regarding ROS homeostasis involvement that are under investigation as mechanism-based therapeutic strategies to counteract the human cancer.

2. ROS Homeostasis

2.1. Production of ROS and RNS. The oxidative metabolism in mitochondria constantly produces a flux of reactive oxygen species (ROS) and a flux of reactive nitrogen species (RNS) as oxidative phosphorylation by-products. The production is estimated on average 1-2% of total rate of oxygen consumption in healthy human body. ROS/RNS are usually named free radicals since they are the most important classes of the free radical family in the majority of living organisms. Free radicals contain an atom or a molecule with one or more unpaired electrons that make them highly reactive, able to bind other radicals or oxidize molecules that they contact. Free radicals share a short life and a generation of chain reactions that ultimately lead to cell structure damage. ROS comprise the singlet oxygen (½ O), the superoxide anion radical (O_2÷) and its metabolites, as the very toxic hydroxyl radical ($^{\bullet}$OH), and the nonradical hydrogen peroxide (H_2O_2) that, in the presence of redox active metals, is partially reduced to ($^{\bullet}$OH), by Fenton reaction [36]. The mitochondrial respiratory chain leaks electrons causing partial oxygen reduction to O_2÷, which is spontaneously, or by superoxide dismutase2 (SOD2), rapidly transformed into H_2O_2. Also, peroxisomal NADPH oxidases (NOXs) are implicated in electron transfer from intracellular NADPH to oxygen generating O_2÷ that is converted into H_2O_2 by superoxide dismutase3 (SOD3). The overall H_2O_2 is turned into reactive $^{\bullet}$OH radicals. RNS were derived from the very dangerous peroxynitrite (ONOO−) generated by O_2÷ and nitric oxide ($^{\bullet}$NO), a highly reactive gaseous molecule, but not a radical, soluble in water and diffusible across cell membranes. The reaction is catalyzed by NO synthases (NOS1–3), a family of constitutive or inducible enzymes with different tissue distribution utilizing arginine and NADPH. $^{\bullet}$NO competes with SOD by directing O_2÷ towards ONOO−, rather than H_2O_2. NO-derived oxidants are endowed with cellular antimicrobial action and act with ROS contributing to establish oxidative conditions [37, 38].

2.2. Antioxidants (ROS Scavenging System). Living organisms have evolved enzymatic and nonenzymatic pathways that prevent oxidative damage to essential macromolecules, including proteins and nucleic acids. The pathways are modulated by several protein-based sensory, while regulatory modules ensure a rapid and appropriate response [39]. Peroxisomal catalase, SODs, glutathione peroxidase, and ascorbate peroxidase are antioxidant enzymes that remove O_2÷, H_2O_2, and peroxides in cell districts, acting as highly efficient antioxidant systems that protect cellular components by variable extent. The enzymes act in concert with other proteins as peroxiredoxins [40–43], thioredoxins (Trx) [44], glutaredoxins (Grx) [45], and metallothionein [46–48] and with low molecular weight, nonenzymatic antioxidants as ascorbate, glutathione [45, 49], tocopherol, carotenoid, and melatonin [50–53]. The oxidative signal is essentially reversed by two potent antioxidant systems the Trx/Trx reductase and Grx/Grx reductase, which reduce disulfides to free thiol groups at the expense of NADPH depletion. Antioxidant systems contribute to scavenge excessive ROS, thus finely controlling their levels and restoring the pools of reduced proteins and lipids (Figure 1).

2.3. ROS/RNS Effects. ROS/RNS exert different effects on the same targets, depending on cell type, with the exception of $^{\bullet}$OH and ONOO− that are always associated to plain toxicity. The basal oxidation level that is necessary for correct cell viability and functions requires a redox homeostasis mechanism. Radical fluctuations are strictly controlled through their continuously balancing in, for instance, increased energetic demand, which intensifies electron flux through mitochondria, or aging, which decreases mitochondrial efficiency. Exogenous ROS/RNS sources, as oxidases and oxygenases, infrared and ultraviolet radiations, dietary nitrosamines, or chemotherapy agents [21], may contribute to redox homeostasis changes. Final effect of ROS/RNS, from now simply referred as ROS, is not exclusively determined by cellular concentration of each species but also by balance between different species, that is, H_2O_2 versus O2÷. Indeed, O_2÷ from mitochondria may drive signaling pathways in

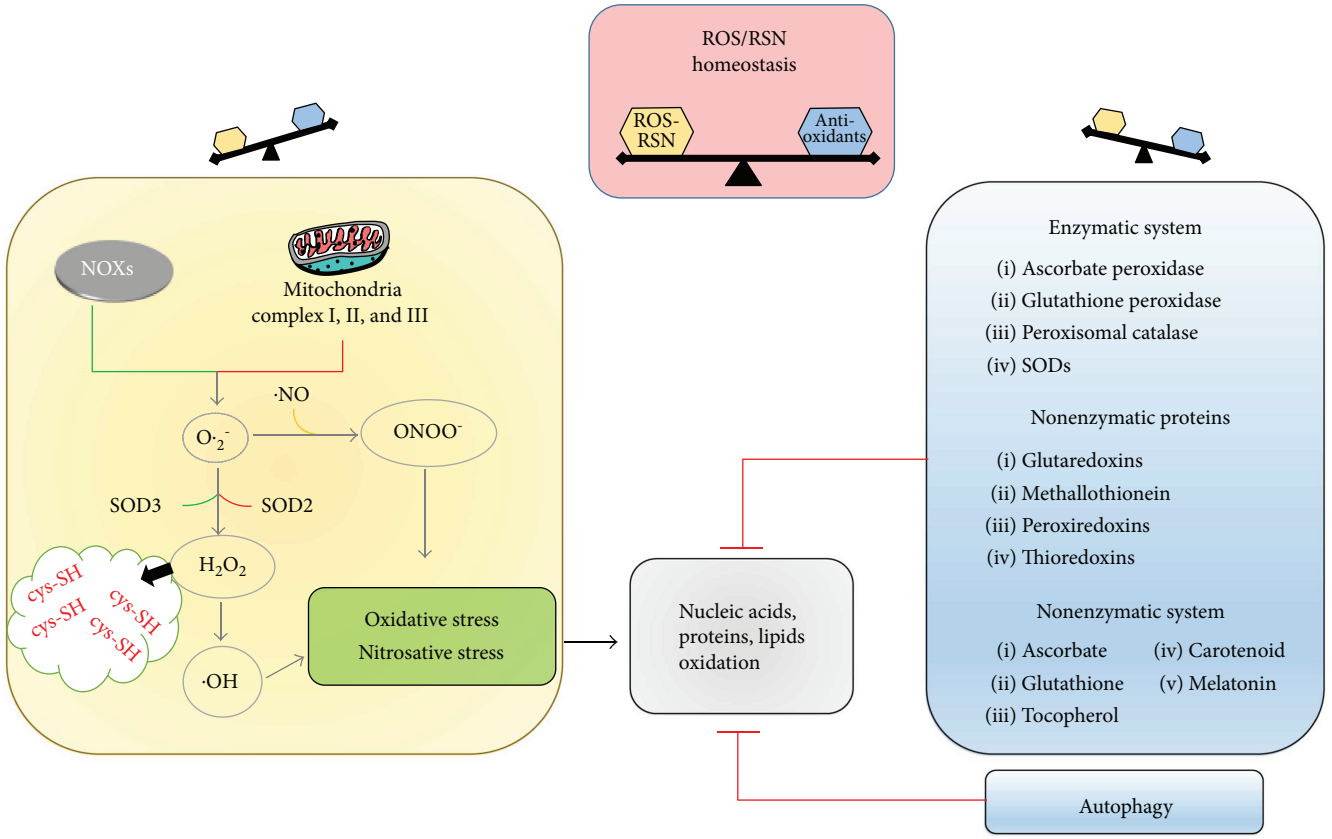

Figure 1: Reactive oxygen species (ROS) and reactive nitrogen species (RNS) balance is critical in maintaining cellular homeostasis. Excessive levels of ROS ($O_2^{\cdot-}$, $^{\bullet}OH$, and H_2O_2) and/or RNS ($ONOO^-$) affect the redox homeostasis, inducing oxidation of cellular nucleic acids, proteins, and lipids. The cells activate several antioxidant systems to maintain the intracellular redox equilibrium, including an enzymatic system (ascorbate peroxidase, glutathione peroxidase, peroxisomal catalase, and SODs) that works in concert with other nonenzymatic proteins (glutaredoxins, metallothionein, peroxiredoxins, and thioredoxins) and an nonenzymatic system (ascorbate, carotenoid, glutathione, melatonin, and tocopherol). In addition, autophagy is a very sensitive antioxidant system. NOXs = NADPH oxidases; cys-SH = cysteine-SH.

cancer onset, development, and amplification. ROS trigger thiol oxidation, glutathionylation, nitrosylation, and carbonylation on specific proteins and enzymes, which consequently act as signal mediators in cell metabolism and signaling, even if the exact mechanisms have to be clarified [38, 54, 55]. Both cytosolic and nuclear proteins are ROS target containing ROS-sensitive cysteine residues that play regulatory rather than structural roles. These cysteines react as molecular switches that transduce redox signals, conferring redox activity to the proteins through their thiol groups. After undergoing oxidative modification and generation of S-hydroxylated derivatives, protein conformation/function is modified by reacting with other cysteines that generate either intra- or intermolecular disulfides, the last promoting complexes to conduct new functions. Redox-activated proteins act as intracellular redox sensors that allow for ROS properly adapting to their functions in the cellular redox equilibrium [21, 56]. Actually, these sensors result useful for studying pathogenesis and progression of multiple diseases [39, 55]. In particular, physiological trace levels of H_2O_2 act as both sensor and second messengers, being able to cross membranes, and induce specific signal transduction pathways in the cell [55]. ROS contribute to cell homeostasis as "second messengers" by modulating the activities of key regulatory molecules, including protein kinases, phosphatases, G proteins, and transcription factors. Periodic oscillations in the cell redox environment regulate cell cycle progression from quiescence (G0) to proliferation (G1, S, G2, and M) and back to quiescence, as a redox cycle. A loss in the redox control of cell cycle could lead to aberrant proliferation, a hallmark of various human pathologies [57]. ROS role is continuously delineated in a variety of physiopathological conditions including cell growth, proliferation, differentiation, aging, senescence, and defense against infectious agents during inflammatory responses [58, 59].

2.4. Oxidative Stress. Excessive ROS ($O_2^{\cdot-}$, $^{\bullet}OH$, and H_2O_2) or RNS (peroxynitrites and nitrogen oxides) and their reactive metabolites may be derived from imbalance between oxidant generation and removal by antioxidants that disrupts the redox homeostasis. The condition, named oxidative/nitrosative stress (OS/NOS, simply referred as OS), is potentially harmful because increasing levels of excessive radicals induce improper signaling or oxidation of the main essential cell molecules. Bases in nucleic acid, amino acid residues in proteins, and fatty acids in lipids show different susceptibility

to OS that allows for a finely organized signaling system. OS consequences depend on cell type so that it is hard to clearly differentiate OS and redox signaling. Cellular OS level moderately overcoming cellular antioxidant level may provide selectivity for specifically targeted molecules and constitute a signaling mechanism, even after generating specific irreversible alterations of definite molecules [60–62]. Metabolic changes from cellular OS include (a) reduced ATP concentration, possibly caused by damaged mitochondria, (b) deactivated glyceraldehyde-3-phosphate dehydrogenase, which causes glycolysis inhibition, (c) increased catabolism of adenine nucleotides, (d) enhanced ATP consumption due to the active transport of oxidized glutathione, (e) increased cytoplasmic calcium concentration from deactivated calcium pumps, (f) cell membrane depolarization, possibly due to deactivation of K, Ca, and Na channels, resulting in increased cell membrane permeability, and (g) decreased glutathione level and ratio between reduced and oxidized glutathione. Another dangerous event is the generation of oxidized glutathione in various connections with xenobiotics, products of lipid peroxidation, or proteins present in the cell. Increased ATP consumption occurs in disposing such products outside the cell that also contributes to reductions in cellular glutathione [63, 64]. Generally, excessive ROS irreversibly damage structures of main macromolecules, membranes, and organelles and hamper signal mediators activity, thereby representing a primary damage source in biological systems. Irreversibly oxidized biomolecules are essentially cleared from cells through the autophagic process that is consequently considered a very sensitive antioxidant system. Autophagy is a converging point of different inputs and underlies cell responses to stressful conditions affecting cellular homeostasis, from biomolecules integrity to cell viability. OS acts as a vital stimulus to sustain autophagy, with ROS being one of the main signal messengers, thus autophagy and ROS coordinate to maintain cellular homeostasis [25, 65]. Although the mechanism by which ROS activates autophagy remains unclear, an essential autophagy-associated protein Atg4 has been shown to be under redox control. S-glutathionylation of the AMP-activated protein kinase AMPK may also contribute to its activation by H_2O_2 exposure, which allows for autophagy progression [28].

2.5. Oxidatively Damaged DNA. The threat of cell molecule oxidation is a consequence of life in an oxygen-rich habitat that differently challenges molecule integrity and cell viability through the intermediate activity of homeostatic processes, mainly based on repair and degradation. Millions of DNA-damaging lesions occur every day in each cell of our bodies due to various stresses. Among which OS represents a major portion as it may induce approximately 10^4 DNA lesions per cell of an organism per day. OS mediates the damage upon different insults such as ultraviolet, X- and γ radiations, pollutants, poisons, or endogenous disequilibria as metabolic imbalance that produce different and characteristic types of lesions. The lesions are particularly significant since they interfere with DNA replication that generates mutations, unless repaired in an error-free process, and alter the expression of protein, including transcriptional factors, and consequently signaling pathways and cellular behavior. Among endogenous and exogenous ROS/RNS, the $O_2\dot{-}$ is considered as a main candidate, responsible for genetic instability and malignant transformation. Oxidative DNA damage on bases of nucleic acid is repaired to a certain extent for maintaining the genome integrity, as evidenced by the DNA repair systems of the cell that are outlined below, but the damage may also escape the repair systems [66–68]. Both nuclear (nDNA) damage and mitochondrial DNA (mtDNA) damage are particularly significant as it can interfere with replication to generate lasting mutations [63, 69]. Although mitochondria possess quality control systems that include antioxidant enzymes, mtDNA is more susceptible to oxygen damage than nDNA, possibly due to (a) lack of nuclear proteins associated with mtDNA, which could protect it from damage, (b) less elaborate and efficacious repair system than nDNA repair machinery, and (c) the proximity of the respiratory chain where ROS/RNS are continuously generated. Two theories attempt to explain the cause of DNA damage: by the first, the damage results from a site-specific Fenton reaction, that is, the generation of a hydroxyl radical in the reaction of transition metal ions present in DNA with H_2O_2 and by the second theory, OS increases intracellular calcium concentration, which in turn activates nucleases digesting DNA [70, 71]. Reactions causing DNA damage and their breakdown products are a multitude exemplified by (a) lesions generated by ½ O as nitrogen modifications in DNA bases, in preference guanine, producing 8-oxo-7,8-dihydroguanine (8-oxoG) and (b) $^{\bullet}$OH that adds double bonds and abstracts a H atom from methyl groups in DNA bases, producing molecules as 5-hydroxymethyl-uracil, C8-OH-adduct guanine radical, and 8-hydroxyguanine; $^{\bullet}$OH targeting C atoms of DNA sugar moiety by abstracting a H from each C–H bond of 2′-deoxyribose, generating various molecules, as 2-deoxypentose-4-ulose, 2-deoxypentonic acid lactone, erythrose, 2-deoxytetradialdose, and glycolic acid [72, 73]. In complex, the above lesions cause base and tandem base modification, leading to DNA intrastrand crosslinks, DNA-protein crosslinks, mismatched pairs with damaged bases, stalled DNA replication forks, clustered lesions, and single- and double-strand breaks (SSB-DSB). SSB are due to modified DNA bases and abasic sites, apurinic/apyrimidinic sites, caused through purine and pyrimidine base damage as well as sugar moiety damage. SSB are the most common lesions that result from genotoxic insults by endogenous ROS [17]. Electrophilic molecules or intrinsic DNA instability or inhibition of topoisomerase, which traps cleaved DNA intermediates, may cause SSB. If not repaired, the damaged site may be bypassed by incorporating a mismatched deoxynucleotide during DNA replication. Many oxidative base lesions in DNA are mutagenic, provoking structural alterations, including transversions: G/T or A/C, or overall conformational changes, which may affect transcription and/or replication processes, leading to chromosome deletions with lethal effects. The most common base oxidations 8-oxoG mispair with adenine (8-oxo-G:A) and 5-hydroxycytosine with thymine thus causing replication stress. The accumulated lesions lead to pathological processes, as they result cytotoxic by causing mitochondrial

dysfunction, mutagenic by causing genetic instability, and finally oncogenic. Also, the marker of inflammation 8-nitroguanine is considered a potential mutagenic [74]. A key cellular response to oxidative damage is the signaling through the JNK pathway. Depending on intensity and duration of the damage signal, this pathway leads to distinct alternative responses including DNA repair, antioxidant production, or cell death. When damage overcomes cell repairing systems, the damage signal (i.e., excessive ROS and products) drives JNK pathways toward proliferation arrest and or cell death that both play a fundamental role in cell homeostasis maintenance. These responses are highly relevant to cancer therapy, as tumors are often under OS that produces elevated JNK levels, and therapy often involves inducing DNA damage with the intention of driving cell death [75]. Generally, oxidative DNA damage is enhanced in tumors where increased metabolism, oncogenic signaling, and mitochondrial dysfunction produce 100-fold more 8-oxoG than in healthy tissues. Inflammation promotes carcinogenesis and generates ROS in tumor cell and its microenvironment that add to a high level of spontaneous DNA base deaminations. A consequent base mispairing is generated that is potentially mutagenic if not rapidly and efficiently repaired. Ever increasing ROS levels lead cells to death (apoptosis). This feature is exploited to exert therapeutic effect against cancer by therapy tailored to augment cellular ROS level. Oxidative damage is believed a potential double-edged sword in cancerogenesis and ROS-based anticancer. Although at low and moderate levels, ROS affect some of the most essential mechanisms of cell survival such as proliferation, angiogenesis, and tumor invasion, at higher levels, these agents can expose cells to detrimental consequences of OS including DNA damage and apoptosis that result in therapeutic effects on cancer. Understanding the new aspects on molecular mechanisms and signaling pathways modulating creation and therapy of cancers by ROS is critical in the development of therapeutic strategies for patients suffering from cancer [30, 76]. Antioxidants protect against genotoxic agents and alleviate their effects by decreasing primary DNA damage that reduces risk of mutation and tumor initiation. ROS enhances the localization of metallothionein (MT) in the nucleus where MT is more efficient than the reduced glutathione in protecting DNA from ROS attacks [76, 77]. The enzyme human mutT homolog detoxifies oxidized nucleotides thus potentially preventing 8-oxoG-induced mutations. It particularly eliminates 8-oxo-7,8-dihydro-2′-deoxyguanosine triphosphate that detoxifies oxidized nucleotides through its pyrophosphatase activity which is a potential target in cancer therapy [78, 79] (Figure 2).

2.6. DNA Repair in Oxidatively Damaged DNA. Cells have evolved several DNA repair pathways to deal with DNA damaged by OS that sense DNA lesions and process them into appropriate structures for DNA damage response (DDR) activation. DNA lesions and corresponding repair mechanisms have been reviewed by Curtin [17] and Chatterjee and Walker [80]. A part from the simplest form of DNA repair that is the direct reversal of the lesion, the cells are equipped with a variety of distinct, although partially compensatory, DNA repair mechanisms, each addressing a specific type of lesion. There are multiple types of DNA damage in humans as well as distinct but interrelated DNA repair mechanisms. Dysregulation of the mechanisms plays a key role in cell genomic instability. Among the repair pathways, tolerance mechanisms are also comprised as the translesion synthesis (TLS) that is composed by specialized DNA polymerases and regulatory proteins able to confer viability in the presence of unrepaired damage. Examples of the most common mechanisms to repair oxidatively damaged DNA regard the repair of modified bases by direct repair and base excision repair (BER) [81, 82], base mismatch repair by mismatch repair pathway, intrastrand crosslinks (ICL) by a complex repair that involves Fanconi anaemia pathway (FA), nucleotide excision repair (NER) [83, 84], TLS and homologous recombination (HR) [85], DNA-protein crosslinks by ICL repair and NER, stalled replication forks by HR, NER, and FA, single-strand breaks (SSB) by BER and HR, double strand breaks (DSB) [85, 86] by HR, and nonhomologous end joining (NHEJ) [87, 88]. The most deleterious lesions produced by many chemotherapeutic agents that block replication and transcription are represented by ICLs. NHEJ is thought to be the primary means of repair for therapeutically induced DSBs resulting from ROS-inducing anticancer treatments. Selective DNA repair inhibitors are considered efficacious in cancer therapy with minimal host toxicity [89–91] (Figure 2).

3. DNA Damage Response (DDR)

The exogenous and endogenous insults upon human DNA result in accumulation of DNA damage that alters the chromatin environment besides increasing the mutagenic and immunogenic properties of the DNA [92–94]. The overall alterations possibly lead to physiological processes as aging and senescence or impact health and modulate disease states [95–97]. DNA damages induce and coordinate a complex signal-transduction network composed by several pathways, collectively named DNA damage response (DDR), that connects the DNA damage signaling to the cell cycle checkpoints maintaining cell homeostasis and functions while the damage is repaired. DDR prevents DNA duplication, cell division, and cell cycling, by arresting transcription process, to preserve genome stability and promote cell survival in front of both reparable or irreparable lesions [98]. If the damage is severe and irreparable, the cell cycle arrest is followed by cell death programs (apoptosis/necrosis) or senescence that eliminate damaged cells and avoid their multiplying. DDR initiates through phosphorylation-driven signaling cascades that sense the DNA damage, being regulated by mediators, and activate downstream effectors that finally determine the cell fate. It has been evidenced a set of 450 genes encoding proteins integral to DDR, among which a "core" group of proteins acts in different steps with some overlapping functions: (a) specialized "sensor proteins" detecting the damage; (b) transcription factors proceeding as "transducer proteins" upon their activation; and (c) "effector proteins" that are recruited by mediators. Other proteins organize and regulate a spectrum of processes that integrate DDR with the cell cycle

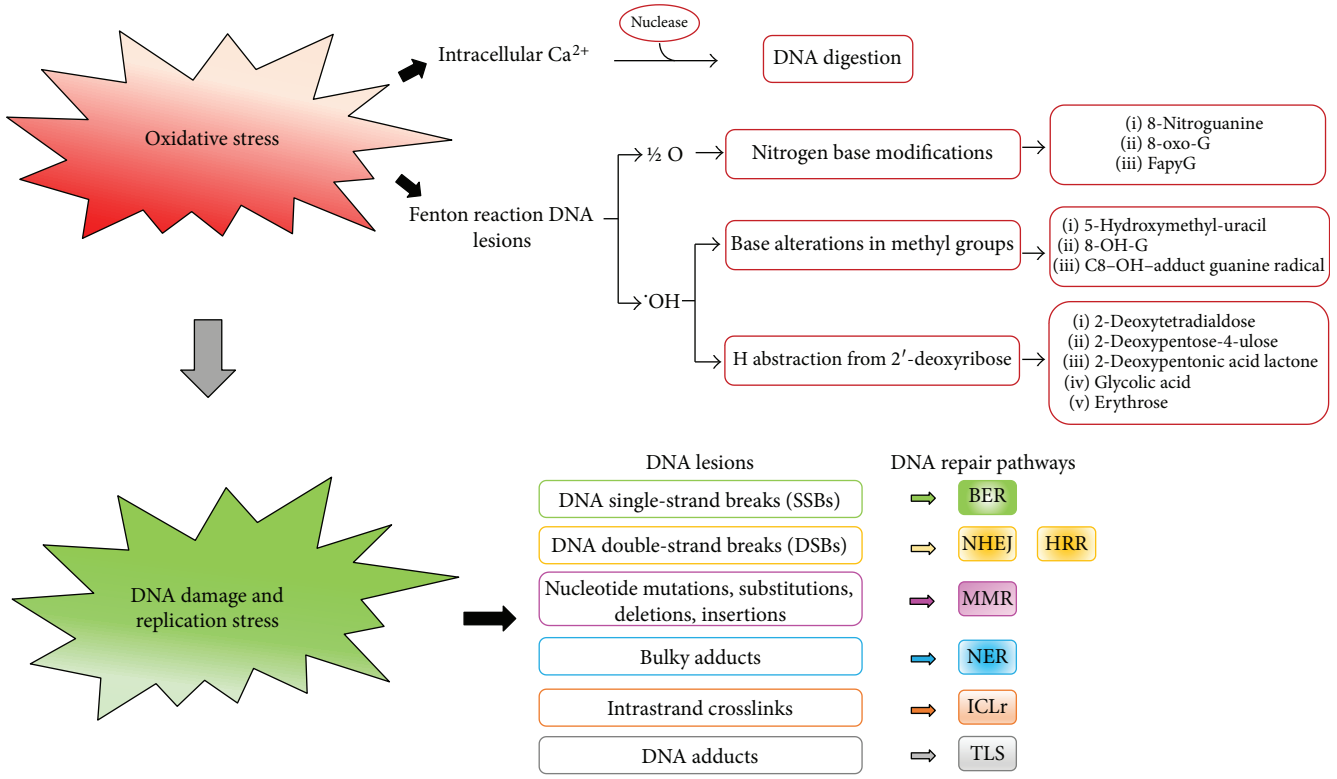

Figure 2: Oxidative stress (OS) causes DNA damage with consequent activation of DNA repair pathways. OS induces DNA damages by two major reactions: increase of the intracellular calcium levels, activating DNA digestion, and Fenton reaction. DNA damage triggers the main DNA repair pathways: BER: base excision repair; NHEJ: nonhomologous end joining; HRR: homologous recombination repair; MMR: mismatch repair; NER: nucleotide excision repair; ICL: intrastrand crosslink; TLS: translation synthesis.

progression allowing for the DNA repair [99, 100]. Each step in DDR is tightly regulated by reversible posttranslational modifications including phosphorylation, ADP-ribosylation, methylation, acetylation, ubiquitylation, sumoylation, and neddylation. Oxidatively induced DNA damage results in robust activation of three protein kinases that belong to the phosphatidylinositol-3-kinase- (PI-3-kinase-) related kinases of the PI-3-kinase/Akt pathway: (i) ataxia telangiectasia-mutated kinase (ATM); (ii) ATM- and Rad3-related kinase (ATR); and (iii) DNA-dependent protein kinase catalytic subunit (DNA-PKcs). The kinases are central components in DDR triggering and act together with the DNA repair machinery to maintain cell genome integrity [101–103]. ATM and ATR are activated through auto-phosphorylation as apical regulators of the response to DSBs and replication stress, respectively, with overlapping but nonredundant activities. A functional crosstalk between the major ATM/ATR pathways controls and coordinates DDR by affecting DNA replication, DNA repair, DNA recombination, mRNA transcription, and RNA processing, as well as protein metabolism and cell cycle. DNA-PKcs interacts with the DNA-binding Ku 70/80 heterodimer to originate the DNA-PK complex, a key regulator in NHEJ pathway that repairs the DSB damage. The first signal transduction wave is conducted by ATM/ATR phosphorylation that acts as DNA damage sensor and transducer. ATM activation is mediated through the Mre11-Rad50-NBS1 (MRN) complex that binds ATM through multiple protein-protein interactions, recruits ATM to DNA lesion as inactive dimer, and unwinds DNA ends to activate ATM. The complex MRN-ATM is located at the damaged DNA foci marked by histone γ-H2AX that is phosphorylated by the complex and regulates various downstream mediators to coordinate the DDR. Despite their distinctive individual activities, ATM, ATR, and DNA-PKcs share many overlapping substrates and roles in the regulation of the cell cycle checkpoints as primary or secondary responders to several DNA lesions. Upon their activation, ATM/ATR phosphorylate the checkpoint kinases CHK2 and CHK1, respectively, that acting as effector proteins, and phosphorylate the A, B, and C isoforms of the Cdc25s phosphatases. The phosphatases lead to inactivate cyclin-dependent kinases (CDK) and arrest cell cycle either at G1/S or G2/M transition, depending on which CDK is inhibited. CHK1 has a double role in CDK1 inactivation, by directly inhibiting Cdc25 and activating the tyrosine kinase Wee1, which specifically inhibits CDK1. Cdc25s control the cell cycle via specific checkpoints in physiological conditions as well as in response to DNA damage. These phosphatases transmit the damage signaling to effectors such as the tumor suppressor p53, a key molecule interconnecting DDR, cell cycle checkpoints, and cell fate decisions in the presence of genotoxic stress; p53 leads to cell cycle arrest or senescence or apoptosis depending on the damage extent and the cellular context. Inactivating mutations in TP53 gene and other genes involved in DDR potentiate cancer development and influence cancer cell sensitivity to anticancer treatments [21]. A

novel genomic stress sensor in the DDR pathway is the AMP-activated protein kinase (AMPK) that is physically associated with the mitotic apparatus and participates in cytokinesis. AMPK has been previously known as a metabolic stress sensor, able to control cellular growth and mediate cell cycle checkpoints in cancer cells in response to low energy levels. AMPK is a key effector of the tumor suppressor liver kinase B1 (LKB1), which inhibits the cell growth mediator mammalian target of rapamycin (mTOR) and activates checkpoint mediators such as p53 and cyclin-dependent kinase inhibitors p21 (cip1) and p27 (kip1). Ionizing radiation and chemotherapy activate AMPK in cancer cells to mediate the signal transduction downstream of ATM that activates p53-p21 (cip1)/p27 (kip1) and inhibits mTOR. AMPK works as a convergence point of metabolic and genomic stress signals, which (i) controls the activity of growth mediators, (ii) propagates DDR, and (iii) mediates the antiproliferative effects of common cytotoxic cancer therapy such as radiation and chemotherapy. This highlights the importance of targeting AMPK with novel cancer therapeutics [104]. Also, it is worthwhile mentioning that the Wnt/beta-catenin signaling pathway, which is pivotal for modulating cell fate, proliferation, and apoptosis, can activate oxidatively induced DDR by regulating various proteins as histone γ-H2AX, p16INK4a, p53, and p21 [105]. Irreparable DNA lesions trigger elimination of damaged cells by apoptotic pathways like the autophagy form named "mitophagy" that leads to lysosomal degradation of damaged mitochondria [106, 107]. ATM links DDR to mitophagy induction by activating the LKB1/AMPK pathway, which in turn activates TSC2 by phosphorylation, thereby inhibiting mTORC1 and removing its inhibitory effect on mitophagy. Since autophagy contributes to clearing the cells of all the irreversibly oxidized biomolecules, it might be included both in the antioxidant system and the DNA damage repair system. Interestingly, it has been recently shown that some DNA repair enzymes can also activate and regulate the autophagy process [108, 109]. The indicated DDR pathways are involved in repairing oxidative DNA damage in healthy as well in cancerous cells, although following a different organization. Cancer cells frequently show several mutated molecules that lead to a reduced DDR activity thus facilitating the generation of further mutations and enhancing the cancer progression. Understanding the mechanism by which DDR is regulated under genotoxic stress should help improving the clinical outcomes [21] (Figure 3).

4. ROS-Sensitive Proteins Involved in DDR

Since when Rotman and Shiloh firstly proposed that ATM may act as a direct sensor and responder in cell OS and damage, accumulating body of studies has been reported. Attention is now focused on identifying the molecular contributions of ATM, ATR, and DNA-PKcs in the interplay between the DDR mechanism and the redox asset that comprehends the redox signaling, besides the oxidative DNA damage generated during the OS conditions [110, 111]. Indeed, several oxidative reactions contribute to redox signaling through finely modulating DDR at different levels, a part from causing oxidative genotoxic lesions. Interestingly, many proteins involved in DDR are endowed with a high number of cysteine residues (indicated in parenthesis) as exemplified by Chk1 (9), Wee1 kinase, a specific CDK1 inhibitor (12), Chk2 (13), Plk1 that allows cell cycle progression recovery after its arrest (13), and caspase 2 that is involved in apoptosis and is inhibited during G2 arrest by Chk1 (18). These ROS-sensitive proteins undergo modifications in their structure and function through cysteine residue oxidation and disulfide generation depending on the cellular ROS levels. In addition, some of these proteins activate pathways as p53 and p21 pathways, which finally lead to cell ROS level regulation. Through this loop mechanism, ROS contribute both to maintain the cell redox equilibrium and calibrate the DDR reactions [21, 112]. ATM is an OS-sensitive protein in which specific cysteine residues originate interprotein disulfides in human cells, upon being oxidized by ROS, thus resulting as an active homodimer. ATM is also activated through phosphorylation, as previously mentioned. The substrates phosphorylated by ATM are different following the MRN- or the OS-dependent activation, suggesting a different substrate specificity in the two conditions. While ATM phosphorylation initiates DDR in the nucleus, disulfide homodimer activates specific transcription factors in the cytosol, thereby leading to induction of antiapoptotic and prosurvival proteins. Through ATM activation, ROS lead to the recruitment of important proteins involved in DDR, including γ-H2AX histone and p53. The roles and localizations of ATM might be due to the presence of separate pools or ways of activation of ATM, or both the conditions that differently sense the cellular ROS levels. As very often OS and DNA damage overlap, the above conditions might collaborate in protecting the damaged cells from apoptosis while their DNA is repaired. It is difficult to discover the degree of overlap between substrates that are phosphorylated by ATM following DNA damage and substrates that are phosphorylated during OS, because the two ATM activities are usually exposed to both the conditions simultaneously. For instance, in anticancer treatments by ionizing radiations, both ROS production and DSB lesions are induced. The roughly 700 ATM targets that have been evidenced by a proteome analysis as probable targets in both DNA repair and oxidation pathways highlight a complicated interplay between oxidized ATM and DSB-activated ATM. The targets are mostly comprised of proteins involved in DNA replication, repair, and cell cycle control, as well as proteins affecting insulin signaling. This suggests that ATM may also function through regulation of metabolic signaling. In conditions that separate DNA from OS damage effects, only a subset of ATM targets that are usually phosphorylated in DDR is also phosphorylated in OS conditions. Now, ATM inhibitors of DDR mechanism are investigated as inhibitors of ATM redox functions. An ATM variant has been identified that is not activated by oxidation while is competent in DNA repair [81, 111, 113]. Interestingly, ROS may activate ATM independently of MRN, indicating that the OS-activated form has a primary role in redox sensing and signaling that may precede DNA damage and does not depend on it. Thus, MRN is not essential for ATM activation by OS, as the ATM pathway may also act separately from the DDR machinery. Evidences are

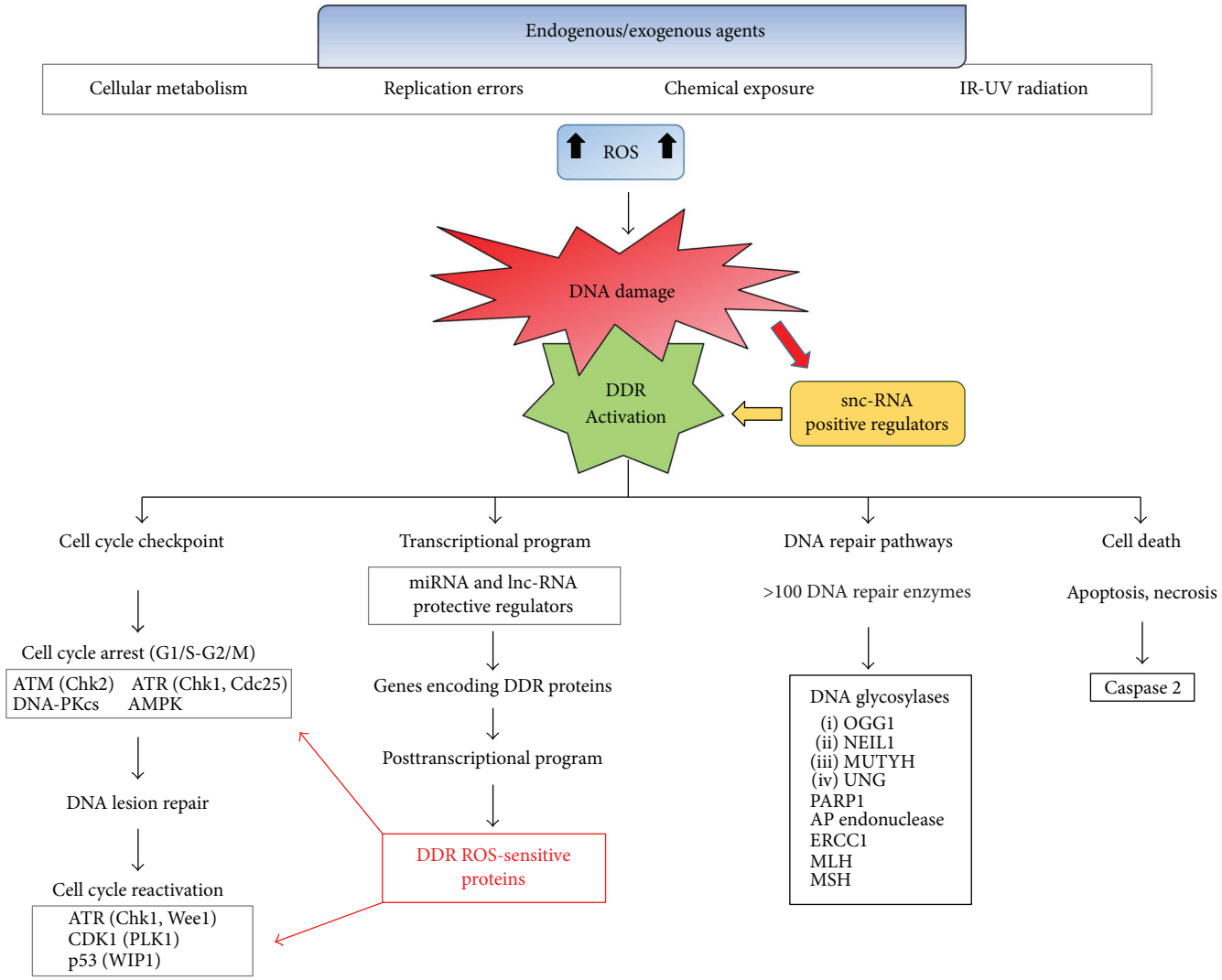

Figure 3: Reactive oxygen species (ROS) generated by endogenous and exogenous agents cause DNA damage and activation of DNA damage response (DDR). DDR activation arrests the cell cycle progression to repair DNA lesions and activate a program encoding ROS-sensitive proteins involved in DDR. ATM, ATR, DNA-PKs, AMPK, Chk1, and Chk2 represent the sensors and transducers that coordinate DDR. Their signals converge on effectors, as tumor suppressor p53, Cdc25 protein phosphatase, and WEE1 tyrosine kinase. DNA repair pathways occur by several DNA repair enzymes such as DNA glycosylases, PARP1, AP endonuclease, ERCC1, MLH, and MSH. DDR triggers apoptosis or necrosis when the DNA damage cannot be repaired. DDR-targeted proteins, whose inhibitors are currently in clinical trials, are indicated in bold. snc-RNAs = small noncoding RNAs; lnc-RNAs = long noncoding RNAs; ATM = ataxia telangiectasia-mutated protein; ATR = ATM- and Rad3-related; AMPK = AMP-activated protein kinase; CDK = cyclin-dependent kinase; DNA-PKcs = dependent protein kinase catalytic subunit; PLK1 = polo-like kinase 1; WIP1 = wild-type p53-induced protein 1; PARP = poly (ADP-ribose) polymerase; AP endonuclease = apurinic/apyrimidinic endonuclease; MLH = MutL homolog; MSH = MutS homolog.

known in which OS activation of ATM occurs in the absence of DNA damage, and OS inhibits ATM activation by MRN through disrupting the MRN-DNA complex [111]. This suggests that the only OS-activated ATM may operate under conditions of high ROS concentrations, playing a protective defense against the oxidative damage. Indeed, ATM deficiency is associated with elevated ROS, and $ATM^{-/-}$ cells are more vulnerable to ROS-mediated OS, in comparison to normal cells [81]. Moreover, ATM inhibition enhances the sensitivity to the radiation therapy that generates ROS in cancer cells. The question is posed whether ATM may regulate global cellular responses to OS. Interestingly, ATM is activated in response to excessive ROS accumulation in vessels where it stimulates the neoangiogenesis of the endothelial cells by acting as a proangiogenic protein. The event is not due to defects in DDR pathway, since it is realized through a different signaling pathway from DDR, that is, the oxidative activation of the mitogen-activated p38α kinase. It is suggested that the pathological proliferating processes might require the ROS defensive system induced by OS activation of ATM. Targeting ATM might suppress tumor angiogenesis and enhance the effect of antitumor ROS-producing therapies. While loss of the activity of MRN-activated ATM may enhance the mutagenic effects of

anticancer treatments and hamper the DDR barrier against tumorigenesis, the inhibition of the OS-activated ATM activity, which mediates oxidative defenses, might be efficacious in controlling malignant cell growth. The targeting of a cysteine residue that is crucial to the ATM activation by OS is believed a potential therapeutic strategy [21, 114]. Another important finding that demonstrates the interplay between ATM and OS is the ATM requirement for the ROS-mediated repression of mTORC1 [115, 116]. In response to elevated ROS, ATM activates the TSC2 tumor suppressor through the LKB1/AMPK metabolic pathway in the cytoplasm to repress mTORC1 and induce autophagy. The pathway acts as a node that integrates cell damage response with key pathways involved in metabolism, protein synthesis, and cell survival. The ATM interactor protein, ATMIN, is involved in the OS-induced ATM activity together with the SUMO (small ubiquitin-related modifier) enzymes as downstream ROS effectors, for cell survival under OS state. Replacement of a SUMO enzyme with a variant fails to maintain activated the ATM-DDR pathway normally induced by H_2O_2. The kinase ATR is also sensitive to modifications of the redox asset, comprising modified O_2 supply and OS conditions. After being activated by replication inhibition during hypoxia conditions, ATR phosphorylates the Chk1 checkpoint signaling, p53, and histone γ-H2AX, activating the cell cycle arrest and the stabilization of stalled replication forks for allowing the subsequent reinitiation of the replication process [110, 112]. Similarly, the ATR-Chk1 checkpoint signaling is triggered by hyperoxic conditions in different in vitro models: human dermal HDF fibroblasts, human monocytes, lung adenocarcinoma cell line A549, and Xenopus egg extracts. In A549 cell line, the Chk1 checkpoint signaling is induced by ATR-mediated phosphorylation in an ATM-independent fashion, while in human monocytes, the ATM and ATR checkpoints are simultaneously activated by ROS-induced DNA damage. Moreover, the antioxidant lycopene, which is able to inhibit gastric pathologies related to oxidative DNA damage as 8-OH-G and DSBs, is also able to prevent ATM and ATR actions induced by ROS in gastric epithelial AGS cells. In summary, OS-activated ATR may precede OS-activated ATM operations showing that OS conditions affect the ATR and ATM interplay in the DNA repair pathways. How ATM and ATR checkpoint pathways regulate each other in response to OS remains to be elucidated [110, 112]. The DNA-PKcs mentioned as basic DDR actors are activated through their auto-phosphorylation by ROS accumulation and stimulate a series of reactions in signaling events typically triggered by OS, similarly to ATM. DNA-PKcs play a direct role in repairing oxidative DNA lesion through the BER repair pathways, although their mechanism in response to OS has to be clarified. Investigations are developing to determine roles and coordination between ATM and DNA-PKcs in OS signaling and oxidative DNA damage repair under both physiological and pathological conditions. This knowledge might offer new possibilities for the treatment of ROS-related diseases, including cancer [110, 111]. Among ROS-sensitive proteins in DDR, Cdc25 phosphatases (Cdc25s) and the checkpoint kinases CDKs are regulated by the intracellular redox milieu. The balance between kinase and phosphatase activity determines the strength of PI-3-kinase/Akt signal that may be modified through favoring kinase or phosphatase activity. Oxidations cooperate with DDR signals to activate kinases and inactivate phosphatases thus favoring the DNA repair. Cdc25s are direct OS targets since oxidation of cysteine residues in their active sites creates intramolecular disulfides causing the enzyme inactivation; thereby the cell cycle is arrested until favorable reducing conditions are restored. Cdc25s are inactivated by both oxidation and phospho-degradation. While oxidation is rapidly reverted, the phospho-degradation implies protein synthesis to be reverted. An oxidizing environment may increase the ratio between Cdc25 oxidation versus Cdc25 phospho-degradation, rendering the mitosis reenter easier and ultimately pushing cells toward proliferation. Cdc25s are overexpressed in tumor cells, which are generally endowed with a prooxidant environment, thus providing a mean for escape from the G2 arrest induced by the DNA damage [117, 118]. Another molecule that acts as OS sensor and cooperates with DDR is the tumor suppressor PTEN, protein tyrosine phosphatases, whose gene results one of the most frequently mutated genes in human cancers. PTEN exerts its tumor suppressor activity by regulating cell growth and survival through negative modulation of the P13-kinase/Akt signaling pathway. PTEN loss and/or inactivation causes abrogation of the checkpoint functions that control the cell cycle thus impairing DNA repair and genomic stability of the cells. Accumulation of DNA lesions and mutations causes tumor promotion. PTEN is inactivated by ROS through formation of an intramolecular disulfide bond between two cysteine residues that involves the protein active site. The inactivated PTEN induces a signal pathway that begins from Akt activation through phosphatidylinositol 3,4,5-trisphosphate, the PTEN physiological substrate, and terminates in the activation of antioxidant enzymes, possibly being an adaptive response to an oxidizing environment. The oxidized asset generally present in cancer cells may inactivate PTEN activity and, at the same time, allow for ROS acting as tumor promoters [118, 119]. A functional interplay between DDR pathways and DNA repair pathways occurs in response to OS, as DDR pathways not only arrest cell cycle progression but also directly participate in and facilitate DNA repair pathways. DNA repair proteins may sense oxidative DNA damage and process the damage into appropriate structures for DDR activation. In conclusion, DDR and redox environment exert a subtle reciprocal interaction, since enzymes participating to DDR are modulated by redox alterations and in turn act to modulate the redox equilibrium. A link between OS and PI-3-kinase/Akt pathway occurs in healthy as well as in cancer cells in which represents an advantage to the tumor survival [120, 121]. More intense investigations need to understand the interplay between ATM/ATR-mediated DDR pathways and DNA damage tolerance pathways in OS response. It is unclear how ATM-Chk2 and ATR-Chk1 pathways crosstalk with each other in response to OS. The new insights into ATM, ATR, and DNA-PKcs roles are a stimulus to identify points that may be redox regulated thus offering possibilities to treat ROS-related pathological conditions and diseases [25, 28].

5. Targeting DDR in Cancer Therapy

Anticancer treatments primarily target DNA damage, both directly and indirectly, in consideration of its role in malignant transformation and related consequences [15, 16]. The potential existence of distinct DNA damage thresholds at various stages of tumorigenesis and the role of the DDR pathway in human cancers are developed by Khanna [97]. DDR is rapidly induced, highly controlled, and regulated in cancer cells as in healthy cells suggesting the possibility of targeting definite DDR steps to hamper the cancer cell growth. The overall proteins of the DDR machinery may provide targetable intervention points for modulating DDR. It is worthwhile noticing that DDR protects and promotes cancer cell survival through restoring their reparable lesions, also when they are induced by DNA-targeted interventions. This event represents a main route to generate resistance against a genotoxic treatment. Dysregulation of DDR through missing or defective canonical pathways in the DNA repair mechanisms can lead to genomic instability that is a fundamental hallmark of cancer. Defective pathways may be eventually compensated for other DDR pathways generating a context, which highly favors cancer and resistance to genotoxic therapies [17]. Indeed, only cancerous tissues, but not healthy tissues, lack DDR components that render them dependent on the remaining compensatory DDR pathways. These compensatory pathways allow for cancer cells surviving in the ROS and replicative stress conditions that are present in cancer tissues. Since the event is cancer-specific, strategies that target compensatory DDR pathways may render a treatment-induced DNA damage more cytotoxic and preferentially eliminate cancer cells, while minimizing the impact on healthy cells. DDR inhibition has become an attractive therapeutic concept in cancer therapy, also for preventing or reversing the resistance to the anticancer treatments. [18, 122–126]. Indeed, dysregulated DDR is exploitable by both ordinary therapy and DDR inhibitors. While upregulated DDR confers resistance to DNA-damaging interventions and has to be inhibited to overcome such refractoriness, downregulated DDR makes tumor more susceptible to specific therapies and DDR inhibitors. In each single patient, the balance between the DNA damage induced by a genotoxic treatment and the consequent DDR is responsible for the effectiveness of the treatment. DNA repair-targeted therapies exploit DNA repair defects in cancer cells to generate their death resulting from simultaneous loss or inhibition of two critical functions. For example, cancer cells defective in one DNA repair pathway rely on alternate repair pathways, if inhibition of a second repair pathway occurs then results in cell death, an effect that selectively targets repair-deficient cancer cells [127–130]. This type of intervention, called synthetic lethality, is actually administered not only to selectively inhibit DDR in cancer cells with deficiencies in DNA repair pathway(s) but also to enhance chemotherapy and radiotherapy efficacy. A number of highly selective inhibitors that inhibit DNA repair pathways are in preclinical development, while others are clinically administered as DDR-targeted therapies in different stages of clinical evaluation. Poly (ADP-ribose) polymerase (PARP) inhibitors (PARPi) are the first clinically approved drugs designed to exploit synthetic lethality in cancer therapeutics that are clinically administered as DDR-targeted therapies to inhibit DNA repair pathways [131, 132]. PARPs are a family of DNA-dependent nuclear enzymes catalyzing the transfer of ADP-ribose moieties from cellular nicotinamide-adenine-dinucleotide to several proteins. This posttranslational modification is involved in cell response to DNA lesions, including DNA damage recognition, signaling, and repair as well as localized replication and transcriptional blockage, chromatin remodeling, and cell death induction. PARPs interact directly/indirectly, or via PARylation with oncogenic proteins and transcription factors, regulating their activity and modulating the carcinogenesis. For instance, PARPs regulate transcription factor-4 (ATF4) responsible for MAP kinase phosphatase-1 (MKP-1), which regulates MAP kinases. Very recent studies show that OS induces DNA breaks and PARP-1 activation causing mitochondrial ROS production and cell death. At the same time, PARPi reduce ROS-induced cell death, suppress mitochondrial ROS production, and protect mitochondrial membrane potential on an ATF4/MKP-1 dependent way, which inactivate JNK- and p38 MAP kinases. JNK is involved in the development of cancer stem cell, while JNK inhibition reduces the stem cell ability in tumor initiating. This could be a novel mechanism contributing to beneficial PARPi effects in combinatory cancer therapy with ROS-modulating drugs [133]. New therapeutic drugs such as PARPi are examples of DDR-targeted therapies that could potentially increase the DNA damage and replication stress imposed by platinum-based agents in tumor cells and provide therapeutic benefit for patients with advanced malignancies [134]. Indeed, many therapies are less effective by using one anticancer drug only, due to refractory properties and drug resistance in advanced cancers. A consensus is that anticancer drug cocktails might better control cancer progresses and metastasis than single drug therapeutics in clinical trials, but the complexity of drug combinations is still a challenge [135]. Investigation on cell cycle checkpoint signaling through ATM/ATR and pathways involved in cancer onset and progression has led to discover potent and selective ATM/ATR inhibitors that are actually in preclinical and clinical development, respectively. Experimental data have provided a strong rationale for administering ATR inhibitors (ATRi) since they cause synthetic lethality in cancers characterized by deficiency of certain DDR components. ATRi are assessed in clinical trials both as single agents and in synergy with various chemo- and radiotherapy therapies, including platinum, PARPi, and immune checkpoint inhibitors [17, 124, 126]. Preclinical data highlight the chromatin-bound phosphatase 2C isoform delta (WIP1) as potential target in human cancer. WIP1 is ubiquitously expressed at basal levels and is potentiated by p53. It acts as a strong negative regulator of p53 pathway thus forming a negative feedback loop that allows for terminating p53 response when DNA repair is completed. Genotoxic stress strongly induces WIP1 in cell lines in a p53-dependent manner (the WIP1 name refers to wild-type p53-induced protein 1). The substrate specificity of WIP1 matches the sites phosphorylated by ATM as p53, γH2AX, and other DDR proteins. When

overexpressed, WIP1 impairs p53 function and contributes to tumorigenesis, usually in combination with other oncogenes. WIP1 loss delays tumor development in mice, allows reactivation of p53 pathway, and inhibits proliferation in tumors endowed with p53. WIP1 is selectively inhibited by the small-molecule GSK2830371 that efficiently reactivates p53 pathway in various cancer types. In combination with DNA damage-inducing chemotherapy or with MDM2 antagonists (such as nutlin-3), WIP1 inhibition promotes cancer cell death or senescence, while healthy cells with basal WIP1 expression are relatively resistant to its inhibition [136].

6. Combinatory Anticancer Strategies Affecting ROS Levels

Most conventional chemo- and radio-therapeutic agents kill cancer cells in patients during cancer therapy by stimulating ROS generation as, at least, one part of their mechanisms of action [137]. ROS-inducing anticancer agents target mitochondria and enzymes in redox pathways resulting in OS conditions that lead to cancer cell death. The mode of cell death depends on the severity of the oxidative damage. Other major mechanisms of these anticancer agents inhibit or disable specific redox pathways and deplete reduced glutathione (GSH) [138]. It is believed that continuous investigations will allow the development of drug combinations for therapies better tailored to patients that cause fewer side effects and drug resistance [139]. Many cancer types may develop strong antioxidant mechanisms and maintain higher ROS levels than normal cells, but, at the same time, excessive OS levels may have tumor-suppressive effects [140]. This aspect offers an interesting therapeutic window because cancer cells might result more sensitive than normal cells to agents that cause further ROS accumulation. Examples of drugs with direct/indirect effects on ROS that are effective in cancer therapies are exemplified in the following sections in combination with DDR inhibitors, basing on the drug function in the cells. For better consulting of the drug combination, Table 1 shows combinatory therapies basing on the DDR target in the cells. Among the vast array of therapies, a single reference is reported either in brackets or as clinical trial number from https://clinicaltrials.gov/ (a database of privately and publicly funded clinical studies conducted on cancer patients).

6.1. DDR Inhibitors and Alkylating-Intercalating Drugs (Combinatory Therapies). Therapies based on platinum coordination complexes (Pt-CC) as cisplatin (cDDP) [141–143], carboplatin (CarboPt) [144], and others, as well as therapies based on anthracyclines like doxorubicin, generate extremely high ROS levels, which may cause tumor cell death by apoptosis but also intolerable therapeutic side effects in the patients. cDDP is an alkylating DNA-damaging agent widely used as anticancer drug. It induces ROS via NADPH oxidase (NOX) and involves, inter alia, the activation of Akt/mTOR pathway, which is regulated by NOX-generated ROS [142, 145]. The combination of a large number of DDR inhibitors with Pt-CC impairs the defensive response of tumor cells against the Pt-CC-induced OS. For instance, the synergy between cDDP and PARP inhibitors (PARPi) that hampers the DNA damage repair may sensitize tumor cells to Pt-CC-induced OS. These combinatory therapies not only generate DNA damage foci and mitochondrial membrane damage in non-small cell lung cancer cells (NSCLC cell line) but also allow for reversing the resistance to the cDDP when it is administered as single agent. Olaparib or veliparib (PARPi) administration with Pt-CC is highly promising in different phases of clinical trials against some cancer types. Olaparib and cDDP administration in combination with radiation therapy (RT), which induces a substantial increase in ROS levels through NOXs activation [146], has been tested in advanced non-small cell lung cancer (NSCLC) (http://clinicaltrials.gov identifier: NCT01562210). In cancer treatments unsuitable for Pt-CC-based therapy as the oesophageal cancer, olaparib has been administered in combination with RT (http://clinicaltrials.gov identifier: NCT01460888). Veliparib and temozolomide [147] have been used to prevent repair processes following the ROS damage generated by CarboPt and paclitaxel [148] in metastatic breast cancer (http://clinicaltrials.gov identifier: NCT01506609). Rucaparib (PARPi) has been administered with CarboPt to advanced solid tumor patients (http://clinicaltrials.gov identifier: NCT01009190). A WEE kinase inhibitor, acting in the DDR mechanism, has amplified the oxidative damage induced by CarboPt, along with other cell killing actions, (http://clinicaltrials.gov identifier: NCT02087176). The compound MCI13E, which inhibits the replication protein A in the DDR mechanism, has also been tested preclinically in combination with cDDP [149]. A negative effect has been observed in the combinatory therapy between B02IR (RAD51 inhibitor) [150] with cDDP and mitomycin C [151], in which the OS caused by cDDP and mitomycin C results aggravated by B021R. Preclinical combinatory therapies between drug-inducing ROS and DDR inhibitors to overcome the resistance to Pt-drugs in solid tumors comprehend cDDP, NU-6027 (ATR inhibitor) [152], and hydroxyurea [153], among others, which is able to induce $O_2^{\cdot-}$ production. The DDR inhibitor VX-970 (ATR inhibitor) sensitizes cancer cells to the combination of CarboPt and the anticancer drug gemcitabine [154], which generates ROS by NOX and via NF-κB activation in diverse cancer types (http://clinicaltrials.gov identifier: NCT02627443). Also, cDDP and gemcitabine have been administered with VX-970 against metastatic cancer (http://clinicaltrials.gov identifier: NCT02567409). Different DDR inhibitors, including ATM inhibitors, have been administered in combination with doxorubicin and other drugs to sensitize tumor cells to doxorubicin-induced OS and DNA damage [155, 156]. Doxorubicin induces oxygen-derived free radicals, particularly H_2O_2, through two main pathways: (i) a nonenzymatic pathway that utilizes iron and (ii) an enzymatic mechanism that involves the mitochondrial respiratory chain [157, 158]. Doxorubicin also inserts into DNA of replicating cells and inhibits topoisomerase II, causing double-strand DNA breaks and preventing DNA and RNA synthesis [159]. In conditions of DNA-PKcs inhibition, doxorubicin has been administered inside pegylated liposomes against advanced solid tumors (http://clinicaltrials.gov identifier: NCT02644278). Doxorubicin has also been

Table 1: DNA damage response (DDR) inhibitors in combination with ROS-inducing treatments for cancer therapy.

DDR target	DDR inhibitors	ROS-inducing treatments (direct/indirect mode of action)		References	Combinatory therapy Preclinical studies and clinical trials
PARP	Olaparib	Radiotherapy	OS increase by mitochondrial dysfunction	[146]	NCT01460888
		Cisplatin + Radiotherapy	ROS increase via NADPH oxidase	[141–143]	NCT01562210
			(♦)	(♦)	
		Cetuximab + Radiotherapy	Glutamine transport inhibition, GSH decrease	[163, 164]	NCT01758731
			(♦)	(♦)	
		Erlotinib	EGFR inhibition, ROS-mediated apoptosis	[173, 174]	[172]
PARP	Veliparib (ABT-888)	Temozolomide + Carboplatin + Paclitaxel	ROS increase, AKT–mTOR signaling disruption	[144]	NCT01506609
			ROS increase via NADPH oxidase	[147]	
			ROS induction	[148]	
		Bevacizumab	ROS and apoptosis increase	[165–167]	NCT02305758
		Rituximab	CD20 binding in B-lymphocytes, O_2^- generation	[170, 171]	[169]
		Auranofin	H_2O_2 and ROS increase by thioredoxin reductase inhibition	[191]	[192]
		Bortezomib	ROS increase by ER stress	[178, 180, 181]	[179]
		Lapatinib	ROS increases	[176]	[176]
		Berberine	OS/NOS decrease	[177]	[177]
PARP	Rucaparib	Carboplatin	(♦)	(♦)	NCT01009190
PARP	Niraparib	Bevacizumab	Cysteine and GSH level reduction	[165–167]	NCT02354131
	4-Iodo-3-nitrobenzamide	Buthionine sulphoximine	Inhibition of glutamate–cysteine ligase complex in GSH synthesis	[187–189]	[190]
RPA	MCI13E	Cisplatin	(♦)	(♦)	[149]
RAD51	B02IR	Mitomycin C + Cisplatin	Stress-mediated ER cell apoptosis by ROS generation	[151]	[150]
			(♦)	(♦)	
APE-1	Methoxyamine	Pemetrexed + Cisplatin	Mitochondrial dysfunction, ROS increase	[161]	NCT02535312
			(♦)	(♦)	
ATM	KU-55933	Radiotherapy	(♦)	(♦)	[155]
		Doxorubicin + Radiotherapy	ROS increase by enzymatic/nonenzymatic pathways	[157]	[156]
			(♦)	(♦)	
ATR	NU-6027	Cisplatin	(♦)	(♦)	[152]
		Hydroxyurea	Increased O_2^- production	[153]	[152]
	VX-970	Topotecan	ROS increase	[182]	NCT02487095
		Cisplatin + Gemcitabine	(♦)	(♦)	NCT02567409
			ROS increase, mitochondria alterations	[154]	
		Carboplatin + Gemcitabine	(♦)	(♦)	NCT02627443
			(♦)	(♦)	
DNA-PKcs	NU-7441	Etoposide	ROS increase, GSH depletion, mitochondrial alterations	[182, 183]	[185]
	KU-60648	Etoposide + Doxorubicin	(♦)	(♦)	[160]
			(♦)	(♦)	
	VX-984	Doxorubicin	(♦)	(♦)	NCT02644278
	UCN-01	5-Fluorouracile	Cellular $O_2^{\bullet -}$ increase	(♦)	NCT00045747
Chk1/Chk2	LY2603618	Pemetrexed	(♦)	(♦)	NCT00988858
		Cisplatin + Pemetrexed	(♦)	(♦)	NCT01139775
			(♦)	(♦)	

Table 1: Continued.

DDR target	DDR inhibitors	ROS-inducing treatments (direct/indirect mode of action)	References	Combinatory therapy Preclinical studies and clinical trials
	Prexasertib (LY2606368)	Cisplatin +	(✦)	(✦)	NCT02124148
		Cetuximab +	(✦)	(✦)	
		Pemetrexed + 5-Fluorouracile	(✦)	(✦)	
			(✦)	(✦)	
		Cisplatin + Radiotherapy + Cetuximab	(✦)	(✦)	NCT02555644
			(✦)	(✦)	
			(✦)	(✦)	

APE1 = AP endonuclease 1; ATM = ataxia telangiectasia-mutated protein; ATR = ATM- and Rad3-related; CHK = checkpoint kinase; DNA-PKcs = DNA-dependent protein kinase catalytic subunit; PARP = poly (ADPribose) polymerase; RPA = replication protein A. References in brackets; clinical trial identifiers (NCT). The effect of the single ROS-inducing drugs is indicated one time, and the following times is indicated with (✦).

combined with etoposide to concur with a dual inhibitor of DNA-PKs and PI-3K to kill tumor cells by causing, inter alia, mitochondria damage, GSH depletion, and ROS increase [160].

6.2. DDR Inhibitors and Folate Cycle Inhibitors (Combinatory Therapies). Pemetrexed (PMX) and 5-FU are folate cycle inhibitors that also promote cytochrome c release from mitochondria and interfere with the electron transport chain, resulting in $O_2^{\cdot-}$ radical production and cell death [161, 162]. A DNA-PKcs inhibitor has been combined to 5-fluorouracil (5-FU) to improve the survival of patients with a form of metastatic pancreatic cancer that is refractory to the anticancer drug gemcitabine (http://clinicaltrials.gov identifier: NCT00045747). The cell reparatory response to the injury caused by PMX and cDDP is prevented by the contemporary administration of methoxyamine, an inhibitor of the DNA repairing AP endonuclease 1, thus resulting in a major efficacy of the therapy (http://clinicaltrials.gov identifier: NCT02535312). Prexasertib (LY2606368) inhibits the Chk1 enzyme involved in the DDR mechanism and has been tested in combination with 5-FU or PMX, or other drugs, against advanced or diffuse metastatic cancer (http://clinicaltrials.gov identifier: NCT02124148). PMX has been administered with the DDR inhibitor LY2603618 (acting against Chk1-Chk2) (http://clinicaltrial.gov identifier: NCT00988858) and in combination with cDDP to improve the survival of patients bearing advanced NSCLC (http://clinicaltrials.gov identifier: NCT01139775).

6.3. DDR Inhibitors, Immuno-Oncology, and Targeted Agents (Combinatory Therapies). Immunotherapy is experiencing a growing interest as witnessed by the number of monoclonal antibodies that are administered in tumor patients as single agents or in combination with therapeutic interventions to prevent resistance to specific drugs. The monoclonal antibody cetuximab, which targets the epidermal growth factor (EGFR), has been combined with prexasertib (prevailing Chk1 inhibitor) or cDDP (http://clinicaltrials.gov identifier: NCT02555644) and the antifolates PMX or 5-FU, or other drugs (http://clinicaltrials.gov identifier: NCT02124148). Cetuximab downregulates the complex glutamine transporter ASCT2-EGFR in the cell membrane of non-small cell lung cancer cells (NSCLC cell lines). This causes that the glutamine necessary for the cellular GSH synthesis decreases, as well as the ROS reducing capacity of the cell. The consequent GSH reduction and OS trigger apoptosis independently of the EGFR-pathway downregulation [163, 164]. This increased sensitivity to OS has been exploited in association with the PARPi olaparib (http://clinicaltrials.gov identifier: NCT01758731). The monoclonal antibody bevacizumab, which causes cysteine and GSH level reduction and OS increase [165–168], has been administered together with the PARPi veliparib against metastatic colorectal cancer, and together with the PARPi niraparib against ovarian cancer (http://clinicaltrials.gov identifier: NCT02305758 and NCT02354131, resp.). The monoclonal antibody rituximab specifically binds to the CD20 antigen of B-cells, causing calcium influx into the cells and apoptotic signaling (reviewed in [167]). The antibody has been associated with veliparib against B-cell lymphoma [169]. In combination therapies, the proapoptotic process induced by rituximab often synergizes with the OS damage and $O_2^{\bullet-}$ production caused by traditional anticancer interventions [170, 171]. Regarding targeted agents administered in combinatory strategies, tyrosine kinase inhibitors (TKIs) can affect the cell redox equilibrium in cancer cell lines and cancer tissues when administered in association with DDR inhibitors [172–174]. For instance, erlotinib enhances ROS production and induces ROS-mediated apoptosis in NSCLC A549 cell lines, via activation of the JNK pathway, leading to epidermal growth factor (EGFR) inhibition [173, 174]. Furthermore, erlotinib causes Nox4-induced H_2O_2 production in head and neck squamous cell cancer (HNSCC) cell lines [175]. The association between the TKIs erlotinib and gefitinib is approved for non-small cell lung cancer (NSCLC) treatment in tumors with specific EGFR mutations (10–15% of Caucasian patients). The TKi lapatinib is the only TKI approved for treating the human breast cancer subtype overexpressing the HER2 oncogene (20–30% of breast cancers). Lapatinib in combination with ABT-888 (PARPi) augments the cytotoxicity to ABT-888 resulting in efficacious synthetic lethality in HER2-positive breast cancer cells in vitro and in vivo

[176]. Interestingly, the combination of lapatinib and the anticancer plant-derived berberine allows for reversing lapatinib resistance through the modulation of the ROS level [177]. In addition, a lapatinib analogue leads to ROS increase in the treatment of inflammatory breast cancer (reviewed in [167]). As a different example of targeted agents, bortezomib is the first ubiquitin-proteasome inhibitor approved as anticancer drug for human use [178]. This compound generates OS and aggravates the endoplasmic reticulum stress, causing apoptotic protein accumulation. Bortezomib has been proposed in association with ABT-888 (PARPi) [179–181].

6.4. DDR Inhibitors and Inhibitors of Topoisomerases I and II (Combinatory Therapies). Inhibitors of topoisomerases I and II, such as topotecan and etoposide, cause single- and double-strand DNA breaks which inhibit DNA function and ultimately lead to cell death. These inhibitors induce OS essentially by increasing the endoplasmic reticulum stress and the oxidative status, as revealed by increased lipid and protein oxidation and decreased GSH and sulfhydryl levels in cancer lines [182, 183]. Evaluation of the chemotherapy improvement of topotecan action along with the drug VX-970 (ATR inhibitor) has been proposed (http://clinicaltrials.gov identifier: NCT02487095). In addition, the enhanced effectiveness of the combination between NU-7441 (DNA-PKcs inhibitor) [184] and etoposide [185], as well as KU-60648 (a dual inhibitor of DNA-PK and PI-3 K) with etoposide and doxorubicin, has been reported [160].

6.5. DDR Inhibitors and Direct Inhibitors of the Redox System (Combinatory Therapies). It is well known that elevated GSH levels trigger chemo-resistance in cancer cells through different pathways: (i) direct interaction with drugs and ROS, (ii) prevention of damage of protein and DNA, and (iii) induction of DNA repair [186]. Several approaches for blocking GSH synthesis in cancer cells have been attempted, but, at the same time, cancer cells with high GSH content are more sensitive to drugs that affect GSH metabolism than normal cells. Buthionine sulphoximine (BSO) is the classical inhibitor of the rate-limiting enzyme in GSH synthesis that is used to increase cancer cell sensitivity to chemotherapeutics [187–189]. To this aim, the combination of 4-I-3 nitrobenzamide (PARPi) with BSO has been investigated in the E-ras 20 cancer cells that express the RAS oncogene, reporting enhanced cell killing [190]. Similarly, to GSH, changes to thioredoxin (Trx) metabolism are implicated in tumor cell resistance to chemotherapy. The gold compound auranofin (AF) is used as Trx inhibitor to induce OS, endoplasmic reticulum stress, and apoptosis in many tumor types, including cisplatin-resistant human ovarian cancer cells [191]. Cotreatment of mantle cell lymphoma (MCL) cells with AF and ABT-888 (PARPi) increases synergistically the apoptosis of ATM-proficient MCL cells, with increased γ-H2AX foci induction in the DNA and depletion of p-Chk1 (a downstream target of ATR signaling) [192].

7. Conclusions and Perspectives

The EU-ROS consortium comprising more than 140 members has worked for four years on the main topics of the redox biology and medicine. The results obtained highlight how synergistic approaches combining a variety of diverse and contrasting disciplines are needed in order to advance the knowledge of redox-associated diseases, including cancer [193]. ROS act as messengers that coordinate intracellular redox signaling in physiological and biological responses, as well as in tumorigenesis, suggesting that ROS-activated oncogenic pathways may also be regulated. Many strategies are under clinical investigations and trials that target the redox adaptation of cancer cells by redox-modulating interventions to both overcome drug resistance and eliminate selectivity cancer cells. Clinical efficacy of anticancer chemotherapies is dramatically hampered by drug resistance dependent on inherited traits, acquired defense against toxins, and adaptive mechanisms mounting in tumors. A heterogeneous cell population with distinct tumorigenic capabilities that complicate and limit the anticancer treatments may compose cancer tissues. Cancer plasticity leads to develop drug resistance by distinct mechanisms: (i) mutations in the target, (ii) reactivation of the targeted pathway, (iii) hyperactivation of alternative pathways, and (iv) cross-talk with the microenvironment. Molecular events leading to drug resistance are regulated by redox mechanisms suggesting redox-active drugs (antioxidants and prooxidants) or inhibitors of the inducible antioxidant defense as a novel approach to diminish the drug resistance. Repair and maintenance of cell genome stability show the cooperation between molecules that are essential to DDR and molecules essential to maintain the redox equilibrium. Ever increasing evidences highlight how the intricate molecular cross-talks between DDR and OS, generally indicated as OS-induced DDR pathways, can provide a useful insight into the drug discovery research aimed at counteracting cancer cell growth. Targeting DNA repair machinery has been a hot topic in anticancer therapy in the last decades. In fact, DDR inhibitors have been developed to increase the efficacy of conventional therapies and utilized in combinatory therapy with common cancer treatment, to overcome the therapeutic resistance to DNA-damaging chemotherapy and radiotherapy. This strategy can be used to selectively kill cancer cells with deficiencies in special DNA repair pathway(s) based on the concept of synthetic lethality. Although targeting DDR pathways is believed a promising therapy to fight solid and hematologic cancers, first early clinical trials with inhibitors in monotherapy have obtained scarce success. Currently, in order to optimize the application of these DDR inhibitors in the combinatory therapies overcoming resistance, massive array of preclinical and clinical trials are evaluating combinations of DDR inhibitors in targeted therapies. The best way to get a personalized medicine, matching the right treatment to the right patient, is based on identifying which patients have which DDR defect. The recent next generation sequencing (NGS) technology, which allows whole genomes to be sequenced in days, will be helpful to this strategy [194]. Today, an ever increasing range of available inhibitors targeting major DDR pathways allows for combining the inhibitors each other and with other targeted therapies and with treatments such as chemotherapy and radiotherapy, aiming at eliminating any escape road for cancer cells. In addition,

there is an emerging impact of the promising immuno-oncology therapies as a new tumor treatment that might synergize with DDR inhibitions [http://clinicaltrials.gov identifier: NCT02484404] [195]. Recently, even the modulation of OS has been considered as a strategy that may affect some DDR pathways in human cancer and the responses to new anticancer therapies. For example, combinatory treatments between DDR inhibitors and agents that regulate indirectly or directly OS are very encouraging. The importance of this therapeutic strategy is supported by the results obtained from several ongoing preclinical and clinical studies exploiting combinations between DDR inhibitors and drugs that modify the ROS homeostasis (Table 1). The complexity of emerging categories of drugs targeting DDR and new strategies for integrating DNA repair-targeted therapies into clinical practice, including combination regimens, is a continuous challenge for both scientist and patients. Indeed, some caution are necessary for DNA repair-targeted agents as treatment with DNA repair inhibitors could increase mutation rates in malignant cells, leading to evolution of metastatic properties and/or drug resistance. Also, systemic DNA damage could increase the risk of secondary malignancies. While maximizing the cellular dependency on DDR inhibition often requires an oxidative DNA damage insult by chemotherapy or radiation, different levels of ROS and enzymes involved in their metabolism can participate in the DDR signaling. They can modulate the activity of key DDR enzymes and regulate the stringency of DDR by rendering the cancer cells more sensible to DDR inhibitors. Thus, lower doses of DDR target therapies might be administered to the patients. At the same time, the capacity of some chemotherapeutic agents to cause temporary perturbations in ROS levels can offer a therapeutic opportunity to both treat cancer and mitigate some toxic side effects of the chemotherapeutic agents. It is believed that the combination of ROS-affecting drugs with DDR inhibitors may help to define better-tailored therapies with fewer side effects and lower probabilities to promote drug resistance development.

Abbreviations

AMPK: AMP-activated protein kinase
ATF4: Transcription factor-4
ATM: Ataxia telangiectasia-mutated protein
ATP: Adenosine triphosphate
ATR: ATM- and Rad3-related
BER: Base excision repair
CDK: Cyclin-dependent kinase
CHK1, CHK2: Checkpoint kinase 1, checkpoint kinase 2
cip1: Cyclin dependent kinase inhibitors p21
DDR: DNA damage response
DNA-PKcs: Dependent protein kinase catalytic subunit
DSB: Double-strand breaks
Grx: Glutaredoxins
HRR: Homologous recombination repair
ICL: Intrastrand crosslink
LKB1: Liver kinase B1
MMR: Mismatch repair
MRN: Mre11-Rad50-NBS1
mtDNA, nDNA: Mitochondrial DNA, nuclear DNA
NER: Nucleotide excision repair
NHEJ: Nonhomologous end joining
NOXs: NADPH oxidases
PARPi: Poly (ADP-ribose) polymerase inhibitor
PLK1: Polo-like kinase 1
PTEN: Phosphatase and tensin homolog
SOD2, SOD3: Superoxide dysmutase2, superoxide dysmutase3
SSB: Single-strand breaks
SUMO: Small ubiquitin-related modifier
TLS: Translation synthesis
Trx: Thioredoxins
WIP1: Wild-type p53-induced protein1
γ-H2AX: Gamma-histone2A.X.

Conflicts of Interest

The authors declare that they have no competing interests.

Acknowledgments

The authors sincerely apologize to colleagues whose works they could not include due to space limitations.

References

[1] R. L. Siegel, K. D. Miller, and A. Jemal, "Cancer statistics, 2017," *CA: a Cancer Journal for Clinicians*, vol. 67, no. 1, pp. 7–30, 2017.

[2] D. Hanahan and R. A. Weinberg, "Hallmarks of cancer: the next generation," *Cell*, vol. 144, no. 5, pp. 646–674, 2011.

[3] F. H. Groenendijk and R. Bernards, "Drug resistance to targeted therapies: déjà vu all over again," *Molecular Oncology*, vol. 8, no. 6, pp. 1067–1083, 2014.

[4] E. Dickreuter and N. Cordes, "The cancer cell adhesion resistome: mechanisms, targeting and translational approaches," *Biological Chemistry*, vol. 398, no. 7, pp. 721–735, 2017.

[5] C. V. Konrad, R. Murali, B. A. Varghese, and R. Nair, "The role of cancer stem cells in tumor heterogeneity and resistance to therapy," *Canadian Journal of Physiology and Pharmacology*, vol. 95, no. 1, pp. 1–15, 2017.

[6] T. Wu and Y. Dai, "Tumor microenvironment and therapeutic response," *Cancer Letters*, vol. 387, pp. 61–68, 2017.

[7] G. Wu, G. Wilson, J. George, C. Liddle, L. Hebbard, and L. Qiao, "Overcoming treatment resistance in cancer: current understanding and tactics," *Cancer Letters*, vol. 387, pp. 69–76, 2017.

[8] A. Tubbs and A. Nussenzweig, "Endogenous DNA damage as a source of genomic instability in cancer," *Cell*, vol. 168, no. 4, pp. 644–656, 2017.

[9] J. H. J. Hoeijmakers, "DNA damage, aging, and cancer," *New England Journal of Medicine*, vol. 361, no. 15, pp. 1475–1485, 2009.

[10] W. P. Roos, A. D. Thomas, and B. Kaina, "DNA damage and the balance between survival and death in cancer biology," *Nature Reviews Cancer*, vol. 16, no. 1, pp. 20–33, 2016.

[11] S. P. Jackson and J. Bartek, "The DNA-damage response in human biology and disease," *Nature*, vol. 461, no. 7267, pp. 1071–1078, 2009.

[12] P. Strzyz, "DNA damage response: cell thriving despite DNA damage," *Nature Reviews Molecular Cell Biology*, vol. 17, no. 7, p. 396, 2016.

[13] L. E. Giono, N. Nieto Moreno, A. E. Cambindo Botto, G. Dujardin, M. J. Muñoz, and A. R. Kornblihtt, "The RNA response to DNA damage," *Journal of Molecular Biology*, vol. 428, no. 12, pp. 2636–2651, 2016.

[14] P. A. Jeggo, L. H. Pearl, and A. M. Carr, "DNA repair, genome stability and cancer: a historical perspective," *Nature Reviews Cancer*, vol. 16, no. 1, pp. 35–42, 2016.

[15] L. H. Pearl, A. C. Schierz, S. E. Ward, B. al-Lazikani, and F. M. G. Pearl, "Therapeutic opportunities within the DNA damage response," *Nature Reviews Cancer*, vol. 15, no. 3, pp. 166–180, 2015.

[16] M. J. O'Connor, "Targeting the DNA damage response in cancer," *Molecular Cell*, vol. 60, no. 4, pp. 547–560, 2015.

[17] N. J. Curtin, "DNA repair dysregulation from cancer driver to therapeutic target," *Nature Reviews Cancer*, vol. 12, no. 12, pp. 801–817, 2012.

[18] S. Bhaskara, "Histone deacetylases 1 and 2 regulate DNA replication and DNA repair: potential targets for genome stability-mechanism-based therapeutics for a subset of cancers," *Cell Cycle*, vol. 14, no. 12, pp. 1779–1785, 2015.

[19] P. Ramos and M. Bentires-Alj, "Mechanism-based cancer therapy: resistance to therapy, therapy for resistance," *Oncogene*, vol. 34, no. 28, pp. 3617–3626, 2015.

[20] Y. Kwon, "Mechanism-based management for mucositis: option for treating side effects without compromising the efficacy of cancer therapy," *OncoTargets and Therapy*, vol. 9, pp. 2007–2016, 2016.

[21] F. Caputo, R. Vegliante, and L. Ghibelli, "Redox modulation of the DNA damage response," *Biochemical Pharmacology*, vol. 84, no. 10, pp. 1292–1306, 2012.

[22] C. Gorrini, I. S. Harris, and T. W. Mak, "Modulation of oxidative stress as an anticancer strategy," *Nature Reviews Drug Discovery*, vol. 12, no. 12, pp. 931–947, 2013.

[23] A. Karimaian, M. Majidiniac, H. Bannazadeh Baghie, and B. Youse, "The crosstalk between Wnt/β-catenin signaling pathway with DNA damage response and oxidative stress: implications in cancer therapy," *DNA Repair*, vol. 51, pp. 14–19, 2017.

[24] A. T. Vessoni, E. C. Filippi-Chiela, C. F. M. Menck, and G. Lenz, "Autophagy and genomic integrity," *Cell Death and Differentiation*, vol. 20, no. 11, pp. 1444–1454, 2013.

[25] G. Filomeni, D. De Zio, and F. Cecconi, "Oxidative stress and autophagy: the clash between damage and metabolic needs," *Cell Death and Differentiation*, vol. 22, no. 3, pp. 377–388, 2015.

[26] H. G. Hambright and R. Ghosh, "Autophagy: in the cROSs-hairs of cancer," *Biochemical Pharmacology*, vol. 126, pp. 13–22, 2017.

[27] M. E. Lleonart, E. Abad, D. Graifer, and A. Lyakhovich, "Reactive oxygen species-mediated autophagy defines the fate of cancer stem cells," *Antioxidants and Redox Signaling*, 2017.

[28] Z. Huang, L. Zhou, Z. Chen, E. C. Nice, and C. Huang, "Stress management by autophagy: implications for chemoresistance," *International Journal of Cancer*, vol. 139, no. 1, pp. 23–32, 2016.

[29] J. N. Moloney and T. G. Cotter, "ROS signalling in the biology of cancer," *Seminars in Cell & Developmental Biology*, 2017.

[30] S. Sabharwal and P. T. Schumacker, "Mitochondrial ROS in cancer: initiators, amplifiers or an Achilles' heel?," *Nature Reviews Cancer*, vol. 14, no. 11, pp. 709–721, 2014.

[31] M. H. Raza, S. Siraj, A. Arshad et al., "ROS-modulated therapeutic approaches in cancer treatment," *Journal of Cancer Research and Clinical Oncology*, vol. 143, no. 9, pp. 1789–1809, 2017.

[32] E. Hatem, N. El Banna, and M. E. Huang, "Multifaceted roles of glutathione and glutathione-based systems in carcinogenesis and anticancer drug resistance," *Antioxidants & Redox Signaling*, vol. 27, no. 15, pp. 1217–1234, 2017.

[33] A. Cort, T. Ozben, L. Saso, C. de Luca, and L. Korkina, "Redox control of multidrug resistance and its possible modulation by antioxidants," *Oxidative Medicine and Cellular Longevity*, vol. 2016, pp. 1–17, 2016.

[34] A. T. Dharmaraja, "Role of reactive oxygen species (ROS) in therapeutics and drug resistance in cancer and bacteria," *Journal of Medicinal Chemistry*, vol. 60, no. 8, pp. 3221–3240, 2017.

[35] L. Tong, C.-C. Chuang, S. Wu, and L. Zuo, "Reactive oxygen species in redox cancer therapy," *Cancer Letters*, vol. 367, no. 1, pp. 18–25, 2015.

[36] C. C. Winterbourn, "Reconciling the chemistry and biology of reactive oxygen species," *Nature Chemical Biology*, vol. 4, no. 5, pp. 278–286, 2008.

[37] S. Di Meo, T. T. Reed, P. Venditti, and V. M. Victor, "Role of ROS and RNS sources in physiological and pathological conditions," *Oxidative Medicine and Cellular Longevity*, vol. 2016, Article ID 1245049, 44 pages, 2016.

[38] J. Zhang, X. Wang, V. Vikash et al., "ROS and ROS-mediated cellular signaling," *Oxidative Medicine and Cellular Longevity*, vol. 2016, Article ID 4350965, 18 pages, 2016.

[39] G. Siedenburg, M. R. Groves, and D. Ortiz de Orué Lucana, "Novel redox-sensing modules: accessory protein- and nucleic acid-mediated signaling," *Antioxidants & Redox Signaling*, vol. 16, no. 7, pp. 668–677, 2012.

[40] A. Nicolussi, S. D'Inzeo, C. Capalbo, G. Giannini, and A. Coppa, "The role of peroxiredoxins in cancer," *Molecular and Clinical Oncology*, vol. 6, no. 2, pp. 139–153, 2017.

[41] S. S. Sabharwal, G. B. Waypa, J. D. Marks, and P. T. Schumacker, "Peroxiredoxin-5 targeted to the mitochondrial intermembrane space attenuates hypoxia-induced reactive oxygen species signalling," *Biochemical Journal*, vol. 456, no. 3, pp. 337–346, 2013.

[42] A. B. Fisher, "Peroxiredoxin 6 in the repair of peroxidized cell membranes and cell signaling," *Archives of Biochemistry and Biophysics*, vol. 617, pp. 68–83, 2017.

[43] A. Matsuzawa, "Thioredoxin and redox signaling: roles of the thioredoxin system in control of cell fate," *Archives of Biochemistry and Biophysics*, vol. 617, pp. 101–105, 2017.

[44] C. Berndt and C. H. Lilli, "Glutathione, glutaredoxins, and iron," *Antioxidants & Redox Signaling*, vol. 27, no. 15, pp. 1235–1251, 2017.

[45] M. Vašák, M. Meloni, and G. Meloni, "Chemistry and biology of mammalian metallothioneins," *JBIC Journal of Biological Inorganic Chemistry*, vol. 16, no. 7, pp. 1067–1078, 2011.

[46] M. T. Rahman, N. Haque, N. H. Abu Kasim, and M. De Ley, "Origin, function, and fate of metallothionein in human blood," *Reviews of Physiology, Biochemistry and Pharmacology*, vol. 173, 2017.

[47] M. Deponte, "The incomplete glutathione puzzle: just guessing at numbers and figures?," *Antioxidants & Redox Signaling*, vol. 27, no. 15, pp. 1130–1161, 2017.

[48] R. Sharafati-Chaleshtori, H. Shirzad, M. Rafieian-Kopaei, and A. Soltani, "Melatonin and human mitochondrial diseases," *Journal of Research in Medical Sciences*, vol. 22, no. 1, p. 2, 2017.

[49] P. Loren, R. Sánchez, and M. E. Arias, "Melatonin scavenger properties against oxidative and nitrosative stress: impact on gamete handling and in vitro embryo production in humans and other mammals," *International Journal of Molecular Sciences*, vol. 18, no. 6, 2017.

[50] S. A. Ganie, T. A. Dar, A. H. Bhat et al., "Melatonin: a potential anti-oxidant therapeutic agent for mitochondrial dysfunctions and related disorders," *Rejuvenation Research*, vol. 19, no. 1, pp. 21–40, 2016.

[51] D. X. Tan, C. L. Manchester, L. Qin, and R. J. Reiter, "Melatonin: a mitochondrial targeting molecule involving mitochondrial protection and dynamics," *International Journal of Molecular Sciences*, vol. 17, no. 12, 2016.

[52] M. Majidinia, A. Sadeghpour, S. Mehrzadi, R. J. Reiter, N. Khatami, and B. Yousefi, "Melatonin: a pleiotropic molecule that modulates DNA damage response and repair pathways," *Journal of Pineal Research*, vol. 63, no. 1, 2017.

[53] M. P. Murphy, A. Holmgren, N. G. Larsson et al., "Unraveling the biological roles of reactive oxygen species," *Cell Metabolism*, vol. 13, no. 4, pp. 361–366, 2011.

[54] W. K. Chiu, A. Towheed, and M. J. Palladino, "Genetically encoded redox sensors," *Methods in Enzymology*, vol. 542, pp. 263–287, 2014.

[55] G. B. Waypa, K. A. Smith, and P. T. Schumacker, "O2 sensing, mitochondria and ROS signaling: the fog is lifting," *Molecular Aspects of Medicine*, vol. 47-48, pp. 76–89, 2016.

[56] C. C. Winterbourn and M. B. Hampton, "Thiol chemistry and specificity in redox signaling," *Free Radical Biology and Medicine*, vol. 45, no. 5, pp. 549–561, 2008.

[57] E. H. Sarsour, M. G. Kumar, L. Chaudhuri, A. L. Kalen, and P. C. Goswami, "Redox control of the cell cycle in health and disease," *Antioxidants & Redox Signaling*, vol. 11, no. 12, pp. 2985–3011, 2009.

[58] P. Davalli, T. Mitic, A. Caporali, A. Lauriola, and D. D'Arca, "ROS, cell senescence, and novel molecular mechanisms in aging and age-related diseases," *Oxidative Medicine and Cellular Longevity*, vol. 2016, Article ID 3565127, 18 pages, 2016.

[59] C. Lopez-Otin, M. A. Blasco, L. Partridge, M. Serrano, and G. Kroemer, "The hallmarks of aging," *Cell*, vol. 153, no. 6, pp. 1194–1217, 2013.

[60] H. Sies, C. Berndt, and D. P. Jones, "Oxidative stress," *Annual Review of Biochemistry*, vol. 86, no. 1, pp. 715–748, 2017.

[61] M. Schieber and N. S. Chandel, "ROS function in redox signaling and oxidative stress," *Current Biology*, vol. 24, no. 10, pp. R453–R462, 2014.

[62] C. Cencioni, F. Spallotta, F. Martelli et al., "Oxidative stress and epigenetic regulation in ageing and age-related diseases," *International Journal of Molecular Sciences*, vol. 14, no. 9, pp. 17643–17663, 2013.

[63] N. Dąbrowska and A. J. Wiczkowski, "Analytics of oxidative stress markers in the early diagnosis of oxygen DNA damage," *Advances in Clinical and Experimental Medicine*, vol. 26, no. 1, pp. 155–166, 2017.

[64] C. Gasparovic, N. Zarkovic, K. Zarkovic et al., "Biomarkers of oxidative and nitro-oxidative stress: conventional and novel approaches," *British Journal of Pharmacology*, vol. 174, no. 12, pp. 1771–1783, 2017.

[65] J. Navarro-Yepes, M. Burns, A. Anandhan et al., "Oxidative stress, redox signaling, and autophagy: cell death versus survival," *Antioxidants & Redox Signaling*, vol. 21, no. 1, pp. 66–85, 2014.

[66] J. Cadet and K. J. A. Davies, "Oxidative DNA damage & repair: an introduction," *Free Radical Biology and Medicine*, vol. 107, pp. 2–12, 2017.

[67] O. A. Sedelnikova, C. E. Redon, J. S. Dickey, A. J. Nakamura, A. G. Georgakilas, and W. M. Bonner, "Role of oxidatively induced DNA lesions in human pathogenesis," *Mutation Research/Reviews in Mutation Research*, vol. 704, no. 1–3, pp. 152–159, 2010.

[68] E. F. Fang, M. Scheibye-Knudsen, K. F. Chua, M. P. Mattson, D. L. Croteau, and V. A. Bohr, "Nuclear DNA damage signalling to mitochondria in ageing," *Nature Reviews Molecular Cell Biology*, vol. 17, no. 5, pp. 308–321, 2016.

[69] A. Cruz-Bermúdez, R. J. Vicente-Blanco, E. Gonzalez-Vioque, M. Provencio, M. Á. Fernández-Moreno, and R. Garesse, "Spotlight on the relevance of mtDNA in cancer," *Clinical and Translational Oncology*, vol. 19, no. 4, pp. 409–418, 2017.

[70] S. D. Cline, "Mitochondrial DNA damage and Its consequences for mitochondrial gene expression," *Biochimica et Biophysica Acta (BBA) - Gene Regulatory Mechanisms*, vol. 1819, no. 9-10, pp. 979–991, 2012.

[71] L. F. Agnez-Lima, J. T. Melo, A. E. Silva et al., "DNA damage by singlet oxygen and cellular protective mechanisms," *Mutation Research*, vol. 751, no. 1, pp. 15–28, 2012.

[72] A. M. Fleming and C. J. Burrows, "Formation and processing of DNA damage substrates for the hNEIL enzymes," *Free Radical Biology & Medicine*, vol. 107, pp. 35–52, 2017.

[73] F. Gullotta, E. De Marinis, P. Ascenzi, and A. di Masi, "Targeting the DNA double strand breaks repair for cancer therapy," *Current Medicinal Chemistry*, vol. 17, no. 19, pp. 2017–2048, 2010.

[74] H. Ohshima, T. Sawa, and T. Akaike, "8-Nitroguanine, a product of nitrative DNA damage caused by reactive nitrogen species: formation, occurrence, and implications in inflammation and carcinogenesis," *Antioxidants & Redox Signaling*, vol. 8, no. 5-6, pp. 1033–1045, 2006.

[75] Z. Shaukat, D. Liu, R. Hussain, M. Khan, and S. L. Gregory, "The role of JNK signalling in responses to oxidative DNA damage," *Current Drug Targets*, vol. 17, no. 2, pp. 154–163, 2016.

[76] S. Kardeh, S. Ashkani-Esfahani, and A. M. Alizadeh, "Paradoxical action of reactive oxygen species in creation and therapy of cancer," *European Journal of Pharmacology*, vol. 735, pp. 150–168, 2014.

[77] X. B. Ling, H. W. Wei, J. Wang et al., "Mammalian metallothionein-2A and oxidative stress," *International Journal of Molecular Sciences*, vol. 17, no. 9, p. 1483, 2016.

[78] G. J. Samaranayake, M. Huynh, and P. Rai, "MTH1 as a chemotherapeutic target: the elephant in the room," *Cancer*, vol. 9, no. 5, 2017.

[79] G. Papeo, "MutT homolog 1 (MTH1): the silencing of a target," *Journal of Medicinal Chemistry*, vol. 59, no. 6, pp. 2343–2345, 2016.

[80] N. Chatterjee and G. C. Walker, "Mechanisms of DNA damage, repair, and mutagenesis," *Environmental and Molecular Mutagenesis*, vol. 58, no. 5, pp. 235–263, 2017.

[81] S. S. Tehrani, A. Karimian, H. Parsian, M. Majidinia, and B. Yousefi, "Multiple functions of long non-coding RNAs in oxidative stress, DNA damage response and cancer progression," *Journal of Cellular Biochemistry*, vol. 119, no. 1, pp. 223–236, 2018.

[82] J. Lukas and M. Altmeyer, "A lncRNA to repair DNA," *EMBO Reports*, vol. 16, no. 11, pp. 1413-1414, 2015.

[83] A. B. Robertson, A. Klungland, T. Rognes, and I. Leiros, "DNA repair in mammalian cells: base excision repair: the long and short of it," *Cellular and Molecular Life Sciences*, vol. 66, no. 6, pp. 981–993, 2009.

[84] A. M. Whitaker, M. A. Schaich, M. R. Smith, T. S. Flynn, and B. D. Freudenthal, "Base excision repair of oxidative DNA damage: from mechanism to disease," *Frontiers of Bioscience*, vol. 22, pp. 1493–1522, 2017.

[85] J. A. Marteijn, H. Lans, W. Vermeulen, and J. H. Hoeijmakers, "Understanding nucleotide excision repair and its roles in cancer and ageing," *Nature Reviews Molecular Cell Biology*, vol. 15, no. 7, pp. 465–481, 2014.

[86] V. Shafirovich and N. E. Geacintov, "Removal of oxidatively generated DNA damage by overlapping repair pathways," *Free Radical Biology and Medicine*, vol. 107, pp. 53–61, 2017.

[87] J. R. Chapman, M. R. G. Taylor, and S. J. Boulton, "Playing the end game: DNA double-strand break repair pathway choice," *Molecular Cell*, vol. 47, no. 4, pp. 497–510, 2012.

[88] D. Huehn, H. A. Bolck, and A. A. Sartori, "Targeting DNA double-strand break signalling and repair: recent advances in cancer therapy," *Swiss Medical Weekly*, vol. 143, 2013.

[89] M. R. Lieber, Y. Ma, U. Pannicke, and K. Schwarz, "Mechanism and regulation of human non-homologous DNA end-joining," *Nature Reviews Molecular Cell Biology*, vol. 4, no. 9, pp. 712–720, 2003.

[90] M. R. Lieber, "The mechanism of double-strand DNA break repair by the nonhomologous DNA end-joining pathway," *Annual Review of Biochemistry*, vol. 79, no. 1, pp. 181–211, 2010.

[91] M. Dizdaroglu, E. Coskun, and P. Jaruga, "Repair of oxidatively induced DNA damage by DNA glycosylases: mechanisms of action, substrate specificities and excision kinetics," *Mutation Research*, vol. 771, pp. 99–127, 2017.

[92] B. Vogelstein, N. Papadopoulos, V. E. Velculescu, S. Zhou, L. A. Diaz, and K. W. Kinzler, "Cancer genome landscapes," *Science*, vol. 339, no. 6127, pp. 1546–1558, 2013.

[93] J. Stadler and H. Richly, "Regulation of DNA repair mechanisms: how the chromatin environment regulates the DNA damage response," *International Journal of Molecular Sciences*, vol. 18, no. 8, 2017.

[94] J. Lukas, C. Lukas, and J. Bartek, "More than just a focus: the chromatin response to DNA damage and its role in genome integrity maintenance," *Nature Cell Biology*, vol. 13, no. 10, pp. 1161–1169, 2011.

[95] J. H. Hoeijmakers, "DNA damage, aging, and cancer," *New England Journal of Medicine*, vol. 361, no. 15, pp. 1475–1485, 2009.

[96] F. Ribezzo, Y. Shiloh, and B. Schumacher, "Systemic DNA damage responses in aging and diseases," *Seminars in Cancer Biology*, vol. 37-38, pp. 26–35, 2016.

[97] A. Khanna, "DNA damage in cancer therapeutics: a boon or a curse?," *Cancer Research*, vol. 75, no. 11, pp. 2133–2138, 2015.

[98] A. Ciccia and S. J. Elledge, "The DNA damage response: making it safe to play with knives," *Molecular Cell*, vol. 40, no. 2, pp. 179–204, 2010.

[99] B. M. Sirbu and D. Cortez, "DNA damage response: three levels of DNA repair regulation," *Cold Spring Harbor Perspectives in Biology*, vol. 5, no. 8, 2013.

[100] Y. Liu, Y. Li, and X. Lu, "Regulators in the DNA damage response," *Archives of Biochemistry and Biophysics*, vol. 594, pp. 18–25, 2016.

[101] A. N. Blackford and S. P. Jackson, "ATM, ATR, and DNA-PK: the trinity at the heart of the DNA damage response," *Molecular Cell*, vol. 66, no. 6, pp. 801–817, 2017.

[102] A. Marechal and L. Zou, "DNA damage sensing by the ATM and ATR kinases," *Cold Spring Harbor Perspectives in Biology*, vol. 5, no. 9, 2013.

[103] F. A. Derheimer and M. B. Kastan, "Multiple roles of ATM in monitoring and maintaining DNA integrity," *FEBS Letters*, vol. 584, no. 17, pp. 3675–3681, 2010.

[104] T. Sanli, G. R. Steinberg, G. Singh, and T. Tsakiridis, "AMP-activated protein kinase (AMPK) beyond metabolism," *Cancer Biology & Therapy*, vol. 15, no. 2, pp. 156–169, 2014.

[105] A. Karimaian, M. Majidinia, H. B. Baghi, and B. Yousefi, "The crosstalk between Wnt/β-catenin signaling pathway with DNA damage response and oxidative stress: implications in cancer therapy," *DNA Repair*, vol. 51, pp. 14–19, 2017.

[106] Y. Hirota, D. Kang, and T. Kanki, "The physiological role of mitophagy: new insights into phosphorylation events," *International Journal of Cell Biology*, vol. 2012, Article ID 354914, 8 pages, 2012.

[107] A. G. Eliopoulos, S. Havaki, and V. G. Gorgoulis, "DNA damage response and autophagy: a meaningful partnership," *Frontiers in Genetics*, vol. 7, 2016.

[108] A. V. Kulikov, E. A. Luchkina, V. Gogvadze, and B. Zhivotovsky, "Mitophagy: link to cancer development and therapy," *Biochemical and Biophysical Research Communications*, vol. 482, no. 3, pp. 432–439, 2017.

[109] M. E. Lleonart, R. Grodzicki, D. M. Graifer, and A. Lyakhovich, "Mitochondrial dysfunction and potential anticancer therapy," *Medicinal Research Reviews*, vol. 37, no. 6, pp. 1275–1298, 2017.

[110] B. P. Chen, M. Li, and A. Asaithamby, "New insights into the roles of ATM and DNA-PKcs in the cellular response to oxidative stress," *Cancer Letters*, vol. 327, no. 1-2, pp. 103–110, 2012.

[111] S. Ditch and T. T. Paull, "The ATM protein kinase and cellular redox signaling: beyond the DNA damage response," *Trends in Biochemical Sciences*, vol. 37, no. 1, pp. 15–22, 2012.

[112] S. Yan, M. Sorrell, and Z. Berman, "Functional interplay between ATM/ATR-mediated DNA damage response and DNA repair pathways in oxidative stress," *Cellular and Molecular Life Sciences*, vol. 71, no. 20, pp. 3951–3967, 2014.

[113] Z. Guo, S. Kozlov, M. F. Lavin, M. D. Person, and T. T. Paull, "ATM activation by oxidative stress," *Science*, vol. 330, no. 6003, pp. 517–521, 2010.

[114] Y. Okuno, A. Nakamura-Ishizu, K. Otsu, T. Suda, and Y. Kubota, "Pathological neoangiogenesis depends on oxidative stress regulation by ATM," *Nature Medicine*, vol. 18, no. 8, pp. 1208–1216, 2012.

[115] A. Alexander, S. L. Cai, J. Kim et al., "ATM signals to TSC2 in the cytoplasm to regulate mTORC1 in response to ROS," *Proceedings of the National Academy of Sciences*, vol. 107, no. 9, pp. 4153–4158, 2010, Erratum in: The Proceedings of the National Academy of Sciences (U.S.A.), vol.109, no. 21, pp. 8352, 2012.

[116] D. N. Tripathi, R. Chowdhury, L. J. Trudel et al., "Reactive nitrogen species regulate autophagy through ATM-AMPK-TSC2-mediated suppression of mTORC1," *Proceedings of the National Academy of Sciences*, vol. 110, no. 32, pp. E2950–E2957, 2013.

[117] J. Rudolph, "Redox regulation of the Cdc25 phosphatases," *Antioxidants & Redox Signaling*, vol. 7, no. 5-6, pp. 761–767, 2005.

[118] E. Tasdemir, M. C. Maiuri, L. Galluzzi et al., "Regulation of autophagy by cytoplasmic p53," *Nature Cell Biology*, vol. 10, no. 6, pp. 676–687, 2008.

[119] V. Stambolic, D. MacPherson, D. Sas et al., "Regulation of PTEN transcription by p53," *Molecular Cell*, vol. 8, no. 2, pp. 317–325, 2001.

[120] J. S. Clerkin, R. Naughton, C. Quiney, and T. G. Cotter, "Mechanisms of ROS modulated cell survival during carcinogenesis," *Cancer Letters*, vol. 266, no. 1, pp. 30–36, 2008.

[121] A. Beillerot, E. Battaglia, A. Bennasroune, and D. Bagrel, "Protection of CDC25 phosphatases against oxidative stress in breast cancer cells: evaluation of the implication of the thioredoxin system," *Free Radical Research*, vol. 46, no. 5, pp. 674–689, 2012.

[122] E. Pons-Tostivint, B. Thibault, and J. Guillermet-Guibert, "Targeting PI3K signaling in combination cancer therapy," *Trends in Cancer*, vol. 3, no. 6, pp. 454–469, 2017.

[123] C. Quan, J. Xiao, L. Liu, Q. Duan, P. Yuan, and F. Zhu, "Protein kinases as tumor biomarkers and therapeutic targets," *Current Pharmaceutical Design*, vol. 23, no. 29, pp. 4209–4225, 2017.

[124] A. M. Weber and A. J. Ryan, "ATM and ATR as therapeutic targets in cancer," *Pharmacology & Therapeutics*, vol. 149, pp. 124–138, 2015.

[125] M. Pospisilova, M. Seifrtova, and M. Rezacova, "Small molecule inhibitors of DNA-PK for tumor sensitization to anticancer therapy," *Journal of Physiology and Pharmacology*, vol. 68, no. 3, pp. 337–344, 2017.

[126] R. Sundar, J. Brown, A. Ingles Russo, and T. A. Yap, "Targeting ATR in cancer medicine," *Current Problems in Cancer*, vol. 41, no. 4, pp. 302–315, 2017.

[127] D. P. McLornan, A. List, and G. J. Mufti, "Applying synthetic lethality for the selective targeting of cancer," *New England Journal of Medicine*, vol. 371, no. 18, pp. 1725–1735, 2014.

[128] C. J. Lord, A. N. Tutt, and A. Ashworth, "Synthetic lethality and cancer therapy: lessons learned from the development of PARP inhibitors," *Annual Review of Medicine*, vol. 66, no. 1, pp. 455–470, 2015.

[129] E. Y. Liu, N. Xu, J. O'Prey et al., "Loss of autophagy causes a synthetic lethal deficiency in DNA repair," *Proceedings of the National Academy of Sciences*, vol. 112, no. 3, pp. 773–778, 2015.

[130] E. H. Stover, P. A. Konstantinopoulos, U. A. Matulonis, and E. M. Swisher, "Biomarkers of response and resistance to DNA repair targeted therapies," *Clinical Cancer Research*, vol. 22, no. 23, pp. 5651–5660, 2016.

[131] A. M. Cseh, Z. Fábián, B. Sümegi, and L. Scorrano, "Poly (adenosine diphosphate-ribose) polymerase as therapeutic target: lessons learned from its inhibitors," *Oncotarget*, vol. 8, no. 30, pp. 50221–50239, 2017.

[132] F. G. Sousa, R. Matuo, D. G. Soares et al., "PARPs and the DNA damage response," *Carcinogenesis*, vol. 33, no. 8, pp. 1433–1440, 2012.

[133] E. Hocsak, V. Szabo, N. Kalman et al., "PARP inhibition protects mitochondria and reduces ROS production via PARP-1-ATF4-MKP-1-MAPK retrograde pathway," *Free Radical Biology and Medicine*, vol. 108, pp. 770–784, 2017.

[134] S. P. Basourakos, L. Li, A. M. Aparicio, P. G. Corn, J. Kim, and T. C. Thompson, "Combination platinum-based and DNA damage response-targeting cancer therapy: evolution and future directions," *Current Medicinal Chemistry*, vol. 24, no. 15, pp. 1586–1606, 2017.

[135] D. Y. Lu, E. H. Chen, H. Wu, T. R. Lu, B. Xu, and J. Ding, "Anticancer drug combinations, how far we can go through?," *Anticancer Agents in Medicinal Chemistry*, vol. 17, no. 1, pp. 21–28, 2017.

[136] S. Pecháčková, K. Burdová, and L. Macurek, "WIP1 phosphatase as pharmacological target in cancer therapy," *Journal of Molecular Medicine*, vol. 95, no. 6, pp. 589–599, 2017.

[137] D. Ivanova, R. Bakalova, D. Lazarova, V. Gadjeva, and Z. Zhelev, "The impact of reactive oxygen species on anticancer therapeutic strategies," *Advances in Clinical and Experimental Medicine*, vol. 40, no. 22, pp. 1934–1940, 2013.

[138] R. Kasiappan and S. Safe, "ROS-inducing agents for cancer chemotherapy," *Reactive Oxygen Species*, vol. 1, no. 1, 2016.

[139] A. Cort, T. Ozben, L. Saso, C. De Luca, and L. Korkina, "Redox control of multidrug resistance and its possible modulation by antioxidants," *Oxidative Medicine and Cellular Longevity*, vol. 2016, Article ID 4251912, 17 pages, 2016.

[140] D. Trachootham, J. Alexandre, and P. Huang, "Targeting cancer cells by ROS-mediated mechanisms: a radical therapeutic approach?," *Nature Reviews Drug Discovery*, vol. 8, no. 7, pp. 579–591, 2009.

[141] S. Y. Saad, T. A. Najjar, and M. Alashari, "Role of non-selective adenosine receptor blockade and phosphodiesterase inhibition in cisplatin-induced nephrogonadal toxicity in rats," *Clinical and Experimental Pharmacology & Physiology*, vol. 31, no. 12, pp. 862–867, 2004.

[142] A. Brozovic, A. Ambriovic-Ristov, and M. Osmak, "The relationship between cisplatin-induced reactive oxygen species, glutathione, and BCL-2 and resistance to cisplatin," *Critical Reviews in Toxicology*, vol. 40, no. 4, pp. 347–359, 2010.

[143] T. Itoh, R. Terazawa, K. Kojima et al., "Cisplatin induces production of reactive oxygen species via NADPH oxidase activation in human prostate cancer cells," *Free Radical Research*, vol. 45, no. 9, pp. 1033–1039, 2011.

[144] T. C. Johnstone, K. Suntharalingam, and S. J. Lippard, "The next generation of platinum drugs: targeted Pt(II) agents, nanoparticle delivery, and Pt(IV) prodrugs," *Chemical Reviews*, vol. 116, no. 5, pp. 3436–3486, 2016.

[145] J. Su, Y. Xu, L. Zhou et al., "Suppression of chloride channel 3 expression facilitates sensitivity of human glioma U251 cells to cisplatin through concomitant inhibition of Akt and autophagy," *Anatomical Record*, vol. 296, no. 4, pp. 595–603, 2013.

[146] T. Yoshida, S. Goto, M. Kawakatsu, Y. Urata, and T.s. Li, "Mitochondrial dysfunction, a probable cause of persistent

oxidative stress after exposure to ionizing radiation," *Free Radical Research*, vol. 46, no. 2, pp. 147–153, 2012.

[147] H. Yin, Y. Zhou, C. Wen et al., "Curcumin sensitizes glioblastoma to temozolomide by simultaneously generating ROS and disrupting AKT/mTOR signaling," *Oncology Reports*, vol. 32, no. 4, pp. 1610–1616, 2014.

[148] H. S. Kim, J. M. Oh, D. H. Jin, K. H. Yang, and E. Y. Moon, "Paclitaxel induces vascular endothelial growth factor expression through reactive oxygen species production," *Pharmacology*, vol. 81, no. 4, pp. 317–324, 2008.

[149] T. M. Neher, D. Bodenmiller, R. W. Fitch, S. I. Jalal, and J. J. Turchi, "Novel irreversible small molecule inhibitors of replication protein A display single-agent activity and synergize with cisplatin," *Molecular Cancer Therapeutics*, vol. 10, no. 10, pp. 1796–1806, 2011.

[150] F. Huang, O. M. Mazina, I. J. Zentner, S. Cocklin, and A. V. Mazin, "Inhibition of homologous recombination in human cells by targeting RAD51 recombinase," *Journal of Medicinal Chemistry*, vol. 55, no. 7, pp. 3011–3020, 2012.

[151] K. Shi, D. Wang, X. Cao, and Y. Ge, "Endoplasmic reticulum stress signaling is involved in mitomycin C(MMC)-induced apoptosis in human fibroblasts via PERK pathway," *PLoS One*, vol. 8, no. 3, article e59330, 2013.

[152] A. Peasland, L. Z. Wang, E. Rowling et al., "Identification and evaluation of a potent novel ATR inhibitor, NU6027, in breast and ovarian cancer cell lines," *British Journal of Cancer*, vol. 105, no. 3, pp. 372–381, 2011.

[153] M. A. Kang, E. Y. So, A. L. Simons, D. R. Spitz, and T. Ouchi, "DNA damage induces reactive oxygen species generation through the H2AX-Nox1/Rac1 pathway," *Cell Death & Disease*, vol. 3, no. 1, article e249, 2012.

[154] S. H. Chen, D. L. Li, F. Yang, Z. Wu, Y. Y. Zhao, and Y. Jiang, "Gemcitabine-induced pancreatic cancer cell death is associated with MST1/cyclophilin D mitochondrial complexation," *Biochimie*, vol. 103, pp. 71–79, 2014.

[155] I. Hickson, Y. Zhao, C. J. Richardson et al., "Identification and characterization of a novel and specific inhibitor of the ataxia-telangiectasia mutated kinase ATM," *Cancer Research*, vol. 64, no. 24, pp. 9152–9159, 2004.

[156] F. S. Shaheen, P. Znojek, A. Fisher et al., "Targeting the DNA double strand break repair machinery in prostate cancer," *PLoS One*, vol. 6, no. 5, article e20311, 2011.

[157] T. Simunek, M. Stérba, O. Popelová, M. Adamcová, R. Hrdina, and V. Gersl, "Anthracycline-induced cardiotoxicity: overview of studies examining the roles of oxidative stress and free cellular iron," *Pharmacological Reports*, vol. 61, no. 1, pp. 154–171, 2009.

[158] H. Mizutani, S. Tada-Oikawa, Y. Hiraku, M. Kojima, and S. Kawanishi, "Mechanism of apoptosis induced by doxorubicin through the generation of hydrogen peroxide," *Life Sciences*, vol. 76, no. 13, pp. 1439–1453, 2005.

[159] T. Ozben, "Oxidative stress and apoptosis: impact on cancer therapy," *Journal of Pharmacological Sciences*, vol. 96, no. 9, pp. 2181–2196, 2007.

[160] J. M. Munck, M. A. Batey, Y. Zhao et al., "Chemosensitization of cancer cells by KU-0060648, a dual inhibitor of DNA-PK and PI-3K," *Molecular Cancer Therapeutics*, vol. 11, no. 8, pp. 1789–1798, 2012.

[161] K. E. Hwang, Y. S. Kim, Y. R. Hwang et al., "Pemetrexed induces apoptosis in malignant mesothelioma and lung cancer cells through activation of reactive oxygen species and inhibition of sirtuin 1," *Oncology Reports*, vol. 33, no. 5, pp. 2411–2419, 2015.

[162] D. B. Longley, D. P. Harkin, and P. G. Johnston, "5-Fluorouracil: mechanisms of action and clinical strategies," *Nature Reviews Cancer*, vol. 3, no. 5, pp. 330–338, 2003.

[163] S. Cao, M. Xia, Y. Mao et al., "Combined oridonin with cetuximab treatment shows synergistic anticancer effects on laryngeal squamous cell carcinoma: involvement of inhibition of EGFR and activation of reactive oxygen species-mediated JNK pathway," *International Journal of Oncology*, vol. 49, no. 5, pp. 2075–2087, 2016.

[164] H. Lu, X. Li, Y. Lu, S. Qiu, and Z. Fan, "ASCT2 (SLC1A5) is an EGFR-associated protein that can be co-targeted by cetuximab to sensitize cancer cells to ROS-induced apoptosis," *Cancer Letters*, vol. 381, no. 1, pp. 23–30, 2016.

[165] H. R. Teppo, Y. Soini, and P. Karihtala, "Reactive oxygen species-mediated mechanisms of action of targeted cancer therapy," *Oxidative Medicine and Cell Longevity*, vol. 2017, article 1485283, 11 pages, 2017.

[166] F. Fack, H. Espedal, O. Keunen et al., "Bevacizumab treatment induces metabolic adaptation toward anaerobic metabolism in glioblastomas," *Acta Neuropathologica*, vol. 129, no. 1, pp. 115–131, 2015.

[167] X. L. Guo, D. Li, K. Sun et al., "Inhibition of autophagy enhances anticancer effects of bevacizumab in hepatocarcinoma," *Journal of Molecular Medicine*, vol. 91, no. 4, pp. 473–483, 2013.

[168] W. A. Hammond, A. Swaika, and K. Mody, "Pharmacologic resistance in colorectal cancer: a review," *Therapeutic Advances in Medical Oncology*, vol. 8, no. 1, pp. 57–84, 2015.

[169] J. D. Soumerai, A. D. Zelenetz, C. H. Moskowitz et al., "The PARP inhibitor veliparib can be safely added to bendamustine and rituximab and has preliminary evidence of activity in B-cell lymphoma," *Clinical Cancer Research*, vol. 23, no. 15, pp. 4119–4126, 2017.

[170] S. Alas, C. P. Ng, and B. Bonavida, "Rituximab modifies the cisplatin-mitochondrial signaling pathway, resulting in apoptosis in cisplatin-resistant non-Hodgkin's lymphoma," *Clinical Cancer Research*, vol. 8, no. 3, pp. 836–845, 2002.

[171] B. Bellosillo, N. Villamor, A. López-Guillermo et al., "Complement-mediated cell death induced by rituximab in B-cell lymphoproliferative disorders is mediated in vitro by a caspase-independent mechanism involving the generation of reactive oxygen species," *Blood*, vol. 98, no. 9, pp. 2771–2777, 2001.

[172] H. Sui, C. Shi, Z. Yan, and H. Li, "Combination of erlotinib and a PARP inhibitor inhibits growth of A2780 tumor xenografts due to increased autophagy," *Drug Design, Development and Therapy*, vol. 9, p. 3183, 2015.

[173] X. Qian, J. Li, J. Ding, Z. Wang, W. Zhang, and G. Hu, "Erlotinib activates mitochondrial death pathways related to the production of reactive oxygen species in the human non-small cell lung cancer cell line A549," *Clinical and Experimental Pharmacology & Physiology*, vol. 36, no. 5-6no. 5-6, pp. 487–494, 2009.

[174] F. Shan, Z. Shao, S. Jiang, and Z. Cheng, "Erlotinib induces the human non-small-cell lung cancer cells apoptosis via activating ROS-dependent JNK pathways," *Cancer Medicine*, vol. 5, no. 11, pp. 3166–3175, 2016.

[175] K. P. Orcutt, A. D. Parsons, Z. A. Sibenaller et al., "Erlotinib mediated inhibition of EGFR signaling induces metabolic

oxidative stress through NOX4," *Cancer Research*, vol. 71, no. 11, pp. 3932–3940, 2011.

[176] S. Nowsheen, T. Cooper, J. A. Stanley, and E. S. Yang, "Synthetic lethal interactions between EGFR and PARP inhibition in human triple negative breast cancer cells," *PLoS One*, vol. 7, no. 10, article e46614, 2012.

[177] R. Zhang, H. Qiao, S. Chen et al., "Berberine reverses lapatinib resistance of HER2-positive breast cancer cells by increasing the level of ROS," *Cancer Biology & Therapy*, vol. 17, no. 9, pp. 925–934, 2016.

[178] Y. S. Hong, S. W. Hong, S. M. Kim et al., "Bortezomib induces G2-M arrest in human colon cancer cells through ROS-inducible phosphorylation of ATM-CHK1," *International Journal of Oncology*, vol. 41, no. 1, pp. 76–82, 2012.

[179] P. Neri, L. Ren, K. Gratton et al., "Bortezomib-induced "BRCAness" sensitizes multiple myeloma cells to PARP inhibitors," *Blood*, vol. 118, no. 24, pp. 6368–6379, 2011.

[180] Z. Chen, E. F. Pittman, J. Romaguera et al., "Nuclear translocation of B cell-specific transcription factor, BACH2, modulates ROS mediated cytotoxic responses in mantle cell lymphoma," *PLoS One*, vol. 8, no. 8, article e69126, 2013.

[181] R. C. Kane, R. Dagher, A. Farrell et al., "Bortezomib for the treatment of mantle cell lymphoma," *Clinical Cancer Research*, vol. 13, no. 18, pp. 5291–5294, 2007.

[182] K. A. Conklin, "Chemotherapy-associated oxidative stress: impact on chemotherapeutic effectiveness," *Integrative Cancer Therapies*, vol. 3, no. 4, pp. 294–300, 2016.

[183] N. Yadav, S. Kumar, T. Marlowe et al., "Oxidative phosphorylation-dependent regulation of cancer cell apoptosis in response to anticancer agents," *Cell Death & Disease*, vol. 6, no. 11, article e1969, 2015.

[184] J. J. J. Leahy, B. T. Golding, R. J. Griffin et al., "Identification of a highly potent and selective DNA-dependent protein kinase (DNA-PK) inhibitor (NU7441) by screening of chromenone libraries," *Bioorganic & Medicinal Chemistry Letters*, vol. 14, no. 24, pp. 6083–6087, 2004.

[185] Y. Zhao, H. D. Thomas, M. A. Batey et al., "Preclinical evaluation of a potent novel DNA-dependent protein kinase inhibitor NU7441," *Cancer Research*, vol. 66, no. 10, pp. 5354–5362, 2006.

[186] N. Traverso, R. Ricciarelli, M. Nitti et al., "Role of glutathione in cancer progression and chemoresistance," *Oxidative Medicine and Cellular Longevity*, vol. 2013, Article ID 972913, 10 pages, 2013.

[187] E. Kun, E. Kirsten, and J. Mendeleyev, "Synergistic anticancer action of reversibly and irreversibly acting ligands of poly (ADP-ribose) polymerase," *International Journal of Molecular Medicine*, vol. 11, no. 2, pp. 191–193, 2003.

[188] O. W. Griffith, "Mechanism of action, metabolism, and toxicity of buthionine sulfoximine and its higher homologs, potent inhibitors of glutathione synthesis," *Journal of Biological Chemistry*, vol. 257, no. 22, pp. 13704–13712, 1982.

[189] F. Lopes-Coelho, S. Gouveia-Fernandes, L. G. Gonçalves et al., "HNF1β drives glutathione (GSH) synthesis underlying intrinsic carboplatin resistance of ovarian clear cell carcinoma (OCCC)," *Tumour Biology*, vol. 37, no. 4, pp. 4813–4829, 2016.

[190] P. I. Bauer, J. Mendeleyeva, E. Kirsten et al., "Anti-cancer action of 4-iodo-3-nitrobenzamide in combination with buthionine sulfoximine: inactivation of poly (ADP-ribose) polymerase and tumor glycolysis and the appearance of a poly (ADP-ribose) polymerase protease," *Biochemical Pharmacology*, vol. 63, no. 3, pp. 455–462, 2002.

[191] C. Marzano, V. Gandin, A. Folda, G. Scutari, A. Bindoli, and M. P. Rigobello, "Inhibition of thioredoxin reductase by auranofin induces apoptosis in cisplatin-resistant human ovarian cancer cells," *Free Radical Biology and Medicine*, vol. 42, no. 6, pp. 872–881, 2007.

[192] S. Ganguly, S. Gunewardena, S. Weir, J. McGuirk, and R. M. Rao, "Synergistic interaction of auranofin with PARP inhibitors in ATM-proficient mantle cell lymphoma," in *Proceedings: AACR 106th Annual Meeting*, Philadelphia, 2015.

[193] J. Egea, I. Fabregat, Y. M. Frapart et al., "European contribution to the study of ROS: a summary of the findings and prospects for the future from the COST action BM1203 (EU-ROS)," *Redox Biology*, vol. 13, pp. 94–162, 2017.

[194] K. W. Derks, J. H. Hoeijmakers, and J. Pothof, "The DNA damage response: the omics era and its impact," *DNA Repair*, vol. 19, pp. 214–220, 2014.

[195] J. F. Liu, W. T. Barry, M. Birrer et al., "Combination cediranib and olaparib versus olaparib alone for women with recurrent platinum-sensitive ovarian cancer: a randomised phase 2 study," *Lancet Oncology*, vol. 15, no. 11, pp. 1207–1214, 2014.

Hindawi
Oxidative Medicine and Cellular Longevity
Volume 2018, Article ID 4950591, 12 pages
https://doi.org/10.1155/2018/4950591

Review Article

Long Noncoding RNAs in Yeast Cells and Differentiated Subpopulations of Yeast Colonies and Biofilms

Derek Wilkinson,[1] Libuše Váchová,[2] Otakar Hlaváček,[2] Jana Maršíková,[1] Gregor D. Gilfillan,[3] and Zdena Palková[1]

[1]*Faculty of Science, Charles University, BIOCEV, 252 50 Vestec, Czech Republic*
[2]*Institute of Microbiology of the Czech Academy of Sciences, BIOCEV, 252 50 Vestec, Czech Republic*
[3]*Department Medical Genetics, Oslo University Hospital and University of Oslo, 0450 Oslo, Norway*

Correspondence should be addressed to Zdena Palková; zdenap@natur.cuni.cz

Received 26 October 2017; Accepted 7 February 2018; Published 25 March 2018

Academic Editor: Paula Ludovico

We summarize current knowledge regarding regulatory functions of long noncoding RNAs (lncRNAs) in yeast, with emphasis on lncRNAs identified recently in yeast colonies and biofilms. Potential regulatory functions of these lncRNAs in differentiated cells of domesticated colonies adapted to plentiful conditions versus yeast colony biofilms are discussed. We show that specific cell types differ in their complements of lncRNA, that this complement changes over time in differentiating upper cells, and that these lncRNAs target diverse functional categories of genes in different cell subpopulations and specific colony types.

1. Introduction

Saccharomyces cerevisiae strains used in the brewing industry and in microbiology and genetics laboratories are often grown as planktonic cells in liquid culture, but yeasts also form multicellular communities such as colonies and biofilms, which reflect a more natural lifestyle and are able to cope with different intrinsic and extrinsic stresses [1]. There is growing evidence of cell differentiation, metabolic reprogramming, activation of various stress-defence mechanisms, and other aspects of primitive multicellularity, not only in the complex colony biofilms of nutritionally challenged wild yeast but also in the less structured, smooth colonies of pampered laboratory strains [2–5]. Ammonia signalling, metabolic reprogramming, mitochondrial retrograde signalling, the presence of extracellular matrix, chromosome rearrangement, and many other processes have been described that contribute towards the colony lifestyle, differentiation processes, stress resistance, adaptation, and longevity of multicellular populations [1, 3–7]. However, lncRNA has, until recently, been overlooked as a potential regulator of processes involved in long-term colony development and differentiation, despite the key roles of regulatory ncRNAs in mammalian cell differentiation [8]. The RNAi machinery, which contributes to the production of regulatory ncRNA in many organisms, has been lost in *S. cerevisiae* [9]. Studies in yeast [10–12] identified large numbers of "cryptic transcripts," "nonannotated transcripts," and "heterogenous unstable RNAs," respectively. These studies established the use of tiling arrays for the identification of yeast long noncoding RNA (lncRNA) and deletion of genes encoding exonucleases, such as *RRP6*, to stabilise unstable transcripts. Loss of RNAi machinery may have triggered the evolution of a large complement of highly expressed lncRNA in yeast [13]. The detection of several thousand lncRNAs in two studies [14, 15] led to an explosion of interest in these poorly understood transcripts.

Here, we present a mini review of yeast lncRNAs and their previously described roles in regulating gene expression under various circumstances. In the second part of the review, we focus in more detail on lncRNAs that we have recently identified in differentiated subpopulations of cells from two distinct types of yeast populations [16, 17], each of which uses unique strategies to cope with stress and ensure

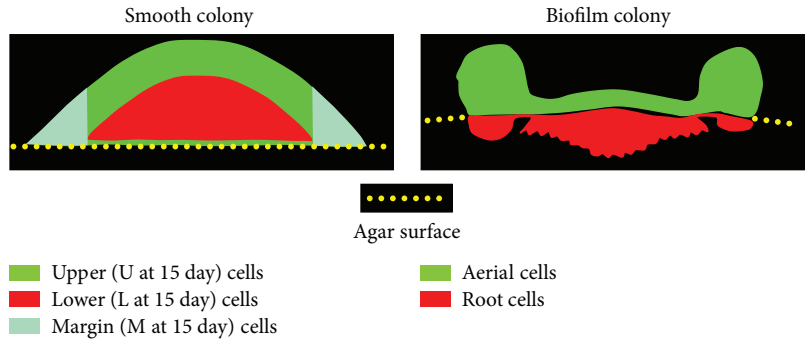

Figure 1: Diagram of cell subpopulations isolated from smooth colonies of BY4742 strain (a) and biofilm colonies of BR-F strain (b).

longevity of the population as a whole. These are complex colony biofilms formed by wild strains of *Saccharomyces cerevisiae* [18] and smooth colonies of *S. cerevisiae* laboratory strains [19] (Figure 1). We present further analyses of these lncRNAs, particularly in relation to their different types and positions in relation to neighbouring genes. We also discuss potential regulatory activities of lncRNAs in ageing smooth colonies and colony biofilms in light of current knowledge of regulatory functions of lncRNAs in yeast cells.

2. Important Messages or Random SPAM?

Transcription of yeast lncRNA occurs largely from bidirectional promoters shared with other loci [10, 14, 20–23]. However, lncRNA accumulation is countered by early termination of unstable antisense transcription, modulation of strand expression via chromatin remodelling, and degradation of lncRNAs [14, 15, 22, 24]. lncRNA/gene expression correlation [25, 26] suggests that some lncRNAs are true cellular regulators. Furthermore, there are numerous examples of the stabilisation (or destabilisation) of lncRNA transcript classes under specific conditions, such as meiosis, respiration or sporulation [26–29], carbon source [14, 30], metal abundance [31], and osmotic stress [32]. It was recently shown that the $5'$–$3'$ exonuclease Xrn1p is localised to eisosomes when glucose is scarce but relocalises to the cytoplasm when glucose is present, where it degrades lncRNAs called XUTs and modulates lncRNA regulation of gene expression [33]. Whether this phenomenon constitutes primary regulation or merely "fine-tuning" of gene expression remains to be determined. Nonetheless, it is clear that the study of lncRNA in yeast may uncover important regulatory mechanisms. On the other hand, some lncRNA transcription may simply be a by-product of bidirectional transcription [15].

3. Classes of lncRNA: Stability and Detection

The identification of different classes of lncRNAs in yeast has been largely determined by the techniques used in their detection. Microarrays, $3'$-long serial analysis of gene expression (SAGE), and *RRP6* deletion were used to identify stable unannotated transcripts (SUTs), lncRNAs that are processed in the cytosol similarly to mRNAs, and cryptic unstable transcripts (CUTs) that are sensitive to the RNA decay machinery and degraded by the nuclear exosome and/or the cytoplasmic $5'$–$3'$ exonuclease Xrn1p [14, 15, 34]. Other lncRNAs follow this stability-based nomenclature (Table 1), which will also be used in this text. MUTs (meiotic unstable transcripts) are a subset of CUTs that are degraded by Rrp6p RNase (a component of the nuclear exosome complex (NEC)) which accumulate predominantly during meiotic development due to decreased levels of Rrp6p [28]. rsCUTs are expressed during respiration and/or sporulation [28]. XUTs (Xrn1p-sensitive unstable transcripts) are another class of CUTs that are degraded in the cytoplasm. Deletion of *XRN1*, which encodes a $5'$–$3'$ exonuclease, stabilises XUTs [34]. Reducing Nrd1p levels in the nucleus inhibits Nrd1p-dependent lncRNA transcription termination [22], allowing identification of Nrd1-unterminated transcripts (NUTs). Telomeric repeat-containing RNA (TERRA), regulating telomere function, is stabilised in *rat1-1* mutants which are defective in $5'$–$3'$ nuclear exonuclease activity [35]. *NAM7* (*UPF1*) encodes an RNA helicase involved in the nonsense-mediated decay (NMD) pathway, and deletion of *NAM7* facilitates accumulation of $5'$-extended transcripts which, because their accumulation depends on inactivation of cytoplasmic degradation, were termed "cytoplasmically degraded CUTs" (CD-CUTs) [31].

Termination of CUT transcription occurs via a different mechanism from that of mRNAs [36]. The Nrd1p-Nab3p complex, which includes helicase and cap-binding proteins, binds specific motifs that are enriched in CUTs and targets nascent lncRNAs for adenylation and degradation via interactions with the TRAMP complex and nuclear exosome [36–39]. CUTs tend to be degraded in the nucleus and are largely sequestered from the cytoplasm under natural conditions, but other classes of lncRNA are exported from the nucleus and degraded in the cytoplasm [39]. Some lncRNA (e.g., CD-CUTs) may even be imported back into the nucleus, following NMD, where they repress gene expression in trans [31, 39]. Once lncRNAs are exported from the nucleus, they may be targeted by several decay pathways [40], including (i) deadenylation, decapping, and degradation by the $5'$–$3'$ exonuclease Xrn1p; (ii) deadenylation, followed by $3'$–$5'$ degradation by the cytoplasmic exosome or via one of the translation-associated pathways; (iii) the nonsense-mediated decay pathway (degrading mRNA

Table 1: Landmarks in the study of yeast lncRNA.

Discovery	lncRNA class*	Strain manipulation	Technique	Reference
Cryptic Pol II transcripts		*RRP6* deletion	Microarray	[12]
Nonannotated transcripts		Wild type	Tiling array	[10]
CUT termination dependent on Nab3p		*NAB3* mutation	Microarray	[37]
Heterogenous unstable RNAs		*RRP6* deletion	Microarray	[11]
Telomeric repeat-containing RNAs (TERRAs)	*TERRAs*	*rat1-1* mutants	RT-PCR, northerns	[35]
Cryptic unstable transcripts (CUTs)	***CUTs***	*RRP6* & *TRF4* deletion	3′-long SAGE	[14]
Stable unannotated transcripts (SUTs) & CUTs	***SUTs***, ***CUTs***	*RRP6* deletion	Microarray	[15]
PHO84 antisense lncRNA can repress in trans		Ectopic *PHO84* expression	qPCR, northerns	[59]
PWR1/*ICR1* lncRNAs and *FLO11* expression		ΔP_{FLO11}, *cit6*, and *sfl1*	Northern blot	[41]
Condition-dependent antisense transcripts		Stationary phase, etc.	Stranded RNA-seq	[26]
Meiotic unannotated transcripts (MUTs), respiration/sporulation unannotated transcripts (rsCUTs)	***MUTs***, *rsCUTs*	Meiotic a/α diploids	Tiling array	[28]
Xrn1-sensitive unstable transcripts (XUTs)	***XUTs***	*XRN1* deletion	RNA-seq	[34]
RME2 lncRNA regulates *IME2* expression		*RME2* promoter deletion	RT-PCR	[27]
CUT repression of metal homeostasis genes	*CD-CUTs*	NMD/CD-CUT mutants	Northern blot	[31]
IME1 and *IME4* expression regulated by lncRNA		set2, set3, haploid/diploid	ChIP, northerns	[29]
lncRNA/gene pairs, coregulated in colonies		GFP-tagged *ATO1*	Microarrays	[66]
Nrd1-unterminated transcripts (NUTs)	*NUTs*	FRB-tagged NRD1	4tU-seq	[22]
Stress/Hog1p-regulated lncRNA transcription		*HOG1* deletion	Tiling arrays	[32]

*Italics: lncRNA classes discovered; bold: classes discussed here in relation to smooth and biofilm colonies.

containing, e.g., spurious stop codons); and (iv) no-go decay (NGD: degrading mRNA with stalled elongation). Wery et al. [40] review the high degree of overlap between lncRNA classes (e.g., between XUTs and both SUTs and CUTs) and suggest that many XUTs are merely SUTs that have been extended at the 3′ end and that these extensions target XUTs for NMD.

4. Regulation of Gene Expression by Annotated lncRNAs

lncRNAs differ in terms of distance from coding regions and orientation with regard to coding genes (Figure 2(a)). Antisense transcripts are transcribed from overlapping loci, located on the opposite strand to sense loci [26] (antisense-overlapping). lncRNA/gene pairs on opposite strands may be transcribed from nearby start points but in opposite directions (antisense-divergent orientation), or their transcription may converge on a common end point (antisense-convergent orientation). Alternatively, the lncRNA locus may occur on the same strand as an upstream or downstream locus (tandem sense orientation) [14].

The functions of most yeast lncRNAs identified so far are unknown, but there are some exceptions, including regulation of *GAL1*, *PHO5*, and *PHO84* expression [23], in which the lncRNA has been assigned a role in regulating the expression of a related gene. In some of these examples, the regulatory function is attributed to the transcription process itself and not to the presence of the lncRNA transcript [39]. For example, lncRNA transcription could be involved in changes in chromatin structure that subsequently influence the binding of transcription factors to promoter regions of the related gene, as was shown for the negative regulation of *IME1* [29] and modulation of expression of *FLO11* [41]. Other known mechanisms of lncRNA function include transcriptional interference in which antisense lncRNA can block/decrease transcription of sense-strand mRNA, for example, in the case of *IME4* mRNA transcription [29]. Many lncRNAs are regulated by the same promoter as a divergent gene on the opposite strand [42], and the lncRNA negatively regulates the expression of an antisense-overlapping gene that lies upstream of the antisense-divergent gene.

Expression of the *FLO11* gene, involved in many processes including colony biofilm formation, is modulated by the expression of a tandem upstream sense locus, *ICR1*. *ICR1* expression is in turn regulated by an antisense-overlapping locus, *PWR1* [41] in a "toggle"-like manner, dependent on two transcription factors: Sfl1p activates *ICR1* expression, inhibiting *FLO11* expression, while Flo8p upregulates *PWR1* expression, inhibiting *ICR1* expression and promoting *FLO11* expression [41]. Rpd3p-mediated chromatin modification may block Sfl1p binding, countering *ICR1*-mediated inhibition of *FLO11* expression. Bumgarner et al. [43] revealed the existence of three expression states within a clonal cell population in which the *FLO11* promoter is (i) silenced, (ii) nonsilenced but lacking transcription factors, and (iii) nonsilenced and bound by transcription factors leading to *FLO11* expression that is absent, low, and high, respectively. *FLO11* expression correlated with *PWR1* expression and anticorrelated with *ICR1* expression and the physical act of *ICR1* transcription

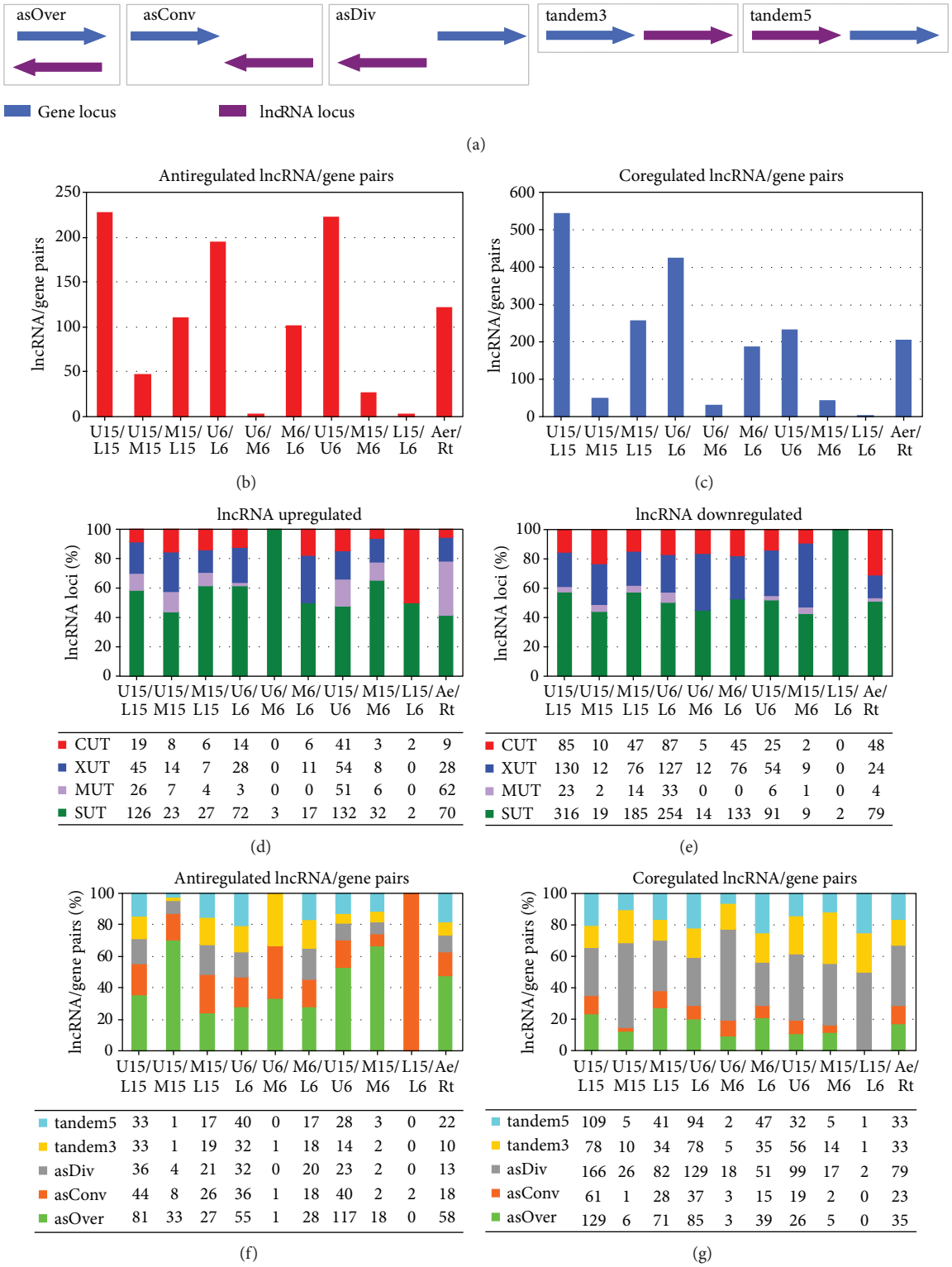

Figure 2: lncRNAs detected in subpopulations of aged yeast colony cells. DE gene and DE lncRNA loci were identified that were located within 1.5 kB of one another in 5 different orientations (a). The numbers of antiregulated (b) and coregulated (c) lncRNA/gene pairs were compared for the different expression comparisons detailed at the bottom of the figure. Percentages (bars) and numbers (boxes underneath) of different classes of lncRNA upregulated (d) or downregulated (e) in each sample as well as the percentages (bars) and numbers (boxes) of antiregulated (f) and coregulated (g) lncRNA/gene pairs are given for each comparison. Abbreviations: asOver: antisense-overlapping; asConv: antisense-convergent; asDiv: antisense-divergent; tandem3: tandem to (sense strand) and downstream of gene; tandem5: tandem to (sense strand) and upstream of gene; SUT: stable unannotated transcript; MUT: meiotic unstable transcript; XUT: Xrn1-dependent unstable transcript; CUT: cryptic unannotated transcript.

displaced transcription factors from the *FLO11* promoter, effectively "resetting" the promoter. Cells with fewer than 5 fluorescent Flo11p dots lacked structured colony morphology, diploid pseudohyphae formation, and haploid adhesion. Since Flo11p drives biofilm formation and biofilm development is a key fungal virulence factor in pathogenic fungi such as *Candida albicans* [44–46], identifying regulators of *FLO11* expression could help to counter the high drug resistance of fungal biofilms or uncover drug targets for treatment of potentially lethal fungemias.

In haploid cells, Rme1p binds upstream of the key meiotic regulator *IME1*, causing the tandem sense locus *IRT1* to express a transcript that recruits histone remodellers that produce a repressive chromatin structure over the *IME1* promoter [29]. In MATa/α diploids, the a1-α2 repression complex blocks *RME1* expression, relieving inhibition of meiosis. Another major regulator of meiosis is *IME4*, encoding a protein that methylates many key sporulation mRNAs [27, 29]. *RME2*, an antisense lncRNA locus overlapping the whole *IME4* ORF, inhibits *IME4* expression in haploid cells. However in diploid cells, the a1-α2 complex binds to the *RME2* promoter, inhibiting lncRNA expression and relieving the block on *IME4* expression [29]. In another example of gene expression regulation via chromatin remodelling, the osmotic stress-induced MAPK, Hog1p binds the 3′ end of *CDC28* (a master regulator of mitosis and meiosis), promoting antisense lncRNA expression that triggers looping of the *CDC28* gene. This looping allows Hog1p to "jump" across the narrow neck of the loop from the 3′ to the 5′ end, where it induces RSC-dependent chromatin remodelling, leading to *CDC28* gene expression [32]. These examples demonstrate how lncRNA regulatory mechanisms can be switched on or off in specific cell subpopulations or in the presence of stress [27, 32].

In some cases, transcription of a lncRNA directly hinders gene expression from a neighbouring target gene [39]. When serine is plentiful, expression from a 5′ tandem sense lncRNA locus, *SRG1*, inhibits expression of the serine biosynthesis gene *SER3* by increasing promoter nucleosome density, which prevents transcription factors from accessing the promoter [47]. Martens et al. [48] showed that serine availability activates binding of the transcription factor Cha4p to the *SRG1* promoter and recruitment the Swi/Snf and SAGA complexes, leading to activation of *SRG1* and thus repression of *SER3*. Such "transcriptional interference" is a common mechanism by which the expression of one locus is attenuated by that of a second, converging locus [49], not only between coding and noncoding loci but also between converging coding loci.

A *GAL10* antisense-overlapping lncRNA (which also sense-overlaps *GAL1*) has been shown to recruit methyltransferase and deacetylase complexes which silence both *GAL10* and *GAL1* [39]. Pinskaya et al. [50] showed that glucose/Reb1-dependent transcription of the antisense transcript $GAL1_{uncut}$ promotes Set1-dependent H3K4 di/trimethylation and facilitates recruitment of the RPD3S histone deacetylase, repressing *GAL1*. A similar mechanism blocks transcription from a "hidden" promoter within *SUC2*, suggesting that H3K4 di/trimethylation might represent a widespread mechanism for maintaining promoter fidelity. lncRNAs are decapped and degraded in a *DCP1*-, *DCP2*-, *XRN1*-, and *RAT1*-dependent manner [51] to facilitate galactose-induced GAL expression. Lenstra et al. [52] showed that lncRNA expression has two modes: spurious and functional. When GAL expression is induced, GAL10 expression is independent of spurious lncRNA expression, but when not induced, tight repression of GAL10 is dependent upon functional lncRNA expression. Cloutier et al. and Beck et al. [53–56] demonstrated that the glucose-dependent DEAD box RNA helicase negatively regulates formation of DNA/RNA hybrid R-loops and that a change of carbon source from glucose to galactose promotes export of Dbp2p to the cytoplasm and lncRNA-dependent R-loop formation and displacement of the Cyc8-Tup1p corepressor from the promoter and derepression of GAL genes. Thus, relieving the block on R-loop formation may be a general mechanism for rapidly derepressing key genes and adapting to changing environmental conditions [55]. Zacharioudakis and Tzamarias [57] further showed that when galactose concentration is high, Gal1p enters a positive feedback loop with Gal4p and the GAL genes are turned on, independently of lncRNA. However, when galactose levels are low, the lncRNA is able to randomly block transition to the on state, delaying the switch to alternative carbon source in a percentage of cells and facilitating metabolic flexibility.

Although most cases of lncRNA regulation identified in budding yeast appear to be *cis*-acting, some examples of *trans*-acting regulators have been described [34, 58, 59]. Reference [34] identifies Xrn1p-sensitive antisense transcripts, some with apparent regulatory roles, and suggests a mechanism whereby XUTs interact with a protein complex to silence target genes and that this activity is promoted by histone H3K4 mono/di-methylation but opposed by histone H3K4 trimethylation. Large numbers of different XUTs are exported from the nucleus and may be degraded by translation-coupled NMD [40], so they may also have posttranscriptional regulatory roles [34]. Ty1 retrotransposon expression is regulated in trans by an antisense CUT [58] which interacts with Ty1, promotes histone deacetylation and Set1-dependent methylation, and effects chromatin silencing. It has been shown [59] that *PHO84* antisense lncRNA is able to act in trans to silence transcription of a second copy of *PHO84* elsewhere in the genome. Silencing of the second *PHO84* copy depends upon a region of homology with the upstream activating sequence and possibly also recruits a silencing complex to the promoter.

A lncRNA overlaps the *PHO5* gene on the antisense strand, and transcription of the lncRNA across the gene promoter plays a role in the activation (not repression) of *PHO5* [60] by increasing the efficiency of histone removal, facilitating access of the polymerase to the TATA box. Bunina et al. [61] showed that starvation-/sporulation-induced expression of the antisense transcript is dependent upon repetitive regions in the 3′UTR and has no effect upon promoter activity but does promote the expression of a long mRNA isoform with enhanced stability.

Chia et al. [62] showed that transcription of an upstream lncRNA, *NDC80*$_{\text{luti}}$, represses *NDC80* expression during meiotic prophase by driving Set1-dependent H3K4Me2 and Set2-dependent H3K36Me3 at the *NDC80* promoter, leading to recruitment of the Set3C and Rpd3S histone deacetylases. The pervasiveness of lncRNA regulation of gene expression in different cell types and under differing conditions has been demonstrated in a number of studies. Kim et al. [63] showed that the promoters of a high percentage of Set2-repressed genes are overlapped by antisense or upstream tandem lncRNA that promote H3K36Me3 and Rpd3S-dependent deacetylation within the promoter region and that many of these genes are regulated by carbon source. A similar mechanism involving Set3C-dependent H3K4me2 was identified previously [30]. McDaniel et al. [64] showed that deleting *SET2* affects the expression of genes involved in stress responses because lack of H3K36Me permits the inappropriate transcription of antisense lncRNA that interferes with gene transcription.

Kwapisz et al. [65] identified CUTs and XUTs, generated from subtelomeric regions (subTERRA) with roles in telomeric silencing and prevention of clustering, respectively, via the formation of DNA-RNA hybrids and by protein scaffolding.

5. Long ncRNAs May Contribute to Gene Regulation within Differentiated Cell Subpopulations of Colonies and Colony Biofilms

Traven et al. [66] provided a first glimpse into the presence of, and potential regulation of genes by, lncRNAs within yeast colonies of laboratory strain BY4741, grown on complete glucose medium and differentiated into two subpopulations of cells on the "outside" and "inside" of the colonies. In this study, transcriptomic differences were identified by microarrays and included 12 SUTs and CUTs on the outside and 53 on the inside of the colonies. In addition, several lncRNA/gene pairs with positively correlating expression were identified that represent possible examples of gene regulation by lncRNA, including the ammonium permease gene *MEP2*.

We performed further studies using the more sensitive RNA sequencing (RNA-seq) technique. RNA-seq provided a detailed transcriptomic view of six cell subpopulations present in smooth BY4742 colonies grown on complete respiratory medium [17]: cells from upper, margin, and lower parts of colonies in two developmental phases (late acidic 6-day-old and alkali-phase 15-day-old). In parallel experiments, two subpopulations (a surface "aerial" cell subpopulation and a subpopulation of invasive "root" cells growing within the agar) from structured colony biofilms grown on the same medium were also studied [16] (Figure 1). Every gene located within 1.5 kB of (or antisense-overlapping) each lncRNA was identified to produce a list of lncRNA/gene pairs in any of the 5 different orientations (Figure 2(a)) considered. Previous expression profiling of subpopulations of smooth colonies and colony biofilms identified some metabolic similarities but even more differences [16, 17]. Whereas some of the expression differences in individual genes may be caused by the fact that laboratory and wild strains forming smooth colonies and colony biofilms, respectively, are not isogenic, most of the differences are in agreement with the different lifestyles of yeast populations in smooth colonies (formed by either laboratory strains or domesticated wild strains) versus colony biofilms [1, 5]. Here, we therefore also compared types of identified lncRNAs as well as lncRNA/gene pairs in smooth colonies and colony biofilms, to see whether any potential lncRNA-related similarities exist among subpopulations of these structures.

5.1. Antiregulation of lncRNA/Gene Pairs Is Highest when Comparing Dissimilar Cell Types. Cells localised to the upper and marginal regions of smooth colonies (Figure 1) are somewhat similar in gene expression, protein production, and so on and are more different from cells localised to the lower regions of central colony areas [17]. lncRNA/gene antiregulation (where gene and lncRNA are antagonistically differentially expressed in the two subpopulations) and coregulation (agonistically differentially expressed) were highest when upper (U) and lower (L) cells were compared and lowest when upper and margin (M) cells were compared (Figures 2(b) and 2(c)). Comparison of aerial and root cells of colony biofilms revealed numbers of antiregulated and coregulated pairs, closest to the numbers identified in marginal/lower cell comparisons in smooth colonies (Figures 2(b) and 2(c)). The numbers of mapped reads were similar for biofilm and smooth colonies (average of 17.1 and 15.4 million reads, resp.); the percentages of mapped reads mapping to lncRNA were 23 and 25%, respectively; and the same read counting and differential expression analysis packages were used in both analyses.

Increased antiregulation and coregulation in the U/L and M/L comparisons, compared with U/M (in both 6- and 15-day-old colonies), is consistent with observed U/M cell similarities (metabolic, gene expression, and other) and differences of both from L cells [17]. High U6/U15 anti- and coregulation agrees with the finding that temporal gene expression changes are most prominent in upper cells of developing colonies [17]. Surprisingly, approximately twice as many antiregulated/coregulated pairs were observed when comparing upper versus lower cells (in smooth colonies) than in root versus aerial parts of biofilm colonies. However, aerial and root parts of colony biofilms are not homogenous and contain small subpopulations of cells with features typical of their counterparts [16]. This fact may dilute the observed aerial-root cell differences. Furthermore, aerial-root cells were separated from younger colony biofilms (3-day-old) than the cells of smooth colonies (6- and 15-day-old), in which upper cells gradually acquire unique metabolic features and gain specific physiology important for longevity [19, 67]. In contrast, only moderate expression changes occur during this time period in slowly growing marginal and lower cells [17]. Accordingly, expression differences between margin and lower cells are more comparable at different developmental time points. However, the aerial versus root and margin versus lower cell comparisons are

similar only in terms of the numbers of co- and antiregulated lncRNA/gene pairs, which may reflect merely the level of similarity/dissimilarity between the respective cell types. As shown below, different lncRNA/gene pairs were identified in smooth colonies and colony biofilms.

5.2. Cell-Type-Specific Expression of lncRNA Classes. Numbers of differentially expressed lncRNAs differ significantly when comparing the various cell subpopulations (Figures 2(d) and 2(e)). The terms upregulation/upregulate (or downregulation/downregulate) are relative, so the observations could be caused by activation (or repression) of transcription in the first subpopulation or by repression (or activation) in the second. Lower cells were found to upregulate the highest number of lncRNAs of all monitored cell types, as shown in Figures 2(d) and 2(e). Margin cells upregulate 10 times as many lncRNA loci as upper cells at 6 days, whereas no difference was observed at 15 days, which is consistent with the finding that the number of upregulated lncRNAs in upper cells increases over time. No differences in the total number of up-/downregulated lncRNAs were observed between aerial and root cells of colony biofilms.

SUTs were the most common lncRNAs in smooth colonies (>50% of both upregulated and downregulated lncRNAs) as well as in colony biofilms (40% of upregulated and >50% of downregulated lncRNAs). Differentially expressed SUTs were similarly distributed between upregulated and downregulated lncRNA categories across most comparisons (Figures 2(d) and 2(e)). CUTs form ~15% of up-/downregulated genes in most comparisons with no significant difference in distribution in smooth colonies. However, significant differences were detected in colony biofilms, where 5.3x as many CUTs were upregulated in roots (forming 30% of all upregulated lncRNAs in roots) as in aerial cells.

The clearest difference in up- and downregulated unstable lncRNAs between smooth colonies and colony biofilms was based on MUTs, forming ~6.5% and ~20% of up-/down regulated lncRNAs, respectively. More MUTs are up- or downregulated in 15-day-old smooth colonies than in 6-day-old colonies, in which MUTs were only identified when comparing L and U cells (10x as many MUTs were upregulated in L cells), indicating increased MUT expression during smooth colony ageing. The largest group of upregulated MUTs occurred in aerial cells of colony biofilms, >14x more than the number of upregulated MUTs in roots. In summary, expression of MUTs is increased in upper (and partially in margin) parts of smooth colonies during ageing, whereas MUTs are already highly expressed in aerial cells of much younger colony biofilms.

Increased MUT expression in aerial cells of biofilm colonies is consistent with the upregulation of a large group of meiotic genes in aerial cells [16]. MUTs accumulate predominantly during meiotic development, possibly due to decreased levels of Rrp6p RNase (a component of NEC), which can degrade MUTs [28] and CUTs [14, 15]. Accordingly, *RRP6* expression is >2-fold upregulated in root cells than in aerial cells. In smooth colonies, *RRP6* expression (which can affect CUT stability) is only moderately upregulated (1.3- to 1.4-fold) in L relative to U or M cells. However, CUT degradation is also dependent upon Nab3p, Nrd1p, and the TRAMP complex (mainly the TRAMP4 complex, which includes Pap2p (Trf4p) [68]). The apparent upregulation of CUT expression in lower cells and MUT expression in upper cells may be due to differential expression of the TRAMP4 and TRAMP5 complexes (which target both shared and unshared transcripts [69]) and of the $3'$–$5'$ exosome components Rrp6p and Dis3p.

5.3. Orientation of lncRNA/Gene Pairs Differs in Antiregulated and Coregulated Pairs. lncRNA/gene pairs were classified according to their mutual position (Figure 2(a)) and expressional relationship (antiregulated, Figure 2(f), and coregulated, Figure 2(g)). The total number of coregulated versus antiregulated lncRNA/gene pairs was slightly higher in both smooth colonies (>1.8x) and colony biofilms (>1.7x), but more prominent differences were observed between specific cell types and among different lncRNA/gene position categories. Coregulated lncRNA/gene pairs were overrepresented as compared with antiregulated pairs in U15/L15 (>2.3x), M15/L15 (>2.3x), U6/L6 (>2.1x), and U6/M6 (>10x) cell comparisons.

Antisense-overlapping (asOver) lncRNAs were the most common category of antiregulated lncRNA/gene pairs both in smooth colonies (>38%) and in colony biofilms (>47%), whereas antisense-divergent (asDiv) lncRNAs were the most prominent category in coregulated lncRNA/gene pairs (>33% in smooth colonies and >38% in colony biofilms). Enrichment of antisense-divergent loci among coregulated and antisense-overlapping loci among antiregulated lncRNA/gene pairs is consistent with previous reports of a positive correlation between the expression of antisense-divergent loci (gene and lncRNA), possibly because of increased bidirectional transcription from a common nucleosome-depleted region [14] and of interference by antisense-overlapping lncRNA in gene expression and thus negative regulation [26]. The distribution of asOver and asDiv lncRNA/gene pairs among different cell comparisons was relatively equal, with the exception of U15/M15 (1.82x more asOver antiregulated pairs than average and 1.65x more asDiv coregulated pairs than average), U6/M6 (1.74x more asDiv coregulated pairs than average), and M15/M6 (1.73x more asDiv coregulated pairs than average) comparisons.

5.4. Different Functional Groups of Genes May Be Negatively Regulated by lncRNA in Smooth and Biofilm Colonies. The numbers of potentially negatively (in antiregulated lncRNA/gene pairs) and positively (in coregulated lncRNA/gene pairs) regulated genes in different functional annotation groups were considered. Antiregulated/coregulated lncRNA/gene pairs were annotated with functional categories using information in SGD (http://www.yeastgenome.org/, [70]) and the literature. Datasets of differentially expressed (DE) genes were then compared using Intervene's UpSet module [71], which visualizes the intersection of multiple data sets in UpSet plots (Figure 3). No common antiregulated and only 6 common coregulated lncRNA/gene pairs were

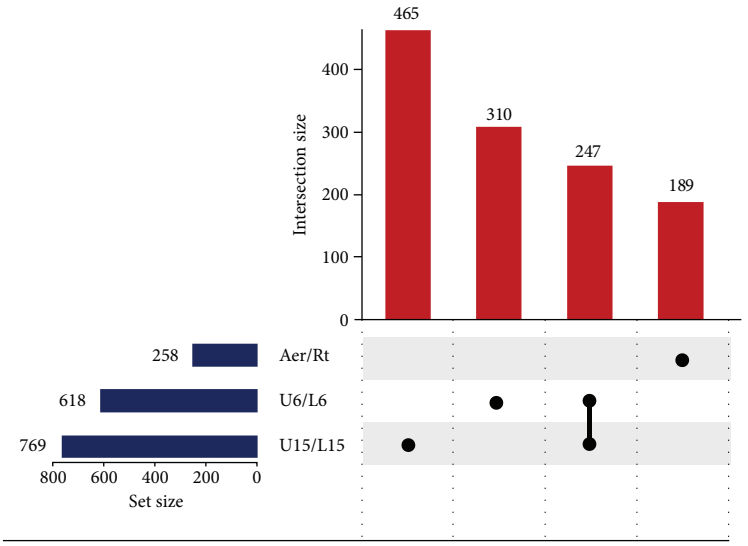

Functional categories	A	C	A	C	A	C	A	C
Amino acid/purine-pyrimidine metabolism	6	10	3	3	1	4	3	9
Carbohydrate metabolism	3	9	0	5	1	12	3	5
Lipid metabolism	4	8	2	5	3	4	1	2
Vitamin/coenzyme metabolism	4	2	4	1	4	4	1	2
Respiration/ATP synthesis	4	6	5	1	0	2	2	0
Metabolism, other	0	2	6	2	0	4	2	0
Transport-amino acids/purine-pyrimidine	0	4	0	3	0	0	4	3
Transport-sugars/carbohydrate	0	3	0	1	0	1	1	5
Ion transport	6	9	6	7	1	6	0	5
Other transport	5	10	2	6	2	1	3	6
Cell wall assembly, maintenance, integrity	7	10	2	6	1	10	0	0
Endocytosis/exocytosis	4	4	2	1	0	1	1	1
Protein trafficking	3	23	5	10	3	11	0	4
Protein maturation/complex assembly	4	7	6	4	0	10	0	1
Organelle assembly/function	0	3	3	2	0	0	0	0
Stress response-DNA damage	4	6	1	3	1	1	0	1
Stress response-oxidative	3	3	2	4	0	4	0	0
Stress response-other	0	3	2	3	0	3	0	2
Cell cycle	9	12	8	5	2	6	3	1
Meiosis/sporulation	12	10	2	4	0	9	7	9
Actin, tubulin, myosin, dynein	0	1	0	0	0	0	1	2
Ribosome biogenesis	5	4	5	4	3	4	2	10
Ribosome subunit	6	9	6	2	8	4	3	7
General transcription	0	4	2	0	1	0	2	1
Translation	9	13	9	9	3	5	7	7
Proteasome/ubiquitin/ubiquitin-like	2	12	0	4	1	9	3	4
Protein degradation, other	1	5	1	3	0	7	0	1
Regulation, transcription	6	13	4	6	1	10	1	4
Regulation, signalling	16	18	10	15	4	14	2	5
Regulation, other	2	6	3	5	4	5	2	0
Retrotransposon	2	2	2	1	0	3	0	0
Other	5	4	1	2	1	3	0	0
Unknown/putative	19	56	21	47	2	36	10	22
Dubious ORF	6	17	1	10	2	5	3	3

Figure 3: UpSet plot of datasets of coregulated and antiregulated genes in the upper and lower parts of biofilm colonies (Aer/Rt) and of 6-day-old (U6/L6) and 15-day-old (U15/L15) smooth colonies. Coregulated and antiregulated gene/lncRNA pairs in three cell comparisons: aerial versus roots of biofilm colonies, upper cells versus lower cells of 6-day-old smooth colonies, and upper cells versus lower cells of 15-day-old smooth colonies [16, 17]. Horizontal blue bar chart indicates numbers of genes, co-/antiregulated (with lncRNA) in each individual comparison. The black dots and lines (intersect "connectors") above the heat map indicate comparisons in which the given number of genes (vertical red bar chart) were co-/antiregulated. Only major intersections are shown. Heat map of genes assigned to functional categories and clustered according to functional category (FC) and co-/antiregulated in different sample comparisons (lower part). Number in heat map cell = number of genes from FC, coregulated or antiregulated with lncRNA in a sample comparison. The higher the number of co-/antiregulated genes, the more intense the colour. A: antiregulated; C: coregulated.

identified in U15 versus L15, U6 versus L6, and aerial versus root cell comparisons, and these include the genes *KSP1*, *PRC1*, *YNL200C*, *LDS2*, *RRT8*, and *NCR1*, encoding a serine/threonine phosphatase with a putative role in TOR signalling, a vacuolar carboxypeptidase Y, a NADHX epimerase, 2 paralogous spore wall assembly proteins, and a vacuolar membrane protein involved in sphingolipid metabolism, respectively. Over 14% of antiregulated lncRNA/gene pairs in upper versus lower cells are shared between 6-day- and 15-day-old smooth colonies, but only 1% is shared by smooth colonies and colony biofilms (6- or 15-day-old). There are major morphological, expression, and metabolic differences between the two colony types [5, 18, 19], the biofilm colony strain BR-F is diploid while the smooth strain BY4742 is haploid, and signalling and coding RNA expression differences between aerial and root cells may outweigh differences in gene expression regulation by lncRNA.

465 lncRNA/gene pairs were coregulated (308) or antiregulated (157) exclusively in U15 versus L15 cells (Figure 3), including antiregulated genes with roles in regulation/signalling, meiosis/sporulation, cell cycle, translation, and cell wall assembly/maintenance/integrity (Figure 3). 310 pairs were coregulated (184) or antiregulated (126) exclusively in U6 versus L6 cells, including antiregulated genes with roles in regulation/signalling, translation, cell cycle, and ribosomal biogenesis as well as those encoding ribosome subunits (Figure 3). These data suggest that development of upper cells may be partially dependent upon the negative expression regulation (by antiregulated lncRNA) of genes with roles in processes such as the mitotic exit network (*AMN1*, *DBF2*, and *NUD1*), bud site selection (*GIC1*, *RSR1*, and *RAX1*), cytokinesis (*AIM44*), mitotic transitions and checkpoints (*SWE1*, *SPC25*, and *HSL1*), Ras signalling (*IRA1* and *BMH2*), glucose signalling (*YCK1* and *YAK1*), and mating signalling (*DIG2*, *MF(ALPHA)2*, and *PPQ1*). 247 pairs were coregulated (198) or antiregulated (49) in both U15/L15 and U6/L6 cell comparisons but not in the aerial-root cell comparison (8 of the antiregulated genes in this group encode ribosome subunits; the others are dispersed among many functional categories). 189 pairs were coregulated (122) or antiregulated (67) exclusively in the colony biofilm cell comparison, including antiregulated genes with roles in meiosis/sporulation and translation (7 each).

In the time point comparisons, 222, 27, and 2 lncRNA/gene pairs, respectively, were antiregulated in the U15/U6, M15/M6, and L15/L6 comparisons. The fact that 89% of these pairs (222 of 251) were antiregulated in upper cells (U15/U6 comparison) suggests that lncRNA regulation of gene expression changes most during development of U cells. This is consistent with the finding that most of the temporal gene-expression changes occur in upper cells, whereas temporal changes in lower cells and, in particular, the margin cell are moderate [17]. Genes encoding ribosome subunits, or involved in ribosome biogenesis or translation, typically appear DE together with neighbouring lncRNA, and while there is some degree of lncRNA/gene pair overlap between 6-day- and 15-day-old colonies, many genes seem to be selectively regulated in 6-day- or 15-day-old colonies. The translation initiation factor gene *TIF1* is upregulated, while its lncRNA is downregulated in U and M relative to L cells in 15-day-old colonies only, suggesting that differentiation may require divergence in fine-tuning of translation rates as colonies age. While *RPL36B* is upregulated (and its lncRNA downregulated) in U and M cells, relative to L cells, of both 6-day- and 15-day-old colonies, repression of its paralog *RPL36A* is relieved (potentially by lncRNA downregulation) only in 15-day-old colonies. Since deletion of the latter decreases fermentative growth but increases respiratory growth, its increased expression as the colony ages is consistent with the utilization by U cells of L cell-derived hexoses in differentiated colonies [72]. Stoichiometric changes in the ribosome subunit make-up may thus represent one aspect of the metabolic remodelling program as cells in ageing colonies differentiate.

Cell cycle progression is regulated under stress conditions by antiregulated noncoding RNAs [73] for genes such as *FAR1* (encoding an inhibitor of cyclin-dependent kinase (CDK) Cdc28p involved in cell cycle phase transitions). In addition, Lardenois et al. [28] suggested that expression of the *CLN2* gene that encodes cyclin G1 may be negatively regulated by promoter-overlapping MUT1465 expression, relieving *CLN2*-dependent repression of *IME1* and allowing meiosis to proceed. In colony biofilms, we observed *FAR1* expression to be upregulated 2.8-fold in aerial cells, and its antisense SUT locus SUT204 was upregulated 1.7-fold in roots. Thus, the Far1p CDK inhibitor may elicit mitotic cell cycle arrest in aerial cells, whereas its expression is repressed in roots to permit cell cycle progression. Furthermore, the cyclin *CLN3* is upregulated 1.7-fold in roots and its antisense-overlapping partner MUT30.1 is upregulated 2.1-fold in aerial cells. Similarly, *CLN2* is upregulated 1.7-fold in roots, and the expression of MUT1465.2, which is located upstream (i.e., over the presumed promoter region) of *CLN2*, is upregulated 3.3-fold in aerial cells. These findings are consistent with previous findings that aerial cells have entered the stationary phase in 40-hour-old colonies, whereas root cells continue to divide [18], indicating that lncRNAs may participate in the regulation of cell division in biofilm colony cell subpopulations. The situation in smooth colonies is less clear because MUT30.1 and MUT1465.2 were not detected in smooth colonies and SUT204 is upregulated 3-fold in L relative to U cells and *FAR1* 2.6-fold in U relative to L cells only in 6-day-old colonies, despite the fact that some dividing cells are present in the very upper layers of these colonies.

6. Conclusions

The complement of lncRNA classes (MUTs, CUTs, etc.) is cell-type-specific, implying that lncRNA expression modulates, and/or is modulated by, cell/colony differentiation. Coregulated expression of antisense-divergent lncRNA/gene pairs appears to be largely the result of bidirectional transcription of a lncRNA and a differentially expressed gene from a common start site [14, 15, 28]. Such coregulation was the most commonly observed lncRNA/coding gene interaction seen in our study of aerial-root cells of colony biofilms and of U/L cells from smooth colonies, also during age-related differentiation. On the other hand, negative

regulation of a coding gene by a lncRNA commonly occurs in the antisense-overlapping orientation. Potential negative regulation of gene expression by antisense-overlapping lncRNAs was most commonly seen in differentiated cell subpopulations, that is, upper and lower cells of 6- and 15-day-old smooth colonies, and changes most over time (between 6 and 15 days) in upper cells. Some potential negative regulations in upper versus lower cells are common to 6-day- and 15-day-old smooth colonies, but few are shared by smooth colonies and colony biofilms, which is consistent with the different lifestyles of these two types of colony populations. Fundamental processes targeted by lncRNA-negative regulation have well-established roles in ageing and differentiation, such as meiosis/sporulation, the cell cycle, cell signalling, ribosome biogenesis, translation, and cell wall assembly/maintenance. Negative regulation of these processes by lncRNAs can enable their fine-tuning during development of yeast smooth colonies and colony biofilms. Further research will be needed to prove and clarify the role of particular lncRNAs in the differentiation of cells within aging multicellular yeast populations.

Conflicts of Interest

The authors declare that they have no conflicts of interest.

Acknowledgments

The research leading to these results has received funding from the Norwegian Financial Mechanism 2009–2014 under Project Contract no. MSMT-28477/2014 (7F14083) and Czech Science Foundation 13-08605S. Derek Wilkinson and Zdena Palková are also supported by LQ1604 NPU II provided by MEYS and Libuše Váchová by RVO61388971, and the research was performed in BIOCEV supported by CZ.1.05/1.1.00/02.0109 BIOCEV provided by ERDF and MEYS.

References

[1] Z. Palkova and L. Vachova, "Life within a community: benefit to yeast long-term survival," *FEMS Microbiology Reviews*, vol. 30, no. 5, pp. 806–824, 2006.

[2] S. Brückner and H. U. Mösch, "Choosing the right lifestyle: adhesion and development in *Saccharomyces cerevisiae*," *FEMS Microbiology Reviews*, vol. 36, no. 1, pp. 25–58, 2012.

[3] S. M. Honigberg, "Cell signals, cell contacts, and the organization of yeast communities," *Eukaryotic Cell*, vol. 10, no. 4, pp. 466–473, 2011.

[4] Z. Palkova and L. Vachova, "Yeast cell differentiation: lessons from pathogenic and non-pathogenic yeasts," *Seminars in Cell & Developmental Biology*, vol. 57, pp. 110–119, 2016.

[5] Z. Palkova, D. Wilkinson, and L. Vachova, "Aging and differentiation in yeast populations: elders with different properties and functions," *FEMS Yeast Research*, vol. 14, no. 1, pp. 96–108, 2014.

[6] K. Podholová, V. Plocek, S. Rešetárová et al., "Divergent branches of mitochondrial signaling regulate specific genes and the viability of specialized cell types of differentiated yeast colonies," *Oncotarget*, vol. 7, no. 13, pp. 15299–15314, 2016.

[7] Z. Tan, M. Hays, G. A. Cromie et al., "Aneuploidy underlies a multicellular phenotypic switch," *Proceedings of the National Academy of Sciences of the United States of America*, vol. 110, no. 30, pp. 12367–12372, 2013.

[8] A. Fatica and I. Bozzoni, "Long non-coding RNAs: new players in cell differentiation and development," *Nature Reviews Genetics*, vol. 15, no. 1, pp. 7–21, 2014.

[9] A. M. Burroughs, Y. Ando, and L. Aravind, "New perspectives on the diversification of the RNA interference system: insights from comparative genomics and small RNA sequencing," *Wiley Interdisciplinary Reviews: RNA*, vol. 5, no. 2, pp. 141–181, 2014.

[10] L. David, W. Huber, M. Granovskaia et al., "A high-resolution map of transcription in the yeast genome," *Proceedings of the National Academy of Sciences of the United States of America*, vol. 103, no. 14, pp. 5320–5325, 2006.

[11] C. A. Davis and M. Ares, "Accumulation of unstable promoter-associated transcripts upon loss of the nuclear exosome subunit Rrp6p in *Saccharomyces cerevisiae*," *Proceedings of the National Academy of Sciences of the United States of America*, vol. 103, no. 9, pp. 3262–3267, 2006.

[12] F. Wyers, M. Rougemaille, G. Badis et al., "Cryptic pol II transcripts are degraded by a nuclear quality control pathway involving a new poly(A) polymerase," *Cell*, vol. 121, no. 5, pp. 725–737, 2005.

[13] E. A. Alcid and T. Tsukiyama, "Expansion of antisense lncRNA transcriptomes in budding yeast species since the loss of RNAi," *Nature Structural & Molecular Biology*, vol. 23, no. 5, pp. 450–455, 2016.

[14] H. Neil, C. Malabat, Y. d'Aubenton-Carafa, Z. Xu, L. M. Steinmetz, and A. Jacquier, "Widespread bidirectional promoters are the major source of cryptic transcripts in yeast," *Nature*, vol. 457, no. 7232, pp. 1038–1042, 2009.

[15] Z. Xu, W. Wei, J. Gagneur et al., "Bidirectional promoters generate pervasive transcription in yeast," *Nature*, vol. 457, no. 7232, pp. 1033–1037, 2009.

[16] J. Maršíková, D. Wilkinson, O. Hlaváček et al., "Metabolic differentiation of surface and invasive cells of yeast colony biofilms revealed by gene expression profiling," *BMC Genomics*, vol. 18, no. 1, p. 814, 2017.

[17] D. Wilkinson, J. Maršíková, O. Hlaváček et al., "Transcriptome remodeling of differentiated cells during chronological ageing of yeast colonies: new insights into metabolic differentiation," *Oxidative Medicine and Cellular Longevity*, vol. 2018, Article ID 4932905, 17 pages, 2018.

[18] L. Váchová, V. Stovícek, O. Hlavácek et al., "Flo11p, drug efflux pumps, and the extracellular matrix cooperate to form biofilm yeast colonies," *The Journal of Cell Biology*, vol. 194, no. 5, pp. 679–687, 2011.

[19] M. Cap, L. Stepanek, K. Harant, L. Vachova, and Z. Palkova, "Cell differentiation within a yeast colony: metabolic and regulatory parallels with a tumor-affected organism," *Molecular Cell*, vol. 46, no. 4, pp. 436–448, 2012.

[20] F. F. Costa, "Non-coding RNAs: meet thy masters," *BioEssays*, vol. 32, no. 7, pp. 599–608, 2010.

[21] T. N. Mavrich, I. P. Ioshikhes, B. J. Venters et al., "A barrier nucleosome model for statistical positioning of nucleosomes throughout the yeast genome," *Genome Research*, vol. 18, no. 7, pp. 1073–1083, 2008.

[22] D. Schulz, B. Schwalb, A. Kiesel et al., "Transcriptome surveillance by selective termination of noncoding RNA synthesis," *Cell*, vol. 155, no. 5, pp. 1075–1087, 2013.

[23] J. Wu, D. Delneri, and R. T. O'Keefe, "Non-coding RNAs in *Saccharomyces cerevisiae:* what is the function?," *Biochemical Society Transactions*, vol. 40, no. 4, pp. 907–911, 2012.

[24] M. Tisseur, M. Kwapisz, and A. Morillon, "Pervasive transcription—lessons from yeast," *Biochimie*, vol. 93, no. 11, pp. 1889–1896, 2011.

[25] J. M. Vera and R. D. Dowell, "Survey of cryptic unstable transcripts in yeast," *BMC Genomics*, vol. 17, no. 1, p. 305, 2016.

[26] M. Yassour, J. Pfiffner, J. Z. Levin et al., "Strand-specific RNA sequencing reveals extensive regulated long antisense transcripts that are conserved across yeast species," *Genome Biology*, vol. 11, no. 8, article R87, 2010.

[27] B. Gelfand, J. Mead, A. Bruning et al., "Regulated antisense transcription controls expression of cell-type-specific genes in yeast," *Molecular and Cellular Biology*, vol. 31, no. 8, pp. 1701–1709, 2011.

[28] A. Lardenois, Y. Liu, T. Walther et al., "Execution of the meiotic noncoding RNA expression program and the onset of gametogenesis in yeast require the conserved exosome subunit Rrp6," *Proceedings of the National Academy of Sciences of the United States of America*, vol. 108, no. 3, pp. 1058–1063, 2011.

[29] F. J. van Werven, G. Neuert, N. Hendrick et al., "Transcription of two long noncoding RNAs mediates mating-type control of gametogenesis in budding yeast," *Cell*, vol. 150, no. 6, pp. 1170–1181, 2012.

[30] T. Kim, Z. Xu, S. Clauder-Munster, L. M. Steinmetz, and S. Buratowski, "Set3 HDAC mediates effects of overlapping noncoding transcription on gene induction kinetics," *Cell*, vol. 150, no. 6, pp. 1158–1169, 2012.

[31] I. Toesca, C. R. Nery, C. F. Fernandez, S. Sayani, and G. F. Chanfreau, "Cryptic transcription mediates repression of subtelomeric metal homeostasis genes," *PLoS Genetics*, vol. 7, no. 6, article e1002163, 2011.

[32] M. Nadal-Ribelles, C. Solé, Z. Xu, L. M. Steinmetz, E. de Nadal, and F. Posas, "Control of Cdc28 CDK1 by a stress-induced lncRNA," *Molecular Cell*, vol. 53, no. 4, pp. 549–561, 2014.

[33] K. Vaškovičová, T. Awadová, P. Veselá, M. Balážová, M. Opekarová, and J. Malinsky, "mRNA decay is regulated via sequestration of the conserved $5'$-$3'$ exoribonuclease Xrn1 at eisosome in yeast," *European Journal of Cell Biology*, vol. 96, no. 6, pp. 591–599, 2017.

[34] E. L. van Dijk, C. L. Chen, Y. d'Aubenton-Carafa et al., "XUTs are a class of Xrn1-sensitive antisense regulatory non-coding RNA in yeast," *Nature*, vol. 475, no. 7354, pp. 114–117, 2011.

[35] B. Luke, A. Panza, S. Redon, N. Iglesias, Z. Li, and J. Lingner, "The Rat1p $5'$ to $3'$ exonuclease degrades telomeric repeat-containing RNA and promotes telomere elongation in *Saccharomyces cerevisiae*," *Molecular Cell*, vol. 32, no. 4, pp. 465–477, 2008.

[36] S. A. Cakiroglu, J. B. Zaugg, and N. M. Luscombe, "Backmasking in the yeast genome: encoding overlapping information for protein-coding and RNA degradation," *Nucleic Acids Research*, vol. 44, no. 17, pp. 8065–8072, 2016.

[37] J. T. Arigo, D. E. Eyler, K. L. Carroll, and J. L. Corden, "Termination of cryptic unstable transcripts is directed by yeast RNA-binding proteins Nrd1 and Nab3," *Molecular Cell*, vol. 23, no. 6, pp. 841–851, 2006.

[38] M. M. Darby, L. Serebreni, X. Pan, J. D. Boeke, and J. L. Corden, "The *Saccharomyces cerevisiae* Nrd1-Nab3 transcription termination pathway acts in opposition to Ras signaling and mediates response to nutrient depletion," *Molecular and Cellular Biology*, vol. 32, no. 10, pp. 1762–1775, 2012.

[39] J. Houseley, "Form and function of eukaryotic unstable non-coding RNAs," *Biochemical Society Transactions*, vol. 40, no. 4, pp. 836–841, 2012.

[40] M. Wery, M. Descrimes, N. Vogt, A. S. Dallongeville, D. Gautheret, and A. Morillon, "Nonsense-mediated decay restricts LncRNA levels in yeast unless blocked by double-stranded RNA structure," *Molecular Cell*, vol. 61, no. 3, pp. 379–392, 2016.

[41] S. L. Bumgarner, R. D. Dowell, P. Grisafi, D. K. Gifford, and G. R. Fink, "Toggle involving *cis*-interfering noncoding RNAs controls variegated gene expression in yeast," *Proceedings of the National Academy of Sciences of the United States of America*, vol. 106, no. 43, pp. 18321–18326, 2009.

[42] Y. Mostovoy, A. Thiemicke, T. Y. Hsu, and R. B. Brem, "The role of transcription factors at antisense-expressing gene pairs in yeast," *Genome Biology and Evolution*, vol. 8, no. 6, pp. 1748–1761, 2016.

[43] S. L. Bumgarner, G. Neuert, B. F. Voight et al., "Single-cell analysis reveals that noncoding RNAs contribute to clonal heterogeneity by modulating transcription factor recruitment," *Molecular Cell*, vol. 45, no. 4, pp. 470–482, 2012.

[44] A. Cassone and R. Cauda, "Candida and candidiasis in HIV-infected patients: where commensalism, opportunistic behavior and frank pathogenicity lose their borders," *AIDS*, vol. 26, no. 12, pp. 1457–1472, 2012.

[45] C. J. Nobile and A. P. Mitchell, "Regulation of cell-surface genes and biofilm formation by the *C. albicans* transcription factor Bcr1p," *Current Biology*, vol. 15, no. 12, pp. 1150–1155, 2005.

[46] G. Ramage, R. Rajendran, L. Sherry, and C. Williams, "Fungal biofilm resistance," *International Journal of Microbiology*, vol. 2012, Article ID 528521, 14 pages, 2012.

[47] J. A. Martens, L. Laprade, and F. Winston, "Intergenic transcription is required to repress the *Saccharomyces cerevisiae* SER3 gene," *Nature*, vol. 429, no. 6991, pp. 571–574, 2004.

[48] J. A. Martens, P. Y. Wu, and F. Winston, "Regulation of an intergenic transcript controls adjacent gene transcription in *Saccharomyces cerevisiae*," *Genes & Development*, vol. 19, no. 22, pp. 2695–2704, 2005.

[49] E. M. Prescott and N. J. Proudfoot, "Transcriptional collision between convergent genes in budding yeast," *Proceedings of the National Academy of Sciences of the United States of America*, vol. 99, no. 13, pp. 8796–8801, 2002.

[50] M. Pinskaya, S. Gourvennec, and A. Morillon, "H3 lysine 4 di- and tri-methylation deposited by cryptic transcription attenuates promoter activation," *The EMBO Journal*, vol. 28, no. 12, pp. 1697–1707, 2009.

[51] S. Geisler, L. Lojek, A. M. Khalil, K. E. Baker, and J. Coller, "Decapping of long noncoding RNAs regulates inducible genes," *Molecular Cell*, vol. 45, no. 3, pp. 279–291, 2012.

[52] T. L. Lenstra, A. Coulon, C. C. Chow, and D. R. Larson, "Single-molecule imaging reveals a switch between spurious and functional ncRNA transcription," *Molecular Cell*, vol. 60, no. 4, pp. 597–610, 2015.

[53] Z. T. Beck, S. C. Cloutier, M. J. Schipma et al., "Regulation of glucose-dependent gene expression by the RNA helicase Dbp2 in *Saccharomyces cerevisiae*," *Genetics*, vol. 198, no. 3, pp. 1001–1014, 2014.

[54] S. C. Cloutier, W. K. Ma, L. T. Nguyen, and E. J. Tran, "The DEAD-box RNA helicase Dbp2 connects RNA quality control with repression of aberrant transcription," *The Journal of Biological Chemistry*, vol. 287, no. 31, pp. 26155–26166, 2012.

[55] S. C. Cloutier, S. Wang, W. K. Ma et al., "Regulated formation of lncRNA-DNA hybrids enables faster transcriptional induction and environmental adaptation," *Molecular Cell*, vol. 61, no. 3, pp. 393–404, 2016.

[56] S. C. Cloutier, S. Wang, W. K. Ma, C. J. Petell, and E. J. Tran, "Long noncoding RNAs promote transcriptional poising of inducible genes," *PLoS Biology*, vol. 11, no. 11, article e1001715, 2013.

[57] I. Zacharioudakis and D. Tzamarias, "Bimodal expression of yeast *GAL* genes is controlled by a long non-coding RNA and a bifunctional galactokinase," *Biochemical and Biophysical Research Communications*, vol. 486, no. 1, pp. 63–69, 2017.

[58] J. Berretta, M. Pinskaya, and A. Morillon, "A cryptic unstable transcript mediates transcriptional *trans*-silencing of the Ty1 retrotransposon in *S. cerevisiae*," *Genes & Development*, vol. 22, no. 5, pp. 615–626, 2008.

[59] J. Camblong, N. Beyrouthy, E. Guffanti, G. Schlaepfer, L. M. Steinmetz, and F. Stutz, "*Trans*-acting antisense RNAs mediate transcriptional gene cosuppression in *S. cerevisiae*," *Genes & Development*, vol. 23, no. 13, pp. 1534–1545, 2009.

[60] J. P. Uhler, C. Hertel, and J. Q. Svejstrup, "A role for noncoding transcription in activation of the yeast *PHO5* gene," *Proceedings of the National Academy of Sciences of the United States of America*, vol. 104, no. 19, pp. 8011–8016, 2007.

[61] D. Bunina, M. Štefl, F. Huber et al., "Upregulation of *SPS100* gene expression by an antisense RNA via a switch of mRNA isoforms with different stabilities," *Nucleic Acids Research*, vol. 45, no. 19, pp. 11144–11158, 2017.

[62] M. Chia, A. Tresenrider, J. Chen, G. Spedale, V. Jorgensen et al., "Transcription of a 5′ extended mRNA isoform directs dynamic chromatin changes and interference of a downstream promoter," *eLife*, vol. 6, article 27420, 2017.

[63] J. H. Kim, B. B. Lee, Y. M. Oh et al., "Modulation of mRNA and lncRNA expression dynamics by the Set2–Rpd3S pathway," *Nature Communications*, vol. 7, article 13534, 2016.

[64] S. L. McDaniel, A. J. Hepperla, J. Huang et al., "H3K36 methylation regulates nutrient stress response in *Saccharomyces cerevisiae* by enforcing transcriptional fidelity," *Cell Reports*, vol. 19, no. 11, pp. 2371–2382, 2017.

[65] M. Kwapisz, M. Ruault, E. van Dijk et al., "Expression of subtelomeric lncRNAs links telomeres dynamics to RNA decay in *S. cerevisiae*," *Non-Coding RNA*, vol. 1, no. 2, pp. 94–126, 2015.

[66] A. Traven, A. Jänicke, P. Harrison, A. Swaminathan, T. Seemann, and T. H. Beilharz, "Transcriptional profiling of a yeast colony provides new insight into the heterogeneity of multicellular fungal communities," *PLoS One*, vol. 7, no. 9, article e46243, 2012.

[67] L. Vachova, L. Hatakova, M. Cap, M. Pokorna, and Z. Palkova, "Rapidly developing yeast microcolonies differentiate in a similar way to aging giant colonies," *Oxidative Medicine and Cellular Longevity*, vol. 2013, Article ID 102485, 9 pages, 2013.

[68] S. San Paolo, S. Vanacova, L. Schenk et al., "Distinct roles of non-canonical poly(A) polymerases in RNA metabolism," *PLoS Genetics*, vol. 5, no. 7, article e1000555, 2009.

[69] J. Houseley and D. Tollervey, "Yeast Trf5p is a nuclear poly(A) polymerase," *EMBO Reports*, vol. 7, no. 2, pp. 205–211, 2006.

[70] J. M. Cherry, "The *Saccharomyces* genome database: advanced searching methods and data mining," *Cold Spring Harb Protoc*, vol. 2015, no. 12, article pdb.prot088906, 2015.

[71] A. Khan and A. Mathelier, "Intervene: a tool for intersection and visualization of multiple gene or genomic region sets," *BMC Bioinformatics*, vol. 18, no. 1, p. 287, 2017.

[72] M. Cap, L. Vachova, and Z. Palkova, "Longevity of U cells of differentiated yeast colonies grown on respiratory medium depends on active glycolysis," *Cell Cycle*, vol. 14, no. 21, pp. 3488–3497, 2015.

[73] C. Sole, M. Nadal-Ribelles, E. de Nadal, and F. Posas, "A novel role for lncRNAs in cell cycle control during stress adaptation," *Current Genetics*, vol. 61, no. 3, pp. 299–308, 2015.

Hindawi
Oxidative Medicine and Cellular Longevity
Volume 2018, Article ID 1898421, 17 pages
https://doi.org/10.1155/2018/1898421

Research Article

Cell Size Influences the Reproductive Potential and Total Lifespan of the *Saccharomyces cerevisiae* Yeast as Revealed by the Analysis of Polyploid Strains

Renata Zadrag-Tecza,[1] **Magdalena Kwolek-Mirek**,[1] **Małgorzata Alabrudzińska**,[2] **and Adrianna Skoneczna**[2]

[1]*Department of Biochemistry and Cell Biology, Faculty of Biology and Agriculture, University of Rzeszow, Rzeszow, Poland*
[2]*Institute of Biochemistry and Biophysics, Polish Academy of Sciences, Laboratory of Mutagenesis and DNA Repair, Warsaw, Poland*

Correspondence should be addressed to Renata Zadrag-Tecza; retecza@ur.edu.pl and Adrianna Skoneczna; ada@ibb.waw.pl

Received 7 September 2017; Revised 4 December 2017; Accepted 1 January 2018; Published 20 March 2018

Academic Editor: Sabrina Büttner

The total lifespan of the yeast *Saccharomyces cerevisiae* may be divided into two phases: the reproductive phase, during which the cell undergoes mitosis cycles to produce successive buds, and the postreproductive phase, which extends from the last division to cell death. These phases may be regulated by a common mechanism or by distinct ones. In this paper, we proposed a more comprehensive approach to reveal the mechanisms that regulate both reproductive potential and total lifespan in cell size context. Our study was based on yeast cells, whose size was determined by increased genome copy number, ranging from haploid to tetraploid. Such experiments enabled us to test the hypertrophy hypothesis, which postulates that excessive size achieved by the cell—the hypertrophy state—is the reason preventing the cell from further proliferation. This hypothesis defines the reproductive potential value as the difference between the maximal size that a cell can reach and the threshold value, which allows a cell to undergo its first cell cycle and the rate of the cell size to increase per generation. Here, we showed that cell size has an important impact on not only the reproductive potential but also the total lifespan of this cell. Moreover, the maximal cell size value, which limits its reproduction capacity, can be regulated by different factors and differs depending on the strain ploidy. The achievement of excessive size by the cell (hypertrophic state) may lead to two distinct phenomena: the cessation of reproduction without "mother" cell death and the cessation of reproduction with cell death by bursting, which has not been shown before.

1. Introduction

The *Saccharomyces cerevisiae* yeast has been one of the most frequently used model organisms in scientific studies, including studies of the mechanism of aging, as it was assumed that this mechanism is universal, at least for *Fungi* and *Metazoa* [1]. The contribution of yeast to such studies is based mainly on the analysis of replicative lifespan (RLS). This parameter is expressed as the number of daughter cells produced by a single "mother" cell during its life. This number is limited, as discovered by Mortimer and Johnston in 1959 [2], equaling an average of 20–30 generations. Having assumed that the number of daughters (buds) formed is a measure of the yeast cell's age, it was acknowledged that factors influencing that number are associated with regulation of the aging process, which is responsible for the limited replicative lifespan of the yeast cells. Thus far, the explanation of the phenomenon of limited reproductive potential of yeast cells has mainly been based on the "senescence factor" accumulation hypothesis [3]. Such an accumulation would lead to a progressive loss of reproductive capabilities by the "mother" cell. The molecules proposed as the "senescence factor" were primarily extrachromosomal rDNA circles [4], oxidatively damaged proteins [5], protein aggregates [6], or damaged mitochondria [7, 8]. Explanations of the phenomenon were also based on genetic regulation [9]. The aforementioned reasons for

the limited reproductive capacity of yeast cells inevitably suggested that this phenomenon should be attributed to the aging process.

An alternative explanation that includes reasons unrelated to aging but that are still determined by cell genotype is offered by the hypertrophy hypothesis, which emphasizes cell size and its important role in the regulation of the reproductive potential of yeast [10, 11]. There exists a clear relationship between cell size and the number of daughter cells produced by a single yeast cell [12–15]. It is connected with an inevitable increase in the cell size observed in successive reproductive cycles, which is a consequence of the evolutionary selection of budding as the mechanism of cytokinesis. Such selection eliminates the possibility for reduction of the size of the mother cell, occurring in most eukaryotic cells in which cytokinesis results in two cells of equal sizes, where each of the cells is approximately half of the cell about to divide. Lack of cell size reduction results in the cell reaching the hypertrophy state after several dozen mitotic cycles, which can limit further reproduction [10]. The hypertrophy hypothesis postulates that the excessive size achieved by the cell—the hypertrophy state—is the reason that prevents the cell from further proliferation. Therefore, the value of reproductive potential is determined as the difference between the maximum size reached by the cell and the threshold value, which allows the cell to enter its first cell cycle, and the rate of the cell size increase per generation [10, 11]. It is worth pointing out that the aforementioned excessive cell size means that the maximum size prevents further reproduction. This maximum size is not universal and may vary depending on the genetic background, genetic changes, or environmental conditions. Therefore, the reproductive potential could be regulated by three parameters: the threshold cell size, the rate of the cell size increase per generation, and the maximum cell size [10, 11]. The relationship between the rate of the cell size increase per generation and the reproductive potential demonstrates that higher rates of cell size increase per generation lead to a decrease in the reproductive potential value and vice versa [15]. This relationship was also confirmed by other studies [12, 13, 16]. The hypothesis that the replicative lifespan of the *S. cerevisiae* yeast cells is not a direct consequence of the aging process is still a matter of debate [17, 18]. An important support for this approach may have come from recently published data showing the evidence of aging-independent causes of limited replicative lifespan in the symmetrically dividing *Schizosaccharomyces pombe* yeast [19]. However, further studies are needed to verify this hypothesis. Here, we present the results of a more comprehensive experimental approach, employing polyploid yeast cells.

In the natural environment, vegetative populations of the *S. cerevisiae* yeast appear in diploid or polyploid forms (autopolyploid and allopolyploid) [20]. In yeast, genome doubling is associated with morphological alterations of cell size and shape, colony organization and growth, generation time, and ecological tolerance. Metabolic changes are also observed, which are mainly associated with an increased rate of cell productivity [21]. The model based on polyploid yeast cells may also be helpful in explaining the causes of limited reproductive capacity of these cells because it provides another opportunity for the analysis of the phenomenon known as replicative aging. First, the use of isogenic cells—from haploid to tetraploid—makes it possible to compare these cells, as they contain the same genetic information but differ in the number of genome copies. Second, while these cells differ in ploidy, they also differ in average size [22]. Under optimum conditions, cell size may be doubled with the doubling of ploidy [23]. Although an increase in cell size may also be observed in the case of certain mutations or as a result of chemical factors, in these cases, such an increase is just one of many other consequences affecting the parameters in question. Another important reason is that in yeast, genome doubling is associated with metabolic changes, which can lead to an increased rate of cell productivity [21]. Because polyploids demonstrate increased productivity, the *Saccharomyces* polyploid has been studied from a biotechnological viewpoint, as many industrial yeast species used in bakery or brewery are polyploids [24, 25]. Therefore, the adopted model allows for a more precise assessment of the role of such factors as cell size or cellular biosynthetic potential in the regulation of the reproductive potential and total lifespan.

The goal of this study was to attempt to verify the role of cell size, both as a physical and physiological parameter, in determining the numeric value of the reproductive potential and its impact on the total lifespan of yeast cells. For that purpose, parameters such as reproductive potential and total lifespan, changes of cell size during the reproductive phase of life, and physiological and genetic parameters of an isogenic set of strains varying in ploidy—from haploid to tetraploid cells—were analyzed. Analyses were performed using three different genetic backgrounds to verify the phenomenon itself and determine its universality.

2. Materials and Methods

2.1. Yeast Strains and Growth Conditions. Yeast strains used in this study are listed in Table 1. Yeast cells were grown on standard liquid YPD medium (1% yeast extract, 1% Bacto Peptone, 2% glucose), unless stated otherwise. Cells were cultivated in a rotary shaker at 150 rpm or on solid YPD medium containing 2% agar, in the temperature of 28°C. In experiments, in which the selective conditions were necessary, the synthetic complete (SC) medium (0.67% yeast nitrogen base, 2% glucose, supplemented with amino acids, uracil, and adenine) was used.

2.2. Yeast Strain Construction. The strains YAS281 (1n), YMR2, YAS288 (α c:L), and YMS14 (2n) were prepared as described previously [26]. Briefly, YAS281 (called for simplicity in this paper BY474X (1n)) was obtained by reconstitution of functional *URA3* locus in BY4741 strain; YMR2 and YAS288 (α c:L) were obtained by disruption of *CAN1* locus with *can1::LEU2* cassette in BY4741 and BY4742, respectively. The diploid YMS14 strain (called later BY474X (2n)) was prepared by mating YAS281 (1n) and YAS288 (α c:L) strains. YAS228 diploid strain resulted from crossing YMR2 and BY4742 haploids of opposite mating types. DNA

Table 1: Yeast *S. cerevisiae* strains used in this study.

Strain	Genotype	Reference
SP4 (1n)	*MATα leu1 arg4*	(Bilinski et al, 1978)
SP4 (2n)	*MAT*a/*MATα* leu1/leu1 arg4/arg4	Lab collection
SP4 (3n)	*MAT*a/*MAT*a/*MATα leu1/leu1/leu1 arg4/arg4/arg4*	Lab collection
SP4 (4n)	*MAT*a/*MAT*a/*MATα*/*MATα leu1/leu1/leu1/leu1 arg4/arg4/arg4/arg4*	Lab collection
BY4741	*MAT*a *his3Δ1 leu2Δ0 met15Δ0 ura3Δ0*	*EUROSCARF*
BY4742	*MATα his3Δ1 leu2Δ0 lysΔ0 ura3Δ0*	*EUROSCARF*
BY4743	*MAT*a/*MATα his3Δ1/his3Δ1 leu2Δ0/leu2Δ0 LYS2/lys2Δ0 met15Δ0/ MET1 ura3Δ0/ura3Δ0*	*EUROSCARF*
YAS288 (α c:L)	*MATα his3Δ1 leu2Δ0 lysΔ0 ura3Δ0 can1::LEU2*	(Alabrudzinska et al., 2011 [26])
YAS228	*MAT*a/*MATα his3Δ1/his3Δ1 leu2Δ0/leu2Δ0 LYS2/lys2Δ0 met15Δ0/ MET15 ura3Δ0/ura3Δ0 can1::LEU2/CAN1*	This work
YAS250	*MAT*a/*MATα his3Δ1/his3Δ1 leu2Δ0/leu2Δ0 LYS2/lys2Δ0 met15Δ0/ MET15 ura3Δ0/ura3Δ0 can1::LEU2/can1::HIS3*	This work
YMR2	*MAT*a *his3Δ1 leu2Δ0 met15Δ0 ura3Δ0 can1::LEU2*	(Alabrudzinska et al., 2011 [26])
YAS281 BY474X (1n)	*Mat*a *his3Δ1 leu2Δ0 met15Δ0 URA3*	(Alabrudzinska et al., 2011 [26])
YMS14 BY474X (2n)	*MAT*a/*MATα his3Δ1/his3Δ1 leu2Δ0/leu2Δ0 LYS2/lys2Δ0 met15Δ0/ MET15 URA3/ura3Δ0 CAN1/can1::LEU2*	(Alabrudzinska et al., 2011 [26])
YAS300 BY474X (3n)	*Mat* a/*MAT*a/*MATα his3Δ1/his3Δ1/his3Δ1 leu2Δ0/leu2Δ0/leu2Δ0 LYS2/LYS2/lys2Δ0 met15Δ0/met15Δ0/MET15 ura3Δ0/ura3Δ0/URA3 can1::LEU2/can1::HIS3/CAN1*	This work
YAS318 BY474X (4n)	*Mat* a/*MAT*a/*MAT*a/*MATα* his3Δ1/his3Δ1/his3Δ1/his3Δ1 leu2Δ0/ leu2Δ0/leu2Δ0//leu2Δ0 LYS2/LYS2/lys2Δ0/lys2Δ0 met15Δ0/ met15Δ0/MET15/MET15 ura3Δ0/ura3Δ0/ura3Δ0/URA3 can1::LEU2/can1::LEU2/can1::HIS3/CAN1	This work
BMA64-1A (1n)	*MAT*a *ura3-52 trp1Δ2 leu2-3112 his3-11 ade2-1 can1-100*	*EUROSCARF*
BMA64 (2n)	*MAT*a/*MATα ura3-52/ura3-52 trp1Δ2/trp1Δ2 leu2-3112/leu2-3112 his3-11/his3-11 ade2-1/ade2-1 can1-100/can1-100*	*EUROSCARF*

fragment carrying *can1::HIS3* deletion cassette was obtained by PCR-amplifying *HIS3* gene from pRS313 plasmid [27] with primers Can1K.up: 5′-CTTCAGACTTCTTAACTCC TGTAAAAACAAAAAAAAAAAAAGGCATAGCATCGG TGATGACGGTGAAAAC-3′ and Can1K.lw: 5′- AGAATG CGAAATGGCGTGGAAATGTGATCAAAGGTAATAAA ACGTCATATAAAAACTTGATTAGGGTGAT-3′. This fragment was introduced into the YAS228 strain to obtain YAS250 strain. Triploid and tetraploid strains were prepared as follows: YAS250 strain was subject of protoplast fusion with YAS281 (1n) resulting in triploid YAS300 strain (i.e., BY474X (3n)). To create tetraploid strain YAS318 (i.e., BY474X (4n)), the protoplast fusion between cells of YMS14 (2n) and YAS250 strains was performed.

2.3. Protoplast Preparation for Fusion. Yeast strains were cultivated in 5 mL YPD medium with agitation at 28°C to the exponential phase (about 1×10^7 cells/mL). The 3 mL aliquots of cell suspensions were spun down in the microcentrifuge (3000 rpm, 30 s) and washed twice with sterile water. Then, the cell pellets were suspended in 1 mL of buffer I (1 M sorbitol, 0.1 M EDTA); Zymolyase® 100T was added to the concentration 40 μg/mL, and cells were incubated at 30°C for an hour. Resulting protoplasts were washed 2-3 times with 0.5 mL of protoplast buffer (0.1 M Pi pH 7.5, 0.8 M sorbitol), with gentle centrifugation (3000 rpm, 30 s) in between. Finally, the pellet was gently resuspended in 100 μL of protoplast buffer.

2.4. Protoplast Fusion. The protoplast fusion was performed according to [28] with some modifications. Briefly, 100 μL suspensions of protoplasts of fusion partners were mixed together and spun down (3000 rpm, 30 s) and after careful removing of the supernatant, the pellet was suspended in fusion buffer (35% PEG 3350, 10 mM $CaCl_2$, and 0.8 M sorbitol) followed by 20 minutes incubation at room temperature. Then, the protoplasts were very gently centrifuged (1000 rpm, 3 min), washed 3 times with protoplasts buffer, and finally resuspended in 1.5 mL of the same buffer. Different volumes (0.1–1 mL) of the fused protoplast suspensions were gently mixed with 10 mL of regeneration medium (0.67% YNB medium, 0.8 M sorbitol, and 0.6% agar) and poured onto the surface of thin layer of synthetic minimal regeneration medium (0.67% YNB medium, 2% glucose, 0.8 M sorbitol, and 2.5% agar). Plates were incubated at 28°C for a week. The resulting colonies were isolated, and the DNA content in the cells of polyploid strains was confirmed by flow cytometry.

2.5. FACS Analysis. The DNA content of *S. cerevisiae* cells was measured by flow cytometry as previously described [29]. Additionally, an analysis of the size of the cells present in the analyzed population of 10,000 cells were performed.

2.6. Determining Reproductive Potential. Reproductive potential of individual yeast cells was determined by a routine procedure [30] on cells placed on agar plates using a micromanipulator. The reproductive potential of each cell was defined as the number of buds formed by the cell. Results of two independent experiments, each on at least 40 cells, were taken at each experimental point.

2.7. Determining Reproductive Potential and Reproductive, Postreproductive and Total Lifespan. Yeast lifespan (reproductive and postreproductive) was determined as described previously [31] with modifications described in Zadrag et al., [32]. Yeast cultures were grown on YPD liquid medium overnight. One-microliter aliquots of culture were dropped on YPD plates with solid medium containing Phloxine B at the concentration of 10 μg/mL, for monitoring the moment of cell death. For each experiment, forty single cells were micromanipulated to the appointed area. The first daughters were chosen as the starting cells, and their successive buddings were followed to determine the reproductive potential and reproductive lifespan expressed in time units. After completion of the buddings, yeast cells were inspected in one-hour intervals to determine the moment of cell death and length of their postreproductive lifespan. Total lifespan was calculated as the sum of hours which cell spent in the reproductive and postreproductive phases of life. During the manipulation, the plates were kept at 28°C for 16 h and at 4°C during the night (8 h). The data represent mean values from two separate experiments.

2.8. ATP Content Estimation. ATP content was assessed with BactTiter-Glo™ Microbial Cell Viability Assay according to the manufacturer protocol (Promega). Cells were suspended in a 100 mM phosphate buffer with pH 7.0, containing 0.1% glucose and 1 mM EDTA. A sample (100 μL) of cell suspension with the density of 10^6 cells/mL was used for determination purposes. Luminescence was recorded after 5 min using a TECAN Infinite 200 microplate reader. The luminescent signal was proportional to the amount of ATP present, which was directly proportional to the number of cells.

2.9. Estimation of Glucose Consumption Rate. Quantitative determination of glucose concentration was performed with copper and molybdenum phosphate reagents by the Somogyi-Nelson method [33]. Glucose reduces the Cu^{2+} ions to Cu^{+} ions. The amount of copper oxide (I) was determined using the arsenomolybdate reagent, which is reduced to molybdenum blue. The intensity of the resulting blue color as a product is proportional to the amount of Cu_2O and therefore the amount of glucose in the analyzed sample.

Yeast cells from the exponential phase of growth were adjusted to the density of 1×10^7 cells/mL, collected by centrifugation (2 min, 7000 rpm) and resuspended in fresh complete medium. After 4 hours of incubation, the cell suspension was centrifuged and supernatant was used for the glucose concentration assay. Samples of media were diluted 100-fold to the volume of 0.5 mL; afterwards, 0.5 mL of the Somogyi-Nelson reagent was added to the media and placed in a boiling water bath for 20 minutes. After cooling of the samples, 0.5 mL of arsenomolybdate reagent was added, and the samples were incubated for 5 min. Then, 3.5 mL of water was added and allowed to stand for another 10 min. Absorbance of the samples was measured at $\lambda = 520$ nm. Glucose content was calculated from a standard curve made for samples with known concentrations of glucose.

2.10. Estimation of Relative RNA Level. Relative RNA content was measured by the method described in [34]. Acridine orange (3,6-dimethylaminopyridine) may bind with nucleic acids forming two types of complexes. The type A complex is formed when molecules of the dye intercalate between bases in a double-stranded DNA and double-stranded RNA fragments. Such a complex shows the green fluorescence. The type B complex is formed when particles of the dye will form aggregates of a single-stranded RNA or denatured single-stranded DNA, which gives the red fluorescence.

Yeast cells from the exponential phase of growth were adjusted to the density of 1×10^8 cells/mL and collected by centrifugation (2 min, 7000 rpm). Cells thus obtained were fixed with 70% cold ethanol for 30 min at room temperature. After fixation, cells were washed twice with cold, sterile PBS and then suspended in a fresh buffer with no alteration in density. 200 μL of cell suspension with a 400 μL of permeabilisation buffer (0.1% Triton X-100, 80 mM HCl, and 150 mM NaCl) was mixed and incubated on ice for 2 min. Afterwards, 1.2 μL of the acridine orange solution (concentration of 6 μg/mL) was added and incubated at low temperature for 10 min. Cells were harvested by centrifugation and suspended in a small volume of PBS. Microscopic observations were carried out using the OLYMPUS BX-51 epifluorescence microscope equipped with the DP-72 digital camera and the cellSens Dimension software at $\lambda_{ex} = 488$ nm and $\lambda_{em} = 650$ nm. The images for all tested cells were performed at exactly the same parameters (the power of lamp and the exposure time) for possibility the comparison of fluorescence signal intensity. To determine the relative value of RNA, the multichannel images were separated into individual color channels (red, green, and blue). Fluorescence intensity (the sum of signal from pixels contained in the cell area) was measured only for the red color channel which corresponded to the relative value of RNA. Analysis was performed for at least 100 cells for each strain and for each biological replication. The quantitative results are presented as mean ± SD from at least three independent experiments.

2.11. Spontaneous Mutagenesis Assay. To determine the mutation frequency at *CAN1* marker gene, the forward mutation assay was employed, as described previously [35]. Briefly, yeast strains were cultured with agitation at 28°C to logarithmic growth phase ($1\text{-}2 \times 10^7$ cells/mL) in SC medium, then the number of Can^R clones were estimated by plating 100 μL of the undiluted cultures on SC medium

lacking arginine but containing 30 μg/mL L-canavanine sulphate (Sigma). Mutant colonies were counted following incubation of the plates for 3 days at 28°C. To calculate the frequency of spontaneous mutations, the number of mutant colonies was normalized to the number of colonies grown on the control SC medium plates. In each experiment, 8 to 10 independent cultures of each yeast strain tested were analyzed. The presented data are the medians calculated from at least three separate experiments. Similar approach was applied to determinate the frequency of 5-FOA^R mutants, except that the *URA3* gene served in this assay as mutagenesis marker, and the selection of mutants was performed on SC media containing 1 g/L of 5-fluoroorotic acid (TRC, Canada).

2.12. Estimation of Cell Volume. Cell volume changes during the reproductive lifespan were estimated through an analysis of microscopic images recorded every fifth cell cycles during a routine procedure of reproductive potential determination. Images were captured with a Nikon Eclipse E200 microscope with 20x lens equipped with a digital camera. Cell diameter was measured four times in various planes for each cell using the MicroImage 3.0 software. For each yeast strain, at least 80 cells were counted. The mean cell volume in the population was estimated by analysis of the microscopic images recorded during the exponential phase of the cell growth. Images were captured with an Olympus BX51 microscope. Cell diameter was measured four times in various planes for each cell using the cellSens Dimension software. In all cases, the mean value of the cell diameter was used for the calculation of the cell volume. Cell volume was estimated using the following formula: $V = 4/3\pi(a^2 b)$, where a and b are the radius calculated as a half of minor and major cell diameters, respectively.

2.13. Statistical Analysis. Statistical analysis of data was performed using the StatSoft Inc. (2011) STATISTICA data analysis software system, version 10.0 (https://www.statsoft.com). The statistical significance of differences between haploid strains (1n) and the 2n-4n strains was estimated using one-way ANOVA and Dunnett's post hoc test for SP4 and BY474X strains. The values were considered significant if $P < 0.05$. In the case of BMA64 yeast strains, the differences between the haploid and diploid strains were assessed using the t-test for independent samples.

3. Results

For the analysis, isogenic groups of yeast strains were prepared representing three independent genetic backgrounds: SP4, BY474X, and BMA64. With an exception of BMA64 yeast strains, each of the groups contained cells varying in the number of genome copies: haploid cells (1n), diploid cells (2n), triploid cells (3n), and tetraploid cells (4n). In the case of BMA64 yeast strains, the cells represented only haploid and diploid forms due to the very high instability of forms with ploidy levels higher than diploid and the quick reversion to the haploid state of such forms. To verify cell ploidy, DNA content was determined for each of the analyzed yeast strains (Figure S1). The purpose of analyses carried out with the use of three genetic backgrounds was to verify if the phenomenon is universal or whether it is closely dependent on the genetic background.

3.1. Reproductive Potential and Total Lifespan of Yeast Cells Differing in Ploidy. The analysis of the reproductive potential of cells differing in ploidy has shown that its value does not directly depend on the number of genome copies. This means that the reproductive capacity of the cell does not increase linearly along with the growth of genome copies. Moreover, the parameter values showed a distinct dependence on the genetic background, and the phenotype of each of the analyzed genetic backgrounds was slightly different. The reproductive potential of SP4 diploid and triploid cells was increased in comparison to haploid cells, but the value for tetraploid cells was clearly lower. Cells in the BY474X genetic background, ranging from diploid to tetraploid, have shown higher values of reproductive potential in comparison to haploid cells; however, the relation was not linear, as the value of the parameter for diploid and tetraploid cells was nearly the same. In contrast, the reproductive potential of diploid cells in the BMA64 genetic background was lower in comparison to haploid cells (Figure 1(a), Table 2).

The total lifespan consists of two phases, reproductive and postreproductive, and each of these phases may be regulated differently. When the reproductive phase of cell life was expressed in units of time (Figure 1(b); Table 2), differences in the reproductive potential between cells differing in ploidy were significantly lower than when the reproductive phase was expressed in the number of daughters produced by these cells (Figure 1(a); Table 2). The reproductive lifespan of diploid cells was comparable to that of haploid cells in both SP4 and BY474X genetic backgrounds. While for tri- and tetraploid SP4 cells, the value of the parameter was lower (the difference was statistically significant for tetraploid cells only); for tri- and tetraploid cells in the BY474X background, the value was significantly higher in comparison to haploid and diploid cells. The reproductive lifespan of diploid cells in the BMA64 genetic background was significantly shorter in comparison to haploid cells. The analysis of postreproductive lifespan (length of life after the end of reproduction phase) showed a negative correlation between the number of genome copies and the length of the postreproductive phase of a cell's life. In particular, in the case of tri- and tetraploid cells of SP4 and BY474X genetic backgrounds, the postreproductive lifespan was significantly shorter (ca. three or four times) in comparison to haploid cells. An extremely short postreproductive lifespan was observed in the case of BMA64 diploid cells: it was approximately seven times shorter in comparison to haploid cells. The shortening of the postreproductive lifespan in the case of diploid and polyploid cells (3n-4n) was observed for each of the analyzed genetic backgrounds (Figure 1(c); Table 2). The total lifespan of diploid cells of the SP4 and BY474X genetic backgrounds was comparable to that of haploid cells. A significant shortening of the postreproductive lifespan in the case of the tri- and tetraploid cells resulted in those cells having clearly shorter total lifespans in comparison to haploid or diploid cells. Similar results were obtained for the SP4 and BY474X genetic backgrounds. The biggest difference between the

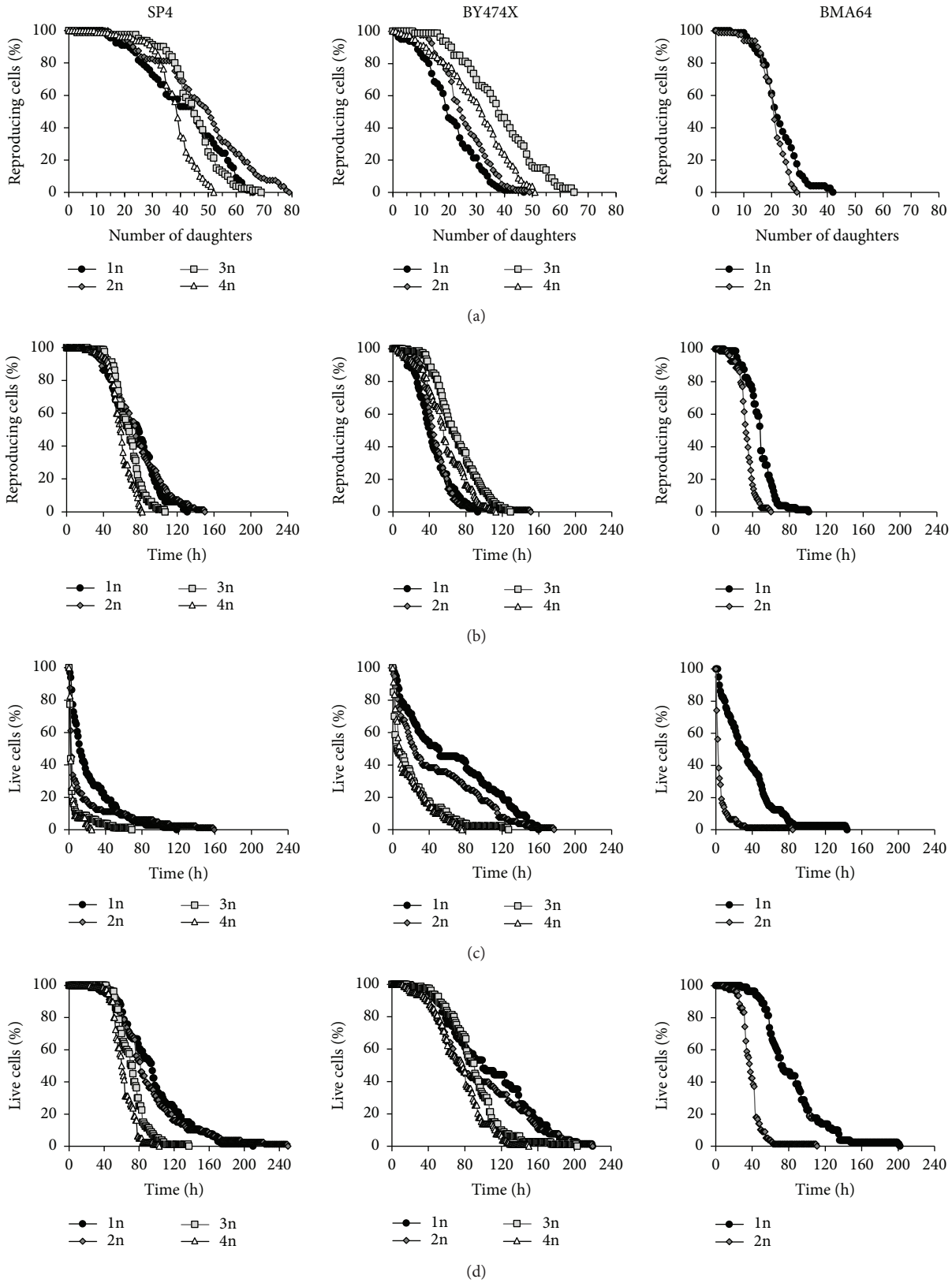

Figure 1: Reproductive potential and time of lifespan of yeast cells differing in ploidy. Budding lifespan (a), reproductive lifespan (b), postreproductive lifespan (c), and total lifespan (d) of yeast strains of different ploidy (from 1n to 4n) representing three genetic backgrounds: SP4, BY474X, and BMA64. Yeast cells during the experiments were grown on solid YPD medium containing 10 μg/mL Phloxine B for cell viability monitoring. The data represent the mean values from two independent experiments of 40 cells each.

Table 2: The budding lifespan (number of generations), reproductive lifespan, postreproductive lifespan, and total lifespan of the yeast strains of different ploidy 1n–4n. Data are presented as the means ± SD from all tested cells during two independent experiments (80 cells). $^{*}P < 0.05$; $^{**}P < 0.01$; and $^{***}P < 0.001$ compared to haploid (1n) strain (one-way ANOVA and Dunnett's post hoc test).

Yeast strain		Budding lifespan Number of daughters	Reproductive lifespan Time (h)	Postreproductive lifespan Time (h)	Total lifespan Time (h)
SP4	1n	41.9 ± 14.9	73.2 ± 26.0	22.5 ± 25.5	95.7 ± 36.3
	2n	48.4 ± 16.3**	75.6 ± 28.0	15.3 ± 31.4	90.7 ± 40.8
	3n	44.7 ± 10.6	66.3 ± 15.2	5.1 ± 11.3***	71.4 ± 16.6***
	4n	38.3 ± 7.8	58.3 ± 12.4***	3.3 ± 5.0***	61.6 ± 12.8***
BY474X	1n	20.8 ± 9.7	43.1 ± 19.7	63.0 ± 51.5	106.1 ± 49.2
	2n	26.1 ± 8.7**	47.5 ± 19.7	46.0 ± 46.8*	93.5 ± 50.5
	3n	37.9 ± 14.1***	73.6 ± 27.9***	23.4 ± 29.9***	96.9 ± 34.4*
	4n	30.5 ± 12.3***	56.3 ± 24.1***	17.1 ± 20.3***	73.43 ± 28.5***
BMA64	1n	23.0 ± 7.0	47.4 ± 15.1	35.3 ± 29.3	82.7 ± 33.2
	2n	21.0 ± 5.6*	32.9 ± 9.3***	5.4 ± 10.8***	38.3 ± 12.8***

analyzed cells was observed in the case of the BMA64 genetic background, where the total lifespan of diploid cells was twice as short as that of haploid cells (Figure 1(d); Table 2). Considering the mean values and the shapes of the curves of the reproductive, postreproductive, and total lifespans, the analyzed cells fall into two groups: the first comprising haploid and diploid cells and the other tri- and tetraploid cells.

3.2. Physiological Parameters of Yeast Cells Differing in Ploidy. An increase in the number of genome copies may have an impact on increasing the cellular biosynthetic potential. Therefore, an analysis was performed of selected parameters that may have an influence on that potential. The ATP level of diploid cells was comparable to that of haploid cells, whereas for tri- and tetraploid cells, the values of the parameter were significantly higher (approximately eight times) in comparison to both haploid and diploid cells. Such a pattern was observed for both SP4 and BY474X genetic backgrounds. For the BMA64 yeast strains, statistically significant differences were already observed in the case of diploid cells (Figure S2A). The ATP level may be associated with the rate of glucose uptake, which is the main source of carbon for yeast cells. This parameter may also be used for estimation of cellular physiology and biosynthetic possibilities. Generally, cells with higher numbers of genome copies showed a higher rate of glucose uptake (as shown by the lower glucose concentration in the medium), but the statistical significance of the observed differences depended on the genetic background (Figure S2B). The haploid and diploid cells of the SP4 genetic background showed a similar rate of glucose uptake. In comparison to those cells, the rate of glucose uptake for tri- and tetraploid cells was significantly higher. In the case of the BY474X genetic background, a higher rate of glucose uptake was shown not only by tri- and tetraploid cells but also by diploid cells. Moreover, these differences compared to haploid cells were statistically significant. The differences in the rate of glucose uptake between haploid and diploid cells of the BMA64 genetic background were not statistically significant. Important information on the fitness of cells and their relative biosynthetic possibilities is also provided through the analysis of the relative RNA content (Figure S3). In each case, the fluorescence intensity indicating the relative level of RNA within the cell increased almost linearly with the increased ploidy. However, the differences were statistically significant in relation to haploid cells only for tri- and tetraploid cells from both SP4 and BY474X genetic backgrounds. For the BMA64 genetic background, the difference was already significant between the haploid and diploid cells (Figure S3D). As the observed relationship between cell ploidy and the relative RNA content might result from differences in cell size, the fluorescence intensity values were segregated by cell size. This approach, in which differences in cell size were considered, showed quite a different outcome. The relative RNA content in cells differing in ploidy was similar for all of the analyzed genetic backgrounds (Figure S3E).

3.3. The Spontaneous Mutagenesis Level in Yeast Cells Differing in Ploidy. Considering the significant shortening of the postreproductive and total lifespans, especially in the case of the tri- and tetraploid cells, we asked if discrepancies in the mutagenesis level could be responsible for such effects. For this reason, the spontaneous mutagenesis level was measured in all four strains from 1n to 4n in the BY474X genetic background. This experiment was only possible for these particular strains out of all strains analyzed in this work. To perform the forward mutation assay, the strain should possess the marker for mutagenesis in its genome. During the construction of BY474X strains, two such markers were introduced: *CAN1* and *URA3*. The presence in the given strain of only one functional copy of the gene, which serves as the mutagenesis marker locus (e.g., *CAN1* in haploid, *CAN1*/can1 in diploid, and *CAN1*/can1/can1 in triploid), allows tracking of the frequency of marker loss. Because *CAN1* encodes arginine permease, growing the cells on the SC medium devoid of arginine and containing canavanine, the toxic analog of arginine, permits positive selection of

mutants. Similar tests could be performed using the *URA3* gene as a marker locus, except that the selection of mutants is performed on the SC medium supplemented with 5-fluoroorotic acid (5-FOA). The *URA3* gene encodes an orotidine-5′-phosphate decarboxylase, the enzyme that converts 5-FOA to toxic 5-fluorouracil. The results of the performed mutagenesis tests are presented in Figure 2. In addition to the already known difference of almost two orders of magnitude in mutation frequency between haploid and diploid strains [26], an additional increase in mutation frequency with the rising ploidy was detected. However, this increase was not as spectacular as between haploid and diploid strains; the mutation levels doubled with each additional genome copy.

3.4. Changes of Cell Size and Shape during the Reproductive Phase of Cell Lifespan. The analyzed yeast strains exhibited differences in cell morphology, which mainly concern cell size. In each of the analyzed genetic backgrounds, the mean cell size in a population increased in a straight line along with cell ploidy. The differences between haploids and cells of higher ploidy (from 2n to 4n) were statistically significant. Moreover, differences were noted regarding the values of the size parameter and the analyzed genetic backgrounds in the ascending sequence from SP4 through BY474X to BMA64 (Figure 3). However, the rate of cell size growth per generation was a more important factor for regulating the reproductive potential of yeast cells than the mean cell size in a population. The analysis of this parameter has shown a clear linear dependence (R^2 in the 0.92 to 1 range) in the case of each strain. For each genetic background, the formula defining the behavior of individual cell types was the same, but the slope of the curves was different, revealing the differences in the growth rate per generation. The cells with higher ploidy showed a higher growth rate per generation. During production of subsequent buds, that is, during the reproductive phase, the cells significantly increased in size. The maximum values reached by the cells were dependent on the time of generation and cell size growth during a single cycle (Figures 4(b), 4(d), and 4(f)). The increase in size may also be accompanied by a change in the cell's shape. For haploid cells, a gradual increase in size was observed, although these cells maintained the same regular shape during the whole reproductive phase of life. By contrast, for diploid cells and especially for tri- and tetraploid cells, an increase in size was accompanied by a change in the shape from ellipsoidal, which was dominant for the major part of the reproductive phase, to spherical, which appeared at the end of that phase. Such changes were observed for the strains in both SP4 and BY474X genetic backgrounds. In turn, the BMA64 cells showed a rapid increase in cell size while maintaining a regular spherical shape (Figure 5(a), Figure S5).

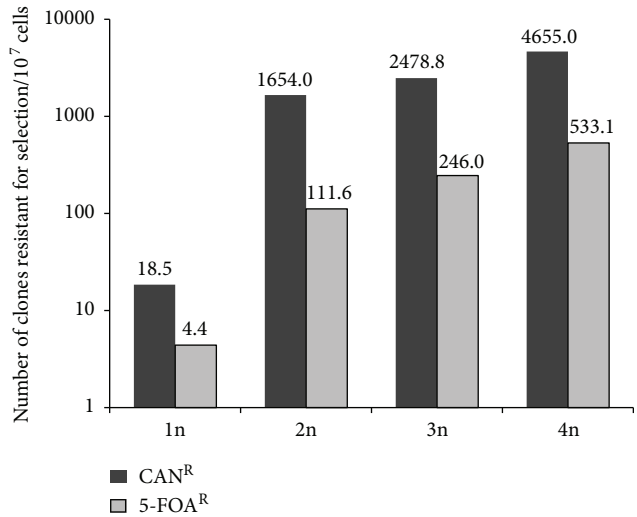

Figure 2: The spontaneous mutagenesis level in yeast cells depends on their ploidy. The changes in spontaneous mutagenesis levels at *CAN1* and *URA3* loci in cells of different ploidy (1n, 2n, 3n, and 4n) in the BY474X background. Spontaneous mutagenesis was measured using a forward mutation assay. Forward mutations leading to canavanine (Can^R) or 5-fluoroorotic acid (5-FOA^R) resistance are median values from at least 30 independent cultures of each strain in three separate experiments. The differences of mutation frequencies between investigated strains were statistically significant ($P < 0.05$).

4. Discussion

The phenomenon of replicative lifespan of the *Saccharomyces cerevisiae* yeast cells has been extensively analyzed but usually only in the context of the aging process. Furthermore, the replicative lifespan represents only a part of the total lifespan, which may be divided into two phases: the reproductive and the postreproductive [32]. Even though the most commonly used explanation for the limited reproductive capacity of these cells is the aging process, it can also be modulated by many aging-independent factors. In addition, both phases may be regulated by these factors through a common mechanism or each phase may be regulated by distinct factors [36]. Increase in genome copies can have an impact on (i) enhanced biosynthetic capacity (physiological efficiency), (ii) genetic stability, and (iii) cell size. Hence, studies based on polyploid cells may provide important information concerning the mechanism regulating the reproductive potential as well as the total lifespan.

4.1. Physiological Efficiency and Genetic Stability in Regulation of Reproductive Potential and Total Lifespan of the Cells. Increase in genome copy number results in an increase in cell productivity [25], which in turn suggests a connection with the reproductive potential. It was confirmed that doubling of the number of genome copies (comparison between haploid and diploid cells) leads to an increase in the reproductive capacities of the cell [9]. However, the experimental data obtained for cells with higher ploidy presented in this paper do not indicate that the reproductive potential increases proportionally to the number of the genome copies. Moreover, in this case, the genetic background may also be an important factor (Figure 1(a)). Indeed, diploid and triploid cells do increase their reproductive potential relative to haploid cells; tetraploid cells, however, exhibit quite different behavior. The reproductive

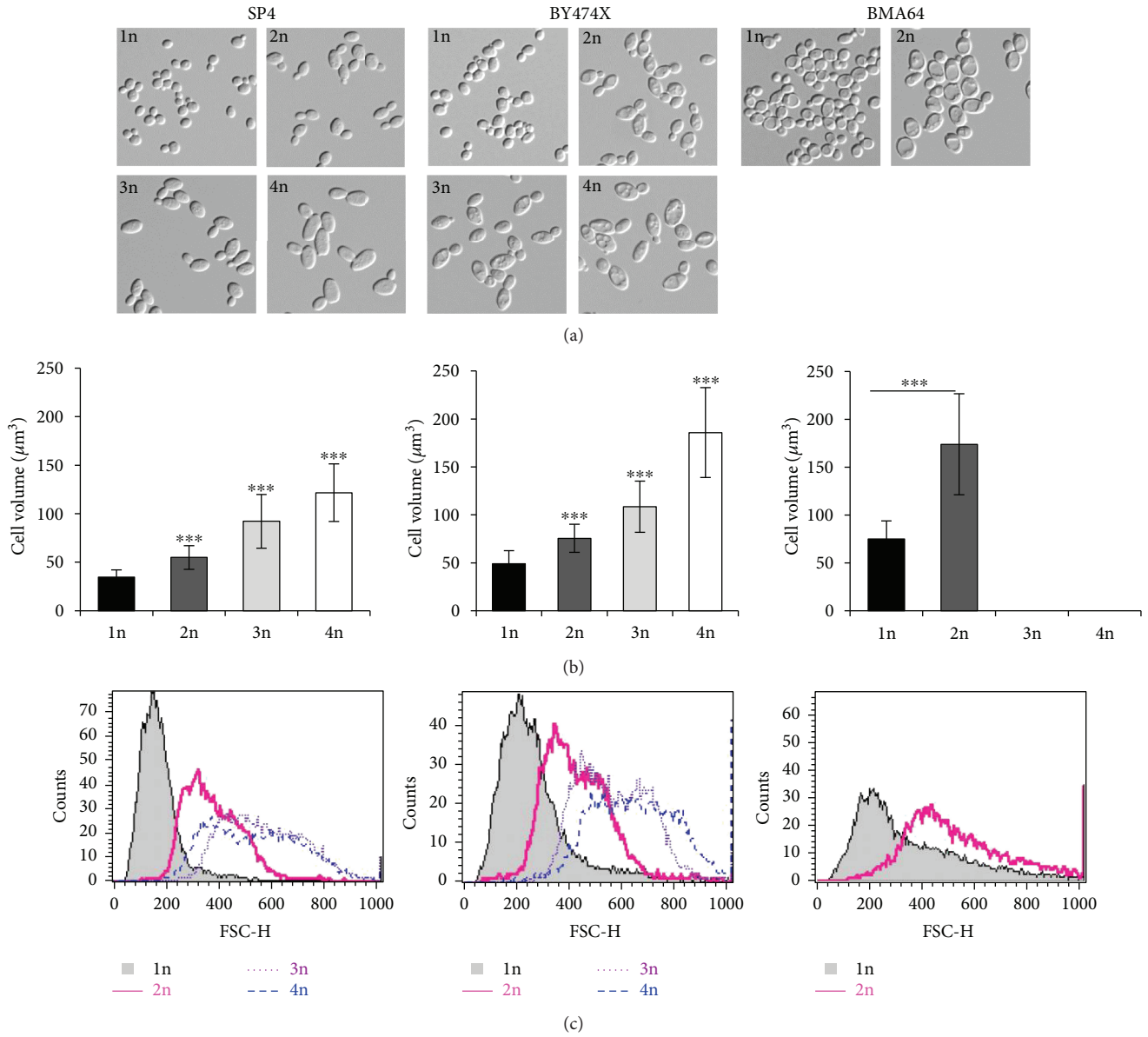

Figure 3: Mean cell size in a population of yeast cells differing in ploidy. (a) Shape and size diversity of yeast cells differing in ploidy. (b) Volume of yeast cells differing in ploidy. Cell volume was estimated by analysis of microscopic images. Data are presented as the mean values for at least 100 cells from each yeast strain. The bars indicate SD from all cells tested in two independent experiments. The stars indicate values that are significantly different from values obtained for the haploid strain (1n) within the same genetic background using one-way ANOVA and Dunnett's post hoc test for SP4 and BY474X strains or *t*-test for BMA64 strain; $^{***}P < 0.001$. (c) Cell size of the yeast strains in the SP4, BY474X, and BMA64 backgrounds as measured by forward scatter (FSC histogram reflects the cells size in the population). The cells were analyzed via FACS as described in the Materials and Methods. Histograms were obtained for 10,000 cells per strain.

potential of these cells can be lower than that of haploid cells or, at best, reach the values achieved by diploid cells depending on the genetic background. Especially intriguing is the significant decrease of the reproductive potential of the BMA64 diploid cells in contrast to the increase of the values of this parameter for the SP4 and BY474X diploid cells (Figure 1(a); Table 2).

Increased numbers of genome copies increase general biosynthetic capabilities, which are an adaptation to the higher demand for cellular constituents resulting from the increase in cell size. Under optimum conditions, the mean cell size in the population doubles with the doubling of ploidy [22, 23], which was also confirmed by the results obtained in these studies (Figure 3). Analysis of biochemical parameters, such as uptake and metabolism of glucose and intracellular ATP levels, which refer to energy metabolism, and the total RNA level referring to the translation efficiency, indicates that increased values of these parameters correlate with increased ploidy, although not always in a proportional manner (Figures S2 and S3). On one hand, the increase of general

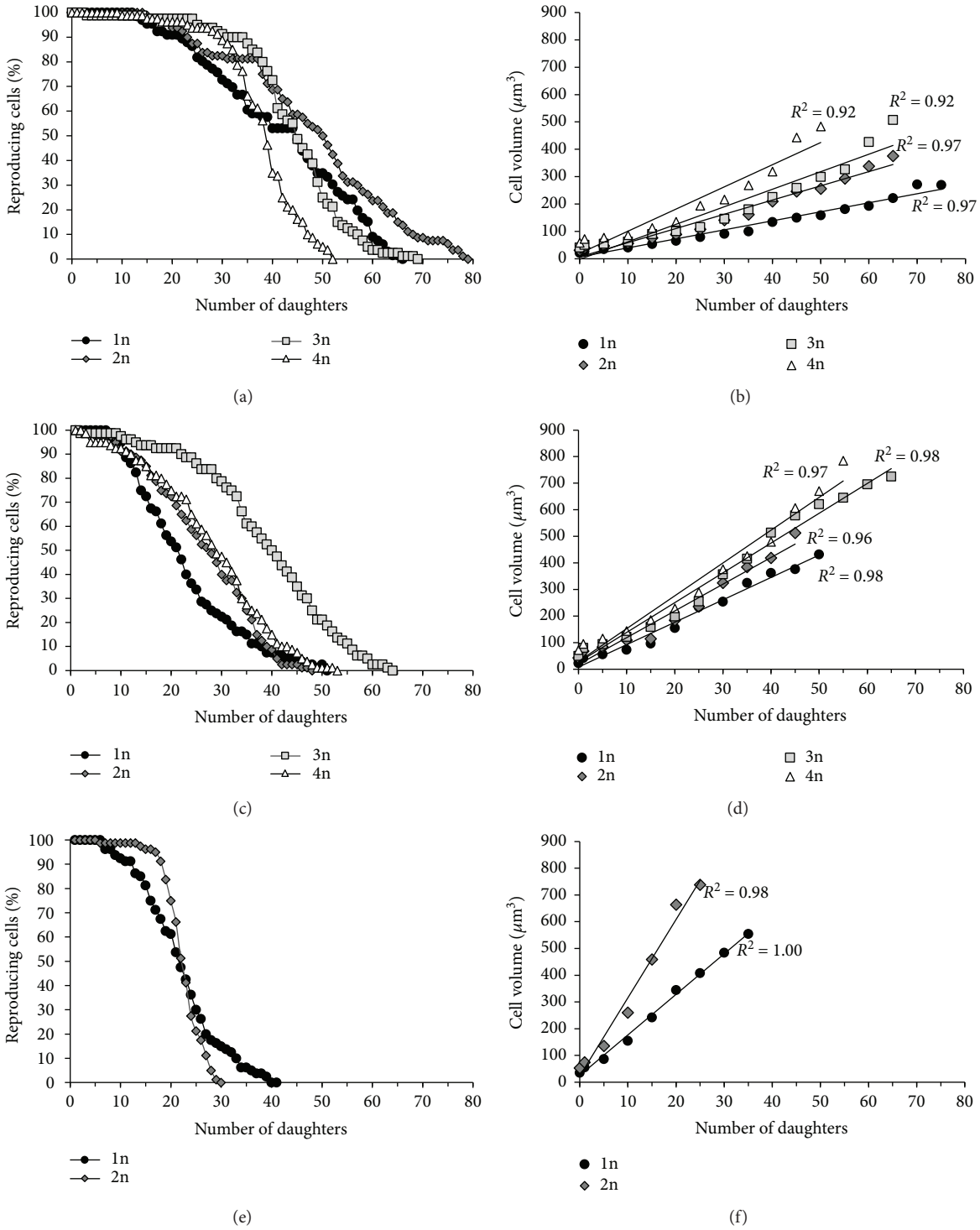

Figure 4: Changes in the size of individual yeast cells during the reproductive phase of life. Reproductive potential of the yeast strains differing in ploidy (from 1n to 4n) representing three genetic backgrounds (a) SP4, (c) BY474X, and (e) BMA64 was determined by the micromanipulation method. Changes in the cell size during the reproductive phase of yeast cell life were estimated by analysis of microscopic images recorded every fifth cell cycle during the determination of reproductive potential of (b) SP4, (d) BY474X, and (f) BMA64. Data were obtained from two independent experiments of 40 cells each.

biosynthetic capabilities, coupled with the increase in the number of genome copies, may be a result of the coordination of intracellular processes to ensure stability in terms of energy and metabolism and their adaptation to the needs arising from the increased cell size [37–40]. On the other hand, such increase may improve the reproductive capacity of cells, especially in the case of tri- and tetraploid cells, as almost 100% of the cells retain the ability to reproduce.

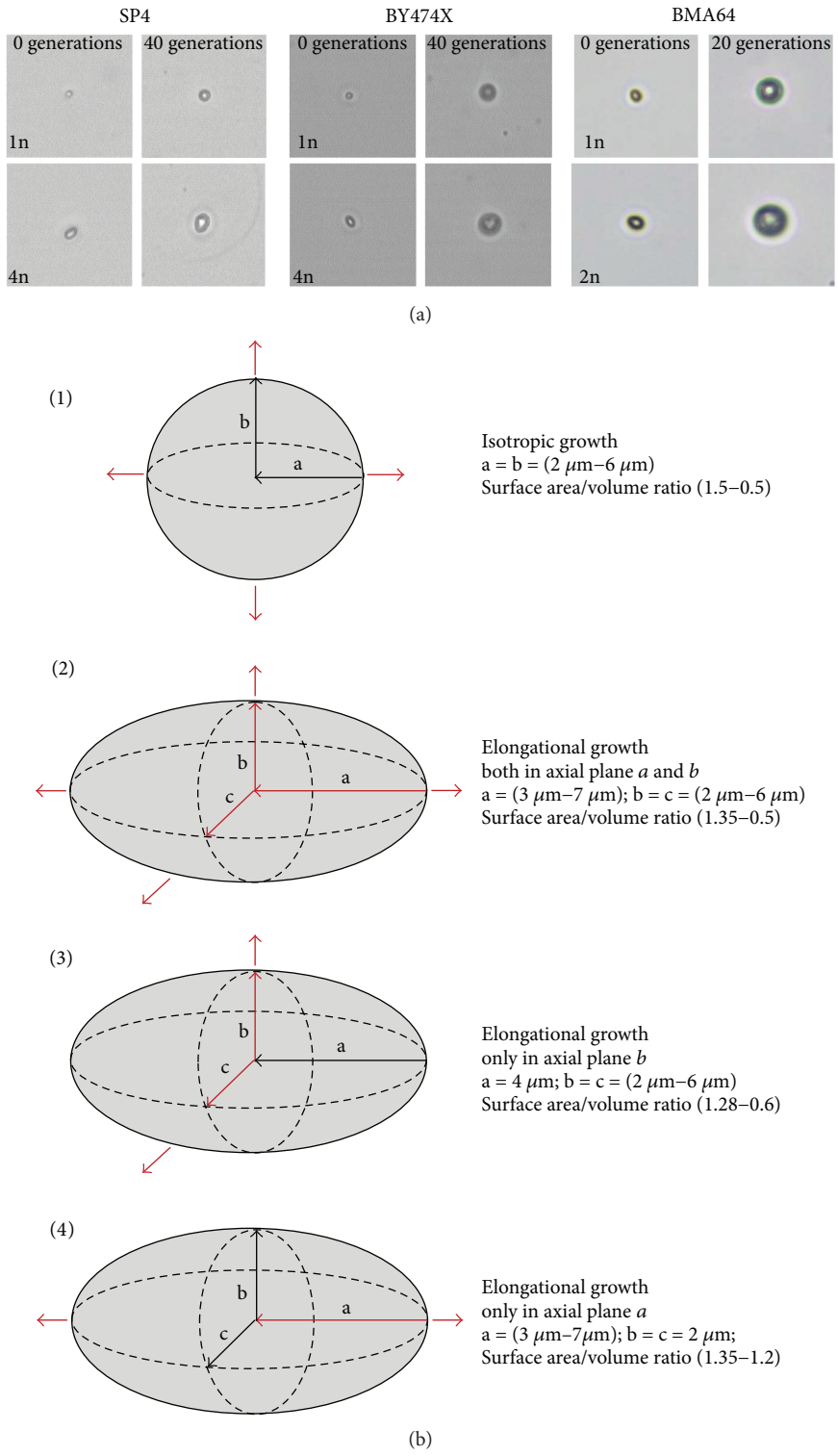

Figure 5: Morphological changes of the yeast cells during the reproductive phase of growth. (a) Changes in the shape of the yeast cell during the reproductive phase of life were assessed by analysis of microscopic images recorded during the reproductive potential determination procedure. The images are representative of all cells analyzed in two independent experiments. (b) The ratio of surface area and cell volume (A/V) changes depending on the shape and type of the cell growth. (1) The isotropic growth of spherical cells leads to fast decrease in the A/V ratio value. (2) The elongational type of growth of ellipsoidal cells when their size is increased in the two axial planes leads to fast decrease in the A/V ratio value. (3) The elongational type of growth of ellipsoidal cells when their size is increased only in axial plane b leads to fast decrease in the A/V ratio value. (4) For the elongational type of growth of ellipsoidal cells when growth occurs in one axial plane, the cell may maintain an almost steady value of the A/V ratio. The red arrows show a growth direction.

Examples of this can be observed mainly at the beginning of the reproductive phase, when di-, tri-, and tetraploid cells have a significant dominance compared to haploid cells (Figures 1(a) and 4, Figure S4). However, this initial dominance quickly wanes and is followed by a clear and rapid decline in the reproductive possibilities of these cells. Such cell behavior may be because the biosynthetic-physiological efficiency of the cells has a significant effect on the reproductive potential but only up to the point at which another factor becomes critical for further reproduction. For explaining this phenomenon, two factors should be considered: genetic stability and cell size.

Increasing the number of genome copies may be beneficial, among other reasons, because of (i) cell protection in the case of damage of one of the gene copies (gene redundancy) [41]; (ii) higher growth rate; and (iii) greater adaptability, including but not limited to higher frequency of beneficial mutations and stronger fitness effects [42]. It is also associated with certain disadvantages that are mainly connected with cell division problems, increased chromosome instability, and DNA repair defects [23, 43], reviewed in [44]. Polyploidization may affect the genetic stability of the cell. Although the frequency of point mutations (such as frameshifts, transversions, or transitions) is the same for haploid and diploid cells, there is as high as a hundredfold difference in the frequency of spontaneous mutagenesis between these cells [26, 45]. This difference is due to various DNA rearrangement events that lead to loss of heterozygosity in diploid strains (namely, gene conversion, allelic crossover, and chromosome loss) [45, 46]. The analysis of spontaneous mutagenesis levels in triploid and tetraploid cells, measured by the frequency of *CAN1* or *URA3* marker loss performed in this work, revealed further increase in spontaneous mutagenesis concomitant with rising cell ploidy (Figure 2). Thus, increases in spontaneous mutagenesis, that is, higher genome instability, likely contribute to the viability of the cells. Surprisingly, a clear correlation between mutagenesis level and reproductive potential of the yeast cells and their survival rates cannot be seen. However, the mutagenesis frequency can be counted only per viable cells in an analyzed population. Therefore, it is highly probable that mutagenesis levels are in fact higher, but some mutagenic events remain invisible because their effects are lethal.

In comparison to haploid cells, tetraploid cells are no more sensitive to various environmental stresses [47]. This is likely because DNA lesions induced by environmental stress that affects an essential gene frequently lead to cell death in haploids, while in diploids or in polyploids, the redundant functional allele of the affected gene is available from another copy of the genome. On the molecular level, the accumulation of DNA lesions provoked by environmental stress stimulates DNA damage response, which encompasses not only recruitment of proper DNA repair proteins to the lesion but also activation of DNA damage checkpoint and cell cycle arrest [48, 49]. If the DNA damage is not repaired properly until mitosis (G2/M checkpoint), it can lead to permanent cell cycle arrest that concludes with cell death (via, e.g., mitotic catastrophe) [44]. That certainly influences, although adversely, both the reproductive potential of the cell and its postreplicative lifespan. The difference in the spontaneous mutagenesis level between haploids and diploids in BY474X background is vast (hundredfold), while between diploids and triploids or tetraploids, it is much lower (about twofold and fourfold, resp.); conversely, a remarkable difference in the reproductive potential is visible between diploids and haploids but not between diploids and tetraploids in this background. This inconsistency of results suggests that it is not genomic instability that limits the reproductive potential of the analyzed cells. However, it is also worth noting that even if no clear relationship is observed when particular factors are considered individually (e.g., impact of point mutation frequency on reproductive potential), their interactions and the resulting additive effect cannot be ruled out. This point of view is similar to that presented by Kaya et al. [50] with regard to mutation accumulation as a cause of haploid yeast aging. The authors emphasize the role of cumulative damage of nuclear and mitochondrial genomes, as opposed to individual damage types, in the regulation of the aging process. For that reason, it is highly probable that both genomic instability and cell size (hypertrophy) may contribute to the decrease of the cell's reproductive potential.

4.2. Cell Size as a Regulator of Reproductive Potential and Total Lifespan. Cell size is an important biological trait that both affects the internal architecture of the cell and determines the range of intracellular biological processes. Increase in cell size results in the need to adjust individual cell components (organelles and macromolecules) to keep them in the right proportions appropriate to the size of the cell [38, 51]. Exceeding a certain size limit may generate problems inter alia with intracellular transport and ensuring of appropriate level of signaling or regulating molecules (e.g., G1 phase cyclin level) necessary to continue reproduction. Processes such as cell growth and cell division are usually closely coordinated to keep the size of a given cell type constant. However, in the case of yeast, the cell size increases along with the subsequent reproductive cycles. This phenomenon is the consequence of budding and the lack of the ability of the cell to reduce its own size, favoring the achievement of an excessive size that makes further reproduction impossible.

The analysis of the reproductive potential of yeast cells shows that the mean value of this parameter does not increase linearly along with the increase in the number of genome copies (Figures 1(a) and 4). However, if we look at the shape of the survival curve, we may notice that along with an increase in ploidy, the part of the whole reproductive phase when almost 100% cells maintain ability to reproduce also increases (Figure 1(a), Figure S4). This suggests that in the absence of other regulators affecting reproductive capabilities of cells, the relationship between ploidy (which corresponds to the biosynthetic abilities of the cells) and the reproductive potential of the cell should be linear. Lack of such a relationship suggests a significant contribution of another factor, such as cell size, in the regulation of the reproductive potential. When analyzing the potential impact of cell size on the

regulation of reproductive potential, it is worth noting the values of the threshold cell size, the rate of the cell size increase per generation, and the maximum cell size, since these values appear to be dependent on the biosynthetic capabilities of cells. This is indicated by the slope of the curve (Figure 4), which shows the rate of an increase in cell size per generation under the reproductive phase of life. These results also emphasize that there is no universal or exact value of cell size causing reproduction cessation because both the maximum cell size and the rate of achievement of the hypertrophy state may be modified through either genome changes or environmental conditions. The maximum cell size allowing for reproduction is higher for tri- and tetraploid cells in comparison to that for haploid and diploid cells (Figure 4), which corresponds to the biosynthetic abilities of these cells and explains the higher reproductive capacity of these cells (except for tetraploid cells). With regard to cells with a significant reduction of the reproductive potential, as in the case of tetraploid cells of the SP4 and BY474X genetic backgrounds and especially the diploid cells of the BMA64 genetic background, a rapid reduction in reproduction capabilities (these cells exhibited high fitness during almost 2/3 of their entire reproductive phase) may actually result from the cell achieving its critical size not only in terms of reproduction purposes but also in terms of cell integrity, which ultimately leads to frequent cell lysis (Figure 4, Figure S4). However, the increased levels of genomic instability due to ineffectiveness of DNA damage response or due to division problems (which might be the case for BMA64 genetic background, which shows signs of endoduplication) (Figure S1) may have enhanced this effect by influencing the rate at which the cells achieved the hypertrophy state.

Cell size is, on the one hand, a physical parameter that, by the surface to volume ratio, determines the size of the cell; on the other hand, it undoubtedly influences the internal architecture and physiological capacity of the cell. The studies conducted demonstrate the existence of two size thresholds: the first leads to cessation of reproduction, but cells are still alive; the second leads to cell death caused by bursting and cell lysis. Hence, cell size may affect not only the reproductive potential but also the total lifespan of cells by shortening the postreproductive phase (Figures 1 and 4). The two size thresholds are related to two distinct phenomena. One is of a physiological nature, because many cellular processes depend directly on cell size, for example, transport across membranes and inside the cell, biosynthetic reactions, and, importantly, the cell cycle. The cell cycle requires the cooperation of many mechanisms to maintain growth homeostasis and optimum cell size. It is therefore possible that a large cell size could affect this cooperation and therefore the ability of cells to reproduce. The other phenomenon occurs because of the obvious lack of strength of the "cell envelope," that is, cell membrane (the lipid composition has an impact on the physicochemical properties) and cell wall. Mechanical strength of the cell wall relies on β-glucan and chitin [52]. During cell growth, the composition of β-glucan increases, which in turn causes an increase in cell wall thickness [53]; however, wall thickness does not affect the elastic properties [54]. Hence, the changes of the internal tension may have an effect on maintaining the integrity of the cell. Diploid BMA64 cells, which show the shortest postreproductive phase, can be used as an example: bursting of these cells occurs almost immediately after the last mitotic cycle. Cell bursting involves almost 90% of all analyzed diploid cells and many haploid cells of these strains. This phenomenon may also explain the behavior of tetraploid yeast cells, which also show a very short postreproductive phase. These cells reach the critical size for reproduction and subsequently the critical size for maintenance of cell integrity faster than haploid cells, which is why their total lifespan is shorter than that of haploid cells (Figures 1 and 4).

When analyzing the causes of cell achieving the size critical for maintaining cell integrity, attention should also be paid to morphological aspects of the cell, that is, cell shape and type of cell size increase. Cells that achieve the size that is critical for their integrity, especially BMA64 strain cells, show a relatively high increase in size during a single cell cycle (slope of the curves, Figure 4(f)). In addition, these cells maintain a very regular spherical shape, which does not change throughout their reproductive and postreproductive phases. In turn, the shape of polyploid yeast cells is more elliptical due to ploidy-dependent cytoskeletal organization. However, this shape may be changed to one that is more spherical, which occurs at the end of the reproductive phase of life (Figures 3(a) and 5(a), Figure S5). Maintenance of a proper surface area and cell volume ratio (A/V ratio) seems to protect the cell against loss of integrity (cell lysis). In general, the A/V ratio is inversely correlated with cell ploidy [55]; however, without cell elongation, the decrease in this ratio might be higher and might lead to reduction of cell functionality. This is confirmed by the data obtained from the analysis of the A/V ratio of cells of different shapes and types of cell size increase. The isotropic growth of spherical cells leads to a rapid decrease in the A/V ratio value. A similar pattern is noted for ellipsoidal cells, whose size is increased in two axial planes. Only when elongational growth occurs in one axial plane may the cell maintain an almost steady value of the A/V ratio (Figure 5(b)). The results obtained by Müller [22] do not indicate that the A/V ratio is the only factor responsible for limiting the reproductive potential of the cells but do not rule out its impact as one of the factors. In turn, the results presented in this paper point to a relevant impact of this parameter to maintenance of proper functionality and cell integrity and therefore the regulation of the reproductive potential and cell death.

Based on these calculations and the observation of the morphological changes of cells during the reproductive phase (Figure 5, Figure S5), two different types of behavior depending on the cell shape may be proposed: (1) the spherical cell, which does not change its shape during the reproductive phase of life; depending on the rate of cell size increase per generation, spherical cells may reach the size that is critical only for further reproduction, for example, haploid cells, or also critical for maintaining cell integrity, for example, diploid cells from the BMA64 strain; (2) the ellipsoidal cell, which at the end of the

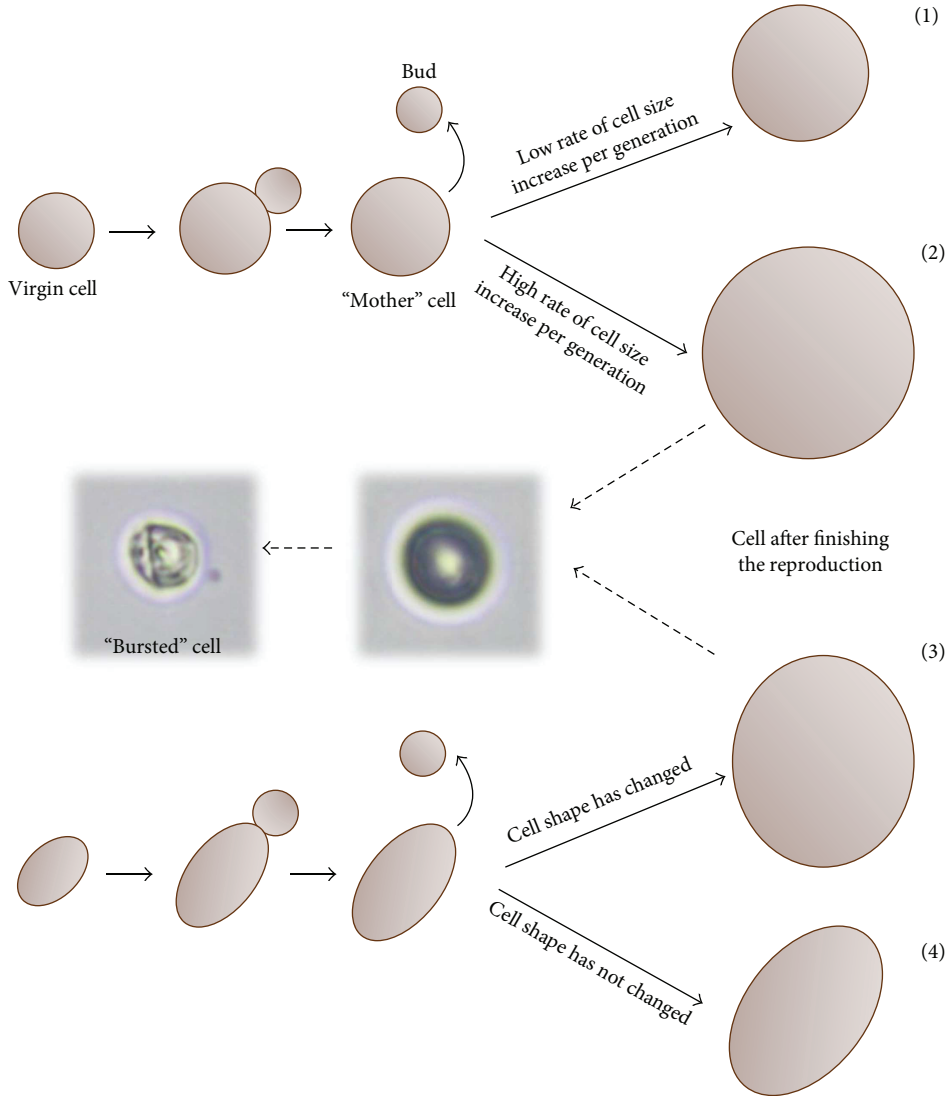

Figure 6: Possible size and shape changes of yeast cells during the reproductive phase of life. (a) The spherical cell with a regular shape. Cell size increases gradually, but its shape does not change during the reproductive phase of life. Depending on the rate of cell size increase per generation, spherical cells may reach the size that is critical only for further reproduction (no cell lysis occurs) (1) or that is also critical for the strength of the cell wall (cell lysis generally occurs) (2). (b) The ellipsoidal cell. Cell size increases gradually during each subsequent reproductive cycle. At the end of the reproductive phase, a cell may change its shape from elliptical to spherical (cell lysis may occur) (3) or maintain the elliptical shape (no cell lysis occurs) (4).

reproductive phase may either change its shape from elliptical to spherical or maintain the elliptical shape (Figure 6). That latter alteration of the cell shape may favor a more rapid achievement of the size critical not only for reproduction but also for maintaining cell integrity. Therefore, in this case, cell lysis may occur, as in the case of tri- and tetraploid cells. The tensile strength of cell walls appears to be lower when the cell assumes a spherical shape. The ellipsoidal cell, even of the same volume as the spherical cell, is better protected against bursting, as it is still able to increase its smaller diameter. The phenomenon of cell bursting was also observed in the case of the *Sc. pombe* yeast cells. For those cells, the change of the cell shape from ellipsoidal to spherical was observed after several mitotic cycles, which also resulted in loss of integrity and cell lysis [56].

The analysis performed with the use of polyploid cells shows a relevant impact of cell size on the regulation of reproductive potential and total lifespan of yeast cells. The total lifespan analysis of cells with the higher-than-haploid number of genome copies has never been performed; therefore, it is an important aspect of discussion on the regulatory role of cell size. The postreproductive phase has a particular influence on the total lifespan [57]. As also shown in these studies, the length of that phase shows an inverted relationship with cell ploidy and is particularly short in the case of tri- and tetraploid cells (or even diploid cells of the BMA64 strain), which may be due to the cell size. This does not mean that accumulation of damage, genetic stability, or changes resulting from the passage of time does not play any role in the regulation of reproductive potential. However, the cessation of reproduction will largely be determined by whichever

factor is first to achieve its critical value. Moreover, their additive effect cannot be ruled out, which may enhance the rate at which the cells achieve the hypertrophy state. The maximum cell size value, which leads to cessation of reproduction, can be regulated among others by biosynthetic possibilities; therefore, its value may differ depending on the number of genome copies. Moreover, the achievement of an excessive size (hypertrophic state) may lead to two distinct phenomena: cessation of reproduction without cell death and cessation of reproduction with cell death by cell bursting.

Abbreviations

WGD: Whole-genome duplication
RLS: Replicative lifespan.

Conflicts of Interest

The authors declare that they have no conflict of interest.

Acknowledgments

The authors are grateful to Professor Tomasz Bilinski for helpful discussions and critical review of the manuscript and Professor Marek Skoneczny for helping in mutagenesis studies and critical review of the manuscript. This work was supported by the Polish National Science Centre (Grant no. DEC-2013/09/B/NZ3/01352).

Supplementary Materials

Figure S1: DNA content of yeast cells differing in ploidy. Cellular DNA content of the yeast strains in the SP4, BY474X, and BMA64 genetic backgrounds. Propidium iodide-stained cells were analyzed via FACS as described in the Materials and Methods. Histograms were obtained for 10,000 cells per strain. Figure S2: ATP content and glucose uptake in yeast cells differing in ploidy. (A) ATP content was determined using BactTiter-Glo Microbial Cell Viability Assay. Luminescence was recorded using the microplate reader. The luminescent signal corresponded to the ATP content, which was directly proportional to the number of cells. (B) Glucose concentration was determined in YPD medium supplemented with glucose (20 mg/mL) using the Somogyi-Nelson method. The YPD medium was collected after 4 hours of cell incubation and used for analysis. Absorbance was recorded using the microplate reader at $\lambda = 520$ nm. The results are presented as the mean values from three independent experiments. The bars indicate SD. The stars indicate values that are significantly different from values obtained for haploid strain (1n) within the same genetic background using one-way ANOVA and Dunnett's post hoc test for SP4 and BY474X strains or *t*-test for BMA64 strain; $^{*}P < 0.05$; $^{**}P < 0.01$; and $^{***}P < 0.001$, respectively. Figure S3: comparison of relative RNA content in yeast differing in ploidy. Relative RNA content of yeast cells was assessed with acridine orange. Fluorescence was examined under the fluorescence microscope at $\lambda_{ex} = 488$ nm and $\lambda_{em} = 650$ nm. For determination of the relative value of RNA, images were separated into individual color channels; fluorescence intensity was measured only for the red channel using the cellSens Dimension software: (A) overlay; (B) red channel; (C) green channel. The results are presented as (D) the mean values of the fluorescence intensity for at least 100 cells from three independent experiments or as (E) calculations of the fluorescence intensity per cell size. The bars indicate SD. The stars indicate values that are significantly different from values obtained for haploid strain (1n) within the same genetic background using one-way ANOVA and Dunnett's post hoc test for SP4 and BY474X strains or *t*-test for BMA64 strain; $^{*}P < 0.05$; $^{**}P < 0.01$; and $^{***}P < 0.001$, respectively. Figure S4: the impact of the number of genome copies on the reproductive possibility of the yeast cells. Calculations illustrating the part of the whole reproductive phase of life when almost all cells (90–100 percent) maintain the ability to reproduce. This value is strictly dependent on the number of the genome copies. Figure S5: changes in yeast cell shape during the reproductive phase of growth. Changes in the shape of the yeast cell during the reproductive phase of life were assessed by analysis of microscopic images recorded every fifth cell cycle during the reproductive potential determination procedure. The images are representative of all cells analyzed in two independent experiments. The analyzed yeast strains differ in ploidy (from 1n to 4n) and represent three genetic backgrounds: SP4, BY474X, and BMA64. *(Supplementary Materials)*

References

[1] M. Polymenis and B. K. Kennedy, "Chronological and replicative lifespan in yeast: do they meet in the middle?," *Cell Cycle*, vol. 11, no. 19, pp. 3531-3532, 2012.

[2] R. K. Mortimer and J. R. Johnston, "Life span of individual yeast cells," *Nature*, vol. 183, no. 4677, pp. 1751-1752, 1959.

[3] N. K. Egilmez and S. M. Jazwinski, "Evidence for the involvement of a cytoplasmic factor in the aging of the yeast *Saccharomyces cerevisiae*," *Journal of Bacteriology*, vol. 171, no. 1, pp. 37–42, 1989.

[4] D. A. Sinclair and L. Guarente, "Extrachromosomal rDNA circles—a cause of aging in yeast," *Cell*, vol. 91, no. 7, pp. 1033–1042, 1997.

[5] H. Aguilaniu, L. Gustafsson, M. Rigoulet, and T. Nystrom, "Asymmetric inheritance of oxidatively damaged proteins during cytokinesis," *Science*, vol. 299, no. 5613, pp. 1751–1753, 2003.

[6] N. Erjavec, L. Larsson, J. Grantham, and T. Nystrom, "Accelerated aging and failure to segregate damaged proteins in Sir2 mutants can be suppressed by overproducing the protein aggregation-remodeling factor Hsp104p," *Genes & Development*, vol. 21, no. 19, pp. 2410–2421, 2007.

[7] C. Y. Lai, E. Jaruga, C. Borghouts, and S. M. Jazwinski, "A mutation in the *ATP2* gene abrogates the age asymmetry between mother and daughter cells of the yeast *Saccharomyces cerevisiae*," *Genetics*, vol. 162, no. 1, pp. 73–87, 2002.

[8] J. R. McFaline-Figueroa, J. Vevea, T. C. Swayne et al., "Mitochondrial quality control during inheritance is associated with lifespan and mother–daughter age asymmetry in budding yeast," *Aging Cell*, vol. 10, no. 5, pp. 885–895, 2011.

[9] M. Kaeberlein, K. T. Kirkland, S. Fields, and B. K. Kennedy, "Genes determining yeast replicative life span in a long-lived

genetic background," *Mechanisms of Ageing and Development*, vol. 126, no. 4, pp. 491–504, 2005.

[10] T. Bilinski, R. Zadrag-Tecza, and G. Bartosz, "Hypertrophy hypothesis as an alternative explanation of the phenomenon of replicative aging of yeast," *FEMS Yeast Research*, vol. 12, no. 1, pp. 97–101, 2012.

[11] T. Bilinski, "Hypertrophy, replicative ageing and the ageing process," *FEMS Yeast Research*, vol. 12, no. 7, pp. 739-740, 2012.

[12] J. Wright, H. Dungrawala, R. K. Bright, and B. L. Schneider, "A growing role for hypertrophy in senescence," *FEMS Yeast Research*, vol. 13, no. 1, pp. 2–6, 2013.

[13] J. Yang, H. Dungrawala, H. Hua et al., "Cell size and growth rate are major determinants of replicative lifespan," *Cell Cycle*, vol. 10, no. 1, pp. 144–155, 2011.

[14] R. Zadrag, G. Bartosz, and T. Bilinski, "Replicative aging of the yeast does not require DNA replication," *Biochemical and Biophysical Research Communications*, vol. 333, no. 1, pp. 138–141, 2005.

[15] R. Zadrag-Tecza, M. Kwolek-Mirek, G. Bartosz, and T. Bilinski, "Cell volume as a factor limiting the replicative lifespan of the yeast *Saccharomyces cerevisiae*," *Biogerontology*, vol. 10, no. 4, pp. 481–488, 2009.

[16] G. E. Janssens and L. M. Veenhoff, "The natural variation in lifespans of single yeast cells is related to variation in cell size, ribosomal protein, and division time," *PLoS One*, vol. 11, no. 12, article e0167394, 2016.

[17] A. R. D. Ganley, M. Breitenbach, B. K. Kennedy, and T. Kobayashi, "Yeast hypertrophy: cause or consequence of aging? Reply to Bilinski et al," *FEMS Yeast Research*, vol. 12, no. 3, pp. 267-268, 2012.

[18] M. Kaeberlein, "Hypertrophy and senescence factors in yeast aging. A reply to Bilinski et al," *FEMS Yeast Research*, vol. 12, no. 3, pp. 269-270, 2012.

[19] E. C. Spivey, S. K. Jones Jr., J. R. Rybarski, F. A. Saifuddin, and I. J. Finkelstein, "An aging-independent replicative lifespan in a symmetrically dividing eukaryote," *eLife*, vol. 6, article e20340, 2017.

[20] Z. Storchova, "Ploidy changes and genome stability in yeast," *Yeast*, vol. 31, no. 11, pp. 421–430, 2014.

[21] D. A. Petrov, "Evolution of genome size: new approaches to an old problem," *Trends in Genetics*, vol. 17, no. 1, pp. 23–28, 2001.

[22] I. Müller, "Experiments on ageing in single cells of *Saccharomyces cerevisiae*," *Archiv für Mikrobiologie*, vol. 77, no. 1, pp. 20–25, 1971.

[23] Z. Storchova, A. Breneman, J. Cande et al., "Genome-wide genetic analysis of polyploidy in yeast," *Nature*, vol. 443, no. 7111, pp. 541–547, 2006.

[24] A. Deregowska, J. Adamczyk, A. Kwiatkowska et al., "Shifts in rDNA levels act as a genome buffer promoting chromosome homeostasis," *Cell Cycle*, vol. 14, no. 21, pp. 3475–3487, 2015.

[25] A. Querol and U. Bond, "The complex and dynamic genomes of industrial yeasts," *FEMS Microbiology Letters*, vol. 293, no. 1, pp. 1–10, 2009.

[26] M. Alabrudzinska, M. Skoneczny, and A. Skoneczna, "Dipoid-specific genome stability genes of *S. cerevisiae*: genomic screen reveals haploidization as an escape from persisting DNA rearrangement stress," *PLoS One*, vol. 6, no. 6, article e21124, 2011.

[27] R. S. Sikorski and P. Hieter, "A system of shuttle vectors and yeast host strains designed for efficient manipulation of DNA in *Saccharomyces cerevisiae*," *Genetics*, vol. 122, no. 1, pp. 19–27, 1989.

[28] F. Farahnak, T. Seki, D. D. Ryu, and D. Ogrydziak, "Construction of lactose-assimilating and high-ethanol-producing yeasts by protoplast fusion," *Applied and Environmental Microbiology*, vol. 51, no. 2, pp. 362–367, 1986.

[29] K. Krol, I. Brozda, M. Skoneczny, M. Bretne, and A. Skoneczna, "A genomic screen revealing the importance of vesicular trafficking pathways in genome maintenance and protection against genotoxic stress in diploid *Saccharomyces cerevisiae* cells," *PLoS One*, vol. 10, no. 3, article e0120702, 2015.

[30] J. Wawryn, A. Krzepilko, A. Myszka, and T. Bilinski, "Deficiency in superoxide dismutases shortens life span of yeast cells," *Acta Biochimica Polonica*, vol. 46, no. 2, pp. 249–253, 1999.

[31] N. Minois, M. Frajnt, C. Wilson, and J. W. Vaupel, "Advances in measuring lifespan in the yeast *Saccharomyces cerevisiae*," *Proceedings of the National Academy of Sciences of the United States of America*, vol. 102, no. 2, pp. 402–406, 2005.

[32] R. Zadrag, G. Bartosz, and T. Bilinski, "Is the yeast a relevant model for aging of multicellular organisms? An insight from the total lifespan of *Saccharomyces cerevisiae*," *Current Aging Science*, vol. 1, no. 3, pp. 159–165, 2008.

[33] M. Somogyi, "Notes on sugar determination," *The Journal of Biological Chemistry*, vol. 195, no. 1, pp. 19–23, 1952.

[34] Z. Darzynkiewicz, G. Juan, and E. F. Srour, "Differential staining of DNA and RNA," *Current Protocols in Cytometry*, 2004, Chapter 7: Unit 7.3.

[35] A. Halas, A. Podlaska, J. Derkacz, J. McIntyre, A. Skoneczna, and E. Sledziewska-Gojska, "The roles of PCNA SUMOylation, Mms2-Ubc13 and Rad5 in translesion DNA synthesis in *Saccharomyces cerevisiae*," *Molecular Microbiology*, vol. 80, no. 3, pp. 786–797, 2011.

[36] R. Zadrag-Tecza and A. Skoneczna, "Reproductive potential and instability of the rDNA region of the *Saccharomyces cerevisiae* yeast: common or separate mechanisms of regulation?," *Experimental Gerontology*, vol. 84, pp. 29–39, 2016.

[37] A. L. Does and L. F. Bisson, "Comparison of glucose uptake kinetics in different yeasts," *Journal of Bacteriology*, vol. 171, no. 3, pp. 1303–1308, 1989.

[38] K. M. Schmoller and J. M. Skotheim, "The biosynthetic basis of cell size control," *Trends in Cell Biology*, vol. 25, no. 12, pp. 793–802, 2015.

[39] A. Szewczyk and S. Pikuła, "Adenosine 5′-triphosphate: an intracellular metabolic messenger," *Biochimica et Biophysica Acta (BBA) - Bioenergetics*, vol. 1365, no. 3, pp. 333–353, 1998.

[40] C. Y. Wu, P. A. Rolfe, D. K. Gifford, and G. R. Fink, "Control of transcription by cell size," *PLoS Biology*, vol. 8, no. 11, article e1000523, 2010.

[41] L. Comai, "The advantages and disadvantages of being polyploid," *Nature Reviews Genetics*, vol. 6, no. 11, pp. 836–846, 2005.

[42] A. M. Selmecki, Y. E. Maruvka, P. A. Richmond et al., "Polyploidy can drive rapid adaptation in yeast," *Nature*, vol. 519, no. 7543, pp. 349–352, 2015.

[43] V. W. Mayer and A. Aguilera, "High levels of chromosome instability in polyploids of *Saccharomyces cerevisiae*," *Mutation Research/Fundamental and Molecular Mechanisms of Mutagenesis*, vol. 231, no. 2, pp. 177–186, 1990.

[44] A. Skoneczna, A. Kaniak, and M. Skoneczny, "Genetic instability in budding and fission yeast—sources and mechanisms," *FEMS Microbiology Reviews*, vol. 39, no. 6, pp. 917–967, 2015.

[45] G. Ohnishi, K. Endo, A. Doi et al., "Spontaneous mutagenesis in haploid and diploid *Saccharomyces cerevisiae*," *Biochemical and Biophysical Research Communications*, vol. 325, no. 3, pp. 928–933, 2004.

[46] M. Hiraoka, K. Watanabe, K. Umezu, and H. Maki, "Spontaneous loss of heterozygosity in diploid *Saccharomyces cerevisiae* cells," *Genetics*, vol. 156, no. 4, pp. 1531–1548, 2000.

[47] A. A. Andalis, Z. Storchova, C. Styles, T. Galitski, D. Pellman, and G. R. Fink, "Defects arising from whole-genome duplications in *Saccharomyces cerevisiae*," *Genetics*, vol. 167, no. 3, pp. 1109–1121, 2004.

[48] J. Heideker, E. T. Lis, and F. E. Romesberg, "Phosphatases, DNA damage checkpoints and checkpoint deactivation," *Cell Cycle*, vol. 6, no. 24, pp. 3058–3064, 2007.

[49] C. D. Putnam, E. J. Jaehnig, and R. D. Kolodner, "Perspectives on the DNA damage and replication checkpoint responses in *Saccharomyces cerevisiae*," *DNA Repair*, vol. 8, no. 9, pp. 974–982, 2009.

[50] A. Kaya, A. V. Lobanov, and V. N. Gladyshev, "Evidence that mutation accumulation does not cause aging in *Saccharomyces cerevisiae*," *Aging Cell*, vol. 14, no. 3, pp. 366–371, 2015.

[51] M. Kafri, E. Metzl-Raz, G. Jona, and N. Barkai, "The cost of protein production," *Cell Reports*, vol. 14, no. 1, pp. 22–31, 2016.

[52] F. M. Klis, S. Brul, and P. W. J. De Groot, "Covalently linked wall proteins in ascomycetous fungi," *Yeast*, vol. 27, no. 8, pp. 489–493, 2010.

[53] A. E. Smith, Z. Zhang, C. R. Thomas, K. E. Moxham, and A. P. J. Middelberg, "The mechanical properties of *Saccharomyces cerevisiae*," *Proceedings of the National Academy of Sciences of the United States of America*, vol. 97, no. 18, pp. 9871–9874, 2000.

[54] M. R. Ahmad, M. Nakajima, S. Kojima, M. Homma, and T. Fukuda, "The effects of cell sizes, environmental conditions, and growth phases on the strength of individual W303 yeast cells inside ESEM," *IEEE Transactions on NanoBioscience*, vol. 7, no. 3, pp. 185–193, 2008.

[55] F. M. Klis, C. G. de Koster, and S. Brul, "Cell wall-related bionumbers and bioestimates of *Saccharomyces cerevisiae* and *Candida albicans*," *Eukaryotic Cell*, vol. 13, no. 1, pp. 2–9, 2014.

[56] M. G. Barker and R. M. Walmsley, "Replicative ageing in the fission yeast *Schizosaccharomyces pombe*," *Yeast*, vol. 15, no. 14, pp. 1511–1518, 1999.

[57] R. Zadrag-Tecza, M. Molon, J. Mamczur, and T. Bilinski, "Dependence of the yeast *Saccharomyces cerevisiae* post-reproductive lifespan on the reproductive potential," *Acta Biochimica Polonica*, vol. 60, no. 1, pp. 111–115, 2013.

Hindawi
Oxidative Medicine and Cellular Longevity
Volume 2018, Article ID 1052413, 17 pages
https://doi.org/10.1155/2018/1052413

Research Article

Changes of *KEAP1/NRF2* and *IKB*/NF-κB Expression Levels Induced by Cell-Free DNA in Different Cell Types

Svetlana V. Kostyuk,[1] Lev N. Porokhovnik,[1,2] Elizaveta S. Ershova,[1,2] Elena M. Malinovskaya,[1] Marina S. Konkova,[1] Larisa V. Kameneva,[1] Olga A. Dolgikh,[1] Vladimir P. Veiko,[3] Vladimir M. Pisarev,[2] Andrew V. Martynov,[1] Vasilina A. Sergeeva,[1] Andrew A. Kaliyanov,[1] Anton D. Filev,[1,2] Julia M. Chudakova,[1] Margarita S. Abramova,[1,4] Serguey I. Kutsev,[1,4] Vera L. Izhevskaya,[1] and Nataliya N. Veiko[1]

[1]*Research Centre for Medical Genetics (RCMG), Moscow 115478, Russia*
[2]*V. A. Negovsky Research Institute of General Reanimatology, Federal Research and Clinical Center of Intensive Care Medicine and Rehabilitology, Moscow 107031, Russia*
[3]*A. N. Bach Institute of Biochemistry, Research Center of Biotechnology, Russian Academy of Sciences, Moscow 119071, Russia*
[4]*N. I. Pirogov Russian National Research Medical University, Moscow 117997, Russia*

Correspondence should be addressed to Lev N. Porokhovnik; lp_soft@mail.ru

Received 19 September 2017; Revised 31 December 2017; Accepted 17 January 2018; Published 20 March 2018

Academic Editor: Sabrina Büttner

Cell-free DNA (cfDNA) is a circulating DNA of nuclear and mitochondrial origin mainly derived from dying cells. Recent studies have shown that cfDNA is a stress signaling DAMP (damage-associated molecular pattern) molecule. We report here that the expression profiles of cfDNA-induced factors NRF2 and NF-κB are distinct depending on the target cell's type and the GC-content and oxidation rate of the cfDNA. Stem cells (MSC) have shown higher expression of *NRF2* without inflammation in response to cfDNA. In contrast, inflammatory response launched by NF-κB was dominant in differentiated cells HUVEC, MCF7, and fibroblasts, with a possibility of transition to massive apoptosis. In each cell type examined, the response for oxidized cfDNA was more acute with higher peak intensity and faster resolution than that for nonoxidized cfDNA. GC-rich nonoxidized cfDNA evoked a weaker and prolonged response with proinflammatory component (NF-κB) as predominant. The exploration of apoptosis rates after adding cfDNA showed that cfDNA with moderately increased GC-content and lightly oxidized DNA promoted cell survival in a hormetic manner. Novel potential therapeutic approaches are proposed, which depend on the current cfDNA content: either preconditioning with low doses of cfDNA before a planned adverse impact or eliminating (binding, etc.) cfDNA when its content has already become high.

1. Introduction

Cell-free DNA (cfDNA) is circulating DNA of both nuclear and mitochondrial origins. Dying cells are the major source of cfDNA [1–4]. For a long time, cfDNA has been studied as a passive marker of cell death after various influences, such as irradiation, and pathologies, especially oncologic [5, 6], or an object for noninvasive diagnostics (liquid biopsy), including prenatal [7–9]. Recently, a novel approach emerged to consider cfDNA as a signaling molecule, which is biologically active regardless of its nucleotide code sequence [1, 10, 11]. The signaling properties of cfDNA depend on two factors. First, it was shown that the GC-content of cfDNA differs from that of the source genomic DNA and depends on the pattern of cell death. In case of a chronic process, circulating cfDNA is enriched with CG-pairs due to the fact that GC-rich regions are more resistant to the endonuclease action [12, 13]. Second, cfDNA is prone to oxidation, mostly

Table 1: Surface marker profiles of MSC used in the study. Cell culture bank of Federal State Budgetary Institution "Research Centre for Medical Genetics."

Number	Cells	Source	Surface markers
1	MSC AT ($N = 9$)	Breast adipose tissue	CD34–, CD45–, HLA-ABC+, HLA-DR–, CD44+, CD29+, CD49b low, CD54 low, CD90+, CD106–, CD105+, CD117–
2	MSC V ($N = 5$)	Umbilical blood and vein	CD34–, CD45–, HLA-ABC+, HLA-DR–, CD44+, CD29+, CD90+, CD105+, CD117–
3	MSC AD (hMADs) ($N = 3$)	Adipose tissue	CD34–, CD15–, HLA-ABC low, HLA-DR–, CD44+, CD13+, CD49b+, CD133–, CD90+, CD105+, CD117–

through the formation of 8-oxodG, and the oxidized cfDNA exerts a stronger signaling action in an oxidation degree-dependent manner [10, 14, 15].

The cfDNA is a DAMP (damage-associated molecular pattern) signaling molecule [16]. The DAMP signaling molecules are hypothesized to serve as messengers of infection or strongly hostile conditions/trauma provoking oxidative stress and cell death. The best-studied receptors for cfDNA are cytosolic AIM2, RIG-1, and DAI and some other DNA sensors [17–26], as well as TLR9 [27, 28]. It is commonly supposed that intrinsic DNA does not activate TLR9; however, our earlier studies have shown that TLR9 reacts for GC-rich endogenous cfDNA [29]. The activation of TLR9 evokes an inflammatory response that implicates the translocation of the transcription factor NF-κB (nuclear factor kappa-light-chain-enhancer of activated B cells) from the cytoplasm to the nucleus with the subsequent launch of transcription of the NF-κB-driven genes [30–33]. This is a tissue-level reaction.

At cellular level, an expression of 100+ genes providing for the cell protection in stress conditions is triggered by another transcription factor, NRF2 (nuclear factor- (erythroid-derived 2-) like factor 2) [34–36]. NRF2 is a master regulator of the antioxidative and anti-inflammatory cell responses [37–39] via the inducible expression of ARE- (antioxidant response element-) driven genes [40]. Thus, NRF2 can provide for the protection against stresses of chemical, infections, and other nature.

The interaction between NF-κB and NRF2 is predominantly antagonistic [40–43]. The underpinning mechanisms are thoroughly reviewed in Discussion. At the same time, a number of stimuli such as reactive oxygen species (ROS), bacterial lipopolysaccharides (LPS), and oxidized low-density lipoproteins induce a simultaneous activation of both NRF2 and NF-κB [44].

In case of protection failure at cellular level, the mechanism of programmed cell death is launched, because the evolutionarily formed strategy prefers to sacrifice the part for the benefit of the whole organism [45]. Both elevated and reduced cell death rates are deleterious and can entail certain pathologic conditions.

The proteins of the BCL2 family play a key role in the regulation of cell death and survival [46, 47]. The BCL-2 protein and four homologous proteins (Bcl-XL, Bcl-W, A1, and Mcl-1) favor cell survival [46].

The inhibitors of apoptosis proteins (IAP) repress caspases 3, 7, and 9 [48]. Under the stress conditions, when the cell survival-oriented processes are activated, expression of the antiapoptotic genes is induced [49].

The aim of this study was to explore the time dynamics of expression of the NF-κB and NRF2 protective factors in response to the action of various kinds of cfDNA and in different cell types and to investigate the effect of cfDNA on cell survival and death.

2. Materials and Methods

Diverse aspects of the biological action of cfDNA were studied on histologically different cultivated cells with different proliferative capacity:

(1) Mesenchymal stem cells (MSC) ($N = 17$) were derived from various sources and characterized by surface markers (Table 1) [15]: normal adipose tissue of surgical material after partial mastectomy (MSC AT), material of umbilical vein and umbilical blood (MSC V), and subcutaneous adipose tissue (MSC AT). The obtained profile of CD markers (Table 1) was typical for MSC [29].

The expression of surface proteins by the cells was studied with the help of flow cytofluorometry using the corresponding antibodies at CyFlow (PARTEC, Germany) [15].

(2) Cultures of human umbilical vein endothelial cells (HUVEC) ($N = 9$) were derived from 9 different specimens of umbilical vein (normal course of pregnancy, successful birth, and healthy newborns) [50]. The HUVEC were characterized by the CD31+ marker.

(3) Human breast adenocarcinoma cells (MCF7) were derived from the cell culture bank of Federal State Budgetary Institution "Research Centre for Medical Genetics" (RCMG), Moscow, Russia. The distinctive molecules of estrogen receptors (ER+) were located on the MCF7 surface [51].

2.1. Model cfDNA Fragment Samples. Based on the conclusions made from the results of our studies of cfDNA properties, we determined the most significant cfDNA parameters, which can evoke biological responses in different cell types:

(1) Elevated GC-rich DNA content of the cfDNA, in particular, elevated ribosomal DNA (rDNA) content [14, 52].

Table 2: Content of the oxidation marker 8-oxodG in DNA samples.

Number	Denomination	Content of 8-oxodG per 10^6 DNA nucleosides
1	gDNA (control)	Less than 0.01
2	DNAoxy1	400
3	DNAoxy2 (or DNAoxy)	1400
4	DNA8-oxodG	700
5	p(rDNA)oxy	50,000

(2) Increased content of oxidized DNA fragments [15, 53].

In order to study the response to the presence of cfDNA in different cell types, model cfDNA fragments were used.

2.1.1. Oxidized Forms of DNA. In case of pathologies and impacts deleterious for the genome, cfDNA contains an increased quantity of oxidized bases. Therefore, to investigate the action of oxidized DNA upon the cells of different types, we prepared *in vitro* samples of model oxidized forms of DNA (Table 2) [15]. We chose gDNA, which had been oxidized by H_2O_2 *in vitro*, as a model molecule in order to exclude the action of other possible factors, such as a changed methylation rate or shifted contents of various motifs that could exert influence on cfDNA properties.

The conditions of gDNA oxidation were chosen in such a way that the final content of the oxidation marker 8-oxo-deoxyguanosine in the oxidized gDNAoxy approximately corresponded to the real 8-oxo-deoxyguanosine content detected in the cfDNA in case of disorders accompanied by oxidative stress. Using mass spectrometry (ESI-MS/MS), we analyzed the 8-oxo-deoxyguanosine content in plasma cfDNA derived from patients with breast cancer and acute myocardial infarction and detected 800 and 2100 8-oxodG, respectively, per 10^6 cfDNA nucleosides [15].

The specimens of oxidized DNA for the experiment were prepared using two methods: either treatment of a genomic DNA (gDNA) sample with 300 mM H_2O_2/Fe^{2+}/EDTA (gDNAoxy 1) or combined treatment of a gDNA sample with 300 mM H_2O_2 and ultraviolet radiation at a wavelength of $\lambda = 312$ nanometers, which induced intense H_2O_2 decomposition and ROS production (gDNAoxy 2) [14]. The content of the oxidation marker 8-oxodG in the obtained DNA specimens was measured using mass spectrometry (ESI-MS/MS) (quantification of 8-oxodG was conducted by Galina V. Baidakova, a senior researcher of Federal State Budgetary Institution "Research Centre for Medical Genetics") [15].

The 8-oxo-deoxyguanosine content in an intact gDNA was below the threshold sensitivity of the method, which was equal to 0.1 (8-oxodG)/10^6 nucleosides, while the first gDNAoxy1 specimen contained ~400 (8-oxodG) per 10^6 nucleosides (lightly oxidized DNA) and the second gDNAoxy2 specimen contained ~2900 (8-oxodG)/10^6 nucleosides (highly oxidized DNA) [15].

When H_2O_2 is applied as an oxidizing agent, not only 8-oxodG but also some other oxidative modifications can be found in the DNA molecule after treatment, because H_2O_2 is a nonspecific oxidant. DNA can be oxidized with the formation of 8-oxodG only, if an oxidation technique based on methylene blue is used [54]. DNA oxidized in this way (DNA8-oxodG) contains solely 8-oxodG in a quantity of ~700 (8-oxodG)/10^6 nucleosides, and we considered this a better model to explore the contribution of the 8-oxodG oxidative modification to the effects evoked by oxidized cfDNA *in vivo*. In addition, we oxidized the sequence of p(rDNA) in order to obtain GC-rich oxidized DNA with a very high oxidation rate of 50,000 per 10^6 nucleosides [15].

2.1.2. GC-Rich Model Fragments, Ligands for TLR9 and TLR9 Blockers. Earlier, we determined that in case of pathology, pregnancy, or damaging exposure, GC-rich rDNA fragments accumulate in the total pool of cfDNA, while the fraction of AT-rich satellite III (SatIII) fragments decreases. The corresponding model fragments were designed as plasmids containing rDNA or SatIII inserts.

A CpG-rich fragment of the transcribed region of the rDNA (from base pair 515 to 5321 in accordance with HSU13369, GeneBank) embedded in pBR322 vector (p(rDNA)) was used as the model GC-DNA. The GC-motif was 9504 bp long [55].

The model DNA samples underwent the same procedure of additional cleaning from lipopolysaccharides via a treatment with Triton X-114 [52] with a subsequent gel filtration on the HW-85 carrier [55].

A computer-aided analysis of the nucleotide composition of p(rDNA) revealed unmethylated CpG motifs within rDNA, which are binding sites for TLR9, a TLR family receptor [55]. We conducted a thorough computer-aided analysis of the model plasmid samples used in the experiments for the existence of TLR9 binding sites and TLR9 blocking sequences.

The ligand for human TLR9 is the sequence GTCGTT and/or TCGTA [56–58]. Generally, R1R2CGY1Y2 is deemed to be an immunostimulating CpG-motif, where R1 stands for a purine (preferably G), R2 is a symbol for a purine or T, and Y1 and Y2 are pyrimidines, which form a complex with human TLR9 having an association constant less than GTCGTT motif [57, 59]. TLR9 blockers can be the motifs Gn ($n > 5$), CCN(A/G/T)(A/G/T)NNGGGN, and CC(A/G/T)(A/G/T)NGGGNN [58, 60, 61].

The plasmid DNA we have chosen carries the pBR322 vector that harbors seven sites being the ligands for human TLR9. The plasmid p(rDNA) carries a CpG-rich fragment of the ribosomal repeat (which contains both binding sites and blocking sequences) [55].

2.2. Cultivation of MSC (Mesenchymal Stem Cells). The technical problem of MSC cultivation is a requirement of the elimination of cells belonging to other tissues, which contaminate the MSC. If the selected cultivation conditions are optimum, the contaminant cells derived from other tissues are eliminated during subsequent passages [29]. The MSC were derived from the adipose tissue of the surgical material of patients with breast adenocarcinoma delivered from Federal State Budgetary Institution N. N. Blokhin Russian Cancer

Research Center (Moscow) in one hour after partial mastectomy [29]. An informed consent for the use of the surgical material was obtained from each patient. The specimen was mechanically disintegrated in DMEM medium (PanEco, Moscow) containing gentamicin at 250 μg/ml, penicillin at 60 units/ml, and streptomycin at 60 units/ml (PanEco); enzymatic dissociation was conducted in DMEM medium by incubating the preparation in the presence of 10% fetal bovine serum (PAA, Austria), 0.04% collagenase (Sigma), and the above-mentioned antibiotics for 16 h at 37°C [29]. The cells were centrifugated at 200g for 10 min, transferred into vials, and cultivated at 37°C in AmnioMax C-100 Basal Medium (Gibco) that contained AmnioMax Supplement C-100, 20 μmol/l HEPES (PanEco) and the antibiotics [29].

2.3. Cultivation of HUVEC (Human Umbilical Vein Endothelial Cells). Endothelial cells were isolated from the umbilical cord (healthy women, normal course of the pregnancy, birth in time and without complications, and healthy newborns). Material sampling and cell isolation were performed in sterile conditions pursuant to an adapted technique [62]. Cultivation was conducted in 199 medium (PanEco, Russia) with penicillin (50 units/ml), streptomycin (50 μg/ml), gentamicin (10 μg/ml), HEPES (20 μl, PanEco, Russia), and growth factors at +37°C (starting density was 500,000 cells per 25 cm^2).

2.4. Cultivation of MCF7 (Human Breast Adenocarcinoma Cells). MCF7 were cultured in DMEM medium supplemented with 10% (v/v) fetal calf serum, 2 mM L-glutamine, 100 units/ml of penicillin, and 100 μg/ml of streptomycin. Cells were grown in a humidified atmosphere with 5% CO_2 in air at 37°C. Before treatment with DNA probes, cells were grown for 24 h or 72 h in slide flasks.

2.5. Measuring Gene Expression Levels Using Real-Time PCR. Expression levels of the genes *NFKB1*, *NRF2*, *BAX*, *BCL2*, *BCL2A1*, *BCL2L1* (*BCL-X*), *BIRC2* (*c-IAP1*), *BIRC3* (*c-IAP2*), *TBP*, and *GAPDH* were measured using real-time PCR.

After the exposure of the cells to extracellular DNA fragments, RNA was extracted from the cells using YellowSolve kits (Clonogen, Russia) or Trizol reagent (Invitrogen) pursuant to the technique attached (http://tools.lifetechnologies.com/content/sfs/manuals/trizol_reagent.pdf) with the subsequent phenol-chloroform extraction and precipitation with chloroform and isoamyl alcohol (49 : 1). RNA concentrations were determined with the help of the dye Quant-iT RiboGreen RNA reagent (MoBiTec, Germany) at a plate reader (EnSpire equipment, Finland) ($\lambda_{excit} = 487$ nm, $\lambda_{flu} = 524$ nm). The reverse transcription reaction was carried out using chemical reagents supplied by Sileks company (Russia) according to the standard procedure.

PCR was carried out using the corresponding primers (Syntol) and the intercalating dye SybrGreen at StepOnePlus instrument (Applied Byosystems, USA). The used primers were as follows (written in the same order (F; R)): *NFKB1* (CAGATGGCCCATACCTTCAAAT; CGGAAACGAAATCCTCTCTGTT); *NRF2* (TCCAGTCAGAAACCAGTGGAT; GAATGTCTGCGCCAAAAGCTG); *TBP* (5′-GCCCGAAACGCCGAATAT-3′; 5′-CCGTGGTTCGTGGCTCTCT-3′); *GAPDH* (GAAGGTGAAGGTCGGAGTC; GAAGATGGTGATGGGATTTC); *BAX* (CCCGAGAGGTCTTTTTCCGAG; CCAGCCCATGATGGTTCTGAT); *BCL2* (TTTGGAAATCCGACCACTAA; AAAGAAATGCAAGTGAATGA); *BCL2A1* (TACAGGCTGGCTCAGGACTAT; CGCAACATTTTGTAGCACTCTG); *BCL2L1* (CGACGAGTTTGAACTGCGGTA; GGGATGTCAGGTCACTGAATG); *BIRC2* (GAATCTGGTTTCAGCTAGTCTGG; GGTGGGAGATAATGAATGTGCAA); and *BIRC3* (AAGCTACCTCTCAGCCTACTTT; CCACTGTTTTCTGTACCCGGA).

The composition of the PCR reaction mix in a volume of 25 μl was the following: 2.5 μl of PCR buffer (700 mM/l Tris-HCl, pH 8.6; 166 mM/l ammonia sulphate, 35 mM/l $MgCl_2$), 2 μl of 1.5 mM/l dNTP solution, and 1 μl of 30 picomol/l solution of each primer and cDNA. The conditions of PCR were chosen individually for each primer pair. The standard conditions for most primers were the following: after denaturation (95°C, 4 min), 40 amplification cycles were conducted in the following mode: 94°C for 20 sec, 56 to 62°C for 30 sec, 72°C for 30 sec, and then, 72°C for 5 min. The PCR procedures were performed at StepOnePlus (Applied Biosystems, USA).

Gene expression levels were analyzed in a series of independent experiments on cells from different donors. Statistical processing of the results was performed using a calibrating curve taking into account the PCR efficiency; the standard error was 2%.

The expression levels of pro- and antiapoptotic genes of interest were normalized to the expression levels of the respective standard gene (TBP) in each cell line analyzed.

Flow cytometry was applied to measure the content of 8-oxo-deoxyguanosine in nuclear DNA using primary (Sc-66036, Santa Cruz, USA) and secondary (anti-mouse-FITC, SC-2010, Santa Cruz, USA) monoclonal antibodies, double-strand DNA break rate via the analysis of gamma focuses of the phosphorylated form of H2AX histone using antibodies to H2AX histones (NB100-78356G, Novus-Bio, USA), and protein expression level using the corresponding monoclonal antibodies BCL2 (Sc-783), BRCA2 (NBP1-88361), NOX4 (SC-30141), NRF2 (ab194984), p53 (sc-126-f), and PCNA (ab2426) according to the common protocol: the exposed cells and control cells were collected from the underlayer, washed with 1% albumin solution in PBS, fixed with 3.7% formaldehyde for 10 min at 37°C, washed off, and permeabilized in 90% methanol at −20°C. Then the cell suspension was incubated with primary antibodies (1 μg/ml) overnight at +4°C (1 μg/ml in PBS in the presence of 1% albumin) and, if necessary, with secondary antibodies (anti-rabbit-FITC Sc-2012, Santa Cruz, USA) for 1 h at room temperature in the dark and assayed with a flow cytofluorometer (CyFlow, Partek, Germany).

2.6. Fluorescence Microscopy. Fluorescence microscopy was conducted using fluorescence microscope AxioImagerA2 (Carl Zeiss). The cultured cells were fixed with 3.7% formaldehyde for 20 min at +4°C and permeabilized with 0.1%

Triton X-100 in PBS (phosphate-buffered saline) with subsequent washing and blocking with 1% albumin solution in PBS and incubated overnight with primary antibodies to NRF2 and p65 subunit of NF-κB at +4°C (1 μg/ml in PBS in the presence of 1% albumin) and then, after washing with PBS, incubated for 1 h with secondary antibodies (Santa Cruz, USA) at room temperature, washed off with PBS and, if required, stained with DAPI.

2.7. Image Analysis. Image processing software "Image 6" was developed in our laboratory and applied in order to measure the fluorescence intensity in and around the nuclei and to calculate the content as compared to controls (in arbitrary units (arb.un.)).

The data were verified with the use of the multifunction system for cell imaging and subsequent automatic processing of the obtained data CyTell (GE Healthcare).

2.8. Annexin V Binding Assays. Cells were detached and washed with PBS. 10,000–50,000 cells were collected by centrifugation, washed in binding buffer (BB) (140 mM NaCl, 4 mM KCl, 0.75 mM MgCl2, 10 mM $CaCl_2$, and 10 mM HEPES), and resuspended in 100 μl of BB.

Annexin V-FITC/propidium iodide staining solution (to 10 samples: 4 μl Annexin V-FITC (ab14082), 10 μl of PI (50 μg/ml), and 90 μl BB, mixed well) was prepared and immediately added to the samples, then incubated at room temperature for 15 min in the dark. After staining, cells were immediately analyzed by flow cytometry using CyFlow Space (Partec, Germany). Annexin V-FITC binding (Ex = 488 nm; Em = 530 nm) was analyzed using the FITC signal detector (FL1) and PI staining by the phycoerythrin emission signal detector (FL2).

2.9. Statistical Analysis. The statistical data analysis was conducted using MS Excel, Statistica 6.0, StatGraph software. The null hypotheses of the absence of the difference between the compared samples were tested with the Mann–Whitney U test. Samples were deemed to be distinct at $p < 0.05$.

2.10. Ethics. The study design was reviewed and approved by the Local Ethics Committee of RSMG (Research Centre for Medical Genetics) to meet the requirements of the Helsinki Declaration of 1975 as revised in 2013. An informed consent for the use of the surgical material had been obtained from each patient, from whom an anonymous cell culture was derived.

3. Results

3.1. Nuclear Translocation of NF-κB and NRF2 after Exposure to cfDNA. The induction of the NF-κB transcription factor by cfDNA fragments is followed by its nuclear translocation with the subsequent activation of target gene expression. The data for NF-κB induction in MSC are shown in Figures 1(a) and 1(b). The translocation of the NRF2 factor under the action of oxidized cfDNA has a similar pattern (Figure 1(c)).

3.2. Profiles of NF-κB and NRF2 Expression in Cells Exposed to cfDNA. Analysis of the dynamics of the expression of NRF2 and NF-κB transcription factors (Figures 2, 3, and 4) corroborates the regularity of mutual inhibition of NF-κB and NRF2 [40–43]. The expression of both factors starts almost simultaneously; however, the expression of NRF2 demonstrated a faster growth followed by NF-κB suppression. Later, NF-κB expression begins to increase, while NRF2 expression decreases. The expression profiles of the two factors overlap to a greater or lesser degree. The dynamics of these processes depends on the types of cells examined and cfDNA used for the induction of expression.

Interestingly, MSC demonstrated the early activation of transcription of *NFKB1* and *NRF2* genes in the presence of oxidized DNA fragments. However, the expression level of the *NFKB1* gene transcription factor only slightly increased in 30 minutes after the start of exposure and then the growth finished soon (in 1 hour), whereas the level of *NRF2* transcription increased (Figure 2(b)).

After the exposure of MSC to GC-rich fragments, the activation of *NFKB1* and *NRF2* gene transcription occurs later. The expression of *NFKB1* gene elevates in 3–24 hours. In contrast, transcription of *NRF2* begins to grow after 10 hours. In this case, we also observed a partial overlapping of the expression profiles of *NFKB1* and *NRF2* genes (Figure 2(a)).

After the exposure of human umbilical vascular endothelial cells (HUVEC) to GC-rich and oxidized fragments, the level of *NRF2* gene increased rapidly in 2-3 hours (Figure 3).

NFKB1 gene transcription during exposure to GC-rich fragments was activated by 3 hours, with the expression level of this gene being approximately twofold higher than the level of transcription of *NRF2* gene—in this case, expression profiles of the two transcription factors under examination markedly overlapped (Figure 3(a)). Under the action of oxidized fragments, the level of *NFKB1* gene transcription peaked much later after 24 hours at the stage of the decreased transcriptional activity of *NRF2* gene (Figure 3(b)).

The human breast adenocarcinoma cells (MCF7) exposed to fragments of oxidized cfDNA and nonoxidized DNA showed a short-time increase in *NRF2* gene expression with the maximum level by 2 hours; then the content of RNA*NRF2* decreased (Figure 4).

Under the action of GC-rich fragments, a late elevation of *NFKB1* gene expression level occurred to have reached the maximum by 24 hours and persisted for a long time (Figure 4(a)). After the exposure to oxidized fragments, the maximum expression was registered in 3 hours, and partial overlapping of the *NFKB1* and *NRF2* gene expression profiles was observed (Figure 4(b)).

3.3. Apoptosis and Expression of Antiapoptotic Proteins under the Action of cfDNA. We observed no signs of massive cell death via necrosis in the cell culture exposed to cfDNA. Therefore, we studied the process of programmed cell death via apoptosis, a long-duration process estimated by specific markers. One of the most frequently used markers of apoptosis intensity is annexin V [63].

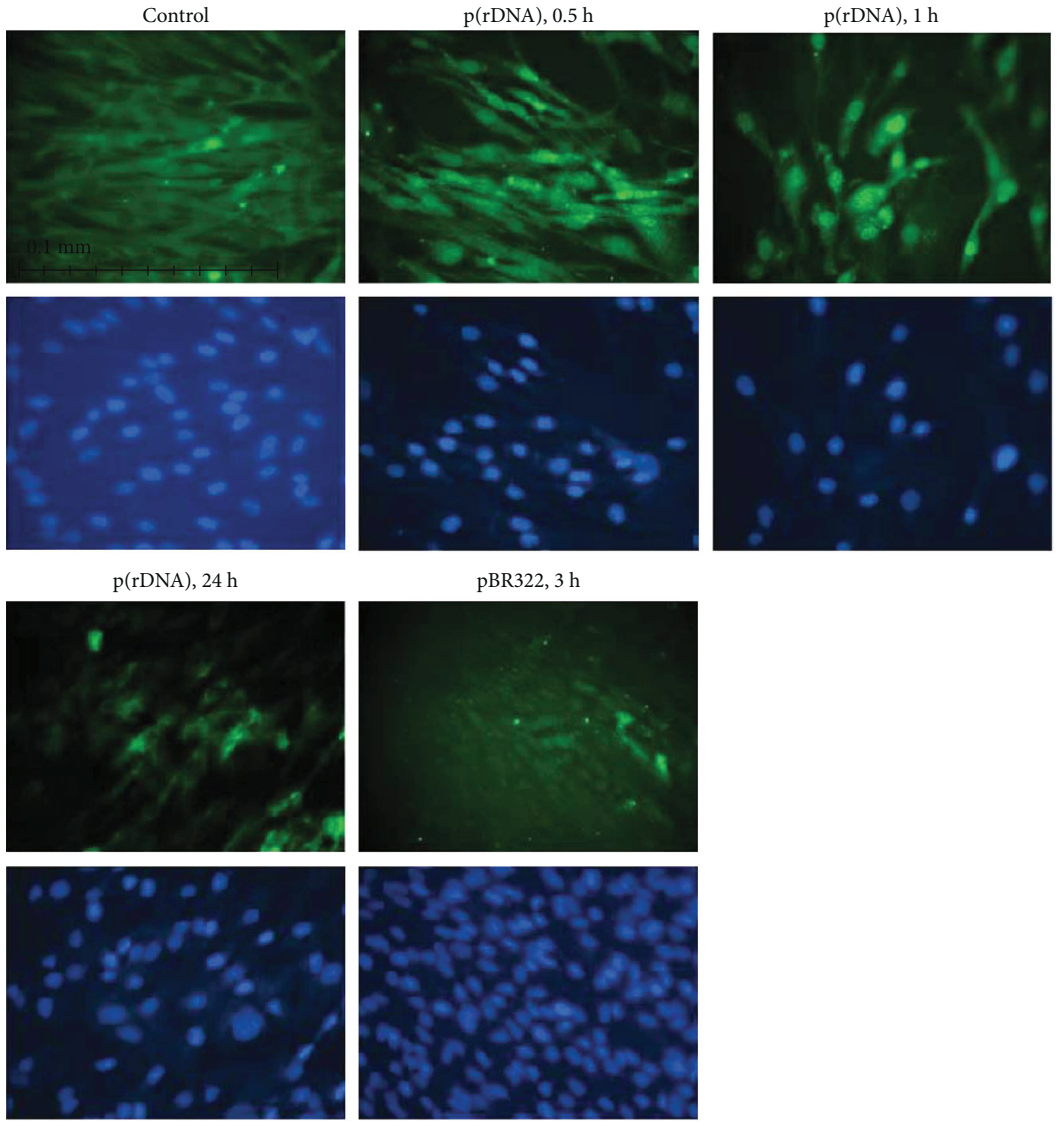

(a)

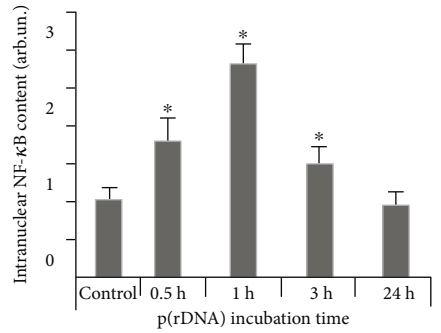

(b)

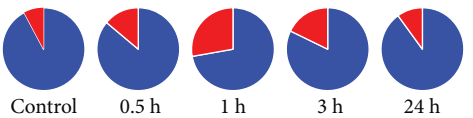

(c)

Figure 1: Continued.

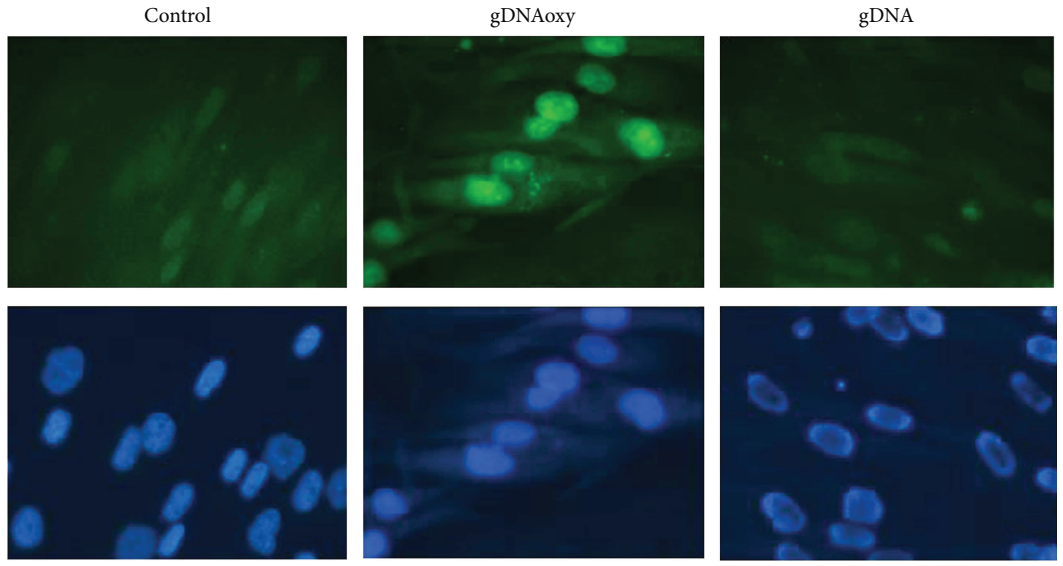

(d)

Figure 1: (a) Intracellular location of the p65 component of NF-κB during cell incubation with GC-rich model DNA (p(rDNA)) and a plasmid vector carrying ribosomal repeats (pBR322) in a concentration of 50 ng/ml. The magnification was ×40; the exposure duration for NF-κB is indicated in the figure. (b) Fraction of cells containing NF-κB in the nucleus. The data were obtained using the Image 6 computer program for image analysis. The expression level of NF-κB was calculated in relation to the control cells cultivated without adding cfDNA fragments. The control cells were taken as a unit. $^{*}p < 0.05$. The experiment was conducted on two MSC cultures. For each culture, multiple measurements (three or more) were performed by different technicians. (c) Reads of the CyTell cell imaging system (GE Healthcare). The red sectors indicate the fraction of NF-κB-positive nuclei, while the blue sectors indicate the fractions of NF-κB-negative cell nuclei. The time of cultivation with p(rDNA) fragments and the vector (50 ng/ml) are indicated in the figure. (d) Intracellular location of NRF2 during cell incubation with oxidized cfDNA fragments (gDNAoxy) and genomic DNA (gDNA) in a concentration of 50 ng/ml. The exposure duration for NRF2 was 1 hour; the magnification was ×100.

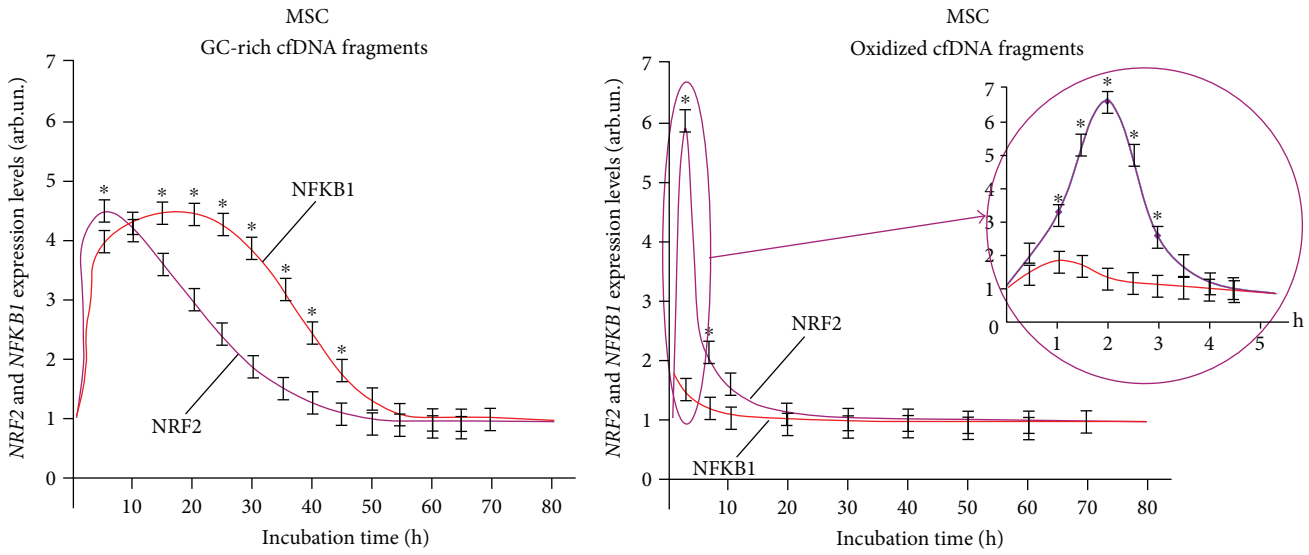

(a) (b)

Figure 2: *NFKB1* and *NRF2* expression curves under the action of (a) GC-rich and (b) oxidized fragments in mesenchymal stem cells (MSC). The expression levels were determined every 5 minutes after adding the corresponding fragments (model GC-rich fragments, model oxidized fragments) using real-time PCR. For each gene, the expression level was calculated relating to the internal standard gene TBP, with a spread in values at every point not exceeding 5%. *Significant difference ($p < 0.05$) between the relative values of NRF2 and NFKB1.

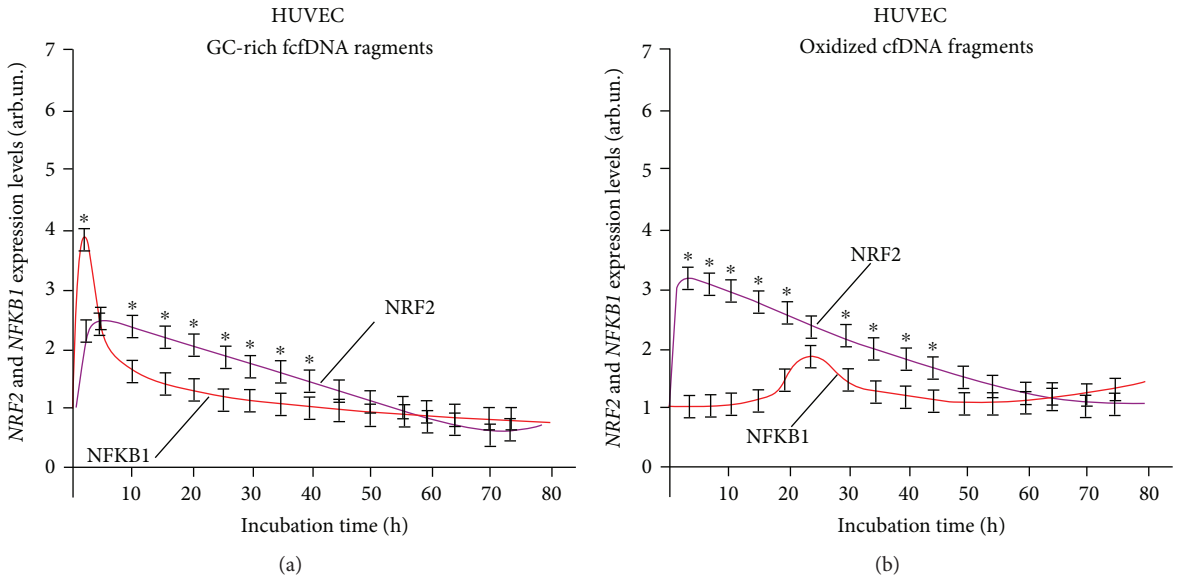

Figure 3: Interaction of two signaling pathways, NRF2 and NFKB1, in human umbilical vascular endothelial cells (HUVEC) exposed to (a) GC-rich and (b) oxidized cfDNA fragments. The expression levels were determined every 5 minutes after adding the corresponding fragments (model GC-rich fragments, model oxidized fragments) using real-time PCR. For each gene, the expression level was calculated relating to the internal standard gene TBP, with a spread in values at every point not exceeding 5%. *Significant difference ($p < 0.05$) between the relative values of NRF2 and NFKB1.

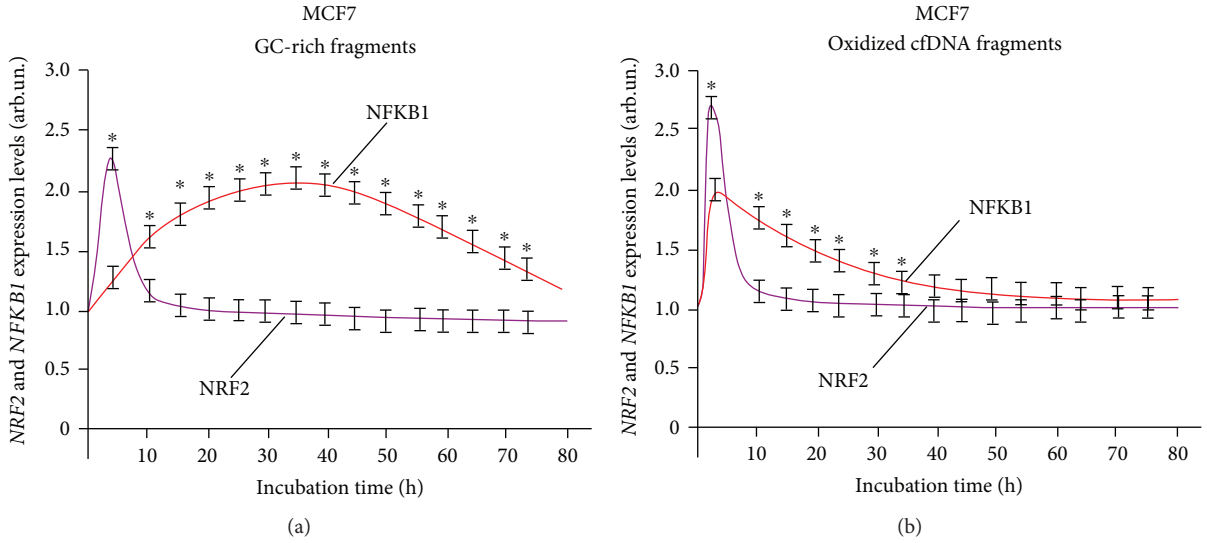

Figure 4: Interaction of two signaling pathways, NRF2 and NFKB1, in human breast adenocarcinoma cells (MCF7) exposed to (a) GC-rich and (b) oxidized cfDNA fragments. The expression levels were determined every 5 minutes after adding the corresponding fragments (model GC-rich fragments, model oxidized fragments) using real-time PCR. For each gene, the expression level was calculated relating to the internal standard gene TBP, with a spread in values at every point not exceeding 5%. *Significant difference ($p < 0.05$) between the relative values of NRF2 and NFKB1.

In 30 minutes after adding DNA fragments in the HUVEC culture medium, the fraction of cells with the signs of apoptosis (fraction *R* framed in Figure 5(a)) diminishes, and this effect is especially prominent in case of exposure to GC-rich DNA (Figure 5(b)). Nonetheless, 3 hours later, the fraction of apoptotic cells increases after the exposure to any type of DNA.

The fraction of MSC with the signs of apoptosis after the exposure to nonoxidized, GC-rich, and oxidized cfDNA fragments was also estimated by the detection of annexin V protein on the cell surface (Figure 6).

A combination of oxidized and nonoxidized cfDNA fragments reduced the level of apoptosis in MSC registered in 3 hours by 40–50%. After a three-hour-long exposure, GC-rich oxidized and nonoxidized fragments (p(rDNA) and p(rDNA)oxy) caused a decrease in the frequency of cells with the signs of apoptosis in a greater degree by 70–80%.

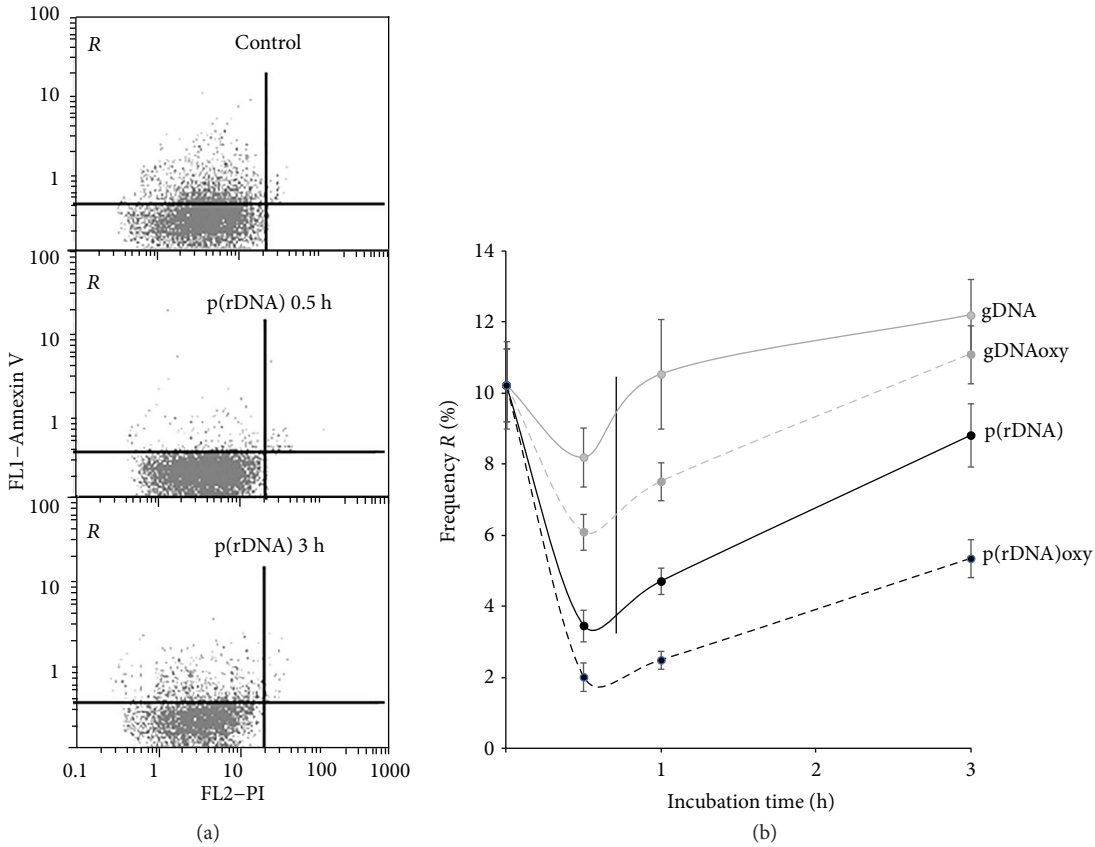

Figure 5: Time profiles of the fraction of apoptotic cells in HUVEC. (a) Annexin V fluorescence is plotted along the y-axis, and PI fluorescence is along the x-axis. From top to bottom: controls, after 1 hour and after 3 hours of exposure to p(rDNA) in a concentration of 50 ng/ml. (b) Temporal course of the frequency of apoptotic cells (cells belonging to the framed R fraction, i.e., with low PI and high annexin V fluorescence) in HUVEC culture according to the detection of cell surface levels of annexin V, a marker of early apoptosis during the cultivation with cfDNA fragments. Every curve significantly differs from the control ($p < 0.05$). gDNA: genomic DNA; p(rDNA): ribosomal repeat on a plasmid; gDNAoxy: oxidized genomic DNA; p(rDNA)oxy: oxidized ribosomal repeat.

A decrease in the fraction of dying cells in the cultures exposed to GC-rich and oxidized DNA is proved by a decrease several times in the content of endogenous extracellular DNA in the cell culture medium. During cultivation, endogenous DNA can be normally found in the medium. The contents are 23 ± 6 ng/ml in HUVEC cultures (a mean for three different cultures), 6 ± 5 ng/ml in MSC lines (a mean for six different cultures), and 140 ± 20 ng/ml in MCF7 cultures. This kind of cfDNA is derived from naturally dying cells during cultivation [16, 52].

Cells from a culture or from a body bind the endogenous extracellular/circulating DNA [64]. Cells seem to adapt to extracellular DNA in the medium and to be in an inactive state. We suppose that potential DNA binding sites, which are not blocked by endogenous DNA, remain on the cell surface in an inactive state. When the cfDNA content increases several times (it occurs *in vitro* after adding exogenous DNA to the culture medium or *in vivo* in case of massive cell death during acute pathologic processes), more DNA will bind to the cell surface. The process of cfDNA binding to the cell surface is rapid. Within the first 30 minutes after emerging the exogenous DNA in the medium, almost the entire amount of cfDNA is located on/in the cells, while the cfDNA content in the culture medium decreases below the control values. In the presence of oxidized (gDNAoxy, p(rDNA)oxy) and unoxidized GC-rich DNA (in a concentration of 50 to 100 ng/ml), the cfDNA content in the culture medium will decrease in 30 minutes by a factor of 2 and 1.5 (HUVEC, $N = 3$), 3.5 and 2 (MSC, $N = 6$), and 3 and 1.8 in the culture (MCF7) in relation to the baseline values measured before the cell exposure to the cfDNA fragments. We are of opinion that unoxidized cfDNA interacts with the cell surface during this process, while oxidized cfDNA is transported to the cytoplasm.

Fragments of GC-rich and oxidized cfDNA also reduced the strength of the apoptotic enzyme caspase 3 in HUVEC, MSC, and lymphocytes ($p < 0.05$). The influence of cfDNA on the strength of caspase 3 depends on the concentration and oxidation degree of the cfDNA fragments: low concentrations of oxidized cfDNA inhibited apoptosis in a greater degree than highly oxidized cfDNA. Fragments of GC-rich cfDNA inhibited apoptosis within a concentration interval of 5 to 100 ng/ml.

We studied the activation of the expression of genes for antiapoptotic proteins of the BCL-2 family (BCL2, BCL2A1, and BCL2L1), BIRC2 (c-IAP1), and BIRC3 (c-IAP2) after the exposure of different cell types to cfDNA.

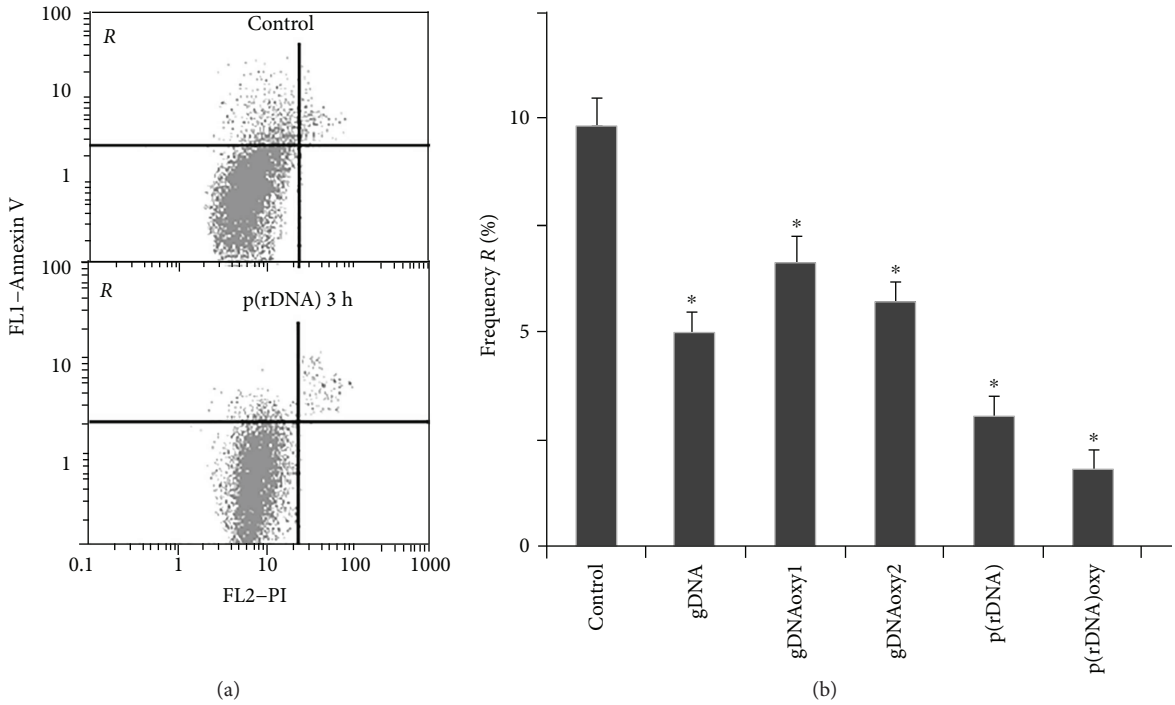

Figure 6: The exposure to cfDNA reduces apoptosis frequency in MSC. (a) Annexin V fluorescence is plotted along the *y*-axis, and PI fluorescence is along the *x*-axis. From top to bottom: controls, after 3 hours of exposure to p(rDNA) in a concentration of 50 ng/ml. *R* area contains cells with low PI and high annexin V fluorescence, that is, apoptotic cells. (b) The percentage frequency of cells belonging to the framed *R* fraction, that is, with the signs of apoptosis. *Significantly different from the control ($p < 0.05$). gDNA: genomic DNA; gDNAoxy1 and gDNAoxy2: oxidized genomic DNA with two different levels of oxidation; p(rDNA): ribosomal repeat; p(rDNA)oxy: oxidized ribosomal repeat.

The analysis of the amount of mRNA for BCL2, BCL2A1 (Bfl-1/A1), BCL2L1 (BCL-X), BIRC2 (c-IAP1), and BIRC3 (c-IAP2) in HUVEC showed that in response to an elevated cfDNA content, processes aimed to apoptosis prevention are considerably activated in the cells. This fact agrees with the data on the absence of significant changes of the total cell count, despite the proliferation arrest. The expression of BCL2 and BIRC family genes increases in 3 hours and remains elevated by a factor of 1.5 to 3 within 72 hours (Figure 7(a)). The activation of the antiapoptotic gene expression was also observed after the exposure of MCF7 culture to cfDNA.

In the presence of oxidized fragments (gDNAoxy and p(rDNA)oxy) and GC-rich fragments of p(rDNA) upon MCF7, the level of mRNA for *BCL2*, *BCL2A1*, and *BCL2L1* increases by a factor of 1.5 to 2 as early as in 0.5 hours, with a 2-fold to 4-fold increase by 48 hours (Figure 7(b)). Nonoxidized gDNA significantly (by a factor of 1.9 to 3.5) induced an increase in the expression of BCL2 family genes in MCF7 as late as 48 hours (Figure 7(b)). GC-rich and oxidized cfDNA fragments heightened *BIRC2* (*c-IAP1*) and *BIRC3* (*c-IAP2*) gene expression by a factor of 2 to 3 (Figure 8(b)). Under the action of cfDNA upon MCF7, the level of expression of the proapoptotic gene *BAX* does not increase or slightly decreases. The facts of the activation of the antiapoptotic genes and suppression of the proapoptotic gene *BAX* agree with the findings suggesting an augmentation of the fraction of the MCF7 pool under the exposure to cfDNA fragments. In MCF7, as well as in HUVEC, cfDNA blocks the process of apoptosis.

The expression of antiapoptotic genes also increases after an exposure of MSC to cfDNA. The expression of *BCL2* gene increased in 1 hour by a factor of 1.5 to 2 on the average after adding oxidized and GC-rich cfDNA fragments; by 3 hours, the expression of *BCL2* gene increased by a factor of 3.5 to 5 and remained on the same level in 24 hours (Figure 8(a)). The level of *BCL2*, *BCL2A1*, *BCL2L1*, *BIRC2* (*c-IAP1*), and *BIRC3* (*c-IAP2*) gene expression in MSC was heightened by a factor of 3 to 6 in 3 hours after the beginning of exposure of MSC to gDNAoxy and GC-rich p(rDNA); an exposure to gDNA increased the expression of the above-mentioned genes, on the average, two times only. Notably, MSC cultures that harbor mutations in *BRCA1* (5382insC) and *TP53* (missense mutation L145p in the fifth exon) genes showed more active expression of the antiapoptotic genes *BCL2*, *BCL2A1*, and *BCL2L1*: the level of expression of these genes raised approximately two times higher than in the MSC cultures carrying no mutation in *BRCA1* and *TP53* genes (data not shown). Apparently, such a strong antiapoptotic response in MSC cultures with mutations in *BRCA1* and *TP53* genes and the activation of the DNA repair gene *BRCA1* are aimed at the survival of cells with the defects in the genes of DNA repair and apoptosis regulation.

Highly oxidized DNA at a high concentration (300 ng/ml and higher) and high contents of p(rDNA) (>350 ng/ml)

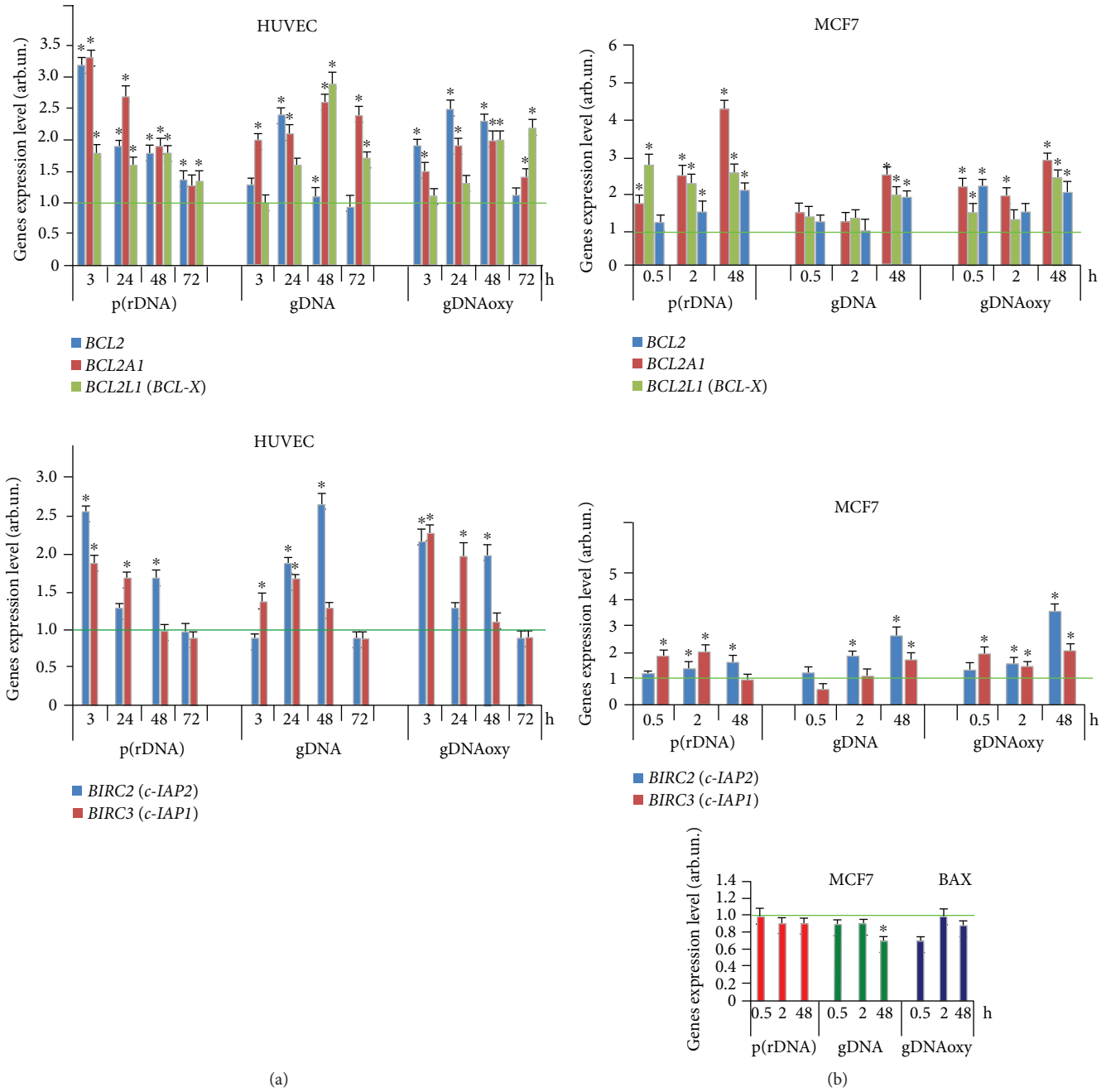

Figure 7: Expression levels of BCL2 family genes *BCL2*, *BCL2A1*, *BCL2L1*, *BIRC2* (*c-IAP1*), and *BIRC3* (*c-IAP2*) after an exposure of HUVEC (a) and MCF7 (b) to oxidized and nonoxidized GC-rich fragments of model cfDNA (50 ng/ml, see the exposure duration in the figure). Averaged values of three independent tests on HUVEC cultures derived from three different donors, and SD values are shown. As an internal standard gene, *TBP* gene was used. The horizontal green lines show the mean gene expression level of intact endothelial cells (1 ± 0.2 arb.un.). *Values are significantly different from the control ($p < 0.05$, Mann–Whitney U test). gDNA: genomic DNA; gDNAoxy: oxidized genomic DNA; p(rDNA): ribosomal repeat.

in the composition of cfDNA-induced cell death processes. So using Countess II FL Automated Cell Counter (TermoFisher) and cell staining with propidium iodide and annexin V-FITC, it was shown that the fraction of apoptotic cells in the MSC pool increased by 40% in 24 hours after the beginning of exposure to highly oxidized DNA in a high concentration (350 ng/ml and higher).

4. Discussion

Every complex metazoan organism maintains its homeostasis at several hierarchic levels: molecular, cellular, and tissue/organ. When the protection at a certain level is insufficient, the protection is activated at the higher level, while the lower level defense mechanisms are switched

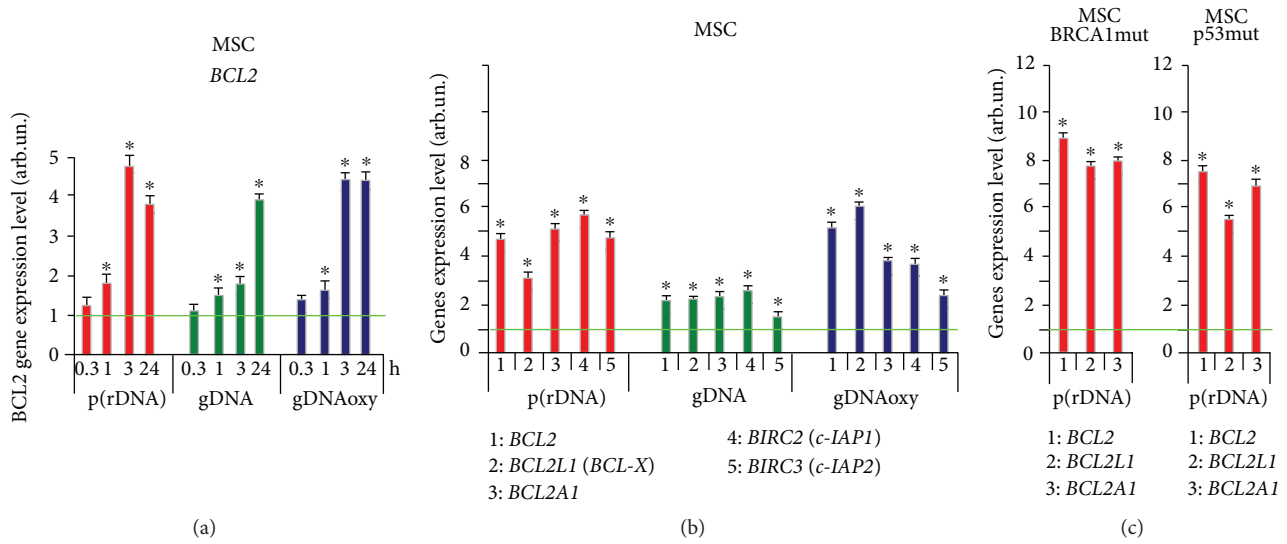

Figure 8: Expression level of *BCL2* gene (a) and *BCL2*, *BCL2A1*, *BCL2L1*, *BIRC2* (*c-IAP1*), and *BIRC3* (*c-IAP2*) genes (b) after an exposure of MSC to oxidized and nonoxidized GC-rich cfDNA fragments (50 ng/ml, see the exposure duration in the figure). Averaged values of three independent tests on MSC cultures derived from three different donors are shown. As an internal standard, TBP gene was used. (c) Expression of *BCL2*, *BCL2A1*, and *BCL2L1* genes in MSC cultures with heterozygous mutations in *BRCA1* (5382insC) and *TP53* (L145p) genes. *Values are significantly different from the control ($p < 0.05$, Mann–Whitney U test). gDNA: genomic DNA; p(rDNA): ribosomal repeat.

off in order to avoid excessive resource expenditures, and "broken" elements of the lower level are sacrificed in order to save the whole system. Similarly, the transition to the lower level of protection inactivates the higher level defense mechanisms and entails saving the lower level elements of the system. A good example of this "save-or-kill" strategy can be the well-investigated crosstalk between NRF2 (cellular level) and NF-κB (tissue/organ level) defense pathways.

Most authors report the operation of the NF-κB and NRF2 signaling pathways in opposition [41, 44, 65, 66]. The published articles propose a variety of mechanisms underpinning the mutual suppression of NRF2 and NF-κB. Some of them are reviewed below.

Binding sites for NF-κB were discovered in a rat *Nrf2* gene promoter [67]. NF-κB binding to the *Nrf2* gene promoter is characterized by a feedback loop: after a long enough period of NF-κB activity, the transcriptional activity of *Nrf2* increases thus suppressing NF-κB [67].

KEAP1 was shown to have some homology to IKB. IKKβ contains an ETGE motif [68]; therefore, it can bind KEAP1 and be targeted for ubiquitination [69]. Sequestration of the IKKβ pool via KEAP1 binding reduces IKBα degradation and may be the elusive mechanism by which NRF2 activation is known to inhibit NF-κB activation. When NRF2 is released due to oxidative signals, it results in an augmentation of the intracellular pool of unbound KEAP1, which can recruit more molecules of intracellular IKKβ thus inhibiting the NF-κB-driven gene expression. A mild oxidative stress entails a reversible KEAP1 alkylation; however, this reaction becomes irreversible under more oxidative conditions thus prohibiting most KEAP1 molecules from returning to the protein-binding conformation [70, 71]. In consequence of that, an abolishment of IKKβ inhibition by KEAP1 is logically expected, which results in growing NF-κB activation as more KEAP1 molecules lose their inhibitory properties. An additional argument in favor of this scheme is an experimentally established fact that the genetically determined decomposition of a KEAP1/CUL3/RBX1 complex with an E3-ubiquitin ligase that regulates both NRF2 and NF-κB signaling pathways appeared to be the key mechanism triggering NF-κB activation in human lung cancer cells [72]. KEAP1 has been shown to physically associate with NFKB-p65 *in vitro* and *in vivo*, and the signal from NF-κB inhibits the NRF2 signaling pathway through the interaction between p65 and KEAP1 [73].

There is evidence for NRF2 modulating the NF-κB signaling pathway at posttranslational level. This response involves IKB kinase and is mediated by the RAC1 signaling protein activated by the TLR4 receptor. This is a small GTPase of the RHO family, which is involved in innate immunity and triggers the NF-κB signaling pathway, as well as activating the NRF2/ARE pathway, which in turn blocks the RAC1-dependent NF-κB activation thus forming a negative feedback loop [74].

Seemingly, NF-κB can repress the *NRF2* gene transcription by a mechanism connected with CREB: NF-κB competes with NRF2 for a transcription coactivator CREB-binding protein (a protein that binds to CREB) [66].

Another scheme accounts for the antagonism because of an interaction of NF-κB with histone deacetylase SIRT1 (Figure 9) [42]. In turn, SIRT1 is an upstream inductor of NRF2 [75–80].

Finally, direct sequestration of free radicals by the NRF2-driven enzymes weakens the action of NF-κB [81].

Major NRF2 functions are xenobiotic detoxification and protection against oxidative stress. The oxidative stress is

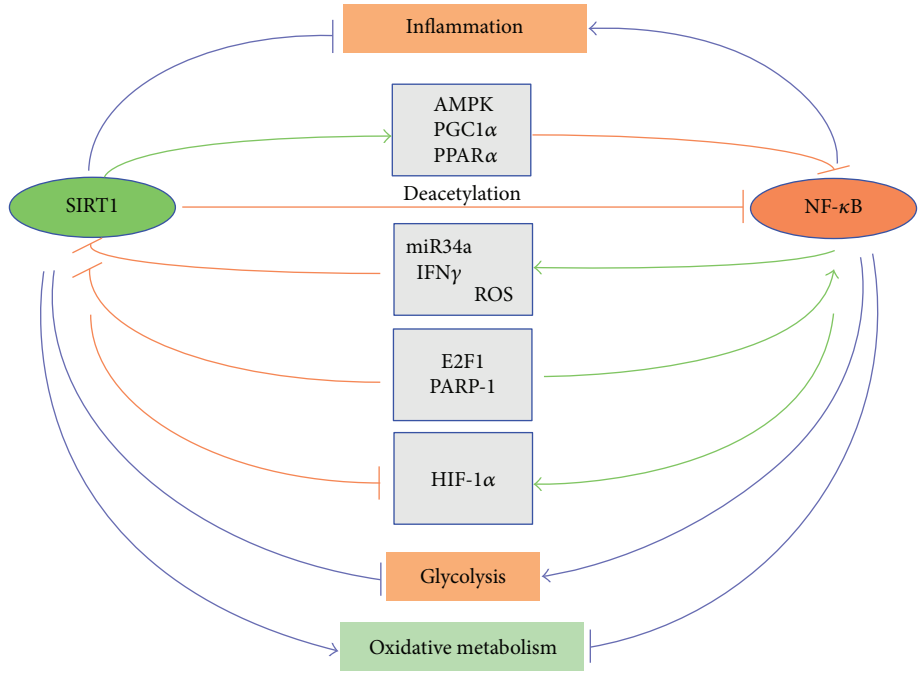

Figure 9: A schematic presentation of the antagonistic regulation between SIRT1 and NF-κB signaling in the control of inflammation and metabolic responses. The major signaling pathways mediating this antagonistic regulation are shown.

involved in the pathogenesis and progress of various diseases. Reactive oxygen species (ROS) alter the reductive-oxidative balance in the cells and apply oxidation-sensitive mechanisms in order to regulate the expression and activity of the transcription factors and genes regulated by the latter [82]. ROS trigger the NF-κB signaling pathway resulting in elevated expression of a large quantity of proinflammatory cytokines such as TNFα, IL-1, IL-2, IL-6, IL-12, and adhesion molecules. The cytokines can induce ROS synthesis to form a vicious circle between oxidative stress and production of the proinflammatory cytokines [67]. This vicious circle can be broken by NRF2 released from the complex with its inactivator KEAP1 [65]. The activated free NRF2 translocates to the nucleus and launches the expression of genes for phase II detoxification enzymes and antioxidative enzymes, including NADP-H:quinone oxidoreductase 1 (NQO1), glutathione S-transferase (GST), heme oxygenase 1 (HO-1), glutathione peroxidase (GSH-Px), glutamate cysteine ligase (GCL), and peroxiredoxin 1 (PRX 1), which play an important role in cell protection by ROS quenching [67, 83]. The NRF2-KEAP1 system is acknowledged as the key mechanism of protection of the cell against oxidative stress. Besides, NRF2 inhibits the expression of proinflammatory cytokines, chemokines, adhesion molecules, matrix metalloproteinase (MMP-9), cyclooxygenase-2, and iNOS [67]. NRF2 modulates a cascade of anti-inflammatory cytokines via NF-κB inhibition and regulates the antioxidant cellular responses [65]. Inducing NRF2 or inhibiting NOX4 as a source of ROS demonstrated therapeutic effectiveness *in vivo* in the therapy of diseases caused by cell senescence [84] or malignant transformation [85], via inhibiting NF-κB.

When the NF-κB-mediated attempt to restore homeostasis fails and oxidative stress rises to extreme levels,

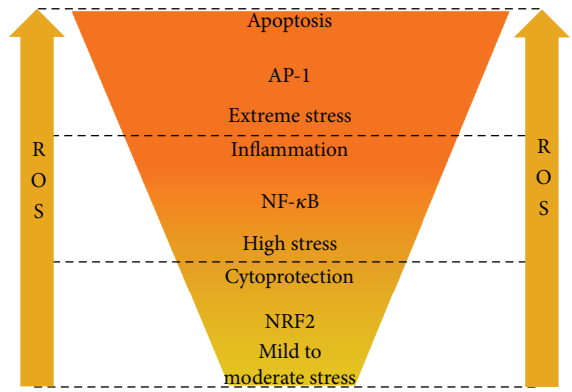

Figure 10: Differential responses to rising oxidative stress.

AP-1-mediated apoptosis is triggered (Figure 10) [86, 87]. Thus, the organism successively implements the "save-or-kill" strategy firstly at the cellular level and, if it failed, then at the tissue level.

We studied the time profiles of activity of the transcription factors NF-κB and NRF2 at the level of expression of their genes. Incubation with cfDNA was accompanied by an apparent increase in NRF2 expression in MSC and HUVEC at the levels of transcription and translation. The maximum effect was observed in case of action of oxidized DNA upon MSC, when the level of RNA*NRF2* showed a 12-fold increase and the protein level showed a 2-fold augmentation. In cancer cells, NRF2 plays an insignificant role in the response for a change of the parameters of cfDNA. The increased expression of NRF2 in MSC and HUVEC is followed by its nuclear translocation suggesting its activation as a transcription factor.

Our findings demonstrate a different intensity of the NRF2-based response in the cells of different types. We hypothesized that the organism's evolutionarily established readiness to sacrifice affected or damaged cells in order to save the tissue integrity depends on the degree of differentiation of the cells. Stem cells are more valuable as a cell depot; therefore, they showed the highest expression of *NRF2* in response to model cfDNA exposure. Perhaps, these peculiarities of MSC determine the anti-inflammatory effect in the MSC-based therapy of autoimmune diseases [88]. Unlike MSC, HUVEC are already differentiated cells; therefore, they easily develop an NF-κB-mediated inflammatory response with the possible transition to massive apoptosis. The same picture was observed in other experiments on fibroblasts (data not shown). In the fibroblasts after serum withdrawal or an exposure to oxidized DNA, the levels of RNA*NRF2* and NRF2 protein increased fivefold.

As far as cancer cells are concerned, they are characterized by a secondary loss of specialization. The cancer cells are known to have constitutive activation of *NRF2* expression [89–93]; therefore MCF7 demonstrated the minimum response of *NRF2* expression to cfDNA, while the NF-κB-mediated proinflammatory response prevailed.

The second regularity, which can be found in all the three cell type studies, consists in different responses for simple GC-rich cfDNA and for oxidized cfDNA. Probably, the evolutionarily established difference of these response patterns is caused by the fact that GC-rich cfDNA accumulates in the body during chronic cell death on a small scale. We showed earlier that under the above-mentioned circumstances, for example, in case of occupational exposure to low-dose ionizing radiation [13] or in case of a disease accompanied by elevated cell death [94], an activation of cfDNA-cleaving nucleases occurs. As a result, total blood cfDNA paradoxically decreases, while the fraction of GC-rich cfDNA with immunostimulatory properties increases. Oxidized cfDNA is a marker of the strong oxidative stress typical for acute conditions. Thus, GC-rich nonoxidized cfDNA is a signal of chronic mild cell death, while cfDNA with high 8-oxodG content is a hallmark of acute and massive cell death. We believe this difference underpins the observed diversity in the expression patterns. In every cell type studied, the response for oxidized cfDNA was more acute, that is, which started earlier and was more intensive, but returned faster to the baseline. GC-rich nonoxidized cfDNA evoked a weaker and elongated response with a predominance of the inflammatory component (NF-κB). It is indeed quite reasonable that an acute oxidative stress requires a cytoprotective response, which can be provided by NRF2-driven genes, whereas the conditions of a chronic stress will transfer the response to the upper tissue level (inflammation).

The exploration of apoptosis rates after adding cfDNA showed that cfDNA with moderately increased GC-content and lightly oxidized DNA promoted cell survival.

The dose survival curves for various types of cfDNA (e.g., Figure 5(b)) are typical hormetic curves. Hormesis is a dose-response phenomenon characterized by a low-dose stimulation and a high-dose inhibition by the same signal [95]. Hence, the strategies of eventual modulation of the cfDNA effect for future therapeutic purposes should be different depending on the current cfDNA concentration: either preconditioning with low doses before a massive impact or measures intended to elimination (binding, etc.) of cfDNA in cases when the cfDNA concentration has become high.

In particular, the revealed effect of low cfDNA concentrations upon MSC suggests an alternative strategy to increase the viability of MSC used in transplantology and therapy of disorders followed by tissue degeneration, a short-time (3 to 24 hours) pretreatment (preconditioning) of MSC culture with a plasmid p(rDNA) in a low concentration (50 ng/ml). The benefits of the plasmid application are low active concentration and high resistance to nuclease cleavage.

Highly oxidized DNA at a high concentration (250 ng/ml and higher) and high contents of GC-rich DNA fraction in the composition of cfDNA induced apoptosis. We have supposed that the introduction of specific antibodies to cfDNA or blocking the cfDNA signal at the level of receptors will be able to neutralize the negative action of high cfDNA concentrations.

Conflicts of Interest

The funding does not lead to any conflict of interests regarding the publication of this manuscript. There is no other possible conflict of interests in the manuscript.

Acknowledgments

The reported study was supported by RFBR (Russian Foundation for Basic Research) within the framework of Research Project no. 16-04-01099A, no. 16-04-00576A, no. 16-04-01541A, and no. 17-04-01587A.

References

[1] S. Gravina, J. M. Sedivy, and J. Vijg, "The dark side of circulating nucleic acids," *Aging Cell*, vol. 15, no. 3, pp. 398-399, 2016.

[2] M. van der Vaart and P. J. Pretorius, "Circulating DNA. Its origin and fluctuation," *Annals of the New York Academy of Sciences*, vol. 1137, no. 1, pp. 18–26, 2008.

[3] H. Lu, J. Busch, M. Jung et al., "Diagnostic and prognostic potential of circulating cell-free genomic and mitochondrial DNA fragments in clear cell renal cell carcinoma patients," *Clinica Chimica Acta*, vol. 452, pp. 109–119, 2016.

[4] V. Brinkmann, U. Reichard, C. Goosmann et al., "Neutrophil extracellular traps kill bacteria," *Science*, vol. 303, no. 5663, pp. 1532–1535, 2004.

[5] E. R. Zaher, M. M. Anwar, H. M. Kohail, S. M. El-Zoghby, and M. S. Abo-El-Eneen, "Cell-free DNA concentration and integrity as a screening tool for cancer," *Indian Journal of Cancer*, vol. 50, no. 3, pp. 175–183, 2013.

[6] Y. I. Elshimali, H. Khaddour, M. Sarkissyan, Y. Wu, and J. V. Vadgama, "The clinical utilization of circulating cell free DNA (ccfDNA) in blood of cancer patients," *International Journal of Molecular Sciences*, vol. 14, no. 12, pp. 18925–18958, 2013.

[7] V. A. Forte, D. K. Barrak, M. Elhodaky, L. Tung, A. Snow, and J. E. Lang, "The potential for liquid biopsies in the precision

medical treatment of breast cancer," *Cancer Biology & Medicine*, vol. 13, no. 1, pp. 19–40, 2016.

[8] S. Tamminga, M. van Maarle, L. Henneman, C. B. Oudejans, M. C. Cornel, and E. A. Sistermans, "Chapter three - maternal plasma DNA and RNA sequencing for prenatal testing," *Advances in Clinical Chemistry*, vol. 74, pp. 63–102, 2016.

[9] A. J. Bronkhorst, J. Aucamp, and P. J. Pretorius, "Cell-free DNA: preanalytical variables," *Clinica Chimica Acta*, vol. 450, pp. 243–253, 2015.

[10] A. V. Ermakov, M. S. Konkova, S. V. Kostyuk, V. L. Izevskaya, A. Baranova, and N. N. Veiko, "Oxidized extracellular DNA as a stress signal in human cells," *Oxidative Medicine and Cellular Longevity*, vol. 2013, Article ID 649747, 12 pages, 2013.

[11] K. Glebova, N. Veiko, S. Kostyuk, V. Izhevskaya, and A. Baranova, "Oxidized extracellular DNA as a stress signal that may modify response to anticancer therapy," *Cancer Letters*, vol. 356, no. 1, pp. 22–33, 2015.

[12] N. N. Veiko, N. A. Bulycheva, O. A. Roginko et al., "Ribosomal repeat in cell free DNA as a marker for cell death," *Biochemistry (Moscow) Supplement Series B: Biomedical Chemistry*, vol. 2, no. 2, pp. 198–207, 2008.

[13] I. B. Korzeneva, S. V. Kostuyk, L. S. Ershova et al., "Human circulating plasma DNA significantly decreases while lymphocyte DNA damage increases under chronic occupational exposure to low-dose gamma-neutron and tritium β-radiation," *Mutation Research/Fundamental and Molecular Mechanisms of Mutagenesis*, vol. 779, pp. 1–15, 2015.

[14] S. V. Kostyuk, V. J. Tabakov, V. V. Chestkov et al., "Oxidized DNA induces an adaptive response in human fibroblasts," *Mutation Research/Fundamental and Molecular Mechanisms of Mutagenesis*, vol. 747-748, pp. 6–18, 2013.

[15] P. Loseva, S. Kostyuk, E. Malinovskaya et al., "Extracellular DNA oxidation stimulates activation of NRF2 and reduces the production of ROS in human mesenchymal stem cells," *Expert Opinion on Biological Therapy*, vol. 12, Supplement 1, pp. S85–S97, 2012.

[16] D. S. Pisetsky, "The origin and properties of extracellular DNA: from PAMP to DAMP," *Clinical Immunology*, vol. 144, no. 1, pp. 32–40, 2012.

[17] Y. H. Chiu, J. B. Macmillan, and Z. J. Chen, "RNA polymerase III detects cytosolic DNA and induces type I interferons through the RIG-I pathway," *Cell*, vol. 138, no. 3, pp. 576–591, 2009.

[18] H. Li, J. Wang, J. Wang, L. S. Cao, Z. X. Wang, and J. W. Wu, "Structural mechanism of DNA recognition by the p202 HINa domain: insights into the inhibition of Aim2-mediated inflammatory signaling," *Acta Crystallographica Section F Structural Biology Communications*, vol. 70, no. 1, pp. 21–29, 2014.

[19] L. Unterholzner, "The interferon response to intracellular DNA: why so many receptors?," *Immunobiology*, vol. 218, no. 11, pp. 1312–1321, 2013.

[20] T. Kawai and S. Akira, "Toll-like receptors and their crosstalk with other innate receptors in infection and immunity," *Immunity*, vol. 34, no. 5, pp. 637–650, 2011.

[21] K. Triantafilou, D. Eryilmazlar, and M. Triantafilou, "Herpes simplex virus 2-induced activation in vaginal cells involves Toll-like receptors 2 and 9 and DNA sensors DAI and IFI16," *American Journal of Obstetrics & Gynecology*, vol. 210, no. 2, pp. 122.e1–122.e10, 2014.

[22] E. Harberts and A. A. Gaspari, "TLR signaling and DNA repair: are they associated?," *Journal of Investigative Dermatology*, vol. 133, no. 2, pp. 296–302, 2013.

[23] H. Kato, K. Takahasi, and T. Fujita, "RIG-I-like receptors: cytoplasmic sensors for non-self RNA," *Immunological Reviews*, vol. 243, no. 1, pp. 91–98, 2011.

[24] S. E. Keating, M. Baran, and A. G. Bowie, "Cytosolic DNA sensors regulating type I interferon induction," *Trends in Immunology*, vol. 32, no. 12, pp. 574–581, 2011.

[25] L. Sun, J. Wu, F. Du, X. Chen, and Z. J. Chen, "Cyclic GMP-AMP synthase is a cytosolic DNA sensor that activates the type I interferon pathway," *Science*, vol. 339, no. 6121, pp. 786–791, 2013.

[26] J. Wu, L. Sun, X. Chen et al., "Cyclic GMP-AMP is an endogenous second messenger in innate immune signaling by cytosolic DNA," *Science*, vol. 339, no. 6121, pp. 826–830, 2013.

[27] W. A. Rose 2nd, K. Sakamoto, and C. A. Leifer, "TLR9 is important for protection against intestinal damage and for intestinal repair," *Scientific Reports*, vol. 2, no. 1, article 574, 2012.

[28] S. Goulopoulou, T. Matsumoto, G. F. Bomfim, and R. C. Webb, "Toll-like receptor 9 activation: a novel mechanism linking placenta-derived mitochondrial DNA and vascular dysfunction in pre-eclampsia," *Clinical Science*, vol. 123, no. 7, pp. 429–435, 2012.

[29] S. Kostjuk, P. Loseva, O. Chvartatskaya et al., "Extracellular GC-rich DNA activates TLR9- and NF-κB-dependent signaling pathways in human adipose-derived mesenchymal stem cells (haMSCs)," *Expert Opinion on Biological Therapy*, vol. 12, Supplement 1, pp. S99–S111, 2012.

[30] N. Carayol, J. Chen, F. Yang et al., "A dominant function of IKK/NF-κB signaling in global lipopolysaccharide-induced gene expression," *Journal of Biological Chemistry*, vol. 281, no. 41, pp. 31142–31151, 2006.

[31] S. Ghosh and J. F. Dass, "Study of pathway cross-talk interactions with NF-κB leading to Its activation via ubiquitination or phosphorylation: a brief review," *Gene*, vol. 584, no. 1, pp. 97–109, 2016.

[32] W. Bao, H. Xia, Y. Liang et al., "Toll-like receptor 9 can be activated by endogenous mitochondrial DNA to induce podocyte apoptosis," *Scientific Reports*, vol. 6, no. 1, article 22579, 2016.

[33] M. Bliksøen, L. H. Mariero, M. K. Torp et al., "Extracellular mtDNA activates NF-κB via Toll-like receptor 9 and induces cell death in cardiomyocytes," *Basic Research in Cardiology*, vol. 111, no. 4, p. 42, 2016.

[34] G. Joshi and J. A. Johnson, "The Nrf2-ARE pathway: a valuable therapeutic target for the treatment of neurodegenerative diseases," *Recent Patents on CNS Drug Discovery*, vol. 7, no. 3, pp. 218–229, 2012.

[35] H. K. Bryan, A. Olayanju, C. E. Goldring, and B. K. Park, "The Nrf2 cell defence pathway: Keap1-dependent and -independent mechanisms of regulation," *Biochemical Pharmacology*, vol. 85, no. 6, pp. 705–717, 2013.

[36] Y. Zhang and Y. Xiang, "Molecular and cellular basis for the unique functioning of Nrf1, an indispensable transcription factor for maintaining cell homoeostasis and organ integrity," *Biochemical Journal*, vol. 473, no. 8, pp. 961–1000, 2016.

[37] A. Lau, N. F. Villeneuve, Z. Sun, P. K. Wong, and D. D. Zhang, "Dual roles of Nrf2 in cancer," *Pharmacological Research*, vol. 58, no. 5-6, pp. 262–270, 2008.

[38] J. D. Hayes and A. T. Dinkova-Kostova, "The Nrf2 regulatory network provides an interface between redox and intermediary metabolism," *Trends in Biochemical Sciences*, vol. 39, no. 4, pp. 199–218, 2014.

[39] M. A. O'Connell and J. D. Hayes, "The Keap1/Nrf2 pathway in health and disease: from the bench to the clinic," *Biochemical Society Transactions*, vol. 43, no. 4, pp. 687–689, 2015.

[40] L. M. Pedruzzi, M. B. Stockler-Pinto, M. J. Leite, and D. Mafra, "Nrf2–keap1 system versus NF-κB: the good and the evil in chronic kidney disease?," *Biochimie*, vol. 94, no. 12, pp. 2461–2466, 2012.

[41] H. Chen, Y. Fang, W. Li, R. C. Orlando, N. Shaheen, and X. L. Chen, "NFκB and Nrf2 in esophageal epithelial barrier function," *Tissue Barriers*, vol. 1, no. 5, article e27463, 2013.

[42] A. Kauppinen, T. Suuronen, J. Ojala, K. Kaarniranta, and A. Salminen, "Antagonistic crosstalk between NF-κB and SIRT1 in the regulation of inflammation and metabolic disorders," *Cellular Signalling*, vol. 25, no. 10, pp. 1939–1948, 2013.

[43] J. D. Wardyn, A. H. Ponsford, and C. M. Sanderson, "Dissecting molecular cross-talk between Nrf2 and NF-κB response pathways," *Biochemical Society Transactions*, vol. 43, no. 4, pp. 621–626, 2015.

[44] N. Wakabayashi, S. L. Slocum, J. J. Skoko, S. Shin, and T. W. Kensler, "When NRF2 talks, who's listening?," *Antioxidants & Redox Signaling*, vol. 13, no. 11, pp. 1649–1663, 2010.

[45] V. N. Manskikh, "Pathways of cell death and their biological importance," *Tsitologiia*, vol. 49, no. 11, pp. 909–915, 2007.

[46] S. Cory, D. C. Huang, and J. M. Adams, "The Bcl-2 family: roles in cell survival and oncogenesis," *Oncogene*, vol. 22, no. 53, pp. 8590–8607, 2003.

[47] W. A. Siddiqui, A. Ahad, and H. Ahsan, "The mystery of BCL2 family: BCL-2 proteins and apoptosis: an update," *Archives of Toxicology*, vol. 89, no. 3, pp. 289–317, 2015.

[48] J. Silke and P. Meier, "Inhibitor of apoptosis (IAP) proteins–modulators of cell death and inflammation," *Cold Spring Harbor Perspectives in Biology*, vol. 5, no. 2, article a008730, 2013.

[49] C. Muñoz-Pinedo, "Signaling pathways that regulate life and cell death: evolution of apoptosis in the context of self-defense," in *Self and Nonself. Advances in Experimental Medicine and Biology*, C. López-Larrea, Ed., vol. 738, pp. 124–143, Springer, New York, NY, USA, 2012.

[50] A. V. Ermakov, M. S. Konkova, S. V. Kostyuk et al., "An extracellular DNA mediated bystander effect produced from low dose irradiated endothelial cells," *Mutation Research/Fundamental and Molecular Mechanisms of Mutagenesis*, vol. 712, no. 1-2, pp. 1–10, 2011.

[51] F. Lu, Y. Yu, B. Zhang, D. Liang, Z. M. Li, and W. You, "Inhibitory effects of mild hyperthermia plus docetaxel therapy on ER(+/−) breast cancer cells and action mechanisms," *Journal of Huazhong University of Science and Technology [Medical Sciences]*, vol. 33, no. 6, pp. 870–876, 2013.

[52] N. N. Veiko, E. A. Kalashnikova, S. N. Kokarovtseva et al., "Stimulatory effect of fragments from transcribed region of ribosomal repeat on human peripheral blood lymphocytes," *Bulletin of Experimental Biology and Medicine*, vol. 142, no. 4, pp. 428–432, 2006.

[53] S. V. Kostyuk, M. S. Konkova, E. S. Ershova et al., "An exposure to the oxidized DNA enhances both instability of genome and survival in cancer cells," *PLoS One*, vol. 8, no. 10, article e77469, 2013.

[54] G. W. Buchko, J. R. Wagner, J. Cadet, S. Raoul, and M. Weinfeld, "Methylene blue-mediated photooxidation of 7,8-dihydro-8-oxo-2′-deoxyguanosine," *Biochimica et Biophysica Acta (BBA) - Gene Structure and Expression*, vol. 1263, no. 1, pp. 17–24, 1995.

[55] S. V. Kostyuk, T. D. Smirnova, L. V. Efremova et al., "Enhanced expression of iNOS in human endothelial cells during long-term culturing with extracellular DNA fragments," *Bulletin of Experimental Biology and Medicine*, vol. 149, no. 2, pp. 191–195, 2010.

[56] J. Vollmer, "TLR9 in health and disease," *International Reviews of Immunology*, vol. 25, no. 3-4, pp. 155–181, 2006.

[57] A. M. Krieg, "CpG still rocks! Update on an accidental drug," *Nucleic Acid Therapeutics*, vol. 22, no. 2, pp. 77–89, 2012.

[58] M. Peter, K. Bode, G. B. Lipford, F. Eberle, K. Heeg, and A. H. Dalpke, "Characterization of suppressive oligodeoxynucleotides that inhibit Toll-like receptor-9-mediated activation of innate immunity," *Immunology*, vol. 123, no. 1, pp. 118–128, 2008.

[59] S. Bauer, "Toll-like receptor 9 processing: the key event in Toll-like receptor 9 activation?," *Immunology Letters*, vol. 149, no. 1-2, pp. 85–87, 2013.

[60] R. F. Ashman, J. A. Goeken, J. Drahos, and P. Lenert, "Sequence requirements for oligodeoxyribonucleotide inhibitory activity," *International Immunology*, vol. 17, no. 4, pp. 411–420, 2005.

[61] A. Trieu, T. L. Roberts, J. A. Dunn, M. J. Sweet, and K. J. Stacey, "DNA motifs suppressing TLR9 responses," *Critical Reviews in Immunology*, vol. 26, no. 6, pp. 527–544, 2006.

[62] J. Ma, J. J. van den Beucken, F. Yang et al., "Coculture of osteoblasts and endothelial cells: optimization of culture medium and cell ratio," *Tissue Engineering Part C: Methods*, vol. 17, no. 3, pp. 349–357, 2011.

[63] D. Wlodkowic, J. Skommer, and Z. Darzynkiewicz, "Cytometry of apoptosis. Historical perspective and new advances," *Experimental Oncology*, vol. 34, no. 3, pp. 255–262, 2012.

[64] E. Y. Rykova, E. S. Morozkin, A. A. Ponomaryova et al., "Cell-free and cell-bound circulating nucleic acid complexes: mechanisms of generation, concentration and content," *Expert Opinion on Biological Therapy*, vol. 12, Supplement 1, pp. S141–S153, 2012.

[65] T. Nguyen, H. C. Huang, and C. B. Pickett, "Transcriptional regulation of the antioxidant response element. Activation by Nrf2 and repression by MafK," *Journal of Biological Chemistry*, vol. 275, no. 20, pp. 15466–15473, 2000.

[66] G. H. Liu, J. Qu, and X. Shen, "NF-κB/p65 antagonizes Nrf2-ARE pathway by depriving CBP from Nrf2 and facilitating recruitment of HDAC3 to MafK," *Biochimica et Biophysica Acta (BBA) - Molecular Cell Research*, vol. 1783, no. 5, pp. 713–727, 2008.

[67] S. Nair, S. T. Doh, J. Y. Chan, A. N. Kong, and L. Cai, "Regulatory potential for concerted modulation of Nrf2- and Nfkb1- mediated gene expression in inflammation and carcinogenesis," *British Journal of Cancer*, vol. 99, no. 12, pp. 2070–2082, 2008.

[68] Y. R. Kim, J. E. Oh, M. S. Kim et al., "Oncogenic *NRF2* mutations in squamous cell carcinomas of oesophagus and skin," *The Journal of Pathology*, vol. 220, no. 4, pp. 446–451, 2010.

[69] D. F. Lee, H. P. Kuo, M. Liu et al., "KEAP1 E3 ligase-mediated downregulation of NF-κB signaling by targeting IKKβ," *Molecular Cell*, vol. 36, no. 1, pp. 131–140, 2009.

[70] H. J. Forman, F. Ursini, and M. Maiorino, "An overview of mechanisms of redox signaling," *Journal of Molecular and Cellular Cardiology*, vol. 73, pp. 2–9, 2014.

[71] L. B. Poole, P. A. Karplus, and A. Claiborne, "Protein sulfenic acids in redox signaling," *Annual Review of Pharmacology and Toxicology*, vol. 44, no. 1, pp. 325–347, 2004.

[72] K. L. Thu, L. A. Pikor, R. Chari et al., "Genetic disruption of KEAP1/CUL3 E3 ubiquitin ligase complex components is a key mechanism of NF-kappaB pathway activation in lung cancer," *Journal of Thoracic Oncology*, vol. 6, no. 9, pp. 1521–1529, 2011.

[73] M. Yu, H. Li, Q. Liu et al., "Nuclear factor p65 interacts with Keap1 to repress the Nrf2-ARE pathway," *Cellular Signalling*, vol. 23, no. 5, pp. 883–892, 2011.

[74] A. Cuadrado, Z. Martín-Moldes, J. Ye, and I. Lastres-Becker, "Transcription factors NRF2 and NF-κB are coordinated effectors of the Rho family, GTP-binding protein RAC1 during inflammation," *Journal of Biological Chemistry*, vol. 289, no. 22, pp. 15244–15258, 2014.

[75] D. S. Yoon, Y. Choi, and J. W. Lee, "Cellular localization of NRF2 determines the self-renewal and osteogenic differentiation potential of human MSCs via the P53-SIRT1 axis," *Cell Death & Disease*, vol. 7, no. 2, article e2093, 2016.

[76] Y. W. Ding, G. J. Zhao, X. L. Li et al., "SIRT1 exerts protective effects against paraquat-induced injury in mouse type II alveolar epithelial cells by deacetylating NRF2 in vitro," *International Journal of Molecular Medicine*, vol. 37, no. 4, pp. 1049–1058, 2016.

[77] F. Xue, J. W. Huang, P. Y. Ding et al., "Nrf2/antioxidant defense pathway is involved in the neuroprotective effects of Sirt1 against focal cerebral ischemia in rats after hyperbaric oxygen preconditioning," *Behavioural Brain Research*, vol. 309, pp. 1–8, 2016.

[78] Y. Kawai, L. Garduño, M. Theodore, J. Yang, and I. J. Arinze, "Acetylation-deacetylation of the transcription factor Nrf2 (nuclear factor erythroid 2-related factor 2) regulates its transcriptional activity and nucleocytoplasmic localization," *Journal of Biological Chemistry*, vol. 286, no. 9, pp. 7629–7640, 2011.

[79] K. Huang, J. Huang, X. Xie et al., "Sirt1 resists advanced glycation end products-induced expressions of fibronectin and TGF-β1 by activating the Nrf2/ARE pathway in glomerular mesangial cells," *Free Radical Biology & Medicine*, vol. 65, pp. 528–540, 2013.

[80] M. T. Do, H. G. Kim, J. H. Choi, and H. G. Jeong, "Metformin induces microRNA-34a to downregulate the Sirt1/Pgc-1α/Nrf2 pathway, leading to increased susceptibility of wild-type p53 cancer cells to oxidative stress and therapeutic agents," *Free Radical Biology & Medicine*, vol. 74, pp. 21–34, 2014.

[81] S. C. Gupta, C. Sundaram, S. Reuter, and B. B. Aggarwal, "Inhibiting NF-κB activation by small molecules as a therapeutic strategy," *Biochimica et Biophysica Acta (BBA) - Gene Regulatory Mechanisms*, vol. 1799, no. 10-12, pp. 775–787, 2010.

[82] Z. A. Massy, P. Stenvinkel, and T. B. Drueke, "The role of oxidative stress in chronic kidney disease," *Seminars in Dialysis*, vol. 22, no. 4, pp. 405–408, 2009.

[83] S. S. Singh, S. Vrishni, B. K. Singh, I. Rahman, and P. Kakkar, "Nrf2-ARE stress response mechanism: a control point in oxidative stress-mediated dysfunctions and chronic inflammatory diseases," *Free Radical Research*, vol. 44, no. 11, pp. 1267–1288, 2010.

[84] L. Hecker, N. J. Logsdon, and D. Kurundkar, "Reversal of persistent fibrosis in aging by targeting Nox4-Nrf2 redox imbalance," *Science Translational Medicine*, vol. 6, no. 231, article 231ra47, 2014.

[85] W. Li, T. O. Khor, C. Xu et al., "Activation of Nrf2-antioxidant signaling attenuates NFκB-inflammatory response and elicits apoptosis," *Biochemical Pharmacology*, vol. 76, no. 11, pp. 1485–1489, 2008.

[86] C. G. Woods, J. Fu, P. Xue, and Y. Hou, "Dose-dependent transitions in Nrf2-mediated adaptive response and related stress responses to hypochlorous acid in mouse macrophages," *Toxicology and Applied Pharmacology*, vol. 238, no. 1, pp. 27–36, 2009.

[87] A. L. Stefanson and M. Bakovic, "Dietary regulation of Keap1/Nrf2/ARE pathway: focus on plant-derived compounds and trace minerals," *Nutrients*, vol. 6, no. 12, pp. 3777–3801, 2014.

[88] V. Pistoia and L. Raffaghello, "Mesenchymal stromal cells and autoimmunity," *International Immunology*, vol. 29, no. 2, pp. 49–58, 2017.

[89] B. Yang, Y. Ma, and Y. Liu, "Elevated expression of Nrf-2 and ABCG2 involved in multi-drug resistance of lung cancer SP cells," *Drug Research*, vol. 65, no. 10, pp. 526–531, 2015.

[90] Y. O. Son, P. Pratheeshkumar, R. V. Roy et al., "Nrf2/p62 signaling in apoptosis resistance and its role in cadmium-induced carcinogenesis," *Journal of Biological Chemistry*, vol. 289, no. 41, pp. 28660–28675, 2014.

[91] E. Reszka, Z. Jablonowski, and E. Wieczorek, "Polymorphisms of NRF2 and NRF2 target genes in urinary bladder cancer patients," *Journal of Cancer Research and Clinical Oncology*, vol. 140, no. 10, pp. 1723–1731, 2014.

[92] S. A. Rushworth, L. Zaitseva, M. Y. Murray, N. M. Shah, K. M. Bowles, and D. J. MacEwan, "The high Nrf2 expression in human acute myeloid leukemia is driven by NF-κB and underlies its chemo-resistance," *Blood*, vol. 120, no. 26, pp. 5188–5198, 2012.

[93] G. M. DeNicola, F. A. Karreth, T. J. Humpton et al., "Oncogene-induced Nrf2 transcription promotes ROS detoxification and tumorigenesis," *Nature*, vol. 475, no. 7354, pp. 106–109, 2011.

[94] N. N. Veiko, N. O. Shubaeva, S. M. Ivanova, A. I. Speranskii, N. A. Lyapunova, and D. M. Spitkovskii, "Blood serum DNA in patients with rheumatoid arthritis is considerably enriched with fragments of ribosomal repeats containing immunostimulatory CpG-motifs," *Bulletin of Experimental Biology and Medicine*, vol. 142, no. 3, pp. 313–316, 2006.

[95] V. Calabrese, C. Cornelius, A. T. Dinkova-Kostova, E. J. Calabrese, and M. P. Mattson, "Cellular stress responses, the hormesis paradigm, and vitagenes: novel targets for therapeutic intervention in neurodegenerative disorders," *Antioxidants & Redox Signaling*, vol. 13, no. 11, pp. 1763–1811, 2010.

Hindawi
Oxidative Medicine and Cellular Longevity
Volume 2018, Article ID 3074769, 11 pages
https://doi.org/10.1155/2018/3074769

Review Article

Yeast Cells Exposed to Exogenous Palmitoleic Acid Either Adapt to Stress and Survive or Commit to Regulated Liponecrosis and Die

Karamat Mohammad, Paméla Dakik, Younes Medkour, Mélissa McAuley, Darya Mitrofanova, and Vladimir I. Titorenko

Concordia University, Department of Biology, Montreal, QC, Canada H4B 1R6

Correspondence should be addressed to Vladimir I. Titorenko; vladimir.titorenko@concordia.ca

Received 2 September 2017; Revised 27 November 2017; Accepted 20 December 2017; Published 31 January 2018

Academic Editor: Paula Ludovico

A disturbed homeostasis of cellular lipids and the resulting lipotoxicity are considered to be key contributors to many human pathologies, including obesity, metabolic syndrome, type 2 diabetes, cardiovascular diseases, and cancer. The yeast *Saccharomyces cerevisiae* has been successfully used for uncovering molecular mechanisms through which impaired lipid metabolism causes lipotoxicity and elicits different forms of regulated cell death. Here, we discuss mechanisms of the "liponecrotic" mode of regulated cell death in *S. cerevisiae*. This mode of regulated cell death can be initiated in response to a brief treatment of yeast with exogenous palmitoleic acid. Such treatment prompts the incorporation of exogenously added palmitoleic acid into phospholipids and neutral lipids. This orchestrates a global remodeling of lipid metabolism and transfer in the endoplasmic reticulum, mitochondria, lipid droplets, and the plasma membrane. Certain features of such remodeling play essential roles either in committing yeast to liponecrosis or in executing this mode of regulated cell death. We also outline four processes through which yeast cells actively resist liponecrosis by adapting to the cellular stress imposed by palmitoleic acid and maintaining viability. These prosurvival cellular processes are confined in the endoplasmic reticulum, lipid droplets, peroxisomes, autophagosomes, vacuoles, and the cytosol.

1. Introduction

Some forms of cell death are classified as "programmed" cell death subroutines; they involve molecular machineries dedicated to commit cellular "suicide" that is aimed at providing certain benefits for development and/or survival of the entire organism [1–6]. Other forms of cell death are actively driven by molecular machineries that attempt to protect cells against certain stresses (without providing benefits for organismal development and/or survival); these forms are known as "regulated" cell death (RCD) subroutines [1, 3]. Cells commit RCD executed by a discrete molecular machinery because (1) the capacity of a molecular machinery dedicated to cell protection against a certain kind of stress is not sufficient to maintain cell viability if the intensity of such extracellular and/or intracellular stress exceeds a threshold and/or (2) molecular machineries driving some cellular processes that (directly or indirectly) contribute to cell protection against a certain kind of exogenous and/or endogenous stress are excessively activated, thereby generating products of these processes in concentrations that are lethal to the cell [1, 3, 7].

S. cerevisiae is a model organism most commonly and productively used for studying different forms of RCD elicited by perturbations in lipid metabolism [8–37]. The detailed knowledge of mechanisms underlying the molecular pathways of various modes of lipotoxic RCD in this yeast is therefore instrumental to our understanding of many human pathologies that are causally linked to dysregulated lipid metabolism, unbalanced lipid homeostasis, lipotoxicity, and lipid-induced cell death [31, 34, 37–41]. Among these human pathologies are obesity, metabolic syndrome, type 2 diabetes, insulin resistance, cardiovascular diseases, hepatic steatosis, liver cirrhosis, and cancer [34, 38–56].

The scope of this review is to analyze mechanisms underlying one of the modes of lipotoxic RCD. It has been discovered in the yeast *S. cerevisiae* and called "liponecrosis."

Liponecrotic RCD can be elicited by a short-term (for 2 h) treatment of yeast cells with exogenous palmitoleic acid (POA), a 16-carbon monounsaturated fatty acid (16 : 1 n-7) [57–59]. We describe different cellular processes that yeast cells exposed to POA use for stress adaptation and viability maintenance. We critically evaluate mechanisms (including POA-induced oxidative stress) through which yeast cells that are exposed to POA die of liponecrosis if the capacities of cellular processes for protection against POA-imposed stress become insufficient to maintain cell viability. We outline the most important unanswered questions and suggest directions for future research.

2. How Do Yeast Cells Die If Treated with POA and How Do They Mount a Protective Stress Response to Survive Such Treatment?

A model for the mechanism of liponecrotic RCD elicited by a short-term treatment of yeast with POA and for the mechanism protecting yeast from such RCD is schematically depicted in Figure 1.

Yeast cells that are briefly exposed to exogenous POA use the lipid-synthesizing and lipid-transporting enzymatic machineries of the endoplasmic reticulum (ER), mitochondria, lipid droplets (LDs), and the plasma membrane (PM) to incorporate this fatty acid into copious amounts of two classes of lipids [34, 59]. One of these POA-containing classes are the so-called "neutral" (uncharged) lipids triacylglycerols (TAGs) and ergosteryl esters (EEs), both of which are first produced in the ER and then deposited in LDs (Figure 1) [37, 40, 60, 61]. The other class are POA-containing phospholipids (Figure 1); they include (1) phosphatidic acid (PA), phosphatidylserine (PS), phosphatidylcholine (PC), and phosphatidylinositol (PI), all of which are synthesized only in the ER and then transferred to mitochondria through mitochondria-ER junctions and to the PM through PM-ER junctions [62–70]; (2) phosphatidylethanolamine (PE), which is produced from ER-derived PS in the inner and outer mitochondrial membranes (IMM and OMM, resp.) and then transferred to the ER through mitochondria-ER junctions and from the ER to the PM through PM-ER junctions [62, 63, 65, 69, 71–75]; and (3) cardiolipin (CL), a signature mitochondrial phospholipid which is generated from ER-derived PA in a series of reactions confined to the IMM and OMM [71, 74, 76–78]. It needs to be emphasized that genetic interventions weakening the incorporation of exogenously added POA into POA-containing phospholipids within the ER have been shown to increase cell resistance to POA-induced liponecrotic RCD [34, 59]. Thus, such incorporation is a pro-death process essential for the commitment of yeast to liponecrotic RCD in response to treatment with exogenous POA.

After being synthesized in the ER, the bulk quantities of POA-containing phospholipids in yeast cells committed to liponecrotic RCD amass in the PM (Figure 1) [34, 59]. Such accumulation of POA-containing phospholipids in the PM activates the alkaline pH- and lipid asymmetry-responsive Rim101 signaling pathway, which orchestrates a series of endocytic internalization and traffic events ultimately promoting transcription of the nuclear *RSB1* gene [79–87]. A protein product of this gene, Rsb1, is known to regulate the bidirectional active transport of PE across the PM bilayer; specifically, Rsb1 stimulates the Lem3-driven transport of PE from the outer monolayer of the PM to its inner monolayer and also slows down the Yor1-driven transport of PE in the opposite direction [86, 88–91]. These effects of Rsb1 elicit a depletion of PE in the outer monolayer of the PM, thereby markedly rising the permeability of the PM to small molecules (Figure 1) [34, 59]. Such increase in the permeability of the PM to small molecules has been shown to play an essential role in committing yeast to POA-induced liponecrotic RCD (Figure 1) [34, 59].

The bulk quantities of POA-containing phospholipids initially synthesized in the ER of yeast cells that are committed to liponecrotic RCD accumulate not only in the PM but also in both membranes enclosing mitochondria (Figure 1) [34, 59]. This buildup of POA-containing phospholipids in the IMM and OMM markedly weakens mitochondrial respiratory capacity, uncouples mitochondria respiratory chain from ATP synthesis, and lowers the electrochemical potential across the IMM (Figure 1) [34, 59]. The resulting decline in mitochondrial functionality plays an essential role in committing yeast to POA-induced liponecrotic RCD, likely because these dysfunctional mitochondria cannot produce enough ATP to support the energy-demanding, prosurvival process of incorporating exogenous POA into neutral lipids (see text below for discussion of this prosurvival process) (Figure 1) [34, 59].

The buildup of POA-containing phospholipids in the IMM and OMM of yeast committed to liponecrotic RCD not only impairs mitochondrial functionality but also considerably increases the intracellular concentration of reactive oxygen species (ROS) that are produced in mitochondria as by-products of respiration (Figure 1) [34, 59]. This rise of ROS concentrations elicits an oxidative damage to different types of molecules in two cellular locations, namely, to (1) protein and lipid components of mitochondria and other cellular organelles and (2) proteins in the cytosol, thereby causing their unfolding and aggregation (Figure 1) [34, 59]. Both these types of cellular oxidative damage are essential contributing factors either to the commitment of yeast to POA-induced liponecrotic RCD or to an execution of this RCD subroutine. Specifically, a massive breakdown of numerous oxidatively damaged and dysfunctional organelles through a nonselective macroautophagic degradation (which is choreographed by the phagophore assembly-specific serine/threonine protein kinase Atg1, adapter protein Atg11, and scaffold protein Atg17 [58, 59, 92–94]) plays a crucial role in executing POA-induced liponecrotic RCD (Figure 1) [34, 58, 59]. Moreover, the buildup of oxidatively damaged, dysfunctional, unfolded, and aggregated proteins in the cytosol of yeast cells treated with POA impairs cellular proteostasis, thus committing these cells to POA-induced liponecrotic RCD (Figure 1) [34, 59].

If the stress imposed by an exposure to POA does not exceed a toxic threshold, yeast cells can use at least four different processes to cope with this stress and maintain viability (Figure 1).

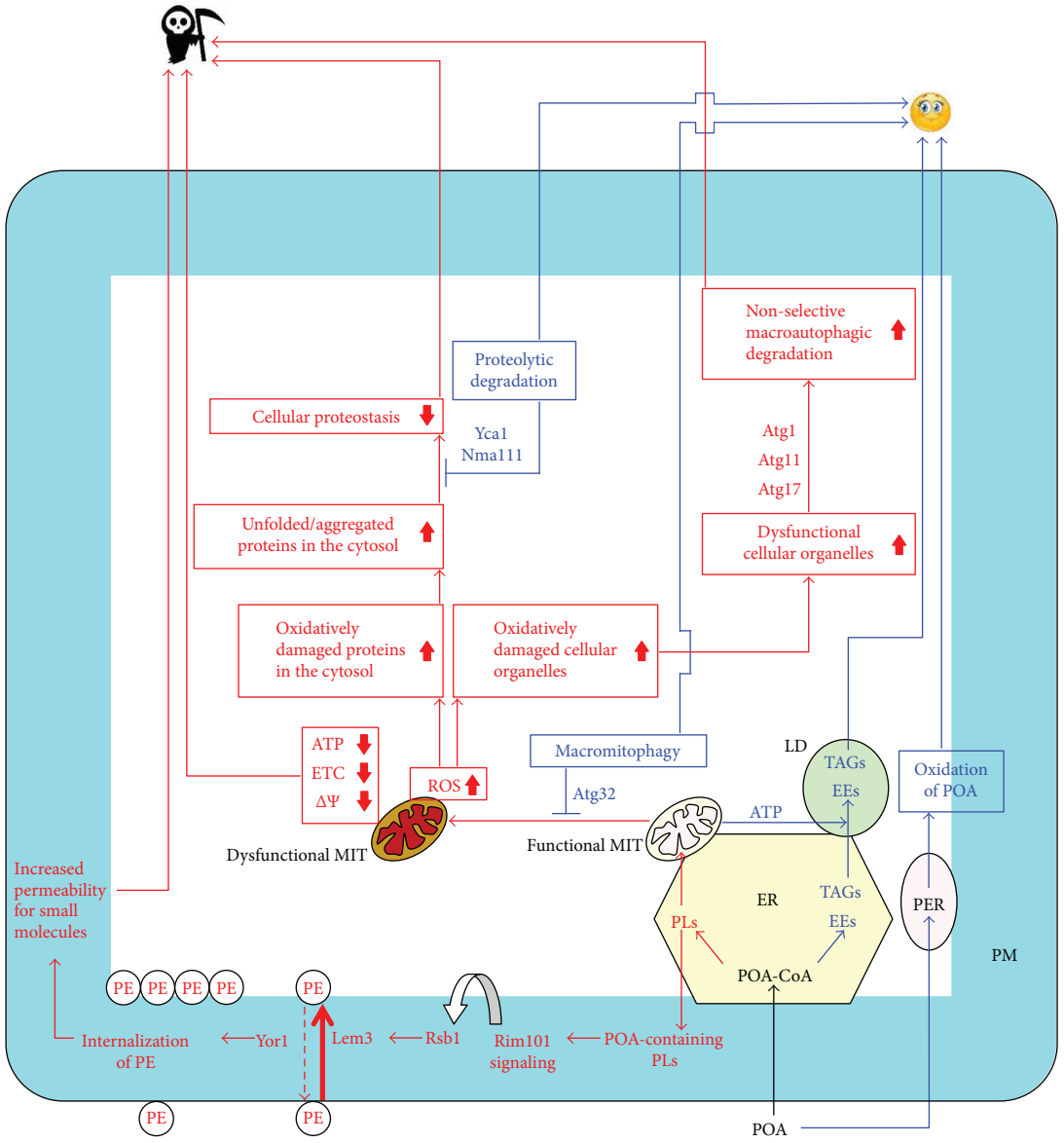

Figure 1: A model for how yeast cells exposed to exogenous palmitoleic acid (POA) either mount a protective stress response and survive or commit to POA-induced regulated liponecrosis and die. Yeast cells briefly exposed to POA can employ four different prosurvival processes to cope with the POA-induced cellular stress and maintain viability. These prosurvival cellular processes include the following: (1) an assimilation of POA into neutral lipids (triacylglycerols (TAGs) and ergosteryl esters (EEs)), in the endoplasmic reticulum (ER) and the subsequent deposition of these neutral lipids in lipid droplets (LD); (2) POA oxidation in peroxisomes (PER); (3) a macroautophagic degradation of dysfunctional or damaged mitochondria (MIT); and (4) a proteolytic degradation of oxidatively damaged, dysfunctional, unfolded, and aggregated proteins that accumulate in the cytosol of yeast cells. Arrows and names displayed in blue color denote prosurvival processes, metabolites, and proteins that protect yeast from POA-induced liponecrotic regulated cell death (RCD). Yeast cells briefly treated with POA can use four different pro-death processes to commit to POA-induced liponecrotic RCD and to execute this RCD subroutine. These pro-death cellular processes include the following: (1) a buildup of POA-containing phospholipids (PLs) in the PM and the ensuing increase in the permeability of the PM to small molecules; (2) the accumulation of POA-containing PLs in both mitochondrial membranes and the resulting decline in mitochondrial functionality, which is needed to support the prosurvival process of incorporating exogenous POA into neutral lipids; (3) a ROS-inflicted oxidative damage to mitochondria and other cellular organelles, which stimulates a nonselective macroautophagic degradation of many kinds of organelles; and (4) a ROS-imposed oxidative damage to cytosolic proteins, which impairs cellular proteostasis because it promotes an accumulation of oxidatively damaged, dysfunctional, unfolded, and aggregated proteins in the cytosol. Arrows and names displayed in red color denote pro-death processes, metabolites, and proteins that commit yeast to POA-induced RCD or execute this RCD subroutine. The up or down arrows in red color denote processes or metabolites whose intensities or concentrations are increased or decreased (resp.) in yeast cells briefly exposed to exogenous POA. See text for more details. ETC, mitochondrial electron transport chain; PE, phosphatidylethanolamine; PLs, phospholipids; PM, plasma membrane; ROS, reactive oxygen species; ΔΨ, electrochemical potential across the inner mitochondrial membrane.

One of these prosurvival cellular processes is an assimilation of POA into neutral lipids (TAGs and EEs), which occurs in the ER and is followed by a buildup of POA-containing neutral lipids in LDs (Figure 1) [34, 58, 59]. This process lowers the extreme cellular stress caused by the accumulation of POA-containing phospholipids in the PM, IMM, and OMM because it attenuates the flow of POA into the pathways for the synthesis of POA-containing phospholipids [34, 58, 59]. The assimilation of POA into neutral lipids is essential for protecting yeast from POA-induced liponecrotic RCD, as demonstrated by the finding that genetic interventions weakening the incorporation of exogenously added POA into POA-containing neutral lipids increase the susceptibility of yeast to this subroutine of RCD [58].

Another prosurvival cellular process is the β-oxidation of POA in peroxisomes of yeast exposed to this monounsaturated free fatty acid (Figure 1) [34, 57–59]. Peroxisomal oxidation of POA mitigates POA-induced liponecrotic RCD because it weakens the incorporation of POA into phospholipids, thereby relieving the excessive cellular stress instigated by the buildup of POA-containing phospholipids in the PM, IMM, and OMM [34, 58, 59]. In support of an essential role of peroxisomal oxidation of POA in the protection of yeast from POA-induced liponecrotic RCD, yeast strains that carry the single-gene-deletion mutations *pex5*Δ and *fox1*Δ attenuating oxidative degradation of POA in peroxisomes are more susceptible to this mode of RCD than an otherwise isogenic wild-type strain [34, 57–59].

Macromitophagy, a macroautophagic degradation of dysfunctional or damaged mitochondria, is also a prosurvival process that allows yeast to cope with the POA-induced cellular stress [34, 58, 59]. Macromitophagy protects yeast from POA-induced liponecrotic RCD because, by selectively degrading dysfunctional mitochondria, it helps to maintain a population of functionally active mitochondria that are needed to generate enough ATP to support the prosurvival process of assimilating POA into neutral lipids (Figure 1) [34, 58, 59]. The *Atg32*Δ-dependent mutational block of macromitophagy impairs the accumulation of LD-deposited neutral lipids and sensitizes yeast to POA-induced liponecrotic RCD [58]; thus, macromitophagy plays an essential role in protecting yeast from this subroutine of RCD.

The degradation of oxidatively damaged, dysfunctional, unfolded, and aggregated proteins that accumulate in the cytosol of yeast cells treated with POA is another prosurvival process in these cells; this proteolytic degradation is catalyzed by the metacaspase Yca1 and serine protease Nma111, two protein components of the caspase-dependent apoptotic RCD pathway (Figure 1) [34, 59, 95–97]. This Yca1- and Nma111-driven proteolysis of oxidatively damaged, dysfunctional, unfolded, and aggregated proteins slows down a progression of POA-induced liponecrotic RCD because it allows to sustain efficient cellular proteostasis, thereby weakening proteostatic cellular stress (Figure 1) [34, 59]. In support of an essential role of such proteolysis in the protection of yeast from POA-induced liponecrotic RCD, lack of Yca1 or Nma111 increases the susceptibility of yeast to this mode of RCD [34, 59].

3. What Are the Relations among Different Processes Involved in Cell Death or Cell Adaptation in Yeast Treated with POA and How Is a Balance between Pro-death and Prosurvival Processes Regulated?

As outlined in the previous section, pro-death cellular processes in yeast treated with POA are direct or indirect due to the initial incorporation of this fatty acid into bulk quantities of POA-containing phospholipids. Two direct pro-death processes include the following: (1) the buildup of POA-containing phospholipids in the PM and the ensuing increase in the permeability of the PM to small molecules and (2) the accumulation of POA-containing phospholipids in both mitochondrial membranes and the resulting decline in mitochondrial functionality, which is needed to support the prosurvival process of incorporating exogenous POA into neutral lipids (Figure 1). Two other pro-death processes only indirectly caused the buildup of POA-containing phospholipids in both mitochondrial membranes because such buildup elicits a rise in the intracellular concentration of ROS initially produced in mitochondria. These indirect pro-death processes are as follows: (1) the ROS-inflicted oxidative damage to mitochondria and other cellular organelles, which stimulates a nonselective macroautophagic degradation of many kinds of organelles and (2) the ROS-imposed oxidative damage to cytosolic proteins, which impairs cellular proteostasis because it promotes the accumulation of oxidatively damaged, dysfunctional, unfolded, and aggregated proteins in the cytosol (Figure 1). Thus, the four pro-death processes relate because they all are initiated in response to the buildup of POA-containing phospholipids. We hypothesize that (1) the direct pro-death processes may precede in time the indirect ones and (2) the relative contribution of each direct or indirect pro-death process into POA-induced liponecrotic RCD may be defined by the relative rates with which POA-containing phospholipids are transferred from the ER to the PM and mitochondria, mitochondria generate ROS, mitochondria and other cellular organelles undergo ROS-inflicted oxidative damage, oxidatively damaged cellular organelles are subjected to nonselective macroautophagic degradation, cytosolic proteins are oxidatively damaged by mitochondrially produced ROS, and oxidatively damaged cytosolic proteins unfold and aggregate. In our hypothesis, none of the pro-death processes may be considered as an individual pro-death pathway. In contrast, our hypothesis posits that all four pro-death processes are likely to be nodes of a branched subnetwork that integrates the flow of POA-containing phospholipids from the ER to the PM and mitochondria, mitochondrial ROS formation, the ROS-imposed oxidative damage to organelles and cytosolic proteins, the nonselective macroautophagic breakdown of different kinds of oxidatively damaged organelles, and the unfolding and aggregation of oxidatively damaged proteins in the cytosol.

Our hypothesis further suggests that prosurvival processes are likely to be nodes of the same branched subnetwork integrating the four pro-death processes. Two direct

Table 1: Some of the morphological and biochemical traits characteristic of palmitoleic acid- (POA-) induced liponecrotic regulated cell death (RCD) are unique to this mode of RCD, whereas other traits are shared by this mode and other (i.e., caspase-dependent apoptotic, autophagic, and necrotic) RCD modes. LDs, lipid droplets; PM, plasma membrane; PS, phosphatidylserine.

Trait	Caspase-dependent apoptotic RCD [references]	Autophagic RCD [references]	Necrotic RCD [references]	POA-induced liponecrotic RCD [references]
Nuclear fragmentation	+ [126]	−	−	− [58]
PS externalization within the PM	+ [126]	−	−	− [58]
Role of Yca1 and Nma111	+ (pro-death role) [106, 107]	−	−	+ (prosurvival role) [59]
Excessive cytoplasmic vacuolization	−	+ [127]	−	− [58]
Massive degradation of various cellular organelles	−	+ [127]	−	+ [58]
Rupture of the PM	−	−	+ [114]	− [58]
Permeability of the PM to small molecules	−	−	+ [114]	+ [59]
Excessive accumulation of LDs	−	−	−	+ [58]

prosurvival processes relieve the extreme cellular stress by preventing the buildup of POA-containing phospholipids in the PM and mitochondria; they include the following: (1) the assimilation of POA into neutral lipids in the ER and the subsequent buildup of POA-containing neutral lipids in LDs and (2) peroxisomal oxidation of POA (Figure 1). Two indirect prosurvival processes are activated to lower the extreme cellular stress created by the buildup of POA-containing phospholipids in both mitochondrial membranes and by the resulting decline in mitochondrial functionality and rise in mitochondrially produced ROS; they are as follows: (1) the selective macroautophagic degradation of oxidatively damaged and dysfunctional mitochondria, which helps to maintain a population of functionally active mitochondria generating sufficient quantities of ATP and producing ROS in nontoxic concentrations and (2) the Yca1- and Nma111-driven proteolysis of oxidatively damaged and aggregated cytosolic proteins, which allows to sustain efficient cellular proteostasis (Figure 1). Akin to pro-death processes, the four prosurvival processes relate because they all are stimulated in attempt to relieve the extreme cellular stress that is generated (directly or indirectly) by the initial incorporation of POA into POA-containing phospholipids. Our hypothesis posits that (1) the direct prosurvival processes may occur earlier than the indirect ones and (2) the relative contribution of each direct or indirect prosurvival process into cell protection from POA-induced liponecrosis may depend on the relative rates with which POA is assimilated into neutral lipids in the ER, POA-containing neutral lipids are transferred from the ER to LDs, POA is oxidized in peroxisomes, oxidatively damaged and dysfunctional mitochondria are subjected to selective macroautophagic degradation, and oxidatively damaged and aggregated cytosolic proteins undergo proteolytic degradation.

In sum, the above hypothesis posits the following: (1) the balance between different pro-death and prosurvival processes may be regulated by their relative rates and (2) these relative rates may be defined by the extracellular and/or intracellular concentrations of POA, nutrient availability, the metabolic state of a yeast cell, and the chronological age of a yeast cell.

4. Is the Subnetwork of Liponecrotic RCD Integrated into a Signaling Network Orchestrating Different RCD Scenarios in Yeast Cells?

Yeast cells undergoing POA-induced liponecrotic RCD exhibit characteristic morphological and biochemical traits [34, 58, 59]. Some of these traits are unique to liponecrotic RCD, whereas other traits are shared by this and certain other modes of RCD (Table 1).

While yeast cells committed to POA-induced liponecrotic RCD do not display such characteristic traits of apoptotic RCD as nuclear fragmentation and PS externalization within the PM bilayer, the metacaspase Yca1 and serine protease Nma111 play essential roles in both liponecrotic and caspase-dependent apoptotic modes of RCD [34, 59]. However, the roles Yca1 and Nma111 play in each of these two RCD modes are quite different (Table 1). As mentioned above, the Yca1- and Nma111-dependent proteolysis of oxidatively damaged, dysfunctional, unfolded, and aggregated proteins in the cytosol of yeast cells is a prosurvival process in POA-induced liponecrotic RCD [34, 59]. Such prosurvival role of Yca1 in sustaining efficient cellular proteostasis is well known [98–105]. In contrast, the Yca1- and Nma111-driven degradation of various cellular proteins is an executing, pro-death process in several caspase-dependent modalities of apoptotic RCD in yeast exposed to certain exogenous stimuli [95–97, 106–110].

While yeast cells undergoing POA-induced liponecrotic RCD do not display such hallmark trait of autophagic RCD as extreme cytoplasmic vacuolization instigated by a buildup of double-membrane vesicles called autophagosomes [34, 58, 59], both liponecrotic and autophagic modes of RCD (1) exhibit a nonselective massive degradation of various cellular organelles and (2) depend on the phagophore assembly-specific serine/threonine protein kinase Atg1 for executing these RCD modes (Table 1) [1, 58, 59, 111–113].

While yeast cells undergoing POA-induced liponecrotic RCD do not exhibit such hallmark feature of necrotic RCD as a severe fracture of the PM [34, 58, 59], both

liponecrotic and necrotic modes of RCD display substantially increased permeability of the PM to small molecules (Table 1) [31, 58, 59, 114–116].

A trait which is unique to POA-induced liponecrotic RCD is a buildup of POA-containing neutral lipids in numerous LDs, a feature that has not been reported for apoptotic, autophagic, or necrotic subroutine of RCD (Table 1) [1, 58, 59, 96, 111–113, 115].

Because POA-induced liponecrotic RCD has several different traits in common with apoptotic, autophagic, and necrotic modes of RCD, we hypothesize that the molecular subnetwork of POA-induced liponecrotic RCD is integrated into a signaling network that orchestrates different RCD scenarios in yeast cells. Other pathways and subnetworks integrated into this signaling network may include apoptotic, autophagic, and necrotic pathways and subnetworks of RCD. In our hypothesis, the molecular subnetwork of POA-induced liponecrotic RCD only partially overlaps with apoptotic, autophagic, and necrotic RCD pathways and subnetworks of the network. Our hypothesis satisfactorily explains the observed existence of several proteins that are common to liponecrotic, apoptotic, autophagic, and necrotic modes of RCD [34, 58, 59]. Furthermore, as our hypothesis suggests, some of the morphological and biochemical traits characteristic of POA-induced liponecrotic RCD are shared by this mode of RCD and other (i.e., apoptotic, autophagic, and necrotic) RCD modes integrated into the network [34, 58, 59]. Moreover, in agreement with our hypothesis on only a partial overlap between liponecrotic and other pathways and subnetworks of RCD, at least one trait characteristic of liponecrotic RCD is unique to this mode of RCD; this trait is the accumulation of POA-containing neutral lipids in many LDs [34, 58, 59].

Our hypothesis on the existence of an RCD signaling network orchestrating different RCD scenarios in yeast cells is reminiscent of the hypothesis on the global programmed cell death (PCD) network that has been proposed and then confirmed for mammalian cells [117–120]. A systems biology platform has been developed for defining the topology of such network operating in mammalian cells; this platform employs cell biological and computational approaches for measuring and computing the effects of single and double genetic interventions on the molecular events characteristic of different PCD modes that are integrated into the network [119]. The use of such platform, possibly in combination with powerful tools of proteomic and metabolomic analyses recently applied for molecular analyses of RCD in yeast [104, 105], will allow to test our hypothesis on the global RCD signaling network in yeast and, perhaps, to dissect the architecture of such network in the near future.

5. Does Liponecrotic RCD Contribute to Yeast Chronological Aging?

POA-induced liponecrotic RCD is an age-related mode of RCD, as the susceptibility of a population of yeast cells to POA-induced liponecrosis increases with the chronological age of this population [34, 58, 59, 121]. Furthermore, the susceptibility of yeast cells to POA-induced liponecrotic RCD can be significantly decreased by some aging-delaying dietary and pharmacological interventions. These interventions include caloric restriction (CR) and lithocholic bile acid (LCA), each implemented at the time of cell inoculation into growth medium [57, 60, 121].

Our recent unpublished findings indicate that in yeast cultured under non-CR conditions on 1% or 2% glucose, the risk of age-related death depends not only on the POA-induced liponecrotic mode of RCD but also on ROS-induced apoptotic RCD mode. Moreover, we found that the liponecrotic and apoptotic modes of RCD have different relative contributions to age-related death of non-CR yeast at different periods of chronological lifespan (CLS). The apoptotic mode of RCD predominates during diauxic (D) phase, apoptotic and liponecrotic RCD modes equally increase the risk of death during post-diauxic (PD) phase, whereas the liponecrotic mode of RCD prevails during stationary (ST) phase of culturing under non-CR conditions (our unpublished data). The longevity-defining mode of liponecrotic RCD is elicited by the accumulation of POA and other free fatty acids in chronologically aging non-CR yeast cells that progress through PD and ST phases of culturing (our unpublished data). In contrast, the longevity-defining mode of apoptotic RCD is caused by the rapid decline of mitochondrial functionality and rise of mitochondrially generated ROS in chronologically aging non-CR yeast cells progressing through D and PD phases of culturing (our unpublished data). CR diet, which is implemented by culturing yeast on 0.2% or 0.5% glucose, decreases the risk of age-related death by attenuating liponecrotic and apoptotic RCD modes during D, PD, and ST phases; these effects of CR are due to its abilities to (1) decrease free fatty acid (including POA) concentrations during PD and ST phases of culturing and to (2) improve mitochondrial functionality and to lessen concentrations of mitochondrially generated ROS during D and PD phases of culturing (our unpublished data).

LCA is a geroprotective chemical compound that delays yeast chronological aging mainly under CR conditions [57]. LCA exhibits the following effects on yeast susceptibility to POA-induced liponecrotic RCD: (1) it decreases such susceptibility only if added to growth medium at the time of cell inoculation, during logarithmic (L) or D phase of culturing; (2) it increases such susceptibility if added during PD phase; and (3) it has no effect on such susceptibility if added during ST phase [121]. Taken together, these findings suggest that liponecrotic RCD may be an essential longevity-limiting (i.e., proaging) factor in chronologically "young" yeast, may somehow contribute to longevity extension (i.e., aging delay) in chronologically "middle-aged" yeast, and may have no influence on longevity (i.e., on the pace of aging) of chronologically "old" yeast. Noteworthy, all these age-related variations in yeast susceptibility to POA-induced liponecrotic RCD coincide with age-related changes in yeast resistance to chronic oxidative, thermal, and osmotic stresses [121]. In the future, it would be important to explore mechanisms that underlie the observed age-related coincidence between yeast susceptibility to POA-induced liponecrotic RCD and yeast resistance to long-term stresses. Moreover, it remains to be determined if and how the concentrations of endogenously

produced free fatty acids (including POA) influence the extent of liponecrotic RCD at different stages of yeast chronological aging.

Of note, LCA decreases yeast susceptibility to the mitochondria-controlled, ROS-induced mode of apoptotic RCD if added to growth medium at the time of cell inoculation and during L, D, PD, or ST phase of culturing [121]. In yeast cultured under CR conditions, exogenous LCA enters cells, is sorted to mitochondria, amasses primarily in the IMM and also resides in the OMM, alters the concentrations of certain mitochondrial membrane phospholipids, elicits a major enlargement of mitochondria, significantly decreases mitochondrial number, prompts an intramitochondrial accumulation of cristae disconnected from the IMM, triggers substantial alterations in mitochondrial proteome, decreases the frequencies of deletion and point mutations in mitochondrial DNA, and leads to changes in vital aspects of mitochondrial functionality [66, 68, 122, 123]. In the future, it would be important to explore how all these aging-delaying effects of LCA are linked to yeast susceptibility to the mitochondria-controlled, ROS-induced mode of apoptotic RCD at different stages of chronological aging.

In sum, it is conceivable that liponecrotic and apoptotic modes of RCD may have different effects on yeast CLS at different periods of life. This is similar to the "P" ("big P") and "p" ("small p") modes of death in the nematode *Caenorhabditis elegans*, which define lifespan earlier or later in life (resp.) [124]. The P mode of death is manifested as a substantial enlargement of the posterior pharyngeal bulb caused by intensified pharyngeal pumping, whereas the p mode of death is due to the complete atrophy of pharynx [124].

6. How Does Liponecrotic RCD Differ from Other Modes of Lipotoxic RCD in Yeast?

Several exogenously added lipids [8–16], as well as different genetic [11–13, 15–25] and pharmacological [24, 26–30] interventions that impair certain aspects of lipid metabolism, have been shown to elicit apoptotic and/or necrotic modes of lipotoxic RCD in yeast. These modes have been extensively reviewed elsewhere [31, 32, 37, 41, 125]. In brief, yeast cells committed to POA-induced liponecrotic RCD exhibit a unique combination of morphological and biochemical traits that is not characteristic of any of these other modes of lipotoxic RCD. Moreover, some of these other modes of lipotoxic RCD differ from each other with respect to (1) structural and/or functional features of yeast committed to a particular mode of RCD; (2) classes of lipids whose concentrations are altered (or are expected to be altered) in yeast committed to a particular mode of RCD; and (3) proteins that are involved in committing to and/or executing a particular mode of RCD [8–32, 37, 41, 125].

Altogether, these findings further support our hypothesis (which is outlined in Section 4) on the possible existence of a global signaling network that integrates partially overlapping molecular pathways and subnetworks of lipotoxic RCD, each pathway and subnetwork being differently responsive to certain perturbations in diverse aspects of lipid metabolism within a yeast cell. The key challenge for the future is to explore mechanisms through which such perturbations in lipid metabolism (1) modulate individual molecular pathways and subnetworks of lipotoxic RCD and (2) orchestrate the integration of these individual pathways and subnetworks into the global signaling network of lipotoxic RCD. To address this challenge, the systems biology platform (which is discussed in Section 4) exploited for mammalian cells [119] can be used in combination with proteomic and metabolomic analyses of molecular signatures [104, 105] characteristic of different lipotoxic RCD modes.

7. Conclusions

To cope with the lipotoxic stress imposed by an exposure to POA, *S. cerevisiae* cells use several different mechanisms to mount a protective stress response and maintain viability. This complex stress response consists in remodeling of at least four cellular processes. If the POA-induced lipotoxic stress exceeds a threshold, yeast cells commit suicide that is assisted by a complex molecular machinery. This molecular machinery alters the spatiotemporal dynamics of several cellular processes to execute a liponecrotic subroutine of RCD. The liponecrotic mode of POA-induced RCD plays an essential role in defining longevity of chronologically aging yeast, likely in coordination with an apoptotic mode of RCD. The molecular subnetwork of POA-induced liponecrotic RCD may be integrated into a global signaling network of partially overlapping molecular pathways and subnetworks, each executing a different mode of lipotoxic or nonlipotoxic RCD.

Conflicts of Interest

The authors declare no conflict of interests.

Acknowledgments

The authors are grateful to other members of the Titorenko laboratory for discussions.

References

[1] L. Galluzzi, I. Vitale, J. M. Abrams et al., "Molecular definitions of cell death subroutines: recommendations of the nomenclature committee on cell death 2012," *Cell Death and Differentiation*, vol. 19, no. 1, pp. 107–120, 2012.

[2] Y. Fuchs and H. Steller, "Live to die another way: modes of programmed cell death and the signals emanating from dying cells," *Nature Reviews Molecular Cell Biology*, vol. 16, no. 6, pp. 329–344, 2015.

[3] L. Galluzzi, J. M. Bravo-San Pedro, O. Kepp, and G. Kroemer, "Regulated cell death and adaptive stress responses," *Cellular and Molecular Life Sciences*, vol. 73, no. 11-12, pp. 2405–2410, 2016.

[4] B. Ke, M. Tian, J. Li, B. Liu, and G. He, "Targeting programmed cell death using small-molecule compounds to improve potential cancer therapy," *Medicinal Research Reviews*, vol. 36, no. 6, pp. 983–1035, 2016.

[5] D. Wallach, T. B. Kang, C. P. Dillon, and D. R. Green, "Programmed necrosis in inflammation: toward identification of

the effector molecules," *Science*, vol. 352, no. 6281, article aaf2154, 2016.

[6] J. Shi, W. Gao, and F. Shao, "Pyroptosis: gasdermin-mediated programmed necrotic cell death," *Trends in Biochemical Sciences*, vol. 42, no. 4, pp. 245–254, 2017.

[7] D. R. Green and B. Victor, "The pantheon of the fallen: why are there so many forms of cell death?," *Trends in Cell Biology*, vol. 22, no. 11, pp. 555-556, 2012.

[8] M. Stratford and P. A. Anslow, "Comparison of the inhibitory action on *Saccharomyces cerevisiae* of weak-acid preservatives, uncouplers, and medium-chain fatty acids," *FEMS Microbiology Letters*, vol. 142, no. 1, pp. 53–58, 1996.

[9] K. Mitsui, D. Nakagawa, M. Nakamura, T. Okamoto, and K. Tsurugi, "Valproic acid induces apoptosis dependent of Yca1p at concentrations that mildly affect the proliferation of yeast," *FEBS Letters*, vol. 579, no. 3, pp. 723–727, 2005.

[10] Q. Sun, L. Bi, X. Su, K. Tsurugi, and K. Mitsui, "Valproate induces apoptosis by inducing accumulation of neutral lipids which was prevented by disruption of the *SIR2* gene in *Saccharomyces cerevisiae*," *FEBS Letters*, vol. 581, no. 21, pp. 3991–3995, 2007.

[11] J. Garbarino, M. Padamsee, L. Wilcox et al., "Sterol and diacylglycerol acyltransferase deficiency triggers fatty acid-mediated cell death," *The Journal of Biological Chemistry*, vol. 284, no. 45, pp. 30994–31005, 2009.

[12] J. Petschnigg, H. Wolinski, D. Kolb et al., "Good fat, essential cellular requirements for triacylglycerol synthesis to maintain membrane homeostasis in yeast," *The Journal of Biological Chemistry*, vol. 284, no. 45, pp. 30981–30993, 2009.

[13] P. Rockenfeller, J. Ring, V. Muschett et al., "Fatty acids trigger mitochondrion-dependent necrosis," *Cell Cycle*, vol. 9, no. 14, pp. 2836–2842, 2010.

[14] D. Carmona-Gutierrez, A. Reisenbichler, P. Heimbucher et al., "Ceramide triggers metacaspase-independent mitochondrial cell death in yeast," *Cell Cycle*, vol. 10, no. 22, pp. 3973–3978, 2011.

[15] S. Fakas, Y. Qiu, J. L. Dixon et al., "Phosphatidate phosphatase activity plays key role in protection against fatty acid-induced toxicity in yeast," *The Journal of Biological Chemistry*, vol. 286, no. 33, pp. 29074–29085, 2011.

[16] L. Galluzzi, I. Vitale, L. Senovilla et al., "Independent transcriptional reprogramming and apoptosis induction by cisplatin," *Cell Cycle*, vol. 11, no. 18, pp. 3472–3480, 2012.

[17] M. M. Nagiec, E. E. Nagiec, J. A. Baltisberger, G. B. Wells, R. L. Lester, and R. C. Dickson, "Sphingolipid synthesis as a target for antifungal drugs. Complementation of the inositol phosphorylceramide synthase defect in a mutant strain of *Saccharomyces cerevisiae* by the *AUR1* gene," *The Journal of Biological Chemistry*, vol. 272, no. 15, pp. 9809–9817, 1997.

[18] H. Kitagaki, L. A. Cowart, N. Matmati et al., "Isc1 regulates sphingolipid metabolism in yeast mitochondria," *Biochimica et Biophysica Acta (BBA) - Biomembranes*, vol. 1768, no. 11, pp. 2849–2861, 2007.

[19] A. M. Aerts, P. Zabrocki, I. E. J. A. François et al., "Ydc1p ceramidase triggers organelle fragmentation, apoptosis and accelerated ageing in yeast," *Cellular and Molecular Life Sciences*, vol. 65, no. 12, pp. 1933–1942, 2008.

[20] T. Almeida, M. Marques, D. Mojzita et al., "Isc1p plays a key role in hydrogen peroxide resistance and chronological lifespan through modulation of iron levels and apoptosis," *Molecular Biology of the Cell*, vol. 19, no. 3, pp. 865–876, 2008.

[21] E. Bener Aksam, H. Jungwirth, S. D. Kohlwein et al., "Absence of the peroxiredoxin Pmp20 causes peroxisomal protein leakage and necrotic cell death," *Free Radical Biology & Medicine*, vol. 45, no. 8, pp. 1115–1124, 2008.

[22] H. Jungwirth, J. Ring, T. Mayer et al., "Loss of peroxisome function triggers necrosis," *FEBS Letters*, vol. 582, no. 19, pp. 2882–2886, 2008.

[23] A. D. Barbosa, H. Osório, K. J. Sims et al., "Role for Sit4p-dependent mitochondrial dysfunction in mediating the shortened chronological lifespan and oxidative stress sensitivity of Isc1p-deficient cells," *Molecular Microbiology*, vol. 81, no. 2, pp. 515–527, 2011.

[24] X. Huang, J. Liu, and R. C. Dickson, "Down-regulating sphingolipid synthesis increases yeast lifespan," *PLoS Genetics*, vol. 8, no. 2, article e1002493, 2012.

[25] J. Tulha, F. Faria-Oliveira, C. Lucas, and C. Ferreira, "Programmed cell death in *Saccharomyces cerevisiae* is hampered by the deletion of *GUP1* gene," *BMC Microbiology*, vol. 12, no. 1, p. 80, 2012.

[26] V. Zaremberg, C. Gajate, L. M. Cacharro, F. Mollinedo, and C. R. McMaster, "Cytotoxicity of an anti-cancer lysophospholipid through selective modification of lipid raft composition," *The Journal of Biological Chemistry*, vol. 280, no. 45, pp. 38047–38058, 2005.

[27] H. Zhang, C. Gajate, L. P. Yu, Y. X. Fang, and F. Mollinedo, "Mitochondrial-derived ROS in edelfosine-induced apoptosis in yeasts and tumor cells," *Acta Pharmacologica Sinica*, vol. 28, no. 6, pp. 888–894, 2007.

[28] V. Cerantola, I. Guillas, C. Roubaty et al., "Aureobasidin A arrests growth of yeast cells through both ceramide intoxication and deprivation of essential inositolphosphorylceramides," *Molecular Microbiology*, vol. 71, no. 6, pp. 1523–1537, 2009.

[29] K. Kajiwara, T. Muneoka, Y. Watanabe, T. Karashima, H. Kitagaki, and K. Funato, "Perturbation of sphingolipid metabolism induces endoplasmic reticulum stress-mediated mitochondrial apoptosis in budding yeast," *Molecular Microbiology*, vol. 86, no. 5, pp. 1246–1261, 2012.

[30] O. Czyz, T. Bitew, A. Cuesta-Marbán, C. R. McMaster, F. Mollinedo, and V. Zaremberg, "Alteration of plasma membrane organization by an anticancer lysophosphatidylcholine analogue induces intracellular acidification and internalization of plasma membrane transporters in yeast," *The Journal of Biological Chemistry*, vol. 288, no. 12, pp. 8419–8432, 2013.

[31] T. Eisenberg and S. Büttner, "Lipids and cell death in yeast," *FEMS Yeast Research*, vol. 14, no. 1, pp. 179–197, 2014.

[32] A. Rego, D. Trindade, S. R. Chaves et al., "The yeast model system as a tool towards the understanding of apoptosis regulation by sphingolipids," *FEMS Yeast Research*, vol. 14, no. 1, pp. 160–178, 2014.

[33] K. V. Ruggles, J. Garbarino, Y. Liu et al., "A functional, genome-wide evaluation of liposensitive yeast identifies the "*ARE2* required for viability" (*ARV1*) gene product as a major component of eukaryotic fatty acid resistance," *The Journal of Biological Chemistry*, vol. 289, no. 7, pp. 4417–4431, 2014.

[34] A. Arlia-Ciommo, V. Svistkova, S. Mohtashami, and V. I. Titorenko, "A novel approach to the discovery of anti-tumor pharmaceuticals: searching for activators of liponecrosis," *Oncotarget*, vol. 7, no. 5, pp. 5204–5225, 2016.

[35] M. Valachovic, M. Garaiova, R. Holic, and I. Hapala, "Squalene is lipotoxic to yeast cells defective in lipid droplet

biogenesis," *Biochemical and Biophysical Research Communications*, vol. 469, no. 4, pp. 1123–1128, 2016.

[36] L. K. Liu, V. Choudhary, A. Toulmay, and W. A. Prinz, "An inducible ER-Golgi tether facilitates ceramide transport to alleviate lipotoxicity," *The Journal of Cell Biology*, vol. 216, no. 1, pp. 131–147, 2017.

[37] D. Mitrofanova, P. Dakik, M. McAuley, Y. Medkour, K. Mohammad, and V. I. Titorenko, "Lipid metabolism and transport define longevity of the yeast *Saccharomyces cerevisiae*," *Frontiers in Bioscience*, vol. 23, no. 3, pp. 1166–1194, 2018.

[38] S. D. Kohlwein and J. Petschnigg, "Lipid-induced cell dysfunction and cell death: lessons from yeast," *Current Hypertension Reports*, vol. 9, no. 6, pp. 455–461, 2007.

[39] P. Rockenfeller and F. Madeo, "Ageing and eating," *Biochimica et Biophysica Acta*, vol. 1803, no. 4, pp. 499–506, 2010.

[40] S. D. Kohlwein, M. Veenhuis, and I. J. van der Klei, "Lipid droplets and peroxisomes: key players in cellular lipid homeostasis or a matter of fat - store 'em up or burn 'em down," *Genetics*, vol. 193, no. 1, pp. 1–50, 2012.

[41] K. Natter and S. D. Kohlwein, "Yeast and cancer cells - common principles in lipid metabolism," *Biochimica et Biophysica Acta (BBA) - Molecular and Cell Biology of Lipids*, vol. 1831, no. 2, pp. 314–326, 2013.

[42] P. G. Kopelman, "Obesity as a medical problem," *Nature*, vol. 404, no. 6778, pp. 635–643, 2000.

[43] R. H. Unger, "Lipotoxic diseases," *Annual Review of Medicine*, vol. 53, no. 1, pp. 319–336, 2002.

[44] J. E. Schaffer, "Lipotoxicity: when tissues overeat," *Current Opinion in Lipidology*, vol. 14, no. 3, pp. 281–287, 2003.

[45] R. H. Unger, "Longevity, lipotoxicity and leptin: the adipocyte defense against feasting and famine," *Biochimie*, vol. 87, no. 1, pp. 57–64, 2005.

[46] R. T. Brookheart, C. I. Michel, and J. E. Schaffer, "As a matter of fat," *Cell Metabolism*, vol. 10, no. 1, pp. 9–12, 2009.

[47] J. Garbarino and S. L. Sturley, "Saturated with fat: new perspectives on lipotoxicity," *Current Opinion in Clinical Nutrition and Metabolic Care*, vol. 12, no. 2, pp. 110–116, 2009.

[48] C. M. Kusminski, S. Shetty, L. Orci, R. H. Unger, and P. E. Scherer, "Diabetes and apoptosis: lipotoxicity," *Apoptosis*, vol. 14, no. 12, pp. 1484–1495, 2009.

[49] S. López, B. Bermúdez, R. Abia, and F. J. Muriana, "The influence of major dietary fatty acids on insulin secretion and action," *Current Opinion in Lipidology*, vol. 21, no. 1, pp. 15–20, 2010.

[50] R. H. Unger and P. E. Scherer, "Gluttony, sloth and the metabolic syndrome: a roadmap to lipotoxicity," *Trends in Endocrinology and Metabolism*, vol. 21, no. 6, pp. 345–352, 2010.

[51] R. Zechner, R. Zimmermann, T. O. Eichmann et al., "FAT SIGNALS - lipases and lipolysis in lipid metabolism and signaling," *Cell Metabolism*, vol. 15, no. 3, pp. 279–291, 2012.

[52] E. Currie, A. Schulze, R. Zechner, T. C. Walther, and R. V. Farese Jr, "Cellular fatty acid metabolism and cancer," *Cell Metabolism*, vol. 18, no. 2, pp. 153–161, 2013.

[53] L. Galluzzi, O. Kepp, M. G. Vander Heiden, and G. Kroemer, "Metabolic targets for cancer therapy," *Nature Reviews Drug Discovery*, vol. 12, no. 11, pp. 829–846, 2013.

[54] G. Zadra, C. Photopoulos, and M. Loda, "The fat side of prostate cancer," *Biochimica et Biophysica Acta (BBA) - Molecular and Cell Biology of Lipids*, vol. 1831, no. 10, pp. 1518–1532, 2013.

[55] J. Park, T. S. Morley, M. Kim, D. J. Clegg, and P. E. Scherer, "Obesity and cancer - mechanisms underlying tumour progression and recurrence," *Nature Reviews Endocrinology*, vol. 10, no. 8, pp. 455–465, 2014.

[56] A. Piano and V. I. Titorenko, "The intricate interplay between mechanisms underlying aging and cancer," *Aging and Disease*, vol. 6, no. 1, pp. 56–75, 2015.

[57] A. A. Goldberg, V. R. Richard, P. Kyryakov et al., "Chemical genetic screen identifies lithocholic acid as an anti-aging compound that extends yeast chronological life span in a TOR-independent manner, by modulating housekeeping longevity assurance processes," *Aging*, vol. 2, no. 7, pp. 393–414, 2010.

[58] S. Sheibani, V. R. Richard, A. Beach et al., "Macromitophagy, neutral lipids synthesis, and peroxisomal fatty acid oxidation protect yeast from "liponecrosis", a previously unknown form of programmed cell death," *Cell Cycle*, vol. 13, no. 1, pp. 138–147, 2014.

[59] V. R. Richard, A. Beach, A. Piano et al., "Mechanism of liponecrosis, a distinct mode of programmed cell death," *Cell Cycle*, vol. 13, no. 23, pp. 3707–3726, 2014.

[60] A. A. Goldberg, S. D. Bourque, P. Kyryakov et al., "A novel function of lipid droplets in regulating longevity," *Biochemical Society Transactions*, vol. 37, no. 5, pp. 1050–1055, 2009.

[61] L. Klug and G. Daum, "Yeast lipid metabolism at a glance," *FEMS Yeast Research*, vol. 14, no. 3, pp. 369–388, 2014.

[62] S. Carrasco and T. Meyer, "STIM proteins and the endoplasmic reticulum-plasma membrane junctions," *Annual Review of Biochemistry*, vol. 80, no. 1, pp. 973–1000, 2011.

[63] J. R. Friedman and G. K. Voeltz, "The ER in 3D: a multifunctional dynamic membrane network," *Trends in Cell Biology*, vol. 21, no. 12, pp. 709–717, 2011.

[64] S. A. Henry, S. D. Kohlwein, and G. M. Carman, "Metabolism and regulation of glycerolipids in the yeast *Saccharomyces cerevisiae*," *Genetics*, vol. 190, no. 2, pp. 317–349, 2012.

[65] A. A. Rowland and G. K. Voeltz, "Endoplasmic reticulum-mitochondria contacts: function of the junction," *Nature Reviews. Molecular Cell Biology*, vol. 13, no. 10, pp. 607–625, 2012.

[66] A. Beach, V. R. Richard, A. Leonov et al., "Mitochondrial membrane lipidome defines yeast longevity," *Aging*, vol. 5, no. 7, pp. 551–574, 2013.

[67] A. Leonov and V. I. Titorenko, "A network of interorganellar communications underlies cellular aging," *IUBMB Life*, vol. 65, no. 8, pp. 665–674, 2013.

[68] V. R. Richard, A. Leonov, A. Beach et al., "Macromitophagy is a longevity assurance process that in chronologically aging yeast limited in calorie supply sustains functional mitochondria and maintains cellular lipid homeostasis," *Aging*, vol. 5, no. 4, pp. 234–269, 2013.

[69] S. Tavassoli, J. T. Chao, B. P. Young et al., "Plasma membrane-endoplasmic reticulum contact sites regulate phosphatidylcholine synthesis," *EMBO Reports*, vol. 14, no. 5, pp. 434–440, 2013.

[70] P. Dakik and V. I. Titorenko, "Communications between mitochondria, the nucleus, vacuoles, peroxisomes, the endoplasmic reticulum, the plasma membrane, lipid droplets and the cytosol during yeast chronological aging," *Frontiers in Genetics*, vol. 7, 2016.

[71] S. E. Horvath and G. Daum, "Lipids of mitochondria," *Progress in Lipid Research*, vol. 52, no. 4, pp. 590–614, 2013.

[72] M. J. Aaltonen, J. R. Friedman, C. Osman et al., "MICOS and phospholipid transfer by Ups2-Mdm35 organize membrane lipid synthesis in mitochondria," *The Journal of Cell Biology*, vol. 213, no. 5, pp. 525–534, 2016.

[73] N. Miyata, Y. Watanabe, Y. Tamura, T. Endo, and O. Kuge, "Phosphatidylserine transport by Ups2-Mdm35 in respiration-active mitochondria," *The Journal of Cell Biology*, vol. 214, no. 1, pp. 77–88, 2016.

[74] K. S. Dimmer and D. Rapaport, "Mitochondrial contact sites as platforms for phospholipid exchange," *Biochimica et Biophysica Acta (BBA) - Molecular and Cell Biology of Lipids*, vol. 1862, no. 1, pp. 69–80, 2017.

[75] C. U. Mårtensson, K. N. Doan, and T. Becker, "Effects of lipids on mitochondrial functions," *Biochimica et Biophysica Acta (BBA) - Molecular and Cell Biology of Lipids*, vol. 1862, no. 1, pp. 102–113, 2017.

[76] M. Connerth, T. Tatsuta, M. Haag, T. Klecker, B. Westermann, and T. Langer, "Intramitochondrial transport of phosphatidic acid in yeast by a lipid transfer protein," *Science*, vol. 338, no. 6108, pp. 815–818, 2012.

[77] M. G. Baile, Y. W. Lu, and S. M. Claypool, "The topology and regulation of cardiolipin biosynthesis and remodeling in yeast," *Chemistry and Physics of Lipids*, vol. 179, pp. 25–31, 2014.

[78] T. Tatsuta and T. Langer, "Intramitochondrial phospholipid trafficking," *Biochimica et Biophysica Acta*, vol. 1862, no. 1, pp. 81–89, 2017.

[79] M. Babst, D. J. Katzmann, E. J. Estepa-Sabal, T. Meerloo, and S. D. Emr, "Escrt-III: an endosome-associated heterooligomeric protein complex required for MVB sorting," *Developmental Cell*, vol. 3, no. 2, pp. 271–282, 2002.

[80] T. M. Lamb and A. P. Mitchell, "The transcription factor Rim101p governs ion tolerance and cell differentiation by direct repression of the regulatory genes *NRG1* and *SMP1* in *Saccharomyces cerevisiae*," *Molecular and Cellular Biology*, vol. 23, no. 2, pp. 677–686, 2003.

[81] W. Xu, F. J. Smith Jr, R. Subaran, and A. P. Mitchell, "Multivesicular body-ESCRT components function in pH response regulation in *Saccharomyces cerevisiae* and *Candida albicans*," *Molecular Biology of the Cell*, vol. 15, no. 12, pp. 5528–5537, 2004.

[82] K. J. Barwell, J. H. Boysen, W. Xu, and A. P. Mitchell, "Relationship of *DFG16* to the Rim101p pH response pathway in *Saccharomyces cerevisiae* and *Candida albicans*," *Eukaryotic Cell*, vol. 4, no. 5, pp. 890–899, 2005.

[83] M. Hayashi, T. Fukuzawa, H. Sorimachi, and T. Maeda, "Constitutive activation of the pH-responsive Rim101 pathway in yeast mutants defective in late steps of the MVB/ESCRT pathway," *Molecular and Cellular Biology*, vol. 25, no. 21, pp. 9478–9490, 2005.

[84] P. Weiss, S. Huppert, and R. Kölling, "Analysis of the dual function of the ESCRT-III protein Snf7 in endocytic trafficking and in gene expression," *The Biochemical Journal*, vol. 424, no. 1, pp. 89–97, 2009.

[85] A. K. Shukla, K. Xiao, and R. J. Lefkowitz, "Emerging paradigms of β-arrestin-dependent seven transmembrane receptor signaling," *Trends in Biochemical Sciences*, vol. 36, no. 9, pp. 457–469, 2011.

[86] T. Maeda, "The signaling mechanism of ambient pH sensing and adaptation in yeast and fungi," *The FEBS Journal*, vol. 279, no. 8, pp. 1407–1413, 2012.

[87] K. Obara, H. Yamamoto, and A. Kihara, "Membrane protein Rim21 plays a central role in sensing ambient pH in *Saccharomyces cerevisiae*," *The Journal of Biological Chemistry*, vol. 287, no. 46, pp. 38473–38481, 2012.

[88] U. Kato, K. Emoto, C. Fredriksson et al., "A novel membrane protein, Ros3p, is required for phospholipid translocation across the plasma membrane in *Saccharomyces cerevisiae*," *The Journal of Biological Chemistry*, vol. 277, no. 40, pp. 37855–37862, 2002.

[89] A. Kihara and Y. Igarashi, "Identification and characterization of a *Saccharomyces cerevisiae* gene, *RSB1*, involved in sphingoid long-chain base release," *The Journal of Biological Chemistry*, vol. 277, no. 33, pp. 30048–30054, 2002.

[90] A. Kihara and Y. Igarashi, "Cross talk between sphingolipids and glycerophospholipids in the establishment of plasma membrane asymmetry," *Molecular Biology of the Cell*, vol. 15, no. 11, pp. 4949–4959, 2004.

[91] M. Ikeda, A. Kihara, A. Denpoh, and Y. Igarashi, "The Rim101 pathway is involved in Rsb1 expression induced by altered lipid asymmetry," *Molecular Biology of the Cell*, vol. 19, no. 5, pp. 1922–1931, 2008.

[92] F. Reggiori and D. J. Klionsky, "Autophagic processes in yeast: mechanism, machinery and regulation," *Genetics*, vol. 194, no. 2, pp. 341–361, 2013.

[93] Y. Feng, D. He, Z. Yao, and D. J. Klionsky, "The machinery of macroautophagy," *Cell Research*, vol. 24, no. 1, pp. 24–41, 2014.

[94] D. J. Klionsky, K. Abdelmohsen, A. Abe et al., "Guidelines for the use and interpretation of assays for monitoring autophagy (3rd edition)," *Autophagy*, vol. 12, no. 1, pp. 1–222, 2016.

[95] A. Beach, A. Leonov, A. Arlia-Ciommo, V. Svistkova, V. Lutchman, and V. I. Titorenko, "Mechanisms by which different functional states of mitochondria define yeast longevity," *International Journal of Molecular Sciences*, vol. 16, no. 3, pp. 5528–5554, 2015.

[96] D. Carmona-Gutierrez, T. Eisenberg, S. Büttner, C. Meisinger, G. Kroemer, and F. Madeo, "Apoptosis in yeast: triggers, pathways, subroutines," *Cell Death and Differentiation*, vol. 17, no. 5, pp. 763–773, 2010.

[97] F. Madeo, D. Carmona-Gutierrez, J. Ring, S. Büttner, T. Eisenberg, and G. Kroemer, "Caspase-dependent and caspase-independent cell death pathways in yeast," *Biochemical and Biophysical Research Communications*, vol. 382, no. 2, pp. 227–231, 2009.

[98] M. A. S. Khan, P. B. Chock, and E. R. Stadtman, "Knockout of caspase-like gene, YCA1, abrogates apoptosis and elevates oxidized proteins in *Saccharomyces cerevisiae*," *Proceedings of the National Academy of Sciences of the United States of America*, vol. 102, no. 48, pp. 17326–17331, 2005.

[99] R. E. C. Lee, S. Brunette, L. G. Puente, and L. A. Megeney, "Metacaspase Yca1 is required for clearance of insoluble protein aggregates," *Proceedings of the National Academy of Sciences of the United States of America*, vol. 107, no. 30, pp. 13348–13353, 2010.

[100] S. Lefevre, D. Sliwa, F. Auchère et al., "The yeast metacaspase is implicated in oxidative stress response in frataxin-deficient cells," *FEBS Letters*, vol. 586, no. 2, pp. 143–148, 2012.

[101] A. Shrestha, L. G. Puente, S. Brunette, and L. A. Megeney, "The role of Yca1 in proteostasis. Yca1 regulates the composition of the insoluble proteome," *Journal of Proteomics*, vol. 81, pp. 24–30, 2013.

[102] S. M. Hill, X. Hao, B. Liu, and T. Nyström, "Life-span extension by a metacaspase in the yeast *Saccharomyces cerevisiae*," *Science*, vol. 344, no. 6190, pp. 1389–1392, 2014.

[103] S. M. Hill and T. Nyström, "The dual role of a yeast metacaspase: what doesn't kill you makes you stronger," *BioEssays*, vol. 37, no. 5, pp. 525–531, 2015.

[104] V. Longo, M. Ždralević, N. Guaragnella, S. Giannattasio, L. Zolla, and A. M. Timperio, "Proteome and metabolome profiling of wild-type and YCA1-knock-out yeast cells during acetic acid-induced programmed cell death," *Journal of Proteomics*, vol. 128, pp. 173–188, 2015.

[105] M. Ždralević, V. Longo, N. Guaragnella, S. Giannattasio, A. M. Timperio, and L. Zolla, "Differential proteome-metabolome profiling of YCA1-knock-out and wild type cells reveals novel metabolic pathways and cellular processes dependent on the yeast metacaspase," *Molecular BioSystems*, vol. 11, no. 6, pp. 1573–1583, 2015.

[106] F. Madeo, E. Herker, C. Maldener et al., "A caspase-related protease regulates apoptosis in yeast," *Molecular Cell*, vol. 9, no. 4, pp. 911–917, 2002.

[107] B. Fahrenkrog, U. Sauder, and U. Aebi, "The *S. cerevisiae* HtrA-like protein Nma111p is a nuclear serine protease that mediates yeast apoptosis," *Journal of Cell Science*, vol. 117, no. 1, pp. 115–126, 2004.

[108] D. Walter, S. Wissing, F. Madeo, and B. Fahrenkrog, "The inhibitor-of-apoptosis protein Bir1p protects against apoptosis in *S. cerevisiae* and is a substrate for the yeast homologue of Omi/HtrA2," *Journal of Cell Science*, vol. 119, no. 9, pp. 1843–1851, 2006.

[109] D. Wilkinson and M. Ramsdale, "Proteases and caspase-like activity in the yeast *Saccharomyces cerevisiae*," *Biochemical Society Transactions*, vol. 39, no. 5, pp. 1502–1508, 2011.

[110] C. Falcone and C. Mazzoni, "External and internal triggers of cell death in yeast," *Cellular and Molecular Life Sciences*, vol. 73, no. 11-12, pp. 2237–2250, 2016.

[111] N. Kourtis and N. Tavernarakis, "Autophagy and cell death in model organisms," *Cell Death and Differentiation*, vol. 16, no. 1, pp. 21–30, 2008.

[112] H. M. Shen and P. Codogno, "Autophagic cell death: Loch Ness monster or endangered species?," *Autophagy*, vol. 7, no. 5, pp. 457–465, 2011.

[113] D. Denton, S. Nicolson, and S. Kumar, "Cell death by autophagy: facts and apparent artefacts," *Cell Death and Differentiation*, vol. 19, no. 1, pp. 87–95, 2012.

[114] T. Eisenberg, H. Knauer, A. Schauer et al., "Induction of autophagy by spermidine promotes longevity," *Nature Cell Biology*, vol. 11, no. 11, pp. 1305–1314, 2009.

[115] T. Eisenberg, D. Carmona-Gutierrez, S. Büttner, N. Tavernarakis, and F. Madeo, "Necrosis in yeast," *Apoptosis*, vol. 15, no. 3, pp. 257–268, 2010.

[116] P. Vandenabeele, L. Galluzzi, T. Vanden Berghe, and G. Kroemer, "Molecular mechanisms of necroptosis: an ordered cellular explosion," *Nature Reviews Molecular Cell Biology*, vol. 11, no. 10, pp. 700–714, 2010.

[117] S. Bialik, E. Zalckvar, Y. Ber, A. D. Rubinstein, and A. Kimchi, "Systems biology analysis of programmed cell death," *Trends in Biochemical Sciences*, vol. 35, no. 10, pp. 556–564, 2010.

[118] E. Zalckvar, S. Bialik, and A. Kimchi, "The road not taken: a systems level strategy for analyzing the cell death network," *Autophagy*, vol. 6, no. 6, pp. 813–815, 2010.

[119] E. Zalckvar, N. Yosef, S. Reef et al., "A systems level strategy for analyzing the cell death network: implication in exploring the apoptosis/autophagy connection," *Cell Death and Differentiation*, vol. 17, no. 8, pp. 1244–1253, 2010.

[120] A. D. Rubinstein and A. Kimchi, "Life in the balance - a mechanistic view of the crosstalk between autophagy and apoptosis," *Journal of Cell Science*, vol. 125, no. 22, pp. 5259–5268, 2012.

[121] M. T. Burstein, P. Kyryakov, A. Beach et al., "Lithocholic acid extends longevity of chronologically aging yeast only if added at certain critical periods of their lifespan," *Cell Cycle*, vol. 11, no. 18, pp. 3443–3462, 2012.

[122] A. Beach, V. R. Richard, S. Bourque et al., "Lithocholic bile acid accumulated in yeast mitochondria orchestrates a development of an anti-aging cellular pattern by causing age-related changes in cellular proteome," *Cell Cycle*, vol. 14, no. 11, pp. 1643–1656, 2015.

[123] A. Leonov, A. Arlia-Ciommo, S. D. Bourque et al., "Specific changes in mitochondrial lipidome alter mitochondrial proteome and increase the geroprotective efficiency of lithocholic acid in chronologically aging yeast," *Oncotarget*, vol. 8, no. 19, pp. 30672–30691, 2017.

[124] Y. Zhao, A. F. Gilliat, M. Ziehm et al., "Two forms of death in ageing *Caenorhabditis elegans*," *Nat Commun*, vol. 8, article 15458, 2017.

[125] S. D. Kohlwein, "Obese and anorexic yeasts: experimental models to understand the metabolic syndrome and lipotoxicity," *Biochimica et Biophysica Acta (BBA) - Molecular and Cell Biology of Lipids*, vol. 1801, no. 3, pp. 222–229, 2010.

[126] F. Madeo, E. Fröhlich, and K. U. Fröhlich, "A yeast mutant showing diagnostic markers of early and late apoptosis," *The Journal of Cell Biology*, vol. 139, no. 3, pp. 729–734, 1997.

[127] A. Abudugupur, K. Mitsui, S. Yokota, and K. Tsurugi, "An ARL1 mutation affected autophagic cell death in yeast, causing a defect in central vacuole formation," *Cell Death and Differentiation*, vol. 9, no. 2, pp. 158–168, 2002.

Hindawi
Oxidative Medicine and Cellular Longevity
Volume 2018, Article ID 4932905, 17 pages
https://doi.org/10.1155/2018/4932905

Research Article

Transcriptome Remodeling of Differentiated Cells during Chronological Ageing of Yeast Colonies: New Insights into Metabolic Differentiation

Derek Wilkinson,[1] Jana Maršíková,[1] Otakar Hlaváček,[2] Gregor D. Gilfillan,[3] Eva Ježková,[1] Ragnhild Aaløkken,[3] Libuše Váchová,[2] and Zdena Palková[1]

[1]*Faculty of Science, Charles University, BIOCEV, 252 50 Vestec, Czech Republic*
[2]*Institute of Microbiology of the Czech Academy of Sciences, BIOCEV, 252 50 Vestec, Czech Republic*
[3]*Department of Medical Genetics, Oslo University Hospital and University of Oslo, 0450 Oslo, Norway*

Correspondence should be addressed to Zdena Palková; zdenap@natur.cuni.cz

Received 13 September 2017; Revised 8 November 2017; Accepted 13 November 2017; Published 11 January 2018

Academic Editor: Karin Thevissen

We present the spatiotemporal metabolic differentiation of yeast cell subpopulations from upper, lower, and margin regions of colonies of different ages, based on comprehensive transcriptomic analysis. Furthermore, the analysis was extended to include smaller cell subpopulations identified previously by microscopy within fully differentiated U and L cells of aged colonies. New data from RNA-seq provides both spatial and temporal information on cell metabolic reprogramming during colony ageing and shows that cells at marginal positions are similar to upper cells, but both these cell types are metabolically distinct from cells localized to lower colony regions. As colonies age, dramatic metabolic reprogramming occurs in cells of upper regions, while changes in margin and lower cells are less prominent. Interestingly, whereas clear expression differences were identified between two L cell subpopulations, U cells (which adopt metabolic profiles, similar to those of tumor cells) form a more homogeneous cell population. The data identified crucial metabolic reprogramming events that arise de novo during colony ageing and are linked to U and L cell colony differentiation and support a role for mitochondria in this differentiation process.

1. Introduction

Yeast colonies are multicellular communities of cells that organize themselves in space and have the ability to differentiate and form specialized subpopulations that fulfill specific tasks during colony development and ageing [1–5]. Despite the fact that mechanisms driving colony development and differentiation are largely unknown, indications exist that the formation of gradients of nutritive compounds such as oxygen and metabolites (including low Mw compounds and waste products) released by cells localized in different positions within the structure contributes to the formation of specialized cell subpopulations [6–8].

Saccharomyces cerevisiae colonies that are grown on complete respiratory medium periodically alter the pH of their surroundings, switching from an acidic phase to a period of alkalization and back. Alkali phase is accompanied by production of volatile ammonia, which functions as a signal that contributes to colony metabolic reprogramming [9–11]. Ammonia (produced by a neighboring colony or even coming from an artificial source) is able to prematurely induce ammonia production (and thus the transition to alkali phase) in acidic-phase colonies [10, 12]. Using microarray transcriptomic analysis and different biochemical and molecular biology approaches, we have previously characterized two major morphologically distinct cell subpopulations that are formed within *S. cerevisiae* colonies during the alkali developmental phase. These subpopulations are differently localized in central areas of the colonies: the U cell subpopulation forms upper-cell layers, whereas L cells form lower layers of these colonies [6, 13]. Despite the fact that U/L cell colony differentiation occurs in relatively old colonies (older

than 12 days) that are composed of mostly stationary-phase cells, U cells behave as metabolically active cells, display a longevity phenotype, and exhibit specific metabolism. For example, U cells activate the TORC1 pathway, which is not typical of stationary-phase cells. These cells also display decreased mitochondrial activity compared with L cells. Several metabolic features of U cells are similar to those of cells of solid tumors [6]. In contrast, L cells, despite being localized from the beginning of colony growth close to nutritive agar, behave as starving and stressed cells that begin losing viability earlier than U cells [6]. These earlier studies showed that L cells release nutritive compounds that are consumed by U cells and are important to U cell survival and long-term viability. In addition to direct measurements of the release and consumption of amino acids and sugars by U and L cells, we showed that mutants with increased viability of L cells often have decreased viability of U cells [6, 7]. Despite prominent differences in the physiology and morphology of U and L cells, we discovered recently that L cells are not homogeneous, but include two subpopulations that differ in the specificity of mitochondrial retrograde signaling. Retrograde signaling, identified in *S. cerevisiae*, mammals, and other organisms [14], is a pathway that signals decreased mitochondrial functionality to the nucleus, where it activates expression of specific genes. Activation, by RTG gene-dependent retrograde signaling (RTG signaling), of expression of genes (such as *CIT2*) involved in anaplerotic pathways was described many years ago in yeast cells grown in liquid cultures [15, 16]. However, we recently showed that RTG signaling in colonies is more complex than that described previously and activates expression of different genes in differentiated cells [17]. We identified three branches of RTG signaling that are specific to U cells (the Ato branch), the upper subpopulation of L cells (the Cit2 branch), and the lower subpopulation of L cells (the cell-viability branch). These signaling branches regulate different gene targets and/or contribute differently to viability of each of the three subpopulations [17].

To extend our knowledge of the similarities and differences of differentiated colony cells and, in particular, the dynamics of their formation, we performed detailed genome-wide transcription profiling by RNA sequencing of cell subpopulations isolated from different areas of acidic- and alkali-phase colonies. We show that upper cells are unique in terms of transcription changes in time and space and also that U cells are a rather homogeneous subpopulation from the point of the view of transcription. Although U cells have significant expression similarities with cells localized to marginal regions, several differences, including those related to mitochondrial functions, contribute to their unique properties. In contrast, lower cells exhibit little temporal transcription dynamics. Furthermore, L cells appear to consist of two subpopulations that differ dramatically in expression, the upper one being in some ways similar to U cells. Altogether, these new findings point towards additional, yet to be identified levels of colony complexity and support the hypothesis of an important role for mitochondria and related signaling in the differentiation of ageing colonies and the escape of specific subpopulations from the stress caused by nutrient depletion.

2. Results and Discussion

2.1. Genome-Wide Transcription Profiling of Cell Subpopulations Separated from 6- and 15-Day-Old Colonies. Three cell subpopulations were separated from 15-day-old alkali-phase giant colonies grown on GMA agar: U cells from the central upper (U15 cells) parts of the colonies, L cells from the central lower (L15 cells) parts of the colonies, and cells that localize to marginal regions (M15 cells) (Figure 1(a)). Similarly, we also separated 6-day-old acidic-phase colonies, that is, colonies in the stage before U/L cell differentiation, into 3 cell subpopulations: cells from the upper (U6 cells) and cells from the lower (L6 cells) regions of the colony centre and cells from the colony margin (M6 cells). To study the composition of fully differentiated U15 and L15 cells, we further separated both U15 and L15 cells into two smaller cell subpopulations: U1 cells from upper and U2 cells from lower layers of U15 cells and L1 cells from upper and L2 cells from lower layers of L15 cells (Figure 1(b)). Total RNA extracted from these ten cell subpopulations was used for RNA sequencing. Altogether, we sequenced 30 transcriptomic libraries, representing three biological replicates of these ten subpopulations (see Materials and Methods for details).

Differential expression (DE) was detected for 7055 loci, reflecting expression differences among the differently localized cell subpopulations and changes in major subpopulations during colony development. Small fold transcription differences between cell types (even if statistically significant in robust sequencing data) usually do not reflect a significant difference in protein/metabolite levels, so we restricted our analysis of differential expression to those genes with an adjusted p value below 0.05 ($p_{\text{adj}} < 0.05$) with expression fold changes of 1.8 or greater. Across 31 comparisons, we found 43,488 differential expressions (DE) involving 5036 unique protein-coding genes fulfilling these criteria. Of these DEs, 32,898 (76%) retain significance when applying the most stringent Bonferroni correction (p value $< 4.8E{-}06$, [18]). The equivalent results for lncRNA are 11,354 (p_{adj} value) and 3599 (Bonferroni correction). The differences in expression of selected genes were confirmed by RT-PCR (Figure 2).

2.2. Differential Expression in Upper, Lower, and Margin Subpopulations and Functional Analysis. Differentially expressed genes were identified in pairs of compared cell subpopulations. To assess overall differences/similarities between the subpopulations, we compared datasets of DE genes using Intervene's UpSet module [19], which visualizes the intersection of multiple datasets in UpSet plots. For clarity, we compared subpopulations of 6- and 15-day-old colonies separately, and, to estimate time-differences, we also compared cells localized to the same position in 6- and 15-day-old colonies (Figures 3–5). Comparison of both U6, L6, and M6 cells (Figure 3) and U15, L15, and M15 cells (Figure 4) revealed at both developmental times the most prominent expression differences between upper and lower cells (2346 and 2594 genes, resp.) and between margin and lower cells (1861 and 1900 genes, resp.). Differences between upper and margin cells were moderate and

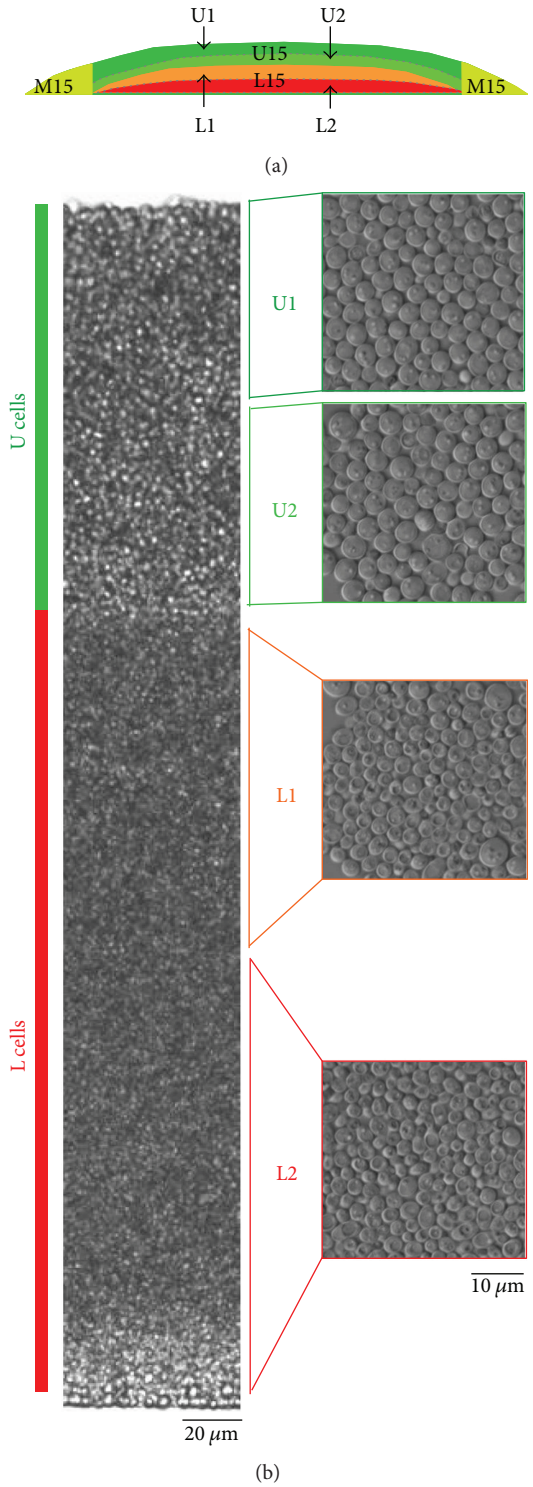

Figure 1: Subpopulations in 15-day-old colonies. (a) Schematic of subpopulations in 15-day-old colonies. (b) Small subpopulations separated from the central part of the colony. (left) Vertical cross section of a 15-day-old colony. (right) Cell subpopulations separated from the colony for RNA sequencing. Cells were visualized by Nomarski contrast. U: upper; L: lower; U1: upper U cells; U2: lower U cells; L1: upper L cells; L2: lower L cells.

more prominent in 15-day-old (420 genes) than in 6-day-old (257 genes) colonies, indicating that upper and margin subpopulations are similar to each other but different from lower cells. Upregulated genes common to both upper and marginal cells relative to lower cells numbered 1554 (6 days) and 1512 (15 days) genes. Unique differences in expression between upper and lower cells were represented by 616 DE genes at day 6 and 711 genes at day 15. Those genes uniquely differing between margin and lower cells numbered 150 genes at day 6 and 180 genes at day 15. Only a few unique DE genes were identified between upper and margin cells in both times (20 and 48 genes, resp.).

Examination of temporal changes in respective colony regions showed (Figure 5) that major changes occur during differentiation from upper cells of 6-day-old colonies to U cells of 15-day-old colonies (1120 DE genes, 703 of which were unique to upper cells). In marginal cells, temporal changes concern the expression of 429 genes, 292 of which were changed in both upper and marginal cells and 67 unique to marginal cells. Temporal changes in lower cells were relatively moderate and regard 245 DE genes, 120 of which were unique to lower cells and 55 jointly changed in lower and upper cells.

Subsequently, we performed global functional grouping of DE genes using gene ontology analysis and hierarchical clustering, further controlled by manual assessment of individual gene functions based upon information in the SGD (http://www.yeastgenome.org/) and the literature. This analysis clustered genes to different functional gene categories (FC) that were upregulated in upper, lower, and margin cell subpopulations as well as during temporal changes in cells localized to particular positions (Figures 3–5). It is worth noting here that the term "upregulation"/"downregulation" of gene expression used throughout the text is usually relative to the opposite subpopulation and does not imply that a gene expression difference is due to an increased rate of transcription in one subpopulation or decreased rate in the other. This functional categorization of DE genes helped us to further identify similarities/differences among the subpopulations and their developmental changes. In parallel with this cluster analysis, we performed statistically supported enrichment analysis of functional categories in our datasets, which confirmed FC enrichment (compared with the genome) in most cases (Figure 6).

In both 6- and 15-day-old-colonies, several prominent FCs were similarly up- and downregulated in upper and margin cells versus lower cells. This finding indicates that cell diversification leading to fully differentiated U and L cells in 15-day-old colonies has already begun in younger colonies, in which cells cannot be clearly distinguished according to morphology. Prominent FCs, the genes of which were upregulated in both upper and margin cells when compared with lower cells at both time points, include genes with functions in vitamin/cofactor metabolism, protein modifications, ribosome biogenesis, translation and tRNA/mRNA processing and modifications, or encoding ribosome or polymerase subunits (Figures 3 and 4). On the other hand, lower cells at both time points upregulated genes involved in metabolism of reserves (storage compounds), respiration and

Target	U6/L6		U6/M6		M6/L6		U15/L15		U15/M15		M15/L15		L15/L6		M15/M6		U15/U6	
	qPCR	RNAseq	qPCR	RNAseq	qPCR	RNAseq	qPCR	RNAseq	qPCR	RNAseq	qPCR	RNAseq	qPCR	RNAseq	qPCR	RNAseq	qPCR	RNAseq
ZRT1	**2.39** ↑	**2.30** ↑	**5.81** ↑	**3.57** ↑	**1.45** ▪	**1.57** ▪	6.33 ↑	**4.17** ↑	**2.55** ↑	**2.07** ↑	2.95 ↑	2.07 ↑	**2.51** ↑	**2.67** ↑	**14.42** ↑	**9.09** ↑	**5.48** ↑	**5.37** ↑
NCE102	**17.99** ↓	**17.04** ↓	**4.71** ↓	**3.25** ↓	**4.60** ↓	**5.35** ↓	19.14 ↓	**16.30** ↓	**3.25** ↓	**3.47** ↓	9.17 ↓	3.92 ↓	**1.67** ▪	**1.72** ▪	**1.96** ↑	**1.74** ▪	**2.01** ↑	**1.49** ▪
STL1	13.84 ↑	3.12 ↑	**2.08** ↓	**2.32** ↓	**12.71** ↑	**8.24** ↑	1.79 ▪	1.58 ▪	**1.41** ▪	**1.93** ↓	**3.29** ↑	**2.84** ↑	**3.44** ↓	**2.43** ↓	**7.21** ↓	**4.44** ↓	**4.91** ↓	**3.79** ↓
CWP1	1.11 ▪	2.24 ↓	**6.29** ↓	**6.78** ↓	7.01 ↑	2.82 ↑	1.02 ▪	5.30 ↓	**1.54** ▪	**2.52** ↓	**1.51** ▪	**1.82** ↓	5.46 ↓	3.19 ↓	**25.37** ↓	**12.07** ↓	**6.20** ↓	**4.38** ↓
INO1	35.37 ↑	5.14 ↑	**2.14** ↑	**1.51** ▪	**7.34** ↑	**3.53** ↑	1.07 ▪	**1.02** ▪	**1.59** ▪	**1.02** ▪	1.43 ▪	**1.14** ▪	**3.55** ↓	**2.07** ↓	100.31 ↓	10.34 ↓	134.70 ↓	17.29 ↓
YDL218w	**5.70** ↓	**3.93** ↓	**2.98** ↑	**1.81** ↑	**12.77** ↓	**7.40** ↓	2.14 ↑	**1.73** ▪	5.13 ↑	2.22 ↑	**1.14** ▪	**1.22** ▪	6.25 ↑	1.96 ↑	**6.96** ↑	**11.59** ↑	171.97 ↑	12.82 ↑
VBA5	**1.78** ▪	**1.90** ↓	36.56 ↑	2.15 ↑	**11.12** ↓	**5.91** ↓	2.85 ↑	**2.86** ↑	**3.38** ↑	**4.99** ↑	**1.56** ▪	**1.79** ▪	6.68 ↑	1.10 ▪	47.06 ↑	2.76 ↑	**3.63** ↑	**6.72** ↑
PDR15	2.78 ↓	7.47 ↓	5.68 ↓	2.26 ↓	2.04 ↓	3.31 ↓	3.93 ↓	17.95 ↓	**2.18** ↓	**2.05** ↓	1.81 ↓	7.15 ↓	**1.46** ▪	**1.57** ▪	5.37 ↓	1.71 ▪	**2.06** ↓	**1.65** ↓
CYC7	**25.50** ↓	**26.16** ↓	**2.18** ↓	**3.66** ↓	95.97 ↓	6.78 ↓	21.22 ↓	**10.30** ↓	**3.44** ↓	**2.46** ↓	8.23 ↓	3.35 ↓	**1.80** ▪	**1.35** ▪	2.81 ↑	1.10 ▪	**1.39** ▪	**1.59** ▪
ANS1	**2.23** ↑	**2.52** ↑	11.24 ↑	3.23 ↑	9.27 ↑	1.26 ▪	2.31 ↓	**1.31** ▪	**1.68** ▪	**1.06** ▪	5.49 ↓	1.22 ▪	**1.90** ↑	**1.18** ▪	**2.27** ↑	**1.86** ↑	**2.37** ↓	**1.80** ↓
MIG2	**2.28** ↓	**1.74** ▪	**1.82** ↓	**2.84** ↓	**1.85** ↑	**1.64** ▪	5.30 ↓	16.84 ↓	2.24 ↑	8.33 ↓	10.23 ↓	1.38 ▪	10.55 ↑	5.32 ↑	1.72 ▪	3.45 ↑	**1.96** ↑	**1.47** ▪
THI5	83.38 ↑	8.58 ↑	**1.47** ▪	**2.04** ↑	56.75 ↑	4.39 ↑	36.25 ↑	6.64 ↑	**1.65** ▪	**1.57** ▪	59.71 ↑	9.86 ↑	**1.00** ▪	**1.25** ▪	**1.05** ▪	**1.67** ▪	**2.30** ↓	**2.10** ↓
CYC1	291.03 ↑	4.18 ↑	**1.27** ▪	**1.43** ▪	228.33 ↑	3.00 ↑	3.85 ↓	1.05 ▪	**5.82** ↓	**2.42** ↓	22.39 ↑	2.34 ↑	1.00 ▪	3.93 ↓	**10.20** ↓	**6.22** ↓	75.67 ↓	24.35 ↓
CTS1	3.61 ↓	19.48 ↓	**2.95** ↓	**3.12** ↓	1.22 ▪	6.21 ↓	13.82 ↓	64.71 ↓	29.28 ↓	9.23 ↓	2.12 ↓	4.78 ↓	**1.41** ▪	**1.77** ▪	**1.84** ↑	**1.48** ▪	5.38 ↓	2.14 ↓
HSP30	8.34 ↓	37.57 ↓	**6.59** ↓	**3.74** ↓	1.27 ▪	8.65 ↓	16.62 ↓	175.93 ↓	54.95 ↓	12.15 ↓	3.31 ↓	7.52 ↓	4.47 ↑	1.79 ↑	**1.07** ▪	**1.24** ▪	8.91 ↓	2.74 ↓

Bold Same or similar expression values
Upregulated in the first population
Downregulated in the first population
Opposite trend of expression

↑ Higher expression in the first population (> 1.8)
▪ No change of expression (< 1.8)
↓ Lower expression in the first population (> 1.8)

Figure 2: RT-qPCR verification of RNA-seq results. RNA-seq results for selected genes were verified using RT-qPCR. First-strand cDNA was synthesized from total RNA using random primers and RT-qPCR carried out in triplicate on 5-fold diluted cDNA. $\Delta\Delta C_T$ values were normalized to those of housekeeping genes (up to 5 genes) to compare fold differences between samples.

mitochondrial ATP synthesis, protein folding and protein quality control, oxidative and other stress responses, proteasome functions, and other protein degradation genes and retrotransposons. The repression of polymerase, ribosome and protein biosynthesis genes on one hand, and induction of protein folding and degradation, respiration and stress response genes on the other, in lower cells compared with upper or marginal cells, is typical of cells subject to environmental stress or the diauxic shift [20, 21]. These data are in agreement with the higher level of reactive oxygen species and other stress-related features of L cells [6] and may indicate that lower cells are already more stressed than upper cells in 6-day-old colonies. Other large FCs of genes, DE at both day 6 and day 15, include genes involved in amino acid, carbohydrate, and lipid metabolism; genes for different transporters; and genes involved in the cell cycle. Each of these FCs is not typical of any particular subpopulation; it includes some genes upregulated in upper/margin cells but also other genes upregulated in lower cells. Often, these FCs also include genes differentially expressed between days 6 and 15 (Figure 5), indicating high spatiotemporal dynamics in expression of genes involved in these cellular processes. Enrichment analysis (Figure 6) confirmed most of the FCs that were differently expressed between different cell types: FCs that are enriched against the background in U/M versus L cell comparisons include those involved in vitamin/cofactor metabolism, protein modification, ribosome biogenesis/subunits, translation, polymerase subunits, and amino acid/purine/pyrimidine metabolism. FC groups that are enriched in L versus U/M cell comparisons include those involved in cell wall, respiration/ATP synthesis, protein folding, stress response, protein degradation, carbohydrate metabolism, other transports and retrotransposons. Interestingly, some FCs (mainly protein modification and ribosome biogenesis/subunit FCs) are significantly underrepresented underrepresented among genes upregulated in L cells versus U and M cells not only that genes from the functional category are repressed but that the functional category itself is generally repressed in L cells versus U or M cells.

2.3. Expression Differences among Small Subpopulations of U and L Cells from Differentiated 15-Day-Old Colonies. In addition to comparing major subpopulations, differential expression results were collected from comparisons of expression data of U1, U2, L1, and L2 subpopulations separated from 15-day-old colonies (Figure 1). At first glance, these comparisons revealed relatively large expression differences between L1 and L2 cells, whereas no DE genes fulfilling our criteria ($p_{adj} < 0.05$; fold change 1.8) were identified between U1 and U2 subpopulations, indicating that in contrast to L cells, U cells are relatively homogeneous. For this reason, we extended our analyses and compared all small subpopulations with U15 and L15 datasets comprising results for major colony subpopulations. Dataset comparisons were then analyzed using Intervene's UpSet module and gene ontology (GO) functional clustering as indicated above. Further statistical analysis confirmed the enrichment of FCs in selected datasets versus the genome (Figure 6). The data obtained provided us with a complex view of the differences/similarities among the subpopulations, as summarized in Figures 6 and 7 and described below.

Comparison of U1 and U2 cells with L15 cells (Figure 7) revealed that most of the genes differentially expressed between U1 and L15 and U2 and L15 are the same 2002 genes. 1627 of these genes were also differentially expressed between U15 and L15 cells. Functional categorization of DE datasets U1/L15 and U2/L15 and their comparison with the U15/L15 dataset showed a high level of FC similarity among both up- and downregulated genes. As expected, comparison of U1 and U2 cells with U15 cells revealed a much lower total number of DE genes (1290 genes) than comparison of U1 and U2 cells with L15 cells (4744 genes) and showed higher expression differences between U2 and U15 (965 genes) than between U1 and U15 (325 genes) cells. Functional categorization of the datasets showed 242 genes upregulated and 83 genes downregulated in U1 versus U15 cells. Of the upregulated genes, 204 genes overlapped with genes upregulated in U2 versus U15 cells. In addition to the largest category of unknown genes/dubious ORFs (55 genes), genes of amino acid, carbohydrate and lipid metabolism (altogether 40 genes), transporter genes (36 genes), and genes related to cell wall function (35 genes) fall into this group. Differences between U2 and U15 were more prominent and regard 336 upregulated and 629 downregulated genes. The largest

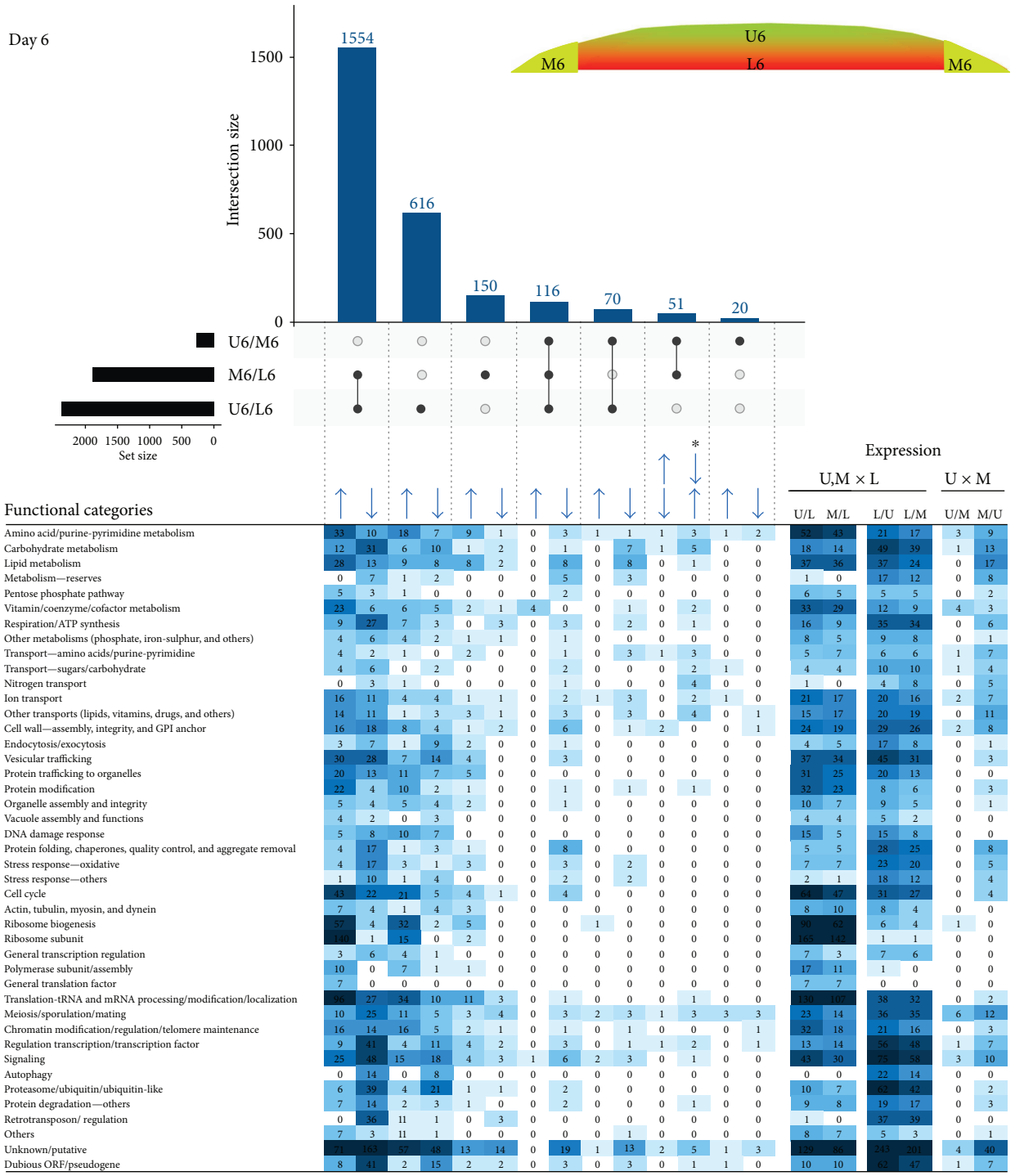

Figure 3: Comparing cell subpopulations in 6-day-old colonies. UpSet plot of datasets of DE genes in upper (U6), lower (L6), and marginal (M6) cells from 6-day-old colonies (upper part). Horizontal black bar chart indicates numbers of genes, DE in each individual comparison. Intersect "connectors" indicate comparisons in which a given number of genes (vertical blue bar chart) were DE. Only major intersections are shown. Heat map of genes assigned to functional categories and clustered according to FC and DE in different sample comparisons (lower part). Number in heat map cell = number of genes from FC, up- or downregulated in sample comparison. The higher the number of up-/downregulated genes, the more intense the color. Arrows indicate upregulation/downregulation in the respective subpopulation ratio(s); asterisk indicates categories of genes that are differently up-/downregulated in the respective subpopulation ratios.

functional category of unique U2-upregulated genes (132 genes) again includes unknown/dubious genes (40 genes). Interestingly, some groups of genes, repressed in U2 versus U15 (567 genes), comprise FCs also typically repressed in L15 versus U15, such as genes for ribosomal subunits (37 genes), ribosome biogenesis (51 genes), translation,

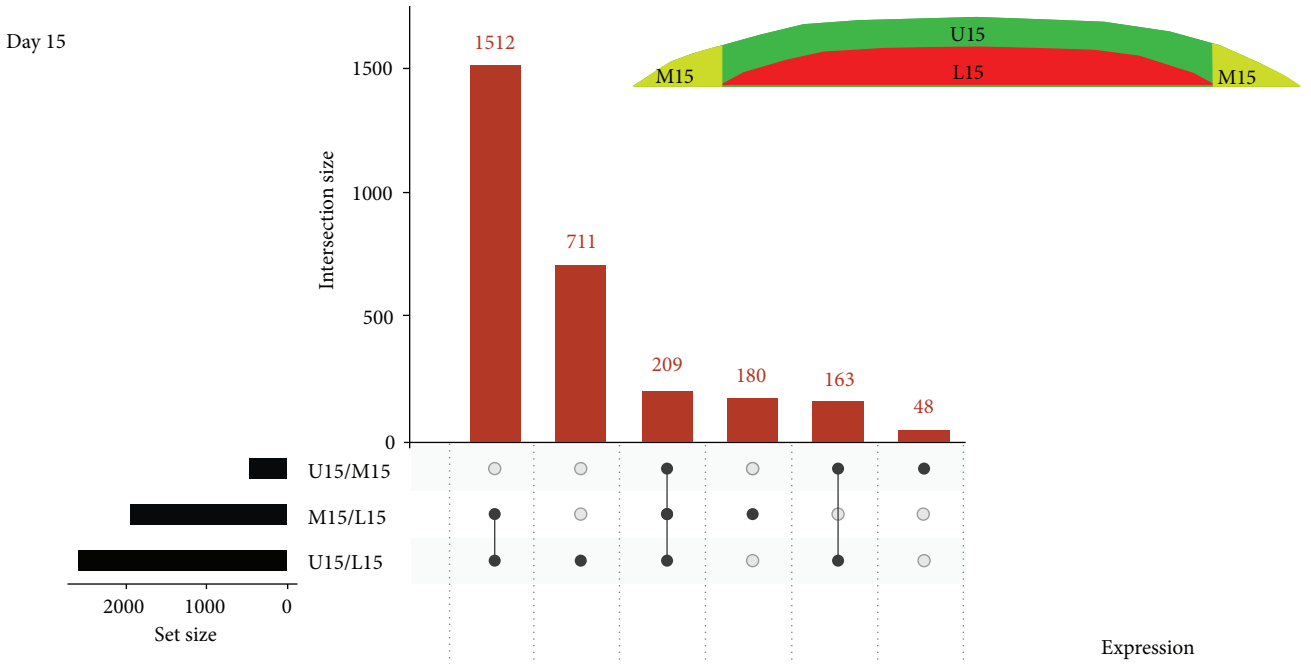

Functional categories													Expression: U, M × L U/L				Expression: U × M U/M	
	↑	↓	↑	↓	↑	↓	↑	↓	↑	↓	↑	↓	U/L	M/L	L/U	L/M	U/M	M/U
Amino acid/purine-pyrimidine metabolism	35	17	9	10	0	4	11	1	0	7	0	4	44	46	38	22	0	15
Carbohydrate metabolism	8	28	2	11	1	12	2	4	3	11	2	2	14	11	62	44	6	25
Lipid metabolism	21	21	6	16	0	3	6	0	1	6	0	3	28	27	46	24	1	12
Metabolism—reserves	1	7	0	1	0	5	0	0	0	0	0	0	1	1	13	12	0	5
Pentose phosphate pathway	2	4	0	0	0	0	3	1	0	0	0	0	2	5	4	5	0	0
Vitamin/coenzyme/cofactor metabolism	20	4	7	8	0	1	5	0	0	1	0	0	27	25	14	5	0	2
Respiration/ATP synthesis	6	12	4	13	0	16	2	1	0	10	0	1	10	8	51	29	0	27
Other metabolisms (phosphate, iron-sulphur, and others)	4	5	3	2	0	2	0	1	0	1	1	0	7	4	10	8	1	3
Transport—amino acids/purine-pyrimidine	2	7	1	4	0	0	3	0	1	1	0	1	4	5	12	7	1	2
Transport—sugars/carbohydrate	2	7	0	7	0	1	0	0	2	4	0	0	4	2	19	8	2	5
Nitrogen transport	2	4	0	0	0	2	0	0	0	2	0	0	2	2	8	6	0	4
Ion transport	12	14	5	9	1	4	5	1	0	3	1	2	18	18	30	19	2	9
Other transports (lipids, vitamins, drugs, and others)	6	15	4	4	0	2	5	4	1	7	0	1	11	11	28	21	1	10
Cell wall—assembly, integrity, and GPI anchor	8	15	6	4	0	15	6	1	0	11	0	0	14	14	45	31	0	26
Endocytosis/exocytosis	3	13	5	4	0	1	0	1	0	2	0	0	8	3	20	15	0	3
Vesicular trafficking	36	18	12	21	0	3	6	1	0	2	0	0	48	42	44	22	0	5
Protein trafficking to organelles	23	13	7	11	0	0	3	0	0	0	0	0	30	26	24	13	0	0
Protein modification	18	5	4	8	0	1	3	0	0	0	0	0	22	21	14	6	0	1
Organelle assembly and integrity	8	7	2	6	0	2	1	0	0	0	0	0	10	9	15	9	0	2
Vacuole assembly and functions	4	0	2	4	0	1	0	0	0	0	0	0	6	4	5	1	0	1
DNA damage response	14	4	9	4	0	2	0	2	0	0	0	0	23	14	10	8	0	2
Protein folding, chaperones, quality control, and aggregate removal	7	14	3	8	0	8	2	2	0	1	0	0	10	9	31	24	0	9
Stress response—oxidative	6	13	1	3	0	1	0	1	1	2	0	0	8	6	19	15	1	3
Stress response—others	2	8	1	4	0	6	0	0	0	2	0	0	3	2	20	14	0	8
Cell cycle	41	17	21	24	0	13	11	0	0	9	0	1	62	52	63	30	0	23
Actin, tubulin, myosin, and dynein	2	5	2	5	0	3	3	1	0	5	0	0	4	5	18	9	0	8
Ribosome biogenesis	72	3	29	3	0	1	7	0	0	0	1	0	101	79	7	4	1	1
Ribosome subunit	149	0	2	1	0	1	2	0	0	0	0	0	151	151	2	1	0	1
General transcription regulation	6	5	2	2	0	0	1	0	0	0	0	0	8	7	7	5	0	0
Polymerase subunit/assembly	11	0	3	0	0	0	1	0	0	0	0	0	14	12	0	0	0	0
General translation factor	7	0	0	0	0	0	1	0	0	0	0	0	7	8	0	0	0	0
Translation-tRNA and mRNA processing/modification/localization	90	23	38	17	0	6	11	1	1	0	0	0	129	101	46	30	1	6
Meiosis/sporulation/mating	17	23	14	6	0	2	4	2	6	3	5	1	37	21	34	27	11	6
Chromatin modification/regulation/telomere maintenance	26	17	17	7	0	3	4	0	0	3	0	1	43	30	30	20	0	7
Regulation transcription/transcription factor	10	38	8	21	0	12	5	0	0	4	0	0	18	15	75	50	0	16
Signaling	21	52	18	22	0	14	5	0	1	2	0	0	40	26	90	66	1	16
Autophagy	0	10	1	1	0	0	0	2	0	0	0	0	1	0	11	12	0	0
Proteasome/ubiquitin/ubiquitin-like	5	36	16	20	0	5	0	1	0	0	0	0	21	5	61	42	0	5
Protein degradation—others	3	15	2	7	0	3	1	0	0	0	0	0	5	4	25	18	0	3
Retrotransposon/ regulation	0	28	0	2	0	9	0	0	0	0	0	0	0	0	39	37	0	9
Others	4	3	4	2	0	0	1	0	0	0	0	0	8	5	5	3	0	0
Unknown/putative	85	137	43	65	1	26	10	10	9	24	7	7	138	96	252	173	17	57
Dubious ORF/pseudogene	11	35	10	21	0	3	2	10	6	8	3	4	27	13	67	48	9	15

Figure 4: Comparing cell subpopulations in 15-day-old colonies. UpSet plot of datasets of DE genes in upper (U15), lower (L15), and marginal (M15) cells from 15-day-old colonies (upper part). Only major intersections are shown. Heat map of genes assigned to functional categories and clustered according to FC and DE in different sample comparisons (lower part). Number in heat map cell = number of genes from FC, up- or downregulated in sample comparison. The higher the number of up-/downregulated genes, the more intense the color. Arrows indicate upregulation/downregulation in the respective subpopulation ratio(s).

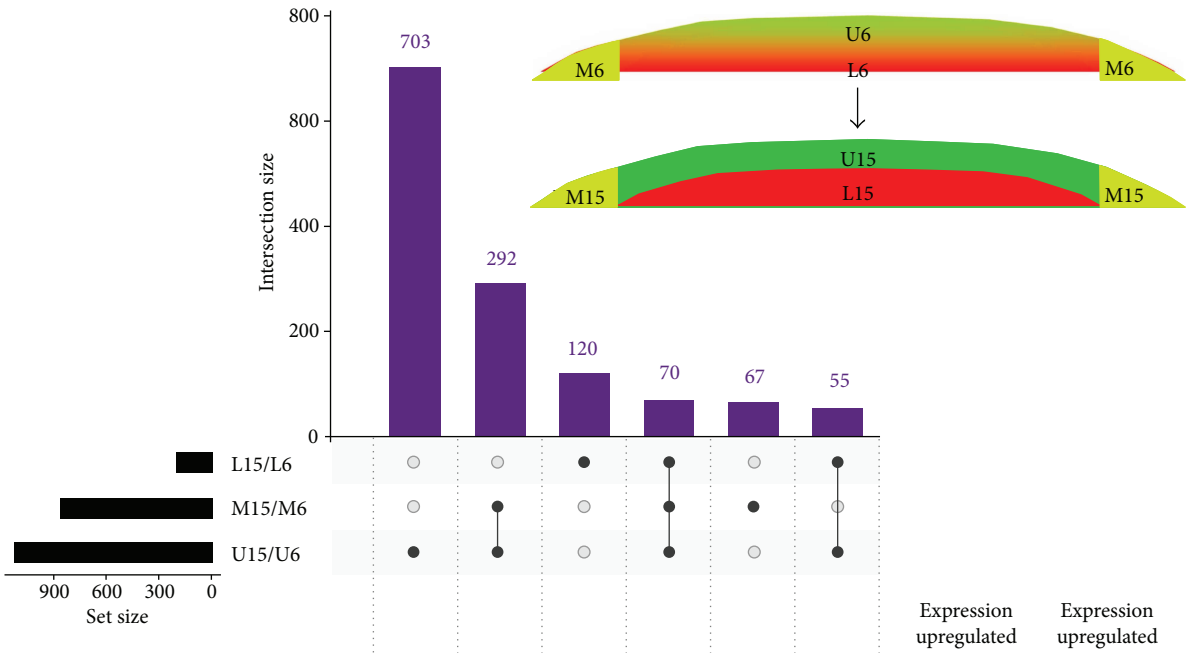

Functional categories	↑	↓	↑	↓	↑	↓	↑	↓	↑	↓	↑	↓	Expression upregulated (day 6) U	M	L	Expression upregulated (day 15) U	M	L
Amino acid/purine-pyrimidine metabolism	5	23	3	13	5	2	1	5	1	3	0	4	45	21	11	9	5	6
Carbohydrate metabolism	10	23	14	13	2	0	5	0	5	1	0	0	36	14	0	29	24	7
Lipid metabolism	6	12	6	16	4	1	4	1	0	0	3	1	30	17	3	19	10	11
Metabolism—reserves	2	0	2	0	0	0	1	0	0	0	1	0	0	0	0	6	3	2
Pentose phosphate pathway	2	1	0	1	0	0	2	0	0	0	0	0	2	1	0	4	2	2
Vitamin/coenzyme/cofactor metabolism	1	10	2	4	1	0	0	1	2	1	0	1	16	6	2	3	4	1
Respiration/ATP synthesis	3	35	2	2	8	1	1	2	0	0	1	1	40	4	4	7	3	10
Other metabolisms (phosphate, iron-sulphur, and others)	0	5	1	3	0	0	0	0	0	0	0	0	8	3	0	1	1	0
Transport—Amino acids/purine-pyrimidine	2	2	2	2	1	0	0	0	0	1	0	0	4	3	0	4	2	1
Transport—Sugars/carbohydrate	3	3	4	3	2	0	0	0	0	0	0	0	6	3	0	7	4	2
Nitrogen transport	1	0	0	4	1	0	1	0	0	0	1	0	4	4	0	3	1	3
Ion transport	4	8	3	6	1	2	5	1	0	1	2	0	15	8	3	14	8	8
Other transports (lipids, vitamins, drugs, and others)	10	7	4	5	2	1	1	1	0	1	1	0	13	7	2	16	5	4
Cell wall—assembly, integrity, and GPI anchor	3	21	1	6	6	2	0	4	1	0	0	1	32	10	7	4	2	6
Endocytosis/exocytosis	1	1	0	1	3	0	0	0	0	1	0	0	2	2	0	1	0	3
Vesicular trafficking	1	4	1	1	0	2	0	0	0	0	0	1	6	1	3	2	1	0
Protein trafficking to organelles	0	11	1	1	2	0	0	0	0	0	0	1	13	1	1	1	1	2
Protein modification	0	12	0	1	0	0	0	1	0	0	0	0	14	2	1	0	0	0
Organelle assembly and integrity	0	10	1	2	1	1	1	0	1	0	0	1	13	2	2	2	3	2
Vacuole assembly and functions	0	3	0	0	0	0	0	0	0	0	0	0	3	0	0	0	0	0
DNA damage response	4	3	1	0	0	0	0	0	2	0	0	0	3	0	0	5	3	0
Protein folding, chaperones, quality control, and aggregate removal	3	4	3	0	0	0	2	0	0	0	0	0	4	0	0	8	5	2
Stress response—oxidative	4	3	2	1	1	0	1	1	2	1	1	0	5	3	1	8	5	3
Stress response—others	2	3	5	0	1	0	0	1	0	0	0	0	4	1	1	7	5	1
Cell cycle	1	40	1	10	5	1	0	0	0	0	0	0	50	10	1	2	1	5
Actin, tubulin, myosin, and dynein	0	13	1	0	1	0	0	0	0	0	0	0	13	0	0	1	1	1
Ribosome biogenesis	2	4	0	2	1	4	0	0	0	1	0	0	6	3	4	2	0	1
Ribosome subunit	0	16	0	4	0	2	0	1	1	1	0	5	26	6	8	0	1	0
General transcription regulation	0	0	0	0	0	0	0	0	0	0	0	0	0	0	0	0	0	0
Polymerase subunit/assembly	1	1	0	0	0	0	0	0	0	0	0	0	1	0	0	1	0	0
General translation factor	0	0	0	0	0	0	0	0	0	0	0	0	0	0	0	0	0	0
Translation-tRNA and mRNA processing/modification/localization	2	17	2	10	5	1	3	0	1	0	0	0	27	10	1	7	6	8
Meiosis/sporulation/mating	26	9	9	3	3	0	1	0	4	1	1	0	12	4	0	37	14	5
Chromatin modification/regulation/telomere maintenance	2	10	0	2	2	2	1	0	0	0	0	0	12	2	2	3	1	3
Regulation transcription/transcription factor	6	12	4	3	4	1	0	1	2	1	0	0	16	5	2	10	6	4
Signaling	9	14	3	5	8	1	3	3	1	1	2	2	24	9	6	17	7	13
Autophagy	5	0	1	0	0	0	0	0	0	0	0	0	0	0	0	6	1	0
Proteasome/ubiquitin/ubiquitin-like	3	5	3	0	3	0	1	0	0	0	0	0	5	0	0	7	4	4
Protein degradation—others	2	6	1	1	1	0	0	0	0	1	0	0	7	2	0	3	1	1
Retrotransposon/ regulation	0	24	0	0	1	0	0	0	0	0	0	0	24	0	0	0	0	1
Others	0	1	0	2	1	0	0	0	0	0	0	0	3	2	0	0	0	1
Unknown/putative	67	83	35	33	13	4	6	4	12	7	5	4	124	44	12	113	53	24
Dubious ORF/pseudogene	29	22	4	7	2	1	1	0	4	5	1	3	32	12	4	35	9	4

Figure 5: Time point comparisons. UpSet plot of datasets of DE genes in upper (U6 and U15), lower (L6 and L15), and marginal (M6 and M15) cells from 6- and 15-day-old colonies, respectively (upper part). Only major intersections are shown. Heat map of genes assigned to functional categories and clustered according to FC and DE in different sample comparisons (lower part). The higher the number of up-/downregulated genes, the more intense the color. Number in heat map cell = number of genes from FC, up- or downregulated in sample comparison. Red cell highlighting: FC upregulated at day 15 relative to day 6. Blue cell highlighting: FC upregulated at day 6 relative to day 15. Arrows indicate upregulation/downregulation in the respective subpopulation ratio(s).

Functional categories	U6/L6	M6/L6	U15/L15	M15/L15	L6/U6	L6/M6	L15/U15	L15/M15	L2/U15	L2/L1	L1/L2	U15/L2	L1/U15	L1/U2	U2/L1	U15/L1
Vitamin/coenzyme/cofactor metabolism	7.7E−09	5.3E−09	4.3E−06	9.4E−07	0.2281	0.3614	0.1911	0.8672	0.5961	0.4150	0.0067	3.1E−06	1.0000	1.0000	0.0002	9E−15
Protein modification	5.5E−13	1.4E−11	1.3E−15	1.8E−13	2.4E−15	2.4E−15	1.6E−15	2.4E−15	2.4E−15	2.4E−15	1.2E−15	1.2E−15	2.3E−14	1.0000	0.0616	0.1618
Ribosome biogenesis	4.3E−12	4.2E−07	1.3E−15	2.3E−12	3E−08	2.1E−07	1.6E−09	2.2E−07	9.3E−09	2.7E−07	1.2E−15	1.2E−15	0.8567	0.2244	0.9259	0.4840
Translation–tRNA and mRNA processing/modification/localization	2.4E−15	2.4E−15	1.3E−15	7.9E−13	0.1025	0.2178	0.0808	0.1366	0.1000	0.0731	1.2E−15	1.2E−15	1.0000	0.3236	1.0000	0.4840
Ribosome subunit	2.4E−15	2.4E−15	1.3E−15	4.8E−15	2.4E−15	2.4E−15	1.6E−15	2.4E−15	2.4E−15	2.4E−15	1.2E−15	1.2E−15	2.3E−08	2.5E−05	0.9259	0.4840
Polymerase subunit	0.0025	0.0408	0.0351	0.0278	0.0538	0.0257	0.0045	0.0289	0.0105	0.0185	0.0001	0.0037	0.2606	1.0000	1.0000	1.0000
Metabolism—reserves	0.3275	0.0904	0.4226	0.5126	6E−05	0.0013	0.0099	0.0011	0.0021	0.0008	0.0761	0.4032	0.6038	0.2242	1.0000	0.4840
Respiration/ATP synthesis	0.0017	0.1575	0.2816	0.2680	3.6E−12	4.7E−14	1.6E−15	4.5E−11	1.4E−13	3.9E−12	0.0977	1.9E−05	5E−05	1.5E−05	1.0000	0.4840
Cell wall—assembly, integrity, and GPI anchor	0.1395	0.1585	0.7511	0.8827	0.0256	0.0083	5.3E−05	0.0003	2.9E−07	8.3E−05	0.9226	1.0000	6.3E−09	0.6496	4.5E−06	0.7399
Protein folding, chaperones, quality control, and aggregate removal	0.0163	0.0949	0.4226	0.6009	0.0154	0.0065	0.0226	0.0098	0.1000	0.0667	0.4558	0.3627	0.0885	0.0003	0.9259	0.7399
Stress response—oxidative/others	0.7398	0.5148	0.5354	0.6811	3.6E−12	6.7E−10	2.2E−09	1.5E−08	1.4E−08	1.5E−05	0.4558	0.0912	0.0158	3.6E−06	0.9234	0.3214
Protein degradation/proteasomes/others	0.0756	0.1217	0.5853	0.0018	1.1E−10	4.5E−07	4.8E−09	1.3E−07	0.0005	0.0010	0.9226	0.0670	1.0000	3.4E−05	0.6844	0.4840
Retrotransposons	2.1E−05	4.3E−05	2.1E−06	2.8E−05	0.0003	5.2E−07	0.0016	3.4E−06	4.5E−05	1.9E−05	1.6E−05	3.8E−07	2.7E−09	1.5E−08	0.9259	0.7399
Amino acid/purine–pyrimidine metabolism	4.9E−07	7.8E−07	0.0001	2.3E−07	1.0000	1.0000	0.0447	0.2965	0.0289	0.4150	4.3E−10	0.0002	0.0370	1.0000	0.5005	0.7399
Carbohydrate metabolism	0.7398	0.7566	0.7511	0.7611	2.9E−08	5E−07	1.4E−10	4.6E−09	1.6E−14	4.1E−13	0.4383	0.5948	0.0026	0.0014	7.8E−08	1.2E−05
Lipid metabolism	0.1314	0.0104	0.8725	0.4837	0.1397	0.7497	0.0605	0.7458	0.0279	0.0271	0.5781	0.7764	0.0255	0.0841	1.0000	0.7510
Transport—amino acids/purine–pyrimidine	0.4346	0.9213	0.3480	0.7611	0.4995	0.9240	0.6455	1.0000	0.8550	0.6946	0.6840	0.2599	0.0129	1.0000	0.9234	0.6156
Transport—sugar/carbohydrate	0.7398	1.0000	0.7511	0.4837	0.1817	0.0825	0.0028	0.2074	1.5E−05	0.0070	0.2652	0.2266	0.0033	0.3542	1.0000	0.4856
Nitrogen transport	0.7398	0.5148	1.0000	0.7611	0.3361	0.0040	0.0229	0.0289	0.0035	0.3151	0.7898	1.0000	0.0002	0.0764	1.0000	1.0000
Ion transport	1.0000	0.9370	0.7511	0.8338	0.8520	0.9390	0.4938	0.7668	0.5576	0.4150	0.4558	0.9165	1.0000	0.2244	0.0671	0.0802
Other transports (lipids, vitamins, drugs, and others)	0.0211	0.0004	0.3476	0.1054	0.0006	0.0001	5.8E−06	1E−05	2.7E−08	3.8E−05	0.0190	0.0349	8.3E−06	0.0034	0.0091	0.3027
Cell cycle	0.3007	0.6161	0.5446	0.4671	0.0017	0.0113	0.7805	0.0524	0.8016	0.2219	0.0334	0.7951	0.6904	1.0000	0.1039	0.4840
Total number of genes in the data set	1154	904	1168	945	1192	957	1414	943	1174	1029	1221	1540	557	328	82	72

Enrichment in dataset, $p_{adj} < 0.01$
Enrichment in dataset, $0.01 < p_{adj} < 0.05$
Underrepresentation in dataset, $p_{adj} < 0.01$
Underrepresentation in dataset, $0.01 < p_{adj} < 0.05$

Figure 6: Statistical analysis of FC enrichment/underrepresentation among DE genes. Fisher's exact test was used to determine whether the percentage of genes in an upregulated dataset that was mapped to a particular FC was significantly higher or lower than the percentage of genes in the yeast genome that was mapped to the same functional category. p values, adjusted for multiple testing using the Benjamini-Hochberg procedure (p_{adj}), are shown for selected FCs of genes, up- or downregulated in individual sample comparisons. Significantly enriched: pink (FDR 0.05) and dark pink (FDR 0.01). Significantly underrepresented: green (FDR 0.05) and dark green (FDR 0.01).

and tRNA/mRNA modification (31 genes). On the other hand, other genes repressed in U2 cells belong to functional categories repressed in U15 versus L15, such as genes involved in respiration (24 genes) and proteasome function (31 genes). These data indicate that U2 cells have more marked downregulation of some functions typically repressed in all U cells, such as respiration. In addition, U2 cells activate, to a lesser extent than U1 cells, some FCs typically upregulated in U15 versus L15 cells, such as those involved in ribosome functions and translation. These data also confirmed that expression differences observed between U2 and L15 cells are not simply caused by U2 sample contamination by L cells.

Comparison of L1 and L2 expression data identified 2144 DE genes, indicating prominent differences in these two cell subpopulations (Figure 8). Further comparison of L1 and L2 with L15 and U15 expression datasets revealed that expression characteristics of L2 cells are similar to those of L15. L2 and L15 cells differ in expression of only 184 genes, whereas, as expected, comparison of L2 and U15 datasets identified 2813 DE genes, which is a number similar to that for the L15/U15 comparison (2595 DE genes). On the other hand, comparison of L1 and L15 datasets identified 1997 DE genes, whereas comparison of L1 and U15 datasets identified only 648 DE genes, indicating more similarities between L1 and U15 than between L1 and L15. Mutual comparison of expression datasets of L1 and L2 with U1 and U2 further supported this conclusion (Figure 9). To gather more information about metabolic differences between L1 and L2 cell subpopulations, we performed functional categorization of expression datasets and compared them with the L15 and U15 functional groups (Figure 8). Comparison of FCs of genes differentially expressed among L1, L2, U15, and L15 confirmed similarity between L2 and L15 functional datasets. Differences between L2 and L15 datasets were small and, apart from unknown genes (41 genes), regard only individual genes spread among different functional groups. In accordance, comparison of L2 with U15 showed a similar profile of up- and downregulated FCs to the comparison of L15 and U15 (Figure 8). Functional categorization of the large number of genes differentially expressed in L1 versus L15 showed an extensive overlap with FCs differentially expressed in L1 versus L2 (1470 genes, 742 up- and 728 downregulated) as well as overlap with FCs up- and downregulated in U15 versus L15 cells (1616 genes, 654 up- and 962 downregulated) (Figure 8) supporting the prediction that L1 cells, in some metabolic aspects, resemble U15 cells. Comparison of L1 and U15 datasets further revealed 72 downregulated genes and 575 upregulated genes; 366 of the latter being also upregulated in L2 versus U15. These data show that cells in upper layers of the L cell subpopulation repress almost no specific genes when compared with U cells, but they increase expression of many L cell typical genes. L cell genes that are upregulated in both L1 and L2 versus U15 cells include genes involved in amino acid, carbohydrate and lipid metabolism, and respiration (altogether 46 genes); genes for several transporters (33 genes); and genes involved in cell wall function (26 genes), protein folding (11 genes), cell cycle (24 genes), signaling and transcription regulation (49 genes), and retrotransposons (33 genes). However, in addition, L1 cells versus U15 partially upregulate FCs comprised of genes that are typically downregulated in L15 cells versus U15 cells, such as genes involved in ribosome biogenesis (27 genes, 24 of which are downregulated in L2 versus U15 and/or L1) and translation and tRNA/mRNA modification (27 genes, 13 of which are downregulated in L2 versus U15 and/or L1). 72 genes downregulated in L1

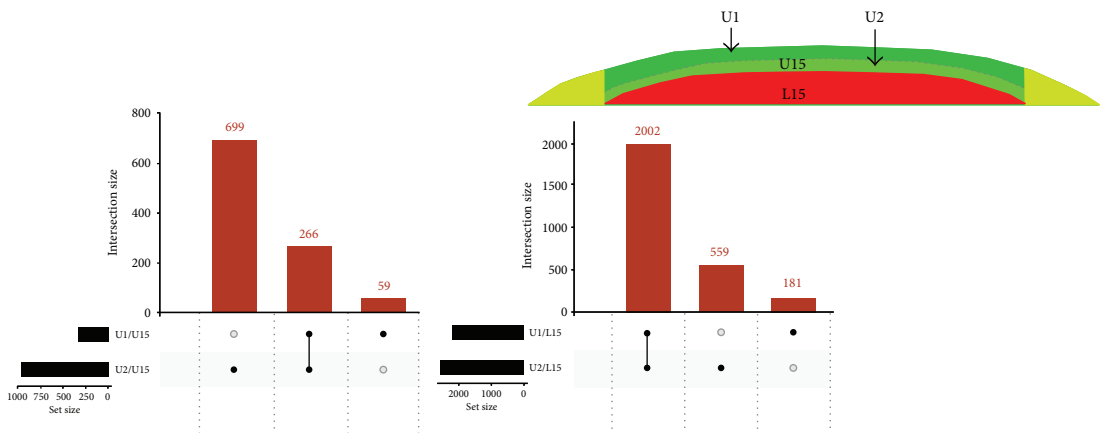

Functional categories	↑ U1/U15	↓ U1/U15	↑ U2/U15	↓ U2/U15	↑ U15/U1	↓ U15/U1	U1/U15	U2/U15	U15/U1	U15/U2	↑ U1/L15	↓ U1/L15	↑ U2/L15	↓ U2/L15	↑ L15/U1	↓ L15/U1	↑ L15/U2	↓ L15/U2	U15/L15	L15/U15
Amino acid/purine-pyrimidine metabolism	7	5	16	0	3	0	19	23	0	5	64	29	11	3	6	3	70	75	32	32	44	38
Carbohydrate metabolism	2	5	7	2	4	1	11	9	3	7	19	50	3	6	1	5	20	22	55	56	14	62
Lipid metabolism	4	4	10	5	0	2	10	14	7	9	27	40	9	6	6	4	33	36	44	46	28	46
Metabolism—reserves	0	2	1	0	0	0	1	1	0	2	1	14	0	1	0	0	1	1	14	15	1	13
Pentose phosphate pathway	0	0	1	0	0	0	1	1	0	0	4	3	0	0	0	1	4	4	4	3	2	4
Vitamin/coenzyme/cofactor metabolism	3	8	2	3	0	0	2	5	3	11	20	12	3	2	4	2	24	23	14	14	27	14
Respiration/ATP synthesis	2	24	3	3	1	0	4	5	3	27	7	52	3	9	1	1	8	10	53	61	10	51
Other metabolisms (phosphate, iron-sulphur, and others)	1	1	1	0	1	0	2	2	0	1	6	6	1	1	2	1	8	7	7	7	7	10
Transport—amino acids/purine-pyrimidine	5	0	6	1	0	0	6	11	1	1	9	6	4	1	1	2	10	13	8	7	4	12
Transport—sugars/carbohydrate	3	3	4	0	2	0	6	7	0	3	5	10	2	3	0	0	5	7	10	13	4	19
Nitrogen transport	2	0	3	0	1	0	4	5	0	0	1	6	2	0	1	0	2	3	6	6	2	8
Ion transport	3	6	10	2	0	1	10	13	3	8	22	16	7	6	4	1	26	29	17	22	18	30
Other transports (lipids, vitamins, drugs, and others)	8	1	10	4	0	0	10	18	4	5	23	22	8	3	1	2	24	31	24	25	11	28
Cell wall—assembly, integrity, and GPI anchor	7	1	35	1	4	0	39	42	1	2	24	21	1	6	1	2	25	25	23	27	14	45
Endocytosis/exocytosis	0	2	1	0	0	0	1	1	0	2	3	19	6	3	1	1	4	9	20	22	8	20
Vesicular trafficking	0	43	3	3	0	1	3	3	4	46	18	47	15	15	7	4	25	23	51	62	48	44
Protein trafficking to organelles	0	13	0	0	0	0	0	0	0	13	24	22	6	9	3	2	27	30	24	31	30	24
Protein modification	1	6	0	0	0	1	0	1	1	6	22	8	4	5	2	2	24	26	10	13	22	14
Organelle assembly and integrity	0	6	0	0	0	0	0	0	0	6	7	13	2	7	0	2	7	9	15	20	10	15
Vacuole assembly and functions	0	4	0	2	1	0	1	0	2	6	3	9	2	1	0	1	3	5	10	10	6	5
DNA damage response	0	17	0	2	0	0	0	0	2	19	5	15	8	2	1	0	6	13	15	17	23	10
Protein folding, chaperones, quality control, and aggregate removal	0	17	1	5	0	2	1	1	7	22	4	28	2	4	0	1	4	6	29	32	10	31
Stress response—oxidative	1	6	0	0	1	1	1	1	1	6	4	21	3	2	3	0	7	7	21	23	8	19
Stress response—others	0	5	4	0	0	0	4	4	0	5	4	16	0	2	1	0	5	4	16	18	3	20
Cell cycle	7	39	7	0	2	1	9	14	1	39	31	48	18	13	2	1	33	49	49	61	62	63
Actin, tubulin, myosin, and dynein	2	8	0	0	0	0	0	2	0	8	3	20	1	1	1	1	4	4	21	21	4	18
Ribosome biogenesis	5	51	1	0	1	0	2	6	0	51	57	8	25	9	2	0	59	82	8	17	101	7
Ribosome subunit	1	37	0	0	0	1	0	1	1	37	120	1	10	1	5	1	125	130	2	2	151	2
General transcription regulation	0	11	0	0	0	1	0	0	1	11	3	7	2	5	0	1	3	5	8	12	8	7
Polymerase subunit/assembly	0	4	1	0	0	0	1	1	0	4	8	1	3	0	0	0	8	11	1	1	14	0
General translation factor	0	1	0	0	0	0	0	0	0	1	6	0	1	0	0	0	6	7	0	0	7	0
Translation-tRNA and mRNA processing/modification/localization	5	31	3	4	2	2	5	8	6	35	78	47	32	12	18	6	96	110	53	59	129	46
Meiosis/sporulation/mating	4	19	6	2	0	1	6	10	3	21	16	34	9	4	1	1	17	25	35	38	37	34
Chromatin modification/regulation/telomere maintenance	1	28	0	0	1	2	1	1	2	28	18	30	16	10	2	1	20	34	31	40	43	30
Regulation transcription/transcription factor	6	14	5	2	0	0	5	11	2	16	10	63	5	10	3	6	13	15	69	73	18	75
Signaling	4	17	6	2	2	1	8	10	3	19	23	78	7	8	3	4	26	30	82	86	40	90
Autophagy	0	6	0	0	1	1	1	0	1	6	0	13	1	0	0	1	0	1	14	13	1	11
Proteasome/ubiquitin/ubiquitin-like	0	31	1	4	0	1	1	1	5	35	14	64	6	12	2	2	16	20	66	76	21	61
Protein degradation—others	1	2	1	1	1	0	2	2	1	3	5	22	5	3	0	1	5	10	23	25	5	25
Retrotransposon/ regulation	5	0	0	0	0	0	0	5	0	0	1	40	0	1	0	0	1	1	40	41	0	39
Others	2	0	0	0	1	0	1	2	0	0	5	1	3	1	2	0	7	8	1	2	8	5
Unknown/putative	27	84	42	13	2	1	44	69	14	97	86	188	41	54	12	14	98	127	202	242	242	252
Dubious ORF/pseudogene	13	5	13	0	6	1	19	26	1	5	17	24	9	22	5	0	22	26	24	46	27	67

Figure 7: Comparing small upper-cell subpopulations. UpSet plot of datasets of DE genes in small upper-cell subpopulations (U1 and U2) and upper (U15) and lower (L15) cells from 15-day-old colonies (upper part). Only major intersections are shown. Heat map of genes assigned to functional categories and clustered according to FC and DE in different sample comparisons (lower part). Number in heat map cell = number of genes from FC, up- or downregulated in sample comparison. The higher the number of up-/downregulated genes, the more intense the color. Arrows indicate upregulation/downregulation in the respective subpopulation ratio(s).

versus U15 are dispersed across many FCs, apart from a cluster of 14 genes involved in vitamin/cofactor metabolism. As expected, FCs upregulated in L1 versus U1 and L1 versus U2 (Figure 9) are similar to those upregulated in L1 versus U15. Interestingly, some FCs such as amino acid and lipid metabolism, cell cycle, signaling, proteasomal function, and unknown gene groups include more upregulated genes in L1 versus U2 than in the L1 versus U1 datasets. In accordance with this, the total number of upregulated genes is higher between L1 and U2 (329 genes) than between the L1 and U1 (208 genes) datasets. This indicates slightly greater expression differences between U2 and L1, despite these subpopulations being localized more closely within the colony than L1 and U1.

2.4. Spatiotemporal Gene Expression in Ageing Colonies. The expression data obtained provide an in-depth view of the functional gene groups, differentially expressed in time and space. In the following paragraphs and in the model (Figure 10), we summarize the major conclusions from these comparisons.

Comparison of the three major cell types (upper, lower, and margin cells) in young acidic-phase and older fully differentiated alkali-phase colonies clearly revealed the most

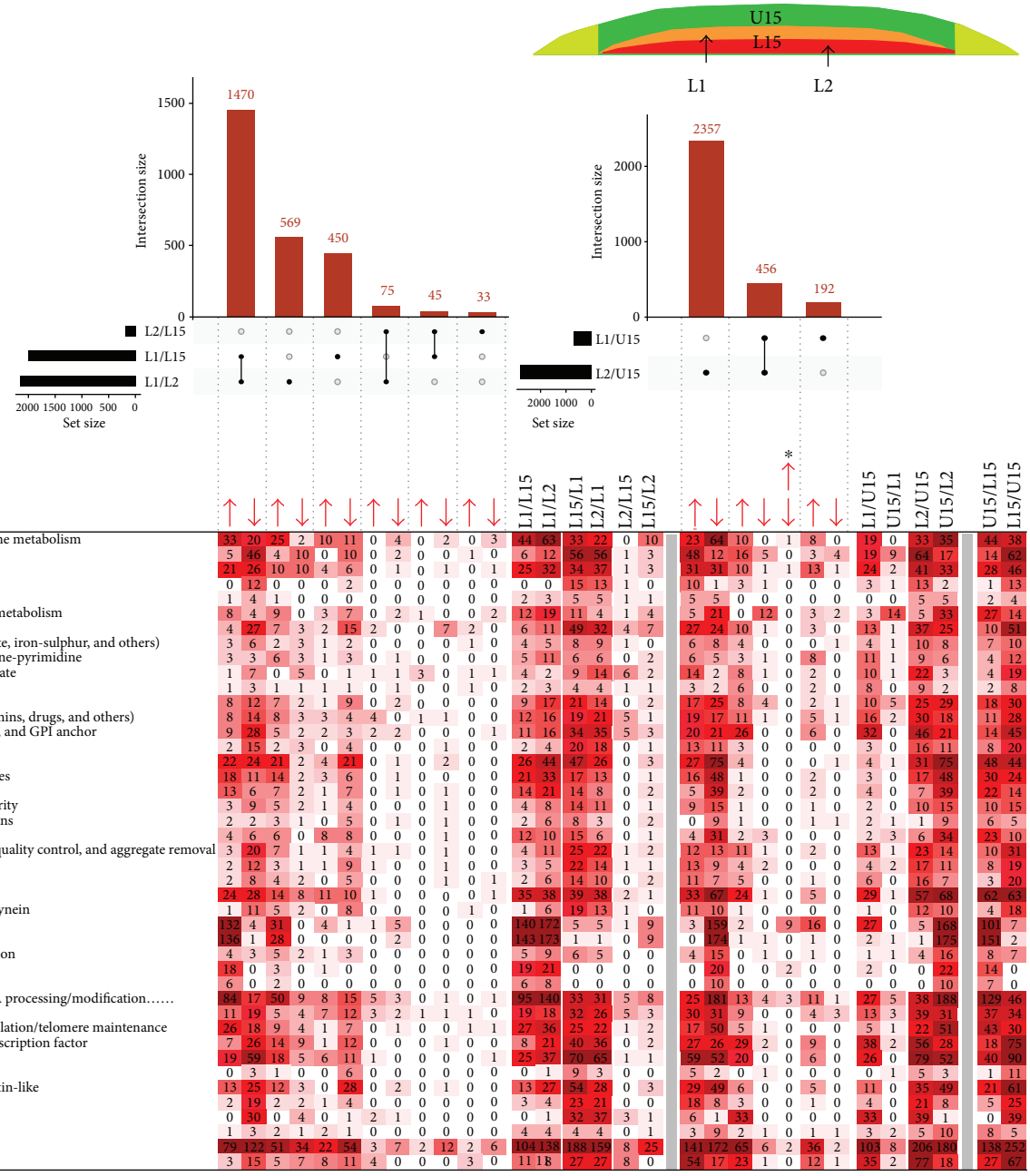

FIGURE 8: Comparing small lower-cell subpopulations. UpSet plot of datasets of DE genes in small lower-cell subpopulations (L1 and L2) and upper (U15) and lower (L15) cells from 15-day-old colonies (upper part). Only major intersections are shown. Heat map of genes assigned to functional categories and clustered according to FC and DE in different sample comparisons (lower part). Number in heat map cell = number of genes from FC, up- or downregulated in sample comparison. The higher the number of up-/downregulated genes, the more intense the color. Arrows indicate upregulation/downregulation in the respective subpopulation ratio(s); asterisk indicates the category of genes that are differently up-/downregulated in the respective subpopulation ratios.

prominent temporal changes in cells localized to upper colony layers (1120 genes), that is, in cells that differentiate during the colony transition from acidic- to alkali-phase into U cells, and which exhibit specific physiology and regulation as described previously [6, 13, 17, 22]. Most of these temporal changes regard genes whose expression changes neither in margin cells nor in lower cells during ageing (~700 genes). Interestingly, about twice as many of these U cell unique genes were repressed than activated in 15-day-old colonies compared to upper cells of younger, 6-day-old acidic-phase colonies. The repressed genes include those involved in respiration, that is, in a process previously shown to be dampened in U cells [6, 13], and are likely involved in determining some of the specific properties of U cells, such as activation of individual branches of RTG signaling subsequently causing changes in gene expression [17]. In contrast to upper cells, many fewer temporal expression changes were observed at the colony margin (442 genes) despite the fact that these cells

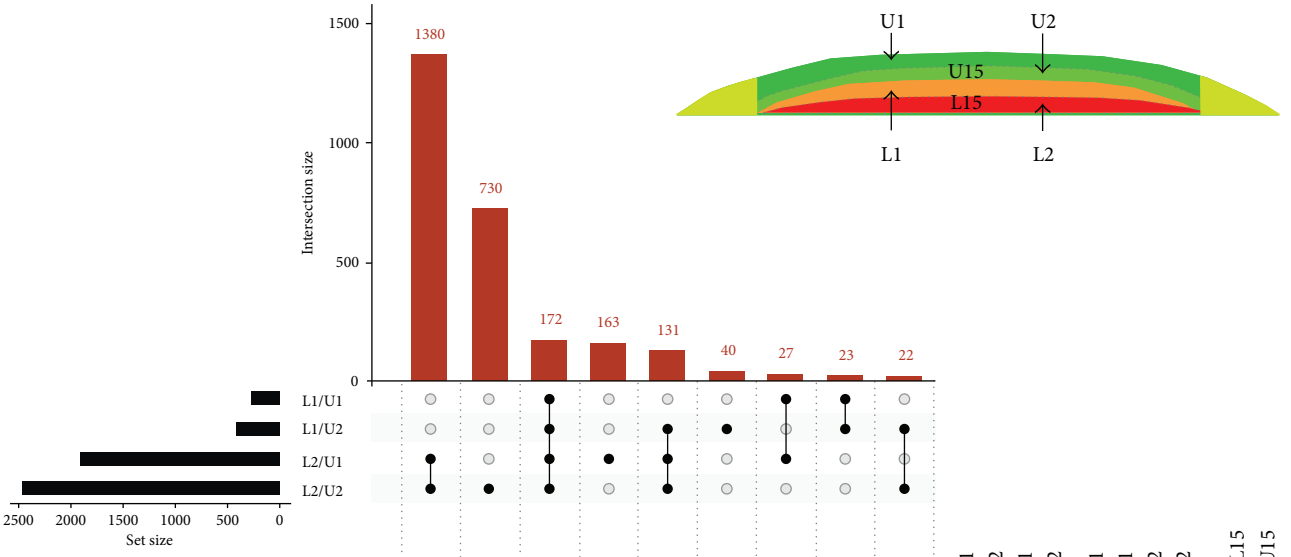

Functional categories	L1/U1	L1/U2	L2/U1	L2/U2	U1/L1	U2/L1	U1/L2	U2/L2	U15/L15	L15/U15
Amino acid/purine-pyrimidine metabolism	5 6 25 27	8 3 71 82	44 38
Carbohydrate metabolism	8 14 56 57	12 12 19 20	14 62
Lipid metabolism	8 14 40 40	2 1 35 39	28 46
Metabolism—reserves	2 3 14 11	0 0 0 1	1 13
Pentose phosphate pathway	0 0 5 5	1 1 5 5	2 4
Vitamin/coenzyme/cofactor metabolism	0 2 7 10	7 6 25 25	27 14
Respiration/ATP synthesis	9 11 39 41	1 0 16 15	10 51
Other metabolisms (phosphate, iron-sulphur, and others)	1 2 6 10	1 1 8 7	7 10
Transport—amino acids/purine-pyrimidine	2 2 7 6	1 1 11 14	4 12
Transport—sugars/carbohydrate	2 3 15 21	0 0 4 4	4 19
Nitrogen transport	2 3 7 5	0 0 2 3	2 8
Ion transport	2 2 12 17	11 5 27 27	18 30
Other transports (lipids, vitamins, drugs, and others)	9 8 24 27	3 4 21 25	11 28
Cell wall—assembly, integrity, and GPI anchor	3 6 21 27	14 10 27 30	14 45
Endocytosis/exocytosis	2 4 19 20	0 0 10 11	8 20
Vesicular trafficking	4 8 32 39	1 0 42 46	48 44
Protein trafficking to organelles	1 3 16 22	0 0 36 38	30 24
Protein modification	1 2 5 8	2 1 30 33	22 14
Organelle assembly and integrity	0 2 13 17	2 0 8 11	10 15
Vacuole assembly and functions	1 0 5 6	0 0 8 5	6 5
DNA damage response	1 1 9 11	0 0 18 15	23 10
Protein folding, chaperones, quality control, and aggregate removal	14 15 27 29	0 0 7 7	10 31
Stress response—oxidative	4 6 16 18	1 0 9 8	8 19
Stress response—others	6 8 12 15	1 1 8 6	3 20
Cell cycle	9 16 42 55	2 0 36 56	62 63
Actin, tubulin, myosin, and dynein	1 2 14 17	1 0 5 6	4 18
Ribosome biogenesis	4 5 6 6	1 1 131 135	101 7
Ribosome subunit	1 1 1 0	4 5 155 153	151 2
General transcription regulation	0 1 4 8	1 0 9 10	8 7
Polymerase subunit/assembly	0 1 0 1	0 0 19 14	14 0
General translation factor	0 0 0 0	0 0 8 8	7 0
Translation-tRNA and mRNA processing/modification…	11 9 33 32	5 3 138 148	129 46
Meiosis/sporulation/mating	3 7 33 35	4 2 22 30	37 34
Chromatin modification/regulation/telomere maintenance	2 7 23 24	0 0 29 35	43 30
Regulation transcription/transcription factor	17 22 52 57	0 0 16 21	18 75
Signaling	9 18 75 77	0 0 37 43	40 90
Autophagy	0 1 6 8	0 0 1 2	1 11
Proteasome/ubiquitin/ubiquitin-like	8 22 48 45	1 0 25 26	21 61
Protein degradation—others	1 3 20 23	0 0 5 11	5 25
Retrotransposon/ regulation	23 24 39 37	0 0 0 1	0 39
Others	0 0 3 2	3 1 8 7	8 5
Unknown/putative	29 59 153 193	20 14 142 160	138 252
Dubious ORF/pseudogene	3 5 26 33	16 10 39 49	27 67

Figure 9: Comparing small upper- and lower-cell subpopulations. UpSet plot of datasets of DE genes in small lower-cell (L1 and L2) and small upper-cell (U1 and U2) subpopulations from 15-day-old colonies (upper part). Only major intersections are shown. Heat map of genes assigned to functional categories and clustered according to FC and DE in different sample comparisons (lower part). Number in heat map cell = number of genes from FC, up- or downregulated in sample comparison. The higher the number of up-/downregulated genes, the more intense the color. Arrows indicate upregulation/downregulation in respective subpopulation ratio(s).

exhibit extensive similarities with U cells as shown by upper-/margin-/lower-cell comparisons in both developmental times. In addition, most of the expression changes occurring in marginal cells between days 6 and 15 also occur in upper cells or in both upper and lower cells over the same time period. Unique temporal changes in margin cells thus concern only ~70 genes, that is, ten times fewer genes than changes in U cells. The lowest number of temporal expression changes occur in lower cells (258 genes in total), but, as in upper cells, many of these changes (~120 genes) involve unique genes that do not change expression in upper and marginal cells during the time period. In contrast to U cells,

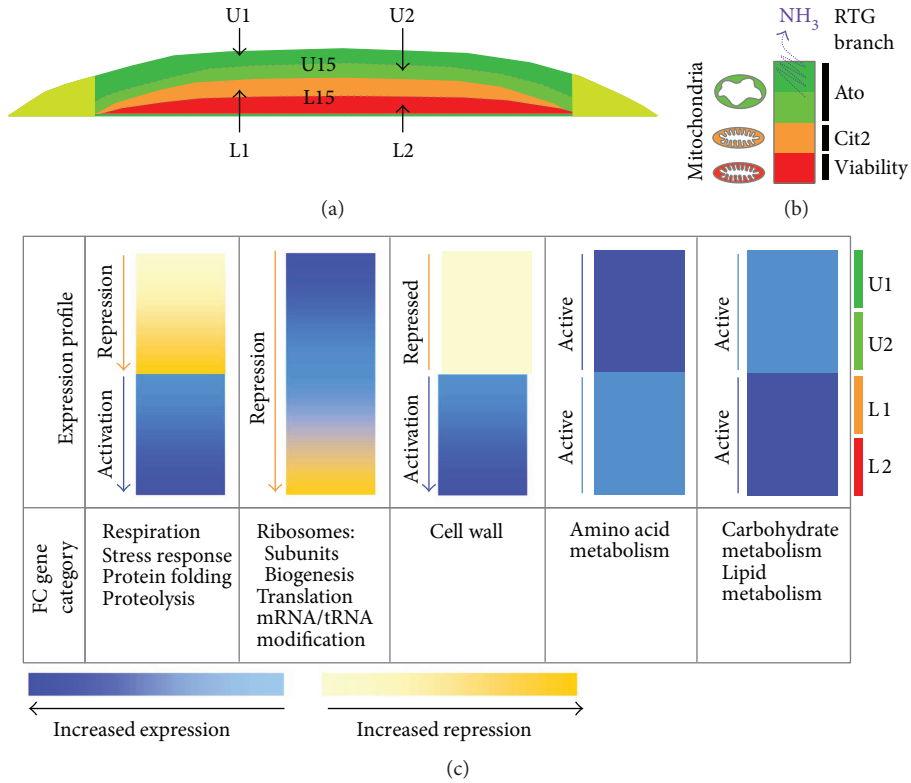

Figure 10: Functional category (FC) expression through a yeast colony. (a) Diagram of 15-day-old colony subpopulations analyzed by RNA-seq in this study. (b) Overview of RTG regulatory pathway branches that are functional in fully differentiated 15-day-old colonies [17, 39]. (c) Based on the differential expression of constitutive genes in different population/subpopulation comparisons in 15-day-old colonies, a schematic was produced indicating expression/repression of various FCs through the colony cross-section from uppermost (U1) to lowest (L2) subpopulation in the colony centre. Increased color density corresponds to increased activation (blue) or repression (yellow) as indicated in bars below the pictures.

three times as many of these unique DE genes were upregulated than downregulated in L cells of 15-day-old colonies. These findings indicate that in contrast to U cells (and, to a lesser extent, also to L cells), marginal cells, which are the most efficiently growing cell subpopulation even in older colonies [23], undergo almost no margin-cell-type-specific changes during colony ageing.

Temporal differences in gene expression of upper, lower, and marginal cells were in agreement with observed differences among these cell subpopulations at individual time points. At both time points (day 6 and day 15), the most prominent cell-type-specific differences were seen between upper and lower cells, where 616 differentially expressed genes were identified only in U6 versus L6 and 711 only in U15 versus L15 cells. On the other hand, a much smaller number of genes exhibited differential expression uniquely between marginal and lower cells (150 and 180 genes at day 6 and day 15, resp.) and negligible expression differences were identified uniquely between upper and marginal cells (20 and 48 genes at days 6 and 15, resp.). The most prominent differences occurring among subpopulations at both time points concerned genes differentially expressed between lower cells and the rest of the colony (i.e., both upper and marginal cells) (1554 and 1512 genes at days 6 and 15, resp.). This finding argues that the greatest similarity exists between upper and marginal cells, which is in accordance with the observation that several protein markers of U cells are also produced in marginal cells, but not in L cells [6, 13, 24]. Although 2.5 times fewer genes were DE relative only to U cells as relative to both U and M, several important FC categories were overrepresented in the former dataset. Examples include genes involved in cell wall function, proteasomes, and meiosis and among U cell-repressed genes involved in respiration, vitamin metabolism, vesicular transport, and cell cycle.

Comparison of small subpopulations derived from U cells (U1 and U2 cell) and from L cells (L1 and L2), to each other and with U15 and L15 cells, provided additional insight into colony complexity (Figure 10). L1 and L2 cells, although morphologically similar, with large vacuoles and other typical characteristics [6, 13, 17], exhibited distinct profiles of DE genes indicating that these cell subpopulations differ significantly. Whereas L2 cells are similar to L15 cells, L1 cells differ from both L2 and L15 in many parameters similar to differences between U15 and L15; L1 cells were thus, to some extent, similar to U15 cells. The L1 to U15 similarity was particularly evident when comparing L1 versus U15 repressed genes, among which only one prominent functional category of genes (involved in vitamin metabolism) was detected. On the other hand, genes belonging to several FCs typically upregulated in L15 cells were also upregulated in L1 cells, including the categories of respiration, cell wall

function, protein folding, proteasomes, and retrotransposons. Thus, L1 cells combine several L cell-specific features with some features typical of U cells, such as expression of many genes encoding ribosome subunits or involved in ribosome biogenesis, translation, and tRNA/mRNA modification. Similar to U and L cells, functional categories of metabolic genes (amino acid, carbohydrate, and lipid metabolism) are active in both L1 and L2 cells and differ regarding the expression of individual genes. In contrast to L1 and L2 cells, differences between U1 and U2 cells were small and no DE genes were identified by direct comparison of these subpopulations. However, comparison of U1 and U2 subpopulations with larger subpopulations of U15 and L15 cells as well as with L1 and L2 revealed some significant differences. The identified U1 and U2 differences in particular concern FCs of genes that are repressed in U2 versus U15 (but not repressed in U1 versus U15). These FCs include on one hand those that are also typically repressed in U15 cells versus L15 cells, such as respiration, protein folding, and proteasomal functions, but on the other hand, also those that are typically repressed in L15 cells versus U15 cells, such as ribosomal subunits or ribosome biogenesis, translation, and mRNA/tRNA modification. Hence, these data show that U2 cells repress some genes similarly to L cells but that, on the other hand, some processes typically repressed in U cells but active in L cells, such as respiration, are more effectively repressed in U2 cells than in U1 (and U15) cells.

2.5. Respiration and Stress-Related Process Exhibit Similar Spatiotemporal Profiles within Developing Colonies. Previous study of the dynamics and development of fully differentiated and morphologically distinct U and L cells [6] showed that the differentiation process lasts several days, starting at about 9-10 days and resulting in fully developed and sharply separated U and L cell layers at ~day 14. Here, we show that metabolic diversification, especially of cells located in upper colony parts, has already started in younger colonies that are in late acidic phase and formed of cells that are still morphologically relatively homogeneous. This concerns particularly the expression of genes involved in ribosome function and translation in upper cells, and genes for proteasomal functions, retrotransposons, and stress response in lower cells of 6-day-old colonies. These differences persist and become more pronounced in fully differentiated U and L cells of 15-day-old colonies, despite the large variation in expression of individual genes being observed within these groups over time. This finding shows that cellular features are to a certain extent determined by cell position within the colony as early as late acidic phase, in which colonies are still linearly growing [23]. This finding also shows that in colonies as young as 6 days, cells located in lower positions closer to agar with better access to nutrients than upper cells already exhibit some features of starvation and stress, such as activation of heat shock genes, stress-defense genes, and genes for proteasomes. Concurrently, colony cells start to diversify the expression of FCs including genes involved in oxidative phosphorylation (OXPHOS) and in respiration-dependent ATP synthesis in mitochondria. When compared with lower cells, most of the DE genes belonging to this FC

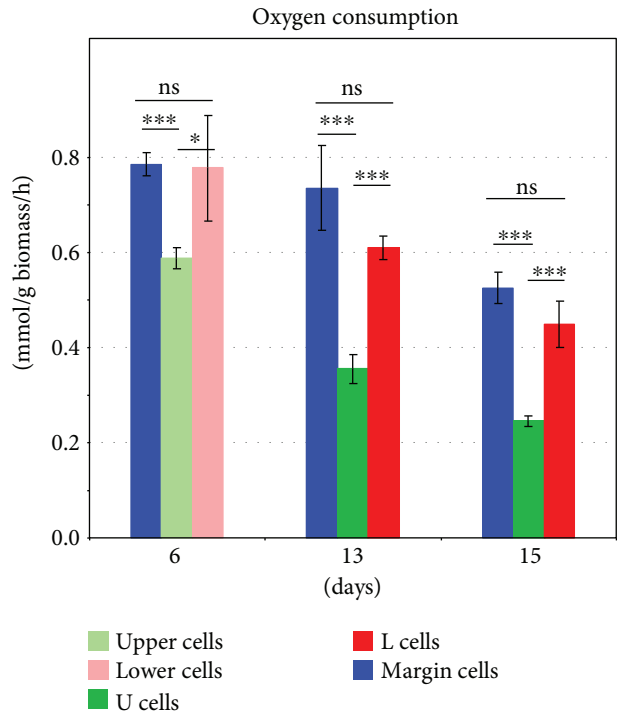

Figure 11: Oxygen consumption by cell subpopulations from 6-, 13-, and 15-day-old colonies. The mean of four biological replicates is shown ±SD. *t*-test *p* values of 0.05 or less were considered statistically significant: $^{*}p < 0.05$ and $^{***}p < 0.001$; ns: not significant.

are downregulated in both upper and marginal cells, indicating reduced mitochondrial activity, despite the facts that both upper and marginal cells have good access to air (and oxygen), that the colonies were grown on complete respiratory medium, and that marginal (and to some extent upper) cells are still dividing in colonies during this developmental stage. Thus, already in 6-day-old colonies, mitochondria may be less active in upper cells that do not exhibit stress features, than in lower cells that are becoming stressed. Simple oxygen consumption experiments (Figure 11) confirmed decreased oxygen consumption by upper cells relative to lower cells of 6-day-old acidic-phase colonies, but did not identify differences between margin and lower cells.

Later on in colony development, U cells of 15-day-old alkali-phase colonies downregulate most of the DE genes of the OXPHOS/ATP synthesis functional category, compared with L cells. This is in agreement with previous findings concerning the differences in mitochondrial morphology and oxygen consumption measured in separated U and L cells as well as in OXPHOS gene expression determined by microarrays [6, 13]. However, the current study revealed a more complex view of the expression of OXPHOS/ATP synthesis genes in differentiated U, M, and L cells and their subpopulations. Expression of these genes was observed in the following degrees: U15 < M15 < L15. Oxygen consumption experiments (Figure 11) confirmed reduced oxygen consumption by U cells compared with both L and M cells of 15-day-old colonies but, similarly to 6-day-old colonies, did not identify significant differences between M and L cells.

Time-line comparison of cells from 6-, 13-, and 15-day-old colonies showed, in addition, a gradual decrease in oxygen consumption by all subpopulations as colonies aged. Transcriptomic comparison of smaller subpopulations showed that U2 cells (which are localized nearer to L1 cells) are the subset of U cells that exhibits the absolutely lowest expression level of OXPHOS/ATP synthesis genes, whereas L2 cells exhibited highest expression (Figure 10(c)). Whether these differences are reflected in differences in oxygen consumption remains to be resolved as our currently used measurements are not suitable for tiny subpopulations. The observed pattern of expression of the FC including OXPHOS/ATP synthesis genes overlaps with that of other FC groups, including a group of stress-related genes (genes involved in protein folding and stress response). This in turn indicates that metabolic reprogramming, leading to a decrease in respiration when nutrients start to be limited (as what happens during colony ageing), may alleviate the stress. Our new data also indicate that the cells at the boundaries of U and L cells (i.e., U2 and L1) differ significantly in the expression of genes belonging to these FCs, as they differ in other prominent features, including cell morphology which shows a sharp demarcation border between U and L cells [6, 13, 17]. On the other hand, the data indicate that at least some of the FCs that are already upregulated in upper cells in late acidic-phase colonies and that continue to be upregulated in alkali-phase colonies, such as FCs related to ribosome functions and translation, exhibit a gradual gradient-like pattern of expression, being most highly upregulated in the upper-most colony cell layers (U1 cells) and decreasing expression towards lower-cell layers (L2 cells) (Figure 10(c)).

In summary, the major differences between cells located near the demarcation border between morphologically distinct U and L cells represent functional gene categories that are upregulated in all L cells and repressed most in U2 cells, such as genes involved in respiration. Expression data of these FCs indicate a gradient of gene repression in U cells in the direction U1 → U2 and conversely a gradient of gene activation in L cells in the direction L1 → L2. On the other hand, L1 cells do not differ dramatically from U2 cells in terms of the expression of functional groups typically upregulated in U cells, such as groups of ribosome and translation-specific genes. The observed pattern of expression of OXPHOS/ATP synthesis genes in 15-day-old colonies indicates that mitochondrial properties may differ not only among U and L cells as described previously [6, 13], but potentially also among the cell layers within these subpopulations. Subsequently, divergent mitochondria may be involved in different cellular processes including the activation of different branches of RTG signaling that contribute to the colony differentiation processes [17]. A link between mitochondrial properties and RTG pathway specificities is also supported by the observation that, despite OXPHOS/ATP synthesis gene expression and oxygen consumption being lowest in upper cells (compared with both lower and marginal cells), oxygen consumption and the expression of genes of this FC differ between days 6 and 15: OXPHOS/ATP synthesis genes are more highly repressed and oxygen consumption reduced in U15 cells (that activate the Ato branch and in parallel repress the Cit2 branch of RTG signaling) compared to U6 cells that have an active Cit2 branch. In addition, the expression of respiratory genes is highest in L2 cells in 15-day-old colonies, that is, in a subpopulation that activates the cell-viability branch of RTG signaling (unrelated to Cit2 and Ato branches) that is necessary for longevity of L2 cells (Figure 10(b) and [17]). Nevertheless, expression data and physiology data do not always correlate, as demonstrated by margin and lower-cell comparisons. Further analyses of the biochemistry and activities of mitochondria from differentiated cell subpopulation, and of their relationship with other specific cellular properties, are therefore needed to demonstrate potential functions of differently altered mitochondria in RTG signaling and in other cellular processes during the colony differentiation process.

3. Conclusions

Genome-wide expression profiling provided us with a complex view of the spatiotemporal changes that occur during chronological ageing of *S. cerevisiae* colonies passing through distinct acidic and alkali developmental phases and undergoing ammonia signaling-related U/L cell differentiation [6, 9, 13]. Major morphological and physiological differences between the U and L cell subpopulations become fully developed within alkali-phase colonies, and U and L cells are sharply demarcated within these colonies [6, 13]. However, new data provides evidence that some of the features typical of U and L subpopulations have already started to develop in earlier phases and that, while prominent expression changes exist in individual genes between day 6 and day 15, especially in upper cells, major DE functional gene categories are relatively preserved. Functional categorization thus shows which metabolic and other processes are important in each of the colony subpopulations, what the relationships between the particular cell types are, and what their similarities and differences are in relation to their age and position within the colony. However, more detailed analyses of individual genes combined with additional biochemical analyses will be needed to understand the dynamics of changes within particular functional groups and thus changes related to particular metabolic processes and functions of individual genes.

4. Materials and Methods

4.1. Strains and Cultivation. *S. cerevisiae* strain BY4742 (*MATa*, *his3*Δ, *leu2*Δ, *lys2*Δ, and *ura3*Δ) was obtained from the EUROSCARF collection. Yeast giant colonies (6 per plate) were grown at 28°C on GMA (1% yeast extract, 3% glycerol, 2% agar, 1% ethanol, 10 mM $CaCl_2$, 0.05% glucose, and 0.002% uracil) with pH dye indicator bromocresol purple.

4.2. Separation of Cell Subpopulations and RNA Isolation. Individual cell layers were harvested from colonies by micromanipulation as described previously [17]. Three particular cell populations were separated from 6-day-old acidic-phase colonies (samples M6, U6, and L6) and from fully

differentiated 15-day-old colonies in the alkali phase (samples M15, U15, and L15). Biomass of each cell sample was harvested from at least 60 colonies (day 6) or 24 colonies (day 15). Cells from 15-day-old colonies were stepwise separated into four smaller subpopulations called U1 ("U upper" cells), U2 ("U lower" cells), L1 ("L upper" cells), and L2 ("L lower" cells), that is, U and L cell layers were equally divided into two individual cell subpopulations. Biomass of each small subpopulation was harvested from at least 24 differentiated colonies. The RNA was isolated from three independent biological replicates. The purity of the cell fractions was controlled by Nomarski contrast microscopy. Total RNA was extracted using the hot-phenol extraction procedure as previously described [25]. To verify the quality and quantity of the RNA extracted, spectrophotometric and electrophoretic analyses were performed. The absorbance of the samples was analyzed at 230, 260, and 280 nm. The total RNA (20 μg) from each replicate was DNase treated using a GenElute™ Mammalian Total RNA Miniprep Kit (Sigma-Aldrich).

4.3. cDNA Library Preparation and RNA Sequencing. Total RNA (4 μg) from each replicate was spiked with 1 μl of ERCC RNA Spike-In Control Mix 1 (Life Technologies) according to manufacturer's instructions. Ribosomal RNA was depleted from all samples using the Ribo-Zero Gold (yeast) rRNA Removal Kit (Illumina Inc., San Diego, CA) followed by purification using Agencourt RNAClean XP reagents (Beckman Coulter, Brea, CA). Efficient rRNA removal was confirmed using a 2100 Bioanalyzer system (Agilent Technologies, Santa Clara, CA). Strand-specific sequencing libraries were prepared from 50% of the depleted rRNA (equivalent to 2 μg total RNA starting material) using a TruSeq Stranded Total RNA Library Prep Kit (Illumina Inc., San Diego, CA) with dual-indexed adapters, employing 15 PCR amplification cycles. A single pool of all samples was sequenced on two lanes of an Illumina HiSeq 3000 system (Illumina, San Diego, CA) with 150 bp paired-end reads, yielding a high-quality, high-coverage transcriptome library with ~12.6 to 23 million sequencing reads per replicate. 96–98% of reads were mapped to 10,409 coding and noncoding loci or to intergenic regions of the yeast genome. For all replicates, 52–72% of mapped reads were mapped to coding or noncoding loci, 16–33% to 5′ and 3′ UTRs, 9–15% to intergenic regions, and 0.3–1% to introns (Figure S1A). 54–82% of reads, mapping to genomic loci, mapped to coding genes and 18–45% to lncRNA (long noncoding RNA) loci (Figure S1B). Retention of strand information was confirmed by visual inspection using the Integrative Genomic Viewer [26].

4.4. Read Mapping, Counting, and Differential Expression Analysis. Reads were mapped to the SacCer3 reference genome and to a custom transcriptome (GTF file), incorporating the coding loci of *S. cerevisiae* build R64 (Ensembl release 76, [27]), ERCC spike-in transcript loci [28], and deduplicated lncRNA loci longer than 200 bp from previous studies [29–33]. Mapping was carried out using the STAR aligner [34]. Mapped reads were counted using "featureCounts" [35] from the Bioconductor RSubreads package v1.22.2. Read counts for technical replicates were added together to produce biological replicate counts. DESeq2 v1.12.3 [36] within R version 3.3.1 was used for differential expression analysis, and normalization/removal of unwanted variation (arising from technical effects) was carried out using RUVseq package v1.10.0 [37] from Bioconductor, using 36 spike-in transcripts, with inter-replicate standard deviation/mean count ratios below 0.3, as negative controls.

4.5. Validation of RNA-seq Analysis by qPCR. qPCR was designed to verify the differences in gene expression of selected target genes identified by RNA-seq analysis. A 1 μg sample of RNA (the same as that used for RNA-seq) was used to synthesize first-strand cDNA. The reverse transcription reactions were performed with Random Primer Mix (S1330S, NEB) using the SuperScript™ III Reverse Transcriptase (Invitrogen) following the manufacturer's instructions. The mRNA levels of target genes were quantified by real-time PCR analysis on LightCycler®480II (Roche) using SYBR® Select Master Mix (Applied Biosystems) with 2 μl of template cDNA (5-fold dilution after RT reaction) in 10 μl reaction volume according to the manufacturer's protocol. All reactions were run in triplicate and cycle threshold (C_T) values for target genes were normalized to up to 5 housekeeping genes (*RPB2*, *TAF6*, *COG1*, *RAD52*, and *RDN25-1*) selected according to their expression profiles in cell populations. 15 genes with different expression in different cell populations were selected as targets. Primers designed for each gene are given in Table S1. The fold change in the expression of the target genes was calculated using the formula: $2^{-\Delta\Delta C_T}$, where ΔC_T = average C_T of the target gene − average C_T of endogenous control (housekeeping gene), and $\Delta\Delta C_T = \Delta C_T$ of the target sample (cell population 1) − ΔC_T of the calibrator sample (cell population 2). The mean of normalized values was used for comparison with RNA-seq data.

4.6. Respiration Rate Measurement. The oxygen consumption of 2 mg of freshly isolated U6, M6, L6, U15, M15, and L15 wet cell biomass was determined at 30°C in 1 ml of water using a 782 oxygen meter with a 1 ml MT-200A cell (Strathkelvin Instruments) as described previously [7].

4.7. FC Enrichment/Reduction among DE Genes. Fisher's exact test was used to assay the significance of FC enrichment/underrepresentation among genes, up- or down-regulated in a particular comparison and the Benjamini-Hochberg procedure used to control the false discovery rate. These steps were carried out using rcompanion package 1.10.1 [38]. A FC was deemed to be enriched/underrepresented among an upregulated gene dataset if the percentage of upregulated genes that were included in the FC was significantly higher/lower ($p_{adj} < 0.05$) than the percentage of genes in the yeast genome that belong to the same FC.

Conflicts of Interest

The authors declare that they have no conflicts of interest.

Authors' Contributions

Jana Maršíková and Otakar Hlaváček contributed equally to this paper.

Acknowledgments

The research leading to these results has received funding from the Norwegian Financial Mechanism 2009–2014 under Project Contract no. MSMT-28477/2014 (7F14083) and from GACR 15-08225S. Jana Maršíková, Derek Wilkinson, and Zdena Palková are also supported by LQ1604 NPU II provided by MEYS and Libuše Váchová by RVO61388971, and part of the research was performed in BIOCEV-supported by CZ.1.05/1.1.00/02.0109 BIOCEV provided by ERDF and MEYS.

Supplementary Materials

Figure S1: Read mapping. For each sample, the percentages of reads, mapping to different genomic features (A), and the percentages of locus-mapped reads, mapping to genes and to lncRNA (B), were calculated and plotted as bar charts. Table S1: List of the primers. (*Supplementary Materials*)

References

[1] J. A. Granek, O. Kayikci, and P. M. Magwene, "Pleiotropic signaling pathways orchestrate yeast development," *Current Opinion in Microbiology*, vol. 14, no. 6, pp. 676–681, 2011.

[2] S. M. Honigberg, "Cell signals, cell contacts, and the organization of yeast communities," *Eukaryotic Cell*, vol. 10, no. 4, pp. 466–473, 2011.

[3] Z. Palkova and L. Vachova, "Life within a community: benefit to yeast long-term survival," *FEMS Microbiology Reviews*, vol. 30, no. 5, pp. 806–824, 2006.

[4] Z. Palkova and L. Vachova, "Yeast cell differentiation: lessons from pathogenic and non-pathogenic yeasts," *Seminars in Cell & Developmental Biology*, vol. 57, pp. 110–119, 2016.

[5] Z. Palkova, D. Wilkinson, and L. Vachova, "Aging and differentiation in yeast populations: elders with different properties and functions," *FEMS Yeast Research*, vol. 14, no. 1, pp. 96–108, 2014.

[6] M. Cáp, L. Stěpánek, K. Harant, L. Váchová, and Z. Palková, "Cell differentiation within a yeast colony: metabolic and regulatory parallels with a tumor-affected organism," *Molecular Cell*, vol. 46, no. 4, pp. 436–448, 2012.

[7] M. Cap, L. Vachova, and Z. Palkova, "Longevity of U cells of differentiated yeast colonies grown on respiratory medium depends on active glycolysis," *Cell Cycle*, vol. 14, no. 21, pp. 3488–3497, 2015.

[8] L. Vachova, M. Cap, and Z. Palkova, "Yeast colonies: a model for studies of aging, environmental adaptation, and longevity," *Oxidative Medicine and Cellular Longevity*, vol. 2012, Article ID 601836, 8 pages, 2012.

[9] Z. Palkova, F. Devaux, M. Ricicova, L. Minarikova, S. Le Crom, and C. Jacq, "Ammonia pulses and metabolic oscillations guide yeast colony development," *Molecular Biology of the Cell*, vol. 13, no. 11, pp. 3901–3914, 2002.

[10] Z. Palkova, B. Janderova, J. Gabriel, B. Zikanova, M. Pospisek, and J. Forstová, "Ammonia mediates communication between yeast colonies," *Nature*, vol. 390, no. 6659, pp. 532–536, 1997.

[11] L. Vachova, H. Kucerova, F. Devaux, M. Ulehlova, and Z. Palkova, "Metabolic diversification of cells during the development of yeast colonies," *Environmental Microbiology*, vol. 11, no. 2, pp. 494–504, 2009.

[12] Z. Palkova and J. Forstova, "Yeast colonies synchronise their growth and development," *Journal of Cell Science*, vol. 113, pp. 1923–1928, 2000.

[13] L. Vachova, L. Hatakova, M. Cap, M. Pokorna, and Z. Palkova, "Rapidly developing yeast microcolonies differentiate in a similar way to aging giant colonies," *Oxidative Medicine and Cellular Longevity*, vol. 2013, Article ID 102485, 9 pages, 2013.

[14] S. M. Jazwinski, "The retrograde response: a conserved compensatory reaction to damage from within and from without," *Mitochondrion in Aging and Disease*, vol. 127, pp. 133–154, 2014.

[15] R. A. Butow and N. G. Avadhani, "Mitochondrial signaling: the retrograde response," *Molecular Cell*, vol. 14, no. 1, pp. 1–15, 2004.

[16] T. Sekito, J. Thornton, and R. A. Butow, "Mitochondria-to-nuclear signaling is regulated by the subcellular localization of the transcription factors Rtg1p and Rtg3p," *Molecular Biology of the Cell*, vol. 11, no. 6, pp. 2103–2115, 2000.

[17] K. Podholova, V. Plocek, S. Resetarova et al., "Divergent branches of mitochondrial signaling regulate specific genes and the viability of specialized cell types of differentiated yeast colonies," *Oncotarget*, vol. 7, no. 13, pp. 15299–15314, 2016.

[18] W. S. Noble, "How does multiple testing correction work?," *Nature Biotechnology*, vol. 27, no. 12, pp. 1135–1137, 2009.

[19] A. Khan and A. Mathelier, "Intervene: a tool for intersection and visualization of multiple gene or genomic region sets," *BMC Bioinformatics*, vol. 18, no. 1, p. 287, 2017.

[20] J. L. DeRisi, V. R. Iyer, and P. O. Brown, "Exploring the metabolic and genetic control of gene expression on a genomic scale," *Science*, vol. 278, no. 5338, pp. 680–686, 1997.

[21] A. P. Gasch, P. T. Spellman, C. M. Kao et al., "Genomic expression programs in the response of yeast cells to environmental changes," *Molecular Biology of the Cell*, vol. 11, no. 12, pp. 4241–4257, 2000.

[22] M. Cap, L. Vachova, and Z. Palkova, "Yeast colony survival depends on metabolic adaptation and cell differentiation rather than on stress defense," *The Journal of Biological Chemistry*, vol. 284, no. 47, pp. 32572–32581, 2009.

[23] L. Vachova and Z. Palkova, "Physiological regulation of yeast cell death in multicellular colonies is triggered by ammonia," *The Journal of Cell Biology*, vol. 169, no. 5, pp. 711–717, 2005.

[24] L. Váchová, O. Chernyavskiy, D. Strachotová et al., "Architecture of developing multicellular yeast colony: spatio-temporal expression of Ato1p ammonium exporter," *Environmental Microbiology*, vol. 11, no. 7, pp. 1866–1877, 2009.

[25] M. Cáp, L. Váchová, and Z. Palková, "Yeast colony survival depends on metabolic adaptation and cell differentiation rather than on stress defense," *The Journal of Biological Chemistry*, vol. 284, no. 47, pp. 32572–32581, 2009.

[26] H. Thorvaldsdottir, J. T. Robinson, and J. P. Mesirov, "Integrative genomics viewer (IGV): high-performance genomics data visualization and exploration," *Briefings in Bioinformatics*, vol. 14, no. 2, pp. 178–192, 2013.

[27] A. Yates, W. Akanni, M. R. Amode et al., "Ensembl 2016," *Nucleic Acids Research*, vol. 44, no. D1, pp. D710–D716, 2016.

[28] L. Jiang, F. Schlesinger, C. A. Davis et al., "Synthetic spike-in standards for RNA-seq experiments," *Genome Research*, vol. 21, no. 9, pp. 1543–1551, 2011.

[29] A. Lardenois, Y. Liu, T. Walther et al., "Execution of the meiotic noncoding RNA expression program and the onset of gametogenesis in yeast require the conserved exosome subunit Rrp6," *Proceedings of the National Academy of Sciences of the United States of America*, vol. 108, no. 3, pp. 1058–1063, 2011.

[30] H. Neil, C. Malabat, Y. d'Aubenton-Carafa, Z. Xu, L. M. Steinmetz, and A. Jacquier, "Widespread bidirectional promoters are the major source of cryptic transcripts in yeast," *Nature*, vol. 457, no. 7232, pp. 1038–1042, 2009.

[31] E. L. van Dijk, C. L. Chen, Y. d'Aubenton-Carafa et al., "XUTs are a class of Xrn1-sensitive antisense regulatory non-coding RNA in yeast," *Nature*, vol. 475, no. 7354, pp. 114–117, 2011.

[32] Z. Xu, W. Wei, J. Gagneur et al., "Bidirectional promoters generate pervasive transcription in yeast," *Nature*, vol. 457, no. 7232, pp. 1033–1037, 2009.

[33] M. Yassour, J. Pfiffner, J. Z. Levin et al., "Strand-specific RNA sequencing reveals extensive regulated long antisense transcripts that are conserved across yeast species," *Genome Biology*, vol. 11, no. 8, article R87, 2010.

[34] A. Dobin, C. A. Davis, F. Schlesinger et al., "STAR: ultrafast universal RNA-seq aligner," *Bioinformatics*, vol. 29, no. 1, pp. 15–21, 2013.

[35] Y. Liao, G. K. Smyth, and W. Shi, "featureCounts: an efficient general purpose program for assigning sequence reads to genomic features," *Bioinformatics*, vol. 30, no. 7, pp. 923–930, 2014.

[36] M. I. Love, W. Huber, and S. Anders, "Moderated estimation of fold change and dispersion for RNA-seq data with DESeq2," *Genome Biology*, vol. 15, no. 12, p. 550, 2014.

[37] D. Risso, J. Ngai, T. P. Speed, and S. Dudoit, "Normalization of RNA-seq data using factor analysis of control genes or samples," *Nature Biotechnology*, vol. 32, no. 9, pp. 896–902, 2014.

[38] S. Mangiafico, "rcompanion: functions to support extension education program evaluation," 2017, https://cran.r-project.org/web/packages/rcompanion/index.html.

[39] Z. Palkova and L. Vachova, "Mitochondria in aging cell differentiation," *Aging*, vol. 8, no. 7, pp. 1287-1288, 2016.

Hindawi
Oxidative Medicine and Cellular Longevity
Volume 2017, Article ID 4064628, 17 pages
https://doi.org/10.1155/2017/4064628

Research Article

Increasing the Fungicidal Action of Amphotericin B by Inhibiting the Nitric Oxide-Dependent Tolerance Pathway

Kim Vriens,[1] Phalguni Tewari Kumar,[2] Caroline Struyfs,[1,3] Tanne L. Cools,[1] Pieter Spincemaille,[4] Tadej Kokalj,[2] Belém Sampaio-Marques,[5,6] Paula Ludovico,[5,6] Jeroen Lammertyn,[2] Bruno P. A. Cammue,[1,3] and Karin Thevissen[1]

[1]*Centre of Microbial and Plant Genetics, KU Leuven, 3001 Heverlee, Belgium*
[2]*BIOSYST-MEBIOS, KU Leuven, 3001 Heverlee, Belgium*
[3]*VIB Department of Plant Systems Biology, 9052 Ghent, Belgium*
[4]*Department of Laboratory Medicine, University Hospitals Leuven, Herestraat 49, 3000 Leuven, Belgium*
[5]*Life and Health Sciences Research Institute (ICVS), School of Health Sciences, University of Minho, Braga, Portugal*
[6]*ICVS/3B's-PT Government Associate Laboratory, Braga/Guimarães, Portugal*

Correspondence should be addressed to Bruno P. A. Cammue; bruno.cammue@biw.kuleuven.be

Received 18 May 2017; Accepted 2 August 2017; Published 10 October 2017

Academic Editor: Reiko Matsui

Amphotericin B (AmB) induces oxidative and nitrosative stresses, characterized by production of reactive oxygen and nitrogen species, in fungi. Yet, how these toxic species contribute to AmB-induced fungal cell death is unclear. We investigated the role of superoxide and nitric oxide radicals in AmB's fungicidal activity in *Saccharomyces cerevisiae,* using a digital microfluidic platform, which enabled monitoring individual cells at a spatiotemporal resolution, and plating assays. The nitric oxide synthase inhibitor L-NAME was used to interfere with nitric oxide radical production. L-NAME increased and accelerated AmB-induced accumulation of superoxide radicals, membrane permeabilization, and loss of proliferative capacity in *S. cerevisiae*. In contrast, the nitric oxide donor S-nitrosoglutathione inhibited AmB's action. Hence, superoxide radicals were important for AmB's fungicidal action, whereas nitric oxide radicals mediated tolerance towards AmB. Finally, also the human pathogens *Candida albicans* and *Candida glabrata* were more susceptible to AmB in the presence of L-NAME, pointing to the potential of AmB-L-NAME combination therapy to treat fungal infections.

1. Introduction

Pathogenic fungi, including *Candida albicans* and *Candida glabrata*, encounter diverse environmental stresses when colonizing human tissues. During the infection process, they are exposed to potent reactive oxygen and nitrogen species (ROS and RNS, resp.), including nitric oxide radical ($NO^{\bullet}$), peroxynitrite ($ONOO^{-}$), superoxide anion radical ($O_2^{-\bullet}$), and hydroxyl radical ($^{\bullet}OH$), generated by the respiratory burst of phagocytic cells [1–3]. ROS and RNS cause damage to DNA, proteins, and lipids and are toxic to most fungi [4, 5]. In contrast to most nonpathogenic fungi, fungal pathogens such as several *Candida* species have developed responses to neutralize these toxic radicals and repair the potential molecular damage [6]. In this respect, various proteins that protect the fungus from oxidative and nitrosative stresses have been identified and include signalling proteins, transcription factors, and a variety of other enzymes such as catalases, superoxide dismutases, peroxidases, and nitric oxide dioxygenase [1, 7]. Hence, antifungals (or combinations thereof) inducing an excess ROS and/or RNS in a pathogenic fungus that cannot be neutralized by its endogenous protection mechanisms are of great interest [8].

Many antifungal agents are reported to induce oxidative (excess ROS) stress in pathogenic fungi. These agents include small molecules, such as miconazole [9, 10], fluconazole [11, 12], amphotericin B (AmB) [12–16], and caspofungin [17], but also antimicrobial peptides, such as protonectin

[18], baicalin [19], and various plant defensins [20–23]. To date, the induction of nitrosative (excess RNS) stress in fungal species has only been demonstrated for AmB in the pathogenic fungus *Cryptococcus gattii* [24] and for the plant defensins NaD1 and PvD1 in *C. albicans* [23, 25]. AmB belongs to the polyene class of antifungals and induces fungal cell death through apoptotic and nonapoptotic pathways [26–29]. Hence, based on the above reports, it seems that AmB can induce both excess ROS and RNS in pathogenic fungi. How the production of these different types of radicals would contribute to AmB's fungicidal action is hitherto not known. Moreover, increased insight in these AmB-induced events may lead to more efficient AmB-based therapies, as exemplified in the current study.

In this study, we further investigated the potential of AmB to induce ROS and RNS and looked at the interplay between these toxic radicals and their accumulation kinetics, thereby linking these events to AmB's killing capacity. To investigate the kinetics of the AmB-induced ROS and RNS, we used a digital microfluidic platform (DMF) in which single cells were captured and monitored over time using time lapse fluorescence microscopy. This DMF platform has been previously optimized for seeding of *Saccharomyces cerevisiae* cells and subsequently for assessing the rate by which AmB-induced membrane permeabilization events occurred at the single cell level [30]. *S. cerevisiae* has been widely used to investigate the mechanisms of action of antifungal agents, including that of AmB [14, 31–35]. Hence, also in this study, we used *S. cerevisiae* as a model organism to better understand the mode of action of AmB and translated the most prominent findings to the fungal pathogens *C. albicans* and *C. glabrata*.

2. Methods

2.1. Strains and Chemical Reagents. *Saccharomyces cerevisiae* strain BY4741, *Candida albicans* strain SC5314, and *Candida glabrata* strain BG2 were used in the cytotoxicity assays. All culture media were purchased from LabM Ltd. (Lancashire, England), unless stated otherwise. Media used were YPD (1% yeast extract; 2% peptone; and 2% glucose), 1/5 YPD (YPD diluted in distilled water), and RPMI-1640 (Roswell Park Memorial Institute-1640 medium; pH 7) with L-glutamine and without sodium bicarbonate (purchased from Sigma-Aldrich, St. Louis, MO, USA), buffered with MOPS (Sigma-Aldrich, St. Louis, MO, USA).

Amphotericin B (AmB), N_ω-Nitro-L-arginine methyl ester hydrochloride (L-NAME), S-nitrosoglutathione, propidium iodide (PI), and dihydroethidium (DHE) were purchased from Sigma-Aldrich (St. Louis, MO, USA). 4-Amino-5-methylamino-2′,7′-difluorofluorescein diacetate (DAF-FM DA) was supplied by Life Technologies (Carlsbad, CA, USA). Peroxide was purchased from VWR chemicals (Radnor, PA, USA).

Fluorinert FC-40 was purchased from 3M (St. Paul, MN, USA), and chemicals for photolithopgraphy were supplied by Rohm and Haas (Marlborough, MN, USA). Fluoroalkylsilane Dynasylan® F 8263 was supplied by Evonik (Essen, Germany). AZ1505 photoresist and Teflon-AF® were obtained from Microchemicals GmbH (Ulm, Germany) and Dupont (Wilmington, DE, USA), respectively. Parylene C dimer and Silane A174 were purchased from Plasma Parylene Coating Services (Rosenheim, Germany).

2.2. Cell Culture Conditions. *S. cerevisiae*, *C. albicans*, or *C. glabrata*, grown overnight in YPD at 30°C and 250 rpm, were diluted to an optical density (OD) of 0.15 measured at $\lambda = 600$ nm in a flask containing 50 mL of fresh YPD and further cultured for 5 h at 30°C and 250 rpm (*S. cerevisiae*) or 37°C and 200 rpm (*Candida* spp.), to obtain exponentially growing cells. Cells were then pelleted by centrifugation (3 min, 4000 rpm), washed and resuspended in 1/5 YPD for *S. cerevisiae* or RPMI-1640 medium for *C. albicans* and *C. glabrata* to an OD of 3 for further use in the experiments.

2.3. Cytotoxicity Assays in Bulk. Exponentially growing cells were supplemented with PI, DHE, or DAF-FM DA to a final concentration of 3 μM, 17 μM, and 5 μM, respectively, and subsequently treated either with DMSO or water (controls), a range of AmB dosages (0.625 μM–10 μM, dissolved in DMSO), 200 mM L-NAME (dissolved in water), or a combination of the above, with a final DMSO concentration of 1% (*v*/*v* %). After mixing, the cell suspensions were transferred to Eppendorf tubes, covered with a layer of silicon oil, placed on a horizontal shaker at 5 rpm, and incubated in the dark for 3 h at room temperature to be compliant with the DMF setup. In case of *C. albicans* and *C. glabrata*, however, the assays were performed at 37°C to be clinically relevant. A plating assay was carried out at the start of the treatment to account for the number of cells at this point. After 3 h, cells were pelleted (3 min, 4000 rpm), washed and resuspended in phosphate buffered saline (PBS), and subsequently plated or subjected to flow cytometry on a BD Influx™ cell sorter. In the plating assay, a 10-fold dilution series of the cell suspensions was prepared in PBS and appropriate cell suspensions were spread in YPD agar plates, after which the plates were allowed to dry for 10 min and incubated for 48 h at 30°C to visualize the number of colony forming units (CFUs). For flow cytometry, cells were monitored for fluorescence at 540/608 nm (FL3 610_20), 485/515 nm (FL1 580_30), or 495/515 nm (FL2 530_40) for detection of membrane permeabilization with PI, detection of superoxide radical accumulation with DHE, or detection of nitric oxide radical accumulation with DAF-FM DA, respectively.

2.4. Cell Cycle Analysis. Aliquots of cells were collected at the indicated time points and cells were pelleted, washed, and fixed with ethanol (70% *v*/*v*) for at least 30 min at 4°C. Cells were then resuspended in sodium citrate buffer (50 mM sodium citrate, pH 7.5), sonicated and treated with RNAse for 1 h at 50°C, followed by subsequent incubation with 20 μg/ml proteinase K for 1 hour at 50°C. Cell DNA was then stained overnight with SYBR Green 10,000 x (Molecular Probes/Invitrogen, Carlsbad, CA), diluted 10-fold in Tris-EDTA (pH 8.0), and incubated overnight at 4°C. Before flow cytometry analysis, samples were diluted 1 : 4 in sodium citrate buffer. The SYBR signals were measured using a BD LSR II™ (Becton Dickinson, NJ, USA) with a 488 nm excitation

laser. Signals from 30,000 cells/sample were captured in FITC channel (530 nm ± 30 nm), at a flow rate of about 1000 cells/s. The percentage of cells in each phase of the cell cycle was determined offline with ModFit LT software (Verity Software House, Topsham, ME).

2.5. Checkerboard Antifungal Assays. AmB (dissolved in DMSO), L-NAME (dissolved in water), and S-nitrosoglutathione (dissolved in water) were 2-fold serially diluted across the columns and rows of a 96-well microtiter plate. Subsequently, AmB dilutions were further diluted 10-fold in 1/5 YPD. Next, 20 μl volumes of these dilutions were transferred to a microtiter plate, allowing the analysis of unique combinations of two compounds. Exponentially growing *S. cerevisiae* cells were diluted to an OD of 0.10, measured at $\lambda = 600$ nm, in 1/5 YPD, and subsequently, 80 μl was added to the microtiter plate, resulting in a final DMSO concentration of 1% (v/v %). In parallel, the number of colony forming units (CFU) of this exponential culture was determined by plating assay. After 24 h of incubation at 30°C, the OD of the checkerboard plate was measured at $\lambda = 600$ nm, to examine the growth of *S. cerevisiae* cells. Subsequently, a plating assay was performed of specific wells of the checkerboard assay to assess cell viability of specific AmB-L-NAME combinations. Based on preliminary data of this experiment, we have performed power calculations ($\alpha = 0.05$; $b = 0.8$) for an AmB concentration of 0.313 μM, which is the tested value closest to the IC50 (0.282 μM AmB for *S. cerevisiae*). These calculations indicated that we needed 2 biological replicates to assure a power of $b = 0.8$. Recalculations of the power calculations, based on data of the 2 biologically independent experiments, confirmed the previously executed power calculations.

2.6. Fabrication of Digital Microfluidic Plates. Digital microfluidic plates were fabricated as described previously [30]. The assembly consists of an actuation plate and a grounding plate, as presented in Supplemental Information S3 Figure available online at https://doi.org/10.1155/2017/4064628. For fabricating the actuation plate (S3 Figure A), cleaned glass wafers (1.1 mm) were sputter coated with chromium (100 nm) and patterned using standard photolithographic processes. After cleaning the plates with acetone and isopropyl alcohol twice, the surface was plasma activated (O_2 plasma, 150 mtorr, 100 W) and the plates were primed with Silane A174 to promote adhesion of the parylene C layer (3 μm) that was subsequently coated using chemical vapour deposition. Next, a thin layer of Teflon-AF (200 nm, using 3% w/w in Fluorinert FC-40) was spin-coated (1200 rpm) on top of the parylene C layer and baked for 5 min at 110°C and 5 min at 200°C. Crenelated actuation electrodes with dimensions of 2.8 mm × 2.8 mm were selectively actuated to manipulate individual droplets of 2.7 μL, using customized software.

For fabrication of the grounding plate (Supplemental Information S3A Figure) of the DMF device, cleaned glass wafers (1 mm) were coated with an aluminium layer (40 nm) using thermal evaporation, leaving two 2.5 × 2.5 mm visualization windows. Fluoroalkylsilane Dynasylan F 8263 was coated on the aluminium to improve adhesion of the subsequent spin-coated Teflon-AF layer (3 μm). Microwells were patterned in the Teflon-AF layer following a hard contact masking procedure, developed by depositing parylene C (1 μm) and aluminium (60–80 nm) layers. A thin layer of AZ1505 photoresist was spin-coated on the aluminium layer, and the aluminium was patterned and etched using standard photolithography processes. The pattern was then transferred from the aluminum to the Teflon-AF using O_2 plasma (150 mtorr, 100 W) for 10 min. Finally, using a dry lift-off method, the aluminium-parylene C mask was peeled off using a pair of forceps, revealing two microwell arrays (1.9 mm × 1.9 mm) on a single grounding plate, consisting of 22,000 microwells each, arranged in a hexagonal pattern with a pitch distance of 14 μm [36]. The dimensions of the microwells were measured to be approximately 5.5 μm in width and 3 μm in depth.

2.7. Cytotoxicity Assays on DMF Platform. A schematic overview of the cytotoxicity assays on the DMF platform is given in Supplemental Information S3B Figure. Exponentially growing cells were supplemented with PI or DHE to a final concentration of 3 μM and 17 μM, respectively, and subsequently treated either with DMSO or water (controls), a range of AmB dosages (5 μM and 10 μM, dissolved in DMSO), 200 mM L-NAME (dissolved in water), or a combination of the above, with a final DMSO concentration of 1% (v/v %). After 5 min, two droplets, one containing the mixed cell suspension and one containing the corresponding composition without cells, were placed on two separate electrodes of the actuation plate. The actuation and grounding plate were assembled, thereby aligning the microwell array with the cell droplet and sandwiching it between the plates. To prevent sticking and evaporation of the droplets, 80 μL of silicon oil was added between the plates by pipetting. The assembled plates were placed in the DMF chip holder, and the device was flipped upside down and incubated for 10 min to allow sedimentation of the cells. This step was followed by automated shuttling of the cell droplet over the microwell array for 15 times, that is, 15 seeding cycles, using software-assisted electrowetting-on-dielectric (EWOD) actuation. After seeding, the cell droplet was actuated away from the array and a droplet without cells was transferred to the array. The cell responses, that is, membrane permeabilization detected by PI or superoxide radical accumulation detected by DHE, were monitored at room temperature for 3 h in 15 min intervals using an inverted fluorescence microscope (IX-71, Olympus, Tokyo, Japan) equipped with a CCD camera. The whole array was scanned in 9 overlapping frames in approximately 15 seconds, in which a single frame covered approximately 4100 wells, using a 20x lens magnification. Both fluorescence and bright field images were collected using the same excitation/emission wavelengths as described above.

2.8. Calculation of Fluorescence Intensity per Cell. The DMF array was imaged for 3 h in 15 min intervals (i.e., 12 time points), and images were processed in ImageJ (v1.47, NIH, MD) for background correction using rolling ball algorithm

with a radius of 50 pixels. Salt-and-pepper noise was removed using the despeckle option in ImageJ. Next, the images were loaded in MATLAB (The Mathworks, Natick, MA), and a custom MATLAB code was executed. The single image captured at 180 min was processed by MATLAB to identify the single fluorescent cells in contrast with the background. The MATLAB code detected the area of a single cell, and a unique numerical digit was allotted to each cell. Within the detected area of a single cell, the maximum pixel value was registered together with its respective coordinate in a vector array. Next, the MATLAB code was executed on all the images captured between 15 min and 165 min. The fluorescence intensity of each individual cell in different time frames was monitored by detecting the pixel values for the registered coordinates. The final output was tabular data with pixel intensities of single cells identified with unique numerical digits, as detected in 12 consecutive time points.

2.9. Data Analysis. Flow cytometric data were normalized to the control data, and DMF data were normalized to the first data point, that is, 15 min. For plating assays, the number of CFUs per mL was displayed in Log scale. Data were analysed with GraphPad Prism 6 SPPS (GraphPad Software, Inc., CA, USA). Two-way ANOVA followed by Dunnett multiple comparison test was performed to analyse statistically significant differences in the number of PI-, DHE-, and DAF-FM DA-positive cells and cells able to proliferate between control and different AmB treatments in *S. cerevisiae*, *C. albicans*, and *C. glabrata*. Pearson's product-moment correlation was performed to analyse the relation between the results obtained in the bulk and the DMF experiments. Survival analyses (Kaplan-Meier) using the Log-rank test were performed on DMF data to compare survival curves and analyse whether treatment significantly affects survival. Two-way ANOVA and subsequent Tukey or Dunnett multiple comparison tests were performed to analyse differences between bulk results for treatment with AmB in the presence or absence of L-NAME for each AmB concentration or to analyse differences in bulk results between the first data point and other data points within the same treatment, respectively. Two-way ANOVA followed by Tukey multiple comparison test was performed to analyse statistically significant differences between different treatments in the cell cycle analyses. Two-way ANOVA followed by Tukey multiple comparison test was performed to analyse statistical differences between the OD measurements for treatment with different concentrations of AmB in the absence or presence of 200 mM L-NAME or 2 mM S-nitrosoglutathione. In all cases, $P < 0.05$ was considered statistically significant. When multiple comparisons were performed, multiplicity-adjusted P values for each comparison are presented, taking into account the total number of groups in the ANOVA and the data in all groups.

3. Results

3.1. Amphotericin B Induced Nitric Oxide and Superoxide Radical Accumulation in Saccharomyces cerevisiae. First, we assessed whether AmB induces accumulation of superoxide and nitric oxide radicals in *S. cerevisiae*. To this end, yeast cultures were treated with AmB for 3 h at room temperature to be compliant with the DMF setup and subjected to flow cytometry to analyse the number of cells with increased superoxide and nitric oxide radical levels using DHE and DAF-FM DA dyes, respectively. The fluorescent probe DHE is typically used for detecting $O_2^{-\bullet}$ due to its relative specificity for this ROS, with minimal oxidation induced by H_2O_2 or hypochlorous acid [37, 38]. Furthermore, in contrast to other intracellular dyes, there is little capacity for the formation of superoxide by DHE due to redox cycling [38]. However, nonspecific oxidation of DHE from other nonsuperoxide sources, such as cytochrome c [38], was not eliminated in this study. The number of cells with compromised plasma membranes was analysed using PI. As PI only enters cells with compromised plasma membrane, it was used as a marker to identify nonapoptotic cell death [39]. To quantify the fungicidal activity of AmB, the treated cultures were subjected to plating assays, thereby assessing the number of cells that was able to proliferate after AmB treatment.

The number of cells that accumulated superoxide (Figure 1(a)) and nitric oxide radicals (Figure 1(b)), as well as the number of cells with permeabilized membranes (Figure 1(c)), was significantly increased by AmB treatment in a dose-dependent manner ($P < 0.05$), while the proliferative capacity of the cells was decreased, yet, not statistically significant (Figure 1(d)). This dose dependency was different for the tested responses: a maximum number of cells producing nitric oxide radicals in AmB-treated yeast cultures were found at AmB concentrations as low as 2.5 μM ($P < 0.0001$) (Figure 1(b)), whereas the highest number of cells with increased superoxide radical accumulation and compromised membranes was observed at 10 μM AmB ($P < 0.0001$) (Figures 1(a) and 1(c), resp.). Hence, it seemed that the production of nitric oxide radicals could be induced at AmB doses that did not trigger the accumulation of superoxide radicals or membrane permeabilization, while this resulted in a reduced proliferative capacity of cells.

3.2. Inhibition of Nitric Oxide Radical Production Resulted in Increased Superoxide Radical Accumulation and Loss of Proliferative Capacity by Amphotericin B. As it was previously shown that superoxide radicals react with nitric oxide radicals, resulting in strongly oxidizing RNS causing damage to proteins and nucleic acids [40–42], we investigated whether the AmB-induced superoxide radical levels could be increased by blocking the production of nitric oxide radicals. To this end, L-NAME was used. L-NAME inhibits nitric oxide synthases in mammalian cells and thus prevents the generation of nitric oxide radicals [43]. Although in yeast, only nitric oxide synthase-like enzymes are identified to date, L-NAME was shown to reduce the levels of nitric oxide radicals in yeast [44–46]. Reduction of the levels of nitric oxide radicals by L-NAME in *S. cerevisiae* was microscopically confirmed (data not shown).

In the presence of L-NAME, the number of cells with AmB-induced accumulation of superoxide radicals significantly increased as compared to that after AmB treatment

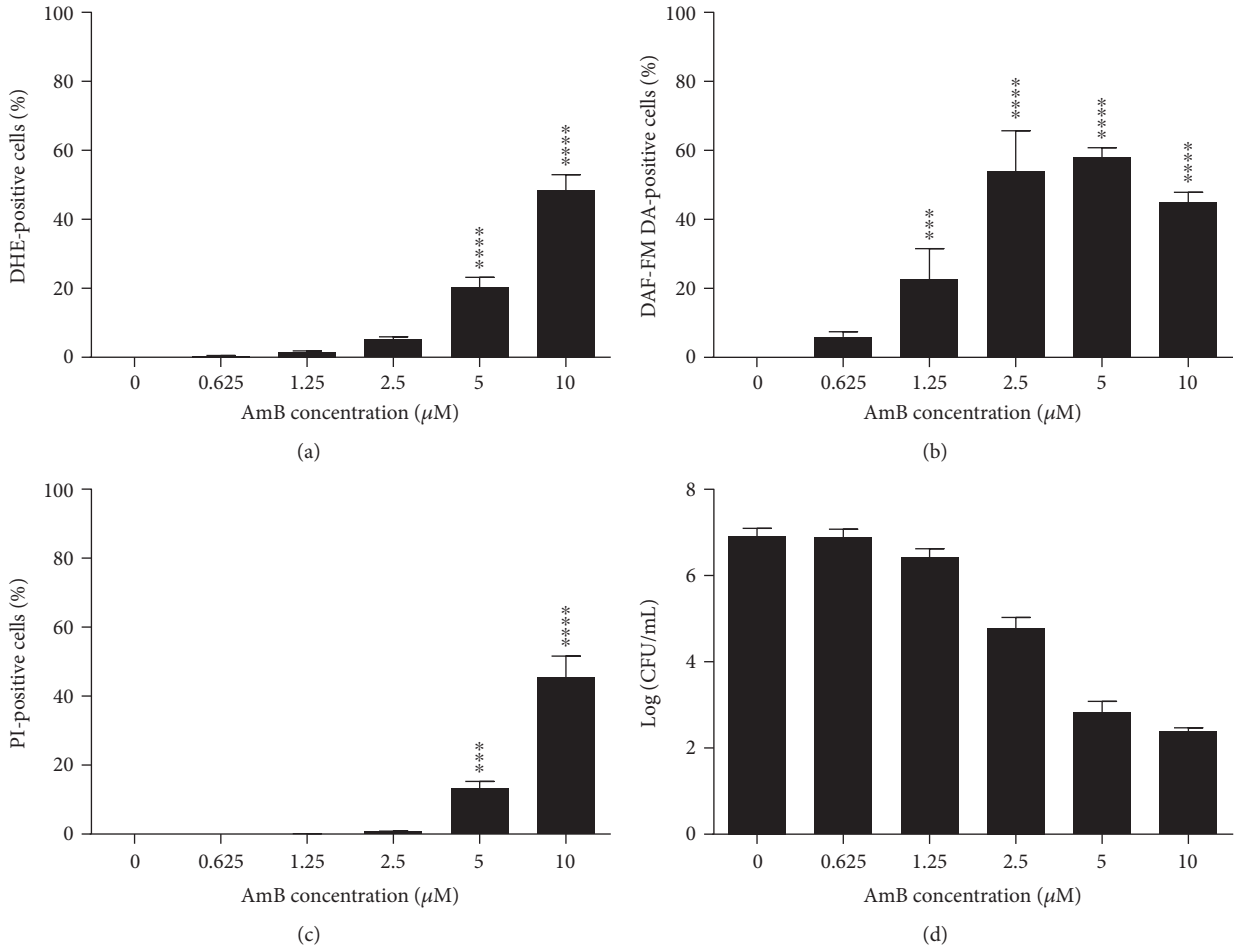

Figure 1: AmB induced accumulation of superoxide and nitric oxide radicals and membrane permeabilization in *S. cerevisiae*. Yeast cultures were treated with different concentrations of AmB for 3 h and subjected to flow cytometry or plating assays. (a) Levels of superoxide radical detected by dihydroethidium (DHE) fluorescence and flow cytometry. (b) Levels of nitric oxide radical detected by 4-amino-5-methylamino-2′,7′-difluorofluorescein diacetate (DAF-FM DA) fluorescence and flow cytometry. (c) Membrane permeabilization events detected by propidium iodide (PI) fluorescence and flow cytometry. (d) Number of CFU/mL in Log-scale, assessed by plating assays and CFU counting. Means and standard errors of the means (SEM) of at least 3 independent biological experiments ($n \geq 3$) are presented. Two-way ANOVA followed by Dunnett multiple comparison test was performed to analyse statistically significant differences in the number of PI-, DHE-, and DAF-FM DA-positive cells and cells able to proliferate between control treatment and treatment with different concentrations of AmB. *** and **** represent $P < 0.001$ and $P < 0.0001$, respectively.

alone, in the case of 2.5 μM or 10 μM AmB (Figure 2(a); $P = 0.05$ and $P < 0.0001$, resp.). Moreover, treatment of yeast with 1.25 μM or 2.5 μM AmB supplemented with L-NAME significantly reduced the number of cells that were able to proliferate, as compared to treatment with AmB alone (Figure 2(c); $P = 0.01$ and $P < 0.0001$, resp.). In contrast, only 10 μM AmB with L-NAME increased the number of cells with a compromised membrane in a significant manner ($P = 0.02$), as compared to that after treatment with AmB alone (Figure 2(b)), suggesting that the combination of low concentrations of AmB with 200 mM L-NAME did not affect membrane permeabilization by AmB. In addition, inhibition of nitric oxide radical production resulted in an increased number of cells that accumulated superoxide radicals and was characterized by membrane permeabilization and inability to proliferate. These findings point towards a potential role of nitric oxide radical production in mediating tolerance towards AmB in yeast. Moreover, we have performed cytotoxicity assays with peroxide in the presence and absence of 200 mM L-NAME and found that L-NAME can only increase the killing activity of AmB but not that of peroxide, implying an AmB-specific effect of L-NAME (Supplemental Information S4 Figure).

3.3. Inhibition of Nitric Oxide Radical Production Resulted in Faster and Increased Superoxide Radical Accumulation and Faster Membrane Permeabilization by Amphotericin B. To gain more insights into the action of L-NAME on the kinetics of AmB-induced superoxide radical accumulation, time lapse experiments were performed on a DMF platform (for a schematic representation of the experimental setup, see Supplemental Information S3 Figure), as described in our previous study [30]. To this end, yeast was treated with either 0 μM (control), 5 μM, or 10 μM AmB in the presence

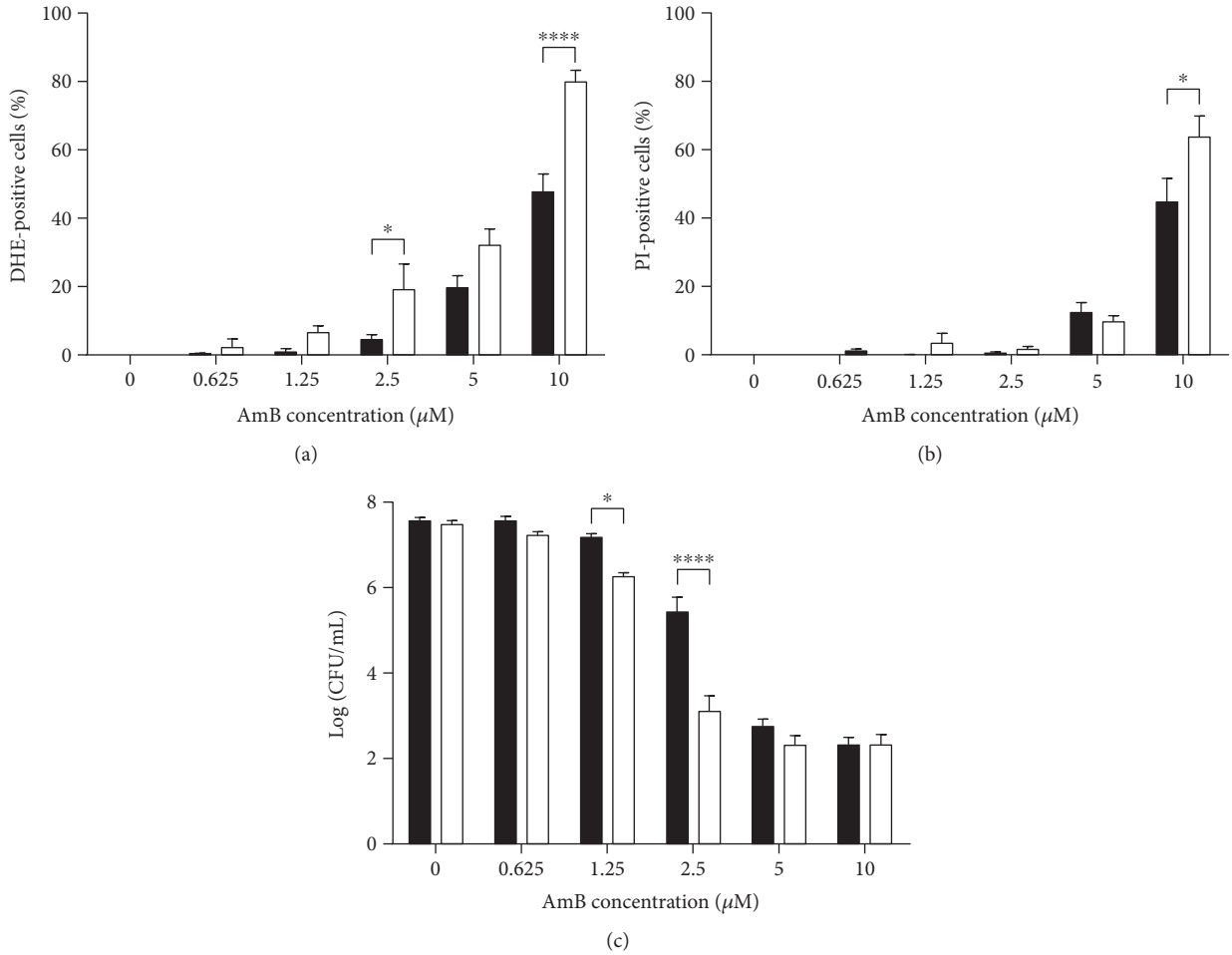

Figure 2: AmB-induced superoxide radical accumulation, membrane permeabilization, and loss of proliferative capacity can be increased by blocking nitric oxide radical production using L-NAME. Exponential yeast cultures were treated with different concentrations of AmB in the presence or absence of 200 mM L-NAME for 3 h. (a) Levels of superoxide radical detected by dihydroethidium (DHE) fluorescence and flow cytometry. (b) Membrane permeabilization events detected by propidium iodide (PI) fluorescence and flow cytometry. (c) Number of CFU/mL in Log-scale, assessed by plating assays and CFU counting. Means and standard errors of the means (SEMs) of at least 3 independent biological experiments ($n \geq 3$) are presented. Black bars represent treatment with AmB alone; white bars represent treatment with AmB supplemented with 200 mM L-NAME. Two-way ANOVA followed by Tukey multiple comparison test was performed to analyse significant differences between the two treatments. $*$ and $****$ represent $P < 0.05$ and $P < 0.0001$, respectively. Multiplicity-adjusted P values are presented in the text.

or absence of 200 mM L-NAME, as these concentrations were shown to have the most profound effect on membrane permeabilization and accumulation of superoxide radicals in the bulk experiments. During treatment, each cell was monitored over time at room temperature for 3 h in 15 min intervals for DHE or PI fluorescence. Validation of the DMF platform to monitor DHE and PI fluorescence at single cell level was performed prior to the assays described above (Supplemental Information S1 Figure).

We found an increased number of DHE- (Figure 3(a)) and PI- (Figure 3(b)) positive cells when yeast was treated with AmB supplemented with 200 mM L-NAME as compared to treatment with AmB alone, starting from 30 min to 45 min incubation, respectively. This observation was in line with the bulk results after 3 h of incubation at room temperature that were obtained by flow cytometry (Figure 2).

Survival analyses were performed to test the hypothesis that different treatments (i.e., AmB in the presence or absence of L-NAME) affect survival in a significantly different manner, in which survival is defined as the occurrence of a specific event [47]. Here, we analysed whether the occurrence of superoxide radical accumulation and membrane permeabilization upon treatment with AmB in the presence and absence of L-NAME was significantly different. The survival curves for treatment with 10 μM AmB in the presence or absence of 200 mM L-NAME were significantly different in both DHE and PI experiments ($P < 0.0001$) (Figures 3(a) and 3(b)), indicating that L-NAME significantly affected the number of superoxide radical accumulating cells and the number of membrane permeabilization events induced by AmB over time. When cells were treated with 10 μM AmB in combination with 200 mM L-NAME, a median survival of 45 min was observed in the DHE experiments, that is,

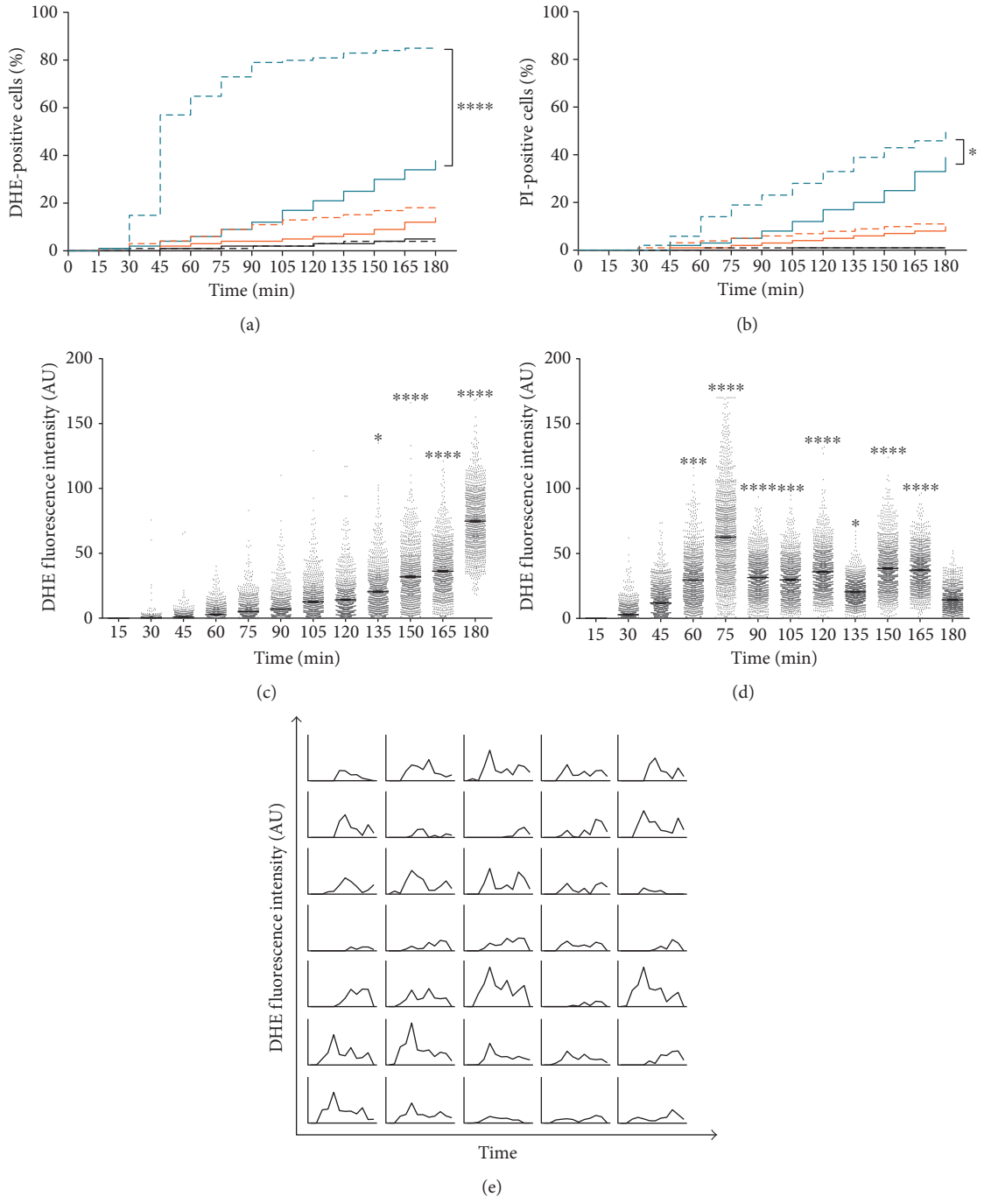

Figure 3: L-NAME increased and accelerated AmB-induced superoxide radical accumulation, membrane permeabilization, and intracellular superoxide radical levels. (a-b) Accumulation of superoxide radicals (a) and membrane permeabilization (b) in *S. cerevisiae* cells treated either with 0 μM (black), 5 μM (orange), or 10 μM (blue) AmB in the presence (dashed lines) or absence (solid lines) of 200 mM L-NAME during 3 h in 15 min intervals. Log-rank tests were performed to analyse significant differences between AmB treatment and treatment of AmB in combination with 200 mM L-NAME for each AmB dose. Data of at least 3 independent biological experiments is presented ($n \geq 3$). $*$ and $****$ represent $P < 0.05$ and $P < 0.0001$, respectively. (c-d) Intracellular DHE fluorescence in *S. cerevisiae* cells treated with 10 μM AmB in the absence (c) or presence (d) of 200 mM L-NAME. Single cells were monitored for their DHE fluorescence during treatment for 3 h in 15 min intervals using fluorescence microscopy and the DMF platform. The fluorescence intensity of each cell is presented as arbitrary units (AU), and each dot represents a single cell. Means and standard errors of the means (SEMs) of at least 3 independent biological experiments ($n \geq 3$), with at least 780 cells each, are presented. Two-way ANOVA followed by Tukey multiple comparison test was performed to analyse significant differences in DHE fluorescence intensity. $*$, $***$, and $****$ represent $P < 0.05$, $P < 0.001$, and $P < 0.0001$, respectively. (e) DHE fluorescence intensity of individual cells over time. A selection of 35 cells was randomly chosen and is representative for more than 3000 cells that were analysed in this study. Each plot represents the DHE fluorescence intensity, measured every 15 min, of one representative cell over the whole duration of the experiment, that is, 180 min.

50% of the cells was DHE positive after 45 min of treatment. In contrast, when AmB was applied alone, 50% of DHE-positive cells in the treated yeast culture was not reached after 180 min (median survival > 180 min), which implied that AmB-induced superoxide radical accumulation occurred faster in cells treated in the presence of L-NAME. Additionally, a hazard ratio (Log-rank) of 4.21 was found when comparing the survival curve of cells treated with 10 μM AmB supplemented with 200 mM L-NAME to that of cells treated with 10 μM AmB, indicating that the rate by which superoxide radicals were formed is 4.21 times faster in the combination treatment, compared to treatment with AmB alone. The same was true for membrane permeabilization events induced by AmB supplemented with L-NAME; upon treatment with the latter, a median survival of 180 min was observed, as compared to >180 min for treatment with AmB alone, and when comparing both survival curves, a hazard ratio of 1.56 was found. This suggested also that membrane permeabilization occurred faster when cells were subjected to AmB in the presence of L-NAME, as compared to treatment with AmB alone.

We further confirmed that the fast increase in superoxide radical levels during AmB-L-NAME combination treatment was linked to a block in the production of nitric oxide radicals. As we were unable to monitor nitric oxide radicals over time using the DMF platform due to an incompatibility of the DAF-FM DA dye and the DMF setup, we opted to further investigate the kinetics of nitric oxide radical production by flow cytometry. Indeed, upon AmB treatment, yeast cells started to produce nitric oxide radicals from 30 min onwards ($P < 0.0001$), and a similar trend was observed to that of superoxide radical accumulation during treatment with AmB supplemented with L-NAME (Supplemental Information S2 Figure).

To further elucidate the variation of superoxide radical levels when cells were subjected to AmB treatment in the presence of L-NAME, we analysed the fluorescence intensity of individual cells. To this end, single cells were monitored over time in 15 min intervals, and hence the fluorescence intensity of each cell, represented by one dot, was reanalysed every 15 min. We found that the DHE fluorescence intensity of cells during AmB treatment gradually increased over time, and the highest fluorescence intensity was measured at 180 min, the end point of this study (Figure 3(c)). Compared to the DHE fluorescence at 15 min, the DHE fluorescence intensity was significantly different from 135 min onwards. In contrast, the DHE fluorescence intensity of cells treated with 10 μM AmB supplemented with 200 mM L-NAME showed two subpopulations, suggesting that superoxide radical accumulation took place in a biphasic manner; the first and highest superoxide radical accumulation peak was observed at approximately 75 min, followed by a rather slow decrease and a second peak at approximately 150 min (Figure 3(d)). Here, the DHE fluorescence intensity was statistically significant from 60 min onwards (compared to DHE fluorescence at 15 min). The kinetics of DHE fluorescence of 35 individual cells, representative for more than 3000 analysed cells, showed different subsets of cells in ROS readouts over time. Some subsets showed an increase in DHE fluorescence, followed by a decrease in fluorescence at certain time points, while other subsets showed a gradual increase in fluorescence over time (Figure 3(e)). Hence, it seemed that not only the number of cells accumulating superoxide radicals increased when subjected to AmB treatment in the presence of L-NAME, but also the intracellular levels of superoxide radicals were altered in a time-dependent manner, as compared to treatment of cells with AmB alone.

Moreover, to further support the data of the single cell analysis via the DMF platform, we performed additional time lapse experiments in bulk via FACS and analysed the subpopulations of DHE- and PI-positive cells of cultures treated with 10 μM AmB in the presence and absence of 200 mM L-NAME for 30, 60, 90, and 180 min. We found an increased number of DHE- and PI-positive cells when yeast was treated with 10 μM AmB supplemented with 200 mM L-NAME as compared to treatment with AmB alone, starting from 30 min to 90 min incubation, respectively (Supplemental Information S5 Figure). These bulk data showed faster and increased ROS accumulation and faster membrane permeabilization by AmB when coincubated with L-NAME and corroborated the data of the single cell analysis via the DMF platform. Note that the number of PI-positive cells induced by AmB in the presence of L-NAME is higher when assessed in bulk as compared to the DMF setup.

3.4. Inhibition of Nitric Oxide Radical Accumulation Resulted in Faster Arrest of Proliferative Capacity of Saccharomyces cerevisiae Cells by Amphotericin B. The results described above indicate that AmB-induced superoxide radical accumulation and membrane permeabilization were significantly altered upon the addition of L-NAME. This tempted us to further investigate whether the proliferative capacity of cells was affected in a time-dependent manner, when comparing both treatments. To this end, plating of *S. cerevisiae* cultures subjected to both treatments was carried out every 15 min, and the number of cells that were able to proliferate (and form CFU) was determined.

At all time points, the proliferative capacity of cells treated with 10 μM AmB and 200 mM L-NAME was significantly reduced as compared to cells treated with 10 μM AmB alone ($P < 0.0001$) (Figure 4(c)). In addition, it seemed that the proliferative capacity of cells subjected to AmB-L-NAME treatment was reduced very fast, that is, within 15 min ($P < 0.0001$), whereas the proliferative capacity of cells upon treatment with AmB alone decreased in a significant manner from 45 min onwards ($P = 0.003$). This suggested that the fast decrease in proliferative capacity of cells within 15 min upon incubation with AmB and L-NAME was independent of superoxide radical accumulation and membrane permeabilization. Similar observations were made in the survival analyses for superoxide radical accumulation and membrane compromising events (Figures 3(a) and 3(b)) and were supported by a second statistical analysis (Two-way ANOVA followed by Dunnett multiple comparison test). Specifically, a significant difference in the number of cells accumulating superoxide radicals (Figure 4(a)) and

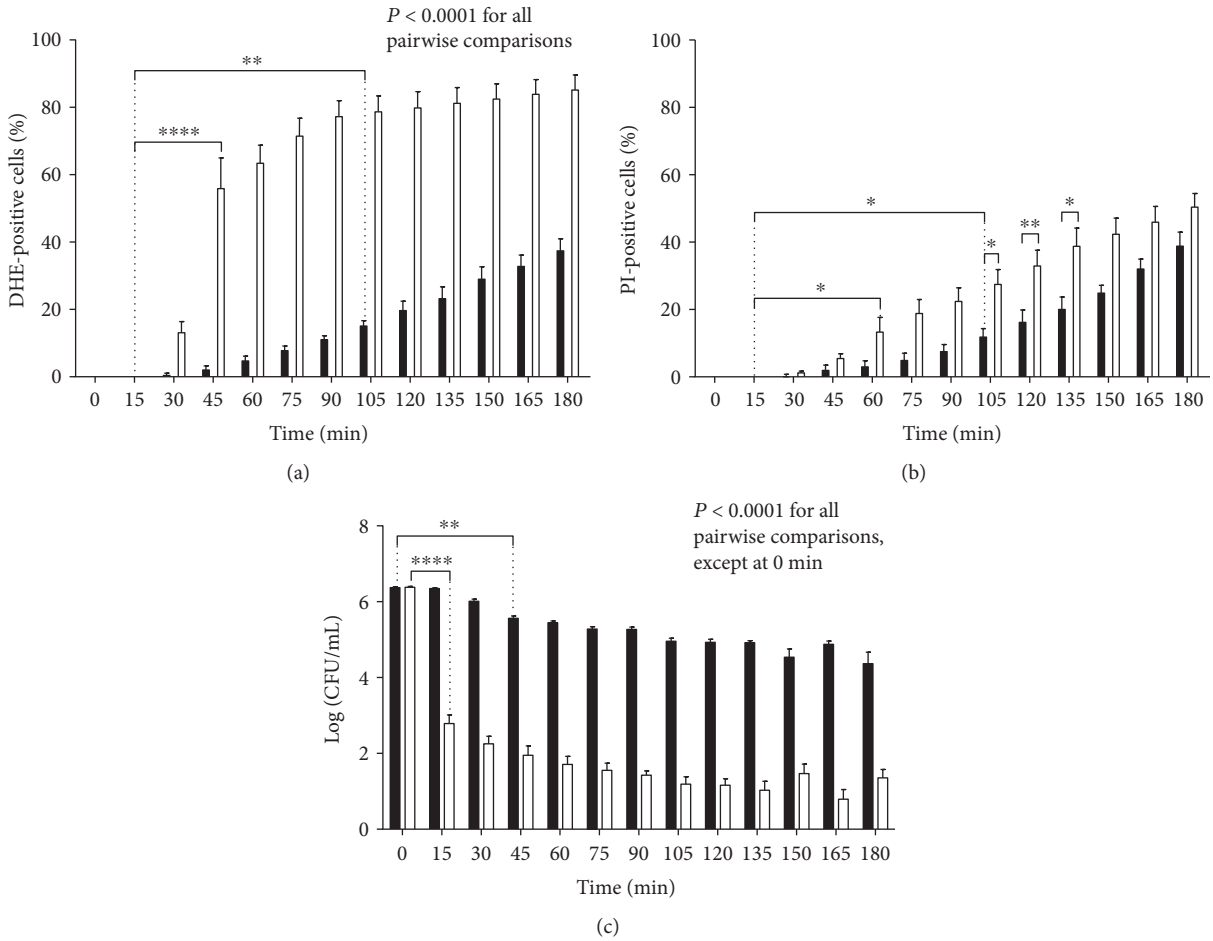

Figure 4: L-NAME decreased the proliferative capacity of cells during AmB treatment, which seems independent of superoxide radical accumulation. Exponential yeast cells were treated with 10 μM AmB in the presence (white bars) or absence (black bars) of 200 mM L-NAME for 3 h. Cells were analysed for their DHE and PI fluorescence in the DMF setup (a and b) or subjected to bulk plating assays (c) every 15 min. Means and standard error of the means (SEMs) of at least 3 independent biological experiments ($n \geq 3$) are presented. Two-way ANOVA followed by Tukey multiple comparison test was performed to analyse significant differences between the two treatments; Two-way ANOVA followed by Dunnett multiple comparison test was performed to analyse significant differences between the first data point (i.e., 0 min (in (c)) or 15 min (in (a) and (b))) and other data points within the same treatment (only the primary significant difference is presented to avoid overcrowding of the figure); $*$, $**$, and $****$ represent $P < 0.05$, $P < 0.01$, and $P < 0.0001$, respectively. A dotted line is shown at 15 min to point out the clear differences between the responses at this time point.

showing membrane permeabilization (Figure 4(b)) was found at earlier time points (i.e., 45 min versus 105 min for superoxide radical accumulation and 60 min versus 105 min for membrane permeabilization) when cells were treated with AmB in the presence of L-NAME, as compared to cells treated with AmB alone.

However, although approximately 99.5% of the treated population was not able to proliferate from 15 min onwards (Figure 4(c)) when subjected to AmB-L-NAME treatment, they were still able to accumulate superoxide radicals at that point, which resulted in a superoxide radical boost starting at 30 min (Figure 4(a)). Hence, it seemed that these cells were still metabolically active and possibly used increased intracellular superoxide radical levels to enter a programmed cell death pathway. In contrast, loss of proliferative capacity of cells treated with AmB alone (Figure 4(c)) might be explained by the gradual increase in the number of membrane permeabilization events; a similar trend in both curves was observed (Figure 4(b)).

To further confirm the crucial role of nitric oxide in modulating AmB's fungicidal activity, we performed checkerboard assays with AmB and the nitric oxide donor, S-nitrosoglutathione. We found that 2 mM S-nitrosoglutathione reduced the activity of AmB (Figure 5). Hence, nitric oxide plays an important role in modulating AmB's activity.

3.5. Amphotericin B Induced Cell Cycle Arrest in Saccharomyces cerevisiae Independently of L-NAME. We further analysed whether the increased loss of proliferative capacity upon combined AmB and L-NAME treatment within 15 min of treatment can be attributed to cell cycle arrest. To this end, we analysed the fraction of cells in the G0/G1, S, and G2/M cell cycle phases at the beginning and

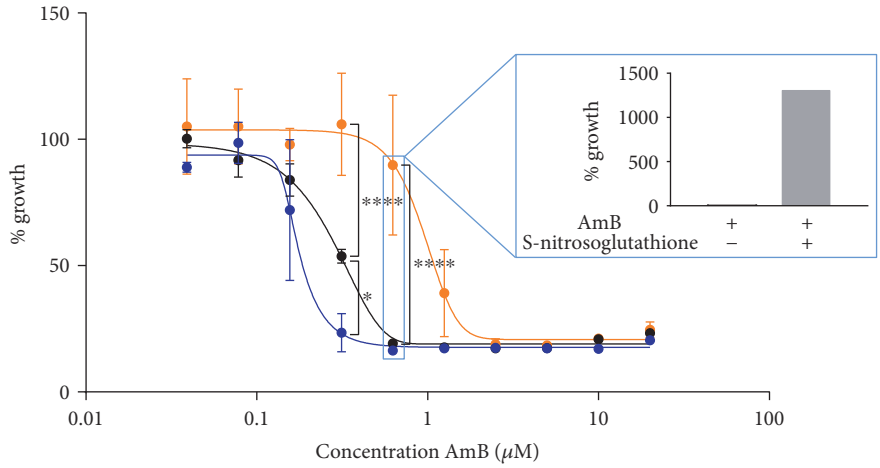

Figure 5: The nitric oxide donor, S-nitrosoglutathione, inhibited the killing activity of AmB. Yeast cells were treated with different concentrations of AmB, in the absence (black) or presence of 200 mM L-NAME (blue) or 2 mM S-nitrosoglutathione (orange). Means and standard errors of the means (SEMs) of at least two independent biological experiments ($n \geq 2$) are presented. The number of CFU/mL for different treatments (insert) was assessed by plating assays and CFU counting and is shown relative to the number of CFU/mL at the start of the experiment. Two-way ANOVA followed by Tukey multiple comparison test was performed to analyse significant differences between the two treatments; $*$ and $****$ represent $P < 0.05$ and $P < 0.0001$, respectively.

after 7.5 and 15 min of incubation with either AmB alone or AmB supplemented with L-NAME.

AmB induced cell cycle arrest in the G2/M phase in yeast at 15 min of treatment, as compared to control cells ($P < 0.0001$) (Figure 6). Interestingly, treatment with L-NAME alone resulted in a decrease in the amount of cells in the S phase at 7.5 and 15 min ($P = 0.03$ and $P = 0.0009$, resp.) and an increase in the amount of cells in the G2/M phase at 15 min ($P = 0.03$), compared to control-treated cells. Yet, L-NAME alone did not increase the other cell cycle phase distributions in a significant manner at both time points, compared to control-treated cells ($P > 0.05$ at 7.5 min and 15 min of treatment). Treatment with AmB-L-NAME did not significantly alter cell cycle phase distributions as compared to those in treatment with AmB alone, suggesting that the observed increased loss of proliferative capacity of yeast cells treated with the AmB-L-NAME combination, compared to AmB treatment alone, was not due to increased cell cycle arrest.

3.6. Candida albicans and Candida glabrata Were More Susceptible to Amphotericin B Treatment in the Presence of Nitric Oxide Radical Production Inhibitors. To validate the results obtained in yeast and in support of the clinical relevance of AmB treatment in the presence of L-NAME, we investigated the effects of this treatment on the human pathogen *Candida albicans*. We confirmed that AmB induced superoxide and nitric oxide radical accumulation ($P < 0.0001$ at 10 μM AmB), associated with loss of proliferative capacity, in *C. albicans*, in a similar dose-dependent way as was observed for *S. cerevisiae* (Figure 7). These results indicated that the range of AmB concentrations used for *S. cerevisiae* was applicable for *C. albicans* as well. Furthermore, we assessed whether treatment at 37°C with AmB in the presence of L-NAME also significantly affected the number of cells that are able to proliferate as compared to treatment with AmB alone. At 37°C, we found that 5 μM AmB resulted in killing of the *C. albicans* culture by 2 Log units (99.00%) and 10 μM AmB by 4 Log units (99.99%). These values are in line with the reported minimal fungicidal concentration (MFC) of AmB (8.66 μM) in a similar experimental setup [48]. Coincubation of 200 mM L-NAME and 5 μM AmB significantly reduced the number of CFUs as compared to treatment with AmB alone ($P < 0.05$) (Figure 8(a)), indicating that L-NAME also enhanced AmB's fungicidal activity against *C. albicans*. Also, in case of *C. glabrata*, we found that 10 μM AmB resulted in killing of *C. glabrata* by 4 Log units (99.99%). These values are in line with the reported MFC of AmB against *C. glabrata* (17 μM) [49]. Also here, 200 mM L-NAME significantly increased AmB's fungicidal activity against *C. glabrata* (Figure 8(b)). All these data point to the clinical potential of combining AmB with L-NAME.

4. Discussion

The aim of this study was to investigate and understand how AmB-induced oxidative and nitrosative stresses (characterized by excess of superoxide radicals and nitric oxide radicals, resp.) are linked to fungal cell death. To inhibit the generation of nitric oxide radicals and nitrosative stress in cells, we used the nitric oxide synthase inhibitor L-NAME. From the bulk studies, we found that superoxide radical accumulation increased when nitric oxide production was inhibited, thereby increasing AmB's antifungal activity. We then further assessed the kinetics of superoxide radical accumulation, membrane permeabilization, and loss of proliferative capacity using a DMF platform in which individual *S. cerevisiae* cells were captured and monitored for their responses over time during treatment. As seeding of *C. albicans* was problematic due to the presence of hyphae, we first tested our hypotheses on *S. cerevisiae* and translated the most

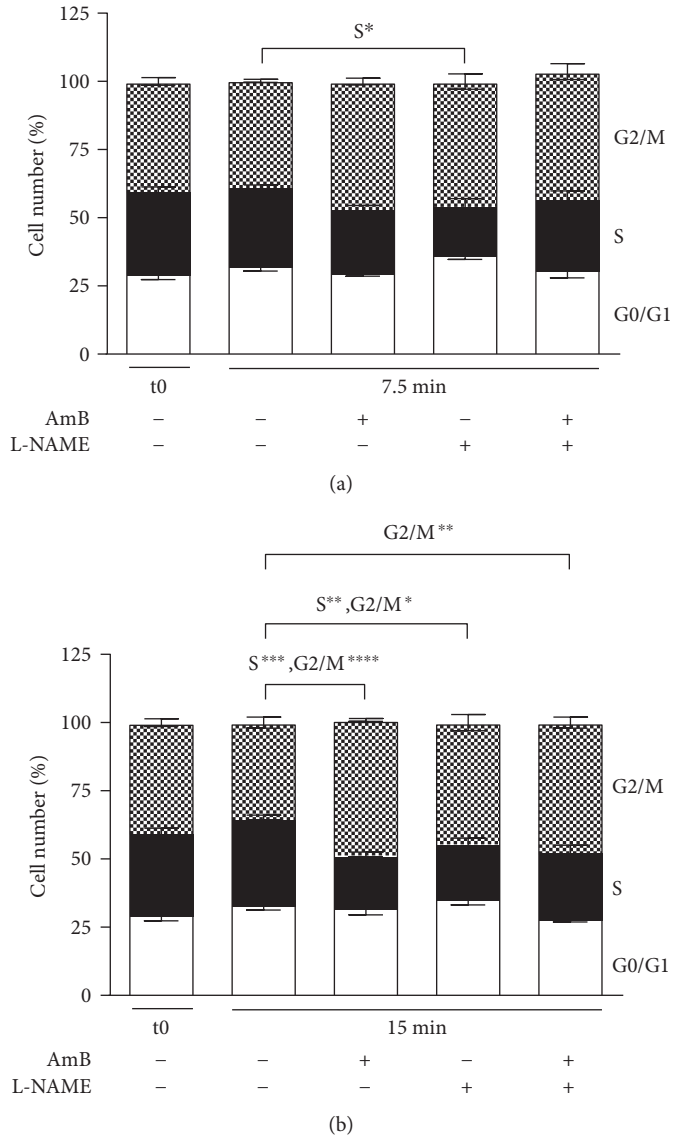

Figure 6: Amphotericin B induced cell cycle arrest in the G2/M phase in yeast. Exponential yeast cultures were treated with either control (1% DMSO; 10% mQ), 200 mM L-NAME (dissolved in mQ), 10 μM AmB (dissolved in DMSO), or a combination of the above for 7.5 min (a) and 15 min (b). After treatment, cells were washed with PBS, fixed in 70% EtOH, stained with PI, and subjected to flow cytometry for cell cycle analysis. White bars represent cells in the G0/G1 phase, black bars represent cells in the S phase, and pixelated bars represent cells in the G2/M phase. Means and standard error of the means (SEMs) of 3 independent biological experiments ($n = 3$) are presented. Two-way ANOVA followed by Tukey multiple comparison test was performed to analyse differences between the cell cycle distributions of control treatment and AmB, L-NAME, or AmB + L-NAME treatment and between cell cycle distributions of AmB treatment and AmB + L-NAME treatment. $*$, $**$, $***$, and $****$ represent $P < 0.05$, $P < 0.01$, $P < 0.001$, and $P < 0.0001$, respectively. Multiplicity-adjusted P values are presented in the main text.

prominent findings to *C. albicans* and *C. glabrata* afterwards using bulk assays. We showed that L-NAME increased and accelerated the effect of AmB on the accumulation of superoxide radicals, membrane permeabilization, and loss of proliferative capacity in *S. cerevisiae*. Moreover, we showed that the data obtained via time lapse experiments in bulk corroborates the data of the single-cell analysis via the DMF platform (Supplemental Information S5 Figure). We revealed that superoxide radicals are important mediators for AmB-induced fungal cell death. However, L-NAME could only increase the killing potential of AmB, but not that of peroxide. This implies an AmB-specific effect of L-NAME and might point to L-NAME's effects via an ergosterol-dependent pathway. Indeed, ROS generation by AmB has been described as a consequence of AmB's spontaneous insertion into ergosterol-containing membranes [50, 51]. In contrast, nitric oxide radicals seemed to play a role in mediating tolerance towards AmB, pointing to a beneficial role of nitric oxide radicals in the yeast response towards AmB. We found that cellular responses are classified into two groups based on the time point that they occur, that is, within 15 min and from 30 to 45 min onwards (Figure 9).

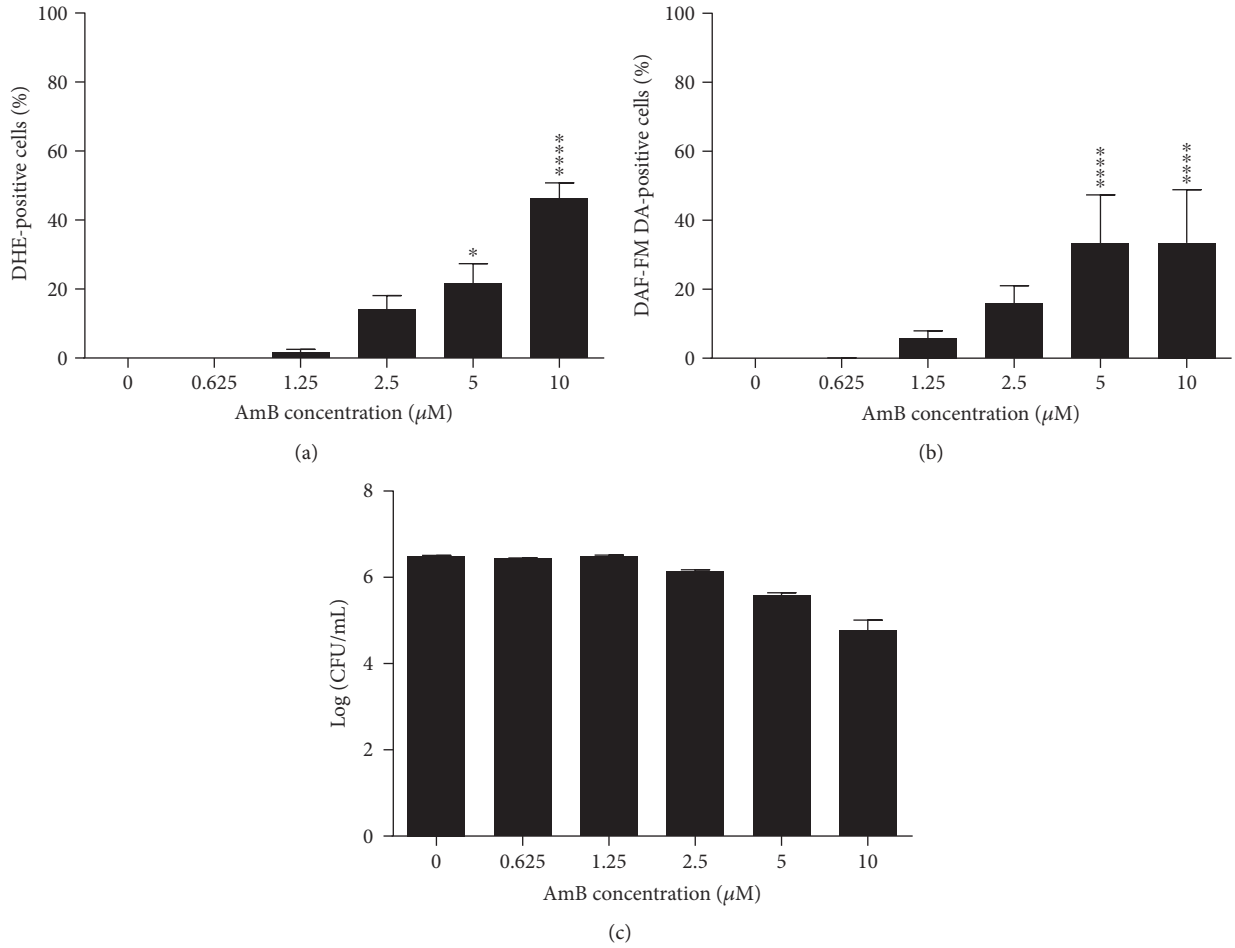

Figure 7: AmB induced accumulation of superoxide and nitric oxide radicals in *C. albicans* and decreased the number of cells that are able to proliferate. Exponential *C. albicans* cultures were treated with different concentrations of AmB for 3 h at room temperature and subjected to flow cytometry or plating assays. (a) Levels of superoxide radical detected by dihydroethidium (DHE) fluorescence and flow cytometry. (b) Levels of nitric oxide radical detected by 4-amino-5-methylamino-2′,7′-difluorofluorescein diacetate (DAF-FM DA) fluorescence and flow cytometry. (c) Number of CFU/mL in Log-scale, assessed by plating assays and CFU counting. Means and standard errors of the means (SEMs) of at least 3 independent biological experiments ($n \geq 3$) are presented. Two-way ANOVA followed by Dunnett multiple comparison test was performed to analyse statistically significant differences in the number of DHE- and DAF-FM DA-positive cells and cells able to proliferate between control treatment and treatment with different concentrations of AmB. $*$ and $****$ represent $P < 0.05$ and $P < 0.0001$, respectively.

Upon treatment of *S. cerevisiae* with AmB in the presence of L-NAME, not only an increased level of superoxide radicals was found as compared to treatment with AmB alone, but also an accelerating effect on these levels was observed (Figures 3(a) and 3(b)). Our DMF approach, allowing a detailed kinetic study at a single-cell level, showed that superoxide radicals accumulated in a biphasic manner during AmB treatment in the presence of L-NAME, resulting in two superoxide radical accumulation peaks at 75 min and 150 min, respectively. This was not observed for cells treated with AmB in the absence of L-NAME, where a superoxide radical accumulation peak seemed to manifest at 180 min, the endpoint of this study (Figures 3(c) and 3(d)). Interestingly, all cell responses, being superoxide radical accumulation, membrane permeabilization, and loss of proliferative capacity, presented themselves significantly faster, as compared to these responses during treatment with AmB alone. Therefore, it might well be that L-NAME solely accelerated AmB action with respect to superoxide radical accumulation and membrane permeabilization, and hence, similar outcomes might be expected for treatment with AmB alone over a longer period of time (i.e., >180 min). Whether, this is the case that requires further investigation. This hypothesis is supported by the fact that L-NAME acts fungistatic (MIC against *S. cerevisiae* of 250 mM), however not fungicidal when administered alone (Supplemental Information S6 Figure), and does not affect the level of superoxide radicals, membrane permeabilization, and proliferative capacity of control cells (Figure 2), suggesting that the observed effect on cell responses is not caused by a similar and dual action of L-NAME and AmB, as is often the case for synergistic interactions.

Secondly, and most notably, L-NAME had a strong enhancing effect on AmB-induced loss of proliferative

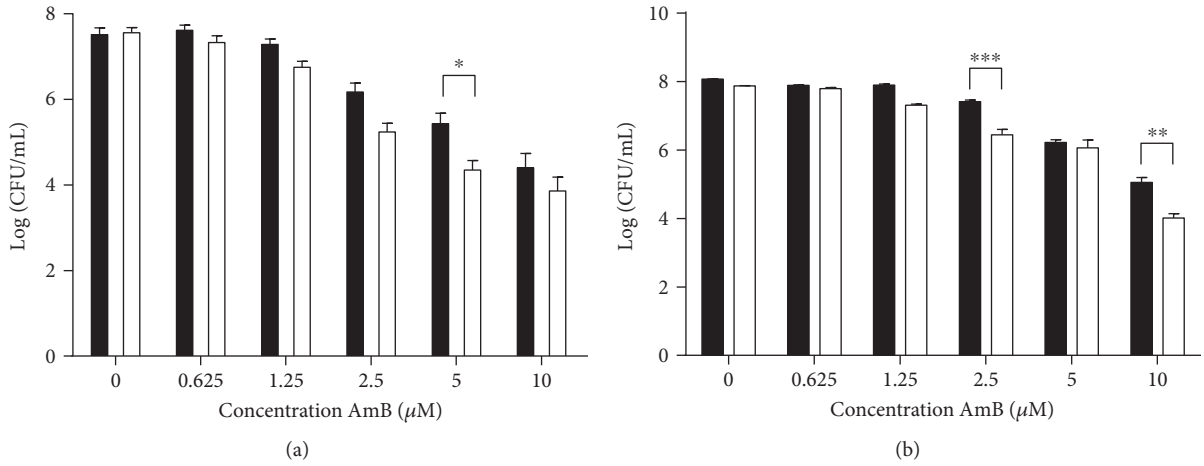

Figure 8: L-NAME significantly decreased the number of AmB-treated cells that are able to proliferate in *C. albicans* (a) and *C. glabrata* (b). Exponential *C. albicans* and *C. glabrata* cultures were treated with different dosages of AmB in the presence (white bars) or absence (black bars) of 200 mM L-NAME for 180 min at 37°C and subjected to plating assays. Means and standard errors of the means (SEMs) of 3 independent biological experiments ($n = 3$) are presented. Two-way ANOVA followed by Tukey multiple comparison test was performed to analyse significant differences between the two treatments; $*$, $**$, and $***$ represent $P < 0.05$, $P < 0.01$, and $P < 0.001$, respectively.

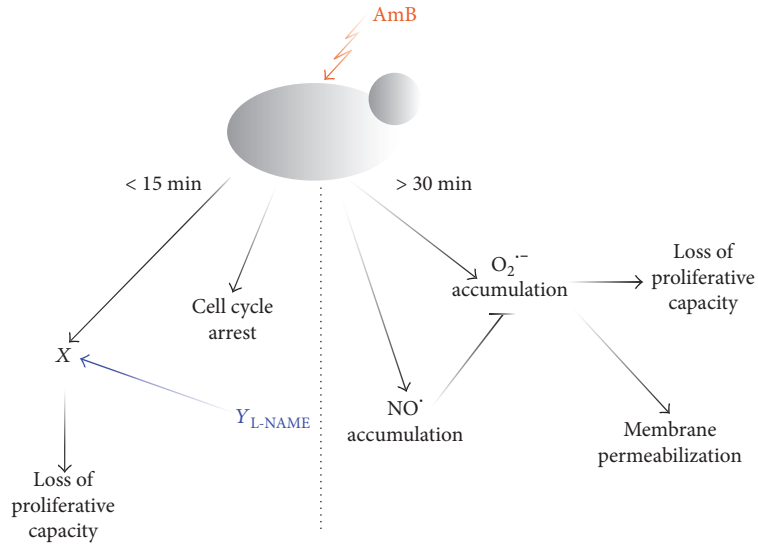

Figure 9: Schematic overview of the major findings on AmB mechanism of action in this study. Within 15 min, AmB caused cell cycle arrest in the G2/M phase and induced a yet to be elucidated event *X*, the latter leading to loss of proliferative capacity in yeast. These effects were independent of nitric oxide radicals, superoxide anion radicals, and membrane permeabilization. After 30 min, AmB induced the accumulation of superoxide radicals, which was associated with membrane permeabilization and loss of proliferative capacity in yeast, and was partially blocked by beneficial action of nitric oxide radicals. Interestingly, the combinatorial action of AmB and L-NAME induced a yet to be identified event *Y* within 15 min, which was independent of nitric oxide radicals, and enhanced the effect of event *X*, leading to enhanced loss of proliferative capacity in yeast.

capacity in yeast: within 15 min, approximately 99.5% of the cells lost their proliferative capacity when subjected to AmB treatment in the presence of L-NAME. In contrast, treatment with AmB alone did not reach a similar negative impact on proliferative capacity of cells within 180 min (Figure 4(c)). This suggest also that here nitric oxide radicals play an important, beneficial, role in the response towards AmB. Yet, we showed that nitric oxide radicals only accumulated from 30 min onwards (Supplemental Information S2 Figure). Hence, L-NAME seemed to have an additional effect apart from inhibiting nitric oxide radical production, resulting in enhancement of AmB fungicidal activity, and this effect occurred within 15 min of treatment (event *Y* in Figure 9). Interestingly, cells receiving treatment with AmB and L-NAME were able to accumulate superoxide radicals only after 30 min, suggesting that these accumulated positive cells were still metabolically active and that AmB-L-NAME-treated cells might use increased levels of superoxide radicals, and thus oxidative stress, to enter a programmed cell death pathway. In addition, as the rapid loss of proliferative

capacity of cells upon combined treatment with AmB and L-NAME could not be explained by superoxide radical accumulation and membrane permeabilization, it seems that mechanisms other than these underlie the negative effect on the proliferative capacity of cells during the first 15 min of AmB treatment in the presence of L-NAME (i.e., event X in Figure 9). A plausible explanation for the loss of proliferative capacity, independent of oxidative stress and nonapoptotic cell death, is cell cycle arrest. We showed that AmB induced cell cycle arrest in the G2/M phase in yeast within 15 min of treatment. These data are in line with other reports on the effect of AmB on the cell cycle in mammalian cell lines [52, 53]. However, this effect was found to be independent of L-NAME, indicating that cell cycle arrest could not account for the observed increased loss of proliferative capacity when cells were treated with the AmB-L-NAME combination.

Overall, it seems that nitric oxide radicals play a beneficial role in AmB antifungal activity, as further demonstrated by the S-nitrosoglutathione-induced inhibition of AmB's killing activity (Figure 5). Nitric oxide radicals were previously shown to protect bacteria against a wide spectrum of antibiotics by alleviating the oxidative stress imposed by them [54]. In addition, nitric oxide radicals were reported to affect fungal cell death, both in beneficial and destructive manners. Specifically, increased intracellular nitric oxide radical levels are suggested to play a cytoprotective role in yeast during stress from heat-shock and hydrostatic pressure [55]. In contrast, PAF26-induced production of nitric oxide radicals was correlated to its antifungal activity, and administering L-NAME partially restored yeast growth in the presence of PAF26, indicating that nitric oxide radicals play an important role in PAF26-induced cell death [44]. In line, Almeida and colleagues showed that nitric oxide is a crucial mediator of H_2O_2-induced apoptosis in yeast and that blockage of nitric oxide radical production by L-NAME decreased the intracellular levels of ROS, thereby increasing survival [46]. Interestingly, in our study, L-NAME increased the accumulation of superoxide radicals during AmB treatment, while decreasing the proliferative capacity of cells in the presence of AmB, and thus decreasing survival. It seems that a nitric oxide radical-dependent tolerance system is switched on upon AmB treatment in yeast, perhaps similar to the system recently described by Nasuno and colleagues [56]. In that study, a downstream pathway of nitric oxide radicals involved in high-temperature stress tolerance in yeast was unravelled. They showed that nitric oxide radicals activated the transcription factor Mac1 that on its turn induced the *CTR1* gene and resulted in increased cellular copper levels, which then resulted in activation of Sod1, a superoxide dismutase [56]. Alternatively, it could also be that nitric oxide activates, potentially via S-nitrosylation, AmB tolerance pathways such as the yeast HOG pathway [57, 58]. How exactly tolerance to AmB via nitric oxide production is mediated requires further investigation.

We further translated the most prominent findings to the human pathogens, *Candida albicans* and *Candida glabrata*, and found that treatment of *C. albicans* or *C. glabrata* with AmB in the presence of L-NAME significantly increases the loss of proliferative capacity, as compared to treatment with AmB alone, suggesting that treatment of AmB in the presence of L-NAME might have a clinical relevance. L-NAME has been extensively studied in *in vitro*, ex vivo, and *in vivo* systems (reviewed in [59]). It was shown to inhibit corneal angiogenesis under chemical growth factor stimulation in rabbits [60] and improve leucocyte adherence and emigration to venular endothelium, characteristic of acute inflammation, in cat jejuni [61]. In addition, L-NAME was found to modulate hemodynamics in dogs [62], ewes [63], and guinea pigs [64] and was shown to reverse sepsis-associated hypotension in various animal models [65]. In humans, L-NAME was tested to treat hypotension, asthma, and sepsis. In view of the latter, L-NAME increased the systemic vascular resistance and blood pressure in septic patients [66, 67]. In treatment of asthma, no adverse effects were found in healthy volunteers and patients with asthma, and results on exhaled nitric oxide levels indicated that L-NAME might be used for treatment of asthma [68]. Finally, L-NAME increased the mean arterial pressure and cerebral blood flow, treating hypotension in patients with tetraplegia. No adverse effects on healthy volunteers or patients were found [69–71]. Hence, although L-NAME as such is not used in a clinical setting to date, it has been studied extensively in humans during the past decades.

AmB, on the other hand, is used in clinical settings to treat invasive fungal infections. However, its applicability is limited due to its nephrotoxicity and hence, it must be used with care [26]. Recent findings indicated that AmB exerts its antifungal action by extracting ergosterol from the plasma membrane, resulting in loss of cell membrane integrity, interference with ergosterol-depending cellular processes, and ultimately cell death [29]. In addition, AmB treatment causes a significant loss of fungal replication competency and numerous morphological and physiological effects on susceptible yeast cells, including cytoplasm shrinking, abnormal nuclear and mitochondrial morphologies, and oxidative stress [72]. Finally, Teixeira-Santos and colleagues showed that pathogenic and nonpathogenic yeast cells develop compensatory responses towards AmB treatment, related to membrane polarization, metabolic activity, and ROS production, depending on the drug concentration and the duration of the treatment [14]. Likewise, we found that treatment of yeast cells with clinically relevant AmB concentrations (i.e., 0.1 μM to 21.6 μM AmB [14, 73]) induces the accumulation of superoxide radicals, in addition to nitric oxide radicals, in *S. cerevisiae* and *C. albicans*. Furthermore, we found that clinically relevant AmB concentrations significantly increase the loss of proliferative capacity of *S. cerevisiae*, *C. albicans*, and *C. glabrata* in the presence of L-NAME.

5. Conclusions

In conclusion, we showed that L-NAME can increase and accelerate AmB-induced superoxide radical accumulation and loss of proliferative capacity in *S. cerevisiae*, the latter was confirmed in the human pathogens *C. albicans* and *C. glabrata*. Moreover, we found that the production of nitric oxide radicals seems to constitute a tolerance mechanism

that is induced by AmB treatment and partially counteracts AmB activity. Moreover, the combinatorial action of AmB and L-NAME induced an additional, yet to be elucidated, event that further enhanced AmB's fungicidal activity. The effects of both AmB and L-NAME have been extensively studied in various *in vitro* and *in vivo* models, pointing towards the potential of AmB-L-NAME combination treatment. However, further research on pharmacology and toxicology of the AmB-L-NAME combination needs to be performed in order to assess its potential clinical relevance.

Conflicts of Interest

The authors declare that there is no conflict of interest regarding the publication of this article.

Authors' Contributions

Kim Vriens, Caroline Struyfs, and Tanne L. Cools performed all cytotoxicity assays in bulk; Phalguni Tewari Kumar performed all cytotoxicities on the DMF platform; Belém Sampaio-Marques carried out cell cycle analysis; Kim Vriens, Phalguni Tewari Kumar, and Caroline Struyfs performed data analysis, and Kim Vriens, Phalguni Tewari Kumar, Caroline Struyfs, and Pieter Spincemaille wrote the manuscript. Tadej Kokalj, Paula Ludovico, Jeroen Lammertyn, Bruno P. A. Cammue, and Karin Thevissen supervised the study. All authors critically read and approved the manuscript. Kim Vriens, Phalguni Tewari Kumar, and Caroline Struyfs contributed equally to this work and hence are the shared first authors.

Acknowledgments

Kim Vriens acknowledges the receipt of a predoctoral grant from the Flanders Innovation & Entrepeneurship Agency (IWT-SB 111016); Karin Thevissen acknowledges the receipt of a mandate of Industrial Research Fund (KU Leuven). In addition, the research leading to these results has received funding from the Research Foundation - Flanders (FWO G086114N and G080016N) and the KU Leuven (OT 13/058 and IDO 10/012, IOF KP/12/009 Atheromix, IOF KP/12/002 Nanodiag). This work was partially developed under the scope of the project NORTE-01-0145-FEDER-000013, supported by the Northern Portugal Regional Operational Programme (NORTE 2020), under the Portugal 2020 Partnership Agreement, through the European Regional Development Fund (FEDER). Belém Sampaio-Marques is supported by the fellowship SFRH/BPD/90533/2012 funded by Fundação para a Ciência e Tecnologia (FCT, Portugal).

References

[1] A. J. Brown, K. Haynes, and J. Quinn, "Nitrosative and oxidative stress responses in fungal pathogenicity," *Current Opinion in Microbiology*, vol. 12, no. 4, pp. 384–391, 2009.

[2] D. Kaloriti, A. Tillmann, E. Cook et al., "Combinatorial stresses kill pathogenic *Candida* species," *Medical Mycology*, vol. 50, no. 7, pp. 699–709, 2012.

[3] C. K. Ferrari, P. C. Souto, E. L. Franca, and A. C. Honorio-Franca, "Oxidative and nitrosative stress on phagocytes' function: from effective defense to immunity evasion mechanisms," *Archivum Immunologiae et Therapiae Experimentalis*, vol. 59, no. 6, pp. 441–448, 2011.

[4] B. S. Hromatka, S. M. Noble, and A. D. Johnson, "Transcriptional response of *Candida albicans* to nitric oxide and the role of the YHB1 gene in nitrosative stress and virulence," *Molecular Biology of the Cell*, vol. 16, no. 10, pp. 4814–4826, 2005.

[5] P. Moradas-Ferreira and V. Costa, "Adaptive response of the yeast *Saccharomyces cerevisiae* to reactive oxygen species: defences, damage and death," *Redox Report*, vol. 5, no. 5, pp. 277–285, 2000.

[6] N. Chauhan, J. P. Latge, and R. Calderone, "Signalling and oxidant adaptation in *Candida albicans* and *Aspergillus fumigatus*," *Nature Reviews Microbiology*, vol. 4, no. 6, pp. 435–444, 2006.

[7] M. Cuellar-Cruz, E. Lopez-Romero, E. Ruiz-Baca, and R. Zazueta-Sandoval, "Differential response of *Candida albicans* and *Candida glabrata* to oxidative and nitrosative stresses," *Current Microbiology*, vol. 69, no. 5, pp. 733–739, 2014.

[8] N. Delattin, B. P. A. Cammue, and K. Thevissen, "Reactive oxygen species-inducing antifungal agents and their activity against fungal biofilms," *Future Medicinal Chemistry*, vol. 6, no. 1, pp. 77–90, 2014.

[9] A. Bink, D. Vandenbosch, T. Coenye, H. Nelis, B. P. Cammue, and K. Thevissen, "Superoxide dismutases are involved in *Candida albicans* biofilm persistence against miconazole," *Antimicrobial Agents and Chemotherapy*, vol. 55, no. 9, pp. 4033–4037, 2011.

[10] D. Vandenbosch, K. Braeckmans, H. J. Nelis, and T. Coenye, "Fungicidal activity of miconazole against *Candida* spp. biofilms," *The Journal of Antimicrobial Chemotherapy*, vol. 65, no. 4, pp. 694–700, 2010.

[11] C. D. Mahl, C. S. Behling, F. S. Hackenhaar et al., "Induction of ROS generation by fluconazole in *Candida glabrata*: activation of antioxidant enzymes and oxidative DNA damage," *Diagnostic Microbiology and Infectious Disease*, vol. 82, no. 3, pp. 203–208, 2015.

[12] C. E. Linares, S. R. Giacomelli, D. Altenhofen, S. H. Alves, V. M. Morsch, and M. R. Schetinger, "Fluconazole and amphotericin-B resistance are associated with increased catalase and superoxide dismutase activity in *Candida albicans* and *Candida dubliniensis*," *Revista da Sociedade Brasileira de Medicina Tropical*, vol. 46, no. 6, pp. 752–758, 2013.

[13] M. Blatzer, E. Jukic, W. Posch et al., "Amphotericin B resistance in *Aspergillus terreus* is overpowered by co-application of pro-oxidants," *Antioxidants & Redox Signaling*, vol. 23, no. 18, pp. 1424–1438, 2015.

[14] R. Teixeira-Santos, E. Ricardo, S. G. Guerreiro, S. Costa-de-Oliveira, A. G. Rodrigues, and C. Pina-Vaz, "New insights regarding yeast survival following exposure to liposomal amphotericin B," *Antimicrobial Agents and Chemotherapy*, vol. 59, no. 10, pp. 6181–6187, 2015.

[15] A. C. Mesa-Arango, N. Trevijano-Contador, E. Román et al., "The production of reactive oxygen species is a universal action mechanism of Amphotericin B against pathogenic yeasts and contributes to the fungicidal effect of this drug," *Antimicrobial Agents and Chemotherapy*, vol. 58, no. 11, pp. 6627–6638, 2014.

[16] F. Sangalli-Leite, L. Scorzoni, A. C. Mesa-Arango et al., "Amphotericin B mediates killing in *Cryptococcus neoformans* through the induction of a strong oxidative burst," *Microbes and Infection*, vol. 13, no. 5, pp. 457–467, 2011.

[17] J. Kelly, R. Rowan, M. McCann, and K. Kavanagh, "Exposure to caspofungin activates cap and hog pathways in *Candida albicans*," *Medical Mycology*, vol. 47, no. 7, pp. 697–706, 2009.

[18] K. Wang, W. Dang, J. Xie et al., "Antimicrobial peptide protonectin disturbs the membrane integrity and induces ROS production in yeast cells," *Biochimica et Biophysica Acta (BBA) - Biomembranes*, vol. 1848, no. 10, Part A, p. 21, 2015.

[19] T. Wang, G. Shi, J. Shao et al., "In vitro antifungal activity of baicalin against *Candida albicans* biofilms via apoptotic induction," *Microbial Pathogenesis*, vol. 87, pp. 21–29, 2015.

[20] K. Vriens, B. P. Cammue, and K. Thevissen, "Antifungal plant defensins: mechanisms of action and production," *Molecules*, vol. 19, no. 8, pp. 12280–12303, 2014.

[21] A. M. Aerts, L. Bammens, G. Govaert et al., "The antifungal plant Defensin HsAFP1 from *Heuchera sanguinea* induces apoptosis in *Candida albicans*," *Frontiers in Microbiology*, vol. 2, p. 47, 2011.

[22] A. M. Aerts, I. E. François, E. M. Meert, Q. T. Li, B. P. Cammue, and K. Thevissen, "The antifungal activity of RsAFP2, a plant defensin from raphanus sativus, involves the induction of reactive oxygen species in *Candida albicans*," *Journal of Molecular Microbiology and Biotechnology*, vol. 13, no. 4, pp. 243–247, 2007.

[23] B. M. E. Hayes, M. R. Bleackley, J. L. Wiltshire, M. A. Anderson, A. Traven, and N. L. van der Weerden, "Identification and mechanism of action of the plant Defensin NaD1 as a new member of the antifungal drug arsenal against *Candida albicans*," *Antimicrobial Agents and Chemotherapy*, vol. 57, no. 8, pp. 3667–3675, 2013.

[24] G. F. Ferreira, L. de Matos Baltazar, J. R. Santos et al., "The role of oxidative and nitrosative bursts caused by azoles and amphotericin B against the fungal pathogen *Cryptococcus gattii*," *The Journal of Antimicrobial Chemotherapy*, vol. 68, no. 8, pp. 1801–1811, 2013.

[25] E. O. Mello, S. F. Ribeiro, A. O. Carvalho et al., "Antifungal activity of *Pv*D1 defensin involves plasma membrane permeabilization, inhibition of medium acidification, and induction of ROS in fungi cells," *Current Microbiology*, vol. 62, no. 4, pp. 1209–1217, 2011.

[26] A. Lemke, A. F. Kiderlen, and O. Kayser, "Amphotericin B," *Applied Microbiology and Biotechnology*, vol. 68, no. 2, pp. 151–162, 2005.

[27] A. J. Phillips, I. Sudbery, and M. Ramsdale, "Apoptosis induced by environmental stresses and amphotericin B in *Candida albicans*," *Proceedings of the National Academy of Sciences of the United States of America*, vol. 100, no. 24, pp. 14327–14332, 2003.

[28] R. S. Al-Dhaheri and L. J. Douglas, "Apoptosis in *Candida* biofilms exposed to amphotericin B," *Journal of Medical Microbiology*, vol. 59, Part 2, pp. 149–157, 2010.

[29] T. M. Anderson, M. C. Clay, A. G. Cioffi et al., "Amphotericin forms an extramembranous and fungicidal sterol sponge," *Nature Chemical Biology*, vol. 10, no. 5, pp. 400–406, 2014.

[30] P. T. Kumar, K. Vriens, M. Cornaglia et al., "Digital microfluidics for time-resolved cytotoxicity studies on single non-adherent yeast cells," *Lab on a Chip*, vol. 15, no. 8, pp. 1852–1860, 2015.

[31] M. E. Cardenas, M. C. Cruz, M. Del Poeta, N. Chung, J. R. Perfect, and J. Heitman, "Antifungal activities of antineoplastic agents: *Saccharomyces cerevisiae* as a model system to study drug action," *Clinical Microbiology Reviews*, vol. 12, no. 4, pp. 583–611, 1999.

[32] T. Edlind, L. Smith, K. Henry, S. Katiyar, and J. Nickels, "Antifungal activity in *Saccharomyces cerevisiae* is modulated by calcium signalling," *Molecular Microbiology*, vol. 46, no. 1, pp. 257–268, 2002.

[33] G. Serhan, C. M. Stack, G. G. Perrone, and C. O. Morton, "The polyene antifungals, amphotericin B and nystatin, cause cell death in *Saccharomyces cerevisiae* by a distinct mechanism to amphibian-derived antimicrobial peptides," *Annals of Clinical Microbiology and Antimicrobials*, vol. 13, p. 18, 2014.

[34] M. E. Cabral, L. I. Figueroa, and J. I. Farina, "Synergistic antifungal activity of statin-azole associations as witnessed by *Saccharomyces cerevisiae*- and *Candida utilis*-bioassays and ergosterol quantification," *Revista Iberoamericana de Micología*, vol. 30, no. 1, pp. 31–38, 2013.

[35] B. Tebbets, D. Stewart, S. Lawry et al., "Identification and characterization of antifungal compounds using a *Saccharomyces cerevisiae* reporter bioassay," *PLoS One*, vol. 7, no. 5, p. 4, 2012.

[36] D. Witters, K. Knez, F. Ceyssens, R. Puers, and J. Lammertyn, "Digital microfluidics-enabled single-molecule detection by printing and sealing single magnetic beads in femtoliter droplets," *Lab on a Chip*, vol. 13, no. 11, pp. 2047–2054, 2013.

[37] A. Gomes, E. Fernandes, and J. L. Lima, "Fluorescence probes used for detection of reactive oxygen species," *Journal of Biochemical and Biophysical Methods*, vol. 65, no. 2-3, pp. 45–80, 2005.

[38] M. M. Tarpey, D. A. Wink, and M. B. Grisham, "Methods for detection of reactive metabolites of oxygen and nitrogen: in vitro and in vivo considerations," *American Journal of Physiology – Regulatory Integrative and Comparative Physiology*, vol. 286, no. 3, pp. R431–R444, 2004.

[39] F. Madeo, E. Frohlich, and K. U. Frohlich, "A yeast mutant showing diagnostic markers of early and late apoptosis," *The Journal of Cell Biology*, vol. 139, no. 3, pp. 729–734, 1997.

[40] J. S. Beckman, T. W. Beckman, J. Chen, P. A. Marshall, and B. A. Freeman, "Apparent hydroxyl radical production by peroxynitrite: implications for endothelial injury from nitric oxide and superoxide," *Proceedings of the National Academy of Sciences of the United States of America*, vol. 87, no. 4, pp. 1620–1624, 1990.

[41] R. Radi, "Nitric oxide, oxidants, and protein tyrosine nitration," *Proceedings of the National Academy of Sciences of the United States of America*, vol. 101, no. 12, pp. 4003–4008, 2004.

[42] R. O. Poyton, K. A. Ball, and P. R. Castello, "Mitochondrial generation of free radicals and hypoxic signaling," *Trends in Endocrinology and Metabolism*, vol. 20, no. 7, pp. 332–340, 2009.

[43] D. D. Rees, R. M. Palmer, R. Schulz, H. F. Hodson, and S. Moncada, "Characterization of three inhibitors of endothelial nitric oxide synthase in vitro and in vivo," *British Journal of Pharmacology*, vol. 101, no. 3, pp. 746–752, 1990.

[44] L. Carmona, M. Gandia, B. Lopez-Garcia, and J. F. Marcos, "Sensitivity of *Saccharomyces cerevisiae* to the cell-penetrating antifungal peptide PAF26 correlates with endogenous nitric oxide (NO) production," *Biochemical and Biophysical Research Communications*, vol. 417, no. 1, pp. 56–61, 2012.

[45] N. S. Osorio, A. Carvalho, A. J. Almeida et al., "Nitric oxide signaling is disrupted in the yeast model for Batten disease,"

Molecular Biology of the Cell, vol. 18, no. 7, pp. 2755–2767, 2007.

[46] B. Almeida, S. Buttner, S. Ohlmeier et al., "NO-mediated apoptosis in yeast," *Journal of Cell Science*, vol. 120, Part 18, pp. 3279–3288, 2007.

[47] D. Collett, *Modelling Survival Data in Medical Research*, Chapman and Hall/CRC, 2 edition, 2003.

[48] T. V. M. Vila, K. Ishida, W. de Souza, K. Prousis, T. Calogeropoulou, and S. Rozental, "Effect of alkylphospholipids on *Candida albicans* biofilm formation and maturation," *The Journal of Antimicrobial Chemotherapy*, vol. 68, no. 1, pp. 113–125, 2013.

[49] E. Cantón, J. Pemán, A. Viudes, G. Quindós, M. Gobernado, and A. Espinel-Ingroff, "*Minimum* Fungicidal concentrations of amphotericin B for bloodstream *Candida* species," *Diagnostic Microbiology and Infectious Disease*, vol. 45, no. 3, pp. 203–206, 2003.

[50] E. B. Cohen, "The role of signaling via aqueous pore formation in resistance responses to amphotericin B," *Antimicrobial Agents and Chemotherapy*, vol. 60, no. 9, pp. 5122–5129, 2016.

[51] E. Thomas, E. Roman, S. Claypool, N. Manzoor, J. Pla, and S. L. Panwar, "Mitochondria influence CDR1 efflux pump activity, Hog1-mediated oxidative stress pathway, iron homeostasis, and Ergosterol levels in *Candida albicans*," *Antimicrobial Agents and Chemotherapy*, vol. 57, no. 11, pp. 5555–5580, 2013.

[52] C. C. Uribe, F. Dos Santos de Oliveira, B. Grossmann et al., "Cytotoxic effect of amphotericin B in a myofibroblast cell line," *Toxicology In Vitro*, vol. 27, no. 7, pp. 2105–2109, 2013.

[53] L. Y. Chen, M. T. Sheu, C. K. Liao, F. C. Tsai, W. Y. Kao, and C. H. Su, "Taiwanofungus camphoratus (Syn Antrodia camphorata) extract and amphotericin B exert adjuvant effects via mitochondrial apoptotic pathway," *Integrative Cancer Therapies*, vol. 12, no. 2, pp. 153–164, 2013.

[54] I. Gusarov, K. Shatalin, M. Starodubtseva, and E. Nudler, "Endogenous nitric oxide protects bacteria against a wide spectrum of antibiotics," *Science*, vol. 325, no. 5946, pp. 1380–1384, 2009.

[55] T. Domitrovic, F. L. Palhano, C. Barja-Fidalgo, M. DeFreitas, M. T. Orlando, and P. M. Fernandes, "Role of nitric oxide in the response of *Saccharomyces cerevisiae* cells to heat shock and high hydrostatic pressure," *FEMS Yeast Research*, vol. 3, no. 4, pp. 341–346, 2003.

[56] R. Nasuno, M. Aitoku, Y. Manago, A. Nishimura, Y. Sasano, and H. Takagi, "Nitric oxide-mediated antioxidative mechanism in yeast through the activation of the transcription factor Mac1," *PLoS One*, vol. 9, no. 11, article e113788, 2014.

[57] R. I. Astuti, D. Watanabe, and H. Takagi, "Nitric oxide signaling and its role in oxidative stress response in *Schizosaccharomyces pombe*," *Nitric Oxide*, vol. 52, pp. 29–40, 2016.

[58] S. H. Qi, L. Y. Hao, J. Yue, Y. Y. Zong, and G. Y. Zhang, "Exogenous nitric oxide negatively regulates the S-nitrosylation p38 mitogen-activated protein kinase activation during cerebral ischaemia and reperfusion," *Neuropathology and Applied Neurobiology*, vol. 39, no. 3, pp. 284–297, 2013.

[59] J. Vitecek, A. Lojek, G. Valacchi, and L. Kubala, "Arginine-based inhibitors of nitric oxide synthase: therapeutic potential and challenges," *Mediators of Inflammation*, vol. 2012, Article ID 318087, 22 pages, 2012.

[60] M. Ziche, L. Morbidelli, E. Masini et al., "Nitric oxide mediates angiogenesis in vivo and endothelial cell growth and migration in vitro promoted by substance P," *The Journal of Clinical Investigation*, vol. 94, no. 5, pp. 2036–2044, 1994.

[61] P. Kubes, M. Suzuki, and D. N. Granger, "Nitric oxide: an endogenous modulator of leukocyte adhesion," *Proceedings of the National Academy of Sciences*, vol. 88, no. 11, pp. 4651–4655, 1991.

[62] M. Sonntag, A. Deussen, and J. Schrader, "Role of nitric oxide in local blood flow control in the anaesthetized dog," *Pflügers Archiv*, vol. 420, no. 2, pp. 194–199, 1992.

[63] G. A. Van Buren, D. S. Yang, and K. E. Clark, "Estrogen-induced uterine vasodilatation is antagonized by L-nitroarginine methyl ester, an inhibitor of nitric oxide synthesis," *American Journal of Obstetrics and Gynecology*, vol. 167, no. 3, pp. 828–833, 1992.

[64] A. Vials and G. Burnstock, "Effects of nitric oxide synthase inhibitors, L-NG-nitroarginine and L-NG-nitroarginine methyl ester, on responses to vasodilators of the guinea-pig coronary vasculature," *British Journal of Pharmacology*, vol. 107, no. 2, pp. 604–609, 1992.

[65] R. G. Kilbourn, C. Szabo, and D. L. Traber, "Beneficial versus detrimental effects of nitric oxide synthase inhibitors in circulatory shock: lessons learned from experimental and clinical studies," *Shock*, vol. 7, no. 4, pp. 235–246, 1997.

[66] A. Petros, D. Bennett, and P. Vallance, "Effect of nitric oxide synthase inhibitors on hypotension in patients with septic shock," *The Lancet*, vol. 338, no. 8782-8783, pp. 1557-1558, 1991.

[67] J. A. Avontuur, R. P. Tutein Nolthenius, J. W. van Bodegom, and H. A. Bruining, "Prolonged inhibition of nitric oxide synthesis in severe septic shock: a clinical study," *Critical Care Medicine*, vol. 26, no. 4, pp. 660–667, 1998.

[68] D. H. Yates, S. A. Kharitonov, P. S. Thomas, and P. J. Barnes, "Endogenous nitric oxide is decreased in asthmatic patients by an inhibitor of inducible nitric oxide synthase," *American Journal of Respiratory and Critical Care Medicine*, vol. 154, no. 1, pp. 247–250, 1996.

[69] J. M. Wecht, J. P. Weir, A. H. Krothe, A. M. Spungen, and W. A. Bauman, "Normalization of supine blood pressure after nitric oxide synthase inhibition in persons with tetraplegia," *The Journal of Spinal Cord Medicine*, vol. 30, no. 1, pp. 5–9, 2007.

[70] J. M. Wecht, J. P. Weir, D. S. Goldstein et al., "Direct and reflexive effects of nitric oxide synthase inhibition on blood pressure," *American Journal of Physiology Heart and Circulatory Physiology*, vol. 294, no. 1, pp. H190–H197, 2008.

[71] J. M. Wecht, M. Radulovic, D. Rosado-Rivera, R. L. Zhang, M. F. LaFountaine, and W. A. Bauman, "Orthostatic effects of midodrine versus L-NAME on cerebral blood flow and the renin-angiotensin-aldosterone system in tetraplegia," *Archives of Physical Medicine and Rehabilitation*, vol. 92, no. 11, pp. 1789–1795, 2011.

[72] B. Chudzik, M. Koselski, A. Czurylo, K. Trebacz, and M. Gagos, "A new look at the antibiotic amphotericin B effect on *Candida albicans* plasma membrane permeability and cell viability functions," *European Biophysics Journal*, vol. 44, no. 1-2, pp. 77–90, 2015.

[73] T. J. Walsh, V. Yeldandi, M. McEvoy et al., "Safety, tolerance, and pharmacokinetics of a small unilamellar liposomal formulation of amphotericin B (AmBisome) in neutropenic patients," *Antimicrobial Agents and Chemotherapy*, vol. 42, pp. 2391–2398, 1998.